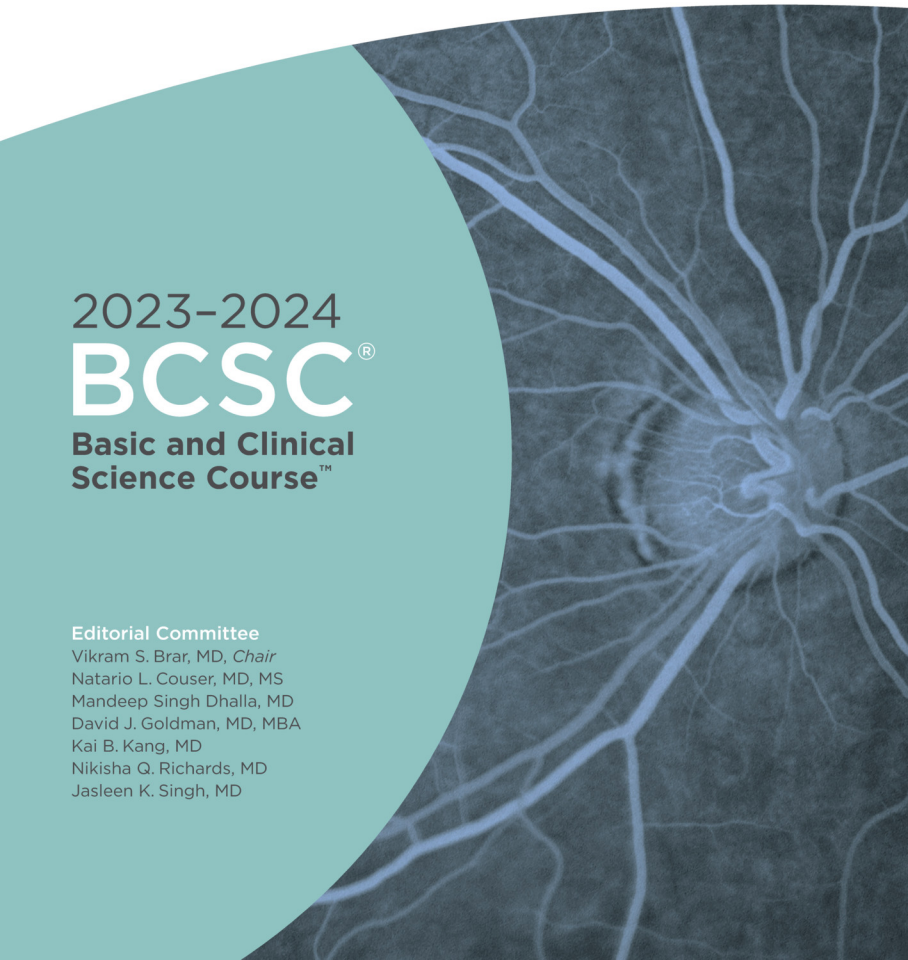
AMERICAN ACADEMY OF OPHTHALMOLOGY®
Protecting Sight. Empowering Lives.

2 | Fundamentals and Principles of Ophthalmology



2023–2024
BCSC®
Basic and Clinical Science Course™

Editorial Committee
Vikram S. Brar, MD, *Chair*
Natario L. Couser, MD, MS
Mandeep Singh Dhalla, MD
David J. Goldman, MD, MBA
Kai B. Kang, MD
Nikisha Q. Richards, MD
Jasleen K. Singh, MD



AMERICAN ACADEMY
OF OPHTHALMOLOGY®
Protecting Sight. Empowering Lives.

2 | Fundamentals and Principles of Ophthalmology

Major Revision Edition

2023–2024
BCSC
Basic and Clinical Science Course™



Published after collaborative review with the European Board of Ophthalmology subcommittee

The American Academy of Ophthalmology is accredited by the Accreditation Council for Continuing Medical Education (ACCME) to provide continuing medical education for physicians.

The American Academy of Ophthalmology designates this enduring material for a maximum of 15 *AMA PRA Category 1 Credits*™. Physicians should claim only the credit commensurate with the extent of their participation in the activity.

CME expiration date: June 1, 2026. *AMA PRA Category 1 Credits*™ may be claimed only once between June 1, 2023, and the expiration date.

BCSC® volumes are designed to increase the physician's ophthalmic knowledge through study and review. Users of this activity are encouraged to read the text and then answer the study questions provided at the back of the book.

To claim *AMA PRA Category 1 Credits*™ upon completion of this activity, learners must demonstrate appropriate knowledge and participation in the activity by taking the posttest for Section 2 and achieving a score of 80% or higher. For further details, please see the instructions for requesting CME credit at the back of the book.

The Academy provides this material for educational purposes only. It is not intended to represent the only or best method or procedure in every case, nor to replace a physician's own judgment or give specific advice for case management. Including all indications, contraindications, side effects, and alternative agents for each drug or treatment is beyond the scope of this material. All information and recommendations should be verified, prior to use, with current information included in the manufacturers' package inserts or other independent sources, and considered in light of the patient's condition and history. Reference to certain drugs, instruments, and other products in this course is made for illustrative purposes only and is not intended to constitute an endorsement of such. Some material may include information on applications that are not considered community standard, that reflect indications not included in approved FDA labeling, or that are approved for use only in restricted research settings. **The FDA has stated that it is the responsibility of the physician to determine the FDA status of each drug or device he or she wishes to use, and to use them with appropriate, informed patient consent in compliance with applicable law.** The Academy specifically disclaims any and all liability for injury or other damages of any kind, from negligence or otherwise, for any and all claims that may arise from the use of any recommendations or other information contained herein.

All trademarks, trade names, logos, brand names, and service marks of the American Academy of Ophthalmology (AAO), whether registered or unregistered, are the property of AAO and are protected by US and international trademark laws. These trademarks include, but are not limited to, AAO; AAOE; AMERICAN ACADEMY OF OPHTHALMOLOGY; BASIC AND CLINICAL SCIENCE COURSE; BCSC; EYENET; EYEWIKI; FOCAL POINTS; FOCUS DESIGN (logo on cover); IRIS; IRIS REGISTRY; ISRS; OKAP; ONE NETWORK; OPHTHALMOLOGY; OPHTHALMOLOGY GLAUCOMA; OPHTHALMOLOGY RETINA; OPHTHALMOLOGY SCIENCE; OPHTHALMOLOGY WORLD NEWS; PREFERRED PRACTICE PATTERN; PROTECTING SIGHT. EMPOWERING LIVES.; THE OPHTHALMIC NEWS AND EDUCATION NETWORK.

Cover image: From BCSC Section 9, *Uveitis and Ocular Inflammation*. Image courtesy of Sam S. Dahr, MD, MS.

MIX
From responsible sources
FSC
www.fsc.org
FSC™ C023083

Copyright © 2023 American Academy of Ophthalmology. All rights reserved. No part of this publication may be reproduced without written permission.

Printed in South Korea.

Basic and Clinical Science Course



Christopher J. Rapuano, MD, Philadelphia, Pennsylvania
Senior Secretary for Clinical Education



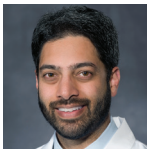
J. Timothy Stout, MD, PhD, MBA, Houston, Texas
Secretary for Lifelong Learning and Assessment



Colin A. McCannel, MD, Los Angeles, California
BCSC Course Chair

Section 2

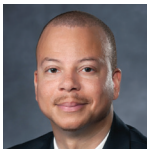
Faculty for the Major Revision



Vikram S. Brar, MD
Chair
Richmond, Virginia



Kai B. Kang, MD
Chicago, Illinois



Natario L. Couser, MD, MS
Richmond, Virginia



Nikisha Q. Richards, MD
Richmond, Virginia



Mandeep Singh Dhalla, MD
Fort Lauderdale, Florida



Jasleen K. Singh, MD
Chesterfield, Missouri



David J. Goldman, MD, MBA
Detroit, Michigan

The Academy acknowledges the following committees for review of this edition:

Vision Rehabilitation Committee: Mona A. Kaleem, MD, Bethesda, Maryland

BCSC Resident/Fellow Reviewers: Sharon L. Jick, MD, *Chair,* St Louis, Missouri; Arpine Barsegian, MD; Sunil Bellur, MD; Hong-Gam T. Le, MD; Michael A. Puente Jr, MD; Nandini Venkateswaran, MD

Practicing Ophthalmologists Advisory Committee for Education: Bradley D. Fouraker, MD, *Primary Reviewer* and *Chair,* Tampa, Florida; George S. Ellis Jr, MD, New Orleans, Louisiana; Kevin E. Lai, MD, Carmel, Indiana; Philip R. Rizzuto, MD, Providence, Rhode Island; J. James Rowsey, MD, Largo, Florida; Gaurav K. Shah, MD, San Francisco, California; Scott X. Stevens, MD, Bend, Oregon; Troy M. Tanji, MD, Waipahu, Hawaii

European Board of Ophthalmology: Anna P. Maino, MBBS, PGCert, *Liaison,* Manchester, England; Rehana Sadia, MBBS, Manchester, England

The Academy also acknowledges the following committee for assistance in developing Study Questions and Answers for this BCSC Section:

Resident Self-Assessment Committee: Evan L. Waxman, MD, PhD, *Chair,* Pittsburgh, Pennsylvania; Amanda D. Henderson, MD, Baltimore, Maryland

Finally, the Academy acknowledges the following consultants for their contributions to the development of Chapter 18: Aaron Y. Lee, MD, Seattle, Washington; J. Peter Campbell, MD, MPH, Portland, Oregon; Thomas S. Hwang, MD, Portland, Oregon; Michael D. Abràmoff, MD, PhD, Iowa City, Iowa.

Recent Past Faculty

Simon K. Law, MD
Jennifer L. Lindsey, MD
David A. Mackey, MD
Robert L. Schultze, MD
Evan Silverstein, MD
Ravi S. J. Singh, MD

The Academy also gratefully acknowledges the contributions of numerous past faculty and advisory committee members who have played an important role in the development of previous editions of the Basic and Clinical Science Course.

American Academy of Ophthalmology Staff

Dale E. Fajardo, EdD, MBA, *Vice President, Education*
Beth Wilson, *Director, Continuing Professional Development*
Denise Evenson, *Director, Brand & Creative*
Susan Malloy, *Acquisitions and Development Manager*
Stephanie Tanaka, *Publications Manager*
Jasmine Chen, *Manager, E-Learning*

Sarah Page, *Online Education and Licensing Manager*
Rayna Ungersma, *Manager, Curriculum Development*
Lana Ip, *Senior Designer*
Amanda Fernandez, *Publications Editor*
Beth Collins, *Medical Editor*
Kenny Guay, *Publications Specialist*
Debra Marchi, *Online Education Specialist*

Financial Disclosures

Academy staff members who contributed to the development of this product state that within the 24 months prior to their contributions to this CME activity and for the duration of development, they have had no financial interest in or other relationship with any entity that produces, markets, resells, or distributes health care goods or services consumed by or used in patients, or with any competing commercial product or service.

The authors and reviewers state that within the 24 months prior to their contributions to this CME activity and for the duration of development, they have had the following financial relationships:*

Dr Campbell: Boston AI Lab (C), Genentech (S)

Dr Couser: Elsevier (P), Retrophin, Inc (S)

Dr Dhalla: Genentech (L)

Dr Fouraker: Addition Technology (C, L), AJL Ophthalmic SA (C, L), Alcon Laboratories (C, L), OASIS Medical, Inc (C, L)

Dr Henderson: Horizon Therapeutics (C)

Dr Lai: Ophthalmology Review (O), Twenty/Twenty Therapeutics (C)

Dr Lee: Carl Zeiss Meditec AG (S), Genentech (C), Gyroscope Therapeutics (C), Johnson & Johnson Vision (C), Microsoft Corporation (S), Novartis (S), NVIDIA GTC (S), Santen, Inc (S), Topcon Medical Systems, Inc (L), Verana Health (C)

Dr Rowsey: HEO3 (P)

Dr Shah: Allergan (C, L, S), DORC International BV (S), Regeneron Pharmaceuticals, Inc (C, L, S)

Dr Venkateswaran: Alcon Laboratories (C), CorneaGen (L), Johnson & Johnson Vision (C)

All relevant financial relationships have been mitigated.

The other authors and reviewers state that within the 24 months prior to their contributions to this CME activity and for the duration of development, they have had no financial interest in or other relationship with any entity that produces, markets, resells, or distributes health care goods or services consumed by or used in patients, or with any competing commercial product or service.

* C = consultant fee, paid advisory boards, or fees for attending a meeting; E = employed by or received a W2 from a commercial company; L = lecture fees or honoraria, travel fees or reimbursements when speaking at the invitation of a commercial company; O = equity ownership/stock options in publicly or privately traded firms, excluding mutual funds; P = patents and/or royalties for intellectual property; S = grant support or other financial support to the investigator from all sources, including research support from government agencies, foundations, device manufacturers, and/or pharmaceutical companies

American Academy of Ophthalmology
655 Beach Street
Box 7424
San Francisco, CA 94120-7424

Contents

Introduction to the BCSC xix

Objectives **1**

PART I Anatomy **3**

1 Orbit and Ocular Adnexa **5**

Highlights 5
Orbital Anatomy 5
- Dimensions of the Adult Orbit 6
- Bony Orbit 6
- Orbital Margin 6
- Orbital Roof 7
- Medial Orbital Wall 8
- Orbital Floor 9
- Lateral Orbital Wall 10
- Orbital Foramina, Canals, and Fissures 11

Periorbital Sinuses 13
Cranial Nerves 16
Ciliary Ganglion 16
- Branches of the Ciliary Ganglion 16
- Short Ciliary Nerves 17

Extraocular Muscles. 17
Extraocular Muscle Origins 18
Extraocular Muscle Insertions 21
Extraocular Muscle Distribution in the Orbit 22
- Blood Supply to the Extraocular Muscles 23
- Innervation of the Extraocular Muscles 24
- Fine Structure of the Extraocular Muscles 24

Vascular Supply and Drainage of the Orbit 24
- Posterior and Anterior Ciliary Arteries 24
- Vortex Veins 27
- Orbital Veins 28

Eyelids 28
- Anatomy 29
- Vascular Supply 38
- Lymphatics 39

Lacrimal Glands and Excretory System 39
- Lacrimal Gland 39
- Accessory Glands 41
- Lacrimal Excretory System 42

Conjunctiva 44
Caruncle 45
Plica Semilunaris 45
Tenon Capsule 45

2 The Eye 47
Highlights 47
Introduction 47
Topographic Features of the Globe 47
Tear Film 49
Cornea 50
Characteristics of the Central and Peripheral Cornea 51
Epithelium and Basal Lamina 52
Bowman Layer 52
Stroma 53
Descemet Membrane 53
Endothelium 54
Corneal Nerves 55
Limbus 56
Sclera 57
Anterior Chamber 60
Trabecular Meshwork 64
Uveal Trabecular Meshwork 65
Corneoscleral Meshwork 65
Juxtacanalicular Meshwork 65
Schlemm Canal 65
Collector Channels 67
Uvea 69
Iris 70
Stroma 72
Vessels and Nerves 73
Dilator Muscle and Anterior Pigmented Epithelium 73
Sphincter Muscle 74
Posterior Pigmented Epithelium 74
Ciliary Body 74
Ciliary Epithelium and Stroma 75
Ciliary Muscle 76
Supraciliary Space 79
Choroid 79
Choriocapillaris and Choroidal Vessels 80
Choroidal Stroma 82
Lens 82
Capsule 83
Epithelium 83
Fibers 85
Zonular Fibers 85

Retina . . . 86
Neurosensory Retina . . . 87
Topography of the Retina . . . 97
Retinal Pigment Epithelium . . . 100
Bruch Membrane . . . 102
Ora Serrata . . . 103
Vitreous . . . 103

3 Cranial Nerves: Central and Peripheral Connections . . . 107
Highlights . . . 107
Olfactory Nerve (First Cranial Nerve) . . . 110
Optic Nerve (Second Cranial Nerve) . . . 110
Intraocular Region . . . 111
Intraorbital Region . . . 116
Intracanalicular Region . . . 118
Intracranial Region . . . 118
Visual Pathway . . . 118
Blood Supply of the Optic Nerve and Visual Pathway . . . 123
Oculomotor Nerve (Third Cranial Nerve) . . . 126
Pathways for the Pupil Reflexes . . . 128
Trochlear Nerve (Fourth Cranial Nerve) . . . 131
Trigeminal Nerve (Fifth Cranial Nerve) . . . 132
Mesencephalic Nucleus . . . 132
Main Sensory Nucleus . . . 133
Spinal Nucleus and Tract . . . 133
Motor Nucleus . . . 134
Intracranial Pathway of Cranial Nerve V . . . 134
Divisions of Cranial Nerve V . . . 135
Abducens Nerve (Sixth Cranial Nerve) . . . 137
Facial Nerve (Seventh Cranial Nerve) . . . 138
Tear Reflex Pathway . . . 141
The Cerebral Vascular System . . . 142
Cavernous Sinus . . . 142
Other Venous Sinuses . . . 142
Circle of Willis . . . 143

PART II Embryology . . . 147

4 Ocular Development . . . 149
Highlights . . . 149
General Principles . . . 149
Eye Development . . . 154
Lens . . . 160
Posterior Segment . . . 161
Uvea . . . 166
Cornea, Anterior Chamber, and Sclera . . . 168

Development of the Extraocular Muscles, Adnexa, and Orbit 168
Extraocular Muscles 168
Adnexa 170
Orbit 171
Genetic Cascades and Morphogenic Gradients 171
Homeobox Gene Program 172
Growth Factors, Diffusible Ligands, and Morphogens 172
Future Directions 173

PART III Genetics 175

Introduction 177
Terminology 177

5 Molecular Genetics 179
Highlights 179
Cell Division and the Cell Cycle 179
Cell Division 179
The Cell Cycle 179
Cell Cycle Regulation 180
Meiosis 181
Genes and Chromosomes 183
Alleles 183
Segregation. 184
Independent Assortment 184
Linkage 185
Gene Structure 185
Noncoding DNA 187
Gene Transcription and Translation: The Central Dogma of Genetics 187
Intron Excision 189
Alternative Splicing and Isoforms 190
Methylation 190
Imprinting 190
X-Inactivation 191
DNA Damage and Repair 191
Repair 191
Apoptosis 192
Pathogenic Variants 192
Polymorphisms 193
Pathogenic Variants Versus Polymorphisms. 193
Genome, Genotype, Phenotype 193
Single-Gene Disorders 194
Cancer Genes. 194
Anticipation 195
Penetrance 195
Expressivity 196
Pleiotropism 196

The Search for Genes in Specific Diseases . . . 197
Polymerase Chain Reaction. . . . 197
Genetic Markers . . . 197
Gene Dosage . . . 198
Linkage and Disease Association . . . 198
Candidate Gene Approaches . . . 199
Pathogenic Variant Screening and Identification . . . 199
Direct Sequencing. . . . 201
Genome-Wide Association Studies . . . 201
Determining Whether Genetic Change Is a Pathogenic Variant . . . 205
Gene Therapy . . . 205
Replacement of an Absent Gene Product in X-Linked and Recessive Diseases . . . 205
Strategies for Dominant Diseases . . . 207

6 Clinical Genetics . . . 211
Highlights . . . 211
Introduction . . . 211
Pedigree Analysis . . . 212
Patterns of Inheritance . . . 214
Dominant Versus Recessive Inheritance . . . 214
Autosomal Recessive Inheritance . . . 215
Autosomal Dominant Inheritance . . . 219
X-Linked Inheritance . . . 221
Maternal Inheritance . . . 225
Terminology: Hereditary, Genetic, Congenital, Familial . . . 225
Chromosome Analysis . . . 227
Aneuploidy of Autosomes . . . 228
Mosaicism . . . 229
Important Chromosomal Aberrations in Ophthalmology . . . 231
Knudson's 2-Hit Hypothesis and the Genetics of Retinoblastoma and the Neurocutaneous Syndromes . . . 233
Racial and Ethnic Concentration of Genetic Disorders . . . 237
Lyonization . . . 238
Mitochondrial Disease . . . 240
Chronic Progressive External Ophthalmoplegia . . . 241
MELAS and MIDD . . . 241
Leber Hereditary Optic Neuropathy . . . 242
Neuropathy, Ataxia, and Retinitis Pigmentosa . . . 243
Complex Genetic Disease: Polygenic and Multifactorial Inheritance . . . 243
Pharmacogenetics . . . 244
Clinical Management of Genetic Disease . . . 245
Accurate Diagnosis . . . 245
Complete Explanation of the Disease . . . 246
Treatment of the Disease Process . . . 246

Genetic Counseling . . . 248
Issues in Genetic Counseling . . . 249
Reproductive Issues . . . 250
Referral to Providers of Support for Persons With Disabilities . . . 251
Recommendations for Genetic Testing of Inherited Eye Disease . . . 252

PART IV Biochemistry and Metabolism . . . 255

Introduction . . . 257

7 Tear Film . . . 259
Highlights . . . 259
Overview of Tear Film . . . 259
Lipid Layer . . . 262
Mucoaqueous Layer . . . 262
Aqueous Component . . . 263
Mucin Component . . . 264
Tear Secretion . . . 265
Tear Dysfunction . . . 267

8 Cornea . . . 271
Highlights . . . 271
Biochemistry and Physiology of the Cornea . . . 271
Epithelium . . . 273
Penetration of the Corneal Epithelium . . . 274
Bowman Layer . . . 275
Stroma . . . 275
Descemet Membrane and Endothelium . . . 277
Descemet Membrane . . . 277
Endothelium . . . 277

9 Aqueous Humor, Iris, and Ciliary Body . . . 281
Highlights . . . 281
Physiology of the Iris and Ciliary Body . . . 281
Dynamics of the Aqueous Humor . . . 282
Blood–Aqueous Barrier . . . 282
Aqueous Humor Formation and Secretion . . . 282
Clinical Implications of Breakdown of the Blood–Aqueous Barrier . . . 284
Composition of the Aqueous Humor . . . 285
Inorganic Ions . . . 287
Organic Anions . . . 287
Carbohydrates . . . 288
Glutathione . . . 288
Proteins . . . 288
Growth-Modulatory Factors . . . 289
Oxygen and Carbon Dioxide . . . 291

10 Lens . . . 293
Highlights . . . 293
Overview . . . 293
Structure of the Lens . . . 293
Capsule . . . 293
Epithelium . . . 294
Cortex and Nucleus . . . 295
Chemical Composition of the Lens . . . 295
Plasma Membranes . . . 295
Lens Proteins . . . 296
Transparency and Physiologic Aspects of the Lens . . . 298
Lens Transparency . . . 298
Lens Physiology . . . 299
Lens Metabolism and Formation of Sugar Cataracts . . . 300
Energy Production . . . 300
Carbohydrate Cataracts . . . 302

11 Vitreous . . . 303
Highlights . . . 303
Overview . . . 303
Composition . . . 304
Collagen . . . 304
Hyaluronan and Chondroitin Sulfate . . . 305
Soluble and Collagen Fiber–Associated Proteins . . . 307
Zonular Fibers . . . 307
Low-Molecular-Weight Solutes . . . 308
Hyalocytes . . . 308
Biochemical Changes With Aging and Disease . . . 309
Vitreous Liquefaction and Posterior Vitreous Detachment . . . 309
Myopia . . . 310
Vitreous as an Inhibitor of Angiogenesis . . . 311
Physiologic Changes After Vitrectomy . . . 311
Injury With Hemorrhage and Inflammation . . . 311
Genetic Disease Involving the Vitreous . . . 313
Enzymatic Vitreolysis . . . 313

12 Retina . . . 315
Highlights . . . 315
Overview . . . 315
Retinal Oxygen Consumption . . . 316
Photoreceptors and Phototransduction . . . 316
Rod Phototransduction . . . 316
Energy Metabolism of Photoreceptor Outer Segments . . . 321
Cone Phototransduction . . . 321
Visual Cycle . . . 322
Trivariant Color Vision . . . 322
Photoreceptor Gene Alterations Causing Retinal Degeneration . . . 323

Classes of Retinal Cells . . . 324
Neurons . . . 326
Glial Cells . . . 328
Vascular Cells. . . . 328
Retinal Electrophysiology . . . 329

13 Retinal Pigment Epithelium . . . 331
Highlights . . . 331
Overview of RPE Structure. . . . 331
Biochemical Composition of the RPE . . . 333
Proteins . . . 333
Lipids . . . 334
Nucleic Acids . . . 334
Major Physiologic Roles of the RPE . . . 334
Vitamin A Regeneration . . . 336
Phagocytosis of Shed Photoreceptor Outer-Segment Discs . . . 338
Transport . . . 338
Pigmentation . . . 341
Retinal Adhesion . . . 341
Secretion. . . . 342
The Role of Autophagy in the RPE . . . 342
The RPE in Disease . . . 343

14 Reactive Oxygen Species and Antioxidants . . . 345
Highlights . . . 345
Overview . . . 345
Reactive Oxygen Species . . . 346
Sources of Reactive Oxygen Species . . . 346
Lipid Peroxidation . . . 347
Reactive Oxygen Species and Defense Mechanisms . . . 349
Oxidative Damage to the Lens and Protective Mechanisms . . . 350
Vulnerability of the Retina to Reactive Oxygen Species . . . 351
Antioxidants in the Retina and Retinal Pigment Epithelium . . . 352
Selenium, Glutathione, and Glutathione Peroxidase . . . 352
Vitamin E . . . 352
Superoxide Dismutase and Catalase . . . 353
Ascorbate . . . 353
Carotenoids . . . 354
The Role of Oxidative Stress in Vision-Threatening Ophthalmic Diseases . . . 354
Glaucoma . . . 355
Diabetic Retinopathy . . . 357
Age-Related Macular Degeneration . . . 358

PART V Ocular Pharmacology 361

15 Pharmacologic Principles 363
Highlights 363
Introduction to Pharmacologic Principles 364
Pharmacokinetics 364
Pharmacodynamics 364
Pharmacotherapeutics 365
Toxicity 365
Pharmacologic Principles and Aging 367
Pharmacokinetics: The Route of Drug Delivery 368
Topical Administration: Eyedrops 368
Topical Administration: Ointments 377
Local Administration: Injections 377
Systemic Administration 380
Ocular Drug Design and Methods of Delivery 382
Prodrugs 382
Sustained-Release and Alternative Methods of Drug Delivery 382
Pharmacogenetics: The Influence of Genetic Variation on Drug Efficacy and Toxicity 386

16 Ocular Pharmacotherapeutics 387
Highlights 387
Legal Aspects of Medical Therapy 388
Compounded Pharmaceuticals 390
Adherence 391
Cholinergic Drugs 392
Muscarinic Drugs 394
Nicotinic Drugs 401
Adrenergic Drugs 402
α-Adrenergic Drugs 402
β-Adrenergic Drugs 408
Carbonic Anhydrase Inhibitors 410
Prostaglandin Analogues 413
Nitric Oxide Donors 414
Rho Kinase Inhibitors 415
Fixed-Combination Medications 417
Osmotic Drugs 417
Actions and Uses 417
Intravenous Drugs 418
Oral Drugs 418
Anti-inflammatory Drugs 419
Glucocorticoids 419
Nonsteroidal Anti-inflammatory Drugs 430
Antiallergic Drugs: Mast-Cell Stabilizers and Antihistamines 434
Antifibrotic Drugs 436

Medications for Dry Eye Syndrome . . . 437
Ocular Decongestants . . . 439
Antimicrobial Drugs . . . 439
Penicillins and Cephalosporins . . . 439
Other Antibacterial Drugs . . . 443
Antifungal Drugs . . . 451
Antiviral Drugs . . . 454
Medications for *Acanthamoeba* Infections . . . 459
Ocular Penetration of Systemically Administered Antimicrobial Agents . . . 459
Local Anesthetics . . . 460
Overview . . . 460
Specific Drugs . . . 463
Anesthetics in Intraocular Surgery . . . 464
Purified Neurotoxin Complex . . . 466
Hyperosmolar Drugs . . . 466
Irrigating Solutions . . . 466
Diagnostic Agents and Surgical Adjuvants . . . 467
Ophthalmic Viscosurgical Devices . . . 468
Fibrinolytic Agents . . . 469
Thrombin . . . 469
Antifibrinolytic Agents . . . 470
Vitamin Supplements and Antioxidants . . . 470
Interferon . . . 470
Growth Factors and Growth Factor Inhibitors . . . 471
Growth Factors . . . 471
Growth Factor Inhibitors . . . 473
Biosimilar Drugs . . . 475

PART VI Imaging and Digital Ophthalmology . . . 477

17 Principles of Radiology for the Comprehensive Ophthalmologist . . . 479
Highlights . . . 479
Overview . . . 479
Computed Tomography . . . 480
Disadvantages . . . 482
Magnetic Resonance Imaging . . . 483
Disadvantages . . . 484
Ultrasonography . . . 488
A-Scan Ultrasonography . . . 489
B-Scan Ultrasonography . . . 490
Ultrasound Biomicroscopy . . . 494
Ordering Imaging Studies . . . 495

18 Digital Ophthalmology 505
Highlights 505
Introduction 505
Data 506
Electronic Health Records 506
Digital Ophthalmology Standards 506
Big Data 507
Teleophthalmology 508
Artificial Intelligence 508
Clinical Example 509
Machine Learning 510
Design, Bias, and Reference Standards 510
Conclusions 512

Additional Materials and Resources 513
Requesting Continuing Medical Education Credit 515
Study Questions 517
Answers 525
Index 533

Introduction to the BCSC

The Basic and Clinical Science Course (BCSC) is designed to meet the needs of residents and practitioners for a comprehensive yet concise curriculum of the field of ophthalmology. The BCSC has developed from its original brief outline format, which relied heavily on outside readings, to a more convenient and educationally useful self-contained text. The Academy updates and revises the course annually, with the goals of integrating the basic science and clinical practice of ophthalmology and of keeping ophthalmologists current with new developments in the various subspecialties.

The BCSC incorporates the effort and expertise of more than 100 ophthalmologists, organized into 13 Section faculties, working with Academy editorial staff. In addition, the course continues to benefit from many lasting contributions made by the faculties of previous editions. Members of the Academy Practicing Ophthalmologists Advisory Committee for Education, Committee on Aging, and Vision Rehabilitation Committee review every volume before major revisions, as does a group of select residents and fellows. Members of the European Board of Ophthalmology, organized into Section faculties, also review volumes before major revisions, focusing primarily on differences between American and European ophthalmology practice.

Organization of the Course

The Basic and Clinical Science Course comprises 13 volumes, incorporating fundamental ophthalmic knowledge, subspecialty areas, and special topics:

1 Update on General Medicine
2 Fundamentals and Principles of Ophthalmology
3 Clinical Optics and Vision Rehabilitation
4 Ophthalmic Pathology and Intraocular Tumors
5 Neuro-Ophthalmology
6 Pediatric Ophthalmology and Strabismus
7 Oculofacial Plastic and Orbital Surgery
8 External Disease and Cornea
9 Uveitis and Ocular Inflammation
10 Glaucoma
11 Lens and Cataract
12 Retina and Vitreous
13 Refractive Surgery

References

Readers who wish to explore specific topics in greater detail may consult the references cited within each chapter and listed in the Additional Materials and Resources section at the back of the book. These references are intended to be selective rather than exhaustive,

chosen by the BCSC faculty as being important, current, and readily available to residents and practitioners.

Multimedia

This edition of Section 2, *Fundamentals and Principles of Ophthalmology,* includes videos related to topics covered in the book and interactive content, or "activities," developed by members of the BCSC faculty. The videos and activities are available to readers of the print and electronic versions of Section 2 (www.aao.org/bcscvideo_section02) and (www.aao.org/bcscactivity_section02). Mobile device users can scan the QR codes below (a QR-code reader may need to be installed on the device) to access the videos and activities.

Videos

Activities

Self-Assessment and CME Credit

Each volume of the BCSC is designed as an independent study activity for ophthalmology residents and practitioners. The learning objectives for this volume are given on pages 1 and 2. The text, illustrations, and references provide the information necessary to achieve the objectives; the study questions allow readers to test their understanding of the material and their mastery of the objectives. Physicians who wish to claim CME credit for this educational activity may do so online by following the instructions at the end of the book.*

Conclusion

The Basic and Clinical Science Course has expanded greatly over the years, with the addition of much new text, numerous illustrations, and video content. Recent editions have sought to place greater emphasis on clinical applicability while maintaining a solid foundation in basic science. As with any educational program, it reflects the experience of its authors. As its faculties change and medicine progresses, new viewpoints emerge on controversial subjects and techniques. Not all alternate approaches can be included in this series; as with any educational endeavor, the learner should seek additional sources, including Academy Preferred Practice Pattern Guidelines.

The BCSC faculty and staff continually strive to improve the educational usefulness of the course; you, the reader, can contribute to this ongoing process. If you have any suggestions or questions about the series, please do not hesitate to contact the faculty or the editors. The authors, editors, and reviewers hope that your study of the BCSC will be of lasting value and that each Section will serve as a practical resource for quality patient care.

* There is no formal American Board of Ophthalmology (ABO) approval process for self-assessment activities. Any CME activity that qualifies for ABO Continuing Certification credit may also be counted as "self-assessment" as long as it provides a mechanism for individual learners to review their own performance, knowledge base, or skill set in a defined area of practice. For instance, grand rounds, medical conferences, or journal activities for CME credit that involve a form of individualized self-assessment may count as a self-assessment activity.

Objectives

Upon completion of BCSC Section 2, *Fundamentals and Principles of Ophthalmology,* the reader should be able to

- identify the bones that make up the orbital walls and the orbital foramina
- identify the origin and pathways of cranial nerves II–VII
- identify the origins and insertions of the extraocular muscles
- describe the distribution of the arterial and venous circulations of the orbit and optic nerve
- describe the anastomoses in the orbit between the external and internal carotid arteries
- describe the venous drainage of the eyelids and orbit, as well as the cavernous sinus
- describe the structural–functional relationships of the outflow pathways for aqueous humor of the eye
- identify various ocular tissues and describe their function and ultrastructural details
- describe the elements of the visual cycle and phototransduction cascade and their relation to vision and inherited retinal diseases
- list the events of embryogenesis that are important for the subsequent development of the eye and orbit
- identify the roles of growth factors, homeobox genes, and neural crest cells in the genesis of the eye
- describe the sequence of events in the differentiation of the ocular tissues during embryonic and fetal development of the eye
- draw a pedigree diagram and identify the main patterns of inheritance
- describe the organization of the human genome and the role of pathogenic variants in health and disease

- explain how appropriate diagnosis and management of genetic diseases can lead to better patient care
- describe the role of the ophthalmologist in the provision of genetic counseling as well as the indications for ordering genetic testing and referring patients for gene therapy
- discuss the biochemical composition of the various parts of the eye and the eye's secretions
- list the various functions of the retinal pigment epithelium, such as phagocytosis, vitamin A metabolism, and maintenance of retinal adhesion
- describe the role of free radicals and antioxidants in the eye
- describe the phases of clinical trials in relation to drug approval by the US Food and Drug Administration
- describe the features of the eye that facilitate or impede drug delivery
- describe the basic principles of ocular pharmacokinetics, pharmacodynamics, and pharmacogenetics
- describe the basic principles underlying the use of autonomic therapeutic agents in a variety of ocular conditions
- list the indications, contraindications, mechanisms of action, and adverse effects of various drugs used in the management of glaucoma
- describe the mechanisms of action of antibiotic, antiviral, and antifungal medications
- describe the mechanisms of action, delivery, and adverse effects of drugs used in corticosteroid and immunomodulatory therapy
- describe available anti–vascular endothelial growth factor agents
- describe the anesthetic agents used in ophthalmology and methods of their delivery
- describe the basic principles of and indications for neuroimaging and ophthalmic ultrasonography as they relate to common ophthalmic and neuro-ophthalmic conditions
- describe the basic principles of artificial intelligence and how artificial intelligence applies to ophthalmology

PART I
Anatomy

CHAPTER 1

Orbit and Ocular Adnexa

This chapter includes a related video. Go to www.aao.org/bcscvideo_section02 or scan the QR code in the text to access this content.

This chapter includes related activities. Go to www.aao.org/bcscactivity_section02 or scan the QR codes in the text to access this content.

Highlights

- Emissary channels in the medial wall of the orbit can facilitate the spread of infection from the ethmoid sinus into the orbit.
- Fractures of the orbital floor can involve the infraorbital groove, which contains the infraorbital nerve, and should be suspected in cases of orbital trauma associated with infraorbital hypoesthesia.
- The optic canal, housed in the lesser wing of the sphenoid, transmits the optic nerve and ophthalmic artery. The shortest, most direct path to the optic nerve and optic canal is along the medial wall.
- At their origin (the annulus of Zinn), the medial and superior rectus muscles are adjacent to the optic nerve sheath. Because of this anatomical relationship, patients with retrobulbar optic neuritis experience pain with eye movement.
- An imaginary line drawn externally between the extraocular muscle insertions approximates the ora serrata internally. Understanding this anatomical relationship is important when assessing the prognosis of and risk for future complications of scleral lacerations in this area.
- The eyelid vasculature includes multiple sites of anastomoses between the external and internal carotid arteries.

Orbital Anatomy

Orbital anatomy, pathology, and changes associated with aging are discussed in detail in BCSC Section 7, *Oculofacial Plastic and Orbital Surgery.* Activity 1-1 demonstrates the critical structures of the orbital walls. Also see Chapter 17, Activities 17-1 and 17-2, which demonstrate normal structures identified on axial and coronal orbital imaging, respectively, with computed tomography (CT) and magnetic resonance imaging (MRI).

ACTIVITY 1-1 Critical structures of the orbital walls.
Developed by Zoë R. Williams, MD. Illustrations by Dave Peace.

Dimensions of the Adult Orbit

Each eye lies within a bony orbit, the volume of which is slightly less than 30 mL. Each orbit is pear shaped; the optic nerve represents the stem. The orbital entrance averages approximately 35 mm in height and 45 mm in width and is widest approximately 1 cm behind the anterior orbital margin. The depth of the orbit, measured from the orbital entrance to the orbital apex, varies from 40 to 45 mm, depending on whether the measurement is made along the lateral wall or the medial wall. Race and sex affect each of these measurements and therefore exophthalmometry, the measurement of the forward globe prominence, varies as well (Table 1-1).

Bony Orbit

The bony orbit, which surrounds the globe and helps protect it from blunt injury, comprises 7 bones (Figs 1-1, 1-2; also see Chapter 1 in BCSC Section 7, *Oculofacial Plastic and Orbital Surgery*):

- ethmoid bone
- frontal bone
- lacrimal bone
- maxillary bone
- palatine bone
- sphenoid bone (greater and lesser wings)
- zygomatic bone

Orbital Margin

The orbital margin, or rim, forms a quadrilateral spiral whose superior margin is formed by the frontal bone, which is interrupted medially by the supraorbital notch (see Fig 1-1A).

Table 1-1 Exophthalmometry Based on Race and Gender

	Women		Men	
Race	Mean (mm)	Upper Limit of Normal (mm)	Mean (mm)	Upper Limit of Normal (mm)
African American	18	23	19	25
Asian[a]	14	19	14	19
Caucasian	15	20	17	22

[a] Based on results seen in a Taiwanese population.

Data from Migliori ME, Gladstone GJ. Determination of the normal range of exophthalmometric values for Black and White adults. *Am J Ophthalmol.* 1984;98(4):438–442; and from Tsai CC, Kau HC, Kao SC, Hsu WM. Exophthalmos of patients with Graves' disease in Chinese of Taiwan. *Eye (Lond).* 2006;20(5):569–573.

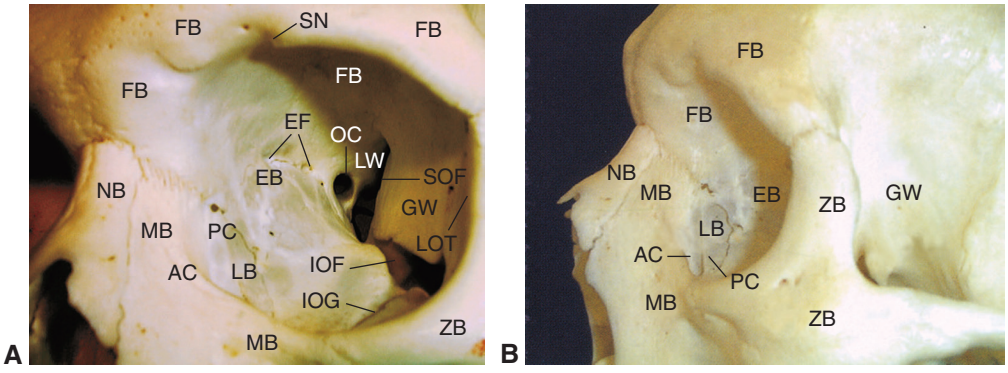


Figure 1-1 Anatomy of left human orbit and skull. **A,** Coronal view of left human orbit. **B,** Sagittal view of left human orbit demonstrating the medial wall. AC = anterior lacrimal crest (part of maxillary bone); EB = ethmoid bone; EF = anterior and posterior ethmoid foramina; FB = frontal bone; GW = greater wing of sphenoid bone; IOF = inferior orbital fissure; IOG = inferior orbital groove; LB = lacrimal bone; LOT = lateral orbital tubercle; LW = lesser wing of the sphenoid bone; MB = maxillary bone; NB = nasal bone; OC = optic canal; PC = posterior lacrimal crest: part of lacrimal bone; SN = supraorbital notch; SOF = superior orbital fissure; ZB = zygomatic bone. *(Modified with permission from Forrester JV, Dick AD, McMenamin PG, Roberts F, Pearlman E.* The Eye: Basic Sciences in Practice. *4th Ed. Elsevier; 2016:Fig 1.5.)*

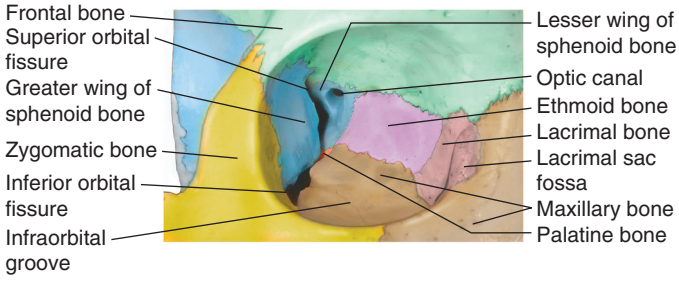


Figure 1-2 Color diagram of bones of the right orbit, coronal view. *(Illustration by Dave Peace.)*

The medial margin is formed above by the frontal bone and below by the posterior lacrimal crest of the lacrimal bone and the anterior lacrimal crest of the maxillary bone. The inferior margin derives from the maxillary and zygomatic bones. Laterally, the zygomatic and frontal bones complete the rim.

Orbital Roof

The orbital roof is formed from 2 bones (Fig 1-3):

- orbital plate of the frontal bone
- lesser wing of the sphenoid bone

The fossa for the lacrimal gland, lying anterolaterally behind the zygomatic process of the frontal bone, resides within the orbital roof. Medially, the trochlea, a curved plate

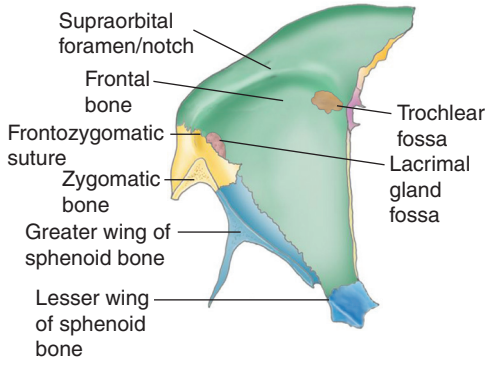


Figure 1-3 Intraorbital view of the right orbital roof. The orbital roof is composed of 2 bones: (1) the orbital plate of the frontal bone; and (2) the lesser wing of the sphenoid bone. The frontal sinus lies within the anterior orbital roof. The supraorbital foramen/notch, located within the medial one-third of the superior orbital rim, transmits the supraorbital nerve, a terminal branch of the frontal nerve of the ophthalmic division of cranial nerve V (CN V_1). Medially, the frontal bone forms the roof of the ethmoid sinus and extends to the cribriform plate. *(Illustration by Dave Peace.)*

of hyaline cartilage, is attached to the trochlear fossa on the frontal bone approximately 4–5 mm behind the orbital margin. The trochlea acts as a pulley for the superior oblique muscle.

Medial Orbital Wall

The medial wall of the orbit is formed from 4 bones (Fig 1-4):

- frontal process of the maxillary bone
- lacrimal bone
- orbital plate of the ethmoid bone
- lesser wing of the sphenoid bone

The orbital plate of the ethmoid bone, which makes up the largest portion of the medial orbital wall, is a paper-thin structure—hence its name, *lamina papyracea*—and is the most common site of fracture following blunt trauma to the orbit. The medial wall contains 2 foramina, the anterior and posterior ethmoidal foramina, which transmit the anterior and posterior ethmoidal arteries, respectively, and can act as conduits for processes involving the ethmoid sinus to enter the orbit.

The fossa for the lacrimal sac is formed by the frontal process of the maxillary bone and the lacrimal bone. Beneath that, the fossa is continuous with the bony nasolacrimal canal, which extends into the inferior meatus (the space beneath the inferior turbinate) of the nose.

CLINICAL PEARL

Due to the thinness of the bone and the presence of emissary channels in the medial wall of the orbit, ethmoid sinusitis is the most common cause of orbital cellulitis.

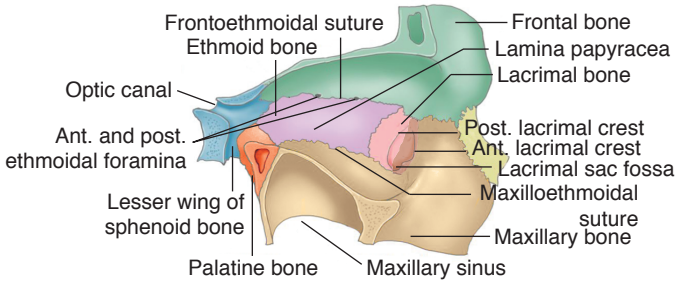


Figure 1-4 Intraorbital view of the right medial orbital wall. The medial orbital wall is formed by 4 bones: (1) maxillary bone (frontal process); (2) lacrimal bone; (3) lesser wing of the sphenoid bone; and (4) orbital plate of the ethmoid bone. The largest component of the medial wall is the lamina papyracea, the orbital plate of the ethmoid bone. Superiorly, the anterior and posterior foramina at the level of the frontoethmoidal suture transmit the anterior and posterior ethmoidal arteries, respectively. The anterior medial orbital wall includes the fossa for the lacrimal sac, which is formed by both the maxillary and lacrimal bones. The lacrimal bone is divided by the posterior lacrimal crest. The anterior part of the lacrimal sac fossa is formed by the anterior lacrimal crest of the maxillary bone. *(Illustration by Dave Peace.)*

CLINICAL PEARL

The most direct path to the optic nerve is along the medial wall: this is relevant for surgical procedures such as enucleation or optic nerve sheath decompression. During orbital surgery, the "rule of twelves" can help guide the surgeon and reduce the risk of optic nerve damage. In general, the distance from the anterior lacrimal crest to the anterior ethmoidal foramen is 24 mm; the distance from the anterior ethmoidal foramen to the posterior ethmoidal foramen is 12 mm; and the distance from the posterior ethmoidal foramen to the optic canal is 6 mm.

Orbital Floor

The floor of the orbit, which is the roof of the maxillary antrum (or sinus), is composed of 3 bones (Fig 1-5):

- orbital plate of the maxillary bone
- palatine bone
- orbital plate of the zygomatic bone

The infraorbital groove traverses the floor and descends anteriorly into the infraorbital canal. Both the groove and the canal house the infraorbital nerve (maxillary division [V_2] of the trigeminal nerve, cranial nerve [CN] V), which emerges at the infraorbital foramen, below the orbital margin of the maxillary bone. Video 1-1 shows orbital blowout fractures and includes both hydraulic and buckling theories.

VIDEO 1-1 Blowout fractures.
Developed by Nikisha Q. Richards, MD.

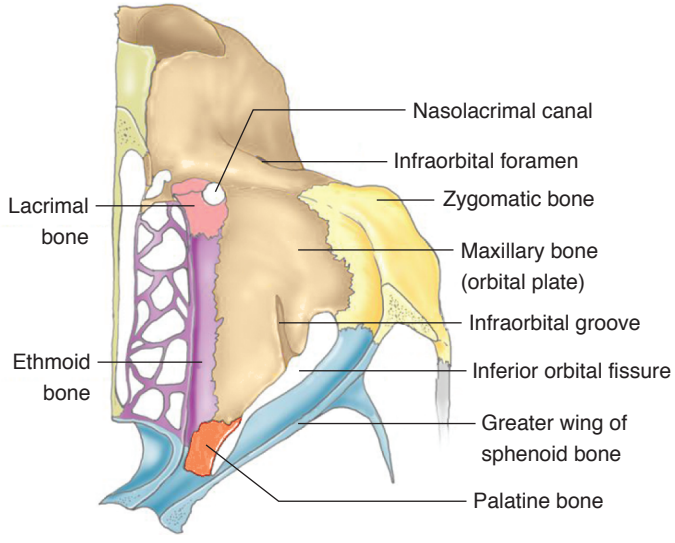


Figure 1-5 Intraorbital view of the right orbital floor. The orbital floor is composed of 3 bones: (1) maxillary bone; (2) orbital plate of zygomatic bone; and (3) palatine bone. The nasolacrimal canal, which houses the nasolacrimal duct, sits in the anterior middle area of the orbital floor, medial to the origin of the inferior oblique muscle. *(Illustration by Dave Peace.)*

Arising from the floor of the orbit just lateral to the opening of the nasolacrimal canal is the inferior oblique muscle, the only extraocular muscle that does not originate from the orbital apex. The floor of the orbit slopes downward approximately 20° from posterior to anterior. Before puberty, the orbital floor bones are immature and more prone to "trapdoor"-type fractures and secondary muscle entrapment.

CLINICAL PEARL

Because the infraorbital nerve is carried by the infraorbital groove, which is housed in the orbital plate of the maxillary bone, it is important to evaluate patients suffering from an orbital floor fracture for numbness or tingling in the area of V_2 distribution (ipsilateral: upper lip, upper posterior teeth, cheek, side of nose, and lower eyelid).

Wei LA, Durairaj VD. Pediatric orbital floor fractures. *J AAPOS.* 2011;15(2):173–180.

Lateral Orbital Wall

The thickest and strongest of the orbital walls, the lateral wall is formed from 2 bones (Fig 1-6):

- zygomatic bone
- greater wing of the sphenoid bone

The lateral orbital tubercle *(Whitnall tubercle),* a small elevation of the orbital margin of the zygomatic bone, lies approximately 11 mm below the frontozygomatic suture (see

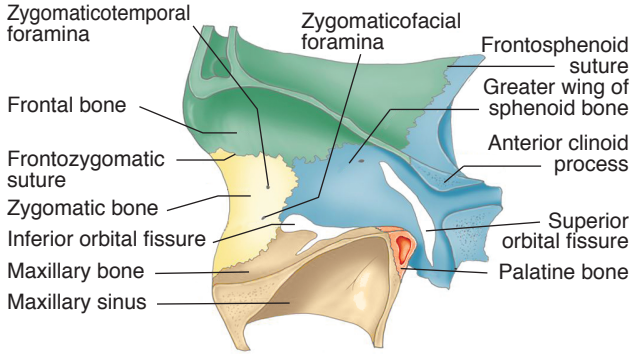


Figure 1-6 Intraorbital view of the right lateral orbital wall. The lateral orbital wall is formed by the zygomatic bone and the greater wing of the sphenoid bone. Within the zygomatic bone, the zygomaticotemporal and zygomaticofacial foramina transmit the zygomaticotemporal and zygomaticofacial nerves and arteries. The junction between the lateral orbital wall and the roof is represented by the frontosphenoid suture. Posteriorly, the wall is bordered by the inferior and superior orbital fissures. The sphenoid wing makes up the posterior portion of the lateral wall and separates the orbit from the middle cranial fossa. Medially, the lateral orbital wall ends at the inferior and superior orbital fissures. *(Illustration by Dave Peace.)*

Fig 1-1A and BCSC Section 7, *Oculofacial Plastic and Orbital Surgery*). This important landmark is the site of attachment for the following structures:

- check ligament of the lateral rectus muscle
- suspensory ligament of the eyeball (Lockwood suspensory ligament)
- lateral canthal tendon
- lateral horn of the levator aponeurosis

Orbital Foramina, Canals, and Fissures

Foramina

The *optic foramen* is the entry point to the optic canal, which leads from the middle cranial fossa to the apex of the orbit (see Figs 1-1, 1-2). The optic canal is directed forward, laterally, and somewhat downward and conducts the optic nerve, the ophthalmic artery, and sympathetic fibers from the carotid plexus. The optic canal passes through the lesser wing of the sphenoid bone.

The *supraorbital foramen* (which, in some individuals, is a notch instead of a foramen) is located at the medial third of the superior margin of the orbit. It transmits blood vessels and the supraorbital nerve, which is an extension of the frontal nerve, a branch of the ophthalmic division (V_1) of CN V. The *anterior ethmoidal foramen* is located at the frontoethmoidal suture and transmits the anterior ethmoidal vessels and nerve. The *posterior ethmoidal foramen* lies at the junction of the roof and the medial wall of the orbit and transmits the posterior ethmoidal vessels and nerve through the frontal bone (see Fig 1-4). The *zygomaticotemporal and zygomaticofacial foramina* lie in the portion of the lateral orbital wall formed by the zygomatic

bone and transmit vessels and branches of the zygomatic nerve, which is also a branch of CN V_1 (see Fig 1-6).

Nasolacrimal canal

The nasolacrimal duct travels inferiorly within the bony nasolacrimal canal from the lacrimal sac fossa into the inferior meatus of the nose (see Figs 1-5, 1-42).

Infraorbital canal

The infraorbital canal continues anteriorly from the infraorbital groove and exits 4 mm below the inferior orbital margin, where it opens into the infraorbital foramen. It transmits the infraorbital nerve, a branch of CN V_2 (the maxillary division) (see Figs 1-1, 1-2, 1-5).

Fissures

The *superior orbital fissure* (Fig 1-7; see also Figs 1-1, 1-2, 1-6) is located between the greater and lesser wings of the sphenoid bone and lies lateral to the optic foramen. It is approximately 22 mm long and is spanned by the tendinous ring formed by the common origin of the rectus muscles *(annulus of Zinn).* Above the ring, the superior orbital fissure transmits the following structures, from lateral to nasal (Figs 1-8, 1-9):

- lacrimal nerve of CN V_1
- frontal nerve of CN V_1
- CN IV (trochlear nerve)
- superior ophthalmic vein

Within the ring or between the heads of the rectus muscle are the following (see Fig 1-8):

- superior and inferior divisions of CN III (the oculomotor nerve)
- nasociliary branch of CN V_1, which also carries the postganglionic sympathetic fibers en route to the ciliary ganglion
- CN VI (the abducens nerve)

The course of the inferior ophthalmic vein is variable; it can travel within or below the ring as it exits the orbit.

The *inferior orbital fissure* lies just below the superior fissure, between the lateral wall and the floor of the orbit, providing access to the pterygopalatine and inferotemporal fossae (see Figs 1-1, 1-2, 1-5, 1-6). Therefore, it is close to the foramen rotundum and the pterygoid canal. The inferior orbital fissure transmits the infraorbital and zygomatic



Figure 1-7 Axial computed tomography (CT) scan of the orbits. The superior orbital fissure (SOF) passes above and below the plane of the optic canal (OC) and is commonly mistaken for the OC. The OC lies in the same plane as the anterior clinoid processes (AClin) and may be cut obliquely in scans so that the entire canal length does not always appear in a single slice. *(Courtesy of William R. Katowitz, MD.)*

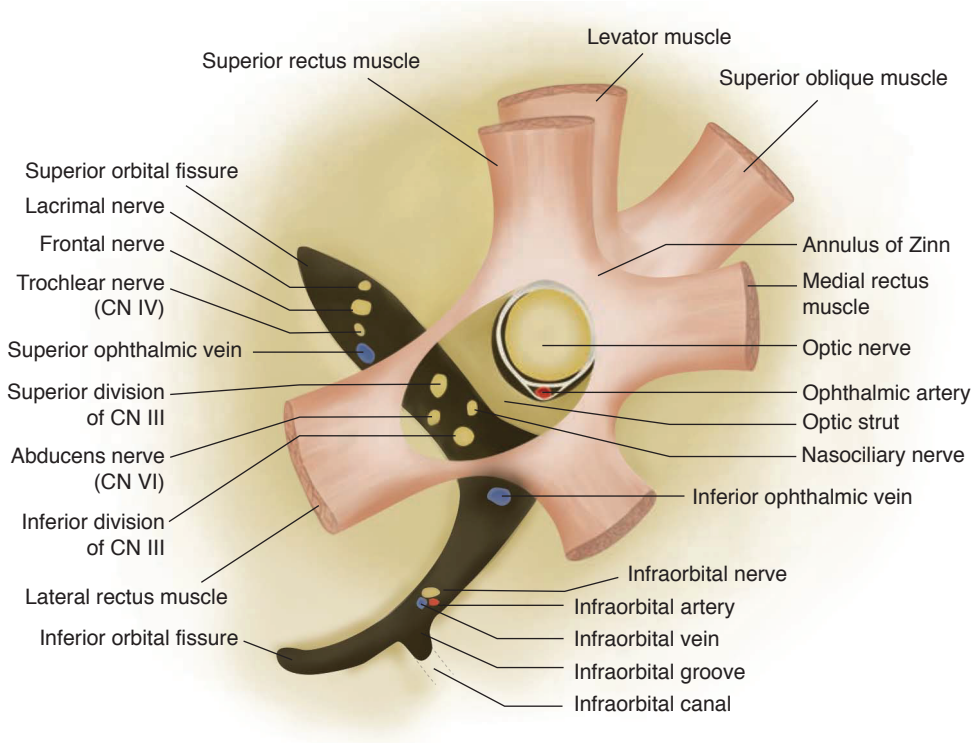


Figure 1-8 Anterior view of the right orbital apex showing the distribution of the nerves as they enter through the superior orbital fissure and optic canal. This view also shows the annulus of Zinn (AZ), the fibrous ring formed by the origin of the 4 rectus muscles. The AZ trisects the superior orbital fissure (SOF). The portion of the SOF above the AZ transmits the trochlear nerve (CN IV), lacrimal and frontal nerves (CN V_1), and the superior ophthalmic vein. The portion of the SOF within the AZ is also known as the oculomotor foramen and transmits the oculomotor nerve (CN III), nasociliary nerve (CN V_1), abducens nerve (CN VI), and sympathetic fibers. The remaining portion of the SOF below the annulus transmits the inferior ophthalmic vein. *(Illustration by Cyndie C.H. Wooley.)*

branches of CN V_2 and an orbital nerve from the pterygopalatine ganglion, and sometimes also the inferior ophthalmic vein. The inferior ophthalmic vein connects with the pterygoid plexus before draining into the cavernous sinus (see the section Vascular Supply and Drainage of the Orbit).

Periorbital Sinuses

The periorbital sinuses have a close anatomical relationship with the orbits (Fig 1-10). The medial walls of the orbits, which border the nasal cavity anteriorly and the ethmoid sinus and sphenoid sinus posteriorly, are almost parallel. In adults, the lateral wall of each orbit forms an angle of approximately 45° with the medial plane. The lateral walls border the middle cranial, temporal, and pterygopalatine fossae. Superior to the orbit are the anterior cranial fossa and the frontal sinus. The maxillary sinus and the palatine air cells are located inferiorly.

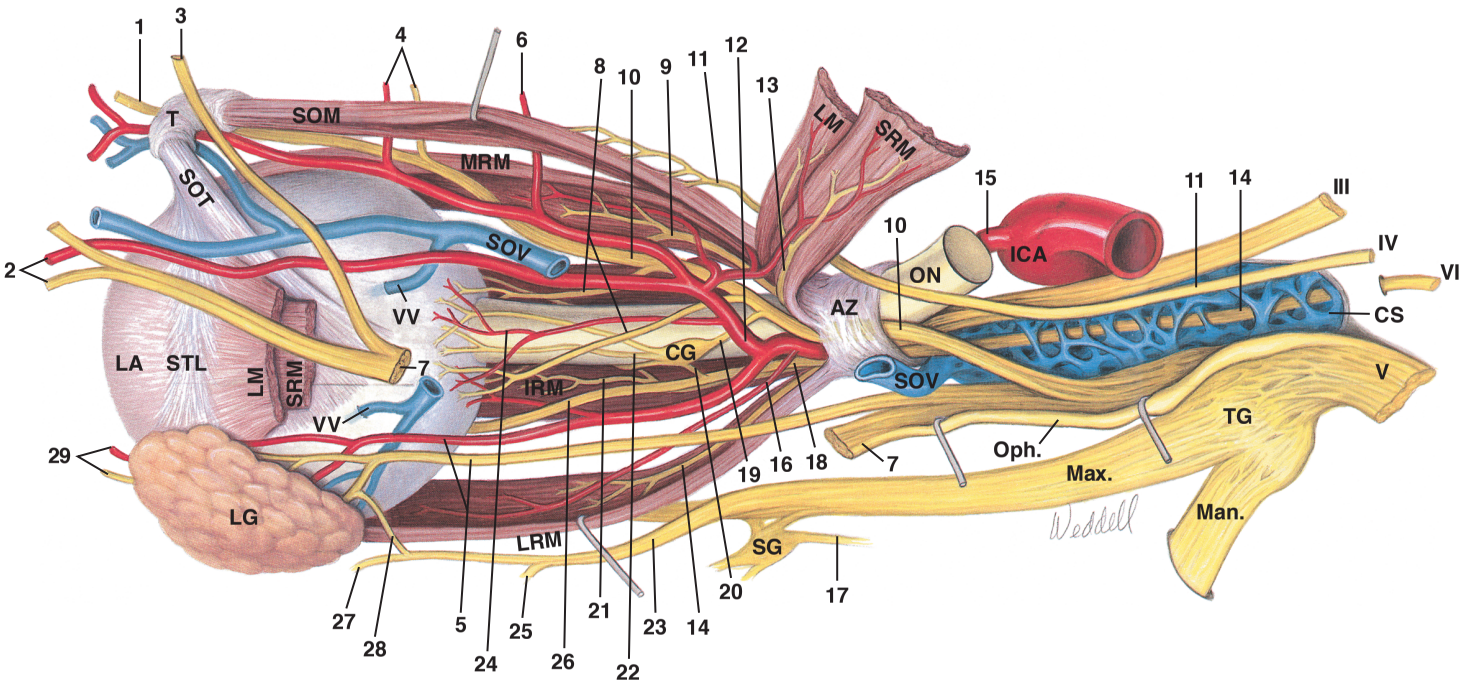


Figure 1-9 Top view of the left orbit. AZ, annulus of Zinn; CG, ciliary ganglion; CS, cavernous sinus; ICA, internal carotid artery; IRM, inferior rectus muscle; LA, levator aponeurosis; LG, lacrimal gland; LM, levator muscle; LRM, lateral rectus muscle; Man., mandibular nerve; Max., maxillary nerve; MRM, medial rectus muscle; ON, optic nerve; Oph., ophthalmic nerve; SG, sphenopalatine ganglion; SOM, superior oblique muscle; SOT, superior oblique tendon; SOV, superior ophthalmic vein; SRM, superior rectus muscle; STL, superior transverse (Whitnall) ligament; T, trochlea; TG, trigeminal (gasserian) ganglion; VV, vortex veins; 1, infratrochlear nerve; 2, supraorbital nerve and artery; 3, supratrochlear nerve; 4, anterior ethmoid nerve and artery; 5, lacrimal nerve and artery; 6, posterior ethmoid artery; 7, frontal nerve; 8, long ciliary nerves; 9, branch of CN III to medial rectus muscle; 10, nasociliary nerve; 11, CN IV; 12, ophthalmic (orbital) artery; 13, superior ramus of CN III; 14, CN VI; 15, ophthalmic artery, origin; 16, anterior ciliary artery; 17, vidian nerve; 18, inferior ramus of CN III; 19, sensory branches from ciliary ganglion to nasociliary nerve; 20, motor (parasympathetic) nerve to ciliary ganglion from nerve to inferior oblique muscle; 21, branch of CN III to inferior rectus muscle; 22, short ciliary nerves; 23, zygomatic nerve; 24, posterior ciliary arteries; 25, zygomaticofacial nerve; 26, nerve to inferior oblique muscle; 27, zygomaticotemporal nerve; 28, lacrimal secretory nerve; 29, lacrimal artery and nerve terminal branches. *(Reproduced from Stewart WB, ed.* Ophthalmic Plastic and Reconstructive Surgery. *4th ed. American Academy of Ophthalmology Manuals Program; 1984.)*

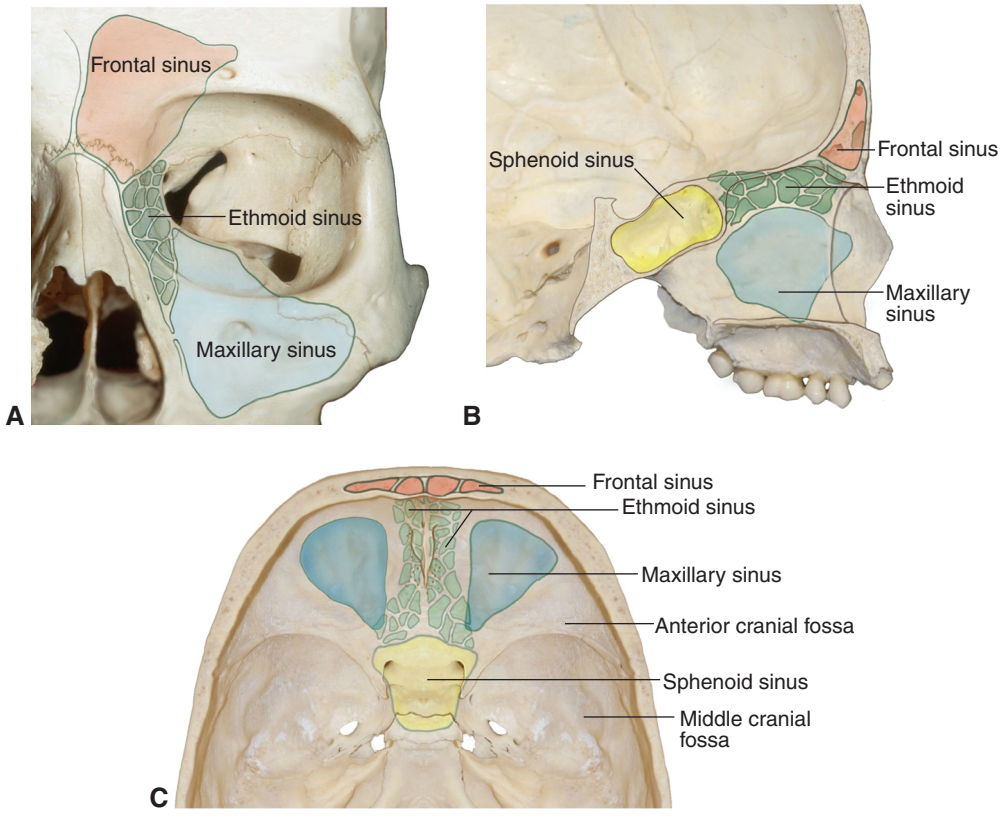


Figure 1-10 Coronal **(A),** sagittal **(B),** and axial **(C)** views of the anatomical relationship of the 4 periorbital sinuses. *(Illustrations by Dave Peace.)*

The inferomedial orbital strut is located along the inferonasal orbit, where the orbital bones slope from the floor to the medial wall. This region is significant because of its proximity to the ostium of the maxillary sinus (Fig 1-11). In addition, the *fovea ethmoidalis,* which forms the roof of the ethmoid sinuses, is a lateral extension of the cribriform plate. The locations of the periorbital sinuses and their relation to anatomical features of the skull are indicated in Figure 1-10 and are discussed further in BCSC Section 7, *Oculofacial Plastic and Orbital Surgery.*

CLINICAL PEARL

When planning for a lacrimal surgery such as dacryocystorhinostomy, it is important to identify and avoid the fovea ethmoidalis to prevent inadvertent cerebral spinal fluid leakage as well as intracranial injury.

Gospe SM 3rd, Bhatti MT. Orbital anatomy. *Int Ophthalmol Clin.* 2018;58(2):5–23.

Zide BM, Jelks GW. *Surgical Anatomy Around the Orbit: The System of Zones.* Lippincott Williams & Wilkins; 2005.

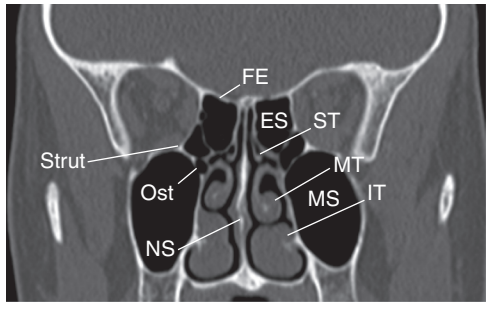


Figure 1-11 Coronal CT scan of the orbits and sinuses showing the maxillary and ethmoid sinuses. ES = ethmoid sinus; FE = fovea ethmoidalis; IT = inferior turbinate; MS = maxillary sinus; MT = middle turbinate; NS = nasal septum; Ost = ostium of the maxillary sinus; ST = superior turbinate; Strut = inferomedial orbital strut. *(Courtesy of William R. Katowitz, MD.)*

Cranial Nerves

Six of the 12 cranial nerves (CNs II–VII) traverse the orbit and directly innervate the eye and periocular tissues. Because certain tumors affecting CN I (the olfactory nerve) can give rise to important ophthalmic signs and symptoms, it is imperative that ophthalmologists also be familiar with the anatomy of this nerve. Chapter 3 discusses CNs I–VII in greater depth; also see BCSC Section 7, *Oculofacial Plastic and Orbital Surgery,* and Section 5, *Neuro-Ophthalmology.*

Ciliary Ganglion

The ciliary ganglion is located approximately 1 cm in front of the annulus of Zinn, on the lateral side of the ophthalmic artery, between the optic nerve and the lateral rectus muscle (Fig 1-12). It receives 3 roots:

- A long (10–12-mm) *sensory root* arises from the nasociliary branch of CN V_1 and contains sensory fibers from the cornea, the iris, and the ciliary body.
- A short *motor root* arises from the inferior division of CN III. It carries preganglionic parasympathetic fibers from the Edinger-Westphal nucleus. The fibers of the motor root synapse in the ganglion, and the postganglionic fibers carry parasympathetic axons to supply the iris sphincter and the ciliary muscle.
- A *sympathetic root* carries postganglionic fibers originating from the superior cervical ganglion, from which they course superiorly with the internal carotid artery. In the cavernous sinus, the sympathetic fibers leave the carotid artery to temporarily join the abducens nerve before entering the orbit either with the nasociliary branch of CN V_1 or as an individual root. The sympathetic root enters the orbit through the superior orbital fissure within the tendinous ring, passes through the ciliary ganglion without synapse, and innervates blood vessels of the eye as well as the dilator muscle of the pupil. Fibers destined for the Müller muscle travel along the frontal and lacrimal branches of CN V_1 and do not pass through the ciliary ganglion.

Branches of the Ciliary Ganglion

Only the parasympathetic fibers synapse in the ciliary ganglion. The sympathetic fibers are postganglionic from the superior cervical ganglion and pass through it without synapsing.

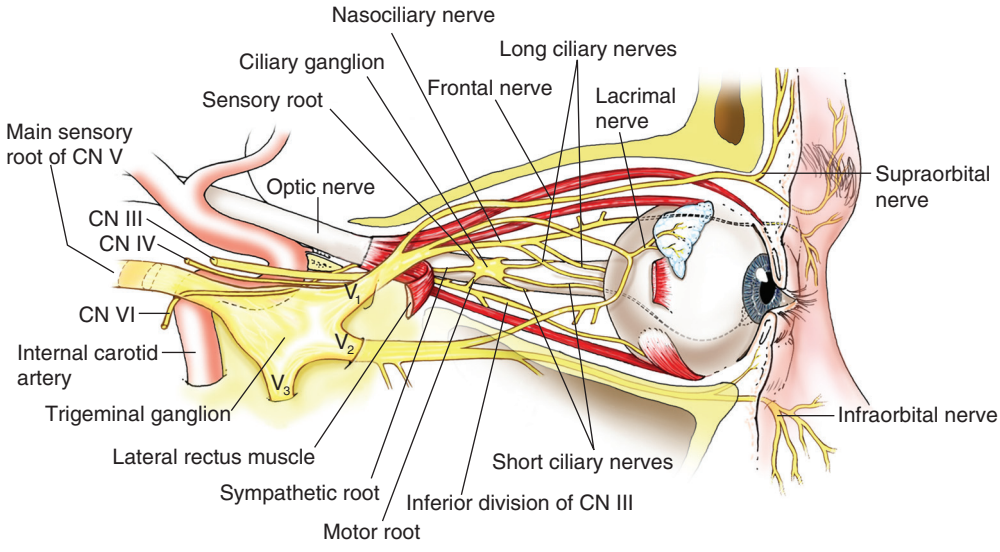


Figure 1-12 Schematic of the lateral orbit demonstrating the ciliary ganglion and CNs II–VI. Note the 3 roots: (1) sensory root, which carries sensation from the globe to the trigeminal ganglion via the nasociliary nerve; (2) sympathetic root carrying postganglionic sympathetic fibers from the superior cervical ganglion and carotid plexus; (3) motor root carrying preganglionic parasympathetic fibers from the inferior division of the oculomotor nerve. *(Illustration by Dave Peace.)*

Sensory fibers from cell bodies in the trigeminal ganglion carry sensation from the eye, orbit, and face. Together, the nonsynapsing sympathetic fibers; the sensory fibers; and the myelinated, fast-conducting postganglionic parasympathetic fibers form the short ciliary nerves (see also Chapter 3, Fig 3-18).

Short Ciliary Nerves

Two groups of short ciliary nerves, totaling 6–10, arise from the ciliary ganglion (see Fig 1-12). They travel on both sides of the optic nerve and, together with the long ciliary nerves, pierce the sclera around the optic nerve (see Fig 1-22). Both long and short ciliary nerves pass anteriorly between the choroid and the sclera to the ciliary muscle, where they form a plexus that supplies the cornea, the ciliary body, and the iris. The long ciliary nerves, which arise directly from the nasociliary branch of CN V_1, are sensory nerves. The short ciliary nerves are both sensory and motor nerves, carrying autonomic fibers to the pupil and ciliary muscles (see Chapter 3).

Extraocular Muscles

There are 7 extraocular muscles (Figs 1-13 through 1-16, Table 1-2, Activity 1-2):

- medial rectus
- inferior rectus
- lateral rectus
- superior rectus
- superior oblique

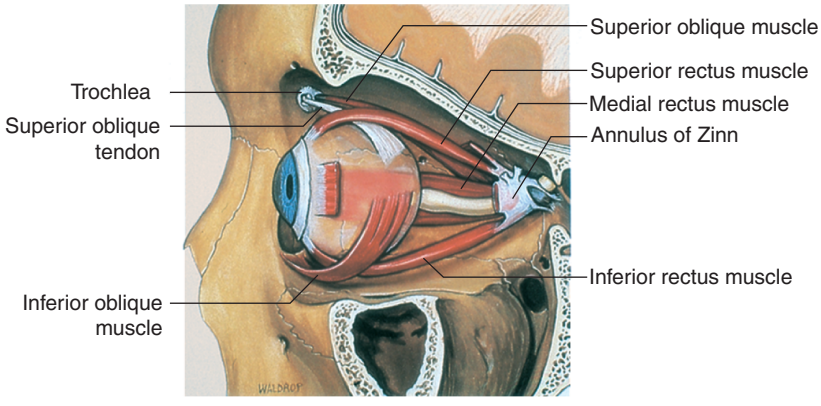


Figure 1-13 Extraocular muscles, lateral composite (sagittal) view of the left eye. Note the insertion points of both oblique muscles posteriorly on the globe in the region of the macula. The annulus of Zinn is a fibrotendinous ring that represents the origin of the 4 rectus muscles. *(Reproduced with permission from Dutton JJ.* Atlas of Clinical and Surgical Orbital Anatomy. *Saunders; 1994.)*

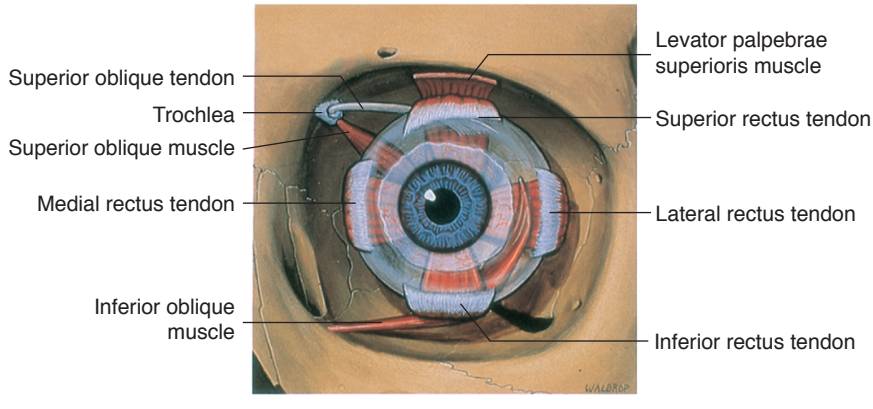


Figure 1-14 Extraocular muscles, frontal view of the left eye, coronal plane. *(Reproduced with permission from Dutton JJ.* Atlas of Clinical and Surgical Orbital Anatomy. *Saunders; 1994.)*

- inferior oblique
- levator palpebrae superioris

Please see Chapter 3 in BCSC Section 6, *Pediatric Ophthalmology and Strabismus*, for discussion of extraocular muscle function.

ACTIVITY 1-2 Interactive model of the extraocular muscles.
Developed by Mary A. O'Hara, MD.

Extraocular Muscle Origins

The annulus of Zinn consists of superior and inferior orbital tendons and is the origin of the 4 rectus muscles (Fig 1-17; also see Figs 1-13, 1-16). The superior tendon of the annulus of Zinn gives rise to the superior rectus muscle and portions of the lateral and medial

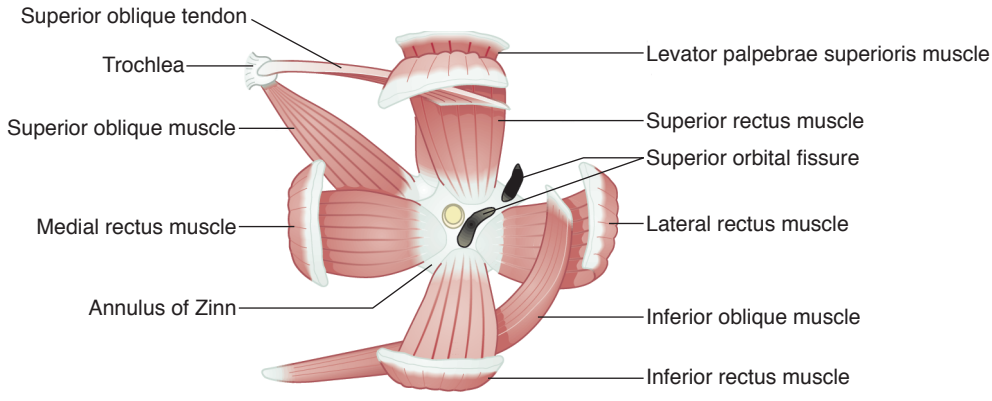


Figure 1-15 Extraocular muscles, coronal view, left eye, with globe removed. *(Reproduced with permission from Dutton JJ.* Atlas of Clinical and Surgical Orbital Anatomy. *Saunders; 1994.)*

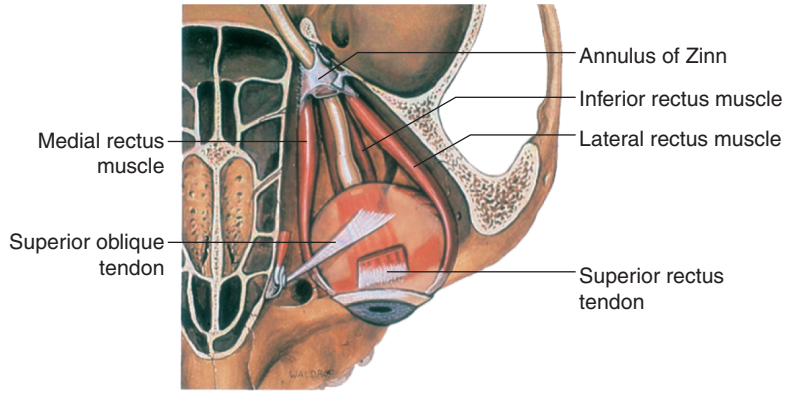


Figure 1-16 Extraocular muscles, superior composite (axial) view. The superior oblique tendon inserts beneath the superior rectus muscle onto the posterior aspect of the globe. The annulus of Zinn is continuous with periorbita around the orbital apex, surrounding dura matter, and part of the optic nerve sheath. *(Reproduced with permission from Dutton JJ.* Atlas of Clinical and Surgical Orbital Anatomy. *Saunders; 1994.)*

rectus muscles. The inferior tendon of the annulus of Zinn gives rise to the inferior rectus muscle and portions of the lateral and medial rectus muscles. The levator palpebrae superioris muscle arises from the lesser wing of the sphenoid bone, at the apex of the orbit, just superior to the annulus of Zinn (see the section "Levator palpebrae superioris muscle" later in the chapter).

The superior oblique muscle originates from the periosteum of the body of the sphenoid bone, above and medial to the optic foramen. The inferior oblique muscle originates anteriorly, from a shallow depression in the orbital plate of the maxillary bone, at the anteromedial corner of the orbital floor, near the fossa for the lacrimal sac (see Table 1-2).

Table 1-2 Comparison of the Extraocular Muscles

Muscle	Origin	Insertion	Size	Blood Supply	Nerve Supply
Medial rectus	Annulus of Zinn	Medially, in horizontal meridian 5.5 mm from limbus	40.8 mm long (tendon: length 3.7 mm, width 10.3 mm)	Medial (inferior) muscular branch of ophthalmic artery	Inferior division of CN III (oculomotor)
Inferior rectus	Annulus of Zinn at orbital apex	Inferiorly, in vertical meridian 6.5 mm from limbus	40 mm long (tendon: length 5.5 mm, width 9.8 mm)	Medial (inferior) muscular branch of ophthalmic artery and infraorbital artery	Inferior division of CN III (oculomotor)
Lateral rectus	Annulus of Zinn spanning the superior orbital fissure	Laterally, in horizontal meridian 6.9 mm from limbus	40.6 mm long (tendon: length 8 mm, width 9.2 mm)	Lateral (superior) muscular branch of ophthalmic artery and lacrimal artery	CN VI (abducens)
Superior rectus	Annulus of Zinn at orbital apex	Superiorly, in vertical meridian 7.7 mm from limbus	41.8 mm long (tendon: length 5.8 mm, width 10.6 mm)	Lateral (superior) muscular branch of ophthalmic artery	Superior division of CN III (oculomotor)
Superior oblique	Medial to optic foramen, between annulus of Zinn and periorbita	To trochlea, through pulley, just behind orbital rim, then hooking back under superior rectus, inserting posterior to center of rotation	40 mm long (tendon: length 20 mm, width 10.8 mm)	Lateral (superior) muscular branch of ophthalmic artery	CN IV (trochlear)
Inferior oblique	From a depression on orbital floor near orbital rim (maxilla)	Posterior inferotemporal quadrant at level of macula; posterior to center of rotation	37 mm long (tendon: length 1 mm, width 9.6 mm at insertion)	Medial (inferior) muscular branch of ophthalmic artery and infraorbital artery	Inferior division of CN III (oculomotor)
Levator palpebrae superioris	Lesser wing of sphenoid bone	Trochlea, supraorbital notch, superior tarsus, lateral orbital tubercle, posterior lacrimal crest	60 mm long (muscle: 40 mm; tendon: 14–20 mm)	Branches of the ophthalmic artery	Superior division of CN III (oculomotor)

CN = cranial nerve.

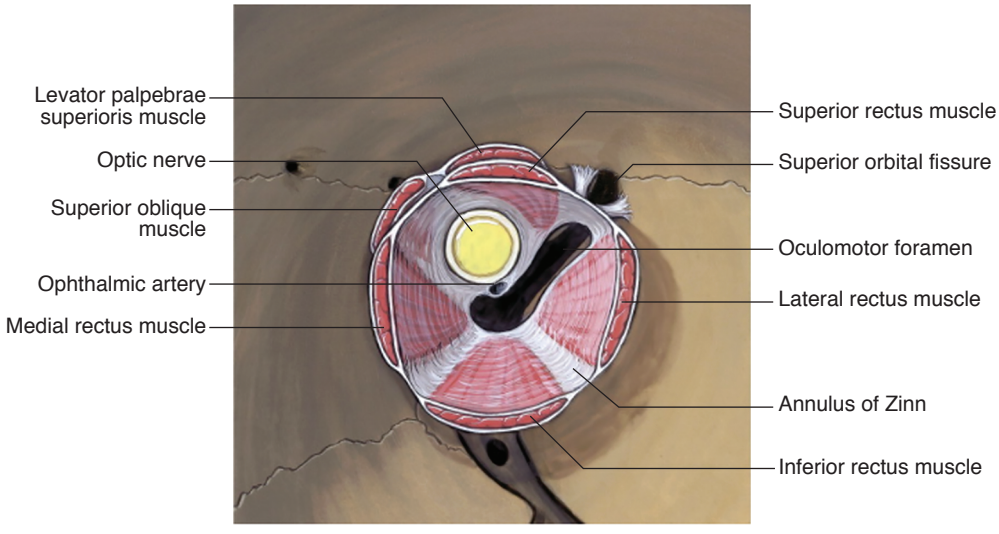


Figure 1-17 Origin of the extraocular muscles. All extraocular muscles, except the inferior oblique, originate in the orbital apex. The 4 rectus muscles share a common fibrotendinous ring known as the *annulus of Zinn*. Note that the superior rectus and medial rectus are juxtaposed to the optic nerve sheath. The oculomotor foramen represents the part of the superior orbital fissure enclosed by the annulus of Zinn. *(Reproduced with permission from Dutton JJ.* Atlas of Clinical and Surgical Orbital Anatomy. *2nd ed. Elsevier/Saunders; 2011:Fig 3-8.)*

CLINICAL PEARL

The relationships of the rectus muscles and the optic nerve sheath at the annulus of Zinn have important clinical implications. For example, patients with retrobulbar optic neuritis may experience pain with extraocular movement because of the connection of the superior and medial rectus muscles to the optic nerve. Additionally, enlargement of these muscles can lead to a compressive optic neuropathy in patients with thyroid eye disease.

Extraocular Muscle Insertions

The 4 rectus muscles insert anteriorly on the sclera. Starting at the medial rectus muscle and proceeding to the inferior rectus, lateral rectus, and superior rectus muscles, the muscle insertions lie progressively farther from the limbus. An imaginary curve drawn through these insertions creates a spiral, called the *spiral of Tillaux* (Fig 1-18).

CLINICAL PEARL

Understanding the relationship between the muscle insertions and the location of the ora serrata is clinically important when suturing to the sclera; a misdirected needle could perforate the retina. It is also important when evaluating trauma patients with scleral lacerations that extend beyond the spiral of Tillaux. In such cases, the risk of retinal incarceration and tractional retinal detachment increase.

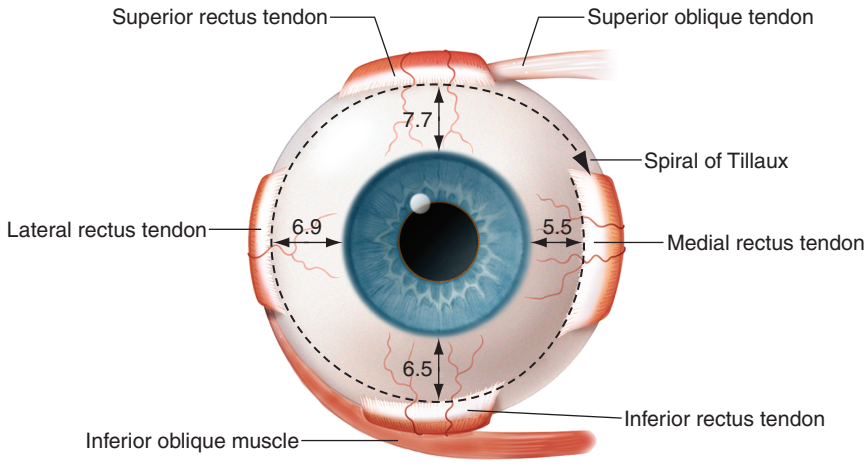


Figure 1-18 The medial rectus tendon is closest to the limbus, and the superior rectus tendon is farthest from it. By connecting the insertions of the tendons beginning with the medial rectus, then the inferior rectus, then the lateral rectus, and finally the superior rectus, a spiral (known as the *spiral of Tillaux*) is obtained. The *dotted line* represents the approximate location of the underlying ora serrata. Measurements are in millimeters. The anterior ciliary arteries are also shown. *(Illustration by Christine Gralapp.)*

The superior oblique muscle, after passing through the trochlea in the superomedial orbital rim, inserts onto the sclera superiorly, under the insertion of the superior rectus. The superior oblique tendon insertion is fanned out so that the anterior fibers provide intorsion and the posterior fibers provide depression and abduction. From its origin, the inferior oblique muscle extends posteriorly, laterally, and superiorly to insert onto the sclera in the posterior inferotemporal quadrant.

Extraocular Muscle Distribution in the Orbit

Figures 1-13 through 1-17 demonstrate the arrangement of the extraocular muscles within the orbit. Note the relationship between the oblique and rectus extraocular muscles. A complex network of tissues interconnects all of the extraocular muscles, the Tenon capsule, and the periorbital tissues. Within the orbit, the extraocular muscles are encased in a fibrous sheath. In the posterior orbit, the muscle sheath is an extension of the annulus of Zinn (see Fig 1-17). Anteriorly, the Tenon capsule surrounds the extraocular muscles as they insert onto the globe (see the section Tenon Capsule at the end of this chapter for further discussion).

The tissues that interact with the extraocular muscle sheath include the check ligaments of the medial and lateral rectus muscles and a pulley system, which consists of collagen, elastin, and smooth muscle. This network of interconnecting tissue, also described as the orbital musculofibrous tissue, functions to stabilize movement of the extraocular muscles within the orbit and in relation to the globe and each other (Fig 1-19). See BCSC Section 6, *Pediatric Ophthalmology and Strabismus,* for further discussion of the pulley system.

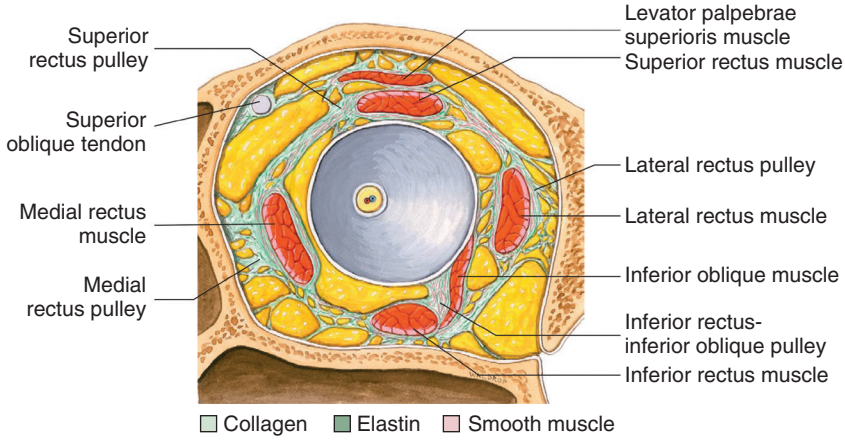


Figure 1-19 Diagram of left orbit demonstrating the orbital musculofibrous tissue, which consists of collagen, elastin, and smooth muscle. This tissue is organized into intermuscular septa and a pulley system, which maintain spatial orientation of the extra-ocular muscles in different aspects of gaze. *(Reproduced with permission from Dutton JJ.* Atlas of Clinical and Surgical Orbital Anatomy. *2nd ed. Elsevier/Saunders; 2011:Fig 3-18.)*

CLINICAL PEARL

Surgical procedures such as scleral buckling and orbital decompression can affect the muscle sheaths and pulley system, respectively. This in turn may affect the postoperative alignment and/or movement of extraocular muscles.

See Chapter 17 in this volume for additional figures depicting the location of the extraocular muscles within the orbit and their relationship to surrounding structures, along with corresponding CT and MRI scans.

Blood Supply to the Extraocular Muscles

The extraocular muscles are supplied by the following (see Table 1-2):

- muscular branches of the ophthalmic artery
- infraorbital artery
- lacrimal artery

The muscular branches of the ophthalmic artery give rise to the anterior ciliary arteries and can be divided into lateral (superior) and medial (inferior) branches. Each rectus muscle has 1–4 anterior ciliary arteries, which eventually penetrate through the muscle belly and the sclera, anastomosing with the major arterial circle. This circle contributes to the blood supply of the anterior segment (see Fig 1-23). The lateral rectus muscle receives part of its blood supply from the lacrimal artery. The inferior oblique and inferior rectus muscles receive part of their blood supply from the infraorbital artery (see Figs 1-20, 1-21, 1-22).

CLINICAL PEARL

Consideration of the anterior segment circulation plays an important role during strabismus surgery because disinsertion of 2 or more rectus muscles can lead to anterior segment ischemia (see BCSC Section 6, *Pediatric Ophthalmology and Strabismus,* Chapter 13). The risk can be mitigated by a fornix approach, a staged surgery, or use of a vessel-sparing technique.

Innervation of the Extraocular Muscles

CN III (the oculomotor nerve) has superior and inferior divisions. The superior division innervates the levator palpebrae superioris and superior rectus muscle. The inferior division innervates the medial rectus, inferior rectus, and inferior oblique muscles (see Table 1-2). The superior oblique muscle is innervated by CN IV (the trochlear nerve). The lateral rectus muscle is innervated by CN VI (the abducens nerve).

Fine Structure of the Extraocular Muscles

The ratio of nerve fibers to muscle fibers in the extraocular muscles is very high (1:3–1:5) compared with the ratio of nerve axons to muscle fibers in skeletal muscle (1:50–1:125). This high ratio enables precise control of ocular movements. The fibers of the extraocular muscles are a mixture of 2 types of muscle fibers. The slow, tonic-type fibers, which are innervated by multiple grapelike nerve endings *(en grappe)*, are used in smooth-pursuit movements. The fast, twitch-type fibers, which have platelike nerve endings *(en plaque),* aid in rapid saccadic movements of the eye.

Porter JD, Baker RS, Ragusa RJ, Brueckner JK. Extraocular muscles: basic and clinical aspects of structure and function. *Surv Ophthalmol.* 1995;39(6):451–484.

Vascular Supply and Drainage of the Orbit

Posterior and Anterior Ciliary Arteries

Approximately 16–20 short posterior ciliary arteries and 6–10 short ciliary nerves enter the globe in a ring around the optic nerve (Figs 1-20 through 1-22). Usually, 2 long posterior ciliary arteries and 2 long ciliary nerves enter the sclera on either side of the optic nerve, close to the horizontal meridian. The long posterior ciliary arteries course anteriorly in the suprachoroidal space, terminating at the major arterial circle of the iris.

The posterior ciliary vessels originate from the ophthalmic artery and supply the entire uvea, the cilioretinal arteries, the sclera, the margin of the cornea, and the adjacent conjunctiva. Occlusion of these vessels (as occurs in giant cell arteritis) may have profound consequences for the eye, such as the development of anterior ischemic optic neuropathy.

The anterior ciliary arteries also arise from the ophthalmic artery and usually supply (in pairs) the superior, medial, and inferior rectus muscles (Figs 1-23, 1-24; also see Fig 1-20). After emerging from the surface of the rectus muscles, the anterior ciliary vessels

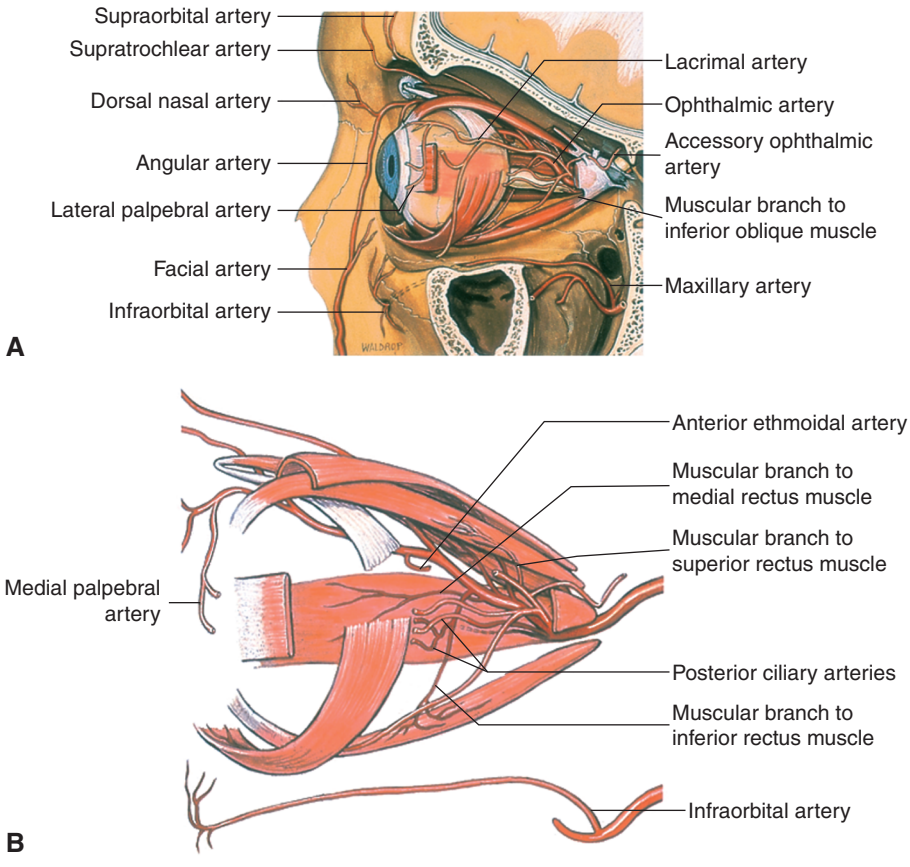


Figure 1-20 Orbital arteries. **A,** Lateral (sagittal) view with extraocular muscles, composite view. The angular artery represents an anastomosis between the external and carotid arteries. **B,** Central dissection. *(Reproduced with permission from Dutton JJ.* Atlas of Clinical and Surgical Orbital Anatomy. *Saunders; 1994.)*

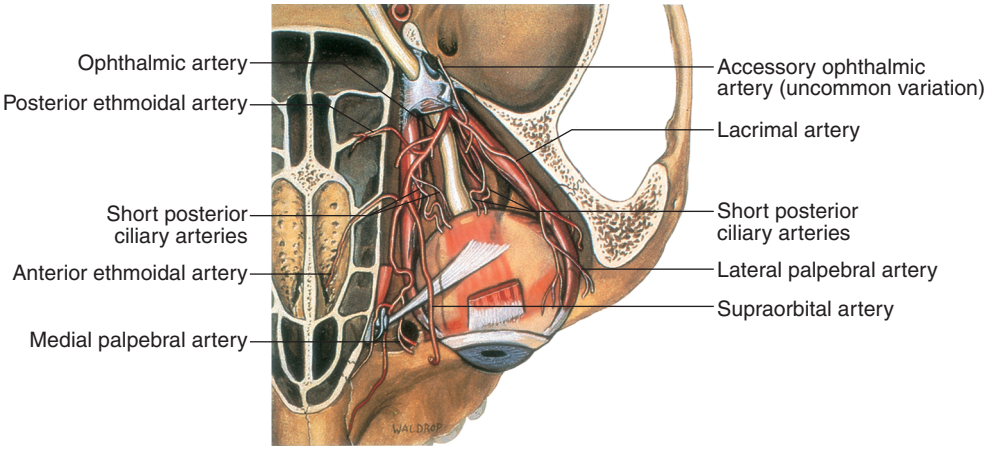


Figure 1-21 Orbital arteries, superior composite (axial) view. The anterior and posterior ethmoidal arteries connect the orbit and the ethmoid sinus through their respective emissaries; this is a common route of extension of an ethmoid sinusitis into the orbit. *(Modified with permission from Dutton JJ.* Atlas of Clinical and Surgical Orbital Anatomy. *Saunders; 1994.)*

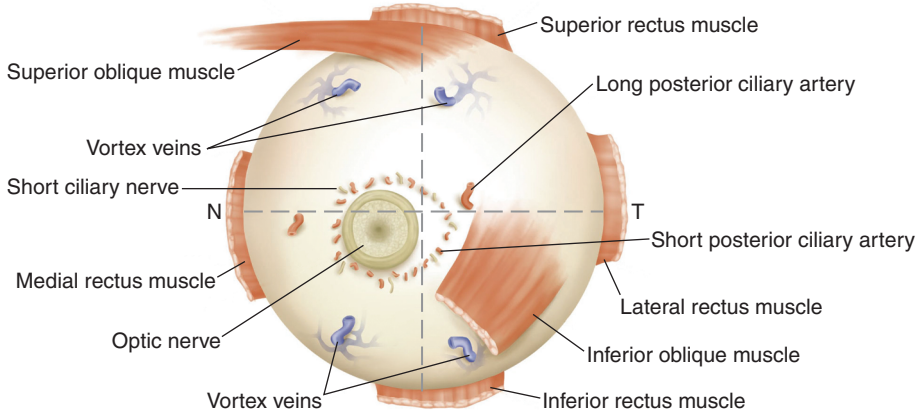


Figure 1-22 Posterior view of the right globe. There are 2 long posterior ciliary arteries and 16–20 short posterior ciliary arteries. The short posterior ciliary arteries are major contributors to the pre-equatorial choroidal circulation. The vortex veins receive venous blood from the uveal tract and eventually join the superior and inferior ophthalmic veins, which primarily drain into the cavernous sinus. Note the insertion of the inferior oblique muscle near the macula. N = nasal; T = temporal. *(Modified by Cyndie C.H. Wooley from an illustration by Thomas A. Weingeist, MD, PhD.)*

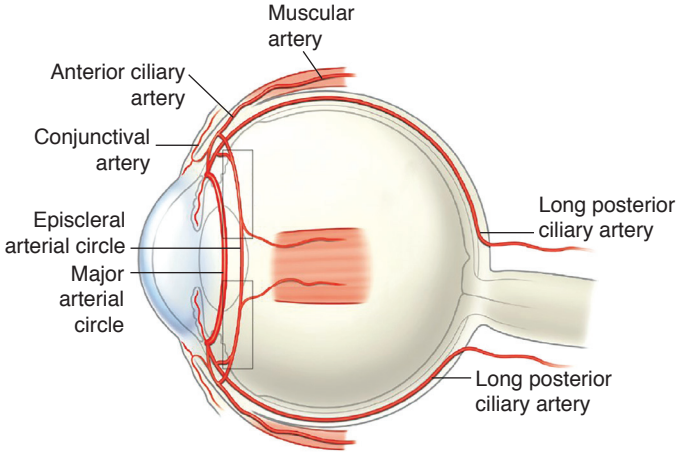


Figure 1-23 Schematic of the anastomoses between the anterior and posterior ciliary circulation. The long posterior ciliary arteries travel in the suprachoroidal space, where they terminate at the major arterial circle of the iris. The anterior ciliary arteries emerge from the surface of the rectus muscles to penetrate the sclera and join the posterior ciliary arteries at the major arterial circle of the iris. The episcleral arterial circle runs on the surface of the sclera, connecting the anterior ciliary arteries. This anatomical relationship is the basis for anterior segment ischemia following strabismus surgery or scleral buckling procedures in certain circumstances. *(Modified with permission from Levin LA, Nilsson SFE, Ver Hoeve J, Wu SM.* Adler's Physiology of the Eye. *11th ed. Elsevier/Saunders; 2011:Fig 4.35.)*

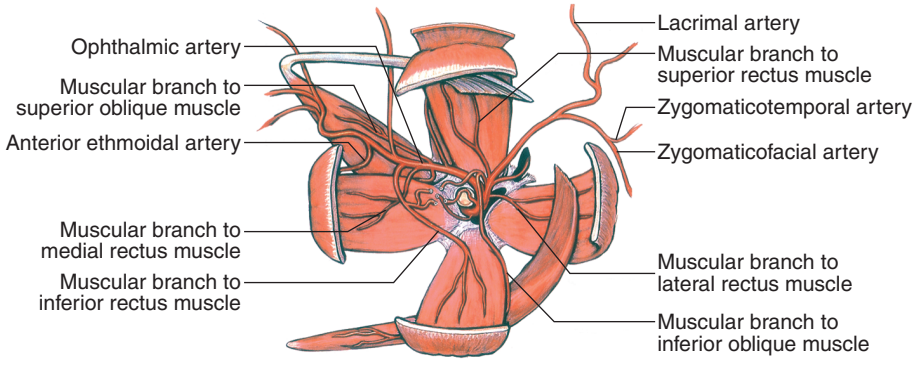


Figure 1-24 Orbital arteries, frontal (coronal) view with extraocular muscles. *(Reproduced with permission from Dutton JJ.* Atlas of Clinical and Surgical Orbital Anatomy. *Saunders; 1994.)*

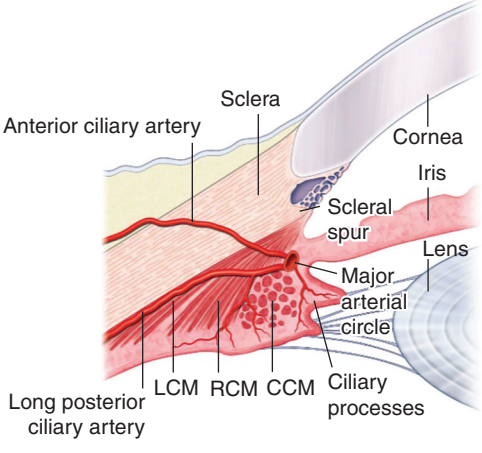


Figure 1-25 Anastomosis of the anterior and posterior ciliary circulation. CCM = circular ciliary muscle; LCM = longitudinal ciliary muscle; RCM = radial ciliary muscle. *(Reproduced with permission from Levin LA, Nilsson SFE, Ver Hoeve J, Wu SM.* Adler's Physiology of the Eye. *11th ed. Elsevier/Saunders; 2011:276.)*

perforate the sclera anterior to the rectus muscle insertions, where they anastomose with the long posterior ciliary arteries at the major arterial circle of the iris (see Fig 1-22).

Within the eye, the posterior ciliary vessel forms the intramuscular circle of the iris, branches of which supply the major arterial circle (which is usually discontinuous). This circle lies within the apex of the ciliary muscle, which it supplies together with the iris (Fig 1-25). The iris vessels have a radial arrangement that, in lightly pigmented blue irises, is visible upon slit-lamp examination. This radial arrangement can be distinguished from the irregular new iris vessels formed in rubeosis iridis.

Vortex Veins

The vortex veins drain the venous system of the choroid, ciliary body, and iris (see Fig 1-22). Each eye contains 4–7 (or more) veins. One or more veins are usually located in each quadrant and exit 14–25 mm from the limbus, between the rectus muscles. The ampullae of the vortex veins are 8–9 mm from the ora serrata and are visible by indirect ophthalmoscopy. A circle connecting these ampullae corresponds roughly to the equator and

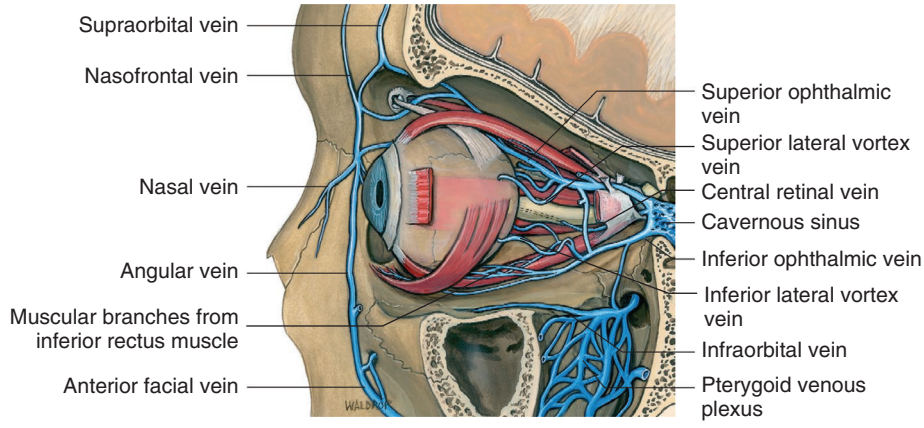


Figure 1-26 Orbital veins, lateral (sagittal) composite view. Note the eventual connection of the facial and ocular venous systems with the cavernous sinus. *(Reproduced with permission from Dutton JJ.* Atlas of Clinical and Surgical Orbital Anatomy. 2nd ed. *Elsevier/Saunders; 2011:Fig 6-8.)*

divides the central or posterior fundus from the peripheral or anterior portion. The vortex veins join the orbital venous system after leaving the eye (Fig 1-26). Venous blood leaving the eye also contains aqueous humor received from the aqueous veins (see Chapter 2).

Orbital Veins

The major veins providing drainage of the orbit and eye are the superior and inferior ophthalmic veins, which primarily empty into the cavernous sinus. In addition to receiving venous blood from the eye via the vortex veins, they also drain the extraocular muscles and portions of the medial face and forehead (see Fig 1-26).

CLINICAL PEARL

Venous drainage from the face anastomoses with that of the orbit, particularly at and above the medial canthus. Infection of the skin in this region can obtain direct access to the cavernous sinus through the orbital venous system, potentially leading to inflammation and cavernous sinus thrombosis. Enlargement of the superior ophthalmic vein may be an indication of cavernous sinus pathology.

Eyelids

The *palpebral fissure* is the exposed ocular surface between the upper and lower eyelids (Fig 1-27). Typically, the adult fissure is 27–30 mm long and 8–11 mm wide. The upper eyelid, which is more mobile than the lower, can be raised 15 mm by the action of the levator palpebrae superioris muscle alone and can be raised another 2 mm by the action of the Müller muscle. If the frontalis muscle of the brow is used, the palpebral fissure can be widened an additional 2 mm. See also BCSC Section 7, *Oculofacial Plastic and Orbital Surgery.*

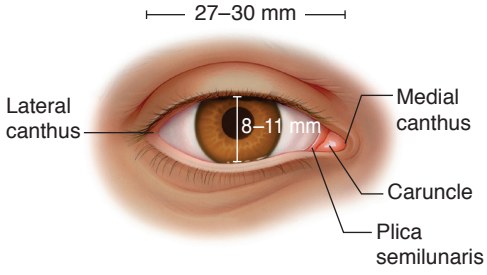


Figure 1-27 Landmarks of the external eye. *(Illustration by Christine Gralapp.)*

Anatomy

Though small in surface area, the eyelid is complex in its structure and function. When the anatomy of the upper eyelid is described, it is helpful to divide it into distinct segments from the dermal surface inward. These segments include the following structures (Fig 1-28, Activity 1-3; see also Figs 1-29 through 1-36):

- skin and subcutaneous connective tissue (more evident distally from the margin)
- muscles of protraction (the orbicularis oculi muscle is the main protractor)
- orbital septum
- orbital fat
- muscles of retraction (levator palpebrae superioris, Müller muscle, capsulopalpebral fascia, inferior tarsal muscle)
- tarsus
- conjunctiva

ACTIVITY 1-3 Upper and lower eyelid anatomy.
Developed by Nikisha Q. Richards, MD.

Eyelid skin and subcutaneous connective tissue

The eyelid skin, one of the thinnest in the body, contains fine hairs, sebaceous glands, and sweat glands. A superior eyelid crease is present near the upper border of the tarsus, where the levator aponeurosis establishes its first insertional attachments. In many individuals of Asian descent, the levator aponeurosis fuses with orbital septum lower along the tarsus, resulting in lower superior eyelid crease. Figure 1-29 depicts the 2 major variations in eyelid anatomy.

The loose connective tissue of the eyelid contains no fat. Blood or other fluids can accumulate beneath the skin and cause rapid and dramatic swelling of the eyelids.

The eyelid margin contains several important landmarks (Fig 1-30). A small opening, the *punctum* of the canaliculus, presents medially at the summit of each lacrimal papilla. The superior punctum, normally hidden by slight internal rotation, is located more medially than the inferior punctum, which is usually apposed to the globe and is not normally visible without eversion.

Along the entire length of the free margin of the eyelid is the *gray line* (or *intermarginal sulcus*), which corresponds on histologic examination to the most superficial portion

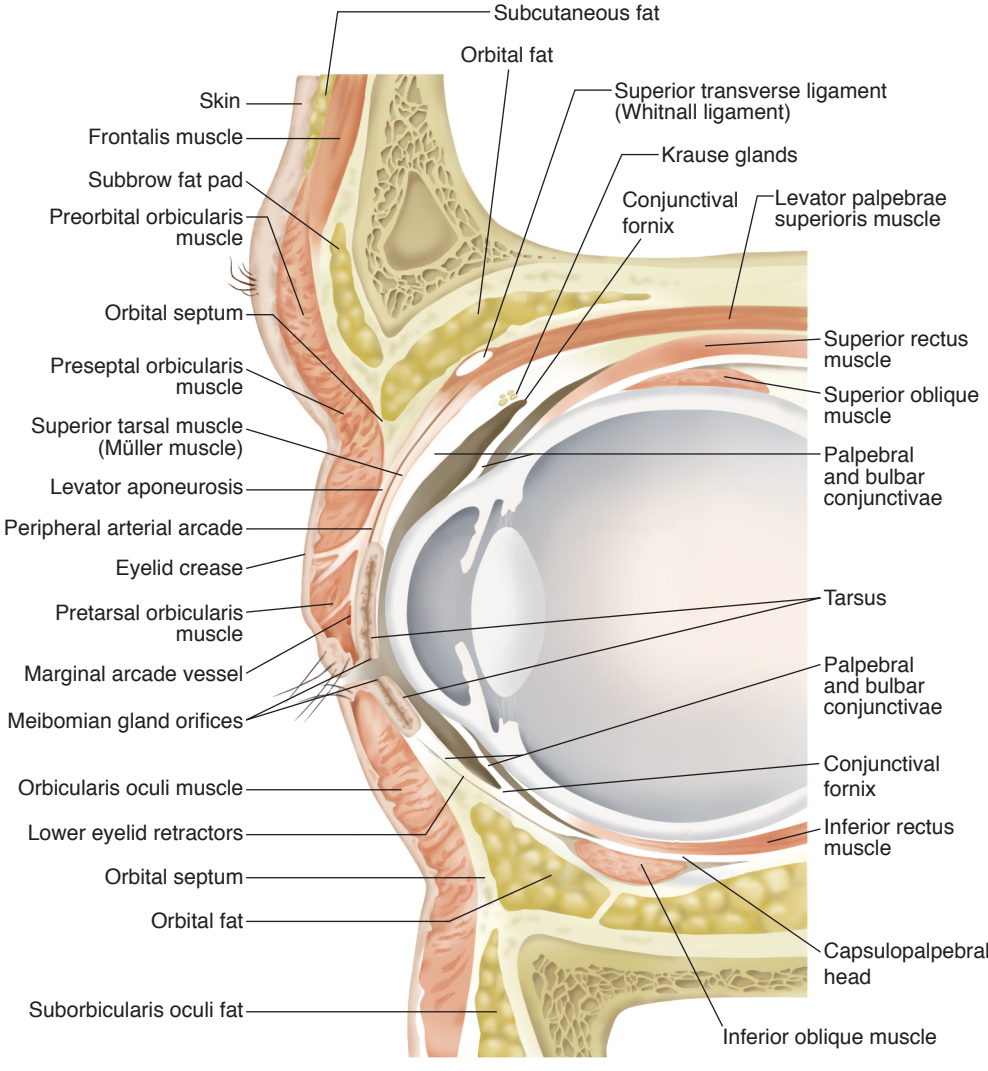


Figure 1-28 Eyelid anatomy: schematic cross section (sagittal) of the upper and lower eyelid area. *(Modified from Stewart WB.* Surgery of the Eyelid, Orbit, and Lacrimal System. *Ophthalmology Monograph 8, vol 2. American Academy of Ophthalmology; 1994:23, 85. Illustration by Cyndie C.H. Wooley.)*

of the preseptal orbicularis oculi muscle, the muscle of Riolan, and to the avascular plane of the eyelid. Anterior to this line, the eyelashes (or cilia) arise, and behind this line are the openings of the meibomian (or tarsal) glands.

The eyelashes are arranged in 2 or 3 irregular rows along the anterior dermal edge of the eyelid margin. They are usually longer and more numerous on the upper eyelid than on the lower one. The margins contain the *glands of Zeis,* which are modified sebaceous glands associated with the cilia, and the *glands of Moll,* which are apocrine sweat glands in the skin (Table 1-3; also see Fig 1-30).

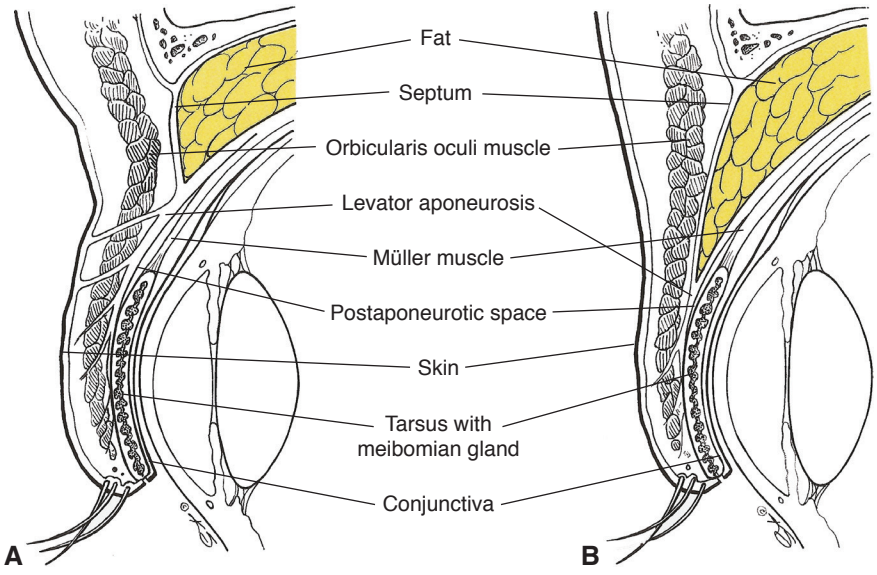


Figure 1-29 Racial variations in eyelid anatomy. **A,** The orbital septum fuses with the levator aponeurosis above the tarsus. **B,** Asian: the orbital septum fuses with the levator aponeurosis between the eyelid margin and the superior border of the tarsus, and there are fewer aponeurotic attachments to the skin. *(Modified with permission from Katowitz JA, ed.* Pediatric Oculoplastic Surgery. *Springer-Verlag; 2002.)*

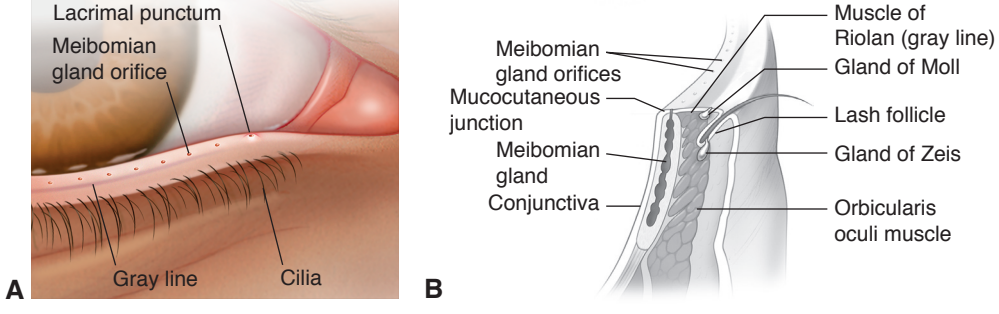


Figure 1-30 Anatomical landmarks of the lower eyelid margin. **A,** The gray line, or intermarginal sulcus, is visible between the bases of the cilia and the orifices of the meibomian glands (tarsal glands). The lower eyelid has been slightly everted to clearly expose the inferior lacrimal punctum. **B,** Cross section of the lower eyelid margin. *(Illustrations by Christine Gralapp.)*

Muscle of protraction: orbicularis oculi muscle

The *orbicularis oculi muscle,* the main protractor of the eyelid, is arranged in several concentric bands around the palpebral fissure and can be divided into orbital and palpebral (preseptal and pretarsal) parts (Fig 1-31). All components of the orbicularis oculi muscle are innervated by CN VII (the facial nerve). The orbital part inserts in a complex way into the medial canthal tendon and into other portions of the orbital margin and the corrugator supercilii muscle. The orbital part acts as a sphincter and functions solely during voluntary closure of the eye.

Table 1-3 Glands of the Eye and Adnexa

Glands	Location	Secretion	Content
Lacrimal	Orbital gland	Exocrine	Aqueous
	Palpebral gland	Exocrine	Aqueous
Accessory lacrimal	Plica, caruncle	Exocrine	Aqueous
Krause	Eyelid	Exocrine	Aqueous
Wolfring	Eyelid	Exocrine	Aqueous
Meibomian	Tarsus	Holocrine	Oil
Zeis	Follicles of cilia	Holocrine	Oil
	Eyelid, caruncle	Holocrine	Oil
Moll	Eyelid	Apocrine	Sweat
Goblet cell	Conjunctiva	Holocrine	Mucus
	Plica, caruncle	Holocrine	Mucus

The palpebral part of the orbicularis oculi muscle functions both voluntarily and involuntarily in spontaneous and reflex blinking. The pretarsal orbicularis muscle adheres firmly to the tarsus; a portion of it attaches to the anterior lacrimal crest and the posterior lacrimal crest (sometimes called the *Horner muscle*) and plays a role in tear drainage. Orbicularis fibers extend to the eyelid margin, where there is the small bundle of striated muscle fibers called the *muscle of Riolan* (Fig 1-32; see also Fig 1-30B). This muscle can be seen on external inspection of the eyelid margin as the gray line. It is thought that this muscle may play a role in tear drainage, inward rotation of eyelashes toward the globe upon eyelid closure, and expression of glandular secretion when blinking.

Orbital septum

The *orbital septum* is a thin sheet of connective tissue that encircles the orbit as an extension of the periosteum of the roof and the floor of the orbit (Fig 1-33). Superiorly, the septum is attached firmly to the periosteum of the superior half of the orbital margin, at the arcus marginalis. It passes medially in front of the trochlea and continues along the medial margin of the orbit, along the margin of the frontal process of the maxillary bone, and onto the inferior margin of the orbit. Centrally, the orbital septum attaches to the aponeurosis of both the upper and lower eyelids. The septum delimits the anterior or posterior spread of edema, inflammation, or blood. Clinical examples include preseptal cellulitis, orbital cellulitis, and retrobulbar hemorrhage.

Orbital fat

Posterior to the septum lie the orbital (preaponeurotic) fat pads: 2 behind the superior septum and 3 behind the inferior septum (see Fig 1-33B).

CLINICAL PEARL

In patients with periorbital lacerations, the presence of orbital fat in the laceration indicates violation of the orbital septum.

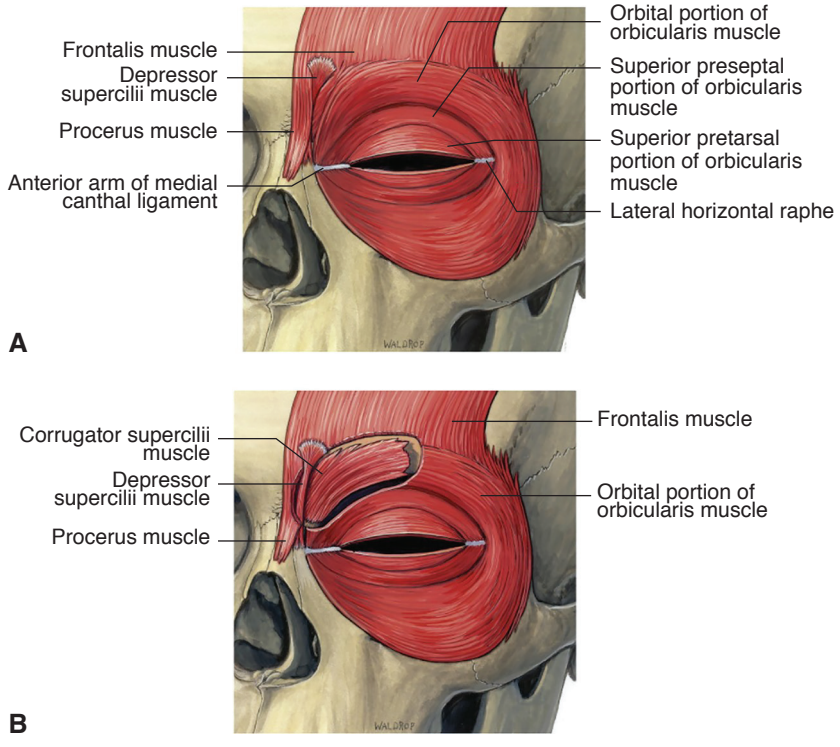


Figure 1-31 The 3 parts of the orbicularis oculi muscle. **A,** Orbital, preseptal, and pretarsal. The preseptal and pretarsal components function in voluntary and involuntary blinking, while the orbital component functions solely in forced lid closure. Note the relationship of the orbicularis oculi with the frontalis, depressor supercilii, and procerus muscles. **B,** The corrugator supercilii muscle with a segment of the orbital portion of the orbicularis oculi muscle removed. *(Modified with permission from Dutton JJ.* Atlas of Clinical and Surgical Orbital Anatomy. *2nd ed. Elsevier/Saunders; 2011:Figs 8-12, 8-13.)*

Muscles of retraction: upper eyelid

In the upper eyelid, the retractors are the *levator palpebrae superioris muscle* with its aponeurosis and the *Müller muscle (superior tarsal muscle).*

Levator palpebrae superioris muscle The levator palpebrae superioris muscle originates from the lesser wing of the sphenoid bone. The body of the levator muscle overlies the superior rectus as it travels anteriorly toward the eyelid. The muscle itself, which is 40 mm long, is innervated by the superior division of CN III, and its action can lift the upper eyelid 15 mm.

The *Whitnall (superior transverse) ligament* is formed by a sleeve of elastic fibers that surrounds the levator muscle (Fig 1-34). It provides support for the upper eyelid and surrounding tissues. At the Whitnall ligament, the levator muscle transitions into the aponeurosis anteriorly and the Müller (superior tarsal) muscle posteriorly. The Whitnall ligament is also where the levator muscle's anterior–posterior vector changes to superior–inferior, toward the aponeurosis.

The *levator aponeurosis,* the tendon of the levator muscle, is 14–20 mm in length and has many attachments to the eyelid and surrounding orbit (see Figs 1-28, 1-34). Anteriorly,

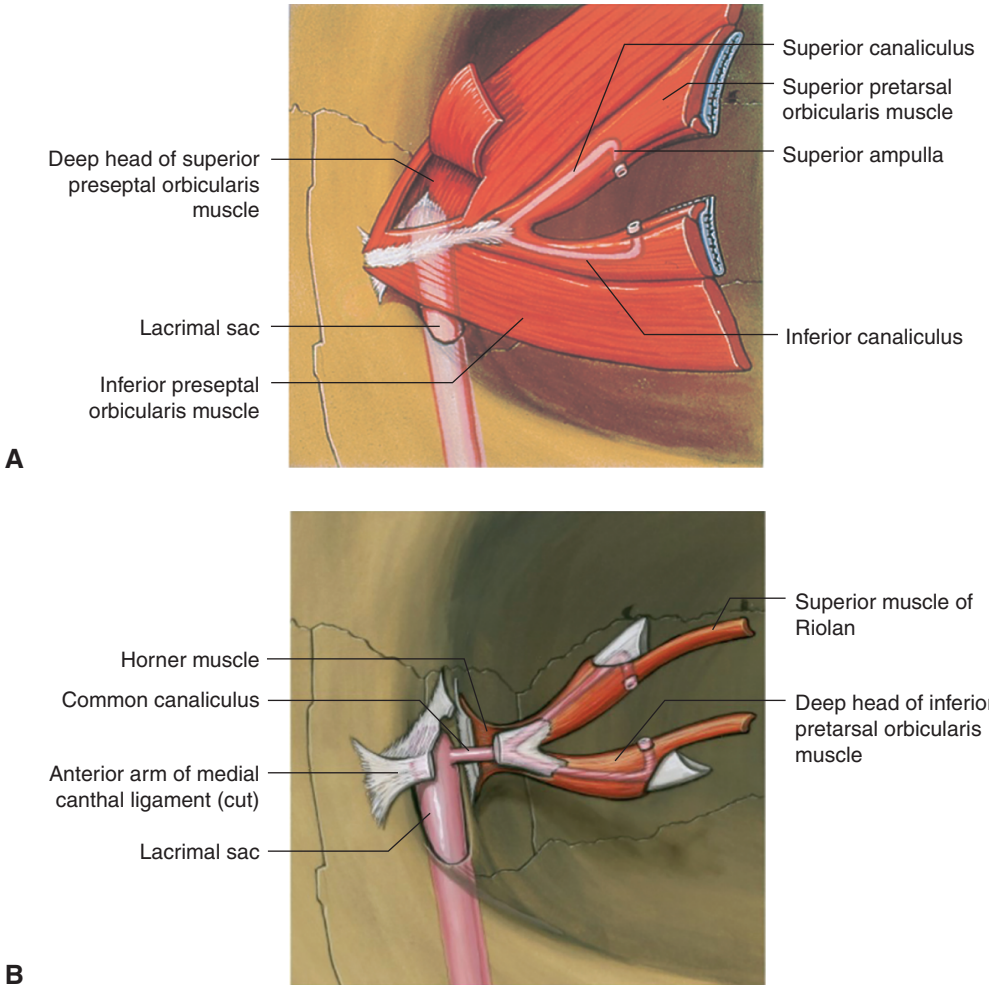


Figure 1-32 Lacrimal drainage system. **A,** Superficial extensions of the orbicularis oculi muscle. **B,** Deep head of the orbicularis oculi muscle; superficial components are reflected. *(Part A reproduced with permission from Dutton JJ.* Atlas of Clinical and Surgical Orbital Anatomy. *Saunders; 1994. Part B reproduced with permission from Dutton JJ.* Atlas of Clinical and Surgical Orbital Anatomy. *2nd ed. Elsevier/Saunders; 2011:Fig 9-3.)*

it passes through the orbicularis oculi muscle and inserts subcutaneously, providing a minor contribution to the superior eyelid crease (see Fig 1-28). Posteriorly, the levator aponeurosis inserts into the surface of the tarsus. The major component forming the eyelid crease is supratarsal fusion of the orbital septum with the aponeurosis (see Fig 1-29). The aponeurosis forms its firmest attachments on the anterior aspect of the tarsus, approximately 3 mm superior to the eyelid margin. The aponeurosis also inserts into the trochlea of the superior oblique muscle and into the fibrous tissue bridging the supraorbital foramen/notch. The lateral horn of the aponeurosis divides the lacrimal gland into orbital and palpebral lobes and inserts at the lateral orbital tubercle. The

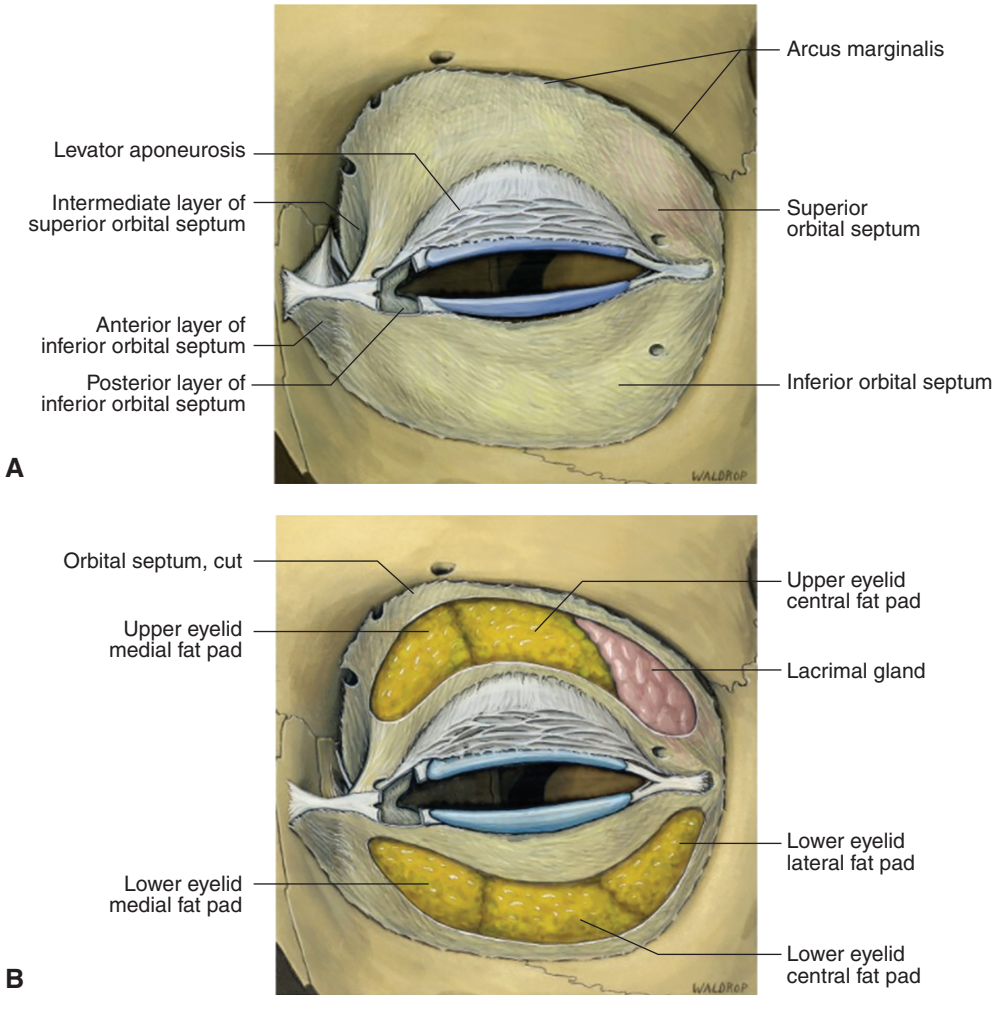


Figure 1-33 Orbital septum. **A,** The orbital septum arises from the periosteum of the bones of the orbital margin (arcus marginalis) and inserts on the aponeurosis of the upper and lower eyelids. **B,** Preaponeurotic fat pads. *(Modified with permission from Dutton JJ.* Atlas of Clinical and Surgical Orbital Anatomy. *2nd ed. Elsevier/Saunders; 2011:Figs 8-8, 8-9.)*

medial horn inserts at the posterior lacrimal crest. Aponeurotic attachments also exist with the conjunctiva of the upper fornix and the orbital septum and also contribute to the superior eyelid crease.

Müller muscle The Müller (superior tarsal) muscle originates from the undersurface of the levator palpebrae superioris muscle in the upper eyelid. This smooth muscle is innervated by the sympathetic nervous system, and its action is responsible for 2 mm of upper eyelid lift. The Müller muscle attaches to the upper border of the upper tarsus and to the conjunctiva of the upper fornix.

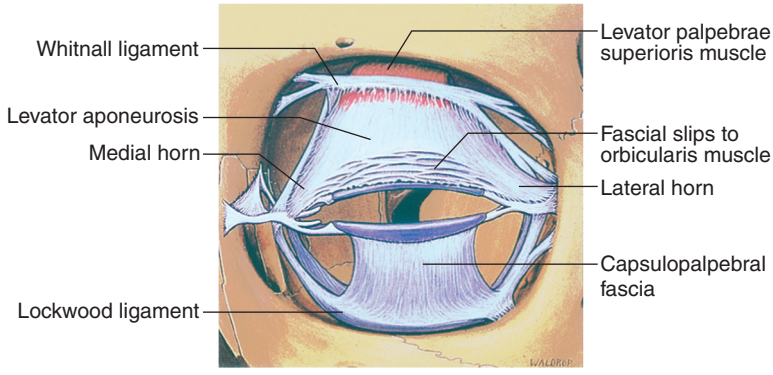


Figure 1-34 Diagram of left orbit demonstrating the levator aponeurosis and the Whitnall ligament, also known as superior transverse ligament. Note the medial and lateral horns of the aponeurosis and the suspensory ligament of Lockwood. *(Modified with permission from Dutton JJ.* Atlas of Clinical and Surgical Orbital Anatomy. *Saunders; 1994.)*

CLINICAL PEARL

When evaluating a patient for blepharoptosis, avoid administering phenylephrine and α-agonists because they may stimulate the Müller muscle, falsely elevating the lid. Ophthalmic oxymetazoline has the same mechanism of action, which is why it may have utility in patients who cannot or choose not to undergo surgical correction of their blepharoptosis. Phenylephrine or other α-agonists may be used to evaluate patients for blepharoptosis repair via a Müller muscle conjunctival resection.

Muscles of retraction: lower eyelid

In the lower eyelid, the retractors are the *capsulopalpebral fascia*, which is analogous to the levator aponeurosis in the upper eyelid, and the *inferior tarsal muscle*. The inferior tarsal muscle arises from the capsulopalpebral head of the inferior rectus muscle in the lower eyelid and attaches to the lower border of the lower tarsus. Like the Müller muscle, the inferior tarsal muscle is smooth muscle, but it is much weaker.

The inferior equivalent to the Whitnall ligament is the suspensory *ligament of Lockwood,* a fusion of the sheath of the inferior rectus muscle, the inferior tarsal muscle, and the check ligaments of the medial and lateral rectus muscles (see Fig 1-34). This ligament provides support for the globe and the anteroinferior orbit.

CLINICAL PEARL

The fusion of the sheath of the inferior rectus muscle, the Lockwood ligament, and the inferior tarsal muscle is an important consideration in surgery, because an operation on the inferior rectus muscle may be associated with palpebral fissure changes.

Tarsus

The *tarsal plates* consist of dense connective tissue, not cartilage. They are attached to the orbital margin by the medial and lateral canthal tendons (see Fig 1-28). Although the upper and lower tarsal plates are similar in width (29 mm) and thickness (1 mm), the height of the upper tarsus (10–12 mm) is almost 3 times greater than that of the lower tarsus (4 mm).

The *meibomian glands* (also called *tarsal glands*) are modified holocrine sebaceous glands that are oriented vertically in parallel rows through the tarsus (Fig 1-35; see also Figs 1-29, 1-30). Their distribution and number within the eyelid can be observed by infrared imaging of the eyelid (Fig 1-36). A single row of 30–40 meibomian orifices is present in the upper eyelid, but there are approximately only 20 orifices in the lower eyelid. Oil (meibum) from meibomian orifices forms a reservoir on the skin of the eyelid margin and is spread onto the tear film with each blink. Alterations in meibomian gland lipid composition and secretion play a role in dry eye. Aging is associated with an alteration in the lipid profile of meibum and with meibomian gland loss.

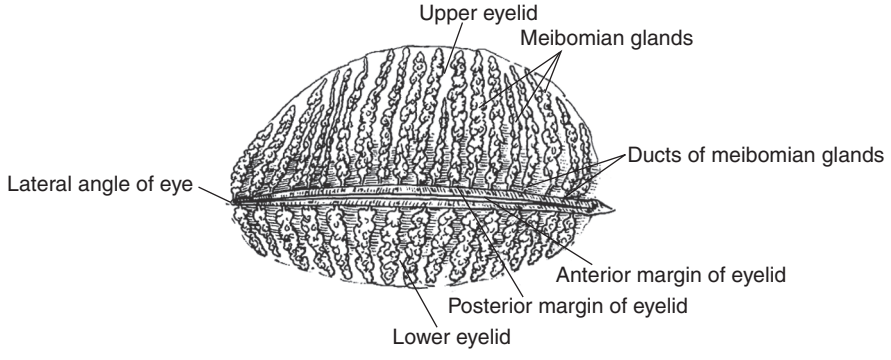


Figure 1-35 Posterior view of the eyelids with the palpebral fissure nearly closed. Note the meibomian (tarsal) glands with their short ducts and orifices. The palpebral conjunctiva has been removed to show these glands in situ. *(Modified with permission from Snell RS, Lemp MA.* Clinical Anatomy of the Eye. *Blackwell; 1989.)*



Figure 1-36 Infrared meibography image of the upper eyelid demonstrates normal meibomian gland architecture. *(Courtesy of Mina Massaro-Giordano, MD.)*

CLINICAL PEARL

The presence of more oil glands in the upper eyelid than in the lower eyelid explains why sebaceous cell carcinoma is more common in the upper eyelid.

Arita R, Itoh K, Inoue K, Amano S. Noncontact infrared meibography to document age-related changes of the meibomian glands in a normal population. *Ophthalmology.* 2008;115(5):911–915.

Sullivan BD, Evans JE, Dana MR, Sullivan DA. Influence of aging on the polar and neutral lipid profiles in human meibomian gland secretions. *Arch Ophthalmol.* 2006;124(9):1286–1292.

Conjunctiva

The palpebral (tarsal) conjunctiva is a transparent vascularized membrane consisting of nonkeratinized stratified squamous epithelium that lines the inner surface of the eyelids. Continuous with the conjunctival fornices (cul-de-sacs), it merges with the bulbar conjunctiva (covering the anterior portion of the sclera) before terminating at the limbus (Fig 1-37). The conjunctiva is discussed further later in this chapter.

Vascular Supply

The blood supply of the eyelids is derived from the facial system, which arises from the external carotid artery, and the orbital system, which originates from the internal carotid artery along branches of the ophthalmic artery. Thus, the eyelid vasculature represents an anastomosis of the external and internal carotid arteries (Fig 1-38).

The *marginal arterial arcade* is located 2 mm from the free border of the eyelid, just above the ciliary follicles. It is either between the tarsal plate and the orbicularis oculi muscle or within the tarsus. A smaller *peripheral arterial arcade* runs along the upper margin of the tarsal plate anterior to the Müller muscle. The superficial temporal artery is a terminal branch of the external carotid artery; BCSC Section 5, *Neuro-Ophthalmology,* discusses the anterior circulation in greater detail. The venous drainage system of the eyelids can be divided into 2 components: a superficial (or preseptal) system, which drains into the internal and external jugular veins, and a deep (or postseptal)

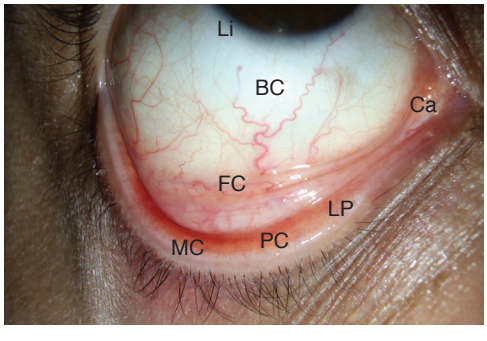


Figure 1-37 The different parts of the conjunctiva: limbus (Li), bulbar conjunctiva (BC), forniceal conjunctiva (FC), palpebral conjunctiva (PC), and marginal conjunctiva (MC). Additional structures include the caruncle (Ca) and the lacrimal punctum (LP). *(Courtesy of Vikram S. Brar, MD.)*

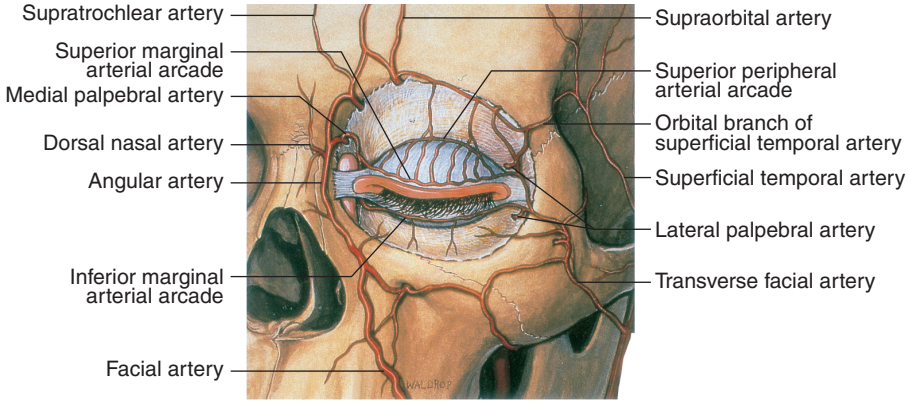


Figure 1-38 Arterial supply of the eyelids. Note the numerous locations where arteries emerging from the orbit anastomose with branches of the facial artery, providing connections between the internal and external carotid arteries. The facial artery gives rise to the angular artery as it travels superiorly, lateral to the nose. The angular artery serves as an important landmark in dacryocystorhinostomy. *(Reproduced with permission from Dutton JJ.* Atlas of Clinical and Surgical Orbital Anatomy. *Saunders; 1994.)*

system, which flows into the cavernous sinus. Thus, the venous circulation of the eyelid connects the face with the cavernous sinus, providing a route for the spread of infection (see Fig 1-26).

Lymphatics

Lymphatic vessels are present in the eyelids, conjunctiva, and orbit. Lymphatic drainage from the eyelids parallels the course of the veins (Fig 1-39). There are 2 groups of lymphatics:

- a medial group that drains into the submandibular lymph nodes
- a lateral group that drains into the superficial preauricular lymph nodes

CLINICAL PEARL

Clinically, swelling of the lymph nodes is a diagnostic sign of several external eye infections, including adenoviral conjunctivitis and Parinaud oculoglandular syndrome.

Lacrimal Glands and Excretory System

Lacrimal Gland

The main lacrimal gland is located in a shallow depression within the orbital part of the frontal bone. The gland is separated from the orbit by fibroadipose tissue and is divided into 2 parts, orbital and palpebral lobes, by the lateral horn of the levator aponeurosis (Fig 1-40). When the upper eyelid is everted, the smaller palpebral lobe can be seen in the superolateral

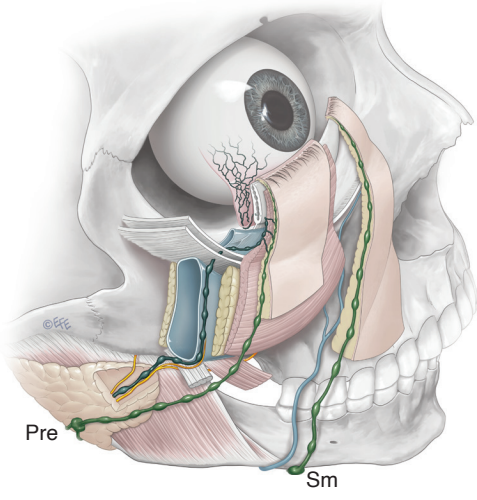


Figure 1-39 Lymphatic drainage *(green)* of the eyelid and conjunctiva. The medial drainage is received by the submandibular lymph node (Sm); the lateral drainage, by the preauricular lymph node (Pre). *(Illustration by Levent Efe Medical Illustration Studios.)*

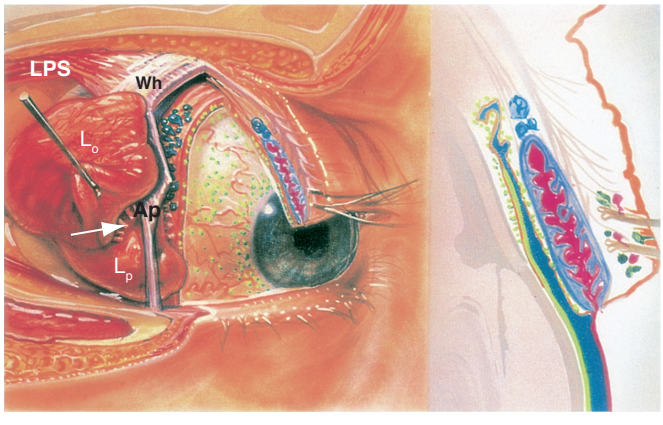


Figure 1-40 The lacrimal secretory system. The conjunctival and tarsal mucin-secreting goblet cells *(green)* contribute to the mucoaqueous and glycocalyx components of the tear film. The accessory lacrimal exocrine glands of Krause and Wolfring are present in the subconjunctival tissues *(blue)* and contribute to the aqueous component of the tear film. Oil-producing meibomian glands and palpebral glands of Zeis and Moll are shown in pink. The orbital lobe of the lacrimal gland (L_o) and the palpebral lobe of the lacrimal gland (L_p) are separated by the lateral horn of the levator aponeurosis (Ap). The tear ducts *(arrow)* from the orbital portion traverse the palpebral portion. The levator palpebrae superioris (LPS) muscle and the Whitnall ligament (Wh) are also shown. *(Modified with permission from Zide BM, Jelks GW.* Surgical Anatomy of the Orbit. *Raven; 1985.)*

conjunctival fornix (Fig 1-41). An isthmus of glandular tissue may exist between the palpebral lobe and the larger orbital lobe.

A variable number of thin-walled excretory ducts, blood vessels, lymphatics, and nerves pass from the orbital lobe into the palpebral lacrimal gland. The ducts continue downward, and between 8 and 12 of them empty into the conjunctival fornix approximately 5 mm above the superior margin of the upper tarsus.



Figure 1-41 Clinical photograph of a palpebral lobe of the lacrimal gland with eyelid manually retracted, right eye. *(Courtesy of Nikisha Q. Richards, MD.)*

CLINICAL PEARL

Because the lacrimal excretory ducts of the orbital and palpebral lobes pass through the palpebral portion of the gland, biopsy of the lacrimal gland is usually performed on the orbital portion to avoid sacrificing the ducts.

The lacrimal glands are exocrine glands that produce aqueous secretions. The body of each gland contains 2 cell types (Fig 1-42):

- glandular epithelial cells, which line the lumen of the gland
- myoepithelial cells, which surround the parenchyma and are covered by a basement membrane

Lacrimal secretions comprise the aqueous component of the mucoaqueous layer of the tear film and include lysozymes, lactoferrin, and immunoglobulin A. The lacrimal gland undergoes structural and functional alterations with age, which may play a role in acquired dry eye syndrome.

The lacrimal artery, a branch of the ophthalmic artery, supplies the gland with blood. The lacrimal gland receives secretomotor cholinergic, vasoactive intestinal polypeptide–ergic, and sympathetic nerve fibers in addition to sensory innervation via the lacrimal nerve (from CN V_1). The gland's extremely complex neuroanatomy governs both reflex and psychogenic stimulation (see BCSC Section 5, *Neuro-Ophthalmology*).

CLINICAL PEARL

Cholinergic innervation helps stimulate secretions from the lacrimal gland. Thus, any medication, including antihistamines, that have anticholinergic properties can create or exacerbate dry eye syndrome.

de Paiva CS. Effects of aging in dry eye. *Int Ophthalmol Clin.* 2017;57(2):47–64.

Accessory Glands

The accessory lacrimal *glands of Krause* and *Wolfring* are located at the proximal margin of the tarsus or in the fornices. They are cytologically identical to the main lacrimal gland

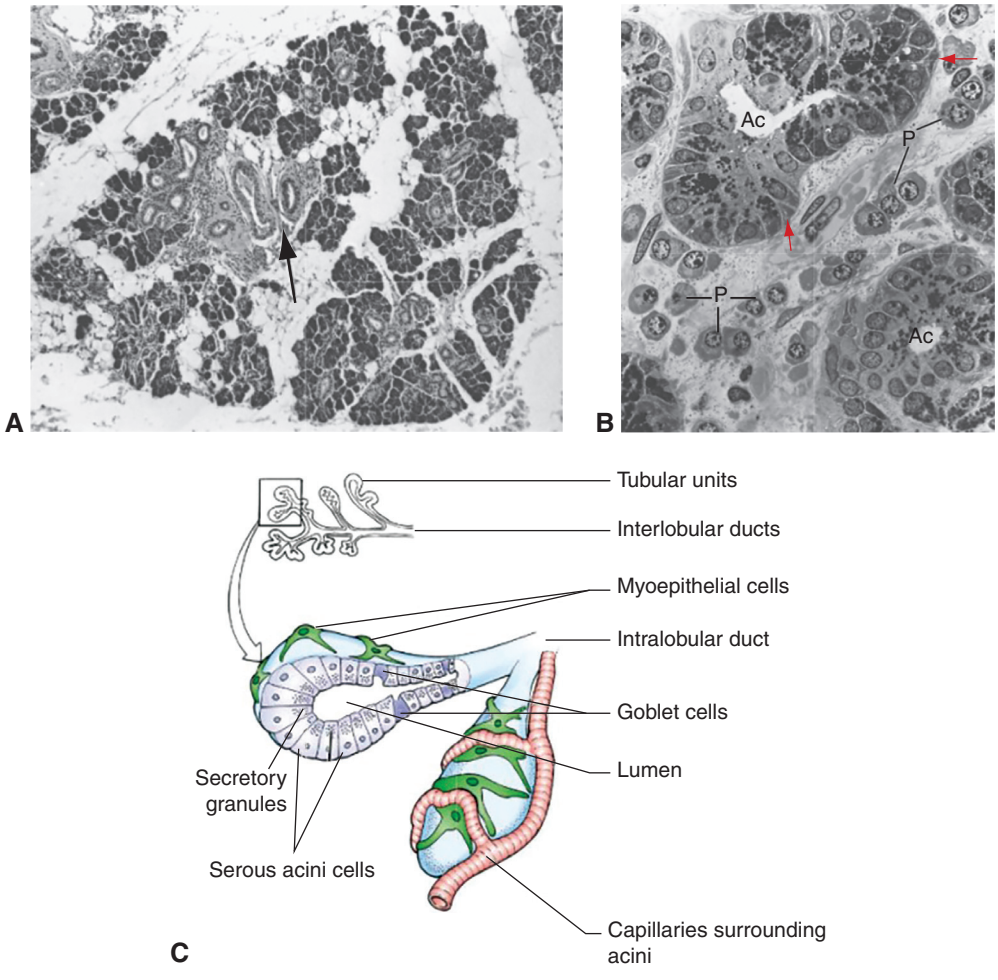


Figure 1-42 Lacrimal gland lobule. **A,** Low magnification of lacrimal gland lobule demonstrating its central duct *(arrow)*. **B,** Histologic section of the lacrimal gland demonstrating acinar units (Ac) made up of a central lumen surrounded by glandular epithelial cells with secretory granules. *Arrows* indicate surrounding myoepithelial cells. The stroma contains blood vessels and numerous plasma (P) cells that produce immunoglobulin A. **C,** Schematic of the lacrimal lobule. *(Modified with permission from Forrester JV, Dick AD, McMenamin PG, Roberts F, Pearlman E.* The Eye: Basic Sciences in Practice. *4th ed. Elsevier; 2016:90.)*

and receive similar innervation (see Figs 1-28, 1-40). These glands account for approximately 10% of the total lacrimal secretory mass.

Lacrimal Excretory System

The lacrimal drainage system includes the upper and lower puncta, the lacrimal canaliculi, the lacrimal sac, and the nasolacrimal duct (Fig 1-43). The *lacrimal puncta* are small (roughly 0.3 mm in diameter) openings on the eyelid margin, located at the extreme nasal border of the eyelids at their junction with the medial canthus (see Fig 1-30A). The inferior punctum is approximately 6.5 mm from the medial canthus; the superior punctum is

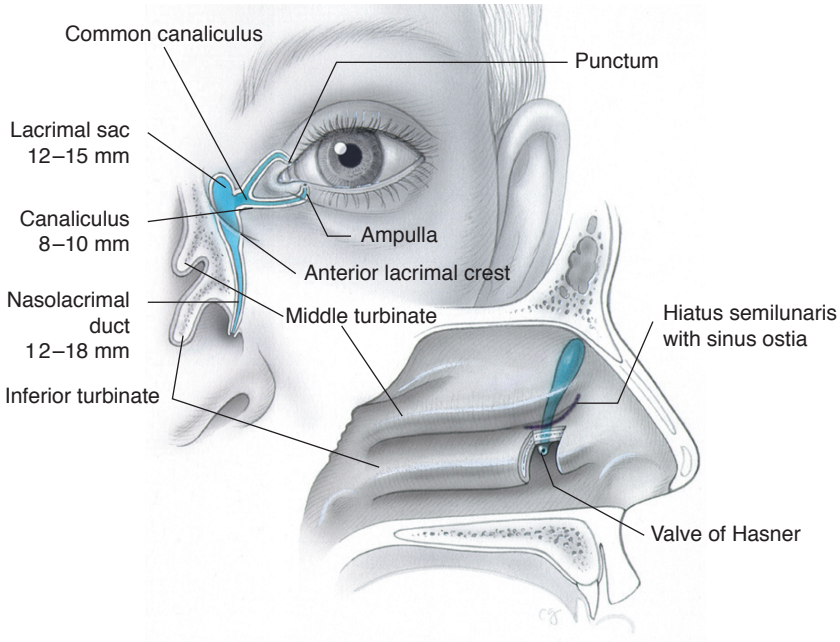


Figure 1-43 Lacrimal excretory system. The measurements given are for adults. *(Illustration by Christine Gralapp.)*

6.0 mm from it. The lower eyelid punctum sits closer to the corneal limbus because of the growth of the maxillary sinus, which draws the lower eyelid punctum laterally. The puncta are directed posteriorly into the tear lake at the inner canthus. The ampulla is a slight dilation at the angle of the canaliculus, just beyond the punctum.

These openings lead to the *lacrimal canaliculi,* the *lacrimal sac,* and finally the *nasolacrimal duct,* which, in turn, leads to the nose. In 90% of people, the canaliculi join to form a common canaliculus prior to entering the lacrimal sac. Fibers of the tarsal orbicularis oculi muscles surround the canalicular system and lacrimal sac, driving the tears into the system and down the duct with blinking (see Fig 1-32).

CLINICAL PEARL

The nasolacrimal duct opens into the nose beneath the inferior turbinate. At this location, a persistent membrane over the valve of Hasner is often associated with excessive tearing and discharge in infants with nasolacrimal duct obstruction. This condition can be treated with massage over the lacrimal sac, which forces contents down the duct, or with lacrimal probing to relieve the obstruction.

The lacrimal puncta and the canaliculi are lined with nonkeratinized stratified squamous epithelium that merges with the epithelium of the eyelid margins. Near the lacrimal sac, the epithelium differentiates into 2 layers:

- a superficial columnar layer
- a deep, flattened cell layer

Goblet cells and occasionally cilia are present. In the canaliculi, the substantia propria consists of collagenous connective tissue and elastic fibers. The wall of the lacrimal sac resembles adenoid tissue and has a rich venous plexus and many elastic fibers.

For further discussion, see BCSC Section 7, *Oculofacial Plastic and Orbital Surgery.*

Conjunctiva

The conjunctiva can be divided into 3 geographic zones: palpebral (tarsal), forniceal, and bulbar (see Fig 1-37). The *palpebral conjunctiva* begins at the mucocutaneous junction of the eyelid and covers the eyelid's inner surface. This part adheres firmly to the tarsus. The palpebral conjunctiva also contains the marginal conjunctiva. In the fornices, the tissue becomes redundant and freely movable *(forniceal conjunctiva);* it becomes enmeshed with fibrous elements of the levator aponeurosis and the Müller muscle in the upper eyelid. In the lower eyelid, fibrous expansions of the inferior rectus muscle sheath fuse with the inferior tarsal muscle, the equivalent of the Müller muscle. The conjunctiva is reflected at the cul-de-sac and attaches to the globe. The delicate *bulbar conjunctiva* is freely movable but fuses with the Tenon capsule as it inserts into the limbus. Loss of the Tenon capsule caused by increasing age can lead to conjunctivochalasis (redundant folds of conjunctiva between the globe and the eyelid margin).

Anterior ciliary arteries supply blood to the bulbar conjunctiva. The palpebral conjunctiva is supplied by branches of the marginal arcades of the eyelids. The superior peripheral arcade, running along the upper border of the eyelid, sends branches proximally to supply the forniceal conjunctiva and then the bulbar conjunctiva, as do the posterior conjunctival arteries. The limbal blood supply derives from the ciliary arteries through the anterior conjunctival arteries. The vascular watershed between the anterior and posterior territories lies approximately 3–4 mm from the limbus.

The innervation of the conjunctiva is derived from the ophthalmic division of cranial nerve V.

The conjunctiva is a mucous membrane consisting of nonkeratinized stratified squamous epithelium with numerous goblet cells and a thin, richly vascularized substantia propria containing lymphatic vessels, plasma cells, macrophages, and mast cells. A lymphoid layer extends from the bulbar conjunctiva to the subtarsal folds of the eyelids. In places, specialized aggregations of *conjunctiva-associated lymphoid tissue (CALT)* correspond to *mucosa-associated lymphoid tissue (MALT)* elsewhere and comprise collections of T and B lymphocytes underlying a modified epithelium. These regions are concerned with antigen processing.

The thickness of the conjunctival epithelium varies from 2 to 5 cells. The basal cells are cuboidal and evolve into flattened polyhedral cells as they reach the surface. The goblet cells (unicellular mucous glands) are concentrated in the inferior and medial portions of the conjunctiva, especially in the region of the caruncle and plica semilunaris. Goblet cells secrete mucin, which is a component of the mucoaqueous layer of the tear film as well as the glycocalyx layer. They are sparsely distributed throughout the remainder of the conjunctiva and are absent in the limbal region. For further discussion of the limbus, see Chapter 8.

Caruncle

The caruncle is a small, fleshy, ovoid structure attached to the inferomedial side of the plica semilunaris (see Figs 1-27, 1-37). Because it is a piece of modified skin, it contains sebaceous glands and fine, colorless hairs. The surface is covered by nonkeratinized stratified squamous epithelium.

> **CLINICAL PEARL**
>
> Because the caruncle is composed of modified cutaneous tissue, it is possible for the caruncle to develop basal cell, squamous cell, and other types of carcinomas.

Plica Semilunaris

The plica semilunaris is a narrow, highly vascular, crescent-shaped fold of the conjunctiva located lateral to and partly under the caruncle (see Fig 1-27). Its lateral border is free and separated from the bulbar conjunctiva, which it resembles on histologic examination. The epithelium of the plica is rich in goblet cells. The plica's stroma contains fat and some nonstriated muscle. The plica is a vestigial structure analogous to the nictitating membrane, or third eyelid, of dogs and other animals.

Tenon Capsule

The Tenon capsule *(fascia bulbi)* is an envelope of elastic connective tissue that fuses posteriorly with the optic nerve sheath and anteriorly with a thin layer of tissue, the *intermuscular septum,* located 3 mm posterior to the limbus (Fig 1-44). The Tenon capsule forms the cavity within which the globe moves. It is composed of compactly arranged collagen fibers and a few fibroblasts.

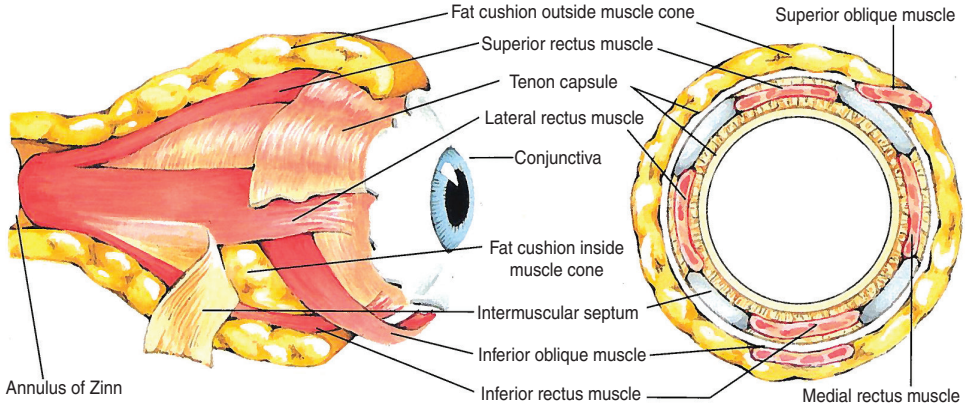


Figure 1-44 Tenon capsule. Note the relationship between Tenon capsule and the extraocular muscles it envelops. This sheath helps establish a pulley system in the orbit where the intermuscular septa, Tenon capsule, check ligaments, and periorbital tissues are interconnected. *(Courtesy of Jordan DR, Anderson RL.* Surgical Anatomy of the Ocular Adnexa: A Clinical Approach. *Ophthalmology Monographs 9. American Academy of Ophthalmogy; 1996.)*

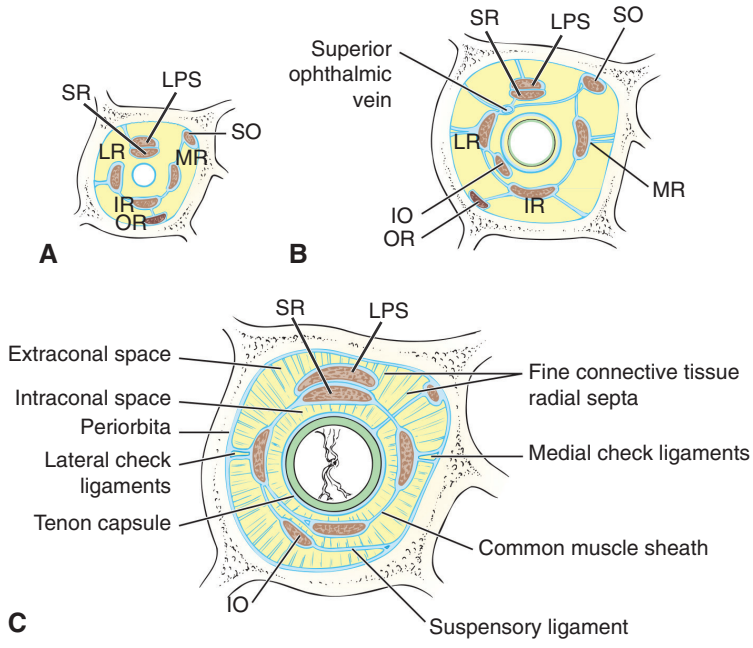


Figure 1-45 Diagram of right orbit with orbital connective tissue demonstrates extraocular muscle sheaths and their relationship to one another; periorbital tissue; and Tenon capsule (also known as the fascia bulbi). **A,** Near orbital apex. **B,** Posterior portion of the globe. **C,** Close to the equator of the globe. Note the intraconal space formed by the septa between the rectus muscles posteriorly **(A, B)** and the check ligaments of the medial and lateral rectus muscles **(C).** The orbital muscle of Müller (OR) is likely a vestigial structure with unknown function. It maintains connections with the inferior ophthalmic vein and may provide a supportive role, like the connective tissue surrounding the superior ophthalmic vein demonstrated in **B.** The orbital fascial tissue (not shown here) also supports other blood vessels and nerves as they traverse the orbit. IO = inferior oblique; IR = inferior rectus; LPS = levator palpebrae superioris; LR = lateral rectus; MR = medial rectus; OR = orbital muscle of Müller; SO = superior oblique; SR = superior rectus. *(Modified with permission from Forrester JV, Dick AD, McMenamin PG, Roberts F, Pearlman E.* The Eye: Basic Sciences in Practice. *4th Ed. Elsevier; 2021:Fig 1.44.)*

The Tenon capsule is thickest near the equator of the globe. Connections between the Tenon capsule and the periorbital tissues help suspend the globe in the orbit. The extraocular muscles penetrate this connective tissue approximately 10 mm posterior to their insertions. The connective tissues form sleeves around the penetrating extraocular muscles, creating pulleys suspended from the periorbita; these pulleys stabilize the position of the muscles relative to the orbit during eye movements. The pulleys are connected to one another and to the Tenon fascia by connective tissue bands (Fig 1-45). Age-related connective tissue degeneration can lead to acquired strabismus such as sagging eye syndrome, which is more common than heavy eye syndrome (see BCSC Section 6, *Pediatric Ophthalmology and Strabismus*). Loss of Tenon capsule with age can also lead to conjunctivochalasis, as mentioned earlier in this chapter.

Demer JL. Mechanics of the orbita. *Dev Ophthalmol.* 2007;40:132–157.

Rutar T, Demer JL. "Heavy eye" syndrome in the absence of high myopia: a connective tissue degeneration in elderly strabismic patients. *J AAPOS.* 2009;13(1):36–44.

CHAPTER 2

The Eye

This chapter includes related videos. Go to www.aao.org/bcscvideo_section02 or scan the QR codes in the text to access this content.

Highlights

- Hemidesmosomes anchor the basal corneal epithelial cells to Bowman layer. Disruption at this level can lead to scarring and recurrent erosion syndrome.
- In addition to housing corneal stem cells, the limbus is the site of passage of the collector channels that link the Schlemm canal to aqueous veins.
- The sclera is an avascular tissue with 2 overlying vascular layers (deep and superficial) in the episclera. Clinically, *episcleritis* refers to inflammation in the superficial layer, and scleritis involves the deep layer.
- The blood–ocular barrier prevents extravasation of intravascular contents into the eye. It consists of intercellular junctions of adjacent cells at various locations in the eye: the blood–aqueous barrier and the blood–retina barrier (inner and outer).
- The retina has a dual circulation; the inner retina is perfused by the retinal vessels seen on routine examination of the fundus, and the outer retina is perfused by the choroid.

Introduction

This chapter discusses the anatomy of the major parts of the human eye. The reader is encouraged to consult other volumes in the BCSC series for further discussion of many of the topics presented here.

Topographic Features of the Globe

The eyeball, or globe, is not a true sphere. The radius of curvature of the cornea is 8 mm, smaller than that of the sclera, which is 12 mm. The anteroposterior diameter of the adult eye is approximately 23–25 mm. The average transverse diameter of the adult eye is 24 mm (Fig 2-1). These dimensions create the oblate spheroid shape of the globe, in which the equatorial radius is greater than the polar radius.

The eye contains 3 compartments: the anterior chamber, the posterior chamber, and the vitreous cavity. The anterior chamber, the space between the iris and the cornea, is filled with aqueous fluid. Anterior chamber depth varies among individuals and in

regional populations; the average depth is 3.11 mm. The average volume of the anterior chamber is 220 μL. The posterior chamber is the anatomical portion of the eye posterior to the iris and anterior to the lens and vitreous face. Like the anterior chamber, it is also filled with aqueous fluid, but the average volume is 60 μL. The largest compartment is the vitreous cavity, which makes up more than two-thirds of the volume of the eye (5–6 mL) and contains the vitreous gel (also called *vitreous, vitreous body,* or *vitreous humor*). The total volume of the average adult eye is approximately 6.5–7.0 mL (Table 2-1).

The eyeball is composed of 3 concentric layers: an outer protective layer, a middle vascular layer, and an inner neural layer. The outermost layer consists of the clear *cornea* anteriorly and the opaque white *sclera* posteriorly. This corneoscleral layer is composed of collagen and protects the internal ocular tissues; the cornea also provides the main refractive power of the eye.

The cornea occupies the center of the anterior pole of the globe. Because the sclera and conjunctiva overlap the cornea anteriorly, slightly more above and below than medially and laterally, the cornea appears elliptical when viewed from the front. The *limbus,* which borders the cornea and the sclera, is blue-gray and translucent.

The middle layer of the globe, the *uvea,* consists of the iris, ciliary body, and choroid. Highly vascular, it serves nutritive and supportive functions, supplying oxygen to the outer retina and producing aqueous humor.

The innermost layer is the *retina.* This photosensitive layer contains the photoreceptors and neural elements that initiate the processing of visual information.

Other important surface features of the globe—such as the vortex veins, the ciliary arteries and nerves, and the extraocular muscles—are discussed in Chapter 1. The optic nerve and its surrounding meningeal sheaths are discussed in Chapter 3.

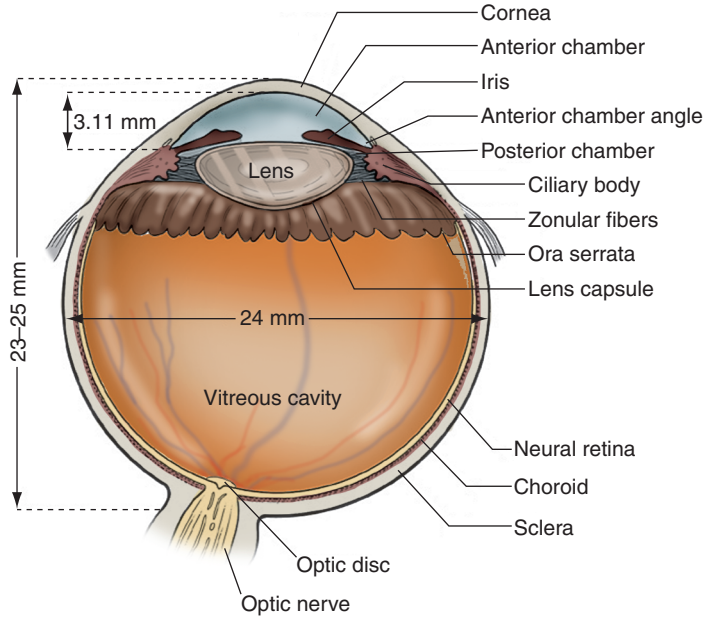


Figure 2-1 Sagittal section of the eye with absent vitreous and major structures identified. Dimensions are approximate and are average for the adult eye. *(Illustration by Christine Gralapp.)*

Table 2-1 Dimensions and Contents of the Adult Eye

	Anterior Chamber	Posterior Chamber	Vitreous Cavity	Eye as a Whole
Average depth (emmetropic eye)	3.11 mm	0.52 mm	16.5 mm	23–25 mm
Volume	220 µL	60 µL	5 to 6 mL	6.5 to 7 mL
Contents	Aqueous	Aqueous	Vitreous	

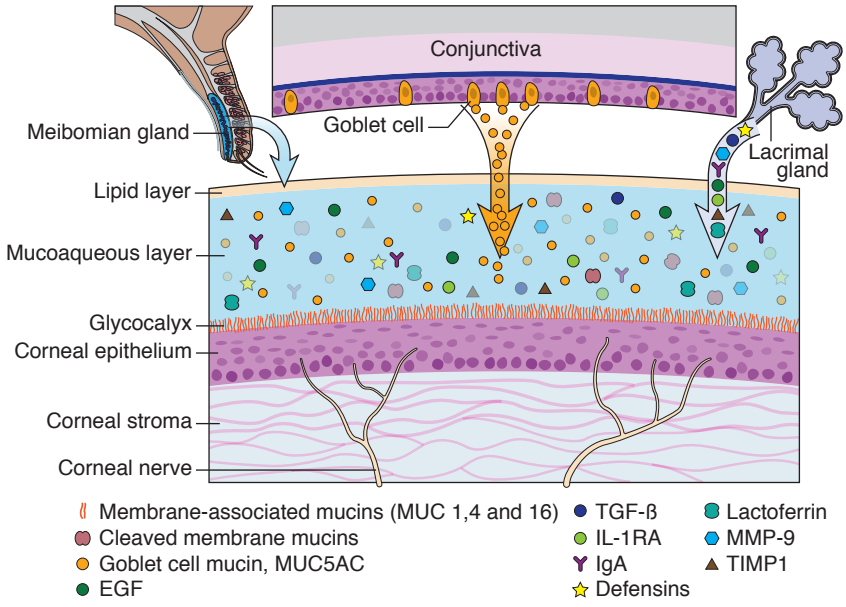


Figure 2-2 Tear film. Derived from meibomian glands, the lipid layer lies on the surface of the tear film and limits evaporation. The middle mucoaqueous layer contains secretions from the lacrimal gland and goblet cells. In addition to providing growth factors, defending against pathogens, and responding to ocular inflammation, the mucoaqueous layer also provides a medium for oxygen to reach the avascular cornea. The glycocalyx covers the surface epithelium and contains membrane-associated mucin, secreted by epithelial cells of the ocular surface. It allows the gel-like mucoaqueous layer to glide smoothly over the ocular surface. *(Adapted from Pflugfelder SC. Tear dysfunction and the cornea: LXVIII Edward Jackson Memorial Lecture.* Am J Ophthalmol. *2011;152(6):902, with permission from Elsevier; and from an illustration by Christine Gralapp. Illustration redrawn by Mark Miller.)*

Tear Film

The cornea and conjunctiva, which comprise the ocular surface, are covered by the *tear film,* which has 3 layers (Fig 2-2):

- outer lipid layer secreted by the meibomian glands: helps reduce evaporation and stabilizes the tear film
- middle hydrophilic mucoaqueous layer secreted by the lacrimal gland/accessory lacrimal glands and conjunctival goblet cells: contains numerous constituents which give it a gel-like consistency

- inner glycocalyx on the ocular surface, secreted by goblet cells as well as conjunctival and corneal epithelial cells: mediates the interaction between the mucoaqueous layer and the surface epithelium, among other functions

Maintenance of the tear film is vital for normal corneal function because it

- provides lubrication for the cornea and conjunctiva
- facilitates the exchange of solutes, including oxygen
- contributes to the antimicrobial defense of the ocular surface
- serves as a medium to remove debris

Further, the air–tear film interface at the surface of the cornea constitutes a major refractive element of the eye, because of the difference in the refractive index of air and that of the tear film. Aberrations in the tear film can profoundly affect the integrity of the ocular surface and, consequently, the patient's vision. See Chapter 7 for in-depth discussion of the tear film.

Cornea

The cornea is a clear avascular tissue consisting of 5 layers (Fig 2-3):

- epithelium
- Bowman layer

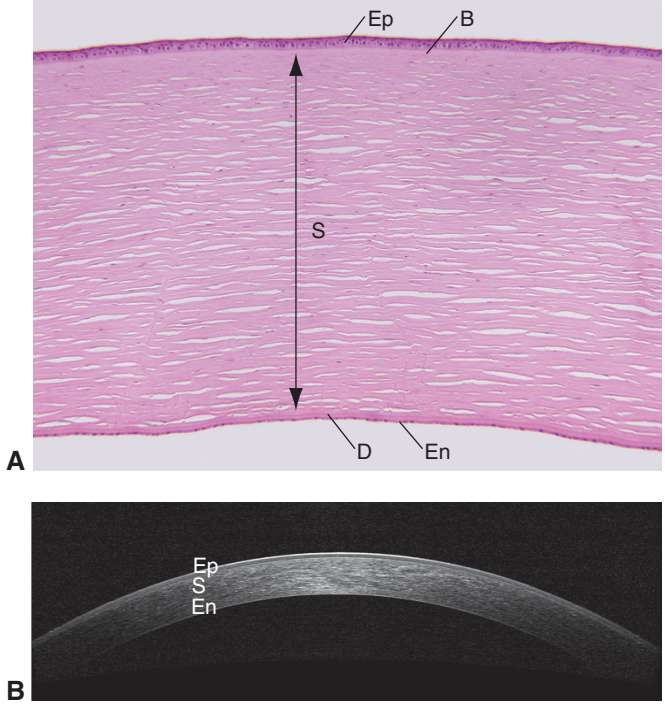


Figure 2-3 Layers of the cornea. **A,** Histologic section showing the 5 layers of the cornea (thickness given within parentheses): epithelium (40–50 µm), Bowman layer (8–15 µm), stroma (470–500 µm), Descemet membrane (10–12 µm), and endothelium (4–6 µm). **B,** Anterior segment optical coherence tomography (AS-OCT) of the cornea. B = Bowman layer; D = Descemet membrane; En = endothelium; Ep = epithelium; S = stroma. *(Part A courtesy of George J. Harocopos, MD; part B courtesy of Vikram S. Brar, MD.)*

- stroma
- Descemet membrane
- endothelium

The cornea covers one-sixth of the surface of the globe. It has a refractive index of 1.376 and an average radius of curvature of 8 mm. With a power of 43.25 diopters (D), the cornea produces most of the eye's refractive power of 58.60 D. Oxygen from the air and from the eyelid vasculature dissolves in tears and is transmitted to the cornea via the tear film. The cornea derives its macromolecules and nutrients from the aqueous humor.

Characteristics of the Central and Peripheral Cornea

In adults, the cornea measures about 11–12 mm in the horizontal meridian and about 10–11 mm in the vertical meridian. Because the posterior surface of the cornea is more curved than the anterior surface, the central cornea is thinner (500–600 μm) than the peripheral cornea (1000 μm).

The typical adult cornea maintains a prolate shape because it is steeper in the center and flattens in the periphery, with more extensive flattening nasally and superiorly than temporally and inferiorly. An understanding of this topography is important when fitting contact lenses or performing refractive surgery (Fig 2-4). For additional discussion, see BCSC Section 3, *Clinical Optics and Vision Rehabilitation*, Section 8, *External Disease and Cornea,* and Section 13, *Refractive Surgery.*

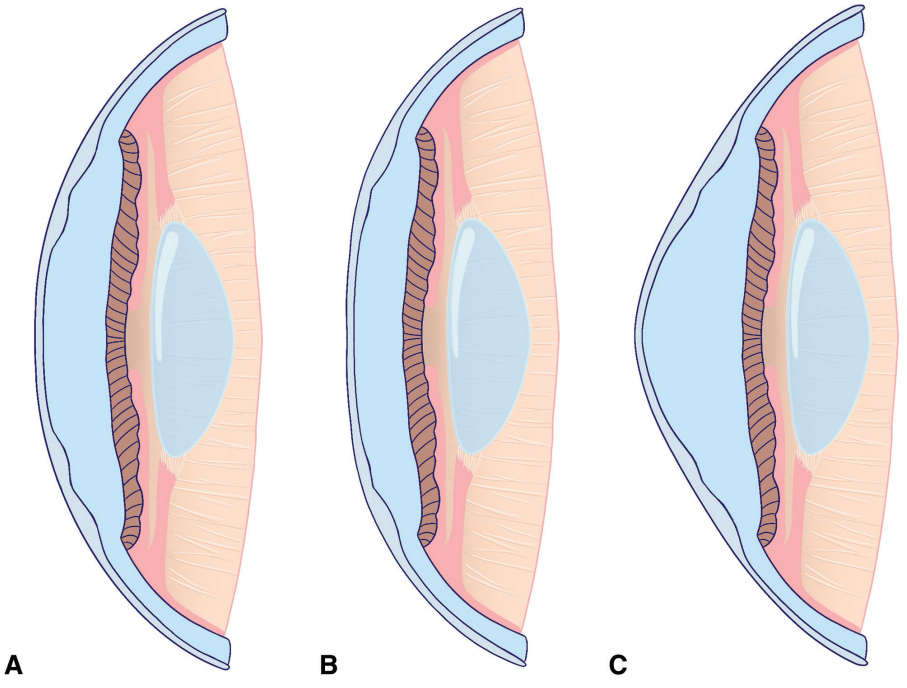


Figure 2-4 Examples of corneal profiles. **A,** Prolate cornea (the typical cornea shape), steeper centrally and flatter in the periphery. **B,** Oblate cornea (eg, after myopic ablation), flatter centrally and steeper in the periphery. **C,** Hyperprolate cornea (eg, after hyperopic ablation). *(Courtesy of Raquel Gouvea and Larissa Gouvea, MD.)*

Epithelium and Basal Lamina

The anterior surface of the cornea is covered by a lipophilic, nonkeratinized, stratified squamous epithelium that is derived from the surface ectoderm, composed of 4–6 cell layers, and is typically 40–50 μm thick (Fig 2-5).

The deepest cell layer is made up of basal cells that have a width of 12 μm and a density of approximately 6000 cells/mm^2. They are attached to the underlying basal lamina by hemidesmosomes. Trauma to the epithelium that disrupts this layer can lead to recurrent corneal erosion due to improper re-formation of these hemidesmosomes.

Overlying the basal cell layer are 2 or 3 layers of polygonal "wing" cells. Superficial to these layers are 1–2 layers of corneal epithelial "surface" cells that are extremely thin (30 μm) and are attached to one another by tight junctions. These junctions allow the surface epithelial cells to act as a barrier to diffusion. Microvilli make the apical membranes of the surface cells highly irregular; however, the tear film renders the surfaces optically smooth.

Although the deeper epithelial cells are firmly attached to one another by desmosomes, they migrate continuously from the basal region toward the tear film, into which they are shed. They also migrate centripetally from their stem cell source at the limbus (see Chapter 8). Diffuse damage to the limbal stem cells (eg, by chemical burns or trachoma) leads to chronic epithelial surface disease.

Del Monte DW, Kim T. Anatomy and physiology of the cornea. *J Cataract Refract Surg.* 2011;37(3):588–598.

Bowman Layer

Beneath the basal lamina of the epithelium is *Bowman layer,* which consists of randomly dispersed collagen fibrils. It is a modified region of the anterior stroma that is 8–15 μm

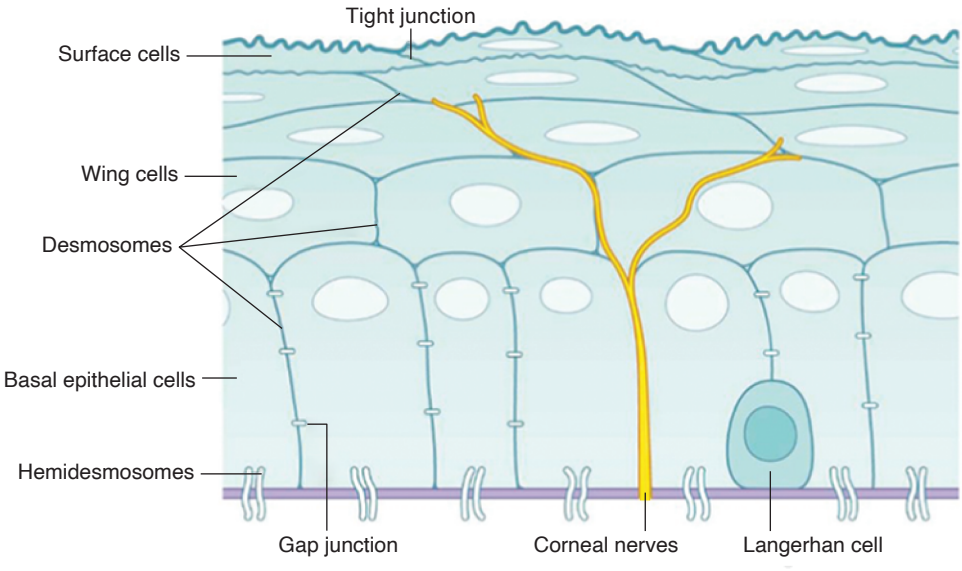


Figure 2-5 Schematic of the corneal epithelium demonstrating adhesion between cells and to the underlying basal lamina *(purple)* and Bowman layer via hemidesmosomes. *(Modified from Hogan MJ, Alvarado JA, Weddell JE.* Histology of the Human Eye: An Atlas and Textbook. *WB Saunders; 1971.)*

thick (see Fig 2-3). Unlike Descemet membrane, it is not restored after injury but is instead replaced by scar tissue.

Stroma

The stroma, which is 470–500 μm thick, constitutes approximately 90% of the total corneal thickness in humans (see Fig 2-3). It is composed of collagen-producing keratocytes, ground substance, and collagen lamellae. Collagen fibrils form obliquely oriented lamellae in the anterior one-third of the stroma (with some interlacing) and perpendicular lamellae in the less compact posterior two-thirds (see Chapter 8, Fig 8-3).

Stromal collagen fibrils extend across the entire diameter of the cornea and are remarkably uniform in size and separation. This uniformity establishes the transparency of the cornea (see Chapter 8). Separation of the collagen fibrils by edema leads to stromal clouding. Stromal collagen fibrils consist of predominantly type I collagen, with some type V. Many other collagen types have been identified in the stroma as well, for example:

- type III collagen, which is associated with stromal wound healing
- type VI collagen, which is intertwined between stromal collagen fibrils, where it acts to bind corneal lamellae to each other
- type VII collagen, which forms the anchoring fibril of the epithelium

The ground substance of the cornea consists of proteoglycans that run along and between the collagen fibrils. Their glycosaminoglycan components (eg, keratan sulfate) are negatively charged and tend to repel each other—as well as draw in sodium and, secondarily, water—producing the swelling pressure of the stroma. The keratocytes lie between the corneal lamellae and synthesize both collagen and proteoglycans. Ultrastructurally, they resemble fibrocytes.

The cornea contains approximately 2.4 million keratocytes, which occupy about 5% of the stromal volume; the density is higher anteriorly (1058 cells/mm^2) than posteriorly (771 cells/mm^2). Keratocytes are highly active cells rich in mitochondria, rough endoplasmic reticula, and Golgi apparatus. They have attachment structures, communicate through gap junctions, and have unusual fenestrations in their plasma membranes. Their flat profile and even distribution in the coronal plane ensure minimal disturbance of light transmission.

The deepest aspect of the stroma forms a thin, acellular layer (10–20 μm) that is highly adherent to the underlying Descemet membrane. This layer, referred to as Dua layer, is an important landmark during deep anterior lamellar keratoplasty (DALK) and is further described in BCSC Section 8, *External Disease and Cornea*.

Müller LJ, Pels L, Vrensen GF. Novel aspects of the ultrastructural organization of human corneal keratocytes. *Invest Ophthalmol Vis Sci.* 1995;36(13):2557–2567.

Mustonen RK, McDonald MB, Srivannaboon S, Tan AL, Doubrava MW, Kim CK. Normal human corneal cell populations evaluated by in vivo scanning slit confocal microscopy. *Cornea.* 1998;17(5):485–492.

Descemet Membrane

The basal lamina of the corneal endothelium, *Descemet membrane,* is periodic acid–Schiff (PAS) positive (Fig 2-6). It is a true basement membrane, and its thickness increases with

age. At birth, Descemet membrane is 3–4 μm thick, increasing to 10–12 μm at adulthood. It is composed of an anterior banded zone that develops in utero (4.6 ± 0.4 μm thick) and a posterior nonbanded zone that is laid down by the corneal endothelium throughout life (the average in adults is 11.8 ± 0.4 μm, increasing about 0.1 μm/year) (Fig 2-7). These zones provide a historical record of the synthetic function of the endothelium. Like other basal laminae, Descemet membrane is rich in type IV collagen.

Peripheral excrescences of Descemet membrane, known as *Hassall-Henle warts,* are common, especially among elderly people. Central excrescences (corneal guttae) are typically found in patients with Fuchs endothelial dystrophy but may also appear with increasing age. See BCSC Section 8, *External Disease and Cornea,* for further discussion of Fuchs endothelial dystrophy.

Endothelium

The corneal endothelium is 4–6 μm thick and is composed of a single layer of hexagonal cells derived from the neural crest (Fig 2-8). Thus, the corneal endothelium is of neuroectodermal origin. In young adult eyes, approximately 500,000 cells are present, at a density of about 3000/mm^2 centrally and up to 8000/mm^2 peripherally. Mitosis of the endothelium is limited in humans, and the overall number of endothelial cells decreases with age.

The size, shape, and distribution of the endothelial cells can be observed by specular microscopy at the slit lamp. The apical surfaces of these cells face the anterior chamber; their

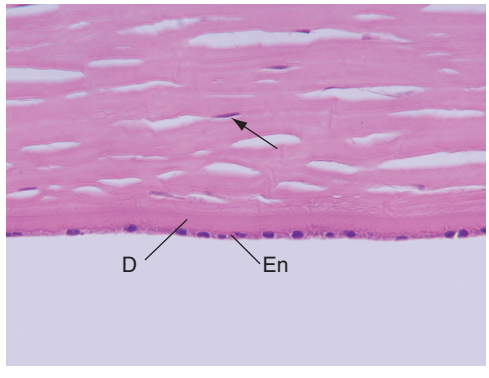


Figure 2-6 Histologic section of the posterior cornea. Higher magnification depicts Descemet membrane (D) and endothelium (En). A keratocyte nucleus *(arrow)* is visible in the posterior stroma. *(Courtesy of George J. Harocopos, MD.)*

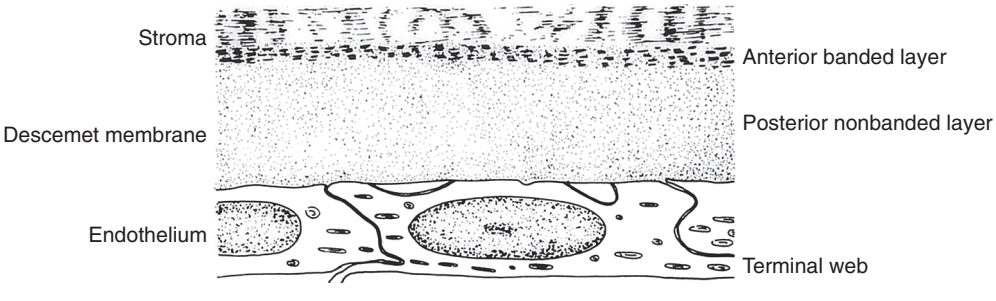


Figure 2-7 Corneal endothelium and Descemet membrane *(Illustration by Thomas A. Weingeist, MD, PhD.)*

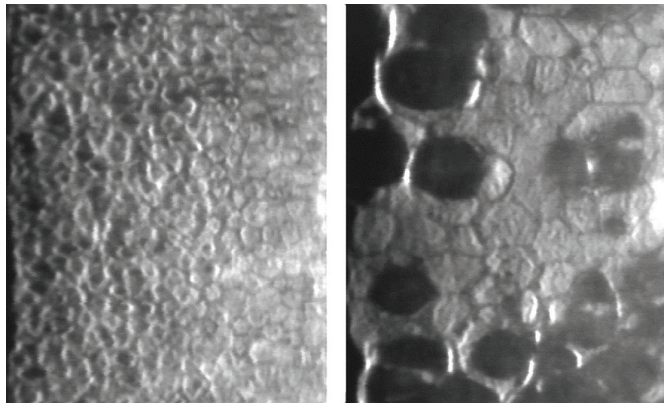


Figure 2-8 Specular microscopy of living corneal endothelium. *Left,* Normal endothelium. Note the hexagonal shape of the endothelial cells. *Right,* The corneal endothelium of a patient with Fuchs endothelial corneal dystrophy. Demonstrated are polymegathism (larger cells), pleomorphism (variability in size and shape of cells), and dark areas of endothelial cell loss (guttae). *(Courtesy of Preston H. Blomquist, MD.)*

basal surfaces secrete Descemet membrane. Typically, young endothelial cells have large nuclei and abundant mitochondria. The active transport of ions by these cells leads to the transfer of water from the corneal stroma and the maintenance of stromal deturgescence and transparency.

Endothelial cell dysfunction and loss—through surgical injury, inflammation, or disease (eg, Fuchs endothelial corneal dystrophy)—may cause endothelial decompensation, stromal edema, and vision loss. Because endothelial mitosis is limited in humans, cell loss causes cell density to decrease and residual cells to spread and enlarge.

Zheng T, Le Q, Hong J, Xu J. Comparison of human corneal cell density by age and corneal location: an in vivo confocal microscopy study. *BMC Ophthalmol.* 2016;16:109. doi:10.1186/s12886-016-0290-5

Corneal Nerves

The cornea is the most densely innervated tissue in the human body. Corneal innervation is derived primarily from branches of the long ciliary nerve (a branch of the nasociliary nerve) that pierce the sclera around the optic nerve to reach the cornea (see Chapter 3, Fig 3-21). The nasociliary nerve is a branch of the ophthalmic division of the trigeminal nerve, cranial nerve (CN) V_1, which is discussed further in Chapter 3.

Corneal nerves are organized into 4 different layers:

- midcorneal stromal nerves
- subepithelial nerve plexus
- subbasal nerve plexus
- intraepithelial nerve terminals

The corneal nerves penetrate the anterior stroma radially, losing their myelin sheath within 1 mm of the limbus. From that point, they arborize to form the subepithelial plexus,

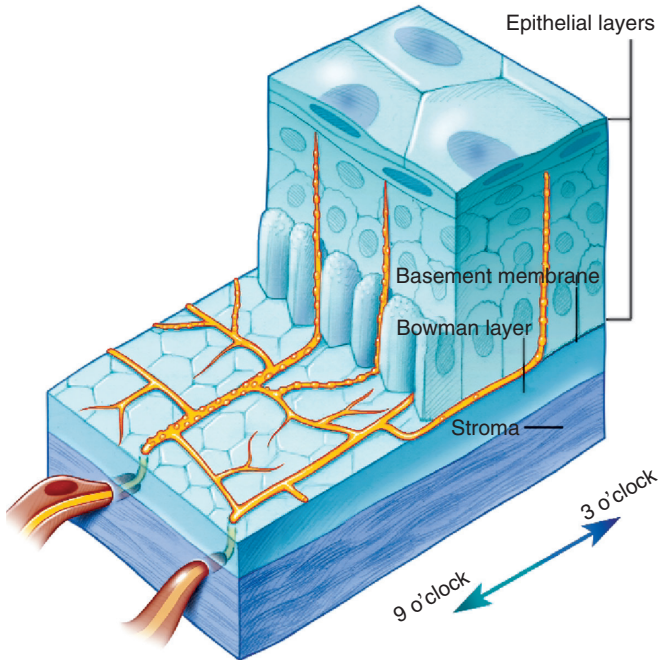


Figure 2-9 Illustration of neural penetration and distribution within the anterior cornea. Corneal nerves are branches of the long ciliary nerves, which branch extensively in the anterior stroma to innervate the epithelium. They provide nociception and help maintain the epithelium. *(From Schultze RL, Singh GD. Neurotrophic keratitis.* Focal Points: Clinical Modules for Ophthalmologists. *American Academy of Ophthalmology; 2003, module 2. Illustration by Christine Gralapp.)*

which gives rise to the subbasal plexus above Bowman layer. Subsequent branching results in nerve terminals that extend throughout the epithelial layers (Fig 2-9). The corneal epithelium has the highest density of nerve terminals of any epithelial tissue in the body. They help create the sensation of pain, touch, and temperature. In addition, they support the epithelium and wound healing through secretion of neuropeptides and growth factors.

Nociception of the ocular surface, afforded by branches of CN V_1, functions in conjunction with the lacrimal system and orbicularis oculi muscle to stimulate reflex tearing and blinking, respectively (see Chapter 3, Video 3-2).

Guerrero-Moreno A, Baudouin C, Melik Parsadaniantz S, Réaux-Le Goazigo A. Morphological and functional changes of corneal nerves and their contribution to peripheral and central sensory abnormalities. *Front Cell Neurosci.* 2020;14: 610342. doi:10.3389/fncel.2020.610342

Marfurt CF, Cox J, Deek S, Dvorscak L. Anatomy of the human corneal innervation. *Exp Eye Res.* 2010;90(4):478–492.

Limbus

The transition zone between the peripheral cornea and the anterior sclera, known as the *limbus* (also called *corneoscleral junction* or *corneal limbus*), is defined differently by anatomists, pathologists, and clinicians (Fig 2-10). The limbus is important for 3 reasons: its

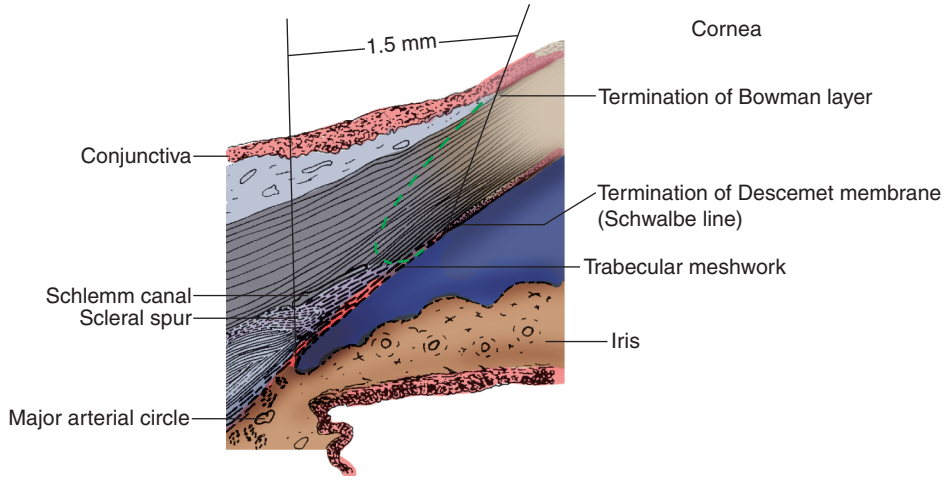


Figure 2-10 Anterior chamber angle and limbus, depicting the concept of the limbus. *Solid lines* represent the limbus as viewed by pathologists; the *green dotted line* represents the limbus as viewed by anatomists. *(Illustration by Thomas A. Weingeist, MD, PhD.)*

relationship to the anterior chamber angle, its use as a surgical landmark, and its supply of corneal epithelial stem cells. The limbus is also the site of passage of the collector channels that link the Schlemm canal to aqueous veins.

The following structures are found at the limbus:

- conjunctiva and limbal palisades of Vogt, which house the corneal stem cells (Fig 2-11A)
- episclera (discussed later in this chapter, in the section Sclera)
- junction of corneoscleral stroma
- aqueous outflow apparatus (collector channels)

The corneoscleral junction begins centrally in a plane connecting the end of Bowman layer and Schwalbe line, which is the termination of Descemet membrane. Internally, its posterior limit is the anterior tip of the scleral spur (see Fig 2-10).

The surgical limbus, an external landmark for incisions in cataract and glaucoma surgery, is sometimes referred to as the *gray* or *blue zone*. Its blue-gray appearance is due to the scattering of light through the oblique interface between cornea and sclera, which occurs gradually over 1–2 mm (Fig 2-11B). The posterior border of the blue-gray zone is a consistent external landmark that corresponds to the internal junction of cornea and sclera overlying the trabecular meshwork in all meridians.

Sclera

The sclera covers the posterior five-sixths of the surface of the globe, with an anterior opening for the cornea and a posterior opening for the optic nerve. The tendons of the rectus muscles insert into the superficial scleral collagen. The Tenon capsule covers the sclera and rectus muscles, anteriorly, and both are overlain by the bulbar conjunctiva. The capsule and conjunctiva fuse near the limbus.

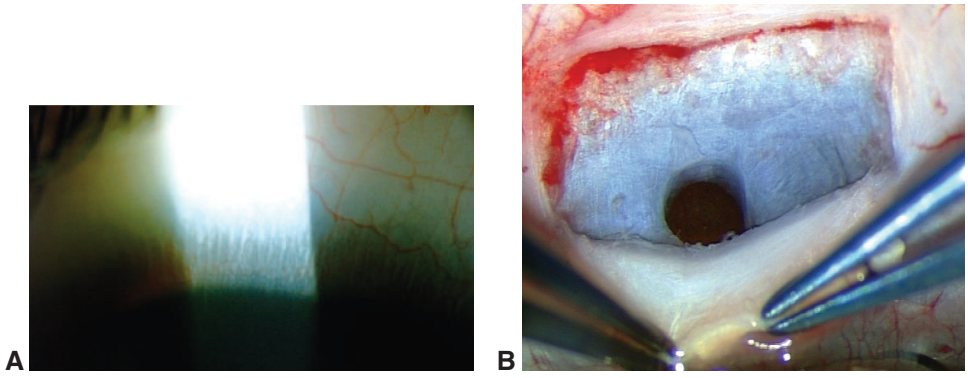


Figure 2-11 Limbus. **A,** Slit-lamp photograph shows the blue-gray corneoscleral limbus. The striations orthogonal to the cornea are the limbal palisades of Vogt, where the corneal stem cells reside. **B,** Photograph of a limbus-based trabeculectomy. Note the exposure of the blue-gray surgical limbus as the conjunctiva is reflected anteriorly over the cornea. The sclerostomy (opening through the sclera to the anterior chamber) is visible. *(Part A courtesy of Cornea Service, Paulista School of Medicine, Federal University of São Paulo; part B courtesy of Keith Barton, MD, and reproduced with permission from Moorfields Eye Hospital.)*

The sclera is thinnest (0.3 mm) just behind the insertions of the rectus muscles and thickest (1.0 mm) at the posterior pole around the optic nerve head. It is 0.4–0.5 mm thick at the equator and 0.6 mm thick anterior to the muscle insertions. Because of the topographic variation in scleral thickness, strabismus and retinal detachment surgery require careful placement of sutures to avoid inadvertent perforation.

CLINICAL PEARL

The most common sites of scleral rupture following blunt trauma are

- in the superonasal quadrant, near the limbus
- in a circumferential arc parallel to the corneal limbus, opposite the site of impact
- behind the insertion of the rectus muscles

Like the cornea, the sclera is essentially avascular except for the vessels of the intrascleral vascular plexus, located just posterior to the limbus, and the episcleral vessels. The episcleral vessels have superficial and deep plexuses (Fig 2-12). The superficial plexus runs beneath Tenon capsule in a radial pattern; in episcleritis, it is this vascular plexus that is involved. The deep episcleral plexus rests on the surface of the sclera and is the layer involved in scleritis.

Numerous channels, or *emissaria,* penetrate the sclera (see Chapter 1, Figs 1-22, 1-23), allowing the passage of arteries, veins, and nerves. These include

- anterior emissaria: penetration of the anterior ciliary arteries, anterior to the rectus muscle insertions
- middle emissaria: exit of vortex veins
- posterior emissaria: lamina cribrosa, penetration of the short and long posterior ciliary vessels and ciliary nerves

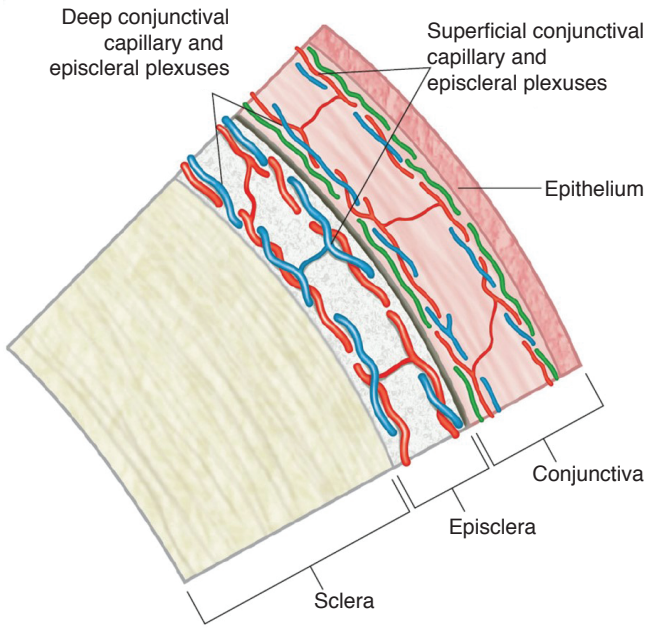


Figure 2-12 Episcleral vessels. The sclera is avascular but has overlying episcleral vessels, which are divided into superficial and deep plexuses. The organization of the conjunctival vasculature, which is also depicted, is similar to that of the episcleral vessels, with the addition of lymphatics, shown in green. *(Modified with permission from Levin LA, Nilsson SFE, Ver Hoeve J, Wu SM.* Adler's Physiology of the Eye. *11th ed. Elsevier/Saunders; 2011:118–119.)*

Extraocular extension of malignant melanoma of the choroid occurs via the middle emissaria.

Branches of the ciliary nerves that supply the cornea sometimes leave the sclera to form loops posterior to the nasal and temporal limbus. These nerve loops, called *Axenfeld loops,* are sometimes pigmented and, consequently, have been mistaken for uveal tissue or malignant melanoma (Fig 2-13).

Anterior to the rectus muscle insertions, the episclera consists of a dense vascular connective tissue that merges deeply with the superficial sclera and superficially with the Tenon capsule and the conjunctiva. The scleral stroma is composed of bundles of collagen, fibroblasts, and a moderate amount of ground substance.

The sclera's collagen fibers vary in size and shape and taper at their ends, indicating that they are not continuous fibers as in the cornea. The inner layer of the sclera *(lamina fusca)* blends imperceptibly with the suprachoroidal and supraciliary lamellae of the uvea. The collagen fibers in this portion of the sclera branch and intermingle with the outer ciliary body and choroid. The opaque, porcelain-white appearance of the sclera, which contrasts markedly with the transparency of the cornea, is primarily due to 2 factors: the greater variation in collagen fibril separation and diameter, and the greater degree of fibril interweaving in the sclera (see also Chapter 8). In addition, the lack of vascular elements contributes to corneal clarity.

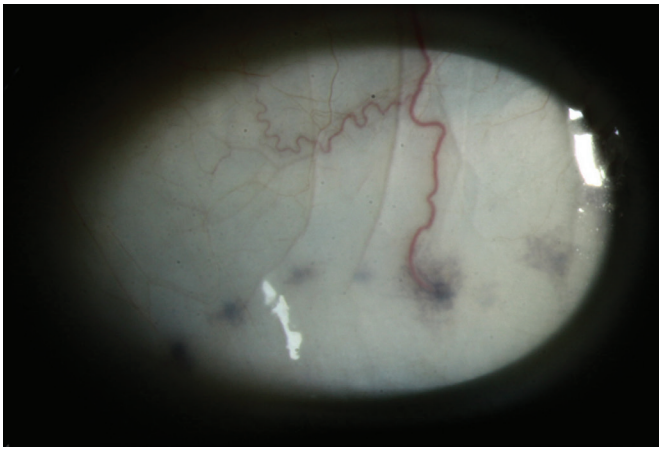


Figure 2-13 External photograph of Axenfeld nerve loops in an arc pattern roughly equidistant from the limbus. *(Reproduced with permission from Jesse Vislisel, MD; EyeRounds.org, University of Iowa. Photograph by Cindy Montague, CRA.)*

Anterior Chamber

The anterior chamber is bordered anteriorly by the cornea and posteriorly by the iris diaphragm and the pupil. The *anterior chamber angle*, which lies at the junction of the cornea and the iris, includes the following structures (Figs 2-14 through 2-19):

- Schwalbe line
- Schlemm canal and trabecular meshwork
- scleral spur
- anterior border of the ciliary body (where its longitudinal fibers insert into the scleral spur)
- peripheral iris

The depth of the anterior chamber averages 3.11 mm; however, it is deeper in eyes with aphakia, pseudophakia, and myopia, and shallower in those with hyperopia. In the average adult eye, the anterior chamber is deepest centrally and reaches its narrowest point slightly central to the angle recess.

The anterior chamber is filled with *aqueous humor,* which is produced by the ciliary body in the posterior chamber. The fluid passes through the pupil aperture and drains via 2 main pathways: 1) the trabecular pathway (ie, through the trabecular meshwork into the Schlemm canal and episcleral veins) and 2) the uveoscleral pathway (ie, through the root of the iris and the ciliary body face, into the suprachoroidal space). The uveoscleral outflow, which is thought to reduce with increasing age, accounts for up to 50% of aqueous outflow in young people (see Fig 2-16).

In both pathways, the aqueous humor eventually joins the venous circulation of the eye, which drains into the cavernous sinus. Intraocular pressure (IOP) is determined by the rate of aqueous production, the resistance offered by the trabecular meshwork, and the pressure of the veins receiving the aqueous. Thus, changes in intrathoracic pressure

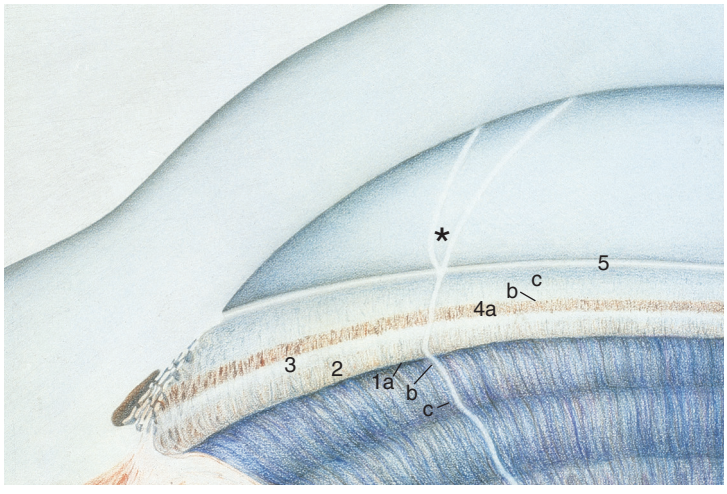


Figure 2-14 Structures of the anterior chamber angle. 1, Peripheral iris: a, insertion; b, curvature; c, angular approach. 2, Ciliary body band. 3, Scleral spur. 4, Trabecular meshwork: a, posterior; b, mid; c, anterior. 5, Schwalbe line. *(*)*, Corneal optical wedge.

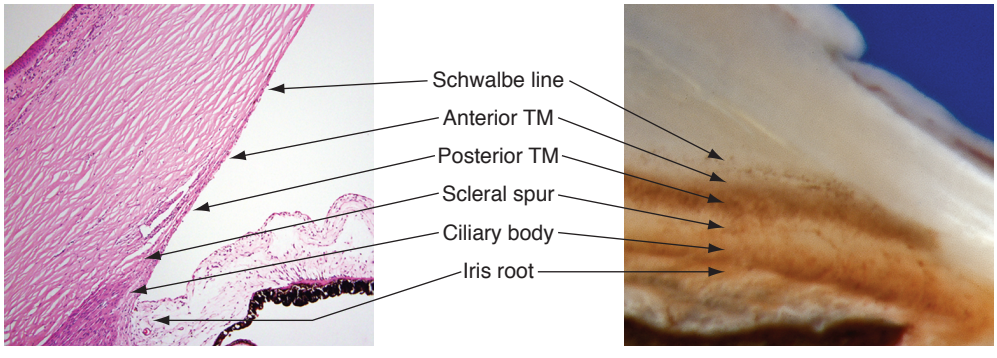


Figure 2-15 Histology and gross photograph of the anterior chamber angle with corresponding structures. TM = trabecular meshwork. *(Courtesy of Tatyana Milman, MD.)*

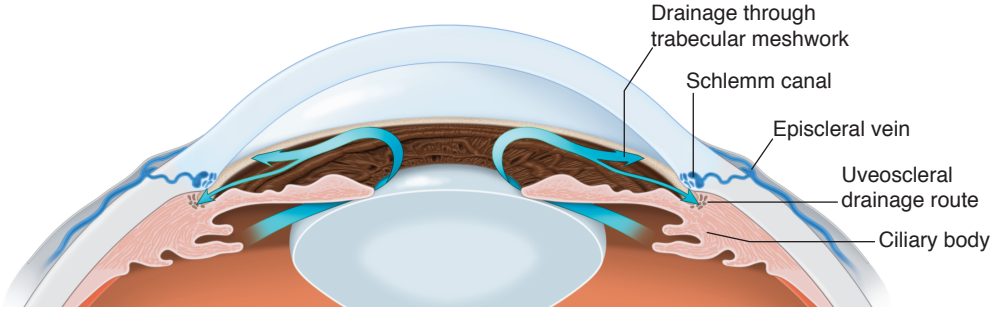


Figure 2-16 Flow of aqueous humor. Aqueous humor is produced in the ciliary body and secreted into the posterior chamber. From there, the aqueous flows through the pupil into the anterior chamber and exits via the trabecular pathway and the uveoscleral pathway. Aqueous is received by the episcleral veins via Schlemm canal and collector channels in the trabecular pathway. In the uveoscleral pathway, aqueous is absorbed by the uveal venous system. *(Illustration by Mark Miller.)*

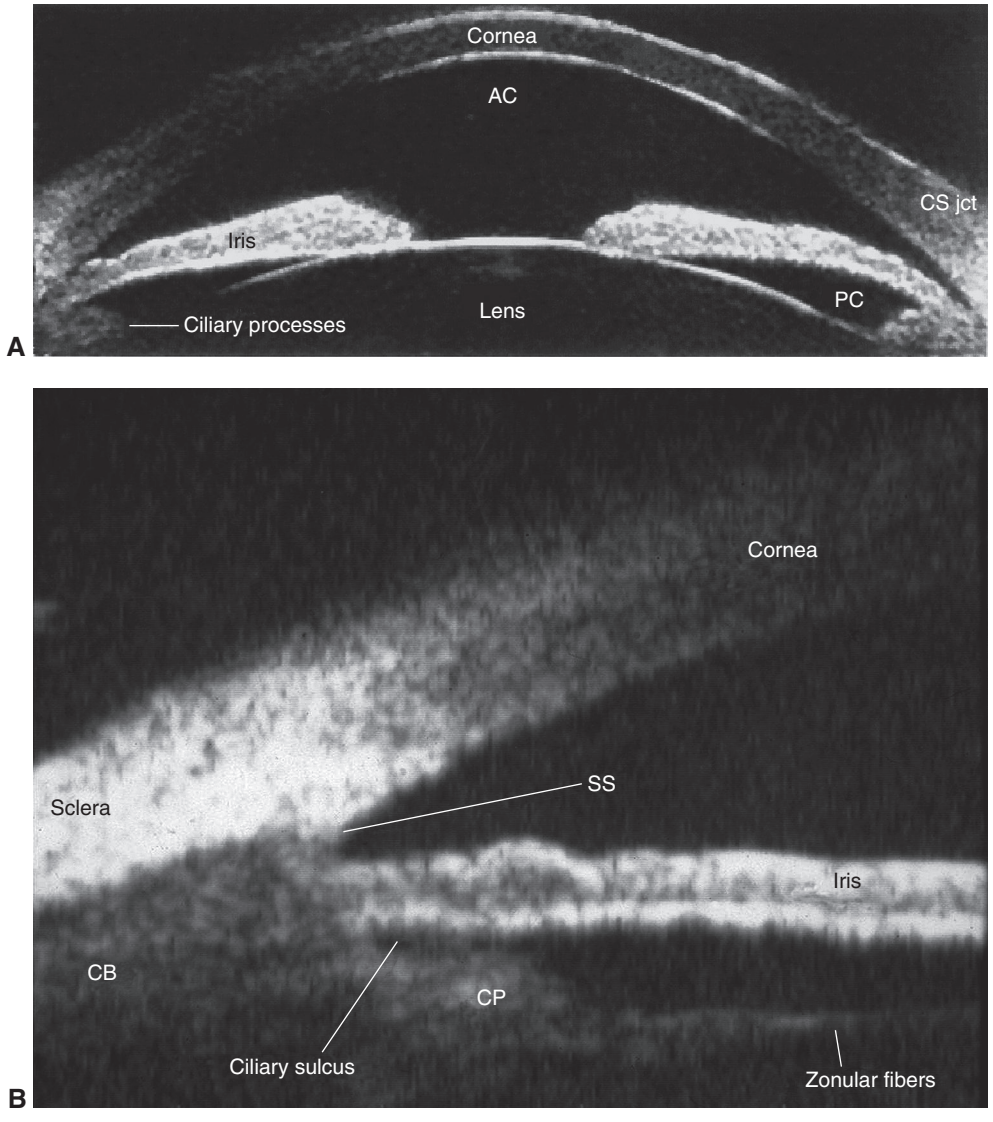


Figure 2-17 Ultrasound biomicroscopy (UBM) imaging of the anterior chamber (AC). **A,** UBM composite image of the anterior segment, including the AC. The iris is slightly convex, indicating a mild pupillary block. The corneoscleral junction (CS jct), ciliary processes, and posterior chamber (PC) region are clearly visible. The angle is narrow but open. Iris–lens contact is small. **B,** UBM image shows typical angle structures. CB = ciliary body; CP = ciliary processes; SS = scleral spur. *(Part A courtesy of Charles Pavlin, MD; part B courtesy of Ken K. Nischal, MD.)*

or within the cavernous sinus can lead to elevated IOP via the venous system. BCSC Section 10, *Glaucoma,* discusses the anterior chamber and aqueous humor in detail.

A third pathway exists in which aqueous humor traverses the vitreous across the retina and into the choroid. Physiologically, this outflow has minimal effect on IOP but is important in maintaining retinal adhesion. See the section Retinal Pigment Epithelium later in this chapter.

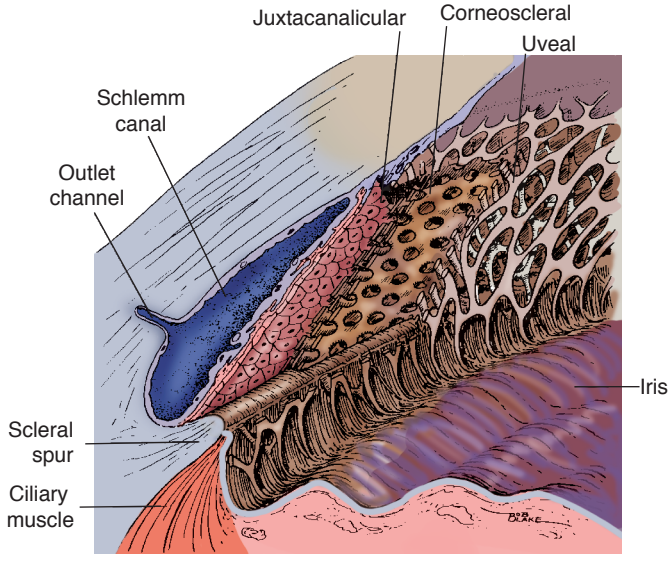


Figure 2-18 Layers of the trabecular meshwork: uveal, corneoscleral, and juxtacanalicular. The point of highest resistance to outflow is at the juxtacanalicular layer. The outlet channel traverses the limbus and drains into an aqueous vein. *(Modified with permission from Shields MB.* Textbook of Glaucoma. *3rd ed. Williams & Wilkins; 1992.)*

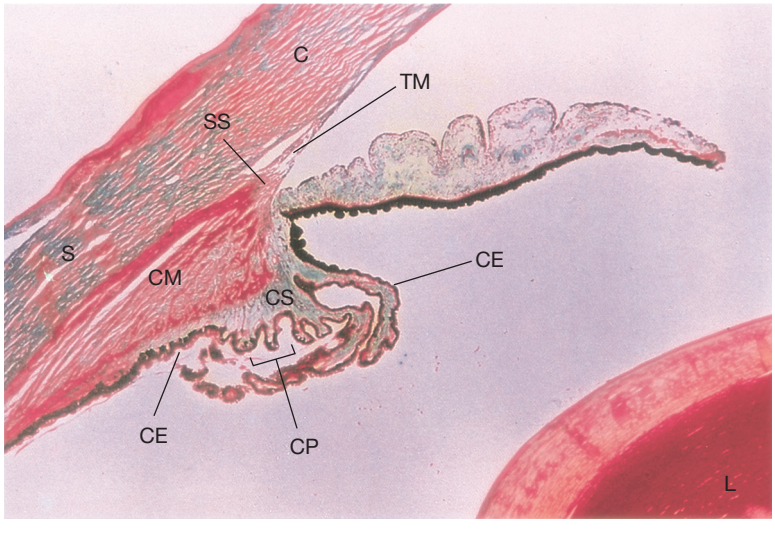


Figure 2-19 Anterior chamber angle, ciliary body, and peripheral lens. Note the triangular shape of the ciliary body. The ciliary muscle fibers (CM) appear red in contrast to the connective tissue. Note the longitudinal fibers inserting into the scleral spur (SS), which is clearly delineated in the region of the trabecular meshwork (TM). The ciliary processes (CP) and ciliary stroma (CS) are lined by the double-layered ciliary epithelium (CE). The lens (L) is artifactually displaced posteriorly. (Masson trichrome stain ×8.) C = cornea; I = iris; S = sclera. *(Courtesy of Thomas A. Weingeist, MD, PhD.)*

High-resolution ultrasound biomicroscopy, performed in vivo, provides detailed 2-dimensional views of the anterior segment of the eye (see Fig 2-17), allowing the clinician to view the relationship of the structures in the anterior segment under different pathologic conditions (Video 2-1).

VIDEO 2-1 Imaging the anterior chamber angle.
Courtesy of Hiroshi Ishikawa, MD.

The internal scleral sulcus accommodates the Schlemm canal externally and the trabecular meshwork internally. Schwalbe line, the peripheral limit of Descemet membrane, forms the anterior margin of the sulcus; the scleral spur is its posterior landmark. The scleral spur receives the insertion of the longitudinal fibers of the ciliary muscle, contraction of which opens up the trabecular spaces (see Fig 2-19).

Myofibroblast-like scleral spur cells with contractile properties are disposed circumferentially within the scleral spur. They resemble mechanoreceptors, receive sensory innervation, and are connected by elastic tissue to the trabecular meshwork. In experiments, stimulation with vasoactive intestinal polypeptide (VIP) or calcitonin gene–related peptide (CGRP) causes an increase in aqueous outflow.

Tamm ER, Braunger BM, Fuchshofer R. Intraocular pressure and the mechanisms involved in resistance of the aqueous humor flow in the trabecular meshwork outflow pathways. *Prog Mol Biol Transl Sci*. 2015;134:301–314.

Trabecular Meshwork

The relationship of the trabecular meshwork and the Schlemm canal to other structures is complex because the outflow apparatus is composed of tissue derived from the cornea, sclera, iris, and ciliary body. The trabecular meshwork is a circular spongework of connective tissue lined by trabeculocytes. These cells have contractile properties, which may influence outflow resistance. They also have phagocytic properties. The shape of the meshwork is roughly triangular when viewed in cross section; the apex is at the Schwalbe line, and the base is formed by the scleral spur and the ciliary body.

The trabecular meshwork can be divided into 3 layers (see Fig 2-18):

- uveal
- corneoscleral
- juxtacanalicular, directly adjacent to the Schlemm canal

The uveal and the corneoscleral layers can be divided by an imaginary line drawn from the Schwalbe line to the scleral spur. The uveal meshwork lies internal and the corneoscleral meshwork external to this line.

Age-related changes to the trabecular meshwork include increased pigmentation, decreased number of trabecular cells, and thickening of the basement membrane beneath the trabecular cells. Trabecular sheets thicken two- to threefold with increasing age. Endothelial cellularity is lost, the amount of connective tissue increases, debris accumulates in the

meshwork, and glycosaminoglycans accumulate in the extracellular space. These changes can increase resistance to aqueous outflow; such changes are exaggerated in case of open-angle glaucoma. This subject is covered in greater depth in BCSC Section 10, *Glaucoma.*

Uveal Trabecular Meshwork

The uveal meshwork faces the anterior chamber. It is composed of cordlike trabeculae and has fewer elastic fibers than does the corneoscleral meshwork. Its trabeculocytes usually contain pigment granules with trabecular apertures that are less circular and larger than those of the corneoscleral meshwork.

Corneoscleral Meshwork

The corneoscleral meshwork consists of a series of thin, flat, perforated connective tissue sheets arranged in a laminar pattern. Each trabecular beam is covered by a monolayer of thin trabecular cells exhibiting multiple pinocytotic vesicles. The basal lamina of these cells forms the outer cortex of the trabecular beam; the inner core is composed of collagen and elastic fibers.

Juxtacanalicular Meshwork

The juxtacanalicular meshwork invests the entire extent of the Schlemm canal and forms its inner wall. On its trabecular aspect, between the outermost layers of the corneoscleral meshwork and the endothelial lining of the Schlemm canal, lies the *endothelial meshwork,* a multilayered collection of cells forming a loose network. Between these cells are spaces up to 10 μm wide through which aqueous humor can percolate to reach the endothelial lining of the Schlemm canal (Fig 2-20). This region of the drainage system contributes the most to outflow resistance, partly because the pathway is narrow and tortuous and partly because of the resistance offered by its extracellular proteoglycans and glycoproteins.

> The endothelial meshwork within the juxtacanalicular trabecular meshwork is the highest point of resistance to aqueous outflow.

Schlemm Canal

The Schlemm canal is a circular tube that closely resembles a lymphatic vessel. It is formed by a continuous monolayer of nonfenestrated endothelium and a thin connective tissue wall. The basement membrane of the endothelium is poorly defined. The lateral walls of the endothelial cells are joined by tight junctions. The apical and basal surfaces of the cells contain micropinocytotic vesicles. Larger vesicles (so-called giant vacuoles) have been observed along the internal canal wall (Fig 2-21). These vacuoles are lined by a single membrane, and their size and number are increased by a rise in IOP. They are thought to contribute to the pressure-dependent outflow of the aqueous humor.

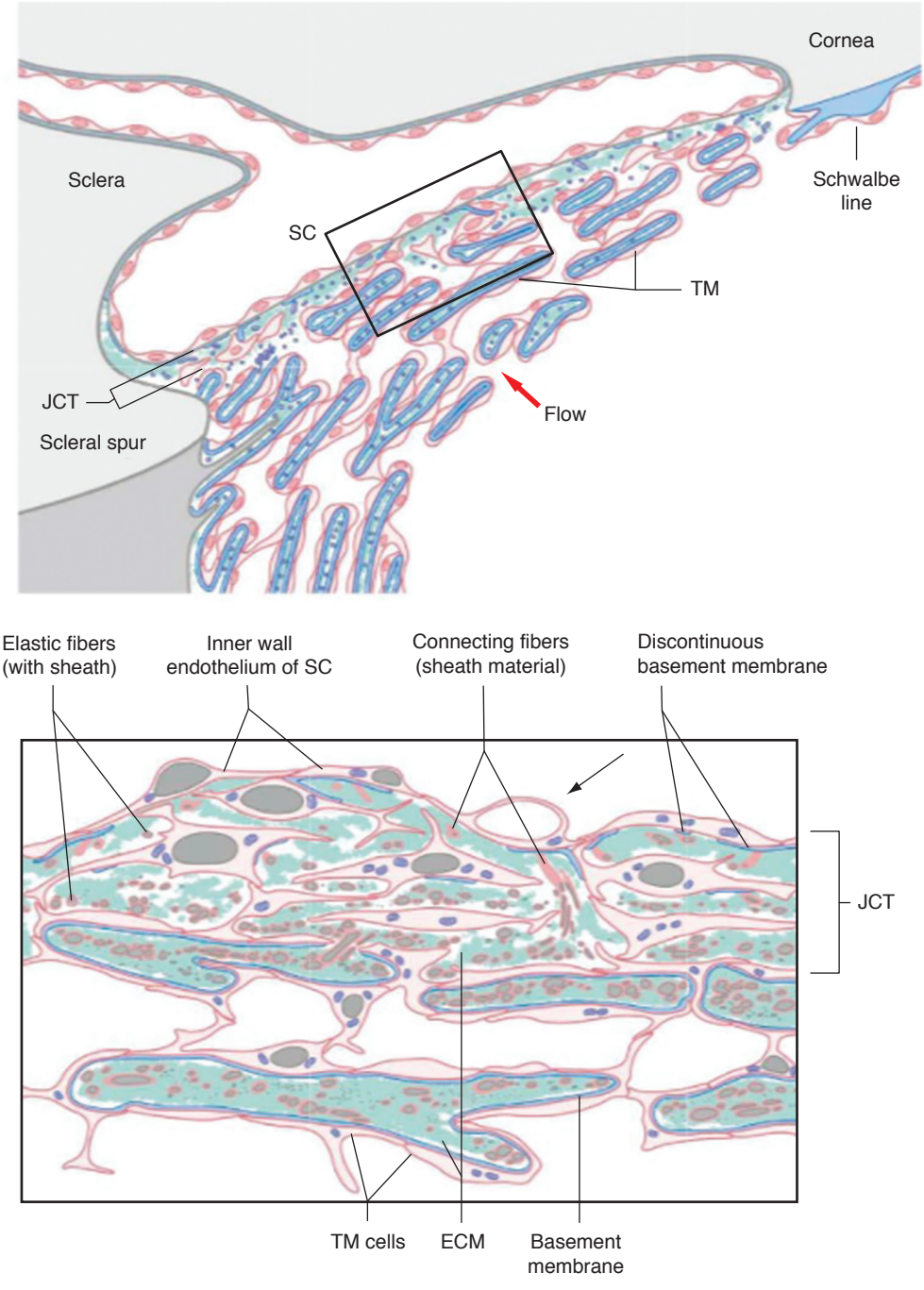


Figure 2-20 Relationship between the juxtacanalicular (JCT) meshwork and the Schlemm canal (SC). *Inset:* The endothelial meshwork (ECM) within the juxtacanalicular meshwork. Note the vacuole along the inner wall of the Schlemm canal *(black arrow).* TM = trabecular meshwork. *(Modified with permission from Levin LA, Nilsson SFE, Ver Hoeve J, Wu SM.* Adler's Physiology of the Eye. *11th ed. Elsevier/Saunders; 2011:285.)*

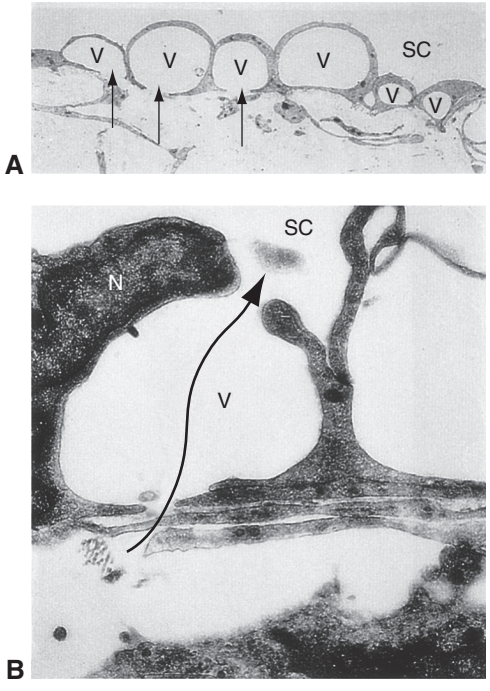


Figure 2-21 Electron micrographs of the Schlemm canal. **A,** Low-magnification electron micrograph of the endothelial lining of the Schlemm canal (SC), showing that most of the vacuolar configurations (V) at this level have direct communication *(arrows)* with the subendothelial extracellular spaces, which contain aqueous humor (×3970). **B,** Electron micrograph of a vacuolar structure that shows both basal and apical openings, thus constituting a vacuolar transcellular channel *(arrow).* Through this channel, the fluid-containing extracellular space on the basal aspect of the cell is temporarily connected with the lumen of the Schlemm canal, allowing bulk outflow of aqueous humor. N = indented nucleus of the cell (×23,825). *(Reproduced with permission from Tripathi RC. The functional morphology of the outflow systems of ocular and cerebrospinal fluids.* Exp Eye Res. *1977;25(Suppl):65–116.)*

CLINICAL PEARL

In one type of microinvasive glaucoma surgery (MIGS), a microstent is implanted in the Schlemm canal to bypass the trabecular meshwork, the point of greatest resistance, thereby increasing aqueous outflow.

Collector Channels

Approximately 25–30 collector channels arise from the Schlemm canal and drain into the deep and midscleral venous plexuses (Fig 2-22). Up to 8 of these channels drain directly into the episcleral venous plexus as aqueous veins (Video 2-2), which are visible in the conjunctiva via biomicroscopy (Fig 2-23).

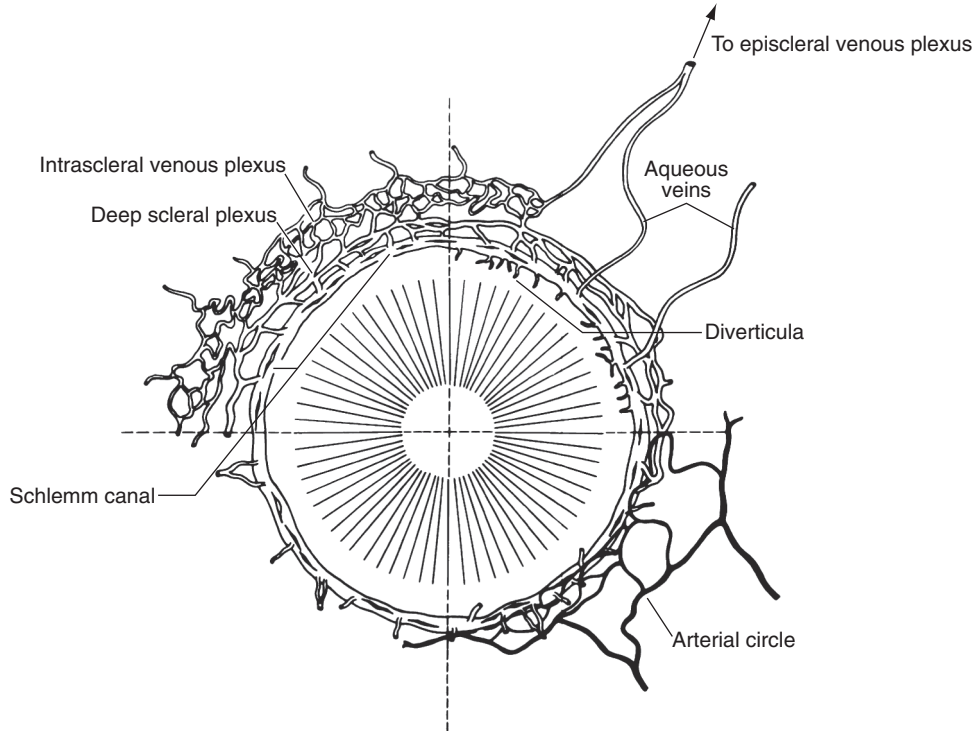


Figure 2-22 Schematic representation of the Schlemm canal and relationships of the arteriolar and venous vascular supply. For clarity, the various systems have been limited to only parts of the circumference of the canal. Small, tortuous, blind diverticula (so-called Sondermann channels) extend from the canal into the trabecular meshwork. Externally, the collector channels arising from the Schlemm canal anastomose to form the intrascleral and deep scleral venous plexuses. At irregular intervals around the circumference, aqueous veins arise from the intrascleral plexus and connect directly to the episcleral veins. The arteriolar supply closely approximates the canal, but no direct communication occurs between them. *(Reproduced with permission from Tripathi RC, Tripathi BJ. Functional anatomy of the anterior chamber angle. In: Jakobiec FA, ed.* Ocular Anatomy, Embryology, and Teratology. *Harper & Row; 1982:236.)*

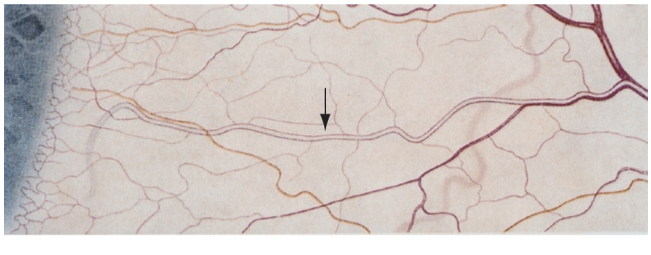


Figure 2-23 Aqueous vein *(arrow).* Collector channels from the Schlemm canal drain into the episcleral venous plexus. With high magnification of the slit-lamp biomicroscope, they are visible near the limbus. Laminar flow and the mixing of aqueous and blood are demonstrated here. *(Reproduced with permission from Thiel R.* Atlas of Diseases of the Eye. *Elsevier; 1963.)*

VIDEO 2-2 Aqueous humor flow through the distal outflow system as seen using indocyanine green aqueous angiography.
Courtesy of Alex Huang, MD, PhD.

Uvea

The uvea (also called the *uveal tract*) is the main vascular layer of the eye. It consists of 3 parts (Fig 2-24):

- iris (located in the anterior uvea)
- ciliary body (located in the anterior pars plicata and the middle pars plana)
- choroid (located in the posterior uvea)

These structures are discussed separately in the next 3 sections.

The uvea is firmly attached to the sclera at only 3 sites:

- scleral spur
- exit points of the vortex veins
- optic nerve

These attachments account for the characteristic anterior dome-shaped choroidal detachment.

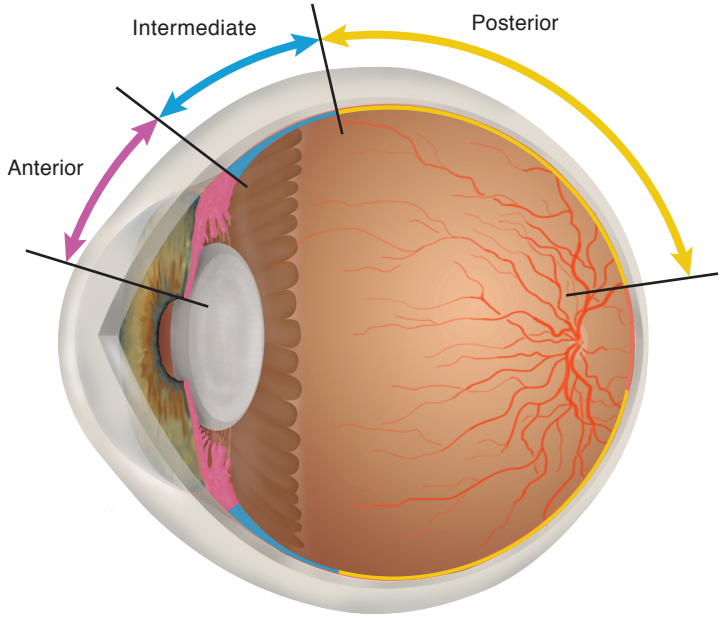


Figure 2-24 The uvea consists of the iris, ciliary body, and choroid. The classification of uveitis, established by the SUN (Standardization of Uveitis Nomenclature) Working Group, is based on the primary site of inflammation. Anterior uveitis *(red)* involves the iris and anterior ciliary body; intermediate uveitis *(blue)* involves the posterior ciliary body and the pars plana and/or the peripheral retina; posterior uveitis *(green)* involves the choroid, either primarily or secondarily from the retina. *(Illustration by Paul Schiffmacher; revised by Cyndie C.H. Wooley.)*

The classification of uveitis, established by the 2005 SUN (Standardization of Uveitis Nomenclature) Working Group anatomical classification system, is based on the *primary anatomical site of inflammation* within the zones of the uvea:

- anterior uveitis (anterior chamber)
- intermediate uveitis (vitreous)
- posterior uveitis (retina or choroid)
- panuveitis (anterior chamber, vitreous, and retina or choroid)

Uveitis is discussed extensively in BCSC Section 9, *Uveitis and Ocular Inflammation*.

Iris

The iris is the most anterior and visible extension of the uvea (Figs 2-25, 2-26). It is made up of mesodermal tissue (blood vessels, connective tissue) and neuroectodermal tissue (smooth muscle, epithelial cells, melanocytes.) The distinctive color of the iris has a genetic component and is determined by the relative density of melanocytes and other pigmented cells. Topographical features of the iris include the pupillary margin, pupillary zone, collarette, crypts, and iris root (Fig 2-27).

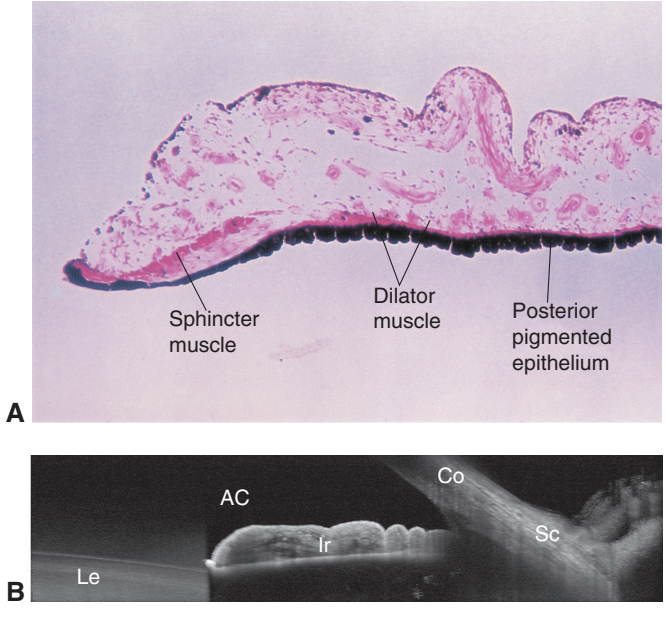


Figure 2-25 Iris. **A,** Histologic section of the iris showing the sphincter muscle, typically found within 1 mm of the pupil border. The dilator muscle, derived from the anterior pigmented layer of the iris epithelium, is found in the mid iris. **B,** AS-OCT scan of the iris. AC = anterior chamber; Co = cornea; Ir = iris; Le = lens; Sc = sclera. *(Part A courtesy of Thomas A. Weingeist, MD, PhD; part B courtesy of Vikram S. Brar, MD.)*

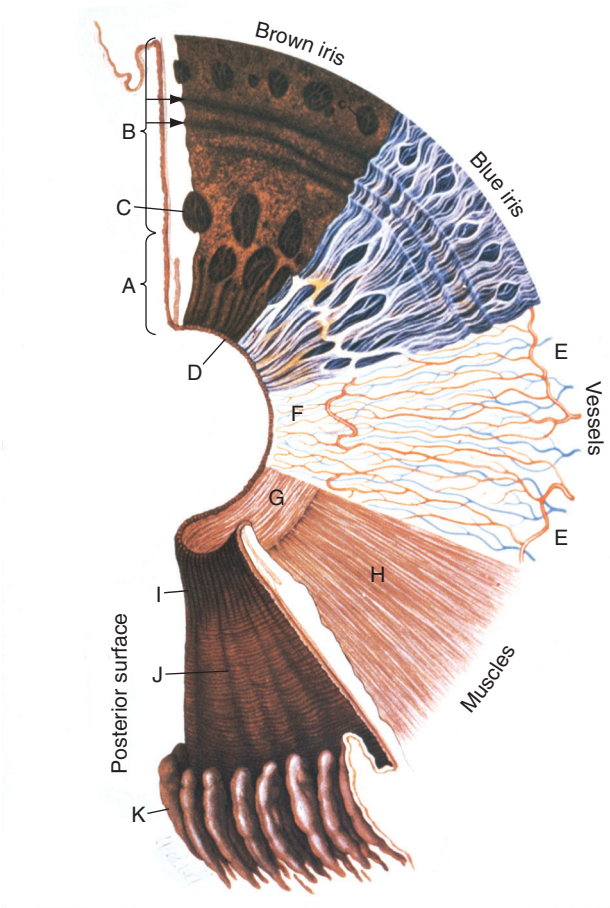


Figure 2-26 Composite drawing of the surfaces and layers of the iris, beginning at the upper left and proceeding clockwise. The iris cross section shows the pupillary (A) and ciliary (B) portions; the surface view shows a brown iris with its dense, matted anterior border layer. Circular contraction furrows are shown *(arrows)* in the ciliary portion of the iris. Fuchs crypts (C) are seen at either side of the collarette in the pupillary and ciliary portions and peripherally near the iris root. The collarette separates the pupillary (A) and ciliary (B) portions. The pigment ruff is seen at the pupillary edge (D). The blue iris surface shows a less dense anterior border layer and more prominent trabeculae. The iris vessels are shown beginning at the major arterial circle in the ciliary body (E). Radial branches of the arteries and veins extend toward the pupillary region. The arteries form the incomplete minor arterial circle (F), from which branches extend toward the pupil, creating capillary arcades. The sector below demonstrates the circular arrangement of the sphincter muscle (G) and the radial processes of the dilator muscle (H). The posterior surface of the iris shows the radial contraction furrows (I) and the structural folds (J) of Schwalbe. Circular contraction folds are also present in the ciliary portion. The pars plicata of the ciliary body is shown at bottom (K). *(Reproduced with permission from Hogan MJ, Alvarado JA, and Weddell JE.* Histology of the Human Eye. *WB Saunders; 1971.)*

CLINICAL PEARL

Because of the relative thinness of the iris root and pupillary margin, they are more susceptible to injury following blunt trauma, resulting in iridodialysis and sphincter tears and/or traumatic mydriasis, respectively.

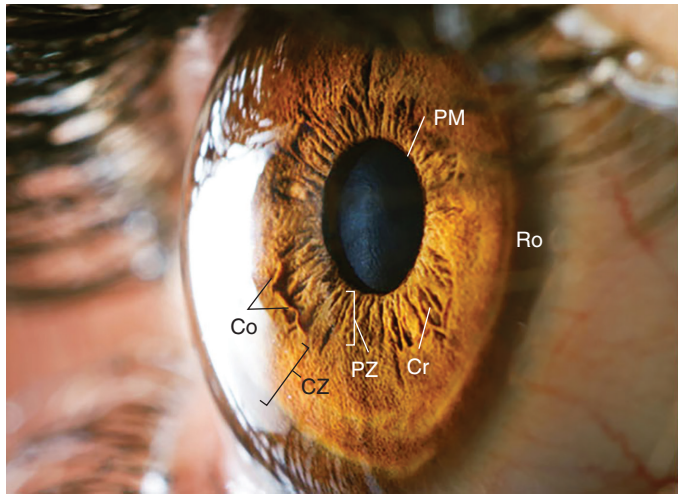


Figure 2-27 Clinical photograph of surface topography of the iris. The collarette divides the iris surface into 2 zones: a peripheral ciliary zone and a central pupil zone. The sphincter muscle lies within the pupil zone and the dilator muscle in the ciliary zone. The collarette can be complete or incomplete and represents the anterior remnant of the hyaloidal system. Iris crypts are areas where the iris is thinned compared with its surroundings. Thus, when located peripherally, crypts are a good target for laser iridotomy. Co = collarette; Cr = crypt; CZ = ciliary zone; PM = pupil margin; PZ = pupil zone; Ro = root. *(Courtesy of Michael Vitek/Shutterstock.com.)*

The mobility of the iris allows the pupil to change size. During mydriasis, the iris is pulled into numerous ridges and folds; during miosis, its anterior surface is smoother.

The major structures of the iris are as follows:

- stroma
- vessels and nerves
- dilator muscle and anterior pigmented epithelium
- sphincter muscle
- posterior pigmented epithelium

Stroma

The iris stroma is composed of pigmented cells (melanocytes), nonpigmented cells, collagen fibers, and a matrix containing hyaluronic acid. The aqueous humor flows freely within the loose stroma along the anterior border of the iris, which contains multiple crypts and crevices that vary in size, shape, and depth. This surface is covered by an interrupted layer of connective tissue cells that merges with the ciliary body.

The overall structure of the iris stroma is similar in irides of all colors. Differences in iris color are related to the amount of pigmentation in the anterior border layer and the deep stroma. The stroma of blue irides is lightly pigmented; brown irides have a densely pigmented stroma.

Vessels and Nerves

Blood vessels form the bulk of the iris stroma. Most follow a radial course, arising from the major arterial circle and passing to the center of the pupil. In the region of the *collarette* (the thickest portion of the iris), anastomoses occur between the arterial and venous arcades to form the minor vascular circle of the iris, which is often incomplete. The major arterial circle is located at the apex of the ciliary body, not the iris (see Chapter 1, Fig 1-23).

The diameter of the capillaries is relatively large. Their endothelium is nonfenestrated and is surrounded by a basement membrane, associated pericytes, and a zone of collagenous filaments. The intima has no internal elastic lamina. Myelinated and unmyelinated nerve fibers serve sensory, vasomotor, and muscular functions throughout the stroma.

Dilator Muscle and Anterior Pigmented Epithelium

The dilator muscle develops from the anterior pigmented epithelium and is derived from the neuroectoderm. It lies parallel and anterior to the posterior pigmented epithelium (Fig 2-28; also see Fig 2-25). The smooth muscle cells contain fine myofilaments and melanosomes. The myofibrils are confined mainly to the basal portion of the cells and extend anteriorly into the iris stroma. The melanosomes and the nucleus are found in the apical region of each myoepithelial cell. The remaining anterior pigmented epithelium is smaller and less pigmented than its posterior counterpart, making it difficult to visualize, even on histologic sections.

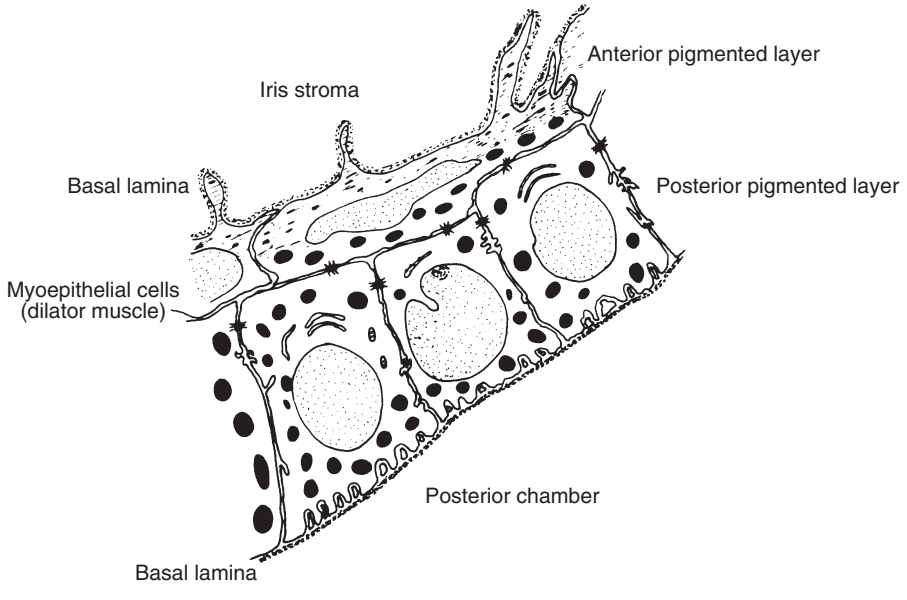


Figure 2-28 Anterior and posterior pigmented epithelia of the iris. The posterior pigmented epithelium is larger than the anterior epithelium and contains more pigment granules than does the latter. *(Illustration by Thomas A. Weingeist, MD, PhD.)*

The muscle has dual sympathetic and parasympathetic innervation. The dilator muscle contracts in response to sympathetic α_1-adrenergic stimulation, and cholinergic parasympathetic stimulation may have an inhibitory role. See BCSC Section 5, *Neuro-Ophthalmology,* for additional discussion of the physiology and pathology of the dilator muscle.

Sphincter Muscle

Like the dilator muscle, the sphincter muscle is derived from neuroectoderm. It is composed of a circular band of smooth muscle fibers and is located near the pupillary margin in the deep stroma, anterior to the posterior pigmented epithelium of the iris (see Fig 2-25). The sphincter muscle receives its primary innervation from parasympathetic nerve fibers that originate in the Edinger-Westphal nucleus and travel with the oculomotor nerve (CN III). It responds pharmacologically to muscarinic stimulation. The reciprocal sympathetic innervation to the sphincter appears to serve an inhibitory role, helping relax the sphincter in darkness. See BCSC Section 5, *Neuro-Ophthalmology,* for additional discussion of physiology and pathology of the sphincter muscle.

Posterior Pigmented Epithelium

The posterior pigmented epithelium of the iris, also called *iris pigment epithelium (IPE),* is densely pigmented and appears velvety smooth and uniform (see Fig 2-25). It is continuous with the nonpigmented epithelium of the ciliary body and thus with the neurosensory portion of the retina. The polarity of its cells is maintained from embryogenesis. The basal surface of the pigmented layer borders the posterior chamber. The apical surface faces the stroma and adheres to the anterior iris epithelium (see Fig 2-28).

The posterior pigmented epithelium of the iris curves around the pupillary margin and extends for a short distance onto the anterior border layer of the iris stroma as the pigment ruff at the pupillary margin. In eyes with rubeosis iridis, the pigmented epithelium may extend farther onto the anterior surface of the iris, a condition called *ectropion.* The term *ectropion uveae,* which refers to an outfolding over the pupil of the IPE, is a misnomer because the IPE is derived from the neuroectoderm (not the neural crest) and therefore is not considered part of the uvea.

Wright KW, Strube YNJ, eds. *Pediatric Ophthalmology and Strabismus.* 3rd ed. Oxford University Press; 2012.

Ciliary Body

The ciliary body, which is triangular in cross section, bridges the anterior and posterior segments of the eye (see Fig 2-19). The apex of the ciliary body is directed posteriorly toward the ora serrata. The base of the ciliary body gives rise to the iris. The only attachment of the ciliary body to the sclera is at its base, via its longitudinal muscle fibers, where they insert into the scleral spur.

The ciliary body has 2 principal functions: aqueous humor formation and lens accommodation. It also plays a role in the trabecular and uveoscleral outflow of aqueous humor.

Ciliary Epithelium and Stroma

The ciliary body is 6–7 mm wide and consists of 2 parts: the pars plana and the pars plicata. The *pars plana* is a relatively avascular, smooth, pigmented zone that is 4 mm wide and extends from the ora serrata to the ciliary processes. The safest posterior surgical approach to the vitreous cavity is through the pars plana, located 3–4 mm from the corneal limbus.

The *pars plicata* is richly vascularized and consists of approximately 70–80 radial folds, or *ciliary processes.* The zonular fibers of the lens attach primarily in the valleys of the ciliary processes but also along the pars plana (see Fig 2-26).

CLINICAL PEARL

In cases of intermediate uveitis, the primary source of inflammation that involves the vitreous arises from the pars plana. Most of these cases are idiopathic, and the term pars planitis is often used.

The capillary plexus of each ciliary process is supplied by arterioles as they pass anteriorly and posteriorly from the major arterial circle; each plexus is drained by 1 or 2 large venules at the crest of each process. Sphincter tone within the arteriolar smooth muscle affects the capillary hydrostatic pressure gradient. In addition, sphincter tone influences whether blood flows into the capillary plexus or directly to the draining choroidal vein, bypassing the plexus completely. Neuronal innervation of the vascular smooth muscle and humoral vasoactive substances may be important in determining regional blood flow, capillary surface area available for exchange of fluid, and hydrostatic capillary pressure. All of these factors affect the rate of aqueous humor formation.

The ciliary body is lined by a double layer of epithelial cells: the inner, nonpigmented ciliary epithelium and the outer, pigmented ciliary epithelium (Fig 2-29). The basal lamina of the nonpigmented epithelium faces the posterior chamber, and the basal lamina of the outer pigmented epithelium is attached to the ciliary stroma and blood vessels. The nonpigmented and pigmented cell layers are oriented apex to apex and are fused by a complex system of junctions and cellular interdigitations. Along the lateral intercellular spaces, near the apical border of the nonpigmented epithelium, are tight junctions (zonulae occludentes) that maintain the blood–aqueous barrier. The basal lamina of the pigmented epithelium is thick and more homogeneous than that of the nonpigmented epithelium.

The pigmented epithelium is relatively uniform throughout the ciliary body. Each of its cuboidal cells has multiple basal infoldings, a large nucleus, mitochondria, an extensive endoplasmic reticulum, and many melanosomes. The nonpigmented epithelium tends to be cuboidal in the pars plana but columnar in the pars plicata. It also has multiple basal infoldings, abundant mitochondria, and large nuclei. The endoplasmic reticulum and Golgi complexes in these cells are important for aqueous humor formation.

The uveal portion of the ciliary body, the stroma, consists of comparatively large fenestrated capillaries, collagen fibers, and fibroblasts.

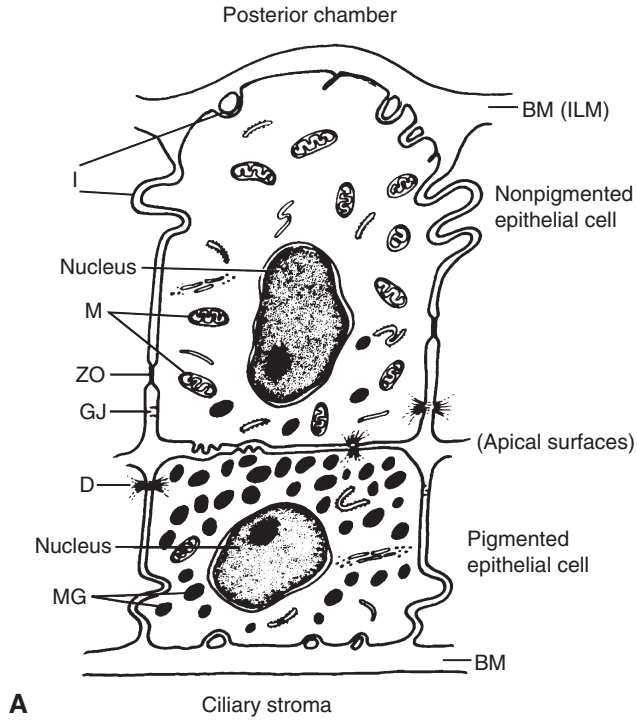


Figure 2-29 Ciliary epithelium. **A,** The 2 layers of the ciliary epithelium, showing apical surfaces in apposition to each other. Basement membrane (BM) lines the double layer and constitutes the internal limiting membrane (ILM) on the inner surface. The nonpigmented epithelium is characterized by large numbers of mitochondria (M), zonula occludens (ZO), and lateral and surface interdigitations (I). The blood–aqueous barrier is established by the intercellular ZOs. The pigmented epithelium contains numerous melanin granules (MG). Additional intercellular junctions include desmosomes (D) and gap junctions (GJ).

(Continued)

The main arterial supply to the ciliary body comes from the anterior and long posterior ciliary arteries, which join to form a multilayered arterial plexus consisting of a superficial episcleral plexus; a deeper intramuscular plexus; and an incomplete major arterial circle. The major arterial circle is often mistakenly attributed to the iris but is actually located posterior to the anterior chamber angle recess, in the ciliary body (see Chapter 1, Figs 1-22, 1-23, 1-25). The major veins drain posteriorly through the vortex system, although some drainage also occurs through the intrascleral venous plexus and the episcleral veins into the limbal region.

Ciliary Muscle

The 3 layers of fibers in the ciliary muscle (Fig 2-30) are

- longitudinal
- radial
- circular

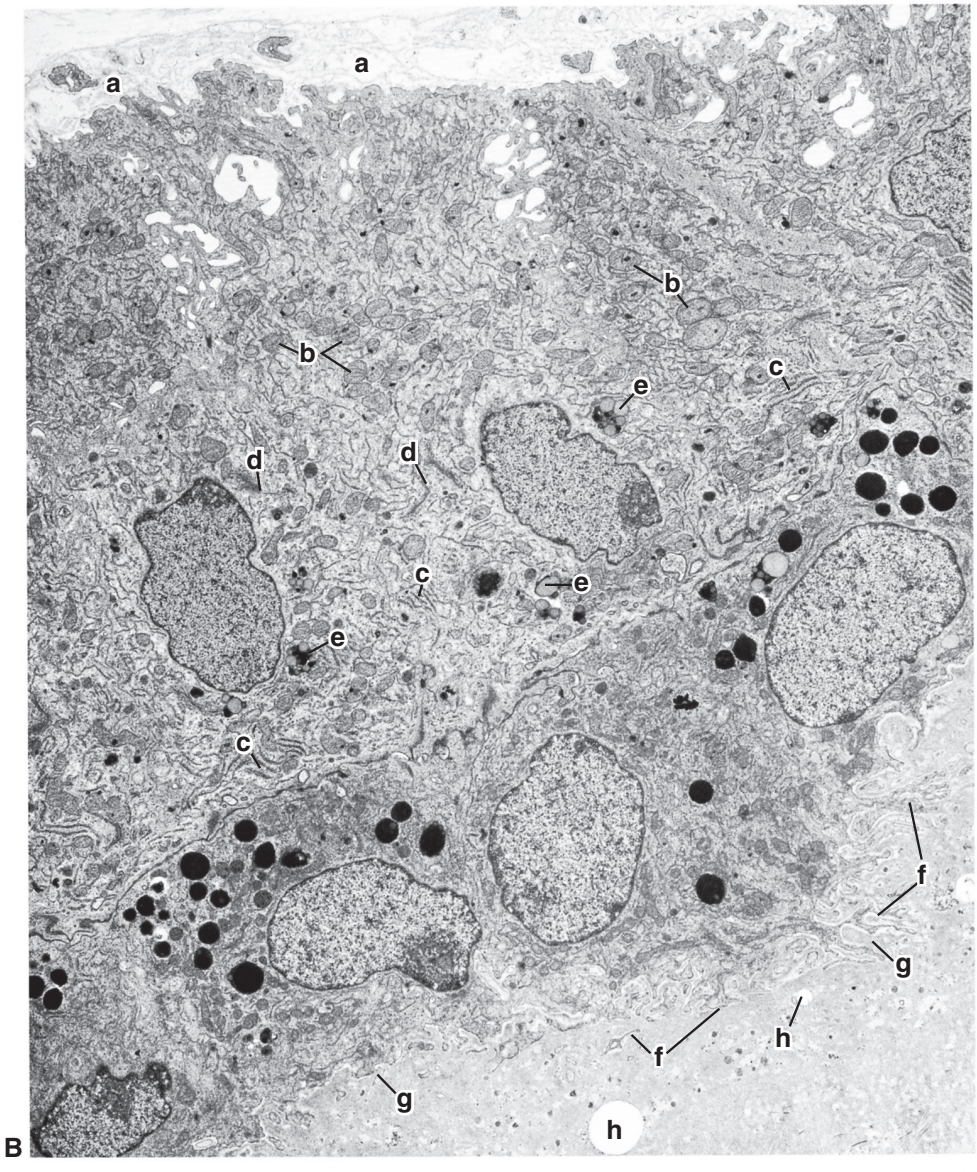


Figure 2-29 *(continued)* **B,** Pars plicata of the ciliary body showing the 2 epithelial layers in the eye of an older person (light microscopy ×5700). The thickened ILM (a) is laminated and vesicular; such thickened membranes are a characteristic of older eyes. The cytoplasm of the nonpigmented epithelium is characterized by its numerous mitochondria (b) and the cisternae of the rough-surfaced endoplasmic reticulum (c). A poorly developed Golgi apparatus (d) and several lysosomes and residual bodies (e) are shown. The pigmented epithelium contains many melanin granules, located mainly in the apical portion. The basal surface is rather irregular, having many fingerlike processes (f). The basement membrane of the pigmented epithelium (g) and a smooth granular material containing vesicles (h) and coarse granular particles are seen at the bottom of the figure. *(Part A reproduced with permission from Shields MB.* Textbook of Glaucoma. *3rd ed. Williams & Wilkins; 1992. Part B modified with permission from Hogan MJ, Alvarado JA, Weddell JE.* Histology of the Human Eye. *Saunders; 1971:283.)*

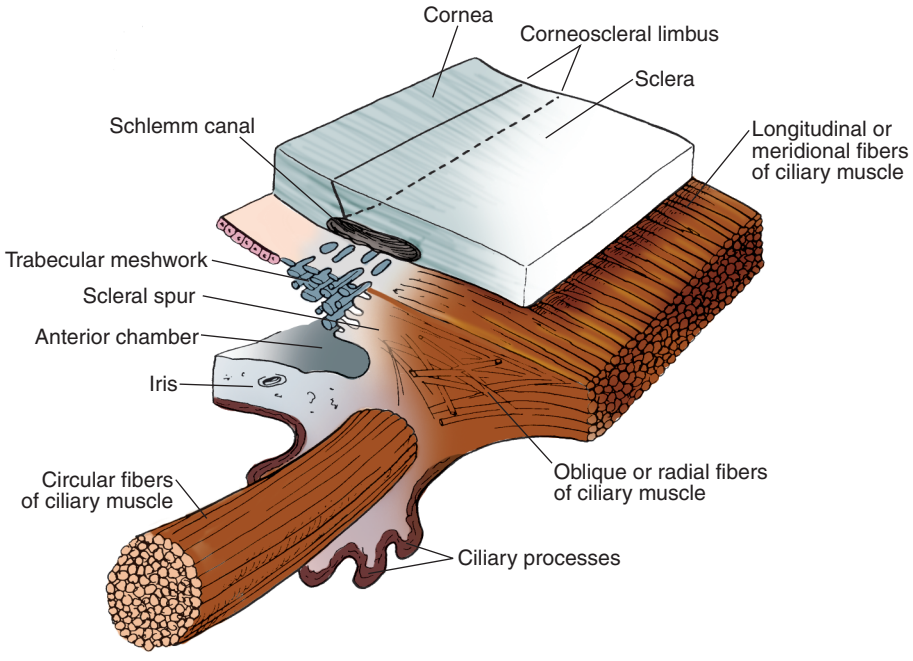


Figure 2-30 Schematic representation of the arrangement of the smooth muscle fibers in the ciliary body. Note the relationship of the ciliary body to the iris, anterior chamber, Schlemm canal, and corneoscleral limbus. The longitudinal fibers insert onto the scleral spur. *(Modified with permission from Snell RS, Lemp MA.* Clinical Anatomy of the Eye. *Blackwell Scientific Publications; 1989.)*

Most of the ciliary muscle is made up of the outer layer of longitudinal fibers that attach to the scleral spur. The radial muscle fibers arise in the midportion of the ciliary body, and the circular fibers are located in the innermost portion. Clinically, the 3 groups of muscle fibers function as a unit. Presbyopia is associated with age-related changes in the lens (discussed in the section Lens, later in this chapter) rather than in the ciliary muscle. Even so, the muscle does change with increasing age: the amount of connective tissue between the muscle bundles increases, and there is a loss of elastic recoil after contraction.

The ciliary muscle fibers behave like other smooth, nonstriated muscle fibers. Ultrastructural studies reveal that they contain multiple myofibrils with characteristic electron-dense attachment bodies, mitochondria, glycogen particles, and a prominent nucleus. The anterior elastic tendons insert into the scleral spur and around the tips of the oblique and circular muscle fibers as they insert into the trabecular meshwork. Both myelinated and unmyelinated nerve fibers are found throughout the ciliary muscle.

Innervation is derived mainly from parasympathetic fibers of CN III via the short ciliary nerves. Approximately 97% of these ciliary fibers are directed to the ciliary muscle, for accommodation, and about 3% are directed to the iris sphincter. Sympathetic fibers have also been observed and may play a role in relaxing the muscle. Cholinergic drugs contract the ciliary muscle. Because some of the muscle fibers form tendinous attachments to the scleral spur, their contraction increases aqueous flow by opening the spaces of the trabecular meshwork.

Supraciliary Space

The supraciliary space is a potential space located below the sclera and above the choroid and ciliary body. This space can expand to accommodate fluid in eyes with certain pathologic conditions (eg, uveal effusion syndrome) and has potential as a possible site for drug delivery.

Choroid

The choroid, the posterior portion of the uvea, nourishes the outer portion of the retina (Fig 2-31). It averages 0.25 mm in thickness and consists of 3 layers of vessels:

- the innermost layer: the choriocapillaris
- the middle layer of small vessels: the Sattler layer
- the outer layer of large vessels: the Haller layer

Perfusion of the choroid comes both from the long and short posterior ciliary arteries and from the perforating anterior ciliary arteries. Venous blood drains through the vortex

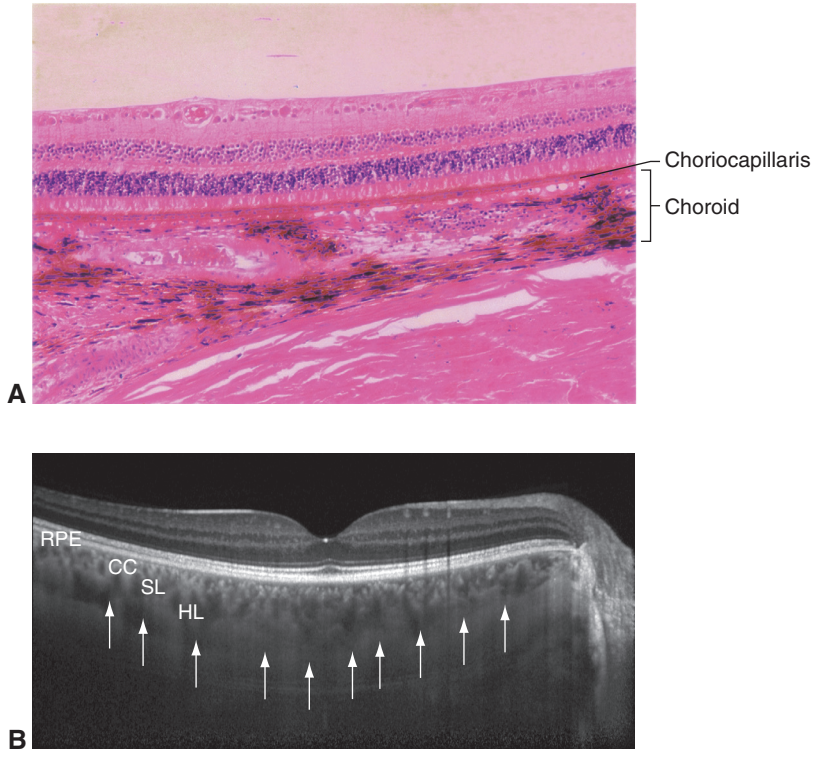


Figure 2-31 Choroid. **A,** Histologic section of the choroid; the choriocapillaris is just below the retinal pigment epithelium (RPE). Beneath the capillaries of the choriocapillaris are the larger middle (Sattler) and outer (Haller) vascular layers. There are scattered melanocytes within the choroid. **B,** OCT image of the choroid (bounded by the RPE and the choroid–sclera junction *[arrows]*) depicts the choriocapillaris (CC), Sattler layer (SL), and Haller layer (HL). *(Part A courtesy of Thomas A. Weingeist, MD, PhD; part B courtesy of Vikram S. Brar, MD.)*

system (Fig 2-32). Blood flow through the choroid is high compared with that through other tissues, exceeding the renal cortex per gram of tissue. As a result, the oxygen content of choroidal venous blood is only 2%–3% lower than that of arterial blood.

Choriocapillaris and Choroidal Vessels

The choriocapillaris is a continuous layer of large capillaries (40–60 μm in diameter) lying in a single plane beneath the retinal pigment epithelium (RPE) (Fig 2-33). The vessel walls are

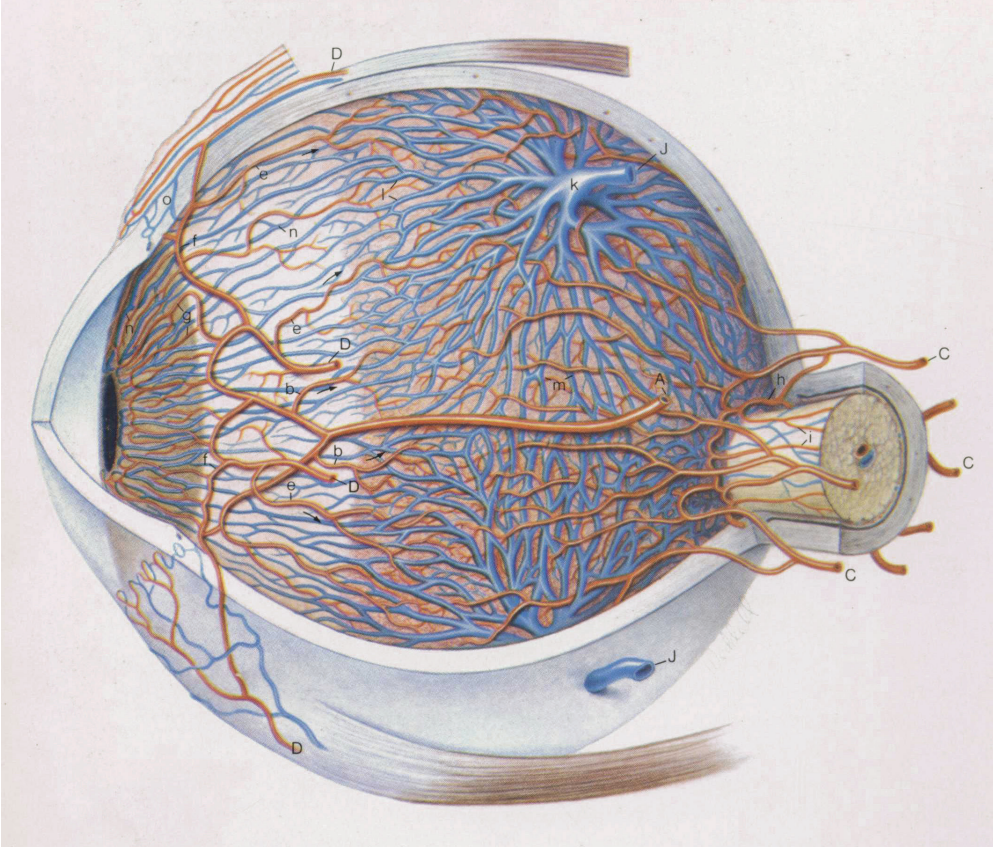


Figure 2-32 Diagram of arterial and venous circulation of the choroid and uveal tract. A = long posterior ciliary artery; b = recurrent branches of the posterior ciliary artery (responsible for supplying the choriocapillaris anterior to the equator); C = short posterior ciliary arteries (responsible for supplying the choriocapillaris from the posterior pole to the equator); D = anterior ciliary artery (note the anastomoses with posterior ciliary circulation and contribution to the episcleral plexus); e = branches of the anterior ciliary artery (contribute to the anterior choriocapillaris); f = major arterial circle of the iris (MAC); g = iris branch of MAC; h = circle of Zinn-Haller; i = pial branches of short posterior ciliary arteries; J = vortex vein (responsible for venous drainage of the eye and uveal tract); k = ampulla of vortex vein; l = choroidal veins (responsible for draining anterior and middle uveal tracts); m = choroidal veins (responsible for draining posterior uveal tract); n = venous return of the iris and ciliary body; o = intrascleral venous plexus (responsible for draining anterior uveal structures into the episcleral system). *(Reproduced with permission from Hogan MJ, Alvarado JA, Weddell JE.* Histology of the Human Eye. *WB Saunders; 1971:326.)*

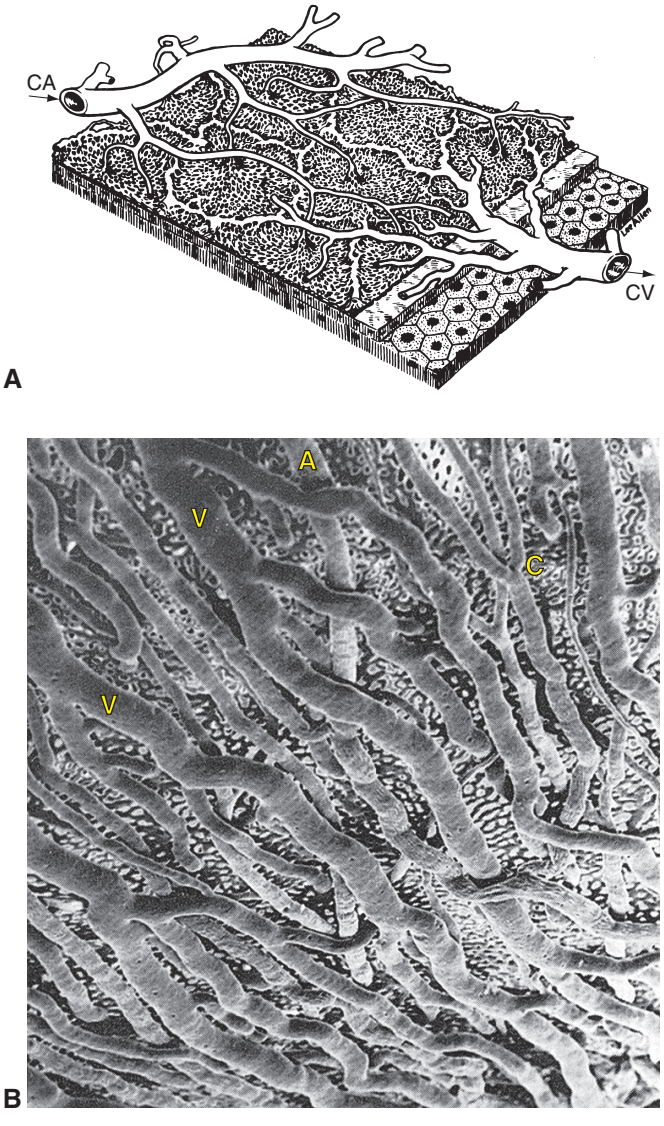


Figure 2-33 Lobular pattern of the choriocapillaris. **A,** Note that the RPE is internal to the choriocapillaris. CA = choroidal arteriole; CV = choroidal venule. **B,** Electron micrograph of the choriocapillaris and larger choroidal vessels. A = arteries; C = choriocapillaris; V = veins. *(Part A reproduced with permission from Hayreh SS. The choriocapillaris.* Albrecht Von Graefes Arch Klin Exp Ophthalmol. *1974;192(3):165–179. Part B courtesy of A. Fryczkowski, MD.)*

extremely thin and contain multiple fenestrations, especially on the surface facing the retina. Pericytes are located along the outer wall.

The middle and outer layers of choroidal vessels are *not* fenestrated. The large vessels, typical of small arteries elsewhere, possess an internal elastic lamina and smooth muscle cells in the media. As a result, small molecules such as those in fluorescein dye, which diffuse

across the fenestrated endothelium of the choriocapillaris, do not leak through medium and large choroidal vessels.

Choroidal Stroma

Abundant melanocytes, as well as occasional macrophages, lymphocytes, mast cells, and plasma cells, appear throughout the choroidal stroma. The intercellular space contains collagen fibers and nerve fibers. In lightly pigmented eyes, pigmentation in the choroid is sparse compared with that of darkly pigmented eyes.

The fenestrations of the choriocapillaris facilitate the exchange of solutes and molecules between the retina/RPE and the choroid. However, these fenestrations are small enough to retain albumin within the intravascular space. The resultant oncotic pressure pulls water across the retina, contributing to retinal adhesion to the RPE.

Lens

The crystalline lens is a biconvex structure located directly behind the posterior chamber and pupil (Fig 2-34). The lens contributes 20.00 D of the 60.00 D of focusing power of the average adult eye. The equatorial diameter is 6.5 mm at birth; it increases in the first 2–3 decades of life and remains approximately 9–10 mm in diameter in adults. The anteroposterior width of the lens is approximately 3 mm at birth and increases after the second decade of life to approximately 6 mm by age 80 years. This growth is accompanied by a shortening of the anterior radius of curvature of the lens, which would increase its optical power if not for a compensatory change in the refractive gradient across the lens substance.

In youth, accommodation for near vision is achieved by ciliary muscle contraction, which moves the ciliary muscle mass forward and inward. This contraction relaxes zonular tension and allows the lens to assume a globular shape, causing its anterior radius of curvature to shorten (Video 2-3, Fig 2-35). With age, accommodative power is steadily lost. At age 8 years, the power is 14.00 D. By age 28 years, the accommodative power decreases to approximately 9.00 D, and it decreases further to 1.00 D by age 64 years. Causes of this power loss include the increased size of the lens, altered mechanical relationships, and the increased stiffness of the lens nucleus secondary to changes in the crystalline proteins of the fiber cytoplasm. Other factors, such as alterations in the geometry of zonular attachments with age and changes in lens capsule elasticity, may also play a role (see Fig 2-35D, E; also see BCSC Section 13, *Refractive Surgery*).



VIDEO 2-3 Computer model of accommodation.
Courtesy of Daniel B. Goldberg, MD.



The lens lacks innervation and is avascular. After regression of the hyaloid vasculature during embryogenesis, the lens depends solely on the aqueous and vitreous for its

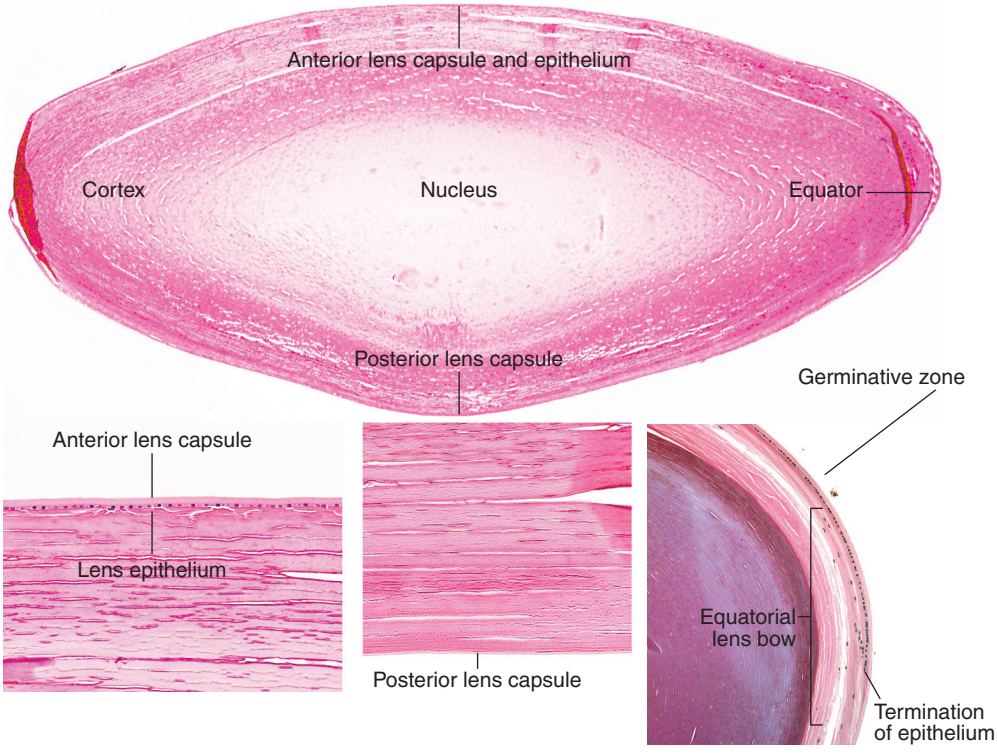


Figure 2-34 Microscopic appearance of the adult lens. *(Courtesy of Tatyana Milman, MD, except for lower right image, which is courtesy of Nasreen A. Syed, MD.)*

nourishment. From embryonic life on, it is entirely enclosed by a basal lamina, the lens capsule. See also BCSC Section 11, *Lens and Cataract*.

Capsule

The lens capsule is a product of the lens epithelium (see Fig 2-34). It is rich in type IV collagen and other matrix proteins. Synthesis of the anterior lens capsule (which overlies the epithelium) continues throughout life so that its thickness increases. Because there are no lens epithelial cells posteriorly, the thickness of the posterior capsule remains constant. Values of 14 µm for the central thickness of the anterior capsule and 4 µm for the central posterior capsule have been cited for the adult lens, although these values may vary among individuals and based on the location within the capsule.

Morphologically, the lens capsule consists of fine filaments arranged in lamellae, parallel to the surface (see Fig 2-35). The anterior lens capsule contains a fibrogranular material, identified as laminin, which is absent from the posterior capsule at the ultrastructural level. The thinness of the posterior capsule creates a potential point of rupture during cataract surgery.

Epithelium

The lens epithelium lies beneath the anterior and equatorial capsule but is absent under the posterior capsule (see Fig 2-34). The basal aspects of the cells abut the lens capsule

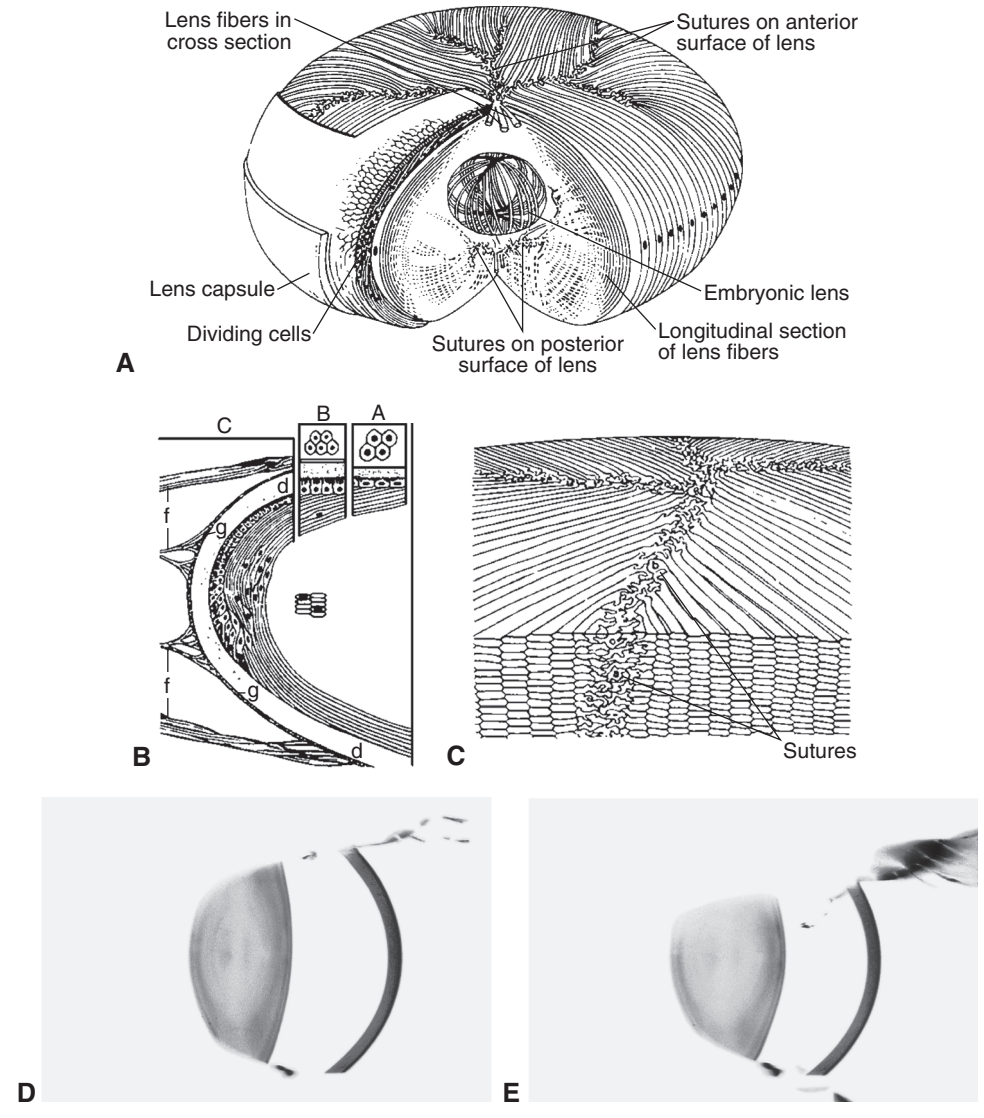


Figure 2-35 Organization of the lens. At areas where lens cells converge and meet, sutures are formed. **A,** Cutaway view of the adult lens showing an embryonic lens inside. The embryonal nucleus has a Y-shaped suture at both the anterior and posterior poles; in the adult lens cortex, the organization of the sutures is more complex. At the equator, the lens epithelium can divide, and the cells become highly elongated and ribbonlike, sending processes anteriorly and posteriorly. As new lens cells are formed, older cells come to lie in the deeper parts of the cortex. **B,** Cross section and corresponding surface view showing the difference in lens fibers at the anterior (A), intermediate (B), and equatorial (C) zones. The lens capsule, or basement membrane of the lens epithelium (d), is shown in relation to the zonular fibers (f) and their attachment to the lens (g). **C,** The diagram shows a closer view of lens sutures. **D** and **E,** Optical sections of the lens of a 25-year-old woman demonstrated by Scheimpflug photography. The cornea is to the right. The lens is in the nonaccommodative state in part **D.** The lens is shown during accommodation in part **E.** Note that the anterior radius of curvature is shortened in the latter case. *(Parts A–C reproduced with permission from Kessel RG, Kardon RH.* Tissues and Organs: A Text-Atlas of Scanning Electron Microscopy. *WH Freeman; 1979. Parts D and E courtesy of Jane Koretz.)*

without specialized attachment sites. The apices of the cells face the interior of the lens, and the lateral borders interdigitate, with practically no intercellular space. Each cell contains a prominent nucleus but relatively few cytoplasmic organelles.

Regional differences in the lens epithelium are important. The central zone represents a stable population of cells whose numbers slowly decline with age. An intermediate zone of smaller cells shows occasional mitoses. Peripherally in the equatorial lens bow area, meridional rows of cuboidal preequatorial cells form the *germinative zone* of the lens (see Figs 2-34, 2-35). In this zone, cells undergo mitotic division, elongate anteriorly and posteriorly, and form the differentiated fiber cells of the lens. In the human lens, cell division continues throughout life and is responsible for the continued growth of the lens.

CLINICAL PEARL

Germinative cells left behind after phacoemulsification can cause posterior capsule opacification due to aberrant proliferation and cell migration. When visually significant, a YAG laser capsulotomy is performed following cataract surgery to create a hole in the opacified capsule to restore vision. Innovations and advancements in surgical techniques and intraocular lens (IOL) designs resulted in less cell migration and lower rates of posterior capsular opacification.

Fibers

As new lens fibers form, they compact previously formed fibers, with the older layers toward the center, surrounding the central embryonic and fetal nuclei formed during embryonic development (see Fig 2-35). There is no definite morphologic distinction between the layers, but rather a gradual transition between the nucleus and cortex of the lens. The terms *endonucleus, nucleus, epinucleus,* and *cortex* refer to potential differences in appearance and behavior of the layers during surgical procedures.

When viewed in optical section with the slit lamp, lamellar zones of discontinuity are visible in the cortex. The fiber cells are hexagonal in cross section, have a spindle shape, and possess numerous interlocking, fingerlike projections. Apart from the most superficial cortical fibers, the cytoplasm is homogeneous and contains few organelles. The high refractive index of the lens results from the high concentration of lens crystallins (α, β, and γ) in the fiber cytoplasm.

Lens sutures are formed by the interdigitation of the anterior and posterior tips of the spindle-shaped fibers. In the fetal lens, this interdigitation forms the anterior Y-shaped suture and the posterior inverted Y–shaped suture. As the lens ages, further branches are added to the sutures; each new set of branch points corresponds to the appearance of a fresh optical zone of discontinuity.

Zonular Fibers

The lens is held in place by a system of zonular fibers *(zonule, suspensory ligament)*; these fibers originate from the basal laminae of the nonpigmented epithelium of the pars plana and pars plicata of the ciliary body. The zonular fibers attach chiefly to the lens capsule

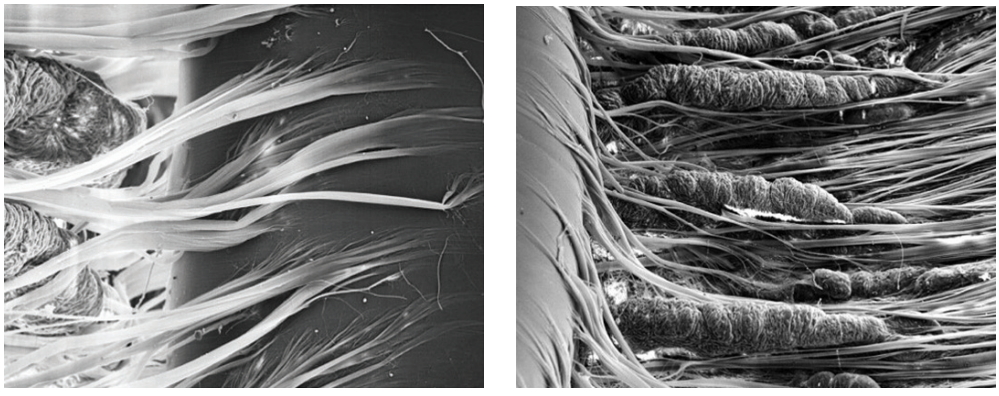


Figure 2-36 Zonular fibers. The zonular fibers insert into the lens capsule anterior and posterior to the equator. Note the ciliary processes between the zonular fibers. *(Courtesy of John Marshall.)*

anterior and posterior to the equator (Fig 2-36). Each fiber is made up of multiple filaments of fibrillin that merge with the equatorial lens capsule (Video 2-4).

VIDEO 2-4 Endoscopic view of ciliary body, zonular fibers, and lens capsule.
Courtesy of Charles Cole, MD.

CLINICAL PEARL

Zonular weakness due to trauma, pseudoexfoliation, uveitis, high myopia, or congenital causes may result in lens subluxation. In patients with Marfan syndrome, pathologic variants in the fibrillin-1 gene lead to weakening of the zonular fibers and subluxation of the lens.

When the eye is focused for distance, the zonule is under tension and the lens form is relatively flattened. During accommodation, contraction of the ciliary muscle moves the proximal attachment of the zonule forward and inward, so the lens becomes more globular, and the eye adjusts for near vision.

Bourge JL, Robert AM, Robert L, Renard G. Zonular fibers, multimolecular composition as related to function (elasticity) and pathology. *Pathol Biol* (Paris). 2007;55(7):347–359.

Goldberg DB. Computer-animated model of accommodation and presbyopia. *J Cataract Refract Surg.* 2015;41(2):437–445.

Retina

The *fundus oculi* is the part of the eye that is visible with ophthalmoscopy (Fig 2-37); it includes the retina, its vessels, and the optic nerve (the anterior surface of which is



Figure 2-37 The fundus oculi. Fundus photograph (wide-field montage) of left eye. The anatomical macula is bounded by the superior and inferior temporal vascular arcades. The central dark area within the macula comprises the fovea. Note the choroidal vessels underlying the retina in the periphery as well as the vortex vein ampullae *(arrows).* The location of ampullae approximate the equator of the eye. *(Courtesy of Vikram S. Brar, MD.)*

visible ophthalmoscopically as the *optic disc*). The reddish color of the fundus is due to the transmission of light reflected from the posterior sclera through the capillary bed of the choroid. The *macula* lies between the temporal vascular arcades. At the macula's center lies the *fovea,* which contains a specialized region in its center known as the *foveola*. The macula and fovea are discussed in greater detail later in the chapter. In the far periphery, the junction between the retina and the pars plana, called the *ora serrata,* can be observed with contact lens examination or indirect ophthalmoscopy, typically with scleral depression.

Embryologically, the retina and its underlying epithelial layer have a common origin, the optic vesicle (see Chapter 4). Thus, the retina can be described as having 2 parts: (1) the neurosensory retina, which contains the photoreceptors, neurons, and other elements; and (2) the retinal pigment epithelium (RPE).

Neurosensory Retina

The *neurosensory retina* is a thin, transparent structure that develops from the inner layer of the optic cup. The neurosensory retina is composed of neuronal, glial, and vascular elements.

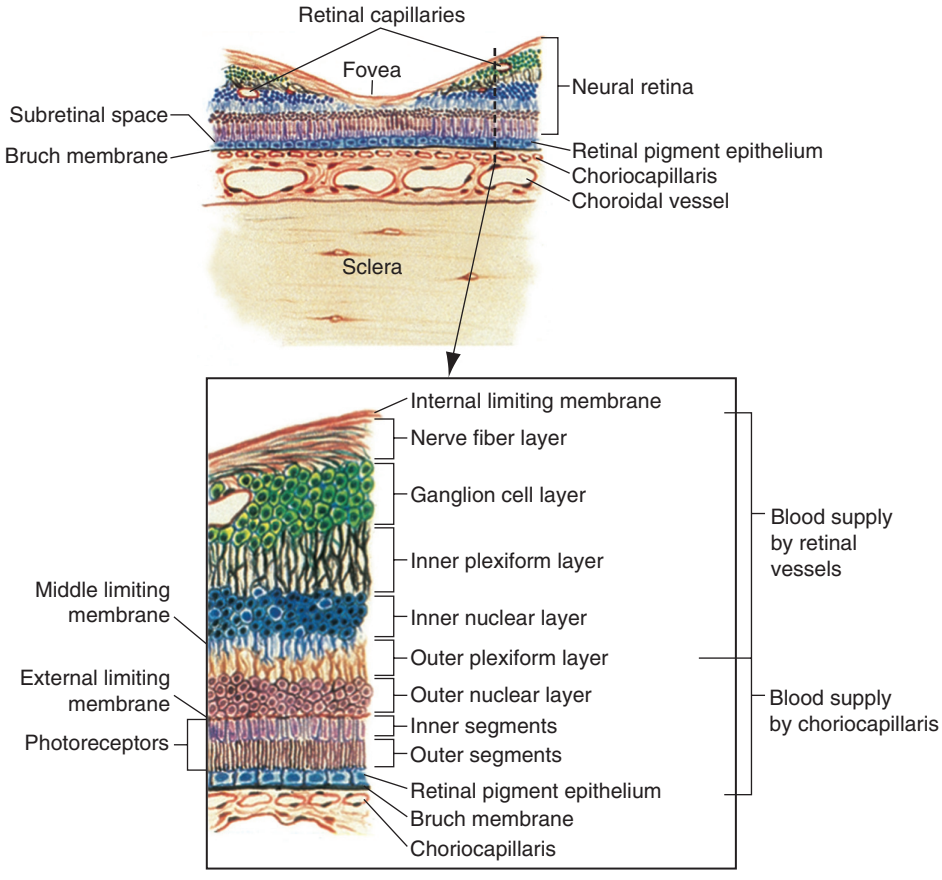


Figure 2-38 Cross section of the retina illustrating its layers and the approximate location of the blood supply to these layers. *(Modified with permission from D'Amico DJ. Diseases of the retina.* N Engl J Med. *1994;331:95–106.)*

In cross section, from inner to outer retina, the layers of the neurosensory retina are as follows (Fig 2-38):

- internal limiting membrane
- nerve fiber layer
- ganglion cell layer
- inner plexiform layer
- inner nuclear layer
- middle limiting membrane (see Fig 2-38)
- outer plexiform layer (referred to as *Henle fiber layer* in the foveal region)
- outer nuclear layer
- external limiting membrane
- rod and cone inner segments
- rod and cone outer segments

These layers are discussed later in the chapter, in the section "Stratification of the neurosensory retina." The retina is also discussed in BCSC Section 12, *Retina and Vitreous.*

Neuronal elements

The photoreceptor layer of the neurosensory retina consists of highly specialized neuroepithelial cells called *rods* and *cones.* There are approximately 100–125 million rods and 6–7 million cones in the human retina, with an approximate ratio of 20:1. Each photoreceptor cell consists of an outer segment and an inner segment. The outer segments, surrounded by a mucopolysaccharide matrix, make contact with the apical processes of the RPE. Tight junctions or other intercellular connections do not exist between the photoreceptor cell outer segments and the RPE. The factors responsible for keeping these layers in apposition are poorly understood but probably involve active transport and other mechanisms, including van der Waals forces, oncotic pressure, and electrostatic forces.

The rod photoreceptor consists of an outer segment that contains multiple laminated discs resembling a stack of coins and a central connecting cilium (Fig 2-39). The microtubules of the cilium have a 9-plus-0 cross-sectional configuration rather than the 9-plus-2 configuration found in motile cilia. The rod inner segment is subdivided into 2 additional elements: an outer ellipsoid containing numerous mitochondria (Fig 2-40), and an inner myoid containing a large amount of glycogen; the myoid is continuous with the main cell body, where the nucleus is located. The inner portion of the cell contains the *synaptic body,* or *spherule,* of the rod, which is formed by a single invagination that accommodates 2 horizontal-cell processes and 1 or more central bipolar dendrites (Fig 2-41). The outer segments of the cones have a different morphology depending on their location in the retina.

The extrafoveal cone photoreceptors of the retina have conical ellipsoids and myoids, and their nuclei tend to be closer to the external limiting membrane than are the nuclei of the rods. Although the structure of the outer segments of the rods and cones is similar, at least 1 important difference exists. Rod discs are not attached to the cell membrane; they are discrete structures. Cone discs are attached to the cell membrane and are thought to be renewed by membranous replacement (see Fig 2-39).

CLINICAL PEARL

Mitochondria within the ellipsoid layer of the inner segment of photoreceptor cells are highly reflective; therefore, this layer is easily visible when the retina is examined in vivo using optical coherence tomography (see Fig 2-40B).

The cone *synaptic body,* or *pedicle,* is more complex than the rod spherule. Cone pedicles synapse with other rods and cones as well as with horizontal and bipolar cell processes (see Fig 2-41). Foveal cones have cylindrical inner segments similar to those in rods but otherwise are cytologically identical to extrafoveal cones.

Horizontal cells make synaptic connections with many rod spherules and cone pedicles; they also extend cell processes horizontally throughout the outer plexiform layer. *Bipolar cells* are oriented vertically. Their dendrites synapse with rod or cone synaptic bodies, and their axons make synaptic contact with ganglion cells and amacrine cells in the inner plexiform layer.

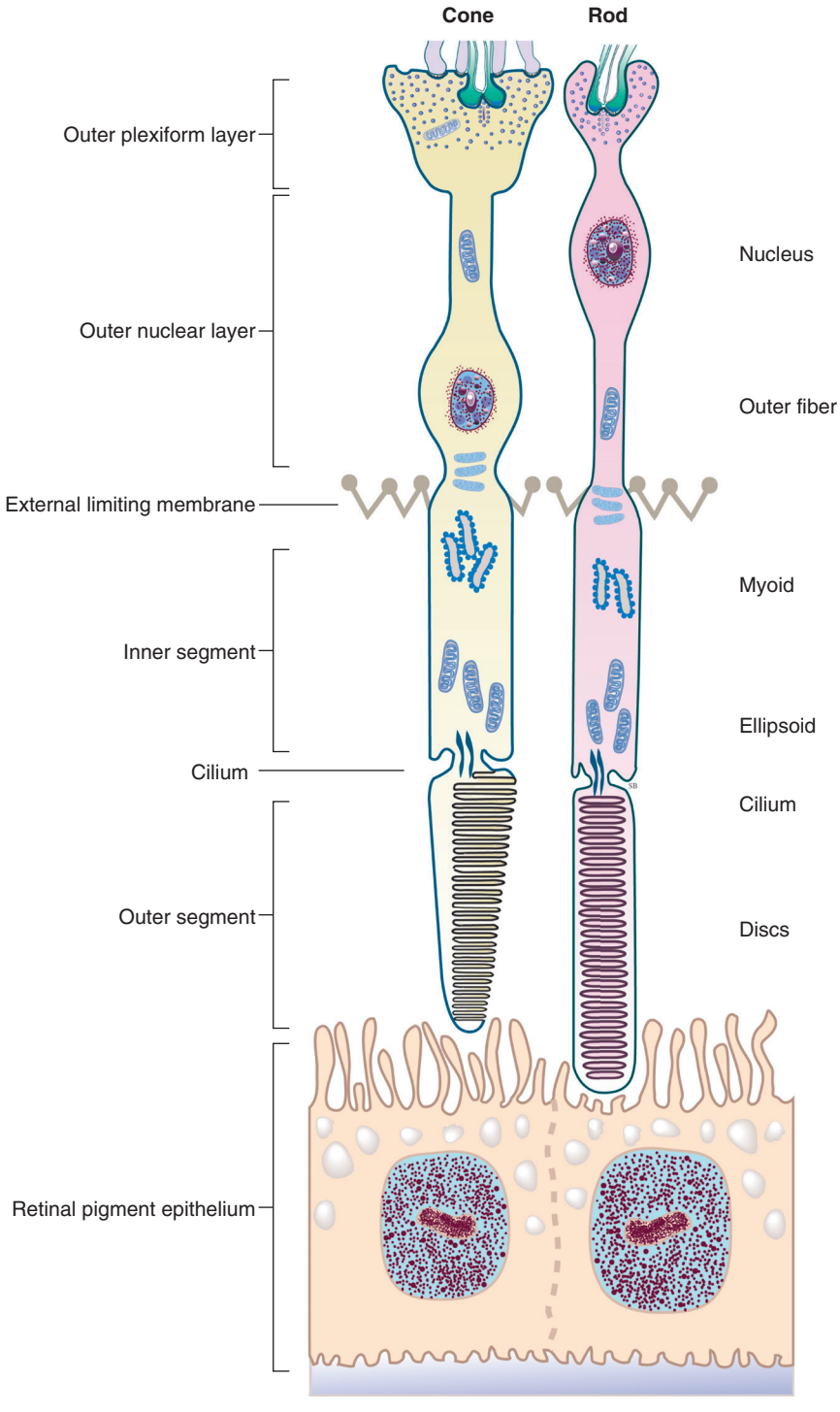


Figure 2-39 Rod and cone photoreceptor cells. *(Illustration by Sylvia Barker.)*

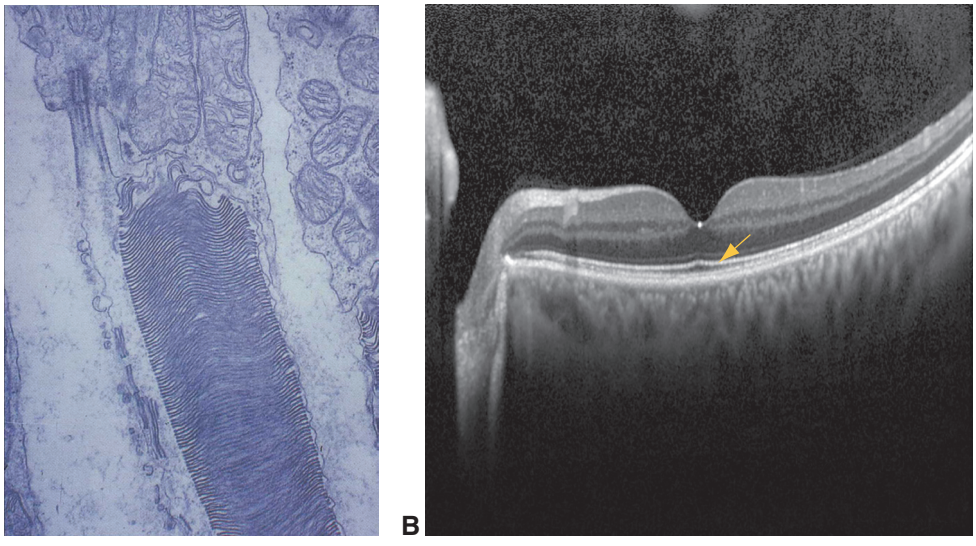


Figure 2-40 Ellipsoid layer. **A,** Electron micrograph of rod photoreceptor cell. Note the cilium connecting the inner and outer segments and the numerous mitochondria in the ellipsoid layer. **B,** OCT section of fovea. *Arrow* designates the ellipsoid layer. *(Part A reproduced with permission from Spalton D, Hitchings R, Hunter P.* Atlas of Clinical Ophthalmology. *3rd ed. Elsevier/Mosby; 2005:400. Part B courtesy of Vikram S. Brar, MD.)*

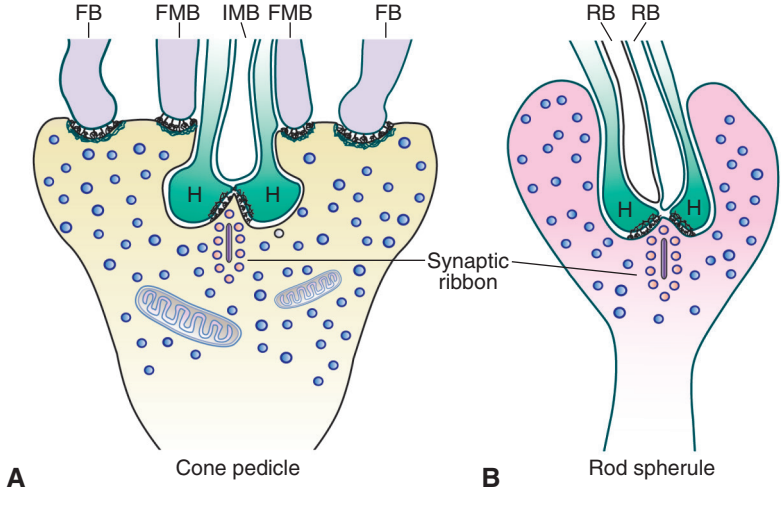


Figure 2-41 Synaptic bodies of photoreceptors. **A,** Cone pedicle with synapses to several types of bipolar cells. **B,** Rod spherule with synapses to bipolar cells. FB = flat bipolar; FMB = flat midget bipolar; H = horizontal cell processes; IMB = invaginating midget bipolar; RB = rod bipolar. *(Illustration by Sylvia Barker.)*

The axons of the ganglion cells bend to become parallel to the inner surface of the retina, where they form the nerve fiber layer and later the axons of the optic nerve. Each optic nerve has more than 1 million nerve fibers. The nerve fibers from the temporal retina follow an arcuate course around the macula to enter the superior and inferior poles of the optic nerve head. The papillomacular fibers travel straight to the optic nerve from the fovea. The nasal axons also pursue a radial course. The visibility of the nerve fibers is enhanced when they are viewed ophthalmoscopically using green (red-free) illumination.

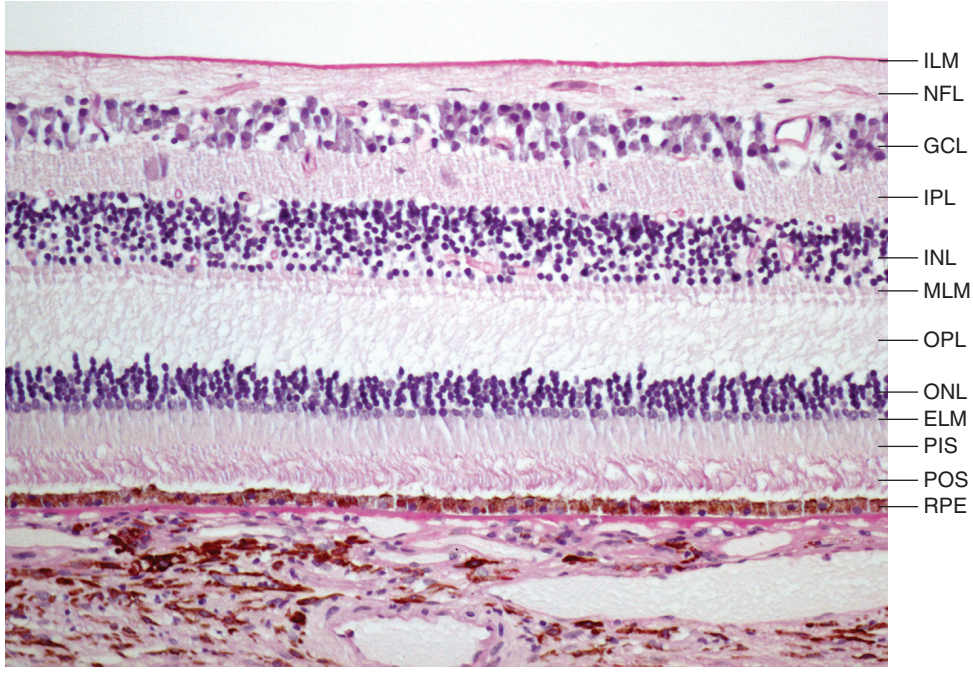
The neuronal elements and their connections in the retina are highly complex (Fig 2-42). Many types of bipolar, amacrine, and ganglion cells exist. The neuronal elements of the rods and cones are interconnected, and signal processing within the neurosensory retina is significant.

Glial elements

Müller cells are glial cells that extend vertically from the external limiting membrane inward to the internal limiting membrane (see Fig 2-42). Their nuclei are located in the inner nuclear layer. Müller cells, along with the other glial elements (the fibrous and protoplasmic astrocytes and microglia), provide structural support and nutrition to the retina and are crucial to normal physiology. In addition, they contribute to the inner blood–retina barrier.

Vascular elements

The retina is a highly metabolic structure, with the highest rate of oxygen consumption per unit weight in the body. The retinal blood vessels are analogous to the cerebral blood vessels and maintain the inner blood–retina barrier. This physiologic barrier is formed by a single layer of nonfenestrated endothelial cells, whose intercellular junctions, under physiologic



A

Figure 2-42 *(Continued)*

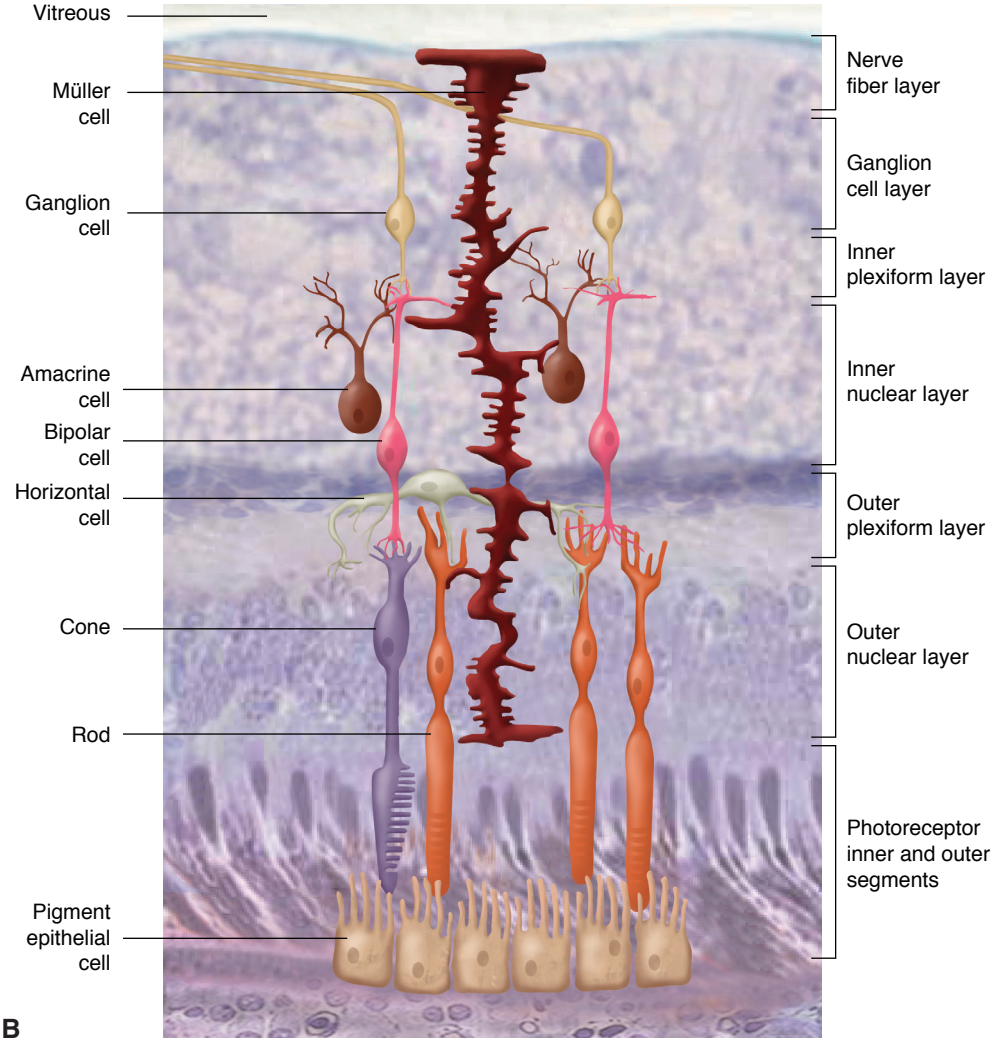


Figure 2-42 *(continued)* Normal retinal layers. **A,** Histology (periodic acid–Schiff [PAS] stain). From vitreous to choroid: ILM = internal limiting membrane; NFL = nerve fiber layer; GCL = ganglion cell layer; IPL = inner plexiform layer; INL = inner nuclear layer; MLM = middle limiting membrane; OPL = outer plexiform layer; ONL = outer nuclear layer; ELM = external limiting membrane; PIS = photoreceptor inner segment; POS = photoreceptor outer segment; RPE = retinal pigment epithelium. **B,** Diagram including cell types of the retina. *(Part A courtesy of Robert H. Rosa, Jr, MD. Part B illustration by Paul Schiffmacher; revised by Cyndie C.H. Wooley.)*

conditions, are impervious to tracer substances such as fluorescein and horseradish peroxidase (Fig 2-43). A basal lamina covers the outer surface of the endothelium and is surrounded by pericytes, or mural cells, which suppress endothelial proliferation and, along with glial cells, contribute to the inner blood–retina barrier (Fig 2-44).

Müller cells and other glial elements are generally attached to the basal lamina of retinal blood vessels. Retinal blood vessels lack an internal elastic lamina and the continuous layer of smooth muscle cells found in other vessels in the body. In the absence of the latter, there is no autonomic regulation of the retinal vessels.

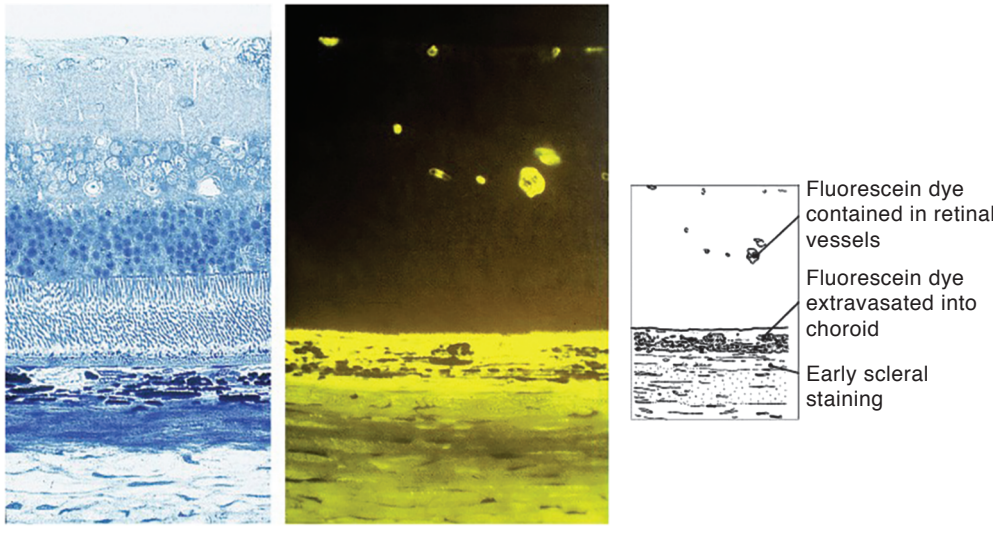


Figure 2-43 Blood–retina barriers. The inner blood–retina barrier is created by intercellular junctions between endothelial cells of the nonfenestrated retinal vessels. The outer blood–retina barrier consists of tight junctions between adjacent RPE cells. *Left:* Normal histologic section of rat retina. *Right:* Section of rat retina following injection of fluorescein. Note the containment of dye within the retinal vessels and the diffuse staining of the choroid by leakage of fluorescein from the fenestrated choriocapillaris. Further extravasation into the outer retina is blocked by the RPE. *(Reproduced with permission from Spalton D, Hitchings R, Hunter P.* Atlas of Clinical Ophthalmology. *3rd ed. Elsevier/Mosby; 2005:409.)*

The retina possesses a dual circulation in which the inner retina is supplied by branches of the central retinal artery, and the outer retina is supplied by the choroid (see Fig 2-38). Retinal arterioles give rise to the superficial capillary plexus and the deep capillary plexus, which supply the ganglion cell layer and inner nuclear layer, respectively (Fig 2-45). The retinal vascular supply is also discussed in BCSC Section 12, *Retina and Vitreous*. The outer nuclear layer and remaining layers of the outer retina are perfused by the choroid. The outer plexiform layer represents a watershed area with regard to perfusion. Perfusion by the 2 circulations can vary with the location in or thickness of the retina, as well as with light exposure. In approximately 18%–32% of eyes, a cilioretinal artery, derived from the posterior ciliary circulation, also supplies the macula. This variation in circulation can result in central visual sparing after central retinal artery occlusion in some cases.

Retinal vessels exhibit several characteristics. In contrast to choroidal vessels, retinal vessels demonstrate dichotomous branching. Also, retinal vessels do not normally cross the horizontal raphe; the occurrence of such suggests the presence of anastomoses, which can often be found in the temporal macula following retinal vein occlusions. Further, retinal arteries do not intersect with other arteries; similarly, retinal veins do not intersect with other veins. At arteriovenous crossings, the 2 vessels share a common sheath, which often represents the site of branch retinal vein occlusions.

Stratification of the neurosensory retina

The neurosensory retina can be divided into several layers (Fig 2-46; also see Figs 2-38, 2-42, 2-45). The photoreceptor outer segments represent the outermost layer and interact

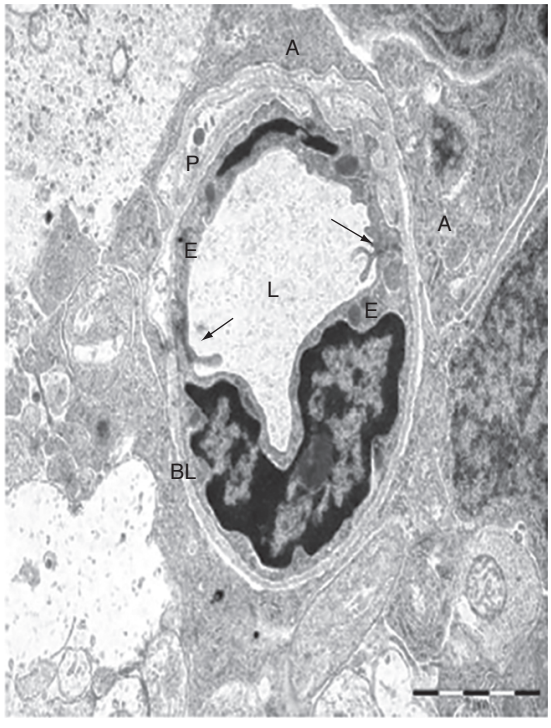


Figure 2-44 Inner blood–retina barrier. Electron micrograph of a retinal capillary in the inner nuclear layer. The inner blood–retina barrier consists of intercellular endothelial junctions (tight, adherens, and gap), pericytes, and contributions from glial cells (Müller cells and astrocytes). A = astrocyte; BL = basal lamina; E = endothelial cell; L = lumen; P = pericyte. *Arrows* = intercellular junctional complexes. *(Modified with permission from Klaassen I, Van Noorden CJ, Schlingemann RO. Molecular basis of the inner blood–retinal barrier and its breakdown in diabetic macular edema and other pathological conditions.* Prog Retin Eye Res. *2013;34:19–48, Fig 3.)*

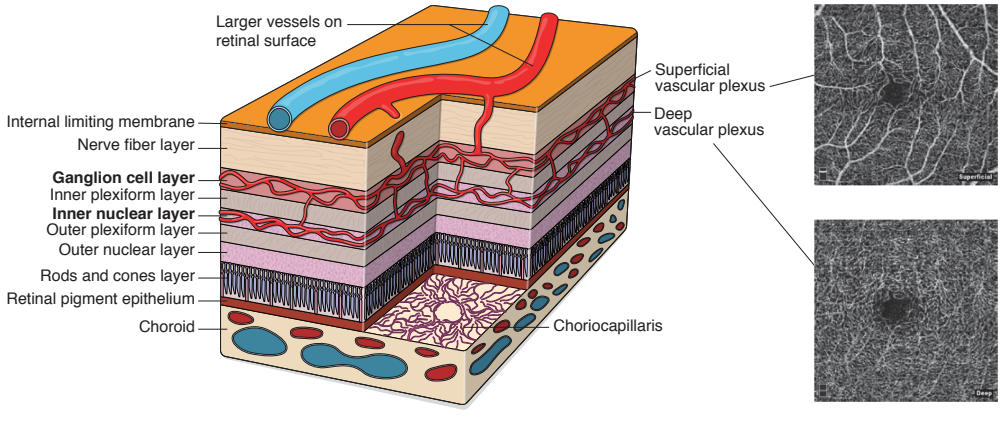


Figure 2-45 Distribution of blood vessels in the retina. OCT angiograms *(right)* demonstrate the superficial vascular plexus and the deep vascular plexus, which arise from retinal arterioles. The schematic *(left)* shows the retinal layers supplied by these plexuses. *(Angiograms courtesy of Vikram S. Brar, MD. Schematic by Mark Miller.)*

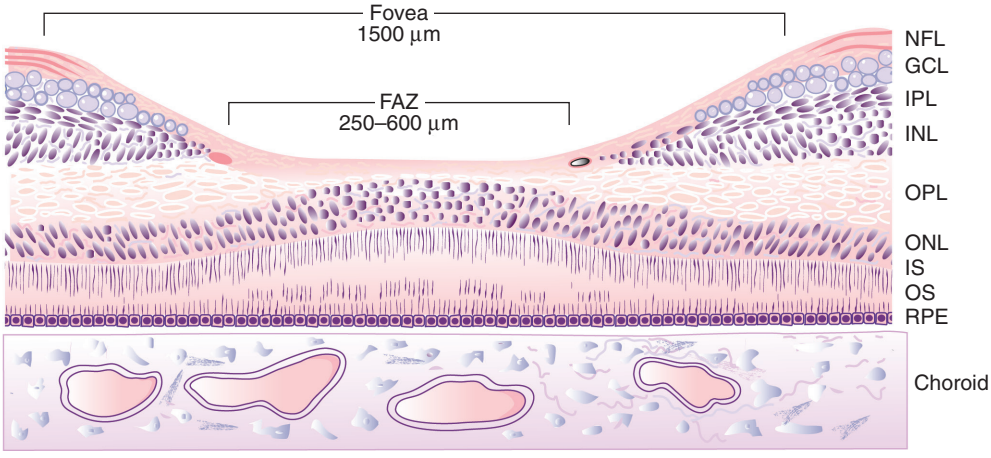


Figure 2-46 Schematic section through the fovea. FAZ = foveal avascular zone; GCL = ganglion cell layer; INL = inner nuclear layer; IPL = inner plexiform layer; IS = inner segment of the photoreceptor; NFL = nerve fiber layer; ONL = outer nuclear layer; OPL = outer plexiform layer (Henle fiber layer); OS = outer segment of the photoreceptors; RPE = retinal pigment epithelium. *(Illustration by Sylvia Barker.)*

with the apical processes of the RPE. A potential space exists between this outermost layer of the neurosensory retina and the RPE and is the plane of separation in retinal detachment. The roof of the subsensory space is demarcated by the *external limiting membrane (ELM),* which separates the photoceptor nucleus from its inner and outer segments (see Fig 2-39). The ELM, which is not a true membrane but is instead a junctional system, is formed by the attachment sites of adjacent photoreceptors and Müller cells. It is highly permeable, allowing the passage of oxygen and macromolecules from the choroid into the outer retina.

Photoreceptor nuclei are found in the *outer nuclear layer (ONL).* The *outer plexiform layer (OPL)* is composed of synapses between the photoreceptors and bipolar cells. Horizontal-cell fibers descend into this region and regulate synaptic transmission. The OPL also accommodates the oblique axons of the rods and cones as they radiate from the foveal center. Because it contains more fibers, the OPL is thicker in the perifoveal region (see Fig 2-46). The radial fibers in this portion of the OPL are known as the *Henle fiber layer.* At the edge of the foveola, the Henle layer lies almost parallel to the internal limiting membrane, resulting in petaloid or star-shaped patterns when these extracellular spaces are filled with fluid or exudate (Video 2-5).

VIDEO 2-5 Foveal architecture and related pathologies.
Developed by Vivian Lee, MD.

Like the ELM, the *middle limiting membrane (MLM)* is not a true membrane but is rather a junctional system in the inner third of the OPL, where synaptic and desmosomal connections occur between photoreceptor inner fibers and processes of bipolar cells. The MLM is sometimes apparent on OCT as a linear density. Retinal blood vessels ordinarily do not extend beyond this point.

The *inner nuclear layer (INL)* contains nuclei of bipolar, Müller, horizontal, and amacrine cells. The *inner plexiform layer (IPL)* consists of axons of the bipolar and amacrine cells and dendrites of the ganglion cells and their synapses. Amacrine cells, like the horizontal cells of the OPL, probably play an inhibitory role in synaptic transmission. The *ganglion cell layer (GCL)* is made up of the cell bodies of the ganglion cells that lie near the inner surface of the retina. The *nerve fiber layer (NFL)* is formed by axons of the ganglion cells. Normally, these axons do not become myelinated until after they pass through the lamina cribrosa of the optic nerve.

Like the ELM and MLM, the *internal limiting membrane (ILM)* is also not a true membrane. It is formed by the footplates of the Müller cells and attachments to the basal lamina. The basal lamina of the retina is smooth on the vitreal side but appears undulatory on the retinal side, where it follows the contour of the Müller cells. The thickness of the basal lamina varies. The ILM is the point of contact of the retina and the cortical vitreous, the vitreoretinal interface.

Overall, cells and their processes in the retina are oriented perpendicular to the plane of the RPE in the middle and outermost layers but parallel to the retinal surface in the innermost layers. For this reason, deposits of blood or exudates tend to form round blots in the outer layers (where small capillaries are found) and linear or flame-shaped patterns in the NFL.

Topography of the Retina

Retinal thickness varies considerably depending upon the location of the area measured (Figs 2-47, 2-48). The retina is thickest in the papillomacular bundle near the optic nerve (0.23 mm) and thinnest in the foveola (0.10 mm) and ora serrata (0.11 mm).

Macula

Clinically, retina specialists tend to regard the macula, which is 5–6 mm in diameter, as the area between the temporal vascular arcades (see Fig 2-38). On histologic examination, it is the region with more than 1 layer of ganglion cell nuclei (Fig 2-49; also see Figs 2-46, 2-47, 2-48). See BCSC Section 12, *Retina and Vitreous,* for further detail.

The name *macula lutea* (which means *yellow spot*) derives from the yellow color of the central retina in dissected cadaver eyes or in eyes with retinal detachment involving the macula. This coloration is due to the presence of carotenoid pigments, located primarily in the Henle fiber layer. There are 2 major carotenoid pigments—zeaxanthin and lutein—whose proportions vary with their distance from the fovea. In the central area (0.25 mm from the fovea), the lutein-to-zeaxanthin ratio is 1:2.4, and in the periphery (2.2–8.7 mm from the fovea), the ratio is greater than 2:1. This variation in pigment ratio corresponds to the rod-to-cone ratio: lutein is more concentrated in rod-dense areas of the retina, and zeaxanthin is more concentrated in cone-dense areas.

Fovea

The *fovea* is a specialized portion of the macula that appears as a central retinal depression. At approximately 1.5 mm in diameter, it is comparable in size to the optic nerve head (see Fig 2-46). Its margins are clinically inexact, but in younger eyes, the fovea is evident

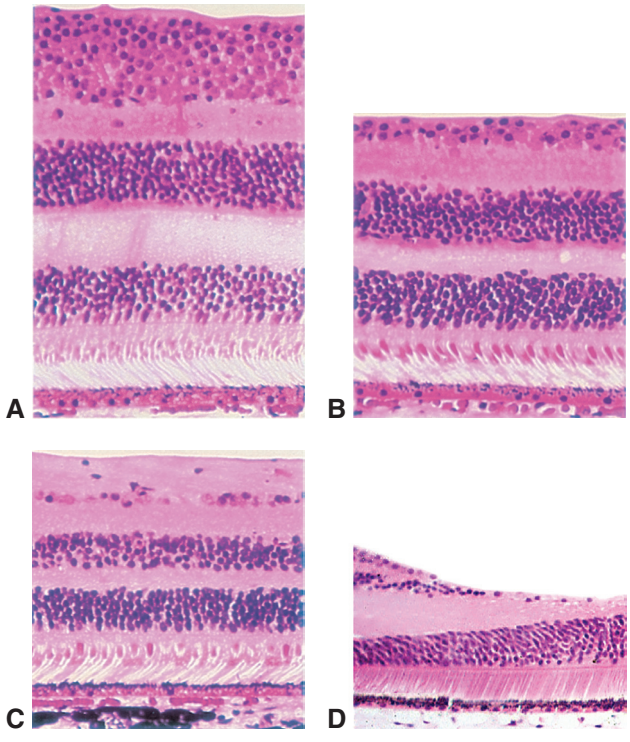


Figure 2-47 Regional differences in the thickness of retinal layers. **A,** Papillomacular bundle, which has the thickest ganglion cell layer. **B,** Macula with a ≥2-cell-thick ganglion cell layer. **C,** Peripheral retina with a single-cell ganglion cell layer and thinner inner and outer nuclear layers. **D,** Fovea, in which only the outer nuclear layer and photoreceptors are present. *(Courtesy of Thomas A. Weingeist, MD, PhD.)*

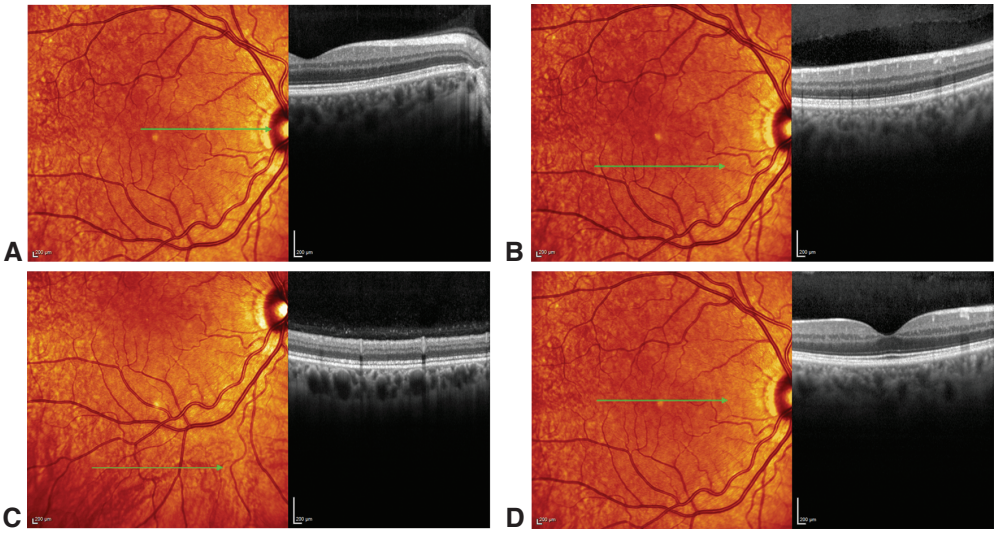


Figure 2-48 OCT images demonstrate the regional differences in retinal layer thickness that are described in Figure 2-47. **A,** Papillomacular bundle. **B,** Macula. **C,** Peripheral retina. **D,** Fovea. *(Courtesy of Vikram S. Brar, MD.)*

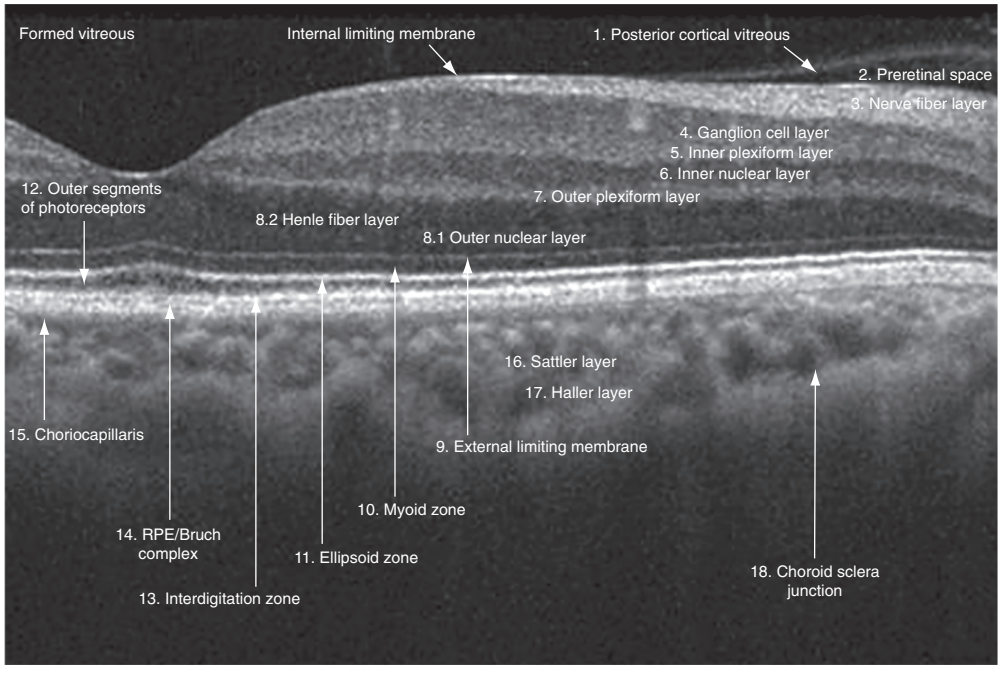


Figure 2-49 OCT image through the fovea. International consensus on segmentation of the normal retina on SD-OCT. *(From Staurenghi G, Sadda S, Chakravarthy U, Spaide RF; International Nomenclature for Optical Coherence Tomography (IN•OCT) Panel. Proposed lexicon for anatomic landmarks in normal posterior segment spectral-domain optical coherence tomography: the IN•OCT consensus.* Ophthalmology. *2014;121(8):1572–1578.)*

ophthalmoscopically as an elliptical light reflex that arises from the slope of the thickened ILM of the retina. From this point inward, the basal lamina rapidly decreases in thickness as it dives down the slopes of the fovea toward the depths of the foveola, where it is barely visible, even by electron microscopy.

The *foveola* is a central depression in the floor of the fovea, located approximately 4.0 mm temporal and 0.8 mm inferior to the center of the optic nerve head. It is approximately 0.35 mm in diameter and 0.10 mm thick at its center. The borders of the foveola merge imperceptibly with the fovea. The nuclei of the photoreceptor cells in the region of the foveola bow forward toward the ILM to form the *fovea externa*. Usually, only photoreceptors, Müller cells, and other glial cells are present in this area.

The photoreceptor layer of the foveola is composed entirely of cones, whose dense packing accounts for the high visual acuity and color vision for which this small area is responsible. The foveal cones are shaped like rods but possess all the cytologic characteristics of extramacular cones. The outer segments are oriented parallel to the visual axis and perpendicular to the plane of the RPE. In contrast, the peripheral photoreceptor cell outer segments are tilted toward the entrance pupil.

The location of the *foveal avascular zone (FAZ),* or capillary-free zone (Fig 2-50; see also Fig 2-46), is approximately the same as that of the foveola. Its appearance in fundus fluorescein angiograms varies greatly. The diameter of the FAZ ranges from 250 to 600 μm or greater; often, a truly avascular, or capillary-free, zone cannot be identified. This area of

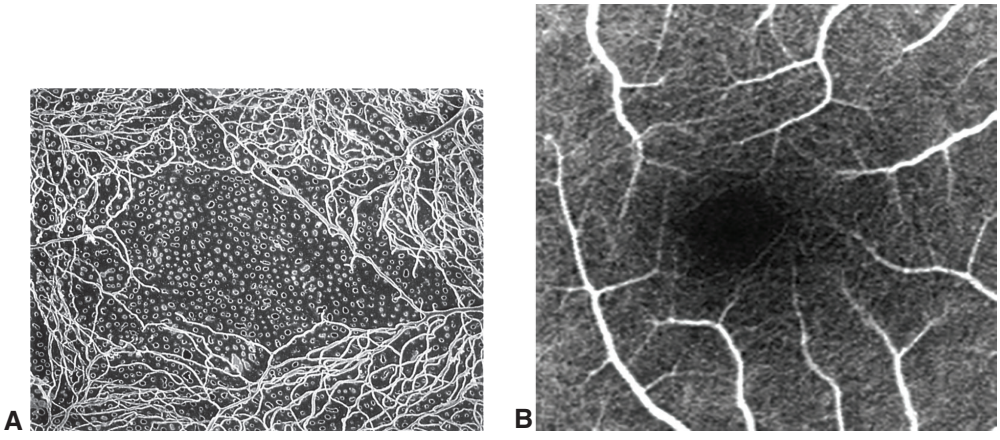


Figure 2-50 Foveal avascular zone (FAZ). **A,** Scanning electron micrograph of a retinal vascular cast at the fovea, showing the FAZ and underlying choriocapillaris, the sole source of oxygen to the retina at this location. **B,** Fluorescein angiogram of the FAZ, obtained during the peak venous phase. Fluorescence from the choriocapillaris is blocked by the RPE. *(Part B courtesy of Vikram S. Brar, MD.)*

the retina is entirely perfused by the choriocapillaris and can be severely affected during retinal detachments that involve the FAZ. Surrounding the fovea is the *parafovea*, which is 0.5 mm wide and is where the GCL, the INL, and the OPL are thickest. Surrounding the parafovea is the most peripheral region of the macula, the 1.5-mm-wide *perifovea*.

Retinal Pigment Epithelium

The retinal pigment epithelium (RPE) develops from the outer layer of the optic cup and consists of a monolayer of hexagonal cells that extends anteriorly from the optic nerve head to the ora serrata, where it merges with the pigmented epithelium of the ciliary body (see Chapter 13). Its structure is deceptively simple considering its many functions:

- vitamin A metabolism
- formation and maintenance of the outer blood–ocular barrier
- phagocytosis of the photoreceptor outer segments
- absorption of light (reduction of scatter)
- formation of the basal lamina of Bruch membrane
- production of the mucopolysaccharide matrix surrounding the outer segments
- maintenance of retinal adhesion
- active transport of materials into and out of the RPE
- management of reactive oxygen species

Like other epithelial and endothelial cells, RPE cells are polarized. The basal aspect is intricately folded and provides a large surface of attachment to the thin basal lamina that forms the inner layer of Bruch membrane. The apices have multiple villous processes that envelop and engage with the photoreceptor outer segments (see Chapter 13). Despite

numerous physical and biochemical interactions between the RPE and photoreceptors, there is no physical connection between the 2 tissues. Separation of the RPE from the neurosensory retina is called *retinal detachment.*

Contiguous RPE cells are firmly attached by a series of lateral junctional complexes. The *zonulae occludentes* and *zonulae adherentes* not only provide structural stability but also play an important role in maintaining the outer blood–ocular barrier (see Chapter 13). The zonula occludens is the junction at which adjacent plasma membranes are fused, forming a circular band or belt around the surface of adjacent cells. A small intercellular space is present between zonulae adherentes.

These junctions establish polarity of molecules within the apical and basal cell membranes, while limiting paracellular transport. This allows the RPE to regulate the transfer of nutrients and macromolecules between the choriocapillaris and outer retina. In addition, the RPE supports unidirectional flow of water (aqueous humor) across the retina and into the choroid.

CLINICAL PEARL

The flow of aqueous humor across the retina and into the choroid helps maintain retinal adhesion. The polarity of water transport is maintained by the tight junctions of the outer blood–retinal barrier and both active and passive processes that direct the flow. In cases of retinal tears (with or without retinal detachment), there is increased flow of aqueous humor across the retinal break. This can lead to reduced IOP in the affected eye.

RPE cell diameter varies from 10–14 μm in the macula to 60 μm in the periphery. In addition, compared with RPE cells in the periphery, RPE cells in the fovea are taller and thinner, contain more melanosomes, and have larger melanosomes. These characteristics account in part for the decreased transmission of choroidal fluorescence observed during fundus fluorescein angiography in the macula.

The eye of a fetus or infant contains between 4 and 6 million RPE cells. Although the surface area of the eye increases appreciably with age, the increase in the number of RPE cells is relatively small. No mitotic figures are apparent within the RPE of the healthy adult eye.

The cytoplasm of the RPE cells contains multiple round and ovoid pigment granules *(melanosomes*; see Chapter 13). These organelles develop in situ during formation of the optic cup and first appear as nonmelanized premelanosomes. Their development contrasts sharply with that of the pigment granules in uveal melanocytes, which are derived from the neural crest and later migrate into the uvea.

CLINICAL PEARL

Loss of melanin production within the RPE and melanocytes within the choroid and iris occurs in patients with ocular and oculocutaneous albinism. Absence of melanin during development can lead to improper neuronal migration and development. In addition, lack of pigmentation within the posterior segment can impair uptake during laser photocoagulation.

RPE cells also possess phagocytic function; they continually ingest the disc membranes shed by the outer segments of photoreceptor cells, enclosing them within *phagosomes*. Several stages of disintegration are evident at any given time. In some species, shedding and degradation of the membranes of rod and cone outer segments follow a diurnal rhythm synchronized with daily fluctuations of environmental light.

Lipofuscin granules within the RPE probably arise from the discs of photoreceptor outer segments and represent residual bodies from phagosomal activity. This so-called "wear-and-tear" pigment is less electron-dense than are the melanosomes, and its concentration increases gradually with age. Clinically, these lipofuscin granules are responsible for the signal observed with fundus autofluorescence imaging.

CLINICAL PEARL

Throughout life, incompletely digested residual bodies, lipofuscin, phagosomes, and other material are excreted beneath the basal lamina of the RPE. These contribute to the formation of *drusen,* which are accumulations of this extracellular material. Drusen can vary in size and are commonly classified by their ophthalmoscopic appearance as hard or soft. They are typically located between the basement membrane of RPE cells and the inner collagenous zone of Bruch membrane. Large soft drusen are associated with intermediate-stage age-related macular degeneration.

The cytoplasm of the RPE cell contains numerous mitochondria (involved in aerobic metabolism), rough-surfaced endoplasmic reticulum, a Golgi apparatus, and a large round nucleus (see Chapter 13). The RPE utilizes all methods of glucose metabolism to generate energy and nicotinamide adenine dinucleotide phosphate (NADPH). The latter assists the RPE in managing reactive oxygen species and regulating oxidative stress. See Chapter 13 for further discussion of the biochemistry of the RPE and Chapter 14 for further discussion of reactive oxygen species and oxidative stress.

Bruch Membrane

Bruch membrane is a PAS-positive lamina resulting from the fusion of the basal laminae of the RPE and the choriocapillaris of the choroid. It extends from the margin of the optic nerve head to the ora serrata. Ultrastructurally, Bruch membrane consists of 5 elements:

- basal lamina of the RPE
- inner collagenous zone
- relatively thick, porous band of elastic fibers
- outer collagenous zone
- basal lamina of the choriocapillaris

It is highly permeable to small molecules such as fluorescein. Defects in the membrane may develop in myopia, pseudoxanthoma elasticum, trauma, or inflammatory conditions and may, in turn, lead to the development of choroidal neovascularization. With age, debris accumulates in and thickens Bruch membrane.

Ora Serrata

The ora serrata separates the retina from the pars plana. Its distance from the Schwalbe line is between 5.75 mm nasally and 6.50 mm temporally. In eyes with myopia, this distance is greater; in hyperopia, shorter. Externally, the ora serrata lies beneath the spiral of Tillaux (see Chapter 1, Fig 1-18).

At the ora serrata, the diameter of the eye is 20 mm and the circumference is 63 mm; at the equator, the diameter is 24 mm and the circumference is 75 mm. Topographically, the margin of the ora serrata is relatively smooth temporally and serrated nasally. Retinal blood vessels end in loops before reaching the ora serrata.

The ora serrata is in a watershed area between the anterior and posterior vascular systems, which may in part explain why peripheral retinal degeneration is relatively common. The peripheral retina in the region of the ora serrata is markedly attenuated. The photoreceptors are malformed, and the overlying retina frequently appears cystic in paraffin sections (Blessig-Iwanoff cysts; Fig 2-51).

Vitreous

The vitreous cavity occupies four-fifths of the volume of the globe. The transparent vitreous humor is important to the metabolism of the intraocular tissues because it provides a route for metabolites used by the lens, ciliary body, and retina. The volume of the vitreous itself is close to 4.0 mL. Although 99% of its volume is water, its viscosity is approximately twice that of water, giving it a gel-like consistency. The viscosity is a result of the presence of the mucopolysaccharide hyaluronic acid (Fig 2-52).

At the ultrastructural level, fine collagen fibrils (chiefly type II) and cells have been identified in the vitreous. The origin and function of these cells, termed *hyalocytes,* are

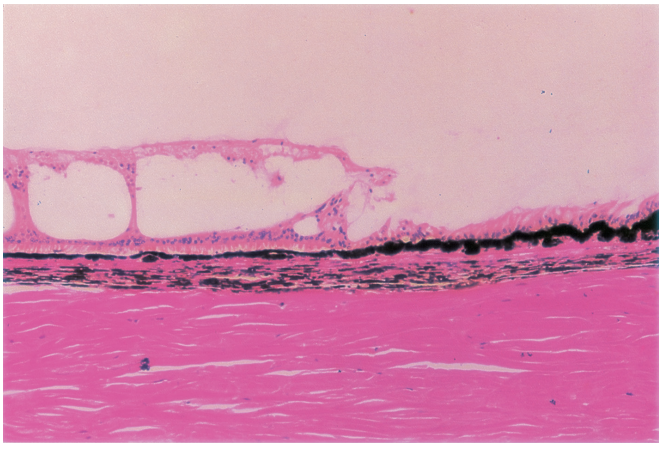


Figure 2-51 Ora serrata. Note the malformed appearance of the peripheral retina and the cystic changes at the junction between the pars plana and the retina (hematoxylin-eosin stain ×32). *(Courtesy of Thomas A. Weingeist, MD, PhD.)*

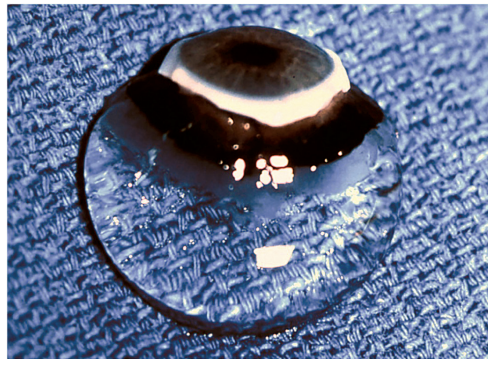


Figure 2-52 Vitreous. Gross photograph of the vitreous with the sclera, choroid, and retina removed from the eye of a 9-month-old child. *(Modified from Sebag J. Posterior vitreous detachment.* Ophthalmology. *2018;125(9):Fig 1.)*

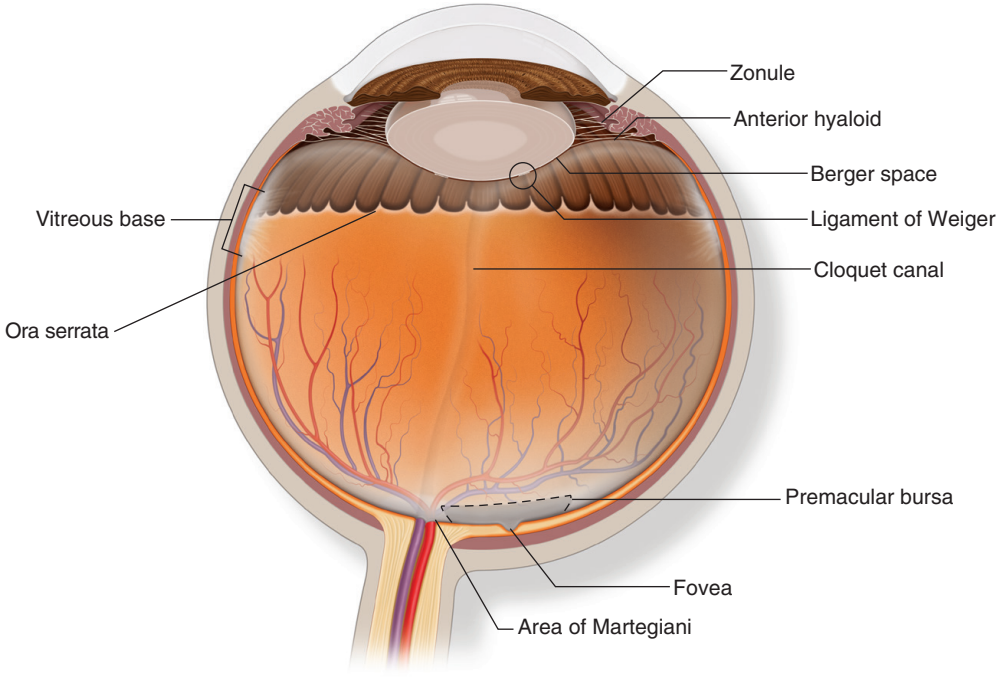


Figure 2-53 Vitreous. The vitreous is most firmly attached to the retina at the vitreous base, which straddles the ora serrata. Additional adhesions exist at the posterior lens capsule (hyaloideocapsular ligament; also known as *ligament of Weiger*), along the retinal vessels, at the perimacular region, and at the optic nerve margin. A prominent area of liquefaction of the premacular vitreous gel is called the *premacular bursa,* or *precortical vitreous pocket. (Illustration by Mark Miller.)*

unknown, but they probably represent modified histiocytes, glial cells, or fibroblasts. The fibrils at the vitreous base merge with the basal lamina of the nonpigmented epithelium of the pars plana and, posteriorly, with the ILM of the retina, the vitreoretinal interface.

The vitreous adheres to the retina peripherally at the vitreous base (Fig 2-53), which extends from 2.0 mm anterior to the ora serrata to approximately 4.0 mm posterior to it.

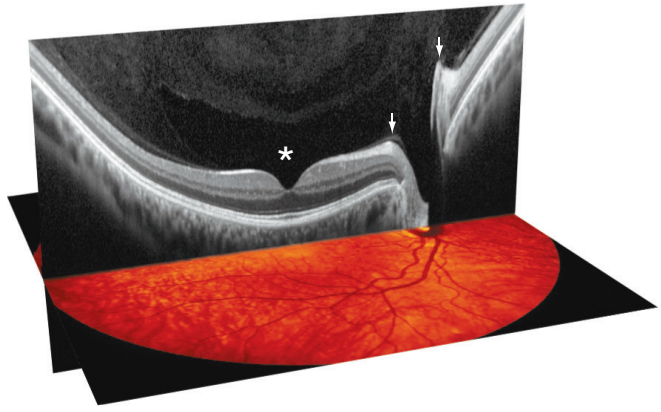


Figure 2-54 Posterior vitreous attachments. OCT image of the fovea and overlying vitreous. Note the adhesion of the vitreous at the margins of the optic nerve *(arrows)* and fovea (perimacular), with overlying premacular bursa *(*)*. *(Courtesy of Vikram S. Brar, MD.)*

Additional attachments exist at the optic nerve head margin, at the perimacular region surrounding the fovea (Fig 2-54), along the retinal vessels, and at the periphery of the posterior lens capsule. See Chapter 11 for further discussion of the vitreous.

Lund-Andersen H, Sander B. The vitreous. In: Levin LA, Nilsson SFE, Ver Hoeve J, Wu SM. *Adler's Physiology of the Eye.* 11th ed. Elsevier/Saunders; 2011:164–181.

CHAPTER 3

Cranial Nerves: Central and Peripheral Connections

This chapter includes related videos. Go to www.aao.org/bcscvideo_section02 or scan the QR codes in the text to access this content.

Highlights

- Cranial nerve (CN) II, the optic nerve, is the only cranial nerve to arise directly from the diencephalon and thus is covered by dura in its extracranial portion.
- CN III—CN III subnuclei supply their respective ipsilateral extraocular muscles. Exceptions are the subnucleus for the superior rectus muscle, which innervates the contralateral superior rectus; and the single, central levator palpebrae subnucleus, which supplies both levator muscles.
- CN IV fascicles completely decussate after leaving the nucleus, thus innervating the contralateral superior oblique muscle. CN IV has the longest intracranial course and is the only CN to exit dorsally from the brainstem.
- CN V, the largest of the CNs, provides sensation to the face and eye, as well as other structures of the head. In orbital floor fractures, the maxillary division can be damaged, leading to dysesthesia in the CN V_2 dermatome.
- CN VI is susceptible to injury from increased intracranial pressure between its point of exit at the pontomedullary junction and where it traverses the Dorello canal formed by the petroclinoid ligament.
- CN VII provides the efferent limb of the tear reflex.

Figure 3-1 depicts cranial nerves I–VI in relation to the bony canals and arteries at the base of the skull. In Figure 3-2, the nerves are shown in relation to the brainstem, cavernous sinus, and orbit. For further study, see BCSC Section 5, *Neuro-Ophthalmology,* which describes these nerves as they apply to specific clinical entities.

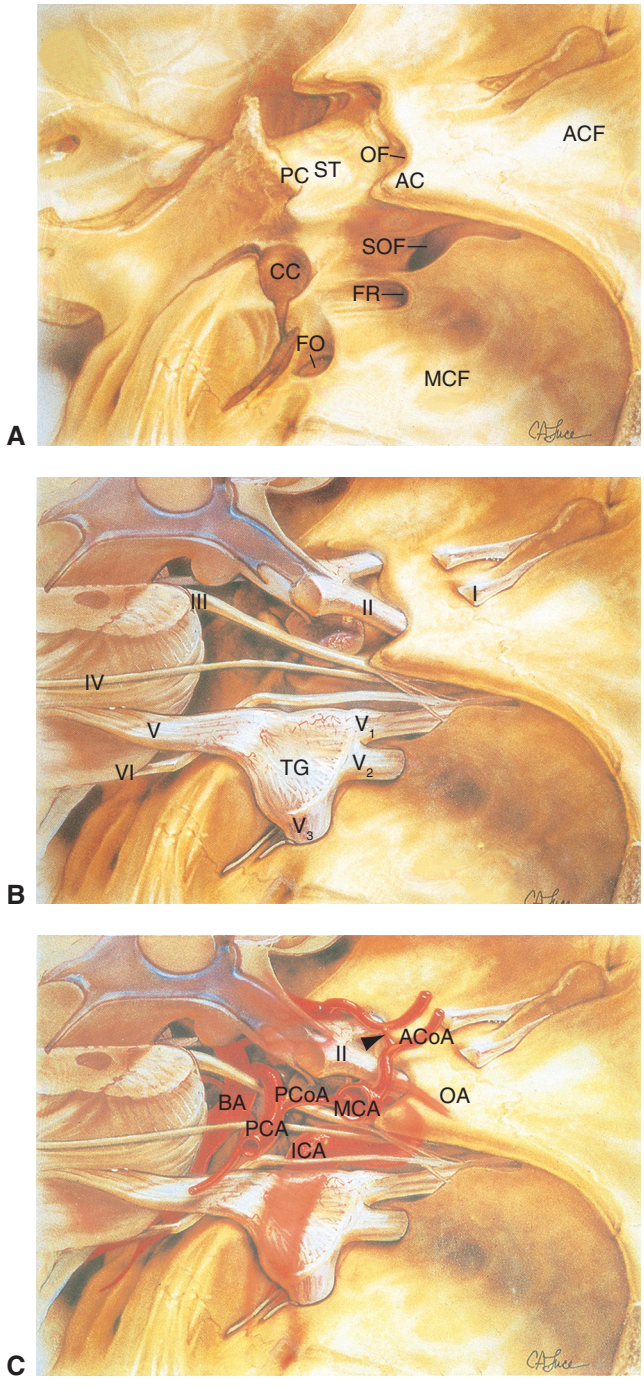


Figure 3-1 View from the right parietal bone looking downward into the skull base. Various anatomical relationships are shown at the base of the skull. The orbits are located to the right, out of the picture (the roof of the orbits is just visible). The floor of the right middle cranial fossa is in the lower part. **A,** The relationship between the bony canals is shown. AC = anterior clinoid; ACF = anterior cranial fossa; CC = carotid canal; FO = foramen ovale; FR = foramen rotundum; MCF = middle cranial fossa; OF = optic foramen; PC = posterior clinoid; SOF = superior orbital fissure; ST = sella turcica. **B,** The relationship between the cranial nerves (with trigeminal ganglion) is depicted. I = olfactory nerve; II = optic nerve; III = oculomotor nerve; IV = trochlear nerve; V = trigeminal nerve, with ophthalmic (V_1), maxillary (V_2), and mandibular (V_3) divisions; VI = abducens nerve; TG = trigeminal ganglion. **C,** The relationship between the arteries is demonstrated. ACoA (and *arrowhead*) = anterior communicating artery; BA = basilar artery; ICA = internal carotid artery; MCA = middle cerebral artery; OA = ophthalmic artery; PCA = posterior cerebral artery; PCoA = posterior communicating artery; II = optic nerve. *(Reproduced with permission from Zide BM, Jelks GW, eds.* Surgical Anatomy of the Orbit. *Raven; 1985:68–69.)*

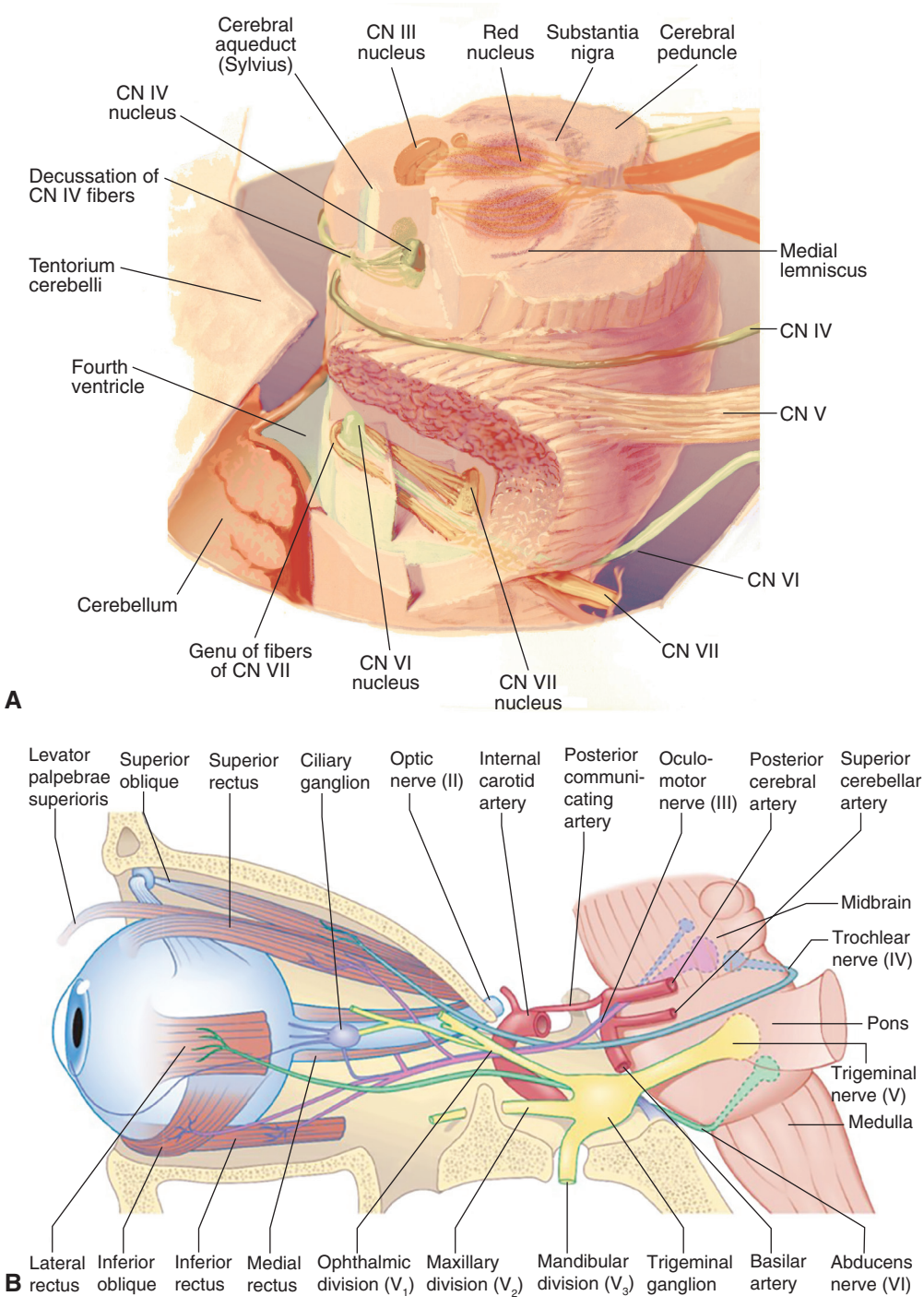


Figure 3-2 Cranial nerves from midbrain to orbit. **A,** Intra-axial course of cranial nerves (CNs) II–VI at the level of the midbrain *(above)* and pons *(below).* Note the relationship to the surrounding cerebellum and CNs V and VII. CN IV has the longest intracranial course and is the only CN that decussates and exits the midbrain dorsally. **B,** Schematic of CNs II–VI from the brainstem to the orbit. *(Part A illustration by Craig A. Luce. Part B modified from Friedman NJ, Kaiser PK, Trattler WB.* Review of Ophthalmology. *3rd ed. Elsevier; 2018:63. Used with permission of Peter K. Kaiser, MD.)*

Olfactory Nerve (First Cranial Nerve)

The olfactory nerve (cranial nerve [CN] I) originates from small olfactory receptors in the mucous membrane of the nose. Unmyelinated CN I fibers pass from these receptors in the nasal cavity through the cribriform plate of the ethmoid bone and enter the ventral surface of the olfactory bulb, where they form the nerve.

The olfactory tract runs posteriorly from the bulb beneath the frontal lobe of the brain in a groove (or sulcus) and lateral to the gyrus rectus (Fig 3-3). The gyrus rectus forms the anterolateral border of the suprasellar cistern. Meningiomas arising from the arachnoid cells in this area can cause important ophthalmic signs and symptoms associated with loss of olfaction.

CLINICAL PEARL

Foster-Kennedy syndrome most commonly arises from meningiomas in the region of the gyrus rectus where the optic chiasm and olfactory nerve are in proximity (see Fig 3-3B). These lesions lead to unilateral optic disc edema with contralateral optic atrophy, as well as anosmia (loss of smell) due to involvement of the nearby olfactory nerve.

Optic Nerve (Second Cranial Nerve)

The optic nerve (CN II) consists of more than 1 million axons that originate in the ganglion cell layer of the retina and extend toward the lateral geniculate nucleus. The optic nerve begins anatomically at the optic nerve head (ONH) but physiologically and functionally within the ganglion cell layer and nerve fiber layer (NFL) that cover the entire retina and continue to the optic chiasm. It may be divided into the following 4 topographic areas (Fig 3-4, Table 3-1):

- intraocular region (ONH, consisting of the NFL [optic disc], prelaminar area, laminar area, and retrolaminar area)
- intraorbital region (located within the muscle cone)
- intracanalicular region (located within the optic canal)
- intracranial region (ending at the optic chiasm)

The optic nerve originates directly from the diencephalon and, developmentally, is part of the brain and central nervous system. Its fibers are surrounded not by Schwann cells but by myelin produced by oligodendrocytes. The intraorbital portion is approximately 25–30 mm long, which is greater than the distance between the back of the globe and the optic canal (18 mm). For this reason, when the eye is in the primary position, the optic nerve runs a sinuous course. Axial proptosis secondary to thyroid eye disease or a retrobulbar tumor will first lead to straightening of the intraorbital optic nerve. Further elongation can lead to stretching of the optic nerve, which may cause chronic nerve injury and optic neuropathy.

Biousse V, Newman NJ. Ischemic optic neuropathies. *N Engl J Med.* 2015;372(25):2428–2436.
Rose GE, Vahdani K. Optic nerve stretch is unlikely to be a significant causative factor in dysthyroid optic neuropathy. *Ophthalmic Plast Reconstr Surg.* 2020;36(2):157–163.

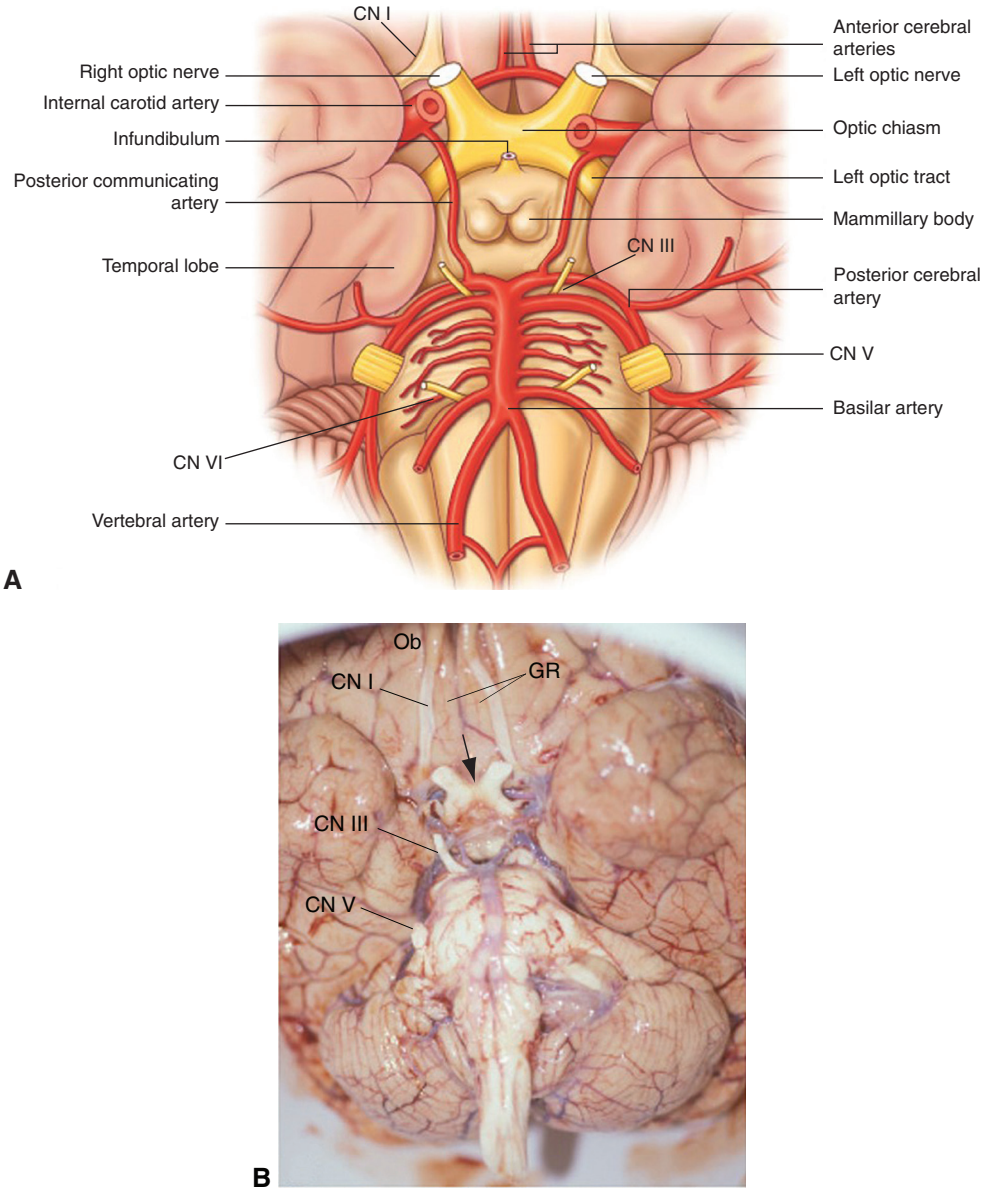


Figure 3-3 Optic chiasm and circle of Willis. **A,** Schematic of the optic chiasm and circle of Willis. Note the relationship of various CNs and adjacent blood vessels. **B,** Photograph of the optic chiasm *(arrow)* in a human brain. CN I = olfactory nerve; CN III = oculomotor nerve; CN V = trigeminal nerve; CN VI = abducens nerve; GR = gyrus rectus; Ob = olfactory bulb. *(Modified with permission from Liu GT, Volpe NJ, Galetta SL.* Neuro-Ophthalmology: Diagnosis and Management. *2nd ed. Elsevier; 2010:238.)*

Intraocular Region

The ONH is the principal site of many congenital and acquired ocular diseases. Its anterior surface is visible ophthalmoscopically as the *optic disc*, an oval structure whose size reflects

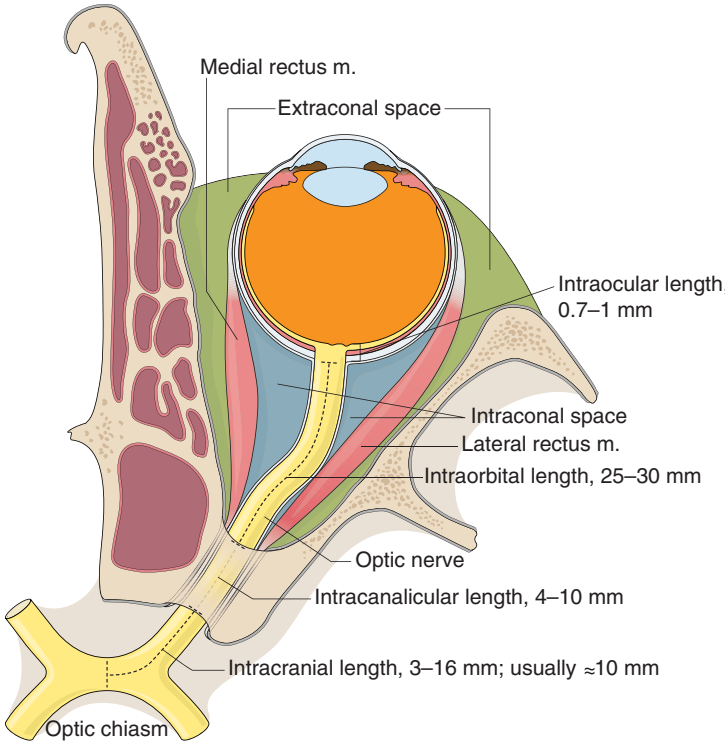


Figure 3-4 The optic nerve. Schematic of the 4 segments of the optic nerve: intraocular, intraorbital, intracanalicular, intracranial. The intraconal *(blue)* and extraconal *(green)* spaces are also depicted. m. = muscle. *(Illustration by Mark Miller.)*

some ethnic and racial variance. The size of the ONH varies widely, averaging 1.76 mm horizontally and 1.92 mm vertically. The central depression, or *cup,* is located slightly temporal to the geometric center of the nerve head and represents an axon-free region. The main branches of the central retinal artery (CRA) and the central retinal vein (CRV) pass through the center of the cup.

The ONH can be divided into 4 topographic areas (Fig 3-5):

- superficial NFL (optic disc)
- prelaminar area
- laminar area
- retrolaminar area

These are discussed in the following sections. *Note:* The term *optic disc* has been used interchangeably in the literature to refer to the superficial NFL and the prelaminar area, or to the entire ONH. This book uses the term *optic nerve head* to refer to all 4 parts.

Garway-Heath DF, Wollstein G, Hitchings RA. Aging changes of the optic nerve head in relation to open angle glaucoma. *Br J Ophthalmol.* 1997;81(10):840–845.

Jonas JB, Gusek GC, Naumann GO. Optic disc, cup, and neuroretinal rim size, configuration and correlations in normal eyes. *Invest Ophthalmol Vis Sci.* 1988;29(7):1151–1158.

Table 3-1 Regional Differences in the Optic Nerve [a]

Segment	Length, mm	Diameter, mm	Blood Supply
Intraocular	0.7–1		Varies by segment
NFL/optic disc [b]		1.76 (horizontal)	CRA
		1.92 (vertical)	Branches of posterior ciliary arteries
Prelaminar			Short posterior ciliary arteries
			Cilioretinal arteries, if present
Laminar			Branches of arterial circle of Zinn-Haller, which arises from the para-optic branches of the short posterior ciliary arteries
Retrolaminar		3	Primary: Pial vessels and short posterior ciliary vessels
			Secondary: CRA and recurrent choroidal arteries
Intraorbital	25–30	3–4	
Distal			Intraneural branches of CRA
Proximal			Pial vessels and branches of ophthalmic artery
Intracanalicular	≈4–10		Branches of ophthalmic artery
Intracranial	3–16, usually ≈10	4–7	Branches of ophthalmic artery, anterior cerebral artery, and superior hypophysial artery

CRA = central retinal artery; NFL = nerve fiber layer.

[a] See also Figure 3-4.

[b] The optic disc refers to the anterior surface of the optic nerve head that is appreciated during clinical examination. It contains the superficial NFL.

Superficial nerve fiber layer

As the unmyelinated ganglion cell axons enter the nerve head, they retain their retinotopic organization, with fibers from the upper retina superiorly and those from the lower retina inferiorly. Fibers from the temporal retina are lateral; those from the nasal side are medial. Macular fibers, which constitute approximately one-third of the nerve, occupy the immediate temporal aspect of the ONH. All other temporal fibers with origins distal to the macula are laterally displaced above or below the macular fibers (Fig 3-6).

Prelaminar area

The ganglion cell axons that enter the nerve head are supported by a "wicker basket" of astrocytic glial cells and are segregated into bundles, or *fascicles,* that pass through the lamina cribrosa (see Fig 3-5). These astrocytes invest the optic nerve and form continuous circular tubes that enclose groups of nerve fibers throughout their intraocular and intraorbital course, separating them from connective tissue elements at all sites. At the edge of the nerve head, the Müller cells that make up the internal limiting membrane (ILM) are replaced by astrocytes. Astrocytes constitute 10% of the nerve head volume and form a membrane that not only covers the surface of the nerve head but is continuous with the ILM of the retina.

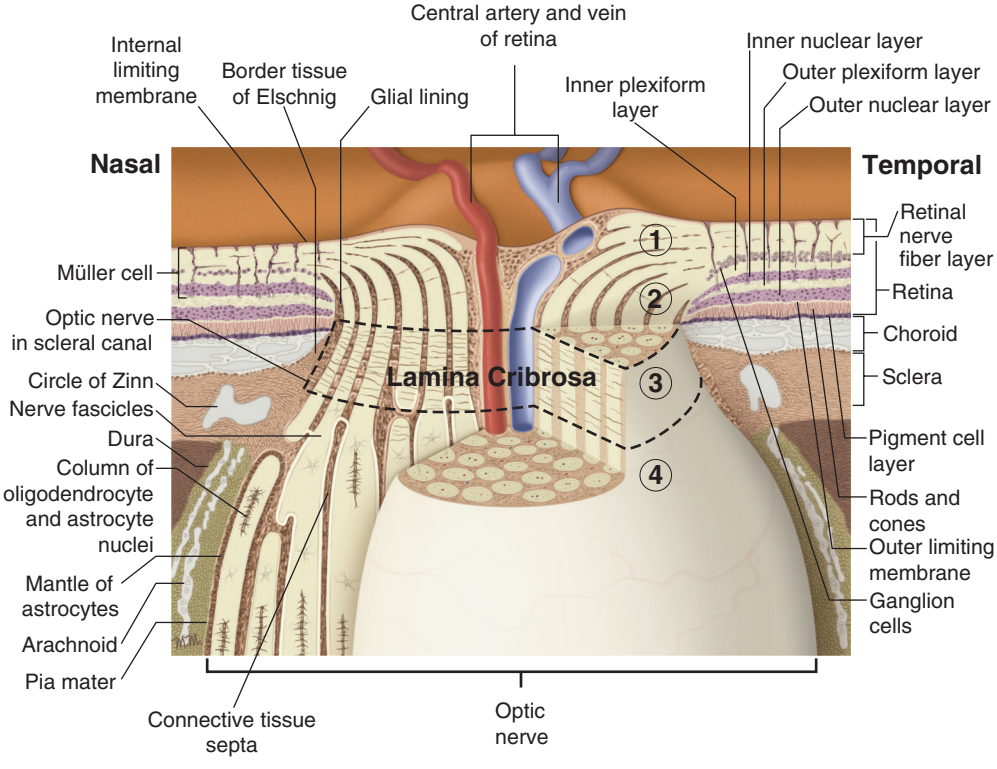


Figure 3-5 Schematic representation of the optic nerve head (ONH). The temporal retina has a thicker layer of ganglion cells, representing the increased ganglion cell concentration found in the macula. Müller glia traverse the neural retina to provide both structural and functional support. Where the retina terminates at the ONH edge, the Müller cells are continuous with the astrocytes, forming the internal limiting membrane. The border tissue of Elschnig is the dense connective tissue that joins the sclera with the Bruch membrane, enclosing the choroid and forming the scleral ring that defines the margin of the ONH. At the posterior termination of the choroid on the temporal side, the border tissue of Elschnig lies between the astrocytes surrounding the optic nerve canal and the stroma of the choroid. On the nasal side, the choroidal stroma is directly adjacent to the astrocytes surrounding the nerve. This collection of astrocytes surrounding the canal is known as the *border tissue,* which is continuous with a similar glial lining at the termination of the retina. The nerve fibers of the retina are segregated into approximately 1000 fascicles by astrocytes. On reaching the lamina cribrosa *(upper dashed line),* the nerve fascicles and their surrounding astrocytes are separated from each other by connective tissue. The lamina cribrosa is an extension of scleral collagen and elastic fibers through the nerve. The external choroid also sends some connective tissue to the anterior part of the lamina. At the external part of the lamina cribrosa *(lower dashed line),* the nerve fibers become myelinated, and columns of oligodendrocytes and a few astrocytes are present within the nerve fascicles. The bundles continue to be separated by connective tissue septa (derived from pia mater and known as *septal tissue*) all the way to the chiasm. A mantle of astrocytes, continuous anteriorly with the border tissue, surrounds the nerve along its orbital course. The dura, arachnoid, and pia mater are shown. The nerve fibers are myelinated. Within the bundles, the cell bodies of astrocytes and oligodendrocytes form a column of nuclei. The central retinal vessels are surrounded by a perivascular connective tissue throughout its course in the nerve. This connective tissue, known as the *central supporting connective tissue strand,* blends with the connective tissue of the lamina cribrosa. 1 = superficial nerve fiber layer; 2 = prelaminar area; 3 = laminar area; 4 = retrolaminar area. *(Illustration by Mark Miller.)*

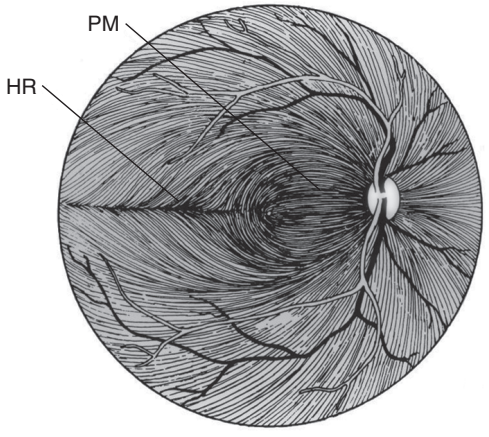


Figure 3-6 The pattern of the nerve fiber layer of axons from retinal ganglion cells to the ONH. Temporal axons originate above and below the horizontal raphe (HR) and take an arching course to the ONH. Axons arising from ganglion cells in the nasal macula project directly to the ONH as the papillomacular bundle (PM). *(Reproduced from Kline LB, Foroozan R, eds.* Optic Nerve Disorders. *2nd ed. Ophthalmology Monographs 10. Oxford University Press, in cooperation with the American Academy of Ophthalmology; 2007:5.)*

The pigment epithelium may be exposed at the temporal margin of the ONH to form a narrow, pigmented crescent. When the pigment epithelium and choroid fail to reach the temporal margin, crescents of partial or absent pigmentation may be noted. The relationship between the choroid and the prelaminar portion of the optic nerve partly accounts for the staining of the ONH normally observed in late phases of fluorescein fundus angiography. The ONH vessels do not leak, but the choroidal capillaries are freely permeable to fluorescein, which can therefore diffuse into the adjacent optic nerve layers.

Laminar area

The *lamina cribrosa* comprises approximately 10 connective tissue plates, which are integrated with the sclera and whose pores transmit the unmyelinated axon bundles of the retinal ganglion cells before they exit as the optic nerve. The openings are wider superiorly than inferiorly, which may imply less protection from the mechanical effects of pressure in glaucoma. The lamina contains type I and type III collagens, abundant elastin, laminin, and fibronectin. Astrocytes surround the axon bundles, and small blood vessels are present.

The lamina cribrosa serves 3 functions:

- scaffold for the optic nerve axons
- point of fixation for the CRA and CRV
- reinforcement of the posterior segment of the globe

Optical coherence tomography and scanning laser ophthalmoscopy help facilitate anatomical study of the lamina cribrosa in pathologic states such as glaucoma and retinal vascular disease.

CLINICAL PEARL

Enucleation may be considered in eyes with large retinoblastoma burden with continued progression despite conservative treatments. The goal of the procedure is to remove as much of the optic nerve as possible in an effort to ensure that the cut end is free from tumor. Postlaminar invasion of the optic nerve is 1 of the pathologic risk factors that determines whether there is extraocular spread.

Retrolaminar area

As a result of myelination of the nerve fibers and the presence of oligodendroglia and the surrounding meningeal sheaths (dural, arachnoid, and pial) (see Figs 3-5, 3-7), the diameter of the optic nerve increases to 3 mm behind the lamina cribrosa. The axoplasm of the neurons contains neurofilaments, microtubules, mitochondria, and smooth endoplasmic reticulum. The retrolaminar nerve transitions to the intraorbital part of the optic nerve.

Intraorbital Region

The intraorbital portion is the longest segment of the optic nerve and takes a sinusoidal path from the posterior aspect of the globe to the orbital apex, where it exits the orbit through the annulus of Zinn to enter the optic canal. Throughout its course, the intraorbital optic nerve remains within the muscle cone and encased by the optic nerve sheath.

Optic nerve sheath (meningeal sheath)

Embryologically, the optic nerve directly emerges from the diencephalon. Thus, the meningeal sheath that surrounds the brain and central nervous system extends to cover the extracranial optic nerve until it fuses with the posterior sclera. The meningeal layers surround the intraorbital and intracanalicular regions of the optic nerve, forming the optic nerve sheath (Fig 3-7).

The optic nerve sheath or meningeal sheath consists of the dura mater (external sheath), arachnoid mater (middle sheath), and pia mater (internal sheath). The pia mater is closely attached to and creates numerous septa in the optic nerve; however, a subdural and subarachnoid space exists beneath those respective meningeal layers. The subarachnoid space that surrounds the optic nerve runs continuous with the subarachnoid space of the brain. Thus, an increase in intracranial pressure (ICP) is also transmitted to the relevant portions of the optic nerve, leading to papilledema.

CLINICAL PEARL

Optic nerve sheath fenestration of the intraorbital optic nerve is performed in certain cases to relieve elevated ICP and limit further optic nerve damage.

The *dural sheath* of the optic nerve, also known as the external sheath, is the outermost meningeal sheath and is continuous with the dura mater in the brain. It is 0.3–0.5 mm thick and consists of dense bundles of collagen and elastic tissue that fuse anteriorly with the outer layers of the sclera. The subdural space is not continuous with the subdural space around the brain.

The *arachnoid sheath* (middle sheath), which is composed of collagenous tissue and small amounts of elastic tissue, lines the dural sheath and is connected to the internal sheath across the subarachnoid space by vascular trabeculae. The subarachnoid space around the optic nerve ends anteriorly at the level of the lamina cribrosa and, as previously mentioned, is continuous with the subarachnoid space of the brain.

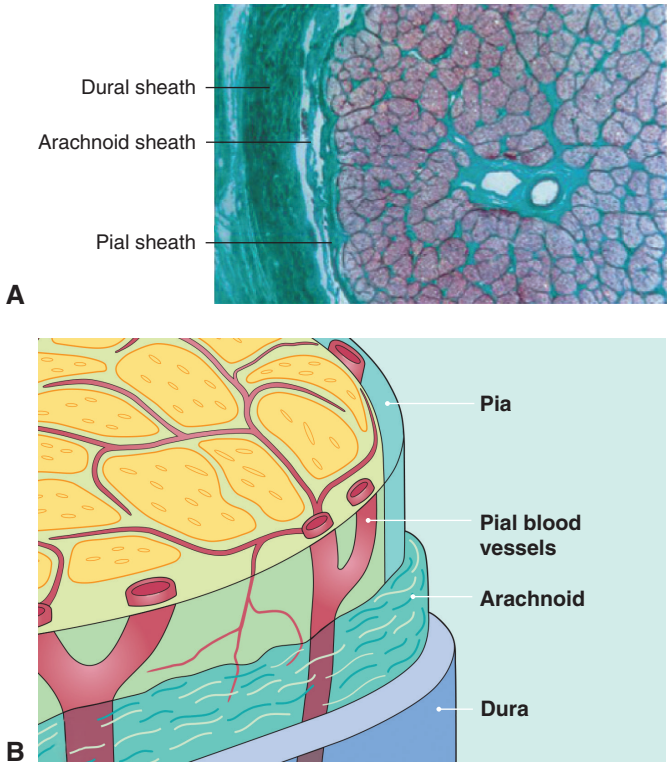


Figure 3-7 Optic nerve sheath. **A,** Photomicrograph. The dural sheath, which is the outer layer, is composed of collagenous connective tissue. The arachnoid sheath, the middle layer, is made up of fine collagenous fibers arranged in a loose meshwork. The pial sheath, the innermost layer, is made up of fine collagenous and elastic fibers and is highly vascularized. Note the pial septa separating the optic nerve into fascicles. These septa contain both connective tissue and vascular elements (Masson trichrome stain, ×64). **B,** Diagram of the optic nerve sheath. Note the close relationship of the pia with the optic nerve and penetrating pial vessels extending along the septa. *(Part A courtesy of Thomas A. Weingeist, MD, PhD; part B reproduced with permission from Salmon JF.* Kanski's Clinical Ophthalmology: A Systematic Approach. *9th ed. Elsevier; 2020:751.)*

CLINICAL PEARL

Because the central retinal vessels cross the subarachnoid space, a rise in ICP can compress the CRV and raise the venous pressure within the retina above the intraocular pressure. This situation causes intraocular venous dilatation and the loss of spontaneous venous pulsation (SVP) at the nerve head (Video 3-1). The presence of SVP indicates normal ICP. However, some individuals have normal ICP and absent SVP. Thus, the loss of previously documented SVP is more indicative of elevated ICP.

VIDEO 3-1 Spontaneous venous pulsations.
Courtesy of Vikram S. Brar, MD.

The innermost meningeal sheath of the optic nerve, the *pial sheath*, is continuous with the pia mater and parts of the arachnoid mater. Both the pia and arachnoid layers contain meningothelial cells, which function in phagocytosis, produce collagen, and participate in wound healing. The meningothelial cells, specifically those of the arachnoid mater, can give rise to optic nerve sheath meningioma.

The pial sheath is a vascular connective tissue coat that sends numerous septa into the optic nerve, dividing its axons into bundles. The septa contain collagen, elastic tissue, fibroblasts, nerves, and small arterioles and venules (see Fig 3-7B). They provide mechanical support for the nerve bundles and nutrition to the axons and glial cells. A mantle of astrocytic glial cells prevents the pia and septa from having direct contact with nerve axons. The septa continue throughout the intraorbital and intracanalicular regions of the nerve and end just before the chiasm. The meninges of the optic nerve are supplied by sensory nerve fibers, which account in part for the pain experienced by patients with retrobulbar neuritis or other inflammatory optic nerve diseases.

Annulus of Zinn

The intraorbital optic nerve lies entirely within the muscle cone. Before passing into the optic canal, the nerve is surrounded by the annulus of Zinn, which is formed by the origins of the rectus muscles. The superior and medial rectus muscles partially share a connective tissue sheath with the optic nerve at this location. This connection may also partially explain why patients with retrobulbar neuritis report symptoms of pain on eye movement. After exiting the orbit, the optic nerve enters the optic canal, which is housed within the lesser wing of the sphenoid bone.

Intracanalicular Region

The optic nerve and surrounding arachnoid sheath are tethered to the periosteum of the bony canal in the intracanalicular region. In blunt trauma, particularly over the eyebrow, the force of injury can be transmitted to the intracanalicular region, causing shearing and interruption of the blood supply to the nerve in this area. Such nerve damage is called *indirect traumatic optic neuropathy.* In addition, optic nerve edema, air, or blood in this area can lead to a compartment syndrome, further compromising the function of the optic nerve within the confined space of the optic canal.

Intracranial Region

After passing through the optic canals, the 2 optic nerves lie superior to the ophthalmic arteries and superior and medial to the *internal carotid arteries* (*ICAs;* see Fig 3-3A). The anterior cerebral arteries cross over the optic nerves and are connected by the anterior communicating artery, which completes the anterior portion of the circle of Willis. The optic nerves then pass posteriorly over the cavernous sinus to join in the optic chiasm.

Visual Pathway

The visual pathway begins in the retina (Fig 3-8); impulses from the photoreceptors are transmitted to the optic chiasm via the optic nerve of each eye. Within the chiasm, the retinal

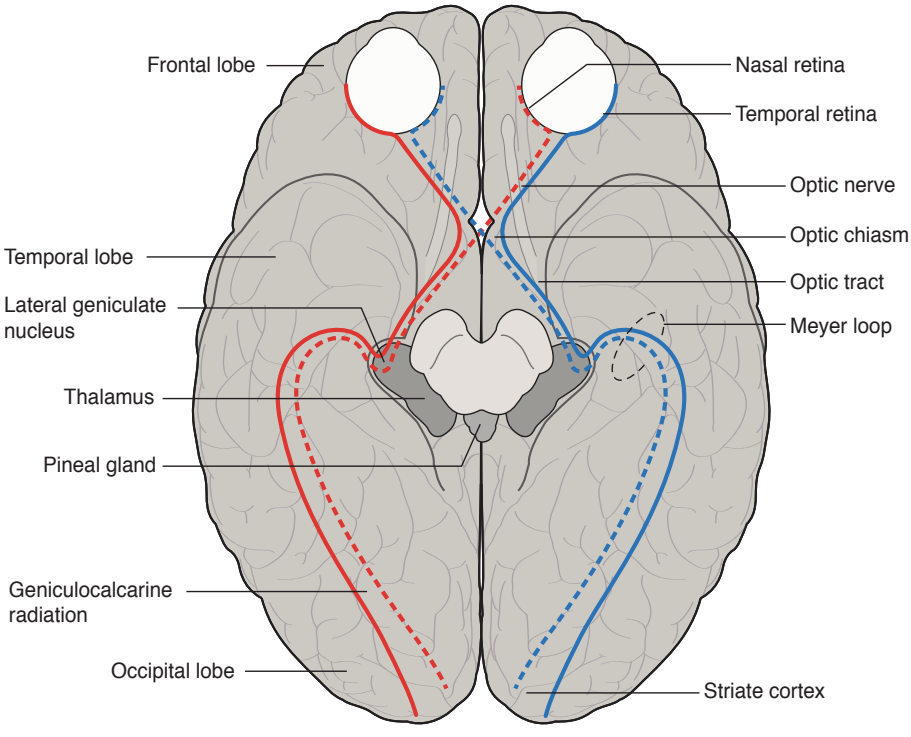


Figure 3-8 The visual pathways. *(Illustration by Mark Miller.)*

fibers segregate into the right and left optic tracts. Each optic tract carries information for its respective field of vision. For example, the right optic tract consists of fibers from the ipsilateral temporal retina and the contralateral nasal retina. The corresponding hemifields represent the left half of the visual field for each eye.

The optic tracts, whose cell bodies lie in the ganglion cell layer of the retina, go on to synapse at the lateral geniculate nucleus (see Fig 3-9). The subsequent fibers further divide as they travel to the primary visual cortex (known variously as *V1, striate cortex,* or *Brodmann area 17*), where they terminate; the most inferior of the fibers (subserving the superior visual field) course through the temporal lobe, and the more superior fibers (subserving the inferior visual field) proceed through the parietal lobe (see Fig 3-10). Lesions along the visual pathway produce characteristic visual field defects that help localize the site of damage. Structures of the visual pathway are described further in the following sections and in BCSC Section 5, *Neuro-Ophthalmology.*

Optic chiasm

The optic chiasm makes up part of the anterior inferior floor of the third ventricle of the brain. It is surrounded by pia and arachnoid mater and is richly vascularized. The chiasm is approximately 12 mm wide, 8 mm long in the anteroposterior direction, and 4 mm thick.

The extramacular fibers from the inferonasal retina cross anteriorly in the chiasm at the "Wilbrand knee" before passing into the optic tract. Extramacular superonasal fibers cross directly to the opposite tract. Extramacular temporal fibers pursue a direct course through the chiasm to the optic tract as a bundle of uncrossed fibers. The macular projections are located centrally in the optic nerve and constitute 80%–90% of the total volume of the optic nerve and the chiasmal fibers. Nasal macular fibers cross in the posterior part of the chiasm. Approximately 53% of the optic nerve fibers are crossed; the remaining 47% are uncrossed.

CLINICAL PEARL

Albinism is associated with aberrant decussation of optic nerve fibers at the chiasm. This can cause crossing of up to 90% of fibers to the contralateral side and may result in strabismus and loss of stereopsis. Aberrant decussation leads to morphologic changes in the optic chiasm, which are visible on magnetic resonance imaging.

Optic tract

Each optic tract is made up of fibers from the ipsilateral temporal retina and the contralateral nasal retina. Fibers (both crossed and uncrossed) from the upper retinal projections travel medially in the optic tract; lower projections move laterally. The macular fibers are dorsolateral within the optic tracts.

Lateral geniculate nucleus

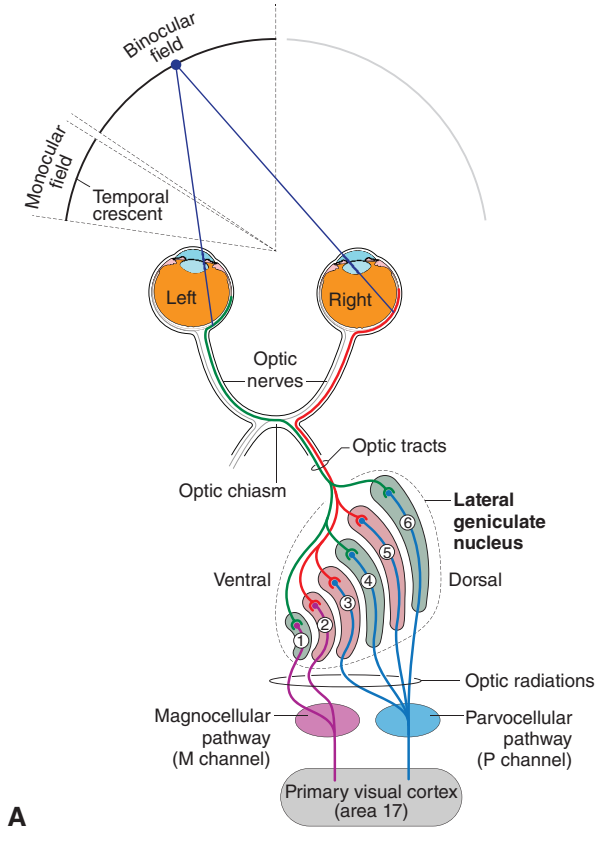
The lateral geniculate nucleus (LGN) is the synaptic zone for the higher visual projections. It is a mushroom-shaped structure in the posterior thalamus that receives approximately 70% of the optic tract fibers within its 6 alternating layers of gray and white matter (the other 30% of the fibers go to the pupillary nucleus). Layers 1, 4, and 6 of the LGN contain axons from the contralateral optic nerve. Layers 2, 3, and 5 arise from the ipsilateral optic nerve. The 6 layers, numbered consecutively from inferior to superior, give rise to the optic radiations (Fig 3-9).

Optic radiations

The optic radiations connect the LGN with the visual cortex of the occipital lobe. From the LGN, inferior fibers (which subserve the superior visual field) travel anteriorly, then laterally and posteriorly, looping around the temporal horn of the lateral ventricles in the temporal lobe (Meyer loop). Superior fibers (which subserve the inferior visual field) travel posteriorly through the parietal lobe (Fig 3-10).

Primary visual cortex

The primary visual cortex is the thinnest area of the human cerebral cortex. It has 6 cellular layers and occupies the superior and inferior lips of the calcarine fissure (also called *calcarine sulcus*) on the posterior and medial surfaces of the occipital lobes. Macular function is extremely well represented in the visual cortex and occupies the most posterior position at the tip of the occipital lobe. The most anterior portion of the calcarine fissure is occupied by contralateral nasal retinal fibers only (Fig 3-11).



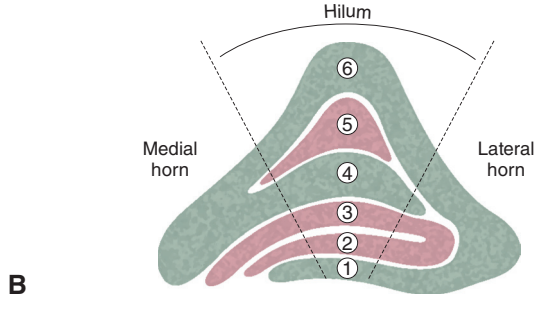
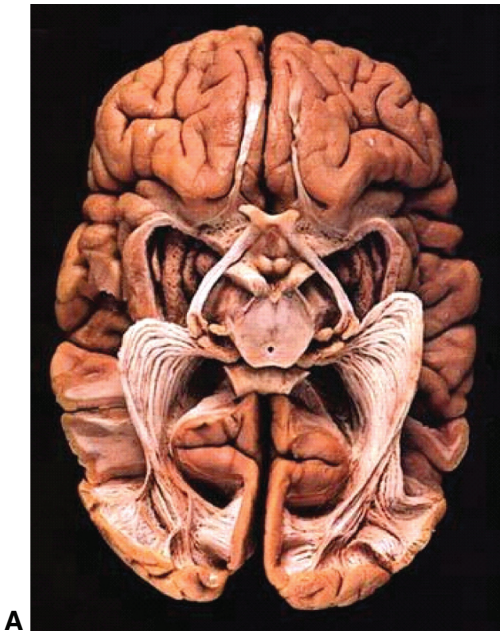
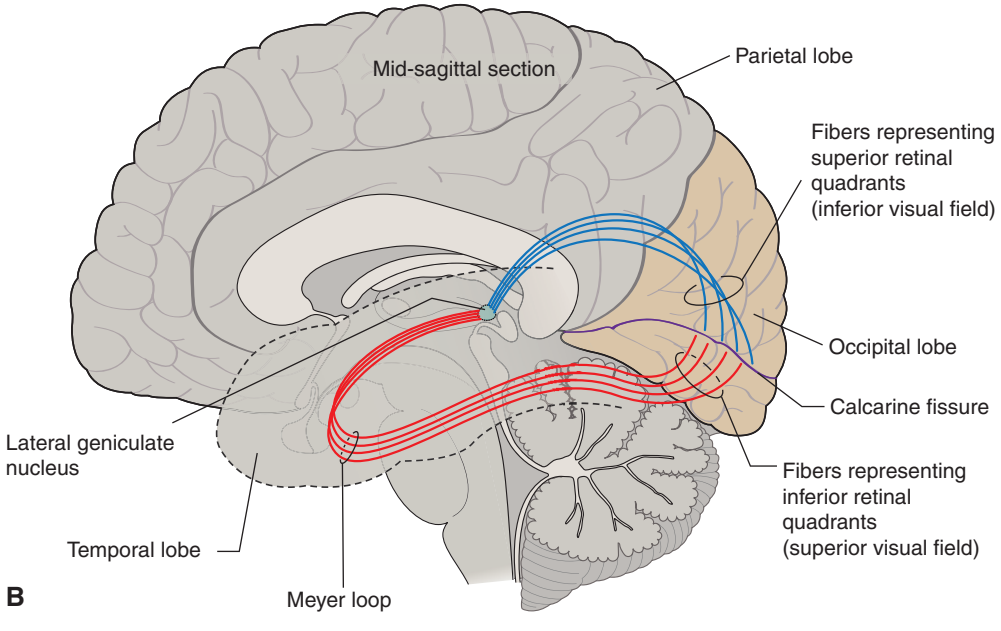


Figure 3-9 Lateral geniculate nucleus (LGN). **A,** The LGN receives the fibers of the corresponding optic tract. Layers 1, 4, and 6 receive input from the crossed fibers of the optic tract; layers 2, 3, and 5 receive input from the uncrossed fibers. Layers 1 and 2 represent the magnocellular pathways, which are concerned with detection of movement. The remaining 4 layers represent the parvocellular pathways, which are responsible for color vision and visual acuity. **B,** The hilum represents central (macular) vision and is perfused by the posterior choroidal artery, the medial horn represents inferior vision, and the lateral horn represents superior vision. These areas are perfused by the anterior choroidal artery. *(Redrawn with permission from Liu GT, Volpe NJ, Galetta SL.* Neuro-Ophthalmology: Diagnosis and Management. *2nd ed. Elsevier; 2010:299–300. Illustration by Mark Miller.)*



A



B

Figure 3-10 Optic radiations. **A,** Axial view of the brain demonstrating the optic chiasm, optic tract, and optic radiations, which connect the LGN to the occipital lobe. **B,** Schematic of the optic radiations, sagittal view. The lower radiations (subserving the superior visual field) course anteriorly before looping posteriorly in the temporal lobe. The upper radiations course dorsally in the parietal lobe to terminate in the occipital lobe above the calcarine fissure. *(Part A reproduced with permission from Sherbondy AJ, Dougherty RF, Napel S, Wandell BA. Identifying the human optic radiation using diffusion imaging and fiber tractography.* J Vis. *2008;8(10):12.1–12.11, Figure 1. Part B redrawn with permission from University of Texas at Dallas. Illustration by Mark Miller.)*

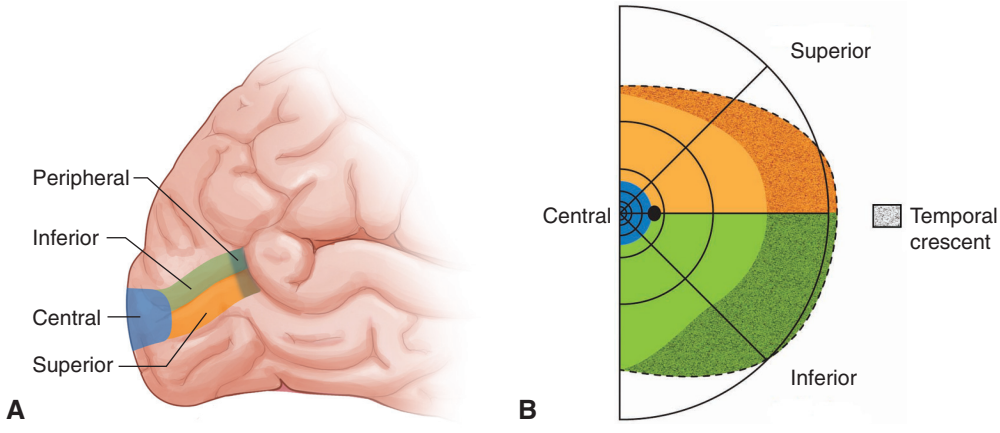


Figure 3-11 Primary visual cortex and corresponding visual field representation. **A,** Left occipital cortex showing the location of the striate cortex within the calcarine fissure. *Blue* represents the macula (central visual field); *green* represents the inferior visual field; and *orange* represents the superior visual field. The most peripheral fibers are represented by the stippled colors. **B,** Right visual hemifield, plotted with kinetic perimetry, corresponds to the regions of the striate cortex in part A. The stippled area corresponds to the monocular temporal crescent, which is mapped in the most anterior 8%, approximately, of the striate cortex. *(Illustrations by Christine Gralapp.)*

Blood Supply of the Optic Nerve and Visual Pathway

Although blood supply of the optic nerve varies widely from 1 segment of the nerve to another, a multitude of studies have revealed a basic pattern (Fig 3-12). The blood supply of the visual pathway is summarized in Table 3-2 and depicted in Figure 3-13. See also Table 3-1, which summarizes the blood supply of the prechiasmal optic nerve. The following sections discuss the vascular supply of the intraocular and intraorbital segments in greater detail.

Intraocular region

The ophthalmic artery lies inferior to the optic nerve. The CRA and, usually, 2 long posterior ciliary arteries branch off from the ophthalmic artery after it enters the muscle cone at the annulus of Zinn.

The lumen of the CRA is surrounded by nonfenestrated endothelial cells with typical zonulae occludens that are similar to those in retinal blood vessels. However, unlike retinal arterioles, the CRA contains a fenestrated internal elastic lamina and an outer layer of smooth muscle cells surrounded by a thin basement membrane. Retinal arterioles have no internal elastic lamina, and they lose their smooth muscle cells shortly after entering the retina. The CRV consists of endothelial cells, a thin basal lamina, and a thick collagenous adventitia.

The lamina cribrosa is supplied by branches of the arterial circle of *Zinn-Haller* (Fig 3-14). This circle arises from the para-optic branches of the short posterior ciliary arteries and is usually embedded in the sclera around the nerve head. It is often incomplete and may be divided into superior and inferior halves. Involvement of the inferior half is the likely cause of altitudinal (superior or inferior hemifield) visual field defects following an episode of nonarteritic anterior ischemic optic neuropathy.

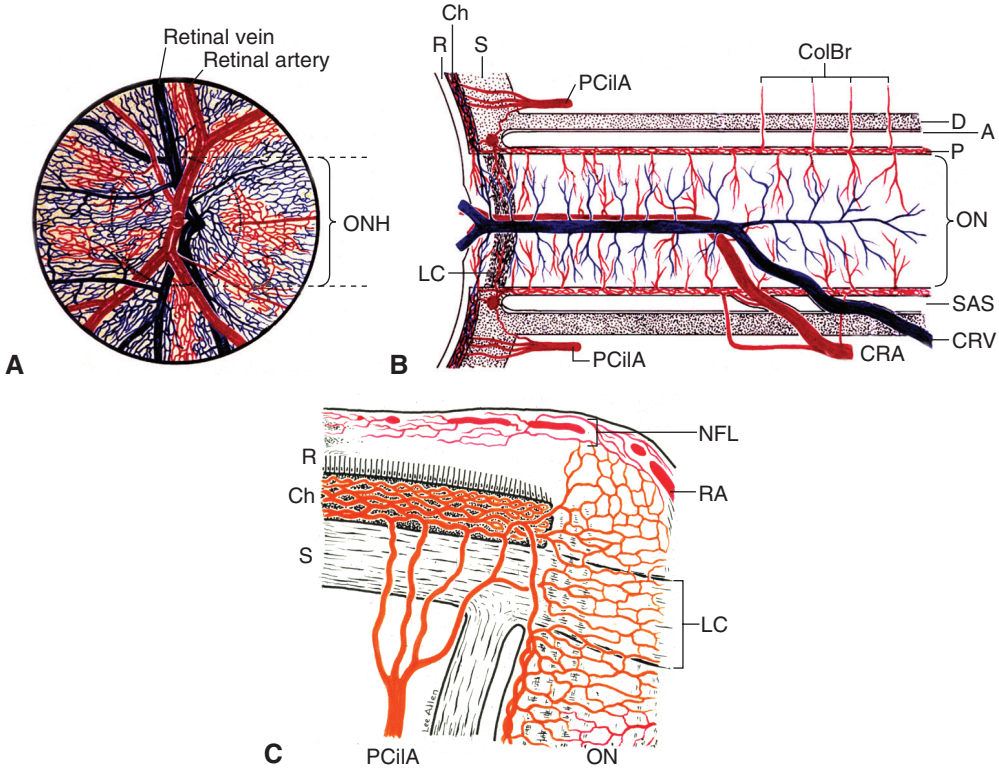


Figure 3-12 Schematic representation of the vascular supply to the optic nerve and ONH. Intraocular view **(A),** lateral view **(B),** and sagittal view **(C)** of the ONH. Short posterior ciliary arteries supply centripetal capillary beds of the anterior ONH. The central retinal artery (CRA) contribution is restricted to nerve fiber layer capillaries and capillaries of the anterior intraorbital optic nerve. Capillary beds at all levels drain into the central retinal vein (CRV). A = arachnoid; Ch = choroid; ColBr = collateral branches; D = dura; LC = lamina cribrosa; NFL = superficial nerve fiber layer of the ONH; ON = optic nerve; ONH = optic nerve head; P = pia; PCilA = posterior ciliary artery; R = retina; RA = retinal arteriole; S = sclera; SAS = subarachnoid space. *(Reproduced with permission from Hayreh SS. The blood supply of the optic nerve head and the evaluation of it—myth and reality.* Prog Retin Eye Res. *2001;20(5):563–593.)*

Table 3-2 Blood Supply of the Visual Pathway

Structure	Blood Supply
Optic chiasm	Branches of anterior cerebral a., superior hypophysial a., internal carotid a., posterior communicating a., and posterior cerebral a.
Optic tract	Branches of posterior communicating a. and anterior choroidal a.
Lateral geniculate nucleus	Branches of anterior and posterior choroidal a.
Optic radiations	Anterior: Anterior choroidal a.
	Posterior: Lateral striate a. (middle cerebral a.) and branches of posterior cerebral a.
Primary visual cortex	Calcarine a. (primarily derived from the posterior cerebral a.) and sometimes branches of the middle cerebral a.

a. = artery.

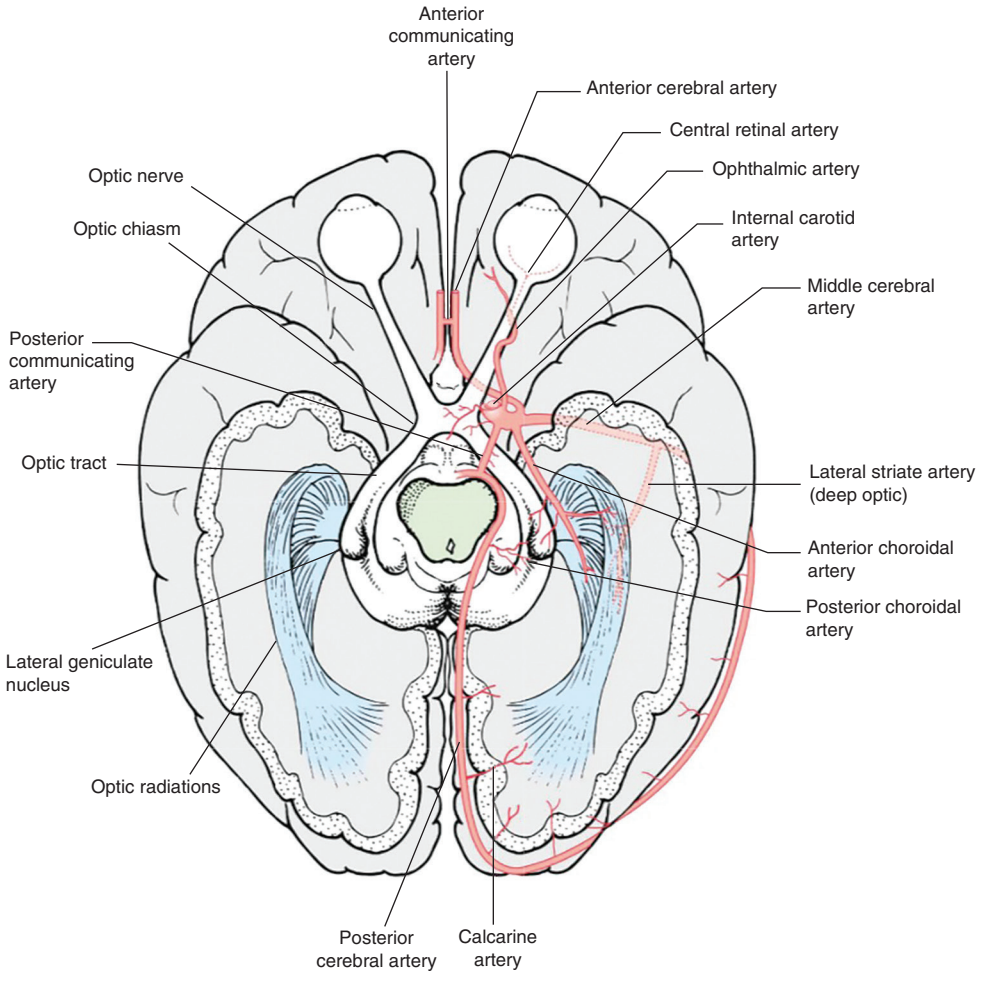


Figure 3-13 Vascular supply of the optic nerve and visual pathway. *(Modified with permission from Forrester JV, Dick AD, McMenamin PG, Roberts F, Pearlman E.* The Eye: Basic Sciences in Practice. *4th ed. Elsevier; 2016:98.)*

The posterior ciliary arteries are terminal arteries, and the area where the respective capillary beds from each artery meet is termed the *watershed zone*. When perfusion pressure drops, the tissue within this area is the most vulnerable to ischemia. Consequences can be significant when the entire ONH or a part of it lies within the watershed zone.

Tan NY, Koh V, Girard MJ, Cheng CY. Imaging of the lamina cribrosa and its role in glaucoma: a review. *Clin Exp Ophthalmol*. 2018;46(2):177–188.

Intraorbital region

The intraorbital region of the optic nerve is supplied proximally by the pial vascular network and by neighboring branches of the ophthalmic artery. Distally, it is supplied by intraneural branches of the CRA. Most anteriorly, it is supplied by short posterior ciliary arteries and infrequently by peripapillary choroidal arteries.

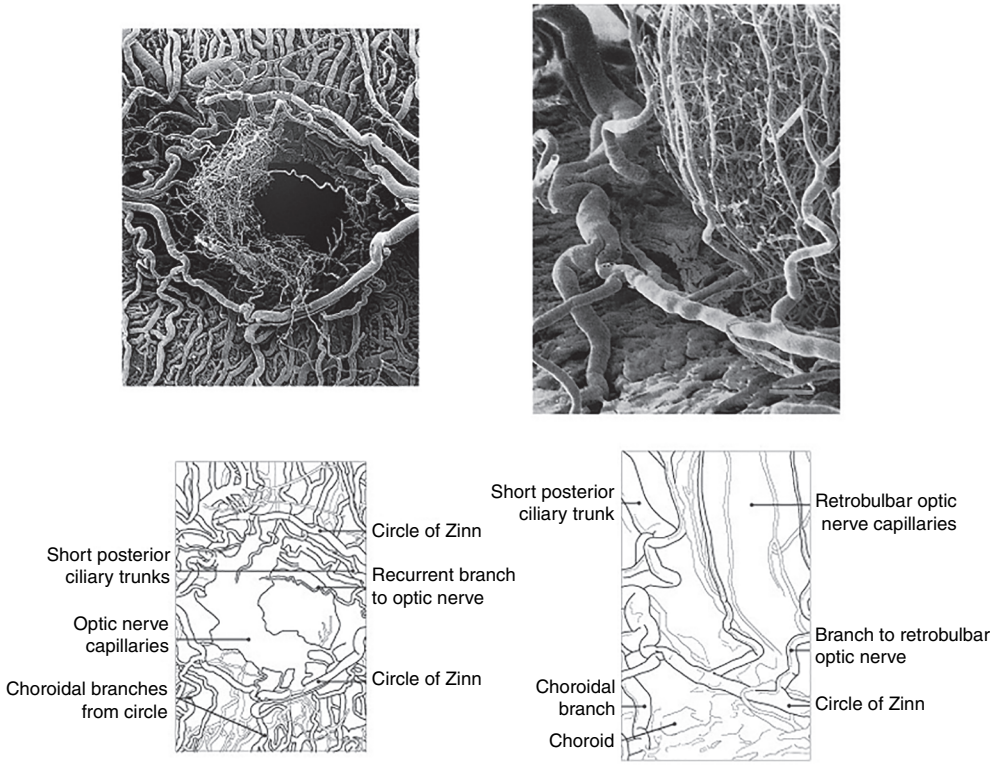


Figure 3-14 Circle of Zinn-Haller. Electron microscopy of the retrolaminar vascular circle *(left).* Branches from the circle to the optic nerve *(right).* *(Reproduced with permission from* Investigative Ophthalmology and Vision Science.*)*

Oculomotor Nerve (Third Cranial Nerve)

Although the oculomotor nerve (CN III) contains only 24,000 fibers, it innervates all the extraocular muscles except the superior oblique and the lateral rectus, which are innervated by the trochlear nerve and abducens nerve, respectively. It also provides parasympathetic cholinergic innervation to the pupillary sphincter and the ciliary muscle.

CN III arises from a complex group of nuclei in the rostral midbrain, or *mesencephalon,* at the level of the superior colliculus. This nuclear complex lies ventral to the periaqueductal gray matter, is immediately rostral to the CN IV nuclear complex, and is bounded inferolaterally by the medial longitudinal fasciculus.

The CN III nucleus consists of several distinct, large motor cell subnuclei, each of which subserves the extraocular muscle it innervates (Fig 3-15). The subnuclei innervate the following:

- ipsilateral inferior rectus muscle
- ipsilateral inferior oblique muscle
- ipsilateral medial rectus muscle
- contralateral superior rectus muscle

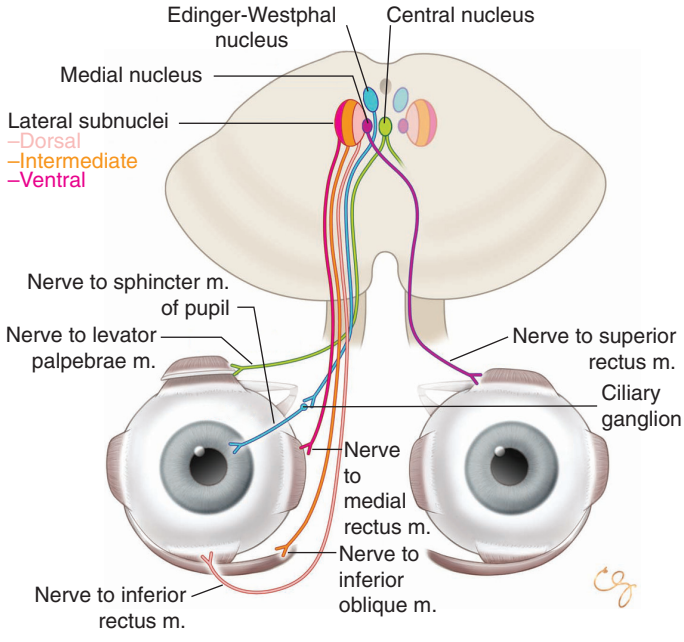


Figure 3-15 Oculomotor nucleus complex. Note that all extraocular muscles served by CN III are innervated by their respective ipsilateral nuclei except the superior rectus muscle. The levator palpebrae muscles of both eyes are controlled by a single central nucleus. Parasympathetic fibers traveling to the pupillary sphincter muscle and ciliary body synapse in the ciliary ganglion in the orbit. m. = muscle. *(Illustration by Christine Gralapp.)*

Except for a single central, caudal subnucleus that serves both levator palpebrae superioris muscles, the cell groups are paired. Notably, the shared innervation of both levator muscles is an example of Hering's law of equal innervation.

CLINICAL PEARL

Hering's law of equal innervation. The paired levator palpebrae superioris muscles receive equal innervation from the single central nucleus of CN III. In cases of unilateral ptosis, both muscles receive increased stimulation to compensate for the single ptotic eyelid. When the ptotic lid is elevated manually, the increased stimulation is released to both eyelids and the contralateral lid becomes relatively more ptotic.

Fibers from the dorsal subnucleus to the superior rectus uniquely cross, or *decussate,* in the caudal aspect of the nucleus and therefore supply the contralateral superior rectus muscles. The Edinger-Westphal nucleus is rostral in location. It provides the parasympathetic preganglionic efferent innervation to the ciliary muscle and pupillary sphincter. The most ventral subnuclei supply the medial rectus muscles. A subnucleus for ocular convergence has been described but is not consistently found in primates.

The fascicular portion of CN III travels ventrally from the nuclear complex, in the area of the red nucleus, between the medial aspects of the cerebral peduncles, and through

the corticospinal fibers (see Fig 3-2). It exits in the interpeduncular space. In the subarachnoid space, CN III passes below the posterior cerebral artery (PCA) and above the superior cerebellar artery, the 2 major branches of the basilar artery (Fig 3-16). The nerve travels forward in the interpeduncular cistern lateral to the posterior communicating artery (PCoA) and penetrates the arachnoid between the free and attached borders of the tentorium cerebelli.

The oculomotor nerve pierces the dura mater on the lateral side of the posterior clinoid process, initially traversing the roof of the cavernous sinus (see Fig 3-26). It runs along the lateral wall of the cavernous sinus, above CN IV, and enters the orbit through the superior orbital fissure (see Fig 3-1).

CN III usually separates into superior and inferior divisions after passing through the annulus of Zinn in the orbit (Fig 3-17). Alternatively, it may divide within the anterior cavernous sinus (see Fig 3-26). The nerve maintains a topographic organization even in the midbrain, so lesions almost anywhere along its course may cause a divisional nerve palsy.

The superior division of CN III innervates the superior rectus and levator palpebrae superioris muscles. The larger inferior division splits into 3 branches to supply the medial rectus, inferior rectus, and inferior oblique muscles.

The parasympathetic fibers wind around the periphery of the nerve, enter the inferior division, and course through the branch that supplies the inferior oblique muscle. They join the ciliary ganglion, where they synapse with the postganglionic fibers, which emerge as many short ciliary nerves (see Chapter 1, Fig 1-12). These nerves pierce the sclera and travel through the choroid to innervate the pupillary sphincter and the ciliary muscle. The superficial location of these fibers makes them more vulnerable to compression (eg, from an aneurysm) than to ischemia.

CLINICAL PEARL

Even in patients with systemic vascular disease, a pupil-sparing CN III palsy is not a perfect indicator of the absence of an enlarging aneurysm. Many neuro-ophthalmologists therefore recommend emergent imaging (by computed tomography/computed tomography angiography or magnetic resonance imaging/magnetic resonance angiography) for any patient with new-onset CN III palsy with incomplete ptosis.

Pathways for the Pupil Reflexes

Pupillary light reflex

The pupillary light reflex (also called *light reflex, pupillary reflex*) consists of a simultaneous and equal constriction of the pupils in response to illumination of 1 eye or the other (Fig 3-18). When the preganglionic parasympathetic fibers leave each Edinger-Westphal nucleus, they run on the superficial surface of CN III as it leaves the brainstem, then spiral downward to lie medially in the nerve at the level of the petroclinoid ligament and inferiorly in the inferior division of CN III as it enters the orbit. These fibers synapse in the ciliary ganglion (see Chapter 1, Fig 1-12) and give rise to postganglionic myelinated short ciliary nerves, approximately 3%–5% of which are pupillomotor. The rest of the fibers are designated for the ciliary muscle and are concerned with the near reflex.

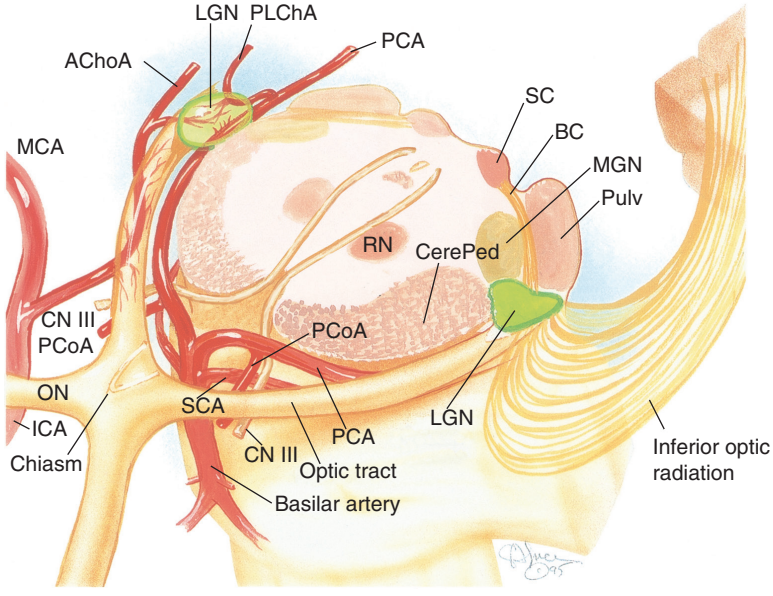


Figure 3-16 At the level of the midbrain, relationship of the LGN to nearby structures and its blood supply. AChoA = anterior choroidal artery; BC = brachium conjunctivum; CerePed = cerebral peduncles; ICA = internal carotid artery; MCA = middle cerebral artery; MGN = medial geniculate nucleus; ON = optic nerve; PCA = posterior cerebral artery; PCoA = posterior communicating artery; PLChA = posterior lateral choroidal artery; Pulv = pulvinar; RN = red nucleus; SC = superior colliculus; SCA = superior cerebellar artery. *(Illustration by Craig A. Luce.)*

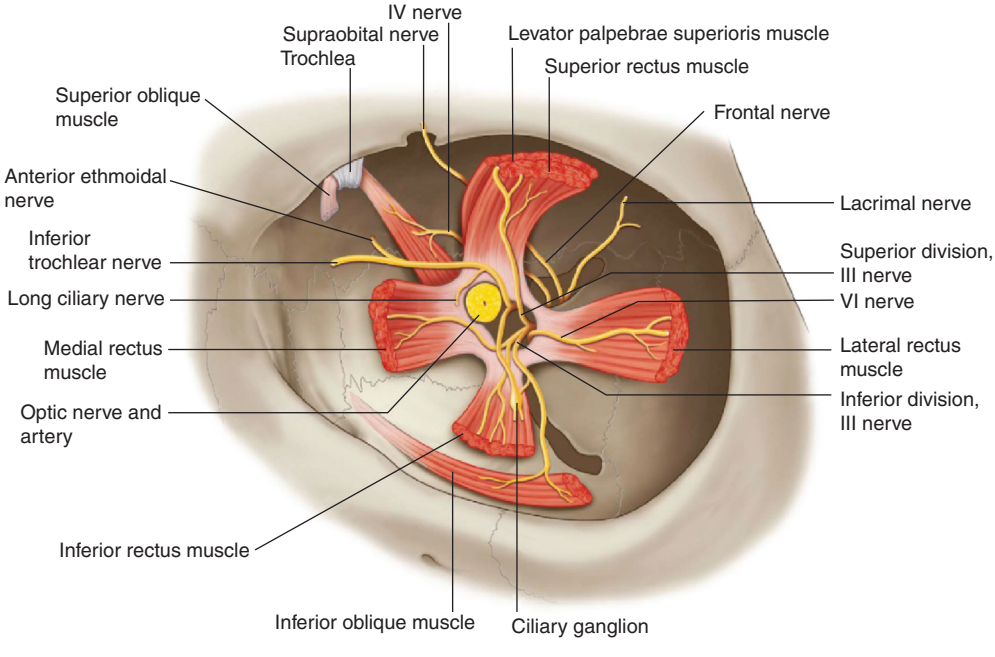


Figure 3-17 Anterior view of the left orbital apex showing the distribution of the nerves as they enter through the superior orbital fissure and optic canal. This view also shows the annulus of Zinn, the fibrous ring formed by the origin of the 4 rectus muscles. *(Reproduced with permission from Jun B, Miller NR. Orbital Apex Inflammation. In: Mukherjee B, Yuen H, eds.* Emergencies of the Orbit and Adnexa. *Springer; 2017:Fig 24.4.)*

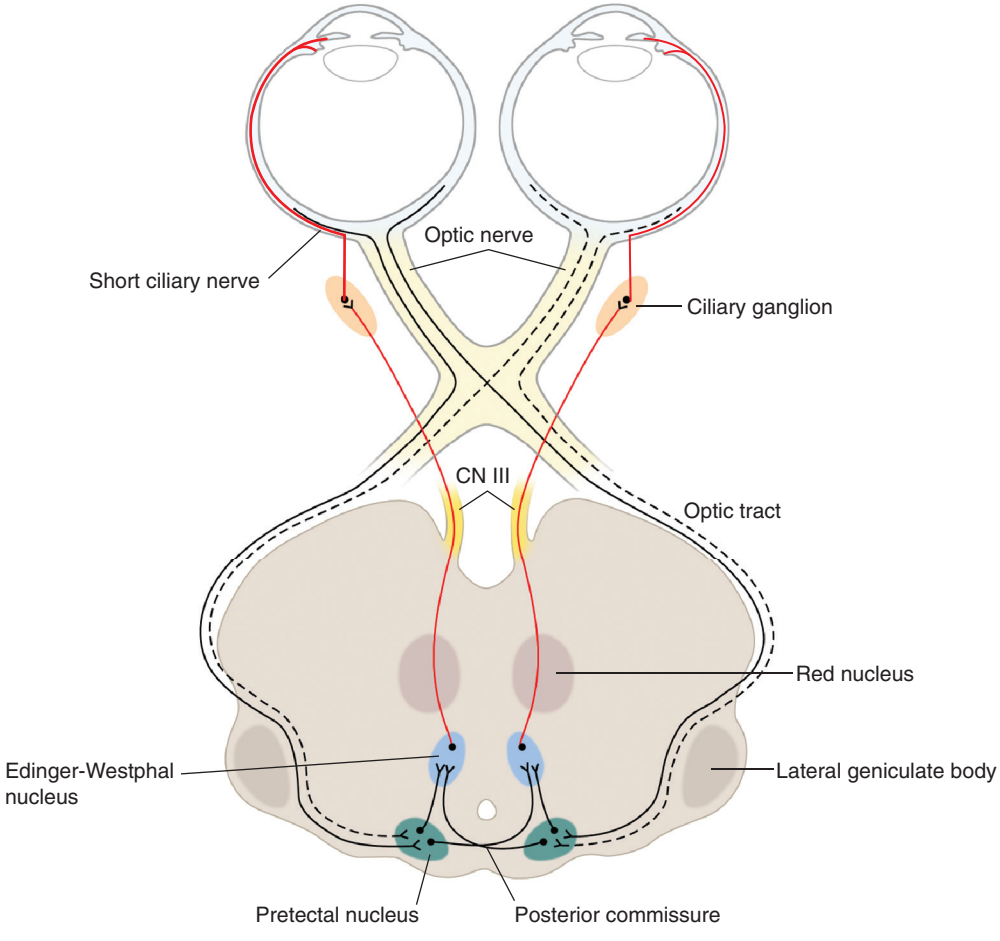


Figure 3-18 Pathway of the pupillary reflexes. *Pupillary light reflex:* Light from each eye passes via electrical signals through the optic nerve, and nasal fibers decussate in the optic chiasm, providing signals in both optic tracts. The pupillary fibers exit the optic tract posteriorly, reaching the pretectal nuclei at the level of the superior colliculus in the midbrain. Efferent fibers project to the ipsilateral and contralateral Edinger-Westphal nuclei. Preganglionic parasympathetic fibers leave each Edinger-Westphal nucleus and run on the superficial surface of the oculomotor nerve as it leaves the brainstem. The fibers follow the inferior division of CN III as it enters the orbit, synapsing in the ciliary ganglion. Postganglionic myelinated short ciliary nerves (3%–5% of which are pupillomotor) then innervate the iris and the ciliary muscle. *Near reflex:* Fibers for the near reflex follow a similar efferent course, inducing miosis, but they also act at the ciliary muscle to induce accommodation. *(Illustration by Christine Gralapp.)*

Near reflex

The near reflex (also called *near synkinesis, near triad*), is a synkinesis that occurs when attention is changed from distance to near. This reflex includes the triad of accommodation, pupil constriction, and convergence. The convergence reflex is initiated in the occipital association cortex, from which impulses descend along corticofugal pathways to relay in pretectal and possibly tegmental areas. From these relays, fibers pass to the Edinger-Westphal

nuclei and both motor nuclei of the medial rectus muscles. Fibers for the near reflex approach the pretectal nucleus from the ventral aspect; thus, compressive dorsal lesions of the optic tectum spare the near pupil reflex relative to the pupillary light reflex (light–near dissociation). Efferent fibers for accommodation follow the same general pathway as do those for the pupillary light reflex, but their final distribution (via the short ciliary nerves) is to the ciliary muscle.

CLINICAL PEARL

Argyll Robertson pupils occur in patients with tertiary syphilis involving the central nervous system. Tertiary syphilis can damage the dorsal aspect of the Edinger-Westphal nucleus, interrupting the pretectal oculomotor light reflex but sparing the more ventrally located fibers of the Edinger-Westphal nuclei, which control the near reflex. Argyll Robertson pupils are therefore characterized by small irregular pupils that have little to no constriction to light but constrict briskly to near targets (light–near dissociation).

Trochlear Nerve (Fourth Cranial Nerve)

The trochlear nerve (CN IV) contains the fewest nerve fibers (approximately 3400) of any CN but has the longest intracranial course (75 mm). The nerve nucleus is located in the caudal midbrain at the level of the inferior colliculus near the periaqueductal gray matter, ventral to the aqueduct of Sylvius. It is continuous with the caudal end of the CN III nucleus and differs histologically from that nucleus only in the smaller size of its cells. Like the CN III nucleus, it is bounded ventrolaterally by the medial longitudinal fasciculus.

The fascicles of CN IV curve dorsocaudally around the periaqueductal gray matter and completely decussate in the superior medullary velum. The nerves exit the brainstem just beneath the inferior colliculus (see Figs 3-1, 3-2). CN IV is the only CN that is completely decussated (the superior rectus subnuclei of CN III project contralaterally; however, the CN III fascicles themselves do not decussate once they leave the nuclear complex), and CN IV is the only CN to exit the dorsal surface of the brainstem (see Fig 3-2). As it curves around the brainstem in the ambient cistern, CN IV runs beneath the free edge of the tentorium, passes between the posterior cerebral and superior cerebellar arteries (like CN III, but more laterally), and then pierces the dura mater to enter the cavernous sinus.

CN IV travels beneath CN III and above the ophthalmic division of CN V (CN V_1) in the lateral wall of the cavernous sinus (see Fig 3-26). It enters the orbit through the superior orbital fissure outside the annulus of Zinn and runs superiorly to innervate the superior oblique muscle (see Fig 3-17).

CLINICAL PEARL

Because of its location outside the muscle cone, CN IV is usually not affected by injection of retrobulbar anesthetics.

Trigeminal Nerve (Fifth Cranial Nerve)

The trigeminal nerve (CN V), the largest CN, possesses both sensory and motor divisions. The sensory portion serves the greater part of the scalp and the forehead, face, eyelids, ocular surface, lacrimal glands, extraocular muscles, ears, dura mater, and tongue. The motor portion innervates the muscles of mastication through branches of the mandibular division.

The CN V nuclear complex extends from the midbrain, through the pons and medulla, to the upper cervical segments, as caudal as the C4 vertebra. It consists of the following 4 nuclei, listed from rostral to caudal:

- mesencephalic nucleus
- main sensory nucleus
- spinal nucleus and tract
- motor nucleus

Important interconnections exist between the different subdivisions of the CN V sensory nuclei and the reticular formation (Fig 3-19).

Mesencephalic Nucleus

The mesencephalic nucleus mediates *proprioception* and *deep sensation* from the masticatory, facial, and extraocular muscles. The nucleus extends inferiorly into the posterior pons as far as the main sensory nucleus.

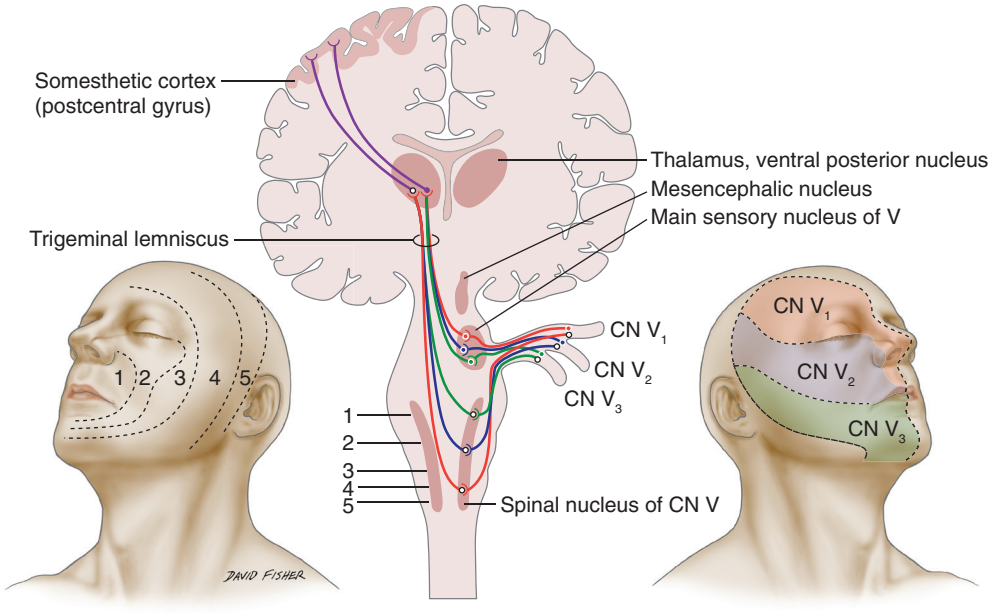


Figure 3-19 Diagram of the central pathways and peripheral innervation of CN V. The numbers 1–5 indicate the locations of dermatomes on the face and their corresponding representation in the brainstem. *(Illustration by David Fisher; used with permission from Kline LB.* Neuro-Ophthalmology Review Manual. *6th ed. Slack; 2008:174.)*

Main Sensory Nucleus

The main sensory nucleus lies in the pons, lateral to the motor nucleus. It is continuous with the mesencephalic nucleus (above) and with the spinal nucleus (below). The main sensory nucleus receives its input from ascending branches of the sensory root, and it serves *light touch* from the skin and mucous membranes. Upon entering the pons, the sensory root of CN V divides into an ascending tract and a descending tract. The ascending tract terminates in the main sensory nucleus, and the descending tract ends in the spinal nucleus.

Spinal Nucleus and Tract

The spinal nucleus and tract extend through the medulla to C4. The nucleus receives *pain* and *temperature* afferents from the descending spinal tract, which also carries cutaneous components of CN VII, CN IX, and CN X that serve sensations from the ear and external auditory meatus. The sensory fibers from the ophthalmic division of CN V (V_1) terminate in the most ventral portion of the spinal nucleus and tract. Fibers from the maxillary division (V_2) end in the midportion of the spinal nucleus (in a ventral–dorsal plane). The fibers from the mandibular division (V_3) end in the dorsal parts of the nucleus (the 3 divisions of CN V are discussed in greater detail later in the chapter).

The cutaneous territory of each of the CN V divisions is represented in the spinal nucleus and tract in a rostral–caudal direction. Fibers from the perioral region are thought to terminate most rostrally in the nucleus; fibers from the peripheral face and scalp end in the caudal portion. The zone between them, the midfacial region, is projected onto the central portion of the nucleus. This "onionskin" pattern of cutaneous sensation (see Fig 3-19) has been demonstrated by clinical studies of patients with damage to the spinal nucleus and tract.

CLINICAL PEARL

Damage to the trigeminal sensory nucleus at the level of the brainstem causes bilateral sensory loss in concentric areas of the face, with the sensory area surrounding the mouth in the center. If a patient verifies this distribution of sensory loss, the lesion is in the brainstem. Conversely, sensory loss that follows the peripheral distribution of the trigeminal sensory divisions (ophthalmic, maxillary, and mandibular) indicates that the lesion lies in the divisions of CN V (V_1, V_2, V_3) and is a fascicular lesion.

Axons from the main sensory and spinal nuclei, as well as portions of the mesencephalic nucleus, relay sensory information to higher sensory areas of the brain. The axons cross the midline in the pons and ascend to the thalamus along the ventral and dorsal trigeminothalamic tracts. They terminate in the nerve cells of the ventral posteromedial nucleus of the thalamus. These cells, in turn, send axons through the internal capsule to the postcentral gyrus of the cerebral cortex.

The afferent limb of the oculocardiac reflex is mediated by CN V_1 (Fig 3-20). It is connected to the efferent limb, which is mediated by the parasympathetic neurons of the vagus nerve, via short internuncial fibers to the reticular formation. The reflex is initiated through pressure on the globe, ocular surface, and/or extraocular muscles and results in 20% or

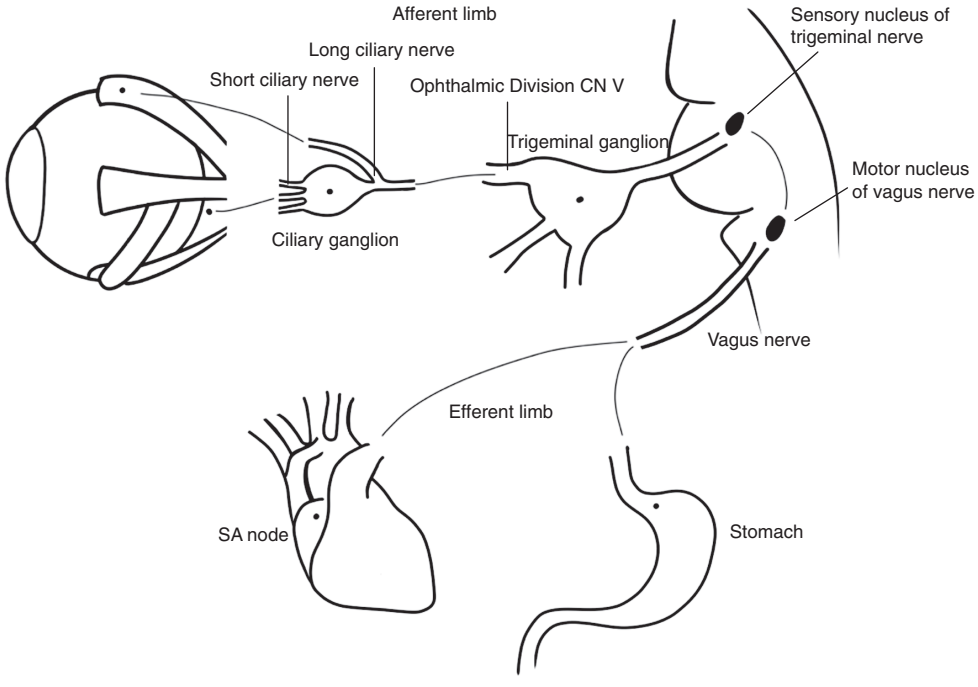


Figure 3-20 Oculocardiac reflex. The afferent limb is mediated by the ophthalmic division of the trigeminal nerve (CN V_1) and the efferent by the vagus nerve (CN X). Stimulation of the eye and/or extraocular muscles can result in bradycardia and nausea. *(Illustration by Lindey Campagne, OD.)*

greater reduction in heart rate. This definition is important when assessing relative change in heart rate, particularly when evaluating an orbital fracture patient for muscle entrapment.

Meuwly C, Golanov E, Chowdhury T, Erne P, Schaller B. Trigeminal cardiac reflex: new thinking model about the definition based on a literature review. *Medicine (Baltimore)*. 2015;94(5):e484. doi:10.1097/MD.0000000000000484

Motor Nucleus

The motor nucleus is located in the pons, medial to the main sensory nucleus. It receives fibers from both cerebral hemispheres, the reticular formation, the red nucleus, the tectum, the medial longitudinal fasciculus, and the mesencephalic nucleus. The motor nucleus gives rise to the axons that form the motor root, which supplies the muscles of mastication (pterygoid, masseter, and temporalis), the tensor tympani muscle, the tensor veli palatini muscle, the mylohyoid muscle, and the anterior belly of the digastric muscle.

Intracranial Pathway of Cranial Nerve V

The intracranial segment of the trigeminal nerve emerges from the upper lateral portion of the ventral pons, passes over the petrous apex (the crest of the petrous part of temporal bone), forms the *trigeminal ganglion,* and then divides into 3 branches (see Figs 3-1, 3-2). The trigeminal ganglion, also called the *gasserian* or *semilunar ganglion,* contains the cell

bodies of origin of all CN V sensory axons. The crescent-shaped ganglion occupies a recess in the dura mater posterolateral to the cavernous sinus. This recess, called the *Meckel cave,* is near the apex of the petrous part of the temporal bone in the middle cranial fossa. Medially, the trigeminal ganglion is close to the ICA and the posterior cavernous sinus.

Divisions of Cranial Nerve V

The 3 divisions of CN V are the ophthalmic division (V_1), the maxillary division (V_2), and the mandibular division (V_3).

Ophthalmic division (CN V_1)

The ophthalmic division enters the cavernous sinus lateral to the ICA and courses beneath CN III and CN IV (see Fig 3-26). Within the sinus, it gives off a tentorial–dural branch, which innervates the cerebral vessels, dura mater of the anterior fossa, cavernous sinus, sphenoid wing, petrous apex, Meckel cave, tentorium cerebelli, falx cerebri, and dural venous sinuses. CN V_1 passes into the orbit through the superior orbital fissure and divides into 3 branches: frontal, lacrimal, and nasociliary (see Fig 3-17).

CLINICAL PEARL

CN V_1 serves as the afferent limb of oculocardiac reflex, whose efferent limb is supplied by the vagus nerve. In cases of supraventricular tachycardia, ocular massage and other vagal maneuvers can help slow the heart rate. In addition to bradycardia, patients experiencing an oculocardiac reflex can also present with nausea. This reflex is often triggered by manipulation of the extraocular muscles, for example during strabismus surgery or following an orbital fracture with entrapment.

Frontal nerve The frontal nerve (see Chapter 1, Fig 1-12) divides into the supraorbital and supratrochlear nerves, which provide sensation to the medial portion of the upper eyelid and the conjunctiva, forehead, scalp, frontal sinuses, and side of the nose. The supratrochlear nerve exits the orbit 17 mm from midline, whereas the supraorbital nerve exits at 27 mm from midline, through either a notch or a true foramen.

Lacrimal nerve The lacrimal nerve innervates the lacrimal gland and the neighboring conjunctiva and skin. The lacrimal gland receives its parasympathetic supply from the retro-orbital plexus (discussed later, in the section Facial Nerve [Seventh Cranial Nerve]). Occasionally, the lacrimal nerve exits the orbit via a lacrimal foramen to supply the lateral forehead. Otherwise, that area is supplied by branches of the supraorbital nerve.

Nasociliary nerve Branches from the nasociliary nerve supply sensation to the middle and inferior turbinates, septum, lateral nasal wall, and tip of the nose. The infratrochlear branch serves the lacrimal drainage system, the conjunctiva, and the skin of the medial canthal region. The ciliary nerves (short and long) carry sensory fibers from the ciliary body, the iris, and the cornea. The short ciliary nerves also carry the sympathetic and parasympathetic fibers from the ciliary ganglion to the iris dilator and sphincter, respectively, and the parasympathetic fibers to the ciliary muscle (Fig 3-21). The sensory short ciliary fibers pass through the ciliary

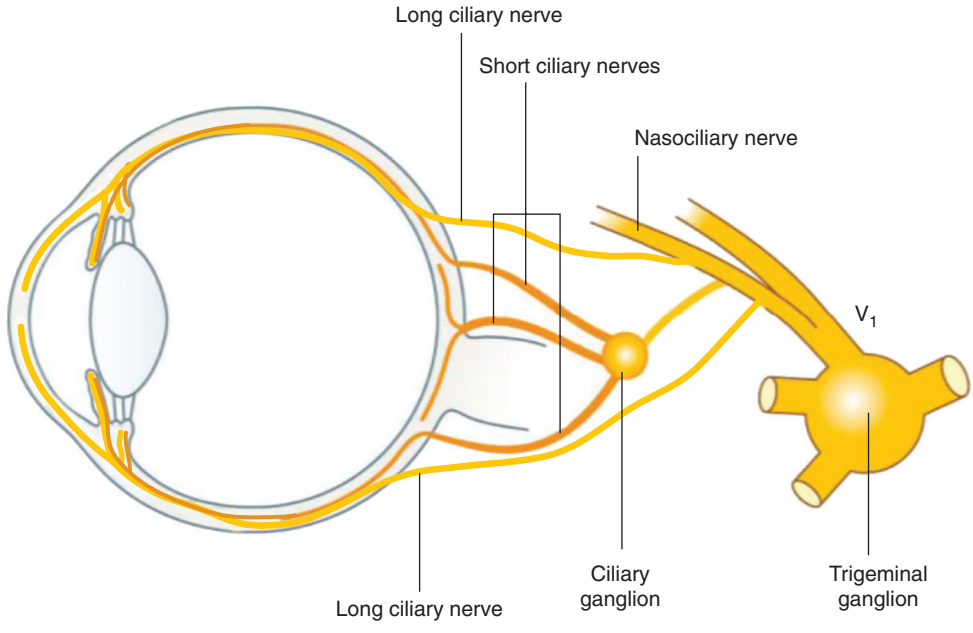


Figure 3-21 Divisions of the nasociliary nerve. The nasociliary nerve is a branch of V_1, the ophthalmic division of CN V. The posterior ciliary nerves supply sensation to the globe. The paired long ciliary nerves innervate the anterior structures and the short ciliary nerves, the posterior structures. The short posterior ciliary nerves also carry sympathetic and parasympathetic fibers to the iris dilator and sphincter muscles, respectively. In addition, they carry parasympathetic fibers to the ciliary muscle, where they induce accommodation. *(Modified with permission from Levin LA, Nilsson SFE, Ver Hoeve J, Wu SM.* Adler's Physiology of the Eye. *11th ed. Elsevier/Saunders; 2011:91.)*

ganglion to join, along with the long ciliary fibers, the nasociliary nerve. Thus, the short ciliary nerves carry sensory (V_1), sympathetic, and parasympathetic fibers (see Chapter 1, Fig -1-12).

CLINICAL PEARL

Hutchinson sign is defined as erythematous skin lesions at the tip, side, or root of the nose. It is a strong predictor of ocular inflammation and corneal denervation in patients with herpes zoster ophthalmicus, especially if both branches of the nasociliary nerve are involved.

Maxillary division (CN V_2)

The maxillary division leaves the trigeminal ganglion to exit the skull through the foramen rotundum, which lies below the superior orbital fissure (see Fig 3-1). CN V_2 courses through the pterygopalatine fossa into the inferior orbital fissure and then passes through the infraorbital canal as the infraorbital nerve. After exiting the infraorbital foramen, CN V_2 divides into an inferior palpebral branch, a nasal branch, and a superior labial branch, supplying the lower eyelid, the side of the nose, and the upper lip, respectively. The teeth, maxillary sinus, roof of the mouth, and soft palate are also innervated by branches of the maxillary division.

These branches can be damaged after fractures of the orbital floor, leading to dysesthesia in the CN V_2 dermatome.

Mandibular division (CN V_3)

The mandibular division contains sensory and motor fibers. It is the only division of CN V that contains motor fibers. It exits the skull through the foramen ovale (see Fig 3-1) and provides motor input for the masticatory muscles. Sensation is supplied to the mucosa and skin of the mandible, lower lip, tongue, external ear, and tympanum.

Standring S, ed. *Gray's Anatomy: The Anatomical Basis of Clinical Practice.* 42nd ed. Elsevier; 2020.

Abducens Nerve (Sixth Cranial Nerve)

The nucleus of the abducens nerve (CN VI) is situated in the floor of the fourth ventricle, beneath the facial colliculus in the caudal pons. The medial longitudinal fasciculus lies medial to the CN VI nucleus. The fascicular portion of CN VI runs ventrally through the paramedian pontine reticular formation and the pyramidal tract and leaves the brainstem in the pontomedullary junction (Fig 3-22; also see Figs 3-1, 3-2).

CN VI then takes a vertical course along the ventral face of the pons and is crossed by the anterior inferior cerebellar artery. It continues through the subarachnoid space along the surface of the clivus to perforate the dura mater below the petrous apex, approximately 2 cm below the posterior clinoid process. It then passes intradurally through or around the inferior petrosal sinus and beneath the petroclinoid (Gruber) ligament through the Dorello canal, after which it becomes extradural and enters the cavernous

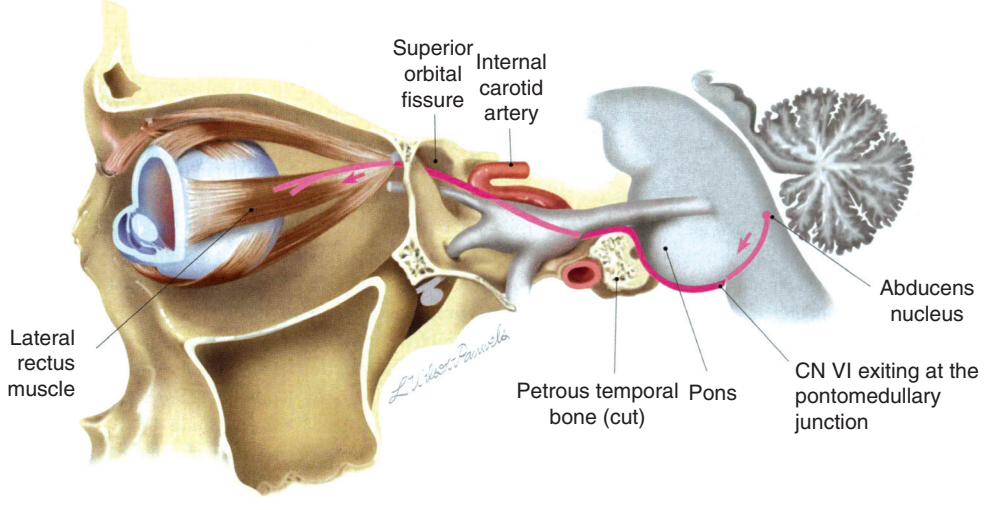


Figure 3-22 Course of the abducens nerve (CN VI). Note the 2 turns the CN VI fascicle takes as it exits the pontomedullary junction and enters the Dorello canal over the petrous component of the temporal bone. Infections extending to this aspect of the petrous bone can result in CN VI palsy. *(Reproduced with permission from Wilson-Pauwels L, Stewart PA, Akesson EJ, Spacey SD.* Cranial Nerves: Function and Dysfunction. *3rd ed. PMPH USA, Ltd; 2010.)*

sinus. The length of the CN VI's route (especially along the surface of the clivus and beneath the petroclinoid ligament) is responsible for this nerve's susceptibility to stretch injury leading to paresis in cases of increased ICP. In the cavernous sinus, CN VI runs below and lateral to the ICA and may transiently carry sympathetic fibers from the carotid plexus (see Fig 3-26). It passes through the superior orbital fissure within the annulus of Zinn to enter the medial surface of the lateral rectus muscle, which it innervates.

CLINICAL PEARL

Gradenigo syndrome is a triad of otitis media, facial pain, and CN VI palsy. CN VI is most susceptible to mastoiditis, otitis, or bone infection at the edge of the tip of the petrous bone toward the clivus (see Fig 3-22).

Facial Nerve (Seventh Cranial Nerve)

The facial nerve (CN VII) is a complex, mixed sensory and motor nerve. The motor root contains special visceral efferent fibers that innervate the muscles of facial expression, including the orbicularis oculi. The sensory root conveys the sense of taste from the anterior two-thirds of the tongue and sensation from the external auditory meatus and the retroauricular skin. It also provides preganglionic parasympathetic innervation by way of the sphenopalatine and submandibular ganglia to the lacrimal, submaxillary, and sublingual glands.

The motor nucleus of CN VII is a cigar-shaped column 4 mm long, located in the caudal third of the pons. It is ventrolateral to the CN VI nucleus, ventromedial to the spinal nucleus of CN V, and dorsal to the superior olivary complex (Figs 3-23, 3-24). The signal for facial movement starts in the primary motor cortex in the precentral gyrus.

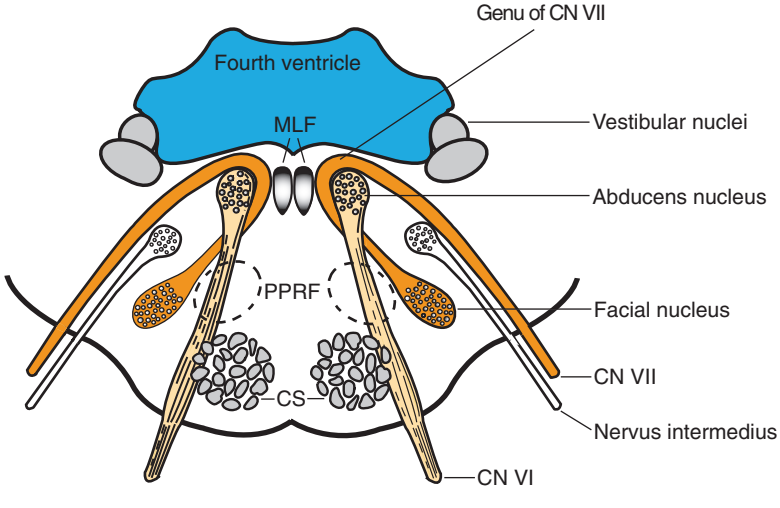


Figure 3-23 Cross section of the pons at the level of CN VI (abducens nerve) nucleus. CS = corticospinal tract; MLF = medial longitudinal fasciculus; PPRF = pontine paramedian reticular formation. *(Illustration by Sylvia Barker.)*

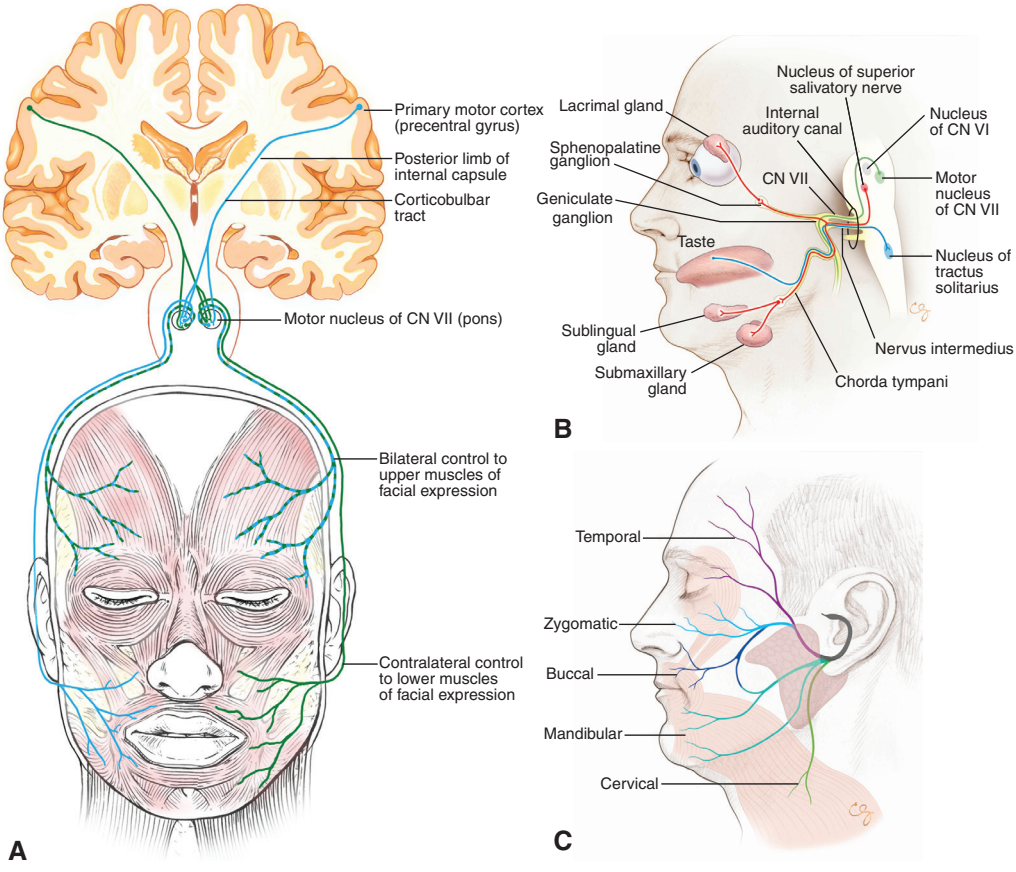


Figure 3-24 Supranuclear, nuclear, and infranuclear anatomy of the facial nerve (CN VII). **A,** The corticobulbar fibers travel through the internal capsule down into the medial one-third of the corticospinal tracts in the cerebral peduncles of the midbrain. The pathways for the upper one-third of facial function (brow and orbicularis muscles) run parallel to but apparently distinct from the pathways for the lower two-thirds along the pyramidal tracts. The corticobulbar fibers travel in the basis pontis; those that control the lower facial muscles decussate at the level of the pons to synapse on the contralateral CN VII nucleus. Corticobulbar fibers that control the upper facial muscles decussate to synapse on the contralateral CN VII nucleus, and some of the fibers do not cross, reaching the ipsilateral CN VII nucleus. **B,** CN VII is predominantly motor in function, with its nucleus located in the caudal pons. CN VII courses dorsomedially and encircles the nucleus of CN VI. After bending around the CN VI nucleus, CN VII exits the pons in the cerebellopontine angle close to CNs V, VI, and VIII. CN VIII, the motor root of CN VII, and the nervus intermedius, the sensory and parasympathetic root of CN VII, enter the internal auditory meatus. Sensory cells located in the geniculate ganglion continue distally as the chorda tympani nerve, which carries taste fibers. Peripheral fibers of the nervus intermedius portion of CN VII initiate salivary, lacrimal, and mucous secretions. **C,** After emerging from the parotid gland, CN VII innervates the muscles of facial expression via 5 peripheral branches. *(Part A reproduced from Bhatti MT, Shiffman JS, Pass AF, Tang RA. Neuro-ophthalmologic complications and manifestations of upper and lower motor neuron facial paresis.* Curr Neurol Neurosci Rep. *2010;10(6):448–458, with permission from Springer. Part A illustration by Dave Peace; parts B and C illustrations by Christine Gralapp.)*

The dorsal motor subnucleus controls the upper half of the face and receives corticobulbar input from *both* cerebral hemispheres, whereas the lateral subnucleus controls the lower half of the face and receives corticobulbar input from the *contralateral* cerebral hemisphere (see Fig 3-24A). Therefore, pathology involving the CN VII nucleus would affect only the contralateral lower face; peripheral CN VII pathology causes an ipsilateral hemifacial palsy.

CLINICAL PEARL

It is important to evaluate patients presenting with a unilateral facial nerve palsy that spares the forehead for an intracranial process of the contralateral side. Patients with a unilateral facial nerve palsy of the upper and lower face should be considered for workup of an underlying disease such as sarcoidosis, carcinoma, Lyme disease, or other conditions that involve the fascicle of the facial nerve.

The facial nerve has several important anatomical relationships with adjacent structures. Fibers from the motor nucleus course dorsomedially to approach the floor of the fourth ventricle and then ascend immediately dorsal to the CN VI nucleus. At the rostral end of the CN VI nucleus, the main facial motor fibers arch over its dorsal surface (forming the internal genu of CN VII) and then pass ventrolaterally between the spinal nucleus of CN V and the CN VII nucleus to exit the brainstem at the pontomedullary junction. The bulge formed by the CN VII genu in the floor of the fourth ventricle is the *facial colliculus* (see Figs 3-2A, 3-23).

CNs VII and VIII (the acoustic nerve) pass together through the lateral pontine cistern in the cerebellopontine angle and enter the internal auditory meatus in a common meningeal sheath.

The main branch of CN VII exits the stylomastoid foramen just behind the styloid process at the base of the mastoid (see Fig 3-24C). It then passes through the superficial and deep lobes of the parotid gland and divides into the superior temporofacial branch (which further divides into the temporal, zygomatic, and buccal subbranches) and the cervicofacial branch. Commonly, the temporal branch supplies the upper half of the orbicularis oculi muscle, and the zygomatic branch supplies the lower half, although the inferior orbicularis is sometimes innervated by the buccal branch. The frontalis, corrugator supercilii, and pyramidalis muscles are usually innervated by the temporal branch.

The temporal (or frontal) branch of the facial nerve crosses the zygomatic arch superficially at the junction of the anterior one-third and posterior two-thirds of the arch. It then enters the more superficial layer of the temporoparietal fascia while staying below the *superficial musculoaponeurotic system (SMAS)*. A good approximation of the course of the nerve across the zygomatic arch follows the point at which a line between the tragus and the lateral eyelid commissure is bisected by a line that begins at the earlobe. The nerve can be injured during perizygomatic or temple surgical approaches, such as Tenzel or Mustardé semicircular flap reconstruction of the eyelid, temporal artery biopsy, and cosmetic forehead and midface surgery.

Tear Reflex Pathway

Reflex lacrimation is controlled by afferents from the sensory nuclei of CN V. The lacrimal reflex arc is shown in Figure 3-25 and demonstrated in Video 3-2. The efferent preganglionic parasympathetic fibers pass peripherally as part of the *nervus intermedius* and divide into 2 groups near the external genu of CN VII (see Fig 3-23). The lacrimal group of fibers passes to the pterygopalatine ganglion in the greater superficial petrosal nerve. The salivatory group of fibers projects through the chorda tympani nerve to the submandibular ganglion to innervate the submandibular and sublingual salivary glands.

VIDEO 3-2 Perception of touch and innervation of the lacrimal functional unit.

Modified with permission from Pflugfelder SC, Beuerman RW, Stern ME, eds. Dry Eye and Ocular Surface Disorders. *Published by CRC Press. © Marcel Dekker; 2004, reproduced by arrangement with Taylor & Francis Books UK.*

The greater superficial petrosal nerve extends forward on the anterior surface of the petrous part of the temporal bone to join the deep petrosal nerve (sympathetic fibers) and form the nerve of the pterygoid canal (vidian nerve). This nerve enters the pterygopalatine fossa; joins the pterygopalatine ganglion; and gives rise to unmyelinated postganglionic

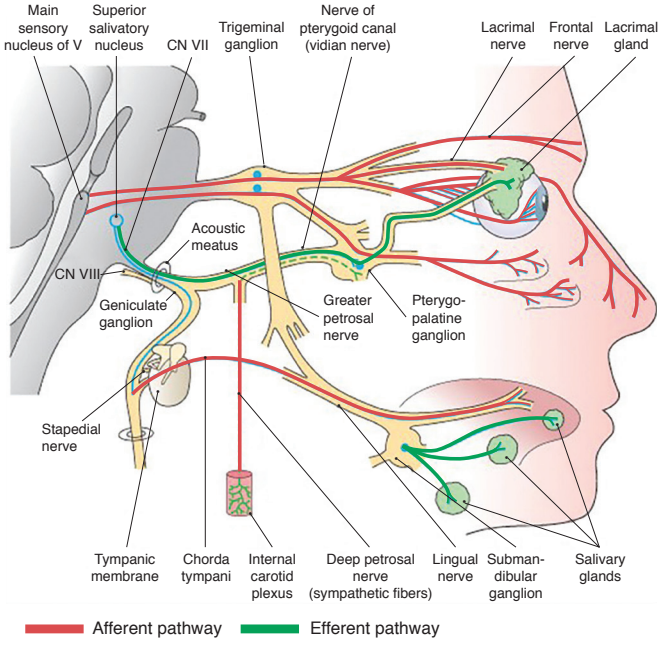


Figure 3-25 Lacrimal reflex arc (after Kurihashi). The afferent pathway is provided by the first and second divisions of CN V. The efferent pathway proceeds from the lacrimal nucleus (close to the superior salivatory nucleus) via CN VII (nervus intermedius), through the geniculate ganglion, the greater superficial petrosal nerve, and the nerve of the pterygoid canal (vidian nerve) (where it is joined by sympathetic fibers from the deep petrosal nerve). The fibers then pass to the pterygopalatine ganglion, where they synapse with postganglionic fibers. These fibers reach the lacrimal gland directly, via the retro-orbital plexus of nerves (particularly CN V_1). The fibers carry cholinergic and vasoactive intestinal polypeptide (VIP)-ergic fibers to the gland. *(Modified with permission from Bron AJ, Tripathi RC, Tripathi BJ.* Wolff's Anatomy of the Eye and Orbit. *8th ed. Hodder Education Publishers; 1997.)*

fibers that innervate the globe, lacrimal gland, glands of the palate, and nose. The parasympathetic fibers destined for the orbit enter it via the superior orbital fissure, along with branches of the ophthalmic nerve (CN V_1). Here, they are joined by sympathetic fibers from the carotid plexus and form a retro-orbital plexus of nerves, whose rami oculares supply orbital vessels or enter the globe to supply the choroid and anterior segment structures. Some of these fibers enter the globe directly; others enter via connections with the short ciliary nerves. The rami oculares also supply the lacrimal gland.

Emotional lacrimation is mediated by parasympathetic efferent fibers originating in the superior salivatory nucleus and the lacrimal nucleus in the caudal pons, both of which lie posterolateral to the motor nucleus. The lacrimal nucleus receives input from the hypothalamus, mediating emotional tearing; there is also supranuclear input from the cortex and the limbic system.

The Cerebral Vascular System

The cranial nerves can be affected by the surrounding cerebrovascular system, which includes both arterial and venous components. CN palsies can be harbingers of life-threatening conditions. Thus, it is imperative to understand the CNs' anatomical relationships with adjacent structures. For further discussion of the cerebral vasculature and the various resultant syndromes of the CNs, see BCSC Section 5, *Neuro-Ophthalmology*.

Cavernous Sinus

The cavernous sinus is an interconnected series of venous channels that drain the eye and orbit and are located just posterior to the orbital apex and lateral to the sphenoid sinus and pituitary fossa. The following structures are located within the venous cavity:

- the ICA, surrounded by the sympathetic carotid plexus
- CNs III, IV, and VI
- the ophthalmic and maxillary divisions of CN V

Figure 3-26 depicts the relative location of these structures in different parts of the cavernous sinus.

Other Venous Sinuses

Other venous sinuses include the superior sagittal, transverse, straight, sigmoid, and petrosal sinuses. The various components of the venous system are depicted in Figure 3-27.

CLINICAL PEARL

Cerebral venous sinus thrombosis or stenosis can result in various neuro-ophthalmic manifestations. Common clinical presentations include acute or chronically elevated ICP, unilateral or bilateral optic nerve edema, and CN VI palsy. Detailed ophthalmic examination and brain imaging are important to avoid delayed diagnosis and treatment.

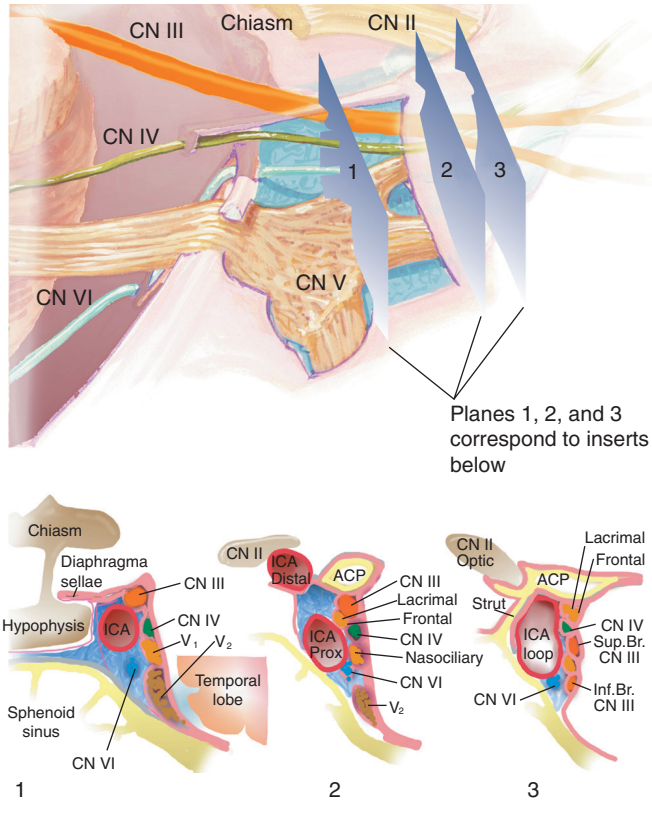


Figure 3-26 Intracavernous course of the ocular motor nerves. CNs III and IV run in the lateral wall of the cavernous sinus along with CN V_1 and CN V_2. CN VI runs in close approximation to the carotid artery within the cavernous sinus itself. As the nerves course toward the anterior aspect of the cavernous sinus and the superior orbital fissure, the ophthalmic division of CN V (CN V_1) divides into 3 branches: the lacrimal, frontal, and nasociliary nerves. ACP = anterior clinoid process; ICA = internal carotid artery; Inf. Br. = inferior branch; Prox = proximal; Sup. Br. = superior branch. *(Illustrations by Craig A. Luce.)*

Circle of Willis

The major arteries supplying the brain are the right and left ICAs (which distribute blood primarily to the rostral portion of the brain, anterior circulation) and the right and left vertebral arteries (which join to form the basilar artery, posterior circulation). The basilar artery distributes blood primarily to the brainstem and the posterior portion of the brain. These arteries interconnect at the base of the brain at the circle of Willis, also called the *cerebral arterial circle* (Figs 3-28, 3-29; see also Figs 3-3, 3-16). These interconnections (anastomoses) help distribute blood to all regions of the brain, even when a portion of the system becomes occluded. CN III, in particular, can be affected by vascular lesions within this region.

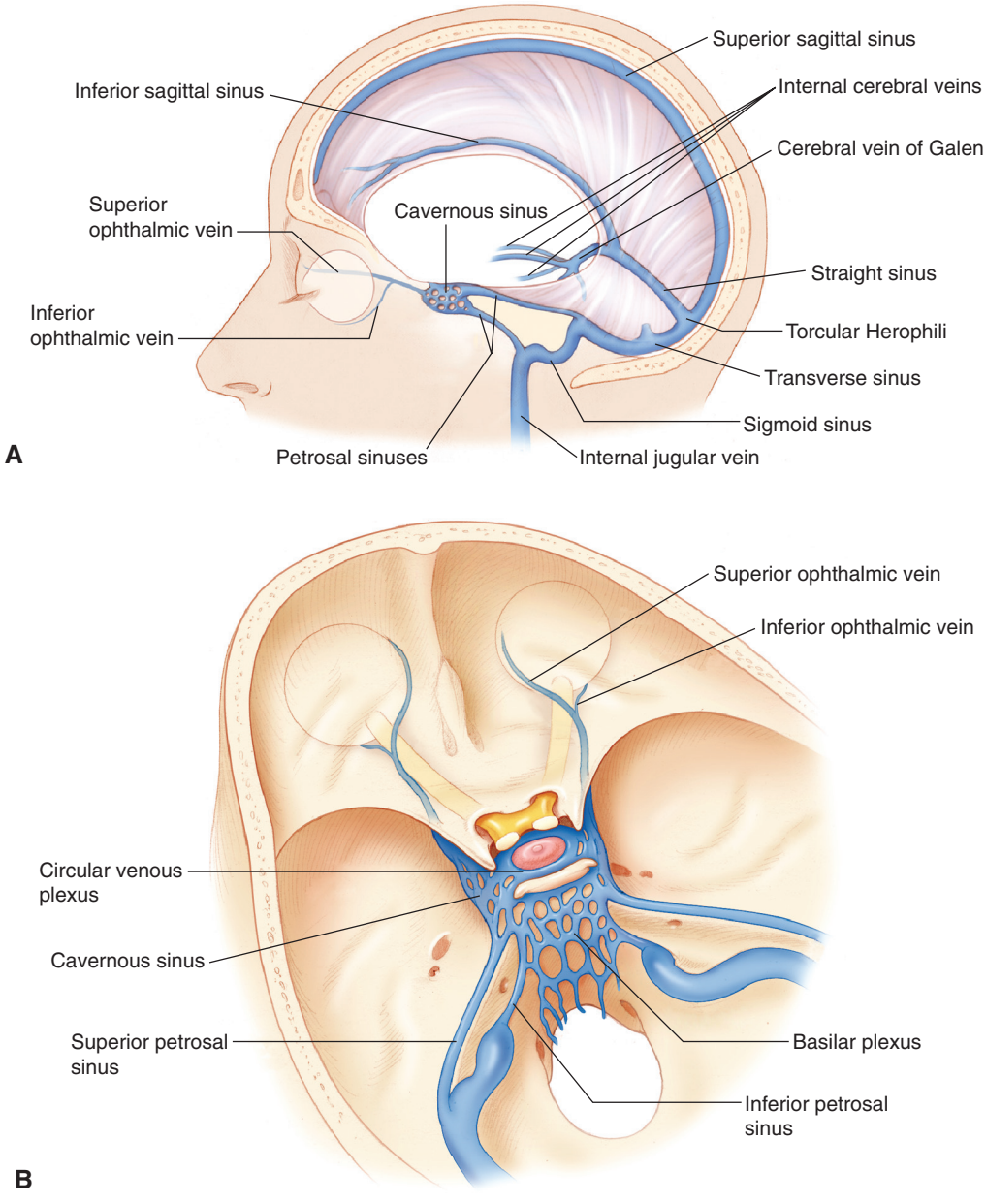


Figure 3-27 Dural venous sinuses. **A,** Cerebral venous sinus system. **B,** Drainage of the cavernous sinus. *(Illustrations by Christine Gralapp.)*

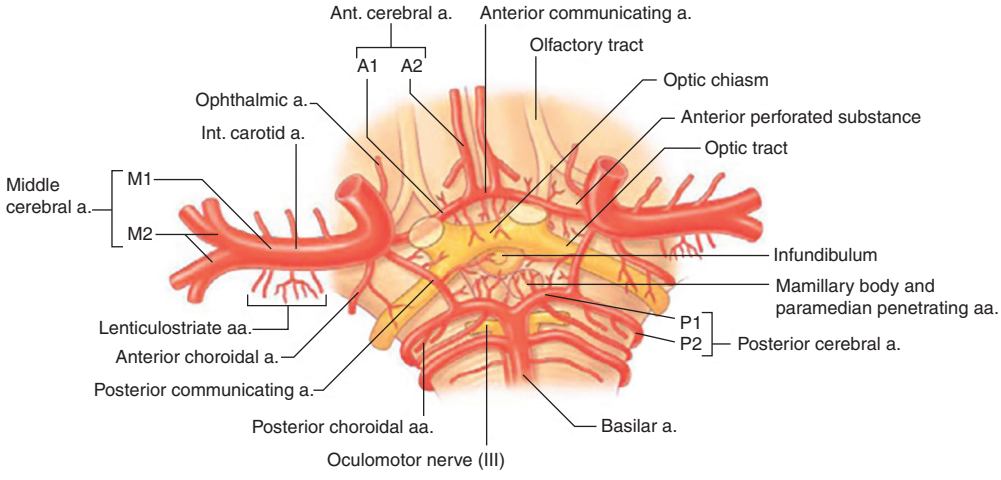


Figure 3-28 The circle of Willis represents an anastomosis of the anterior, middle, and posterior cerebral arteries. Branches from these vessels supply the distal segment of the intracranial optic nerves, optic chiasm, and optic tract. a. = artery; aa. = arteries; Ant. = anterior; Int. = internal. *(Modified with permission from Liu GT, Volpe NJ, Galetta SL.* Neuro-Ophthalmology: Diagnosis and Management. *2nd ed. Elsevier; 2010:295.)*

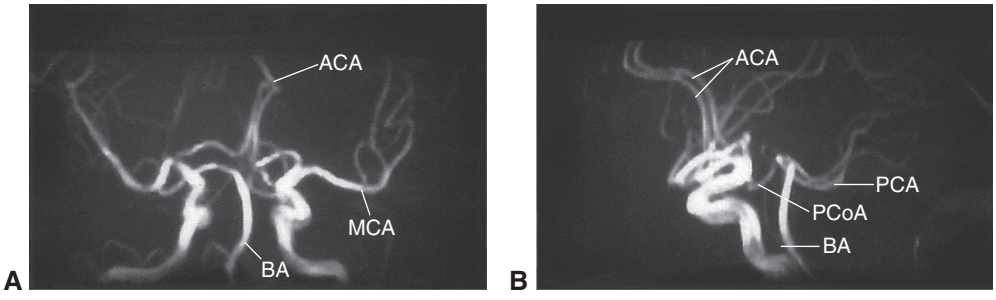


Figure 3-29 Magnetic resonance angiogram (MRA) of the circle of Willis. **A,** MRA shows the circle of Willis in an anteroposterior view. **B,** MRA of oblique view from the same patient. ACA = anterior cerebral artery; BA = basilar artery; MCA = middle cerebral artery; PCA = posterior cerebral artery; PCoA = posterior communicating artery. *(Courtesy of T. Talli, MD, and W. Yuh, MD.)*

CLINICAL PEARL

Most cerebral aneurysms are found at predictable locations around the circle of Willis; the 3 most common are the junction of the anterior communicating artery with the anterior cerebral artery (30%–35%), the junction of the PCoA with the ICA (30%–35%), and the middle cerebral artery bifurcation (20%). CN III is rostral enough to be affected by these aneurysms. About 20% of patients with PCoA aneurysms have isolated CN III palsy on presentation, and about 80% of aneurysms occurring in patients with CN III palsy are located in the PCoA—usually at the junction of the PCoA and the ICA.

Love BB, Biller J. Stroke in children and young adults: overview, risk factors, and prognosis. In: Biller J, ed. *Stroke in Children and Young Adults.* 2nd ed. Elsevier/Saunders; 2009:1–14.

PART II
Embryology

CHAPTER 4

Ocular Development

This chapter includes a related video. Go to www.aao.org/bcscvideo_section02 or scan the QR code in the text to access this content.

Highlights

- The eye develops from 2 germ layers, the ectoderm and the mesoderm.
- Most of the eye forms from different types of ectoderm: surface ectoderm, neuroectoderm, and neural crest cells.
- A series of genetic cascades guide ocular development; alteration of these cascades results in ocular malformations.
- Advances in stem cell research may lead to novel treatments in the future.

General Principles

Embryogenesis is the successive development of cells into more defined structures through a specific series of steps regulated by genetic programs. These genetic programs consist of cascades of genes that are expressed in response to external cues. Often, the same genes participate in different cascades and play different roles in different contexts.

For example, gene products that activate transcription in a particular program may repress transcription in the context of another program, depending on the position of the program within the overall developmental cascade. The cascades are regulated by diffusible ligands (growth factors and hormones) that create overlapping zones of concentration gradients, which in turn allow cells to orient their position within the developing embryo and determine what program to activate. Misactivation of genetic cascades causes embryologic abnormalities that can give rise to congenital abnormalities or be lethal. Such misactivation can be caused by a pathogenic variant or exposure to a teratogen.

During gastrulation (development from a single-layered blastula to a multilayered gastrula), 3 germ layers form in all animal embryos (Figs 4-1, 4-2):

1. ectoderm (superficial layer of cells)
2. mesoderm (middle layer)
3. endoderm (inner layer)

In addition, vertebrate embryos have neural crest cells, an ectomesenchymal cell population that arises from the neuroectoderm at the dorsal edge of the neural tube. These cells

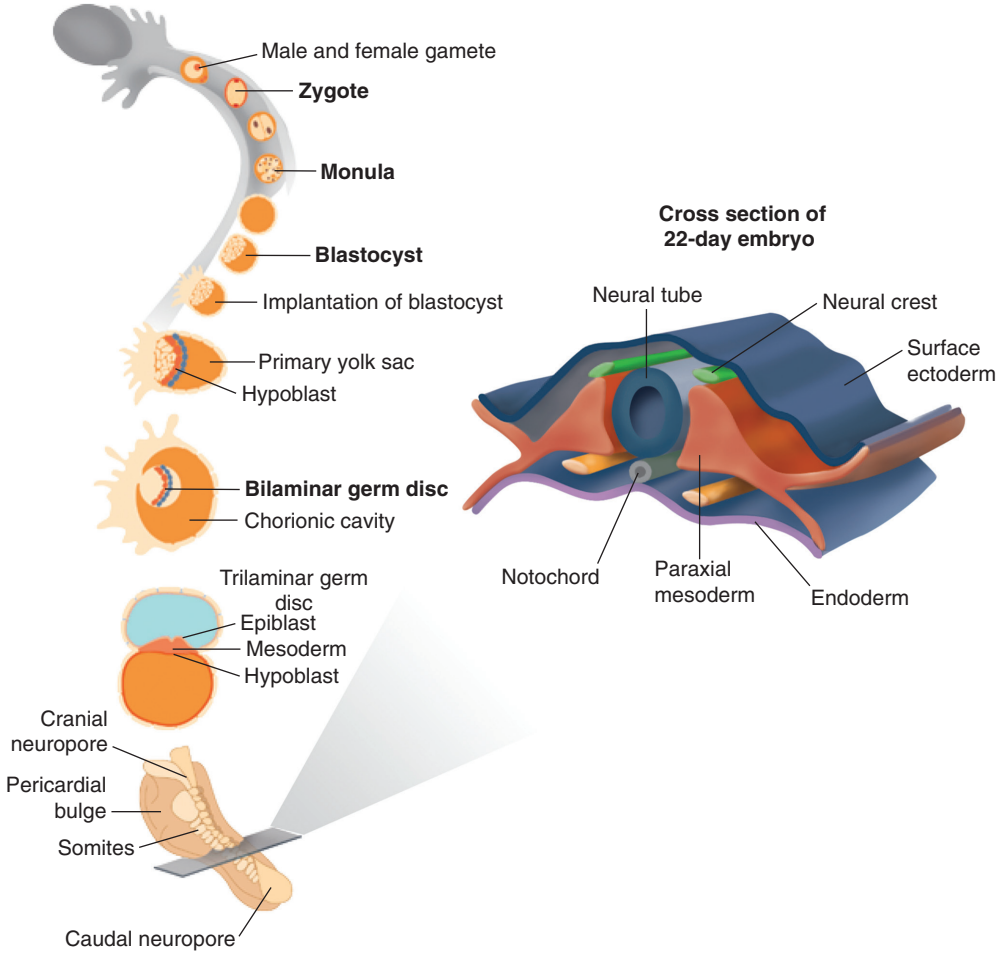


Figure 4-1 Early stages of embryonic development. The cross section demonstrates the neural tube and underlying notochord with adjacent neural crest cells *(green)* and mesoderm *(red)*. There is overlying surface ectoderm and underlying endoderm. The optic sulci develop within the neuropore at day 22. *(Illustration by Paul Schiffmacher. Adapted with permission from Forrester JV, Dick AD, McMenamin PG, Roberts F, Pearlman E.* The Eye: Basic Sciences in Practice. *4th ed. Elsevier; 2016:eFig 2-1.)*

are transient migratory stem cells that can form tissues with ectodermal and mesodermal characteristics (Fig 4-3). Several types of neural crest cells can be distinguished according to their location and contributions. Ocular structures are derived from cranial neural crest cells (referred to as *neural crest cells* throughout this chapter).

The eye and orbital tissues develop from ectoderm, mesoderm, and neural crest cells, with the neural crest cells making the largest contribution. In addition, neural crest cells contribute significantly to facial, dental, and cranial structures (Fig 4-4). For this reason, syndromes that arise from neural crest maldevelopment often involve the eye as well as these structures.

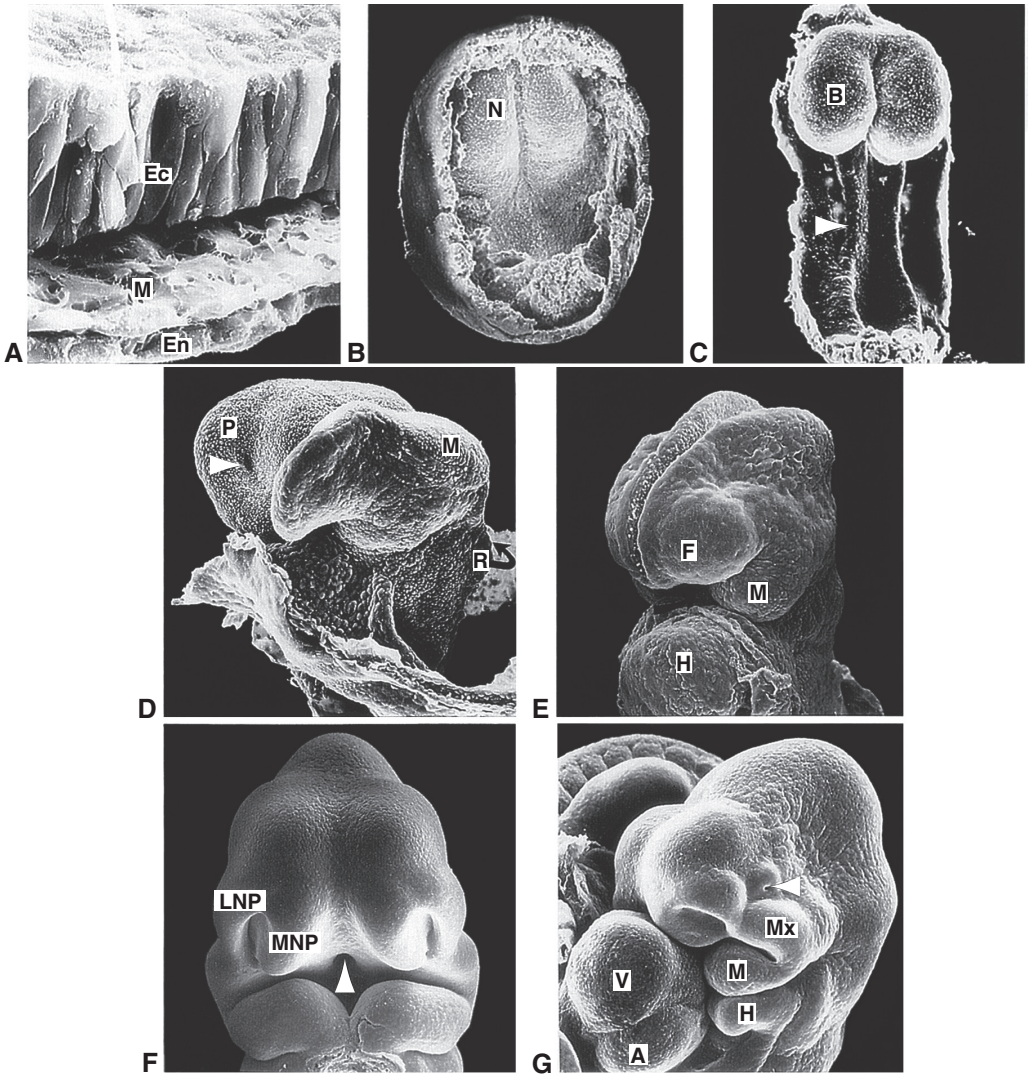


Figure 4-2 Scanning electron micrographs of normal craniofacial development. **A,** A parasagittal section through the cranial aspect of a gastrulation-stage mouse embryo. The cells of the 3 germ layers—ectoderm (Ec), mesoderm (M), and endoderm (En)—have distinct morphologies. **B,** The developing neural plate (N) is apparent in a dorsal view of this presomite mouse embryo. **C,** Neural folds *(arrowhead)* can be observed in the developing spinal cord region. The lateral aspects of the brain (B) region have not yet begun to elevate in this mouse embryo in the head-fold stage. **D,** Three regions of the brain can be distinguished at this 6-somite stage: prosencephalon (P), mesencephalon (M), and rhombencephalon (R, *curved black arrow*). Optic sulci *(arrowhead)* are visible as evaginations from the prosencephalon. **E,** The neural tube has not yet fused in this 12-somite embryo. The stomodeum, or primitive oral cavity, is bordered by the frontonasal prominence (F), the first visceral arch (mandibular arch, M), and the developing heart (H). **F,** Medial and lateral nasal prominences (MNP, LNP) surround olfactory pits in this 36-somite mouse embryo. The Rathke pouch *(arrowhead)* can be distinguished in the roof of the stomodeum. **G,** In this lateral view of a 36-somite mouse embryo, the first and second (hyoid, H) visceral arches are apparent. The region of the first arch consists of maxillary (Mx) and mandibular (M) components. Note the presence of the eye with its invaginating lens *(arrowhead)*. Atrial (A) and ventricular (V) heart chambers can be distinguished. *(Reproduced from Sulik KK, Johnston MC. Embryonic origin of holoprosencephaly: interrelationship of the developing brain and face.* Scan Electron Microsc. *1982;(Pt 1):311.)*

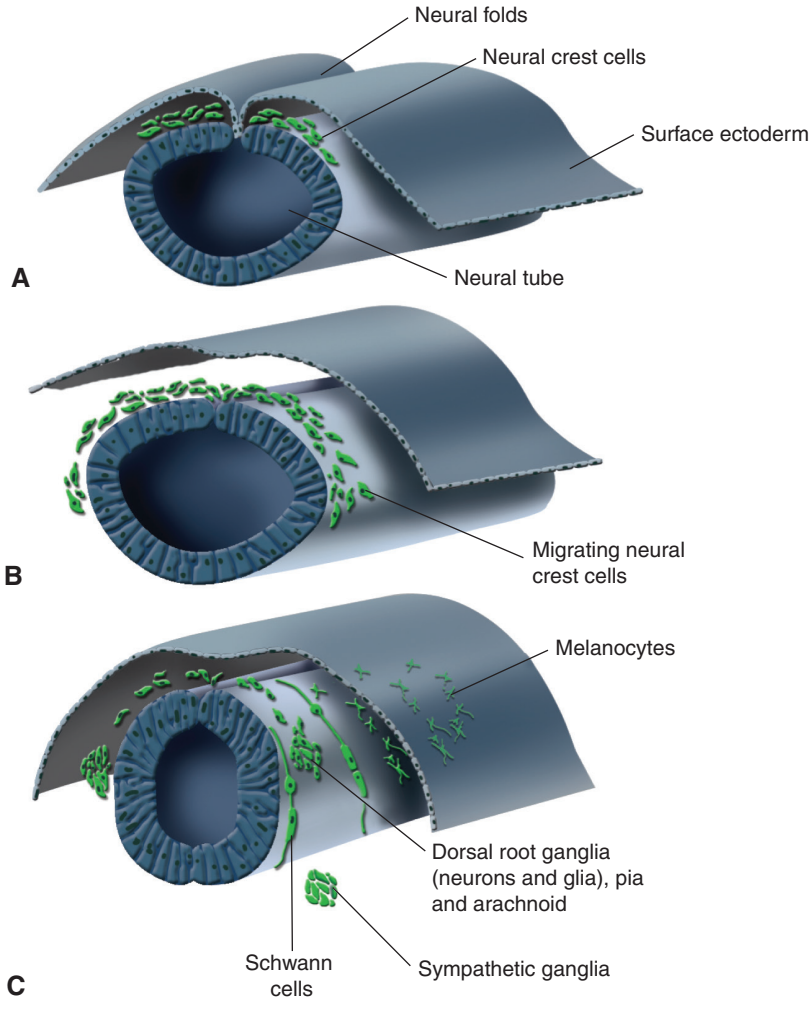


Figure 4-3 Migration of neural crest cells. **A,** Origin of neural crest cells from the junction of surface ectoderm and neuroectoderm *(light blue)* at the dorsal edge of the neural tube. **B,** Lateral/ventral migration. **C,** Differentiation of neural crest cells; note the development of melanocytes, dorsal root ganglia (including sensory ganglia of cranial nerve V), and autonomic ganglia. *(Illustration by Paul Schiffmacher. Adapted with permission from Forrester JV, Dick AD, McMenamin PG, Roberts F, Pearlman E.* The Eye: Basic Sciences in Practice. *4th ed. Elsevier; 2016:eFig 2-2.)*

CLINICAL PEARL

Oculoauriculovertebral dysplasia (also known as *Goldenhar syndrome*) arises from neural crest cell maldevelopment within the first 2 branchial arches. In this condition, numerous reported abnormalities affect different organ systems. Common clinical manifestations include hemifacial microsomia, limbal dermoids, cleft palate, preauricular skin tags, hearing loss, and eyelid coloboma.

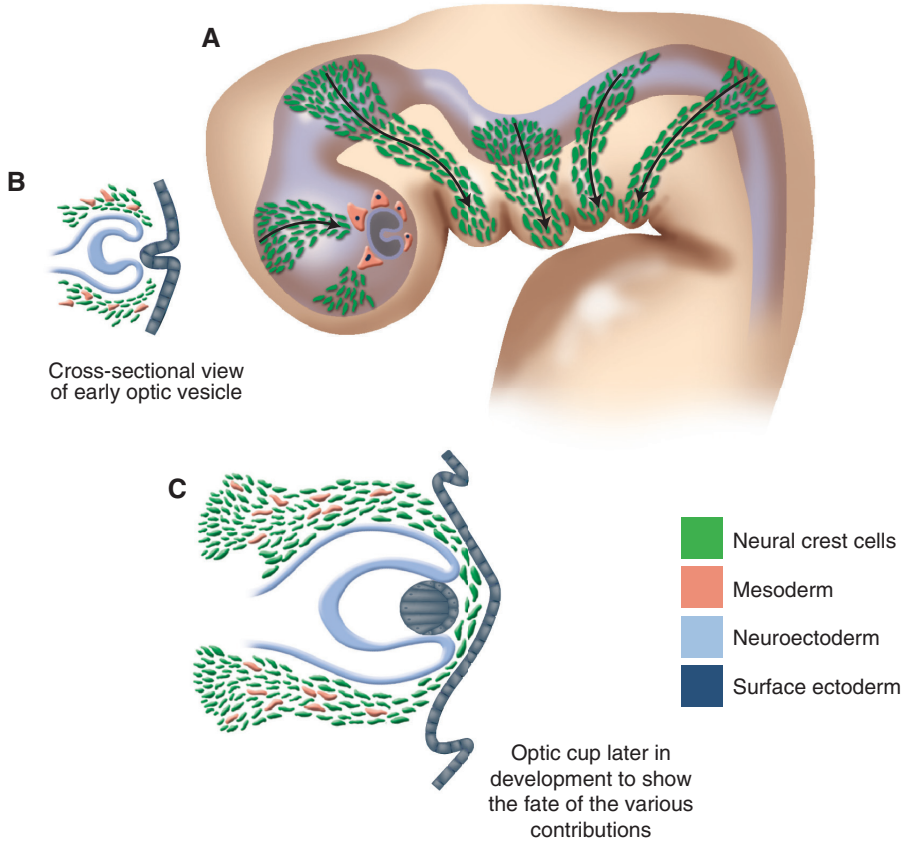


Figure 4-4 Migration of neural crest cells. **A,** Lateral and ventral migration of neural crest cells that will contribute to the development of the face and eye. In the head, neural crest cells contribute to tissues initially thought to be of mesodermal origin only. This does not occur in the trunk. Note the optic vesicle at the rostral ventral aspect. **B,** Cross section of the optic vesicle with invagination of the neuroectoderm (which will contribute to the retina, retinal pigment epithelium, and optic nerve) and overlying surface ectoderm (which contributes to the lens). **C,** The neural crest cells and mesoderm surrounding the neuroectoderm will contribute to the sclera, cornea, and uvea (melanocytes), among numerous other ocular structures. *(Illustration by Paul Schiffmacher. Adapted with permission from Forrester JV, Dick AD, McMenamin PG, Roberts F, Pearlman E.* The Eye: Basic Sciences in Practice. *4th ed. Elsevier; 2016:113.)*

Following gastrulation, the ectoderm separates into surface ectoderm and neuroectoderm. Each makes a key contribution to the development of the eye (Fig 4-5, Table 4-1).

Billon N, Iannarelli P, Monteiro MC, et al. The generation of adipocytes by the neural crest. *Development.* 2007;134(12):2283–2292.

Bogusiak K, Puch A, Arkuszewski P. Goldenhar syndrome: current perspectives. *World J Pediatr.* 2017;13(5):405–415.

Foster CS, Sainz de la Maza M, Tauber J. *The Sclera.* Springer Science + Business Media LLC; 2012.

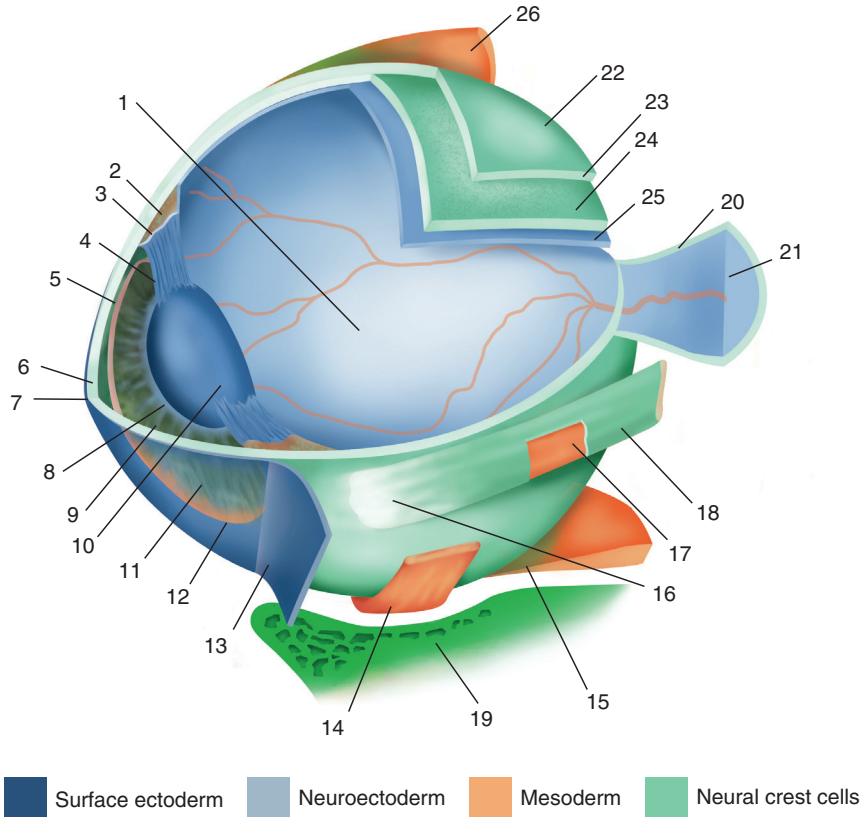


Figure 4-5 Embryologic origin of the ocular tissues. 1, Vitreous body; 2, ciliary muscle; 3, ciliary body epithelium; 4, zonular fibers; 5, corneal endothelium; 6, corneal stroma; 7, corneal epithelium; 8, iris sphincter; 9, iris dilator; 10, lens; 11, iris stroma; 12, trabecular meshwork; 13, conjunctiva; 14, inferior oblique muscle; 15, inferior rectus muscle; 16, medial rectus tendon; 17, medial rectus muscle; 18, medial rectus muscle sheath; 19, inferior orbital bones; 20, optic nerve sheath; 21, optic nerve; 22, bulbar sheath; 23, sclera (portions of the temporal sclera are derived from the mesoderm); 24, choroid; 25, neurosensory retina and retinal pigment epithelium; 26, superior rectus muscle. *(Developed by Evan Silverstein, MD, and Vikram S. Brar, MD. Illustration by Cyndie C.H. Wooley; original art by Paul Schiffmacher.)*

Eye Development

Figure 4-6 and Table 4-2 outline the timeline of ocular development. Video 4-1 presents a guided animation of ocular embryology.

VIDEO 4-1 Ocular embryology.
Animation developed by Evan Silverstein, MD.

The optic primordium appears in neural folds at 22 days. Two optic sulci, derived from neuroectoderm, develop on either side of the midline and eventually deepen to form an optic pit, which subsequently forms the *optic vesicles* (see Fig 4-6A, B). The narrow neck of

Table 4-1 Derivatives of Embryonic Tissues

Ectoderm			Mesoderm
Neuroectoderm	**Neural crest cells**	**Surface ectoderm**	
Ciliary body epithelium (nonpigmented and pigmented)	Bones: midline and inferior orbital bones; parts of orbital roof and lateral rim	Epithelium, glands, cilia of skin of eyelids, and caruncle	Extraocular muscle fibers
Iris epithelium (nonpigmented and pigmented)	Cartilage	Lacrimal drainage system	Orbital fat
Iris sphincter and dilator muscles	Connective tissue of orbit	Lacrimal gland	Vascular endothelium
Vitreous	Ciliary ganglion	Conjunctival epithelium	Ciliary body
Neurosensory retina	Orbital fat	Corneal epithelium	Iris stroma
Retinal pigment epithelium	Lacrimal gland	Lens	Temporal sclera
Optic nerve, axons, and glia	Extraocular muscle sheaths and tendons Vasculature: muscle and connective tissue sheaths of ocular and orbital vessels Corneal stroma and endothelium Melanocytes (uveal and epithelial) Schwann cells of ciliary nerves Sclera, except temporal sclera Trabecular meshwork Iris stroma Vitreous Choroid Meningeal sheaths of the optic nerve	Vitreous	Vitreous Choroid

each vesicle directly connects it to the developing forebrain. Once the optic vesicle touches the inner aspect of the surface ectoderm, the vesicle invaginates to form a bilayered embryologic optic cup. The inner layer forms the neural retina, and the outer layer forms the retinal pigment epithelium (RPE) (see Fig 4-6B–D).

As the optic cup forms, 2 processes take place. First, the surface ectoderm begins to invaginate to form the lens (see Fig 4-6B–D). Second, the area between the cup and the surface ectoderm fills with a combination of mesodermal and neural crest–derived cells, collectively termed the *ectomesenchyme,* which will form much of the anterior segment of the eye (see Fig 4-6E). In the area surrounding the posterior aspect of the optic cup, the same group of cells will give rise to the hyaloid vessels, choroid, and sclera (see Fig 4-6C–E).

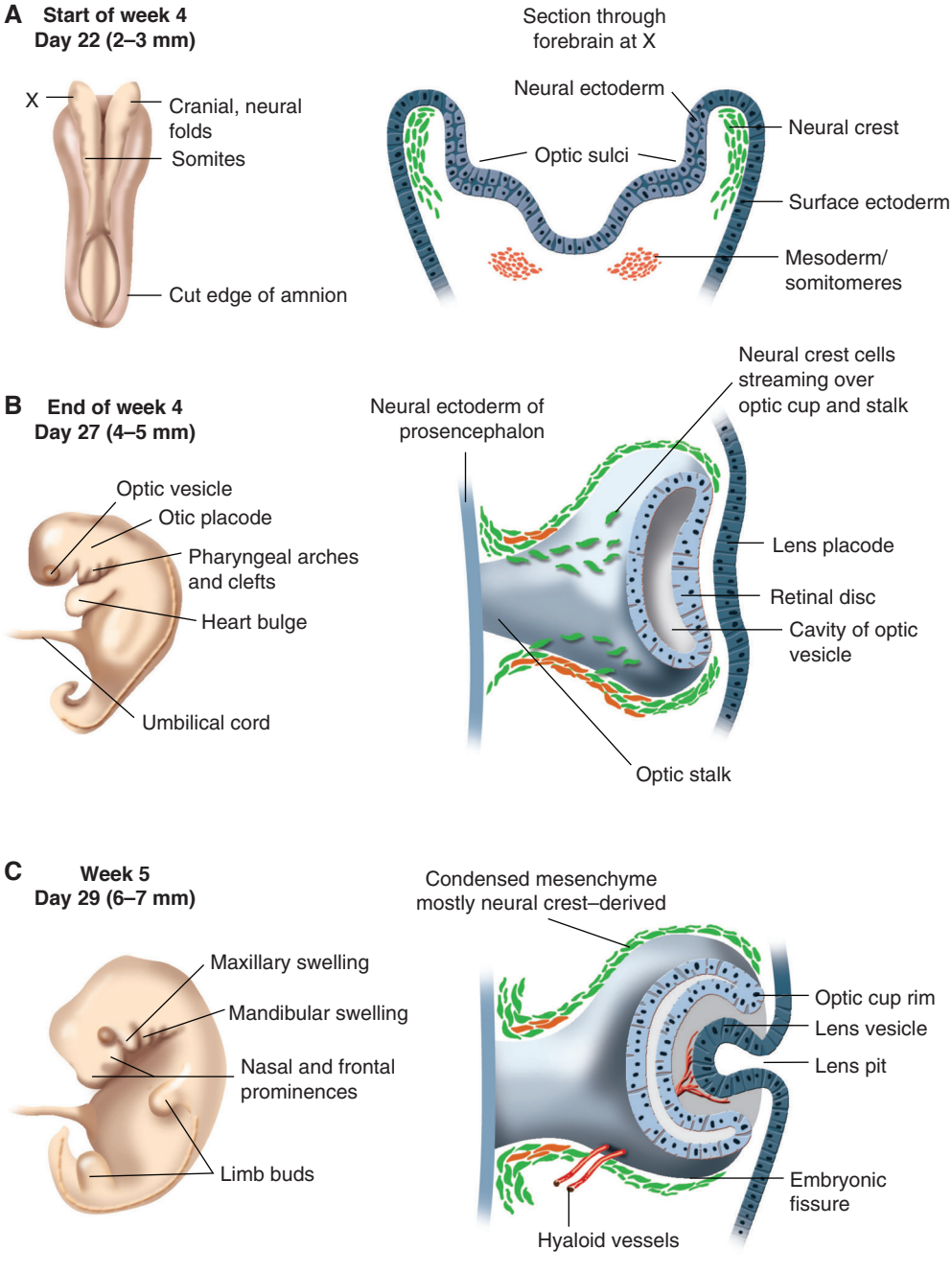


Figure 4-6 Embryonic development of the eye. The contributions of the surface ectoderm, neuroectoderm, neural crest cells, and mesoderm are shown. RPE = retinal pigment epithelium. *(Illustration by Paul Schiffmacher. Adapted from Forrester JV, Dick AD, McMenamin PG, Roberts F, Pearlman E.* The Eye: Basic Sciences in Practice. *4th ed. Elsevier; 2016:104–105.)*

(Continued)

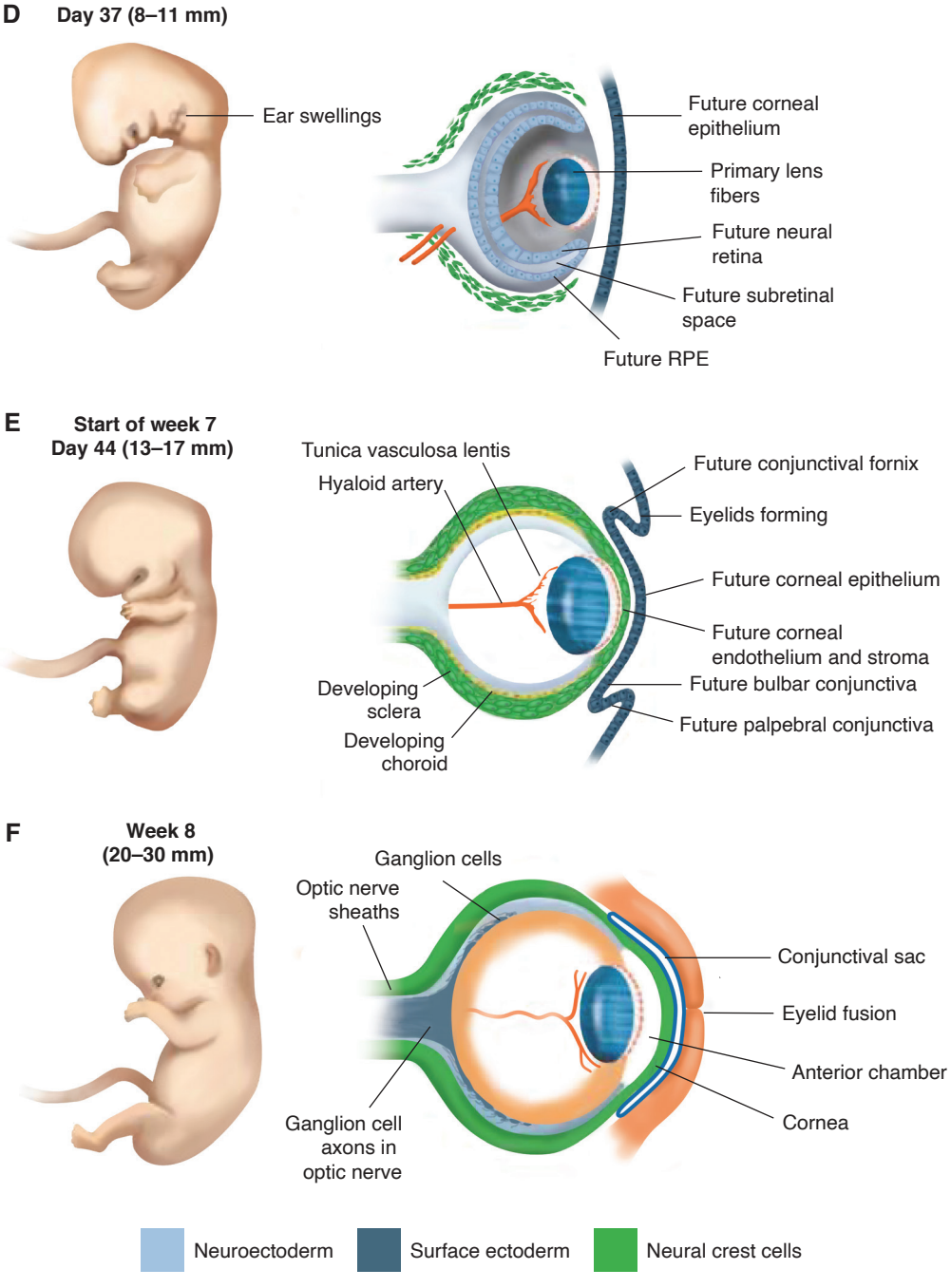


Figure 4-6 *(continued)*

Table 4-2 Chronology of Embryonic and Fetal Development of the Eye

22 days	Optic primordium appears in neural folds (1.5–3.0 mm).
25 days	Optic vesicle evaginates. Neural crest cells migrate to surround vesicle.
28 days	Vesicle induces lens placode.
4–5 weeks	Eyelid folds appear.
Second month	Invagination of optic and lens vesicles occurs. Hyaloid artery enters the eye via embryonic fissure. Closure of embryonic fissure begins. Pigment granules appear in retinal pigment epithelium. Primordia of lateral rectus and superior oblique muscles grow anteriorly. Eyelid folds meet and fuse. Nasolacrimal groove begins to form. Retinal differentiation begins with nuclear and marginal zones. Migration of retinal cells begins. Neural crest cells of corneal endothelium migrate centrally. Corneal stroma follows. Cavity of lens vesicle is obliterated. Secondary vitreous surrounds hyaloid system. Choroidal vasculature develops. Axons from ganglion cells migrate to optic nerve. Glial lamina cribrosa forms. Bruch membrane appears.
Third month	Precursors of rods and cones differentiate. Anterior rim of optic vesicle grows forward, and ciliary body starts to develop. Sclera condenses. Vortex veins pierce sclera.
Fourth month	Retinal vessels grow into nerve fiber layer near optic nerve head. Folds of ciliary processes appear. Iris sphincter develops. Descemet membrane forms. Schlemm canal appears. Hyaloid system starts to regress. Glands and cilia develop.
Fifth month	Photoreceptors develop inner segments. Choroidal vessels form layers. Iris stroma is vascularized. Eyelids begin to separate.
Sixth month	Retinal ganglion cells thicken in macula. Recurrent arterial branches join the choroidal vessels. Dilator muscle of iris forms.
Seventh month	Outer segments of photoreceptors differentiate. Central fovea starts to thin. Fibrous lamina cribrosa forms. Choroidal melanocytes produce pigment. Circular muscle forms in ciliary body.
Eighth month	Anterior chamber angle completes formation. Hyaloid system disappears.
Ninth month	Retinal vessels reach the periphery. Myelination of optic nerve fibers to lamina cribrosa is complete. Pupillary membrane disappears.

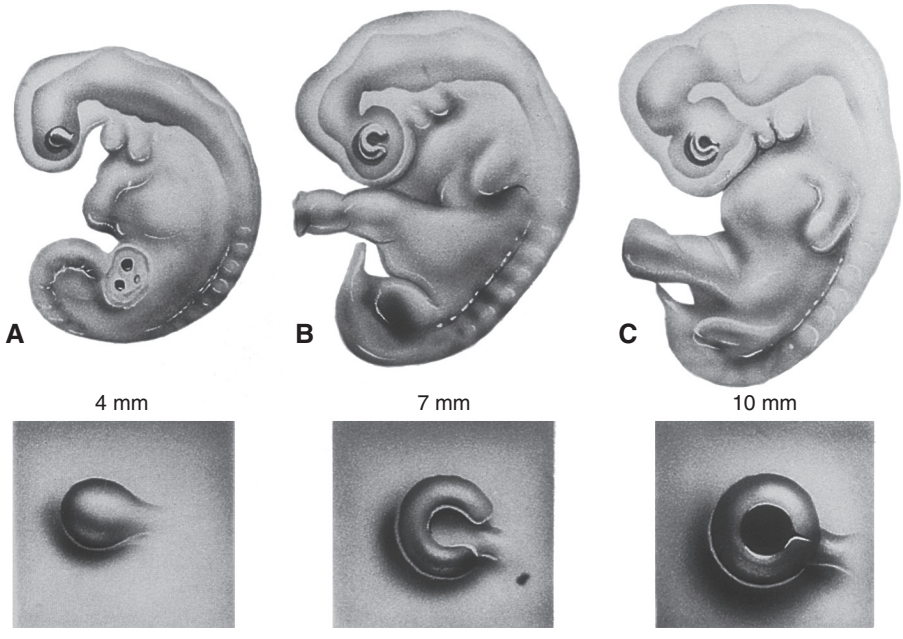


Figure 4-7 Ocular and somatic development. **A,** Flexion of the neural tube and ballooning of the optic vesicle. **B,** Upper-limb buds appear as the optic cup and embryonic fissure emerge. **C,** Completion of the optic cup with closure of the fissure. Convolutions appear in the brain, and leg buds appear. Measurements show the size of the embryo. *Bottom (left to right):* Optic vesicle; optic cup with open embryonic fissure; cup with fissure closing.

The invagination of the optic cup occurs asymmetrically (Fig 4-7). It contains a ventral fissure, the embryonic fissure of the optic cup, that facilitates entry of mesodermal and neural crest cells. The fissure closes at its center first and then "zips" both anteriorly and posteriorly. Failure of the embryonic fissure to close leads to a coloboma of the iris, lens, retina, and/or optic nerve. See BCSC Section 6, *Pediatric Ophthalmology and Strabismus,* for further discussion of congenital and developmental ocular diseases. The following sections discuss the development of individual ocular structures.

CLINICAL PEARL

Anterior colobomas (which cause iris and occasionally anterior scleral defects) are the most common type; central colobomas are the least common; and posterior colobomas (which cause optic nerve head, retinal, and choroidal defects) occur with a frequency somewhere in between. The location of fissure closure correlates with the inferonasal quadrant, which is where colobomas are found clinically (Fig 4-8).

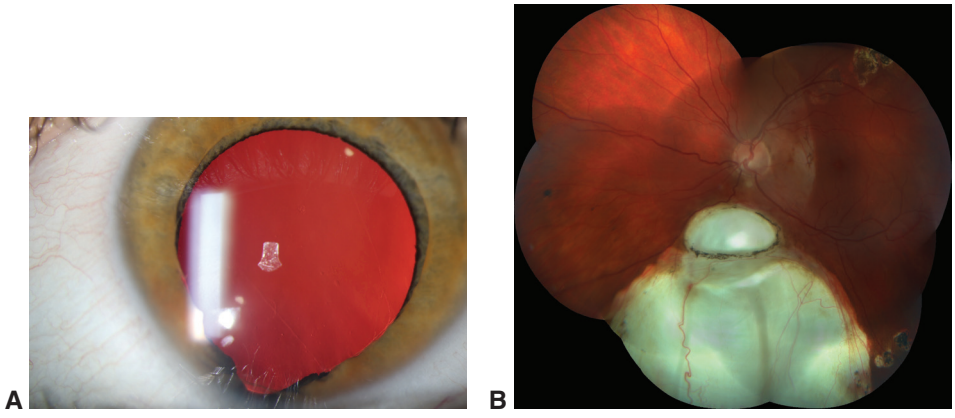


Figure 4-8 Ocular coloboma. Color photographs of the left eye of the same patient. The embryonic fissure correlates to the inferior nasal aspect of the eye. Colobomas of different ocular structures arise in this axis when the fissure fails to close. **A,** Anterior segment photograph demonstrating iris coloboma. The red reflex also demonstrates irregular development of the inferior lens equator and absence of zonules. **B,** Fundus photograph demonstrating coloboma in the inferior nasal quadrant with absence of retina and choroid. The optic nerve is also enlarged. *(Courtesy of Vikram S. Brar, MD.)*

Lens

Lens formation begins with proliferation of surface ectoderm cells to form a lens plate, followed by inward invagination of the plate to form a lens pit. As the pit deepens, it closes anteriorly and detaches to form the lens vesicle (see Fig 4-6C, D). The remaining cells at the surface form the corneal epithelium (see Fig 4-6D). Invading neural crest cells form the corneal endothelium and stroma, along with other anterior segment structures (see Fig 4-6E).

The lens vesicle is a single-layer structure composed of cuboidal cells surrounding a large lumen, and it sits within the optic cup. The anterior cells remain cuboidal and single layered throughout life, but the rest of the lens epithelium cells become elongated, and their proliferation fills the optic vesicle. These cells make up the primary lens fibers that eventually form the embryonal nucleus. The remaining outer cells create a true basement membrane known as the *lens capsule* (Fig 4-9).

Development of the lens vesicle is supported by a branching network of vessels, derived from the hyaloid artery, known as the *tunica vasculosa lentis*. Failure of this tissue to regress can lead to conditions ranging from pupillary membranes, seen on routine slit-lamp examination, to a malformation called *persistent fetal vasculature,* which can be associated with lenticular opacity and abnormal development of the eye. See also BCSC Section 6, *Pediatric Ophthalmology and Strabismus.*

The lens is a unique structure in that its basement membrane surrounds its cellular component. The lens capsule is transparent, thickest at its equator, and thinnest posteriorly. It is composed of type IV collagen and glycosaminoglycans (GAGs). The elasticity of the lens capsule is key to facilitating changes in lens shape to achieve accommodation. The anterior

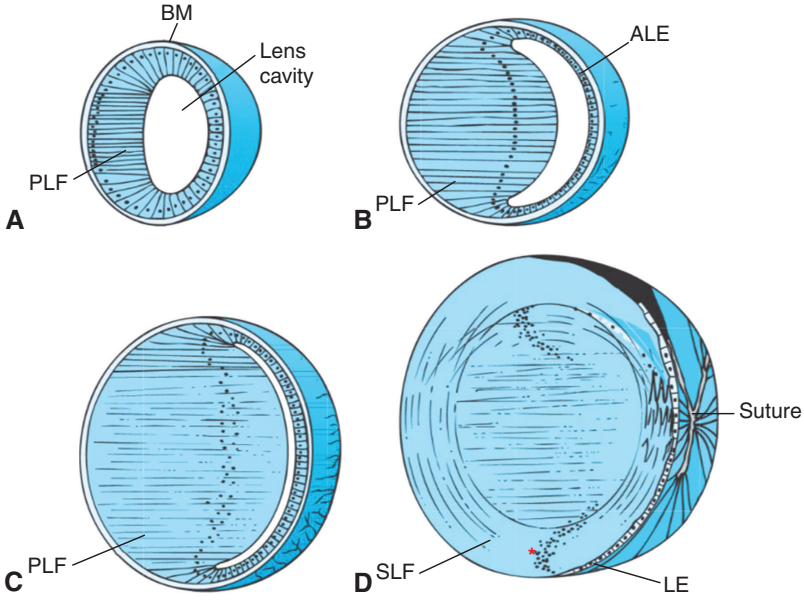


Figure 4-9 Lens formation. **A,** Lens vesicle. **B,** Anterior cells remain cuboidal, whereas the posterior cells elongate. **C,** The posterior cells eventually fill the lens vesicle, giving rise to the embryonic nucleus. **D,** The anterior cells give rise to the lens epithelium (LE). Note the lens bow region *(red asterisk)* extending from the epithelial cells, giving rise to the secondary lens fibers (SLF). ALE = anterior lens epithelium; BM = basement membrane; PLF = primary lens fibers. *(Modified with permission from Forrester JV, Dick AD, McMenamin PG, Roberts F, Pearlman E.* The Eye: Basic Sciences in Practice. *4th ed. Elsevier; 2016:115.)*

lens (cuboidal) epithelium continues to form new lens fibers throughout life (see Fig 4-9D), leading to the lenticular thickening observed with age. The zonular fibers of the lens form as part of the tertiary vitreous, consisting mostly of mesoderm and ectoderm.

Posterior Segment

Retina

The inner layer of the optic cup forms the neural retina, and the outer layer forms the RPE (Fig 4-10). These opposing surfaces are ciliated. The inner-layer cilia develop into the photoreceptors, while the outer-layer cilia regress.

CLINICAL PEARL

Embryologically, the neurosensory retina and RPE eventually appose; however, they lack covalent linkage. Throughout life, the retina remains attached to the RPE through a combination of hydrogen bonds, electrostatic forces, and osmotic gradient. In certain conditions, fluid accumulates in this subsensory potential space, leading to retinal detachment.

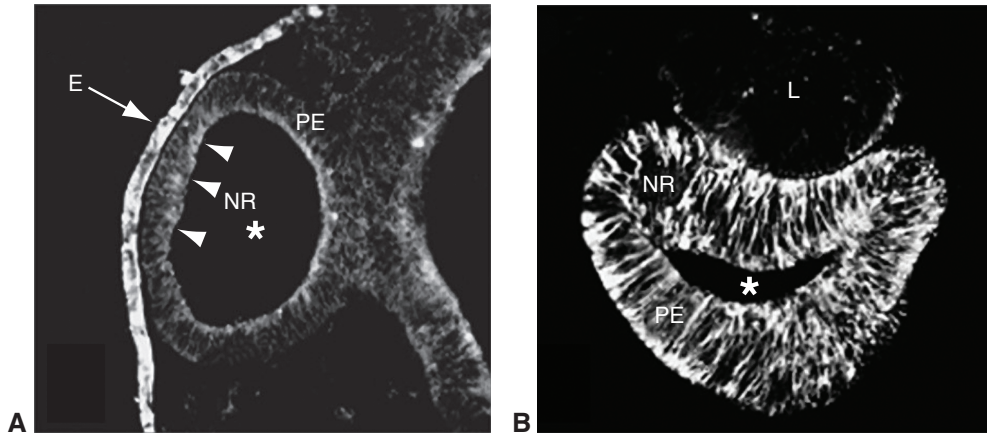


Figure 4-10 Development of the retina and the retinal pigment epithelium. **A,** Apposition of the surface ectoderm (E) with the inner wall of the optic cup *(arrowheads);* the neural retina (NR) is separated from the outer wall and the pigment epithelium (PE) by the subretinal space *(asterisk).* **B,** Further invagination of the optic cup with induction of the overlying lens (L) by the NR. The intervening subretinal space *(asterisk)* separates the NR from the PE. *(Modified with permission from Ryan SJ, Ogden TE, Hinton DR, Schachat AP, Wilkinson CP.* Retina. *3rd ed. Mosby; 2001:5.)*

Neural (inner) retinal development is driven by overlapping cascades of genetic programs. Several "master" switches help determine lineages and drive cell fate. These include Nrl (neural retina leucine zipper), a transcription factor that serves as an intrinsic regulator of rod photoreceptor development. Retinal development occurs concentrically, beginning in the center of the optic cup and extending peripherally. Lamination of the neural retina occurs at approximately 8–12 weeks of gestation with the formation of inner and outer neuroblastic layers. Ganglion cells appear to be the first to differentiate; early in the second trimester, they proliferate rapidly (Fig 4-11). The internal and external limiting membranes develop when cells cease to proliferate and begin to differentiate.

Retinal vasculature develops from remnants of the hyaloid artery; this artery is retained within the optic nerve and eventually becomes the central retinal artery (Fig 4-12). Blood vessel development at this stage occurs from mesenchymal precursors (ie, vasculogenesis) or from existing blood vessels (ie, angiogenesis). In the developing eye under normal conditions, angiogenesis is not pathologic. Endothelial cells organize posteriorly, with vessel development following the same concentric pattern as retinal development.

CLINICAL PEARL

The concentric pattern of retina vascular development from the optic nerve to the ora is the basis for the zone I–III designations in the classification of retinopathy of prematurity.

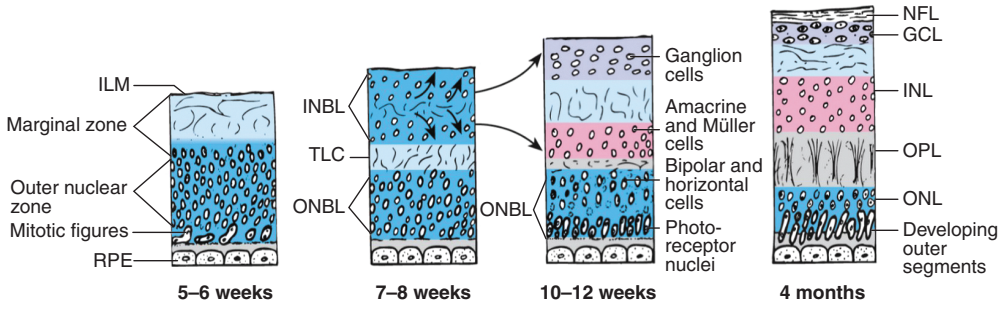


Figure 4-11 Development of the neural retina. The inner neuroblastic layer (INBL) gives rise to ganglion, Müller, and amacrine cells. The outer neuroblastic layer (ONBL) gives rise to bipolar and horizontal cells. Later, the cell bodies and outer segments of the photoreceptors develop. GCL = ganglion cell layer; ILM = internal limiting membrane; INL = inner nuclear layer; NFL = nerve fiber layer; ONL = outer nuclear layer; OPL = outer plexiform layer; RPE = retinal pigment epithelium; TLC = transient layer of Chievitz. *(Reproduced with permission from Forrester JV, Dick AD, McMenamin PG, Roberts F, Pearlman E.* The Eye: Basic Sciences in Practice. *4th ed. Elsevier; 2016:115.)*

Retinal pigment epithelium

The RPE forms from proliferating columnar epithelial cells that create lateral tight junctions and deposit a basement membrane, which later becomes the inner layer of Bruch membrane. The RPE is the only pigmented tissue in the body that is not derived from neural crest cells, although these cells are located at the anterior-most edge of the neural crest, suggesting shared origins.

Optic nerve

The optic nerve develops from the optic stalk, the narrow isthmus that connects the optic vesicles with the forebrain (see Fig 4-6B, C). The optic stalk is highly active in regulating cell migration into and around the developing eye, mostly through release of ligands and expression of growth factor receptors. It initially forms from neuroectodermal cells surrounded by neural crest cells. In the sixth week of gestation, neuroectodermal cells begin to vacuolate and degenerate, providing space for axons from the ganglion cells of the inner retina (see Fig 4-12). The surrounding neural crest cells form meninges, whereas neuroectodermal cells form surrounding oligodendrocytes (to form myelin sheaths). Peripheral nerves, including most cranial nerves, are surrounded by myelin supplied by Schwann cells. The exception is the optic nerve, which is surrounded by oligodendrocytes. This difference is an important reason for the optic nerve's susceptibility to neuritis.

Vitreous

The vitreous probably develops from both mesodermal and ectodermal components. Neural crest cells of the inner optic cup probably contribute the connective fibers of the vitreous. The hyaloid vasculature develops from mesodermally derived cells (Fig 4-13; see also Fig 4-6C, D and Fig 4-12). The primary vitreous, the earliest vitreous in the embryo, forms a central conical structure that contains the hyaloid vasculature (Fig 4-14; see also Fig 4-13) and is surrounded by secondary vitreous. The secondary vitreous forms from hyalocytes as

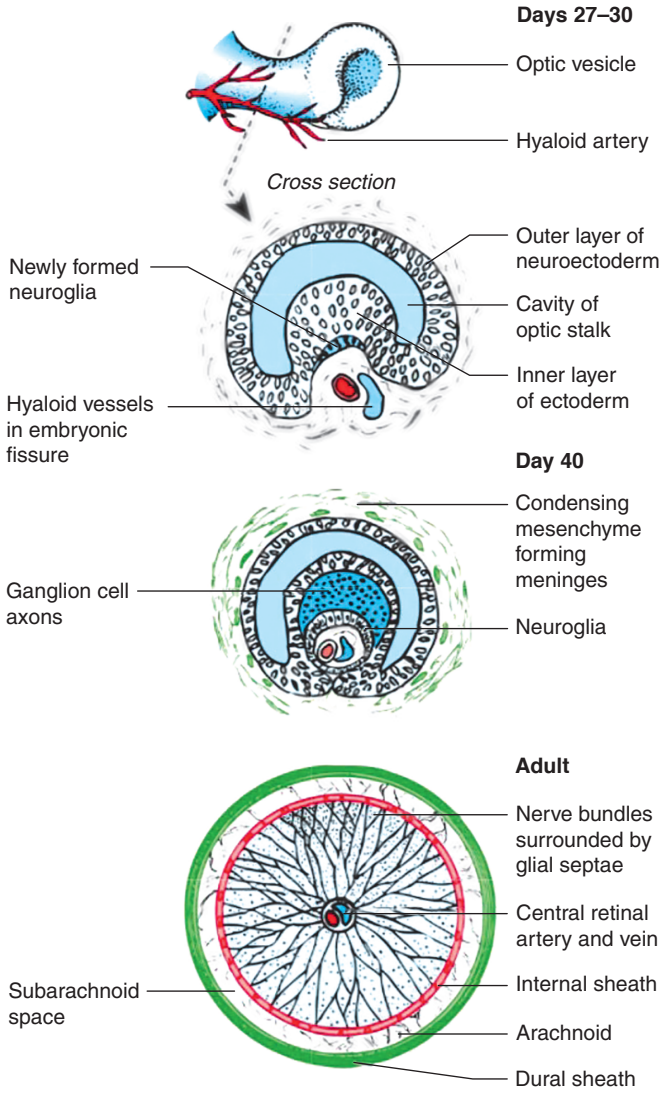


Figure 4-12 Development of the optic nerve. The hyaloid artery enters the eye via the embryonic fissure. As the fissure closes, the artery is retained within the optic nerve stalk and becomes the central retinal artery. Condensation of the surrounding neural crest cells and mesoderm form the optic nerve sheath and pial vessels. The developing ganglion cells grow toward the optic nerve stalk along the inner layer of ectoderm. The outer layer will form the lamina cribrosa. Astroglia generate the septae around the nerve bundles. These cells later give rise to oligodendrocytes, which myelinate the postlaminar axons of the retinal ganglion cells. *(Modified with permission from Forrester JV, Dick AD, McMenamin PG, Roberts F, Pearlman E.* The Eye: Basic Sciences in Practice. *4th ed. Elsevier; 2016:117.)*

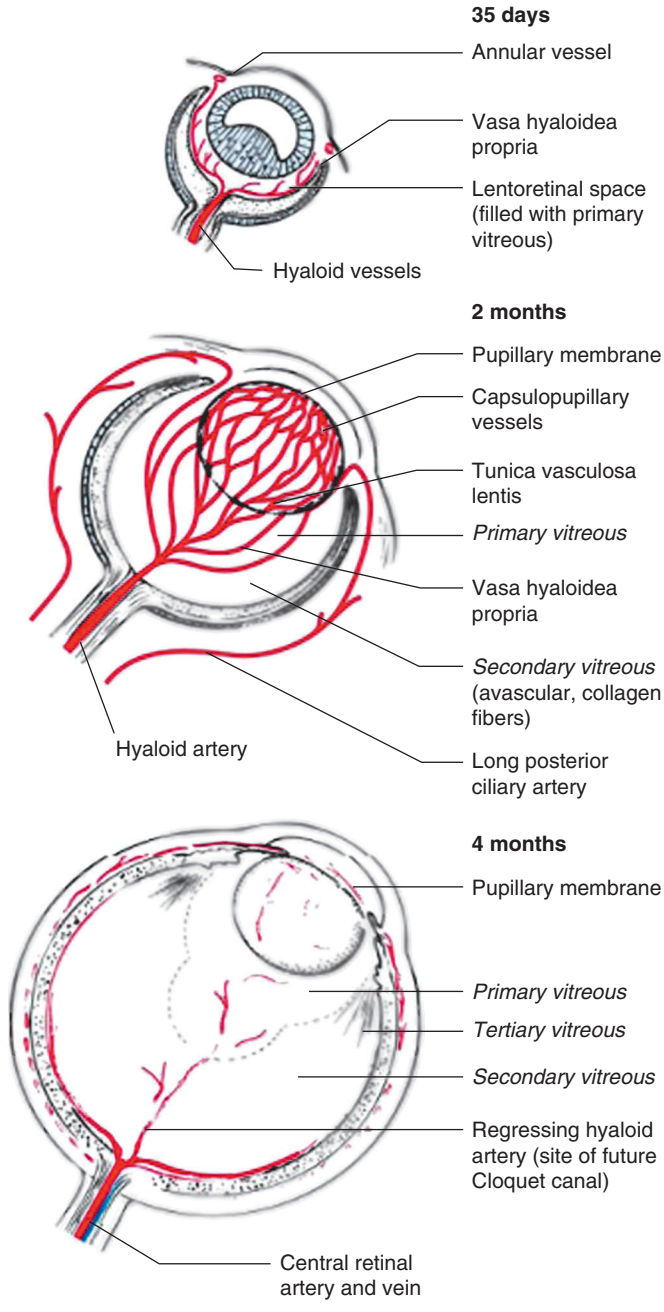


Figure 4-13 Development of the vitreous. The mesoderm gives rise to the hyaloid artery, which is contained within the primary vitreous. This vascular system supplies the tunica vasculosa lentis. The secondary vitreous forms from hyalocytes as the primary vitreous regresses. The zonular fibers develop from the tertiary vitreous. *(Modified with permission from Forrester JV, Dick AD, McMenamin PG, Roberts F, Pearlman E.* The Eye: Basic Sciences in Practice. *4th ed. Elsevier; 2016:123.)*

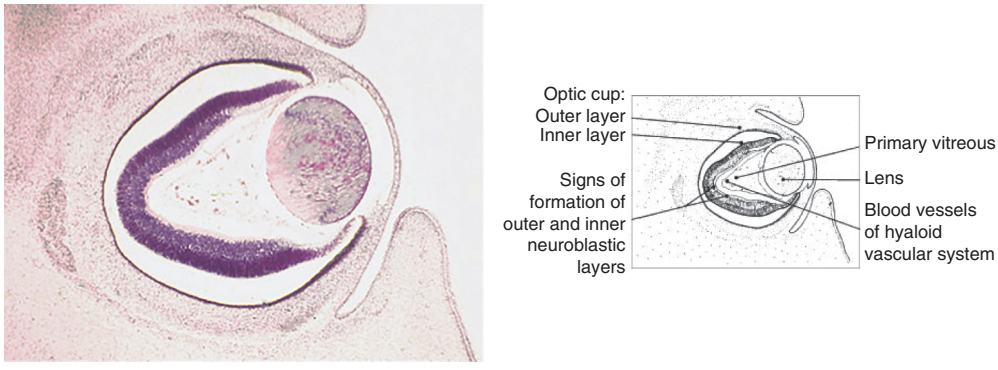


Figure 4-14 Histologic image and corresponding illustration showing the relationship between the optic cup, primary vitreous, and lens. Note the vasculature of the primary vitreous. The ciliary body and iris have not developed. Note the corneal epithelium and eyelids developing from surface ectoderm. *(Reproduced with permission from Spalton D, Hitchings R, Hunter P.* Atlas of Clinical Ophthalmology. *3rd ed. Elsevier/Mosby; 2005:398.)*

the primary vitreous begins to regress, eventually (by the sixth fetal month) enveloping the regressed primary vitreous. Between months 4 and 6, the zonular fibers of the lens develop from tertiary vitreous and are distinct from the primary and secondary vitreous. Remnants of the primary vitreous include the Cloquet canal and its anterior extension, the hyaloideocapsular ligament (also known as *ligament of Weiger*).

CLINICAL PEARL

Persistent fetal vasculature is a congenital disorder that arises when the hyaloid vasculature fails to regress. It can manifest as a unilateral cataract with microphthalmia and sometimes retinal detachment.

Uvea

The uvea (also called *uveal tract*) is the pigmented vascular layer of the eye and develops from a combination of mesoderm and neural crest cells. It comprises the iris, ciliary body, and choroid. The corresponding epithelial layers of the ciliary body and iris are derived from the neuroectoderm and are not considered part of the uvea. The uvea obtains its dark color from the neural crest–derived melanocytes residing within it. Its blood vessels and ciliary muscles are derived from the mesoderm.

Ciliary body and iris

At the anterior aspect of the optic cup, the surrounding mesoderm proliferates, pushing the neuroectoderm inward and centrally between the corneal endothelium and the anterior lens surface. This process, in turn, gives rise to the ciliary body and iris epithelium (Fig 4-15).

Mesodermal proliferation results in formation of the ciliary muscle and leads to infolding of the neuroectoderm. These folds give rise to the ciliary processes, which are

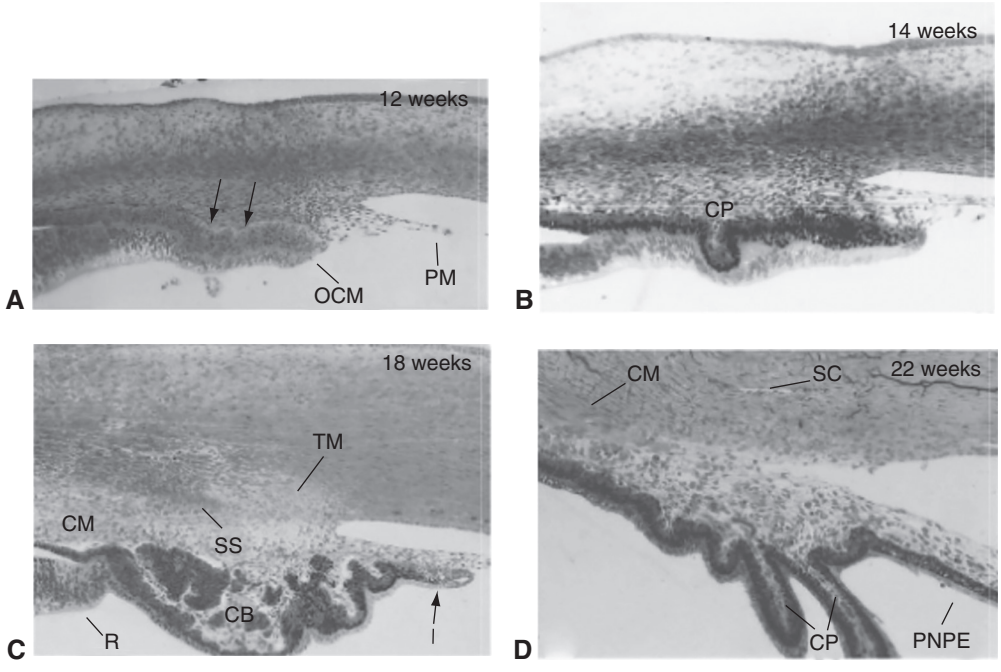


Figure 4-15 Development of the iris and ciliary body in a human fetal eye from 12 to 22 weeks. **A,** *Arrows* indicate proliferating vascular mesoderm behind the neuroectoderm at the optic cup margin (OCM). **B,** Continued growth of the mesoderm, with infolding of the neuroectoderm and development of a ciliary process (CP). Note the inner pigmented and outer nonpigmented layers of the ciliary epithelium. **C,** Anteriorly, the neuroectoderm forms the epithelial layers of the iris (I). At this stage, the angle recess is present, with developing trabecular meshwork (TM), ciliary muscle (CM), and intervening scleral spur (SS). **D,** Developing CPs and iris. Note that the posterior nonpigmented epithelium of the iris (PNPE) is continuous with the nonpigmented ciliary epithelium. The PNPE will acquire pigment as the iris develops. CB = ciliary body; PM = pupillary membrane; R = retina; SC = Schlemm canal. *(Modified with permission from Forrester JV, Dick AD, McMenamin PG, Roberts F, Pearlman E.* The Eye: Basic Sciences in Practice. *4th ed. Elsevier; 2016:125.)*

lined by 2 layers of epithelium: (1) an inner, nonpigmented layer, facing the posterior chamber; and (2) an outer, pigmented layer. The inner, nonpigmented layer of the ciliary body is continuous with the retina posteriorly and the nonpigmented posterior epithelium of the iris anteriorly. The latter acquires pigment over the course of development, starting at the pupil margin and progressing radially to the iris root, giving rise to the posterior iris pigment epithelium found in the adult eye. Pigmentation does not occur in the anterior epithelial layer of the iris. The outer, pigmented layer of the ciliary body is continuous with the RPE posteriorly.

Anteriorly, the neuroectoderm incorporates surrounding mesenchymal elements from the tunica vasculosa lentis. The subsequent anterior component, of mesodermal origin, gives rise to the iris stroma and vasculature. Posteriorly, the neuroectoderm continues as the epithelial layers of the iris and forms the sphincter and dilator muscles. The dilator muscles are a direct extension of the anterior iris epithelium (Fig 4-16).

Choroid

Condensation of the neural crest cells and mesoderm surrounding the optic cup produces the choroid on the inner aspect of the cup as well as the sclera and cornea on its outer aspect (see Fig 4-6D, E). A layer of small blood vessels, the *choriocapillaris,* forms first and is fenestrated. This process is followed by the development of an outer layer of larger vessels, which gives rise to the vortex veins and branches of the posterior ciliary circulation. Subsequently, a middle layer of arterioles forms between the choriocapillaris and the outer layer of larger vessels. Melanocytes develop in the choroid later in gestation.

Cornea, Anterior Chamber, and Sclera

Cornea and anterior chamber

Surface ectoderm closes over the lens pit and gives rise to the corneal epithelium (see Fig 4-6D). This process is followed by 3 successive waves of migration of neural crest–derived cells (Fig 4-17; see also Fig 4-6E). The *first wave* gives rise to the corneal endothelium, passing between the surface ectoderm and the anterior lens vesicle. The *second wave* passes between the endothelium and epithelium to give rise to the keratocytes of the corneal stroma. The *third wave*, consisting of cells of neural crest and mesodermal origin, contributes to iris development (Table 4-3).

The corneal endothelial cells meet with the developing iris, forming the angle recess. The trabecular meshwork and the Schlemm canal develop from mesenchymal cells posterior to the recess. The endothelial cells that line the canal and collector channels are derived from adjacent capillaries, which eventually form the episcleral venous plexus. The resultant aqueous veins receive aqueous humor and deliver it to the venous circulation (see Chapter 2, Figs 2-22, 2-23). The trabecular beams undergo further maturation and stratification to form the layered trabecular meshwork. Changes in this process have been implicated in the development of congenital glaucoma and anterior chamber dysgenesis. The scleral spur forms between the trabecular meshwork and the ciliary muscle as the anterior chamber angle develops (see Fig 4-15C, D).

Sclera

The sclera forms from mesodermal (temporal sclera) and neural crest–derived ectomesenchymal elements. The sclera joins the developing cornea near the equator of the eye but continues to develop and expand to surround the developing optic cup. The scleral spur and Tenon capsule form later, at the time of extraocular muscle insertion.

Development of the Extraocular Muscles, Adnexa, and Orbit

Extraocular Muscles

The extraocular muscles (EOMs) form from paraxial and prechordal mesoderm, following cues from the developing eye as well as from the surrounding neural crest–derived mesenchyme. Interactions among the optic cup, mesoderm, and neural crest cells are crucial to the proper development and organization of the EOMs. If the optic cup fails to form and the eye vesicle turns into a cyst (microphthalmia spectrum), the EOMs often develop anomalously.

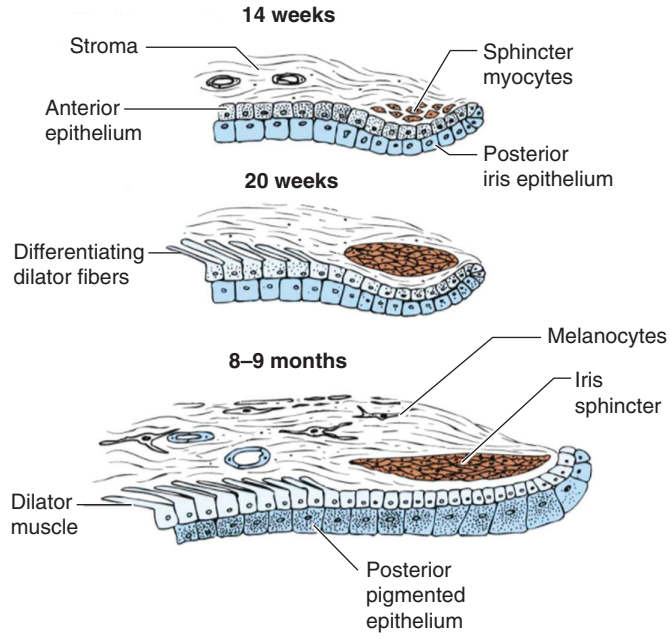


Figure 4-16 Development of the iris. The iris sphincter and dilator muscles are derived from neuroectoderm. The dilator muscle arises directly from the anterior iris epithelium. *(Modified with permission from Forrester JV, Dick AD, McMenamin PG, Roberts F, Pearlman E.* The Eye: Basic Sciences in Practice. *4th ed. Elsevier; 2016:126.)*

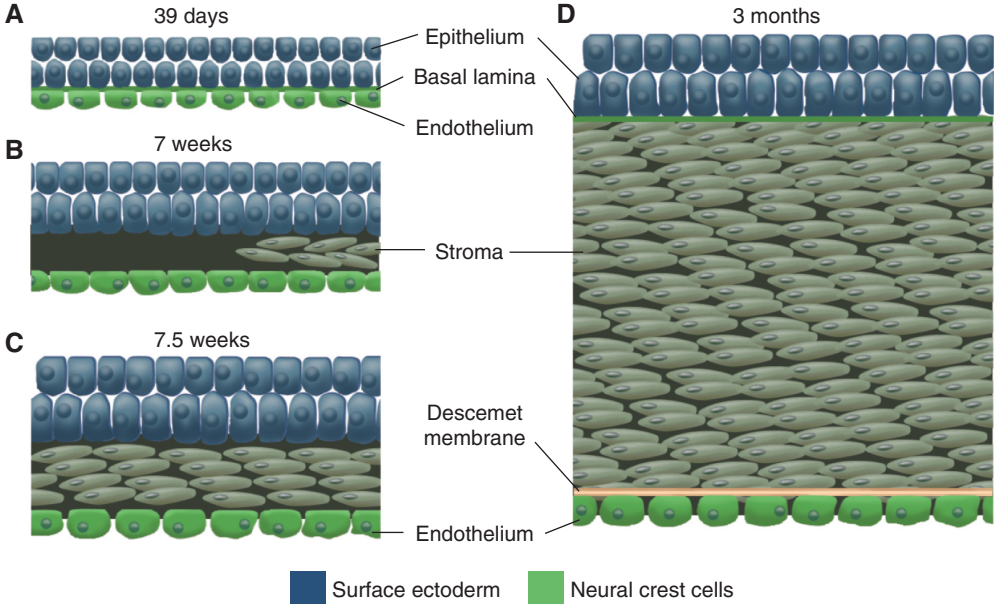


Figure 4-17 Development of the cornea in the central region. **A,** At day 39, 2-layered epithelium rests on the basal lamina and is separated from the endothelium (first wave) by a narrow acellular space. **B,** At week 7, neural crest–derived ectomesenchymal cells from the periphery migrate into the space between the epithelium and the endothelium (second wave). **C,** Mesenchymal cells (future keratocytes) are arranged in 4–5 incomplete layers by 7.5 weeks of gestation; a few collagen fibrils are present among the cells. **D,** By 3 months, the epithelium has 2–3 layers of cells, and the stroma has approximately 25–30 layers of keratocytes that are arranged more regularly in the posterior half. Thin, uneven Descemet membrane lies between the most posterior keratocytes and the single layer of endothelium. *(Illustration by Cyndie C.H. Wooley.)*

Table 4-3 Waves of Migration of Neural Crest–Derived Cells in the Anterior Segment

Wave	Cell Type	Tissue
1	Ectomesenchymal	Endothelium
2	Ectomesenchymal	Keratocytes of corneal stroma
3	Neural crest Mesodermal	Iris (melanocytes/stroma) Pupillary membrane/iris vessels

Data from Eghrari AO, Riazuddin SA, Gottsch JD. Overview of the cornea: structure, function, and development. *Prog Mol Biol Transl Sci.* 2015;134:7–23; and Forrester JV, Dick AD, McMenamin PG, Roberts F, Pearlman E. Embryology and early development of the eye and adnexa. In: *The Eye: Basic Sciences in Practice.* 4th ed. Elsevier; 2016:119.

This is likely because signals from the optic cup are necessary for proper migration of neural crest cells into the eye and surrounding tissues, and subsequent signals from these neural crest–derived cells are required for proper development and organization of the EOMs.

Congenital cranial dysinnervation disorders involving the EOMs include Duane syndrome, Marcus Gunn jaw-winking syndrome, Möbius syndrome, and congenital fibrosis of the EOMs (see BCSC Section 6, *Pediatric Ophthalmology and Strabismus*). Genetic studies have identified pathogenic variants in genes for neuron biology and axon guidance (eg, *KIF21A, PHOX2A, TUBB3*) that cause these EOM syndromes.

Congenital ptosis and other congenital EOM disorders probably result from delays in muscle innervation. Current models suggest that as the muscle mesenchyme and associated nerve jointly develop, a delay in innervation of the muscle mesenchyme can cause premature differentiation of the mesenchyme into connective tissue (ie, fibrosis). The extent of the delay may correlate with the severity of fibrosis (eg, severity of the congenital ptosis and levator muscle dysfunction). Furthermore, the delay in, or absence of, innervation may provide a window for inappropriate innervation by another cranial nerve, such as trigeminal innervation of the levator muscle (Marcus Gunn jaw-winking syndrome) or oculomotor innervation of the lateral rectus muscle (Duane syndrome).

Bohnsack BL, Gallina D, Thompson H, et al. Development of extraocular muscles requires early signals from periocular neural crest and the developing eye. *Arch Ophthalmol.* 2011;129(8):1030–1041.

Engle EC. Human genetic disorders of axon guidance. *Cold Spring Harb Perspect Biol.* 2010;2(3):a001784.

Adnexa

The upper eyelid begins to develop at 4–5 weeks of gestation as a proliferation of surface ectoderm in the region of the future outer canthus. During the second month, both the upper and the lower eyelids become discernible as undifferentiated skinfolds that surround mesenchyme of neural crest origin (see Fig 4-6E, F and Fig 4-14). Later, mesodermal mesenchyme infiltrates the eyelids and differentiates into the palpebral musculature. The eyelid folds grow toward each other as well as laterally. Starting near the inner canthus, the margins of the folds fuse

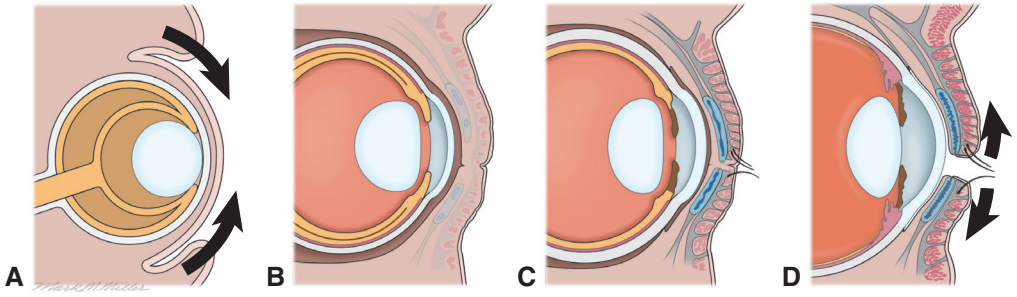


Figure 4-18 Development of the eyelids. **A,** During the seventh week, the upper and lower eyelid folds grow over the developing eye. **B,** Eyelid folds fuse during weeks 8 to 10; fusion starts along the nasal margin. **C**, Subsequently, cilia and glandular structures develop. **D,** From the fifth to seventh months, the eyelids gradually separate. *(Original illustration by Paul Schiffmacher; revised illustration by Mark Miller.)*

between weeks 8 and 10 of gestation. As the folds adhere to each other, development of the cilia and glands begins. The orbicularis muscle condenses in the fold during week 12. The eyelid adhesions begin to gradually break down late in the fifth month (Fig 4-18), coincident with the secretion of sebum from the sebaceous glands and cornification of the surface epithelium.

The lacrimal gland begins to develop between the sixth and seventh weeks of gestation. Solid cords of epithelial cells proliferate from the basal cell layer of the conjunctiva in the temporal region of the fornix. Neural crest–derived mesenchymal cells aggregate at the tips of the cords and differentiate into acini. At approximately 3 months, ducts of the gland form by vacuolation of the cord cells and the development of lumina. Lacrimal gland (reflex) tear production does not begin until 20 or more days after birth. Therefore, newborn infants cry without tears.

Orbit

Orbital development involves key contributions from ectodermal, mesodermal, and neural crest–derived elements. By the fourth week of gestation, the frontonasal and maxillary processes of neural crest cells occupy the space that surrounds the optic cups. The bones, cartilage, fat, and connective tissues of the orbit develop from these cells. All bones of the orbit are membranous except the sphenoid, which is initially cartilaginous. Ossification begins during the third month of gestation, and fusion occurs between the sixth and seventh months.

Genetic Cascades and Morphogenic Gradients

The embryonic genome is not transcribed until the stage of midblastula transition, which takes place several hours after fertilization. Instead, maternal messenger RNA (mRNA) within the oocyte provides the initial set of genetic instructions to the fertilized egg. Once embryonic transcription begins, it follows a set of predefined genetic programs.

Homeobox Gene Program

The blueprint for the embryonic program involves the homeobox genes *(HOX)*. These genes are so named because they contain a distinctive and highly conserved segment of DNA, approximately 180 base pairs long, that encodes a conserved 60–amino acid sequence constituting the homeodomain. The homeodomain provides a protein with specific DNA-binding capabilities.

The function of *HOX* genes as master regulators arises from their ability to regulate the expression of downstream genes through homeodomain binding to DNA promoter sequences, wherein they act as switches of gene transcription. Each set of switches drives a particular cell fate, and transcriptional cascades of these switches lead to the development of different tissues and organs.

As expected, specific *HOX* genes are crucial for the development of the eye. The paired box 6 gene *(PAX6),* in particular, appears to be a master switch for eye development. The PAX6 transcription factor is expressed in a band in the anterior neural plate, very early in the primordial eye field, and ectopic expression of *PAX6* can lead to ectopic eyes and aniridia (Fig 4-19), Peters anomaly, coloboma, and microphthalmia.

The following *HOX* genes also play key roles in development of the eye, and pathogenic variations in these genes have been reported in patients with the conditions given within parentheses: paired box 2 (*PAX2;* renal coloboma syndrome), retina and anterior neural fold homeobox (*RAX;* eg, microphthalmia), and paired-like homeodomain 2 (*PITX2;* eg, Peters anomaly, Axenfeld-Rieger syndrome).

Shaham O, Menuchin Y, Farhy C, Ashery-Padan R. PAX6: a multi-level regulator of ocular development. *Prog Retin Eye Res.* 2012;31(5):351–376.

Growth Factors, Diffusible Ligands, and Morphogens

Gene-expression cascades are crucial for development of the eye, just as they are for development of most organs. However, to respond to cues in real time, cells in the developing

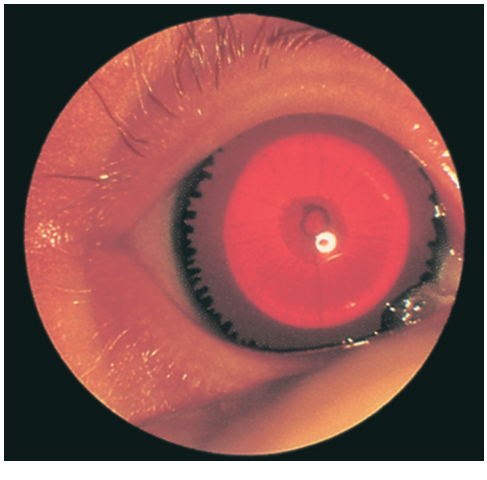


Figure 4-19 Aniridia in an infant. There is minimal iris root with ciliary processes visible.

eye require additional signals. These signals take the form of diffusible extracellular factors (termed *morphogens*) that are active in the earliest stages of embryonic development.

The most important of these factors include retinoic acid (RA), Wnt, fibroblast growth factors (FGFs), the hedgehog family members Shh and Ihh, and insulin-like growth factor (IGF). These factors fall into 2 broad groups. Group 1 ligands (eg, RA) interact with intracellular receptors that directly regulate gene expression. Group 2 ligands (eg, Wnt, FGFs) interact with cell-surface receptors that initiate an intracellular signaling cascade, often involving protein phosphorylation cascades, to eventually influence gene expression and intracellular remodeling (eg, cytoskeleton), cell motility, protein trafficking, and other processes.

CLINICAL PEARL

Defects in Wnt signaling cause familial exudative vitreoretinopathy (incomplete vascularization of the peripheral retina), leading to vitreous bleeding, tractional retinal detachments, and severe visual impairment.

Cells respond differently to ligands depending on ligand concentration in the context of a concentration gradient (also termed *morphogenic gradient*). In many cases, cells and tissues that have multiple potential fates use these diffusible ligands to activate a particular fate. For example, FGF signaling in the optic vesicle regulates expression of the basic helix-loop-helix transcription factor microphthalmia-associated transcription factor (MITF) in the optic cup, which in turn regulates the balance between development of neural retina and pigment epithelium. The interested reader is referred to several excellent reviews on the topic of eye development and diffusible ligands in embryogenesis.

Kish PE, Bohnsack BL, Gallina D, Kasprick DS, Kahana A. The eye as an organizer of craniofacial development. *Genesis*. 2011;49(4):222–230.

Rogers KW, Schier AF. Morphogen gradients: from generation to interpretation. *Annu Rev Cell Dev Biol*. 2011;27:377–407.

Sadler TW. *Langman's Medical Embryology*. 13th ed. Lippincott Williams & Wilkins; 2014.

Tabata T. Genetics of morphogen gradients. *Nat Rev Genet*. 2001;2(8):620–630.

Williams AL, Bohnsack BL. What's retinoic acid got to do with it? Retinoic acid regulation of the neural crest in craniofacial and ocular development. *Genesis*. 2019;57(7–8):e23308. doi:10.1002/dvg.23308

Future Directions

The embryologic study of how a single cell (zygote) develops into a multitude of cell and tissue types gave rise to the field of stem cell biology. The first successful culture of human embryonic stem cell (hESC) lines derived from spare in vitro fertilization blastocysts was reported in 1998. Stem cells range from totipotent to pluripotent to multipotent as they become more limited in their potential to form the entire range of cell and tissue types.

The strict definition of *stem cells* refers to cells that can self-renew via asymmetric cell division; the more colloquial and common definition refers to multipotent but lineage-restricted progenitor cells (eg, limbal stem cells). Although stem cell research has generally depended on the study of hESCs, the advent of induced pluripotent stem cell (iPSC)

technology has allowed stem cells to be grown from a small sample of adult somatic cells, such as skin cells, and provided a more easily accessible and less politically charged model for the study of pluripotency. Stem cell models have been extremely useful in the study of organogenesis, tissue differentiation, and associated genetic cascades.

The ability to generate 3-dimensional neural retina from hESCs, called *retinal organoids,* has been demonstrated in vitro. As they grow, retinal organoids follow the steps of normal embryonic development, including invagination of the optic vesicle and formation of the optic cup, in giving rise to complex, stratified retinal tissue opposed by the RPE. These organoids allow researchers to study human retinal development and disease outside the organism by using simple retinal networks that function like a developing human retina. Human retinal organoids have already been successfully used to model retinal diseases and conditions affecting the retina, such as microphthalmia, Best vitelliform macular dystrophy, gyrate atrophy, Leber congenital amaurosis, and retinitis pigmentosa.

The use of stem cell lines has expanded beyond the retina to other ocular tissues, such as corneal epithelium, and endothelial regeneration. Future therapies employing regenerative transplantation approaches, however, are more likely to utilize lineage-restricted progenitor cells so as to increase the likelihood of successful regeneration of function while reducing the risk of cancer.

Eiraku M, Takata N, Ishibashi H, et al. Self-organizing optic-cup morphogenesis in three-dimensional culture. *Nature.* 2011;472(7341):51–56.

Forrester JV, Dick AD, McMenamin PG, Roberts F, Pearlman E. Embryology and early development of the eye and adnexa. In: *The Eye: Basic Sciences in Practice.* 5th ed. Elsevier; 2020:106–134.

Gage PJ, Zacharias AL. Signaling "cross-talk" is integrated by transcription factors in the development of the anterior segment in the eye. *Dev Dyn.* 2009;238(9):2149–2162.

Graw J. The genetic and molecular basis of congenital eye defects. *Nat Rev Genet.* 2003;4(11):876–888.

Nakano T, Ando S, Takata N, et al. Self-formation of optic cups and storable stratified neural retina from human ESCs. *Cell Stem Cell.* 2012;10(6):771–785.

Sun B, Bikkuzin T, Li X, Shi Y, Zhang H. Human-induced pluripotent stem cells-derived cornea endothelial-like cells promote cornea transparency in a rabbit model of bullous keratopathy. *Stem Cells Dev*. 2021;30(17):856–864.

Swaroop A, Kim D, Forrest D. Transcriptional regulation of photoreceptor development and homeostasis in the mammalian retina. *Nat Rev Neurosci.* 2010;11(8):563–576.

PART III
Genetics

Introduction

Genetics is the study of heredity and the variations in inherited characteristics and diseases. Although genetics is a relatively new science compared with such disciplines as anatomy and physiology, its significance in expanding our overall understanding of human life cannot be overstated. Genetic knowledge can enhance our understanding of the processes of cellular function, embryology, and development, as well as our concepts of disease. As many as 90% of medical diseases either have a major genetic component or involve genetic factors that may significantly influence disease manifestations and severity.

Some 20,000–25,000 human genes involving about 180,000 exons are known. The discovery of previously unknown genes, such as the *homeobox-containing genes* (eg, the *HOX* and *PAX* gene families; see the section Homeobox Gene Program in Chapter 4)—which regulate, guide, and coordinate early embryologic development and differentiation—has broadened our understanding of physiology at the cellular and tissue levels. Similarly, the identification of genes that appear to be transcribed as initiating events in the process of *apoptosis* (programmed cell death) has facilitated the elucidation of the mechanisms of normal embryogenesis as well as degenerative disease and cancer progression.

Genetic disorders affect about 5% of live-born infants in the United States. Clinical findings are limited to the eye in 10%–15% of known genetic diseases. Most hereditary eye diseases are relatively rare; however, genetic factors play a central role in healthy ocular development and are not infrequently an underlying cause of childhood blindness and visual impairment in adults. By establishing a solid foundation in medical genetics, the reader may acquire a better understanding of the evolving role of genetics and genomics in ophthalmology, which, in turn, may improve the clinical care of affected individuals.

Terminology

Familiarity with the vocabulary of genetics and molecular biology will greatly enhance the reader's understanding of the following 2 chapters on molecular and clinical genetics. The reader is thus encouraged to review the genetics glossary in the online appendix of this book (www. aao.org/bcscappendix_section02) and consult online resources, such as the 2 examples that follow, to help reinforce concepts.



APPENDIX Genetics Glossary.



National Cancer Institute Dictionary of Genetics Terms. Accessed February 1, 2023. www.cancer.gov/publications/dictionaries/genetics-dictionary
National Human Genome Research Institute Talking Glossary of Genomic and Genetic Terms. Accessed February 1, 2023. www.genome.gov/glossary

CHAPTER 5

Molecular Genetics

Highlights

- Cell division occurs via a complex process known as the cell cycle. The function of tumor suppressor genes is to regulate this cycle. Alterations in these genes result in numerous conditions with ophthalmic manifestations, such as certain neurocutaneous disorders (phakomatoses) and retinoblastoma.
- Approximately 99% of DNA does not code for proteins and may be involved in the regulation of gene expression. The term epigenetics refers to the study of heritable processes that alter gene expression without changing the DNA sequence.
- Transcription factors determine the rate of messenger RNA production from DNA. The family of *PAX* genes encodes transcription factors, pathogenic variants (mutations) of which are involved in the development of numerous ophthalmic conditions.
- New gene therapies, such as AAV (adeno-associated virus) vector gene therapy and the CRISPR–Cas9 system, hold great potential to treat many previously untreatable eye diseases.

Cell Division and the Cell Cycle

Cell Division

A cell may undergo 2 types of division: mitosis and meiosis. Mitosis refers to somatic cell division, whereas meiosis refers to germinal cell replication.

The Cell Cycle

The cell cycle is the series of events that leads to cellular duplication and division (Fig 5-1). The 4 distinct phases are

- G_1 (growth, preparation for DNA synthesis)
- S (DNA synthesis/chromosome replication)
- G_2 (growth, preparation for mitosis)
- M (mitosis and cytokinesis)

During the M phase of the cell cycle, mitosis gives rise to the multiple generations of genetically identical cells needed for the growth and maintenance of an organism. The M phase consists of 2 processes: *mitosis,* in which the cell's replicated chromosomes divide into

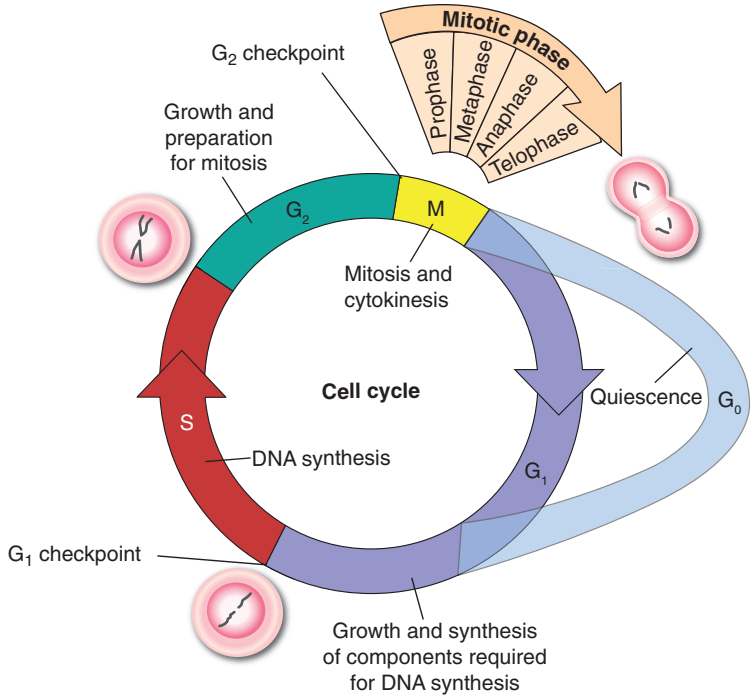


Figure 5-1 In the cell cycle, the progression from DNA synthesis (S) to mitosis (M) includes growth phases before (G_1) and after (G_2) the replication of DNA. Upon receiving signals to differentiate, cells leave the cycle and enter the final stage of cell differentiation, terminal differentiation. Cell-cycle regulation occurs at numerous checkpoints before the cell progresses from one phase to another. Under certain circumstances, cells may return to quiescence (G_0) or enter the pathway to programmed cell death (apoptosis).

2 identical groups, followed by *cytokinesis,* in which the cell's cytoplasm divides in half and forms 2 distinct, genetically identical daughter cells, each with the same diploid chromosome number and genetic information as the parent cell.

The M phase can be subdivided into several distinct, sequential phases:

- *prophase* (chromatin is condensed into chromosomes)
- *metaphase* (chromosomes align in the middle of the cell)
- *anaphase* (chromosomes split and migrate to opposite poles of the cell)
- *telophase* (2 daughter nuclei form at the poles of the cell)

Cells that have temporarily stopped dividing are said to have entered a state of quiescence called the *G_0 phase.*

Cell Cycle Regulation

In the cell cycle, transition from 1 phase to the next is regulated at checkpoints (see Fig 5-1). Important checkpoints occur at the following phase transitions:

- G_1: transition from G_1 to S
- G_2: transition from G_2 to M

At these checkpoints, the successful, error-free completion of the previous phase is verified. At the G_1 checkpoint, cell size and nutrient and growth factor availability are assessed, and the DNA is checked for damage. After the G_1 checkpoint is completed, the cell is committed to proceeding with cell division; otherwise, it enters the quiescent G_0 phase. At the G_2 checkpoint, further inspection of the DNA occurs before the cycle progresses to the M phase. If DNA damage is detected at either checkpoint, it may be repaired or programmed cell death (see the section Apoptosis) may be initiated.

Checkpoint regulation occurs via a family of proteins known as *cyclins* and *cyclin-dependent kinases (CDKs)*. At the G_1 checkpoint, CDK phosphorylation of proteins of the retinoblastoma (Rb) family facilitates downstream transcription in preparation for the S phase. Tumor suppressor genes like the Rb family often have a role in the regulation of the cell cycle, dysregulation of which can lead to cancer (see the section "Tumor suppressor genes").

CLINICAL PEARL

Checkpoint inhibitors represent a class of medication known as immunotherapy, which is used in the treatment of various cancers. In general, checkpoint inhibitors work by increasing the ability of our immune system to attack tumor cells. Enhanced immune activity can result in ocular side effects ranging from dry eyes to multifocal choroiditis.

Fortes BH, Liou H, Dalvin LA. Ophthalmic adverse effects of immune checkpoint inhibitors: the Mayo Clinic experience. *Br J Ophthalmol.* 2021;105(9):1263–1271.

Sun A, Bagella L, Tutton S, Romano G, Giordano A. From G_0 to S phase: a view of the roles played by the retinoblastoma (Rb) family members in the Rb-E2F pathway. *J Cell Biochem.* 2007;102(6):1400–1404.

Meiosis

Meiosis is a specialized type of cell division that consists of 2 successive cell divisions (meiosis I and meiosis II) and produces the ova and sperm necessary for sexual reproduction in eukaryotes (Fig 5-2). Unlike in mitosis, the chromosomes undergo recombination in meiosis, shuffling the genes from each parent to produce a different genetic combination in each gamete. Meiosis produces 4 genetically unique haploid cells, whereas mitosis produces 2 genetically identical diploid cells.

Interphase consists of the G_1 and S phases (there is no G_2 phase in meiosis) and is followed by meiosis I and then meiosis II. Both meiosis I and II are divided into prophase, metaphase, anaphase, and telophase stages, as in the mitotic cell cycle. In the G_1 phase, each chromosome consists of a single (very long) molecule of DNA. At this stage in humans, the cells contain 46 chromosomes, the same number as in somatic cells. During the S phase, each of the 46 chromosomes duplicates, becoming a complex of 2 identical sister chromatids.

During meiosis I, homologous chromosomes (a matched pair, 1 derived from each parent) separate into 2 cells. Each of the resulting daughter cells contains the entire haploid content of each chromosome; the first meiotic division thus reduces the ploidy of the original cell by half.

During meiosis II, each chromosome's sister strands (the chromatids) are decoupled, and the individual chromatids are segregated into haploid daughter cells. The 2 cells resulting from meiosis I divide during meiosis II, creating 4 haploid daughter cells.

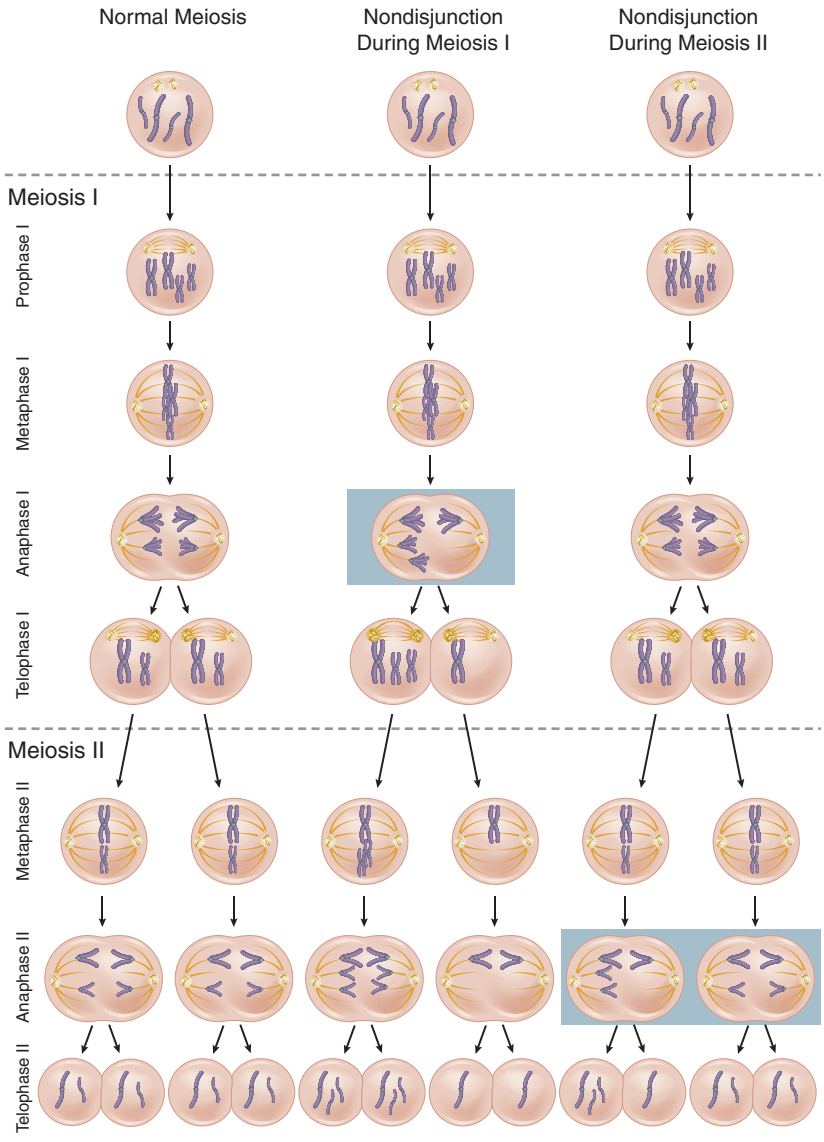


Figure 5-2 Normal meiosis and chromosomal nondisjunction *(blue boxes)* occurring at different phases of meiosis. See Chapter 6 in this volume for discussion of chromosomal nondisjunction. *(Illustration by Cyndie C.H. Wooley.)*

The specialized cells that arise from meiosis, called gametes, participate in sexual reproduction. The male gamete is a sperm, and the female gamete, an ovum. At conception, a sperm and an ovum unite, forming a zygote, a single cell containing 46 chromosomes. Because both parents contribute equally to the genetic makeup of their offspring, new and often advantageous gene combinations may emerge.

Chromosomal *crossing over* is the exchange of genetic material between homologous chromosomes that results in recombinant chromosomes. Crossing over occurs during the

prophase of meiosis I (prophase I), usually when matching regions on matching chromosomes break off and connect to the other chromosome. Although the same genes appear in the same order, the alleles are different. Thus, theoretically, offspring can have any combination of the parental alleles. This theory of the *independent assortment* of alleles is fundamental to genetic inheritance (see the sections Genes and Chromosomes and Independent Assortment in this chapter).

Genes and Chromosomes

The word *gene* comes from the Greek *genes* ("giving birth to") and is used as a term for individual units of hereditary information. Genes are the basic units of inheritance, and each carries a sequence of nucleotides that encodes a single trait or a single polypeptide chain and its associated regulatory regions. Human genes vary substantially in size, from approximately 500 base pairs (bp) to more than 2 million bp. However, more than 98% of human genes range in size from less than 10 kilobase pairs (kb; 1 kb = 1000 bp) to 500 kb.

While a single human cell contains enough DNA for 6 million genes, the 23 pairs of known chromosomes contain approximately 20,000–25,000 genes. The remaining 99% of genetic material is likely to be involved in the regulation of gene expression (see the section Noncoding DNA later in this chapter). The relative sequence of the genes, which are linearly arranged along the chromosome, is called the *genetic map.* A *locus* is the physical position or region occupied by a single gene on a chromosome. The physical contiguity of various gene loci becomes the vehicle for close associations between genes *(linkages)* and gene clustering in groups that characteristically move together or separately *(segregation)* from one generation to the next.

Each normal human somatic cell has 46 chromosomes composed of 23 pairs. Each member of a homologous pair carries matched, though not necessarily identical, genes in the same sequence. One member of each chromosome pair is inherited from the father, and the other is inherited from the mother. Each normal sperm or ovum contains 23 chromosomes, 1 representative from each pair; thus, each parent transmits half of their genetic information to each child. Of the 46 chromosomes, 44 are called *autosomes* because they provide information on somatic characteristics; the remaining 2 are the X and Y chromosomes (see the section X-Linked Inheritance in Chapter 6).

In the past, when only a few eye disease genes—or only the gene location—were known, clinicians often remembered the chromosomal locations. Now, it is known that numerous genes are involved in certain diseases, such as retinitis pigmentosa (RP). Information on genes, including their chromosomal locations, can be readily found in electronic databases, such as Online Mendelian Inheritance in Man (OMIM; www.omim.org).

Alleles

The alternative forms of a particular gene at the same locus on each chromosome of an identical pair are called *alleles* (Greek for *reciprocals*). If both members of a pair of alleles for a given autosomal locus are identical (ie, the DNA sequence is the same), the individual is *homozygous* (a *homozygote*). If the allelic genes are distinct (ie, the DNA sequence differs), the

individual is *heterozygous* (a *heterozygote*). Different gene defects can generate dramatically different phenotypes and still be allelic. For example, sickle cell disease (SS hemoglobinopathy), caused by homozygosity of 1 pathogenic variant, is substantially different from the phenotypic expression of SC hemoglobinopathy, yet the *Hb S* gene and the *Hb C* gene are allelic.

The term *polyallelism* refers to the many possible variants of a single gene. Protein variants that correspond to allelic variants frequently possess biochemical properties that slightly differ from those of the normal gene product. In mucopolysaccharidoses (MPSs), for example, the enzyme α-L-iduronidase is defective in both severe MPS I (Hurler syndrome) and attenuated MPS I (Scheie syndrome). These disorders arise from abnormalities of the same enzyme that stem from variations of the same gene. However, the clinical severity of these 2 disorders (age at onset; age at detection; and severity of affliction of the skeleton, liver, spleen, and cornea) is entirely different, presumably because the function of the enzyme variant is less altered by the MPS I variation. Because the affected enzyme is a protein composed of hundreds of amino acids, a variation resulting in a base substitution within a certain codon might cause a change in 1 or more amino acids in a portion of the enzyme remote from its active site, limiting the effect on the enzyme's function. However, the substitution of 1 amino acid at a crucial location in the enzyme's active site might abolish most or all enzymatic activity.

Several examples of allelic disorders appear in MPS. The phenotype of the usual heterozygote is determined by 1 allelic variant and 1 "normal" allele. However, the genotype of a compound heterozygote comprises 2 different allelic variants at the same locus. The genetic compound heterozygote in attenuated MPS is biochemically proven and clinically manifests as features intermediate to those observed in the homozygotes of the 2 alleles. When detailed biochemical analyses are performed, the products of the 2 alleles manifest slightly different properties (eg, rates of enzyme activity or electrophoretic migration).

Ashworth JL, Biswas S, Wraith E, Lloyd IC. Mucopolysaccharidoses and the eye. *Surv Ophthalmol*. 2006;51(1):1–17.

Fenzl CR, Teramoto K, Moshirfar M. Ocular manifestations and management recommendations of lysosomal storage disorders I: mucopolysaccharidoses. *Clin Ophthalmol*. 2015;9:1633–1644.

Segregation

Two allelic genes occupying the same gene locus on 2 homologous chromosomes are separated during the division of the 2 chromosomes during meiosis, with each going to a different gamete. Thus, the allelic genes are said to *segregate*, meaning they cannot occur together in a single offspring of the bearer. For example, if a parent is a compound heterozygote for both hemoglobin S and hemoglobin C, which occupy the same genetic locus on homologous chromosomes, none of their offspring will inherit both hemoglobins from that parent; each will inherit either one or the other.

Independent Assortment

Genes on different *(nonhomologous)* chromosomes may or may not separate together during meiotic cell division. In this random process, called *independent assortment,* nonallelic genes assort independently of one another. Because *crossing over* (chromosomal material exchange

between the members of a pair of homologous chromosomes) can occur in meiosis, 2 nonallelic genes originally on opposite members of the chromosomal pair may end up together on either of the 2 chromosomes or may remain separated, depending on their original positions and the sites of genetic interchange. Thus, the gametes of an individual with 2 nonallelic dominant traits, or *syntenic traits,* located on the same chromosome could produce 4 possible offspring. A child may inherit

- both traits, if the separate alleles remain on the same chromosome and the child inherits this chromosome
- neither trait, if the genes remain on 1 chromosome, but the child inherits the opposite chromosome with neither allele
- only 1 of the 2 alleles, if crossing over occurred between the loci, and the child receives the chromosome with that particular allele

This scheme for nonallelic traits depends on the independent assortment of chromosomes in the first division of meiosis. Approximately 50 crossovers (1–3 per chromosome) occur during an average meiotic division.

Linkage

Linkage is the major exception or modification to the law of independent assortment. Genes located reasonably close together on the same chromosome tend to be transmitted together, from generation to generation, more frequently than chance alone would allow; therefore, they are said to be linked. The closer together the 2 loci are, the less likely they are to be affected by crossovers. The genetic distance between genes is described in centimorgans (cM; named for Thomas Hunt Morgan, who described crossing over), and a distance of 1 cM (~1 million bp) between genes represents a 1% chance that these genes will cross over independently of one another. Linear physical proximity along a chromosome cannot be considered an automatic guarantor of linkage, however. Certain sites on each chromosome may be more vulnerable to homologous crossing over than others. *Linkage disequilibrium* occurs when combinations of alleles are present in a population more or less frequently than would be expected based on their distances from each other.

Gene Structure

Composed of DNA, *genes* are the molecular units of heredity and are located primarily in the cell nucleus, where they are assembled into *chromosomes* of varying sizes. Humans have 22 pairs of numbered chromosomes, which are numbered from largest (1) to smallest (22), and an additional pair of sex chromosomes (XY or XX). The 4 bases present in DNA—adenine (A), cytosine (C), guanine (G), and thymine (T)—are combined into a double-helix structure that allows replication, transcription, and translation. The genetic structure (Fig 5-3) can be likened to the sections of an encyclopedia, where genes are the chapters, *exons* the sentences, *trinucleotides* the words, and *nucleotides* the letters.

Mitochondria, the site of oxidative phosphorylation, are the power plants of the cell. Mitochondria are a vestige of a symbiotic relationship between 2 primitive unicellular

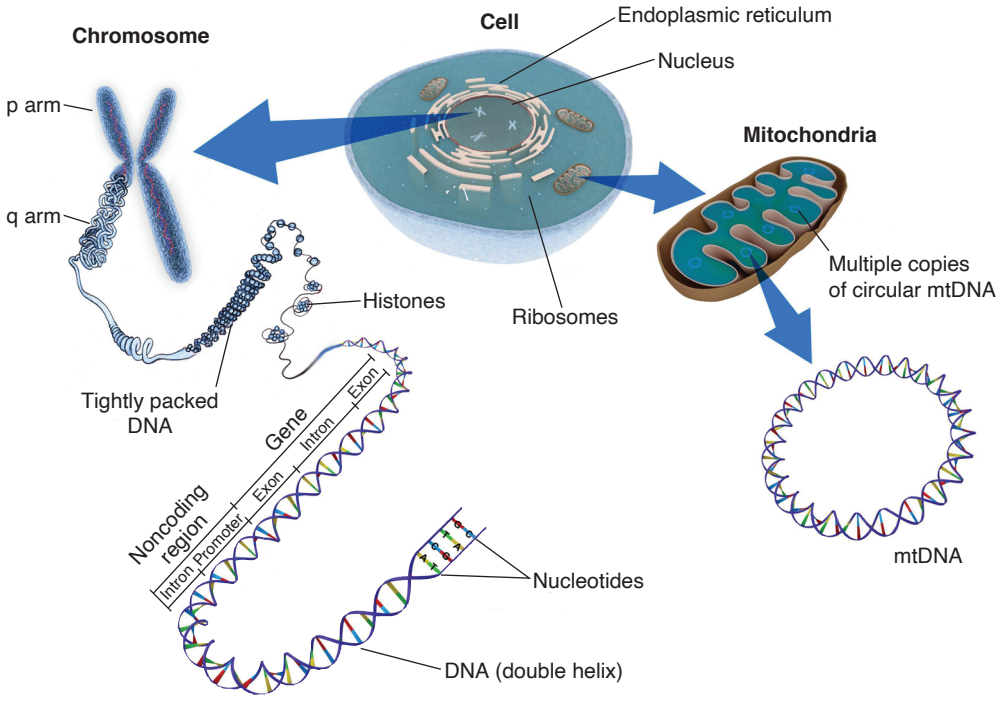


Figure 5-3 Structures of the cell showing the location of DNA within chromosomes and mitochondria. The basic double helix of nucleotides is divided into noncoding regions, including introns and promoter regions, and coding exons, which form genes. The figure shows a noncoding intron between 2 exons. The intron is spliced out before the segment is translated. This modification occurs following transcription, though before messenger RNA (mRNA) is finalized.

organisms that merged to form eukaryotic organisms (most animals and plants). The fact that mitochondria still contain their own DNA is a reminder of their independent origin. Each mitochondrion contains 2–10 copies of a short, circular DNA segment containing 13 protein-coding genes involved in oxidative phosphorylation. Because mitochondria contain several segments of DNA and each cell contains several mitochondria, mitochondrial DNA (mtDNA) may vary within a cell and between cells of the same person, a state known as *heteroplasmy.* Humans acquire mitochondria from the ovum; thus, mtDNA follows maternal line inheritance.

Chromosomal DNA replication and RNA synthesis (transcription) occur within the nucleus (see the section Gene Transcription and Translation: The Central Dogma of Genetics for further details). Messenger RNA (mRNA) is transported to ribosomes in the cytoplasm for translation to the amino acid sequences of proteins. Following the mRNA molecule's initiation codon (start sequence) is the structural *open reading frame,* which is composed of *exons* (sequences that code for amino acids that will be present in the final protein) and *introns* (sequences that are spliced out during mRNA processing). Following the last exon is the *3' untranslated region,* the function of which is partly regulatory.

The development of introns in higher organisms may have provided evolutionary benefits. The compartmentalization of coding segments into exons may have promoted rapid protein evolution by allowing for the alternative processing of precursor RNA (alternative splicing) and rearrangements of exons during gene duplication (exon shuffling). Some introns contain complete, separate genes, and some may cause disease or influence the expression of other genes. The expansion of unstable repeats within introns can cause abnormal splicing and result in genetic disease. Small insertions and deletions are very common and referred to as *indels.*

Noncoding DNA

The majority of DNA—approximately 99% of the base sequences in human DNA—does not code for proteins. Noncoding DNA comprises introns, promoters, and other regions within chromosomes and mitochondria and is involved in regulating gene expression and exon splicing. Noncoding DNA contains highly repetitive sequences, some of which include *satellites, microsatellites, short interspersed elements*, and *long interspersed elements.* The 300 bp *Alu* sequence, named after the restriction enzyme used to identify it, is the most frequently appearing repetitive DNA sequence.

Some repetitive noncoding DNA sequences form *telomeres,* which are essential for the correct formation and maintenance of chromosomes. Loss of telomeric DNA correlates with cell senescence, and defects in telomeric DNA maintenance have been proposed to be associated with carcinogenesis. In addition, RNA transcribed from noncoding DNA may directly influence the transcription of other sequences and participate in normal genome repair and regulation.

Telomeres Mendelian Randomization Collaboration; Haycock PC, Burgess S, Nounu A, et al. Association Between Telomere Length and Risk of Cancer and Non-Neoplastic Diseases: A Mendelian Randomization Study. *JAMA Oncol.* 2017;3(5):636–651.

Gene Transcription and Translation: The Central Dogma of Genetics

The central dogma of gene transcription and translation is that DNA code is transcribed to an mRNA sequence and then translated as the amino acid code of the resulting protein (Fig 5-4). Because the trinucleotides that correspond to amino acids have some redundancy in the system, a nucleotide change may not necessarily change the amino acid. The coding region of DNA is composed of exons, several of which are spliced together to construct the full RNA coding sequence. Although the central dogma specifies that DNA determines RNA sequences and that RNA determines amino acid sequences, gene expression is also modulated by both genetically and environmentally determined feedback and regulatory mechanisms. These mechanisms, such as methylation and histone formation, can silence gene expression. In addition, small segments of RNA, known as small or short interfering RNA (siRNA), can block mRNA translation.

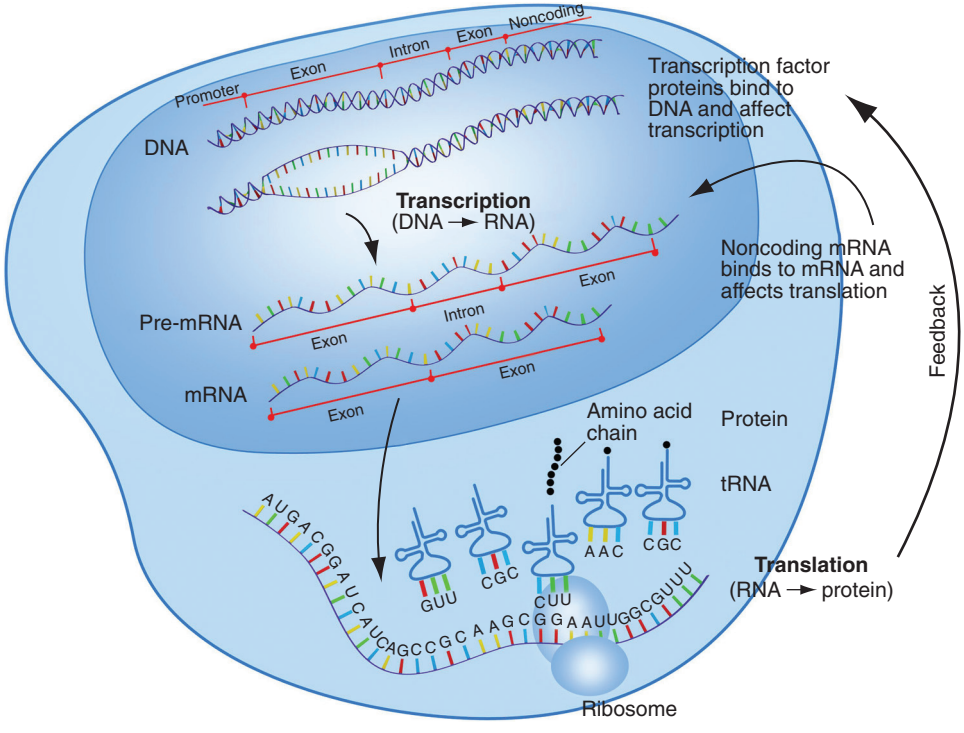


Figure 5-4 The central dogma of genetics, as represented schematically, is that the DNA sequence code is transcribed to an mRNA sequence, and then the mRNA transcription is translated into the amino acid sequence of the coded protein. However, proteins in the form of transcription factors and complementary short RNA sequences can modify translation and transcription. These proteins are being investigated as potential forms of therapy.

Epigenetics is the study of the influence of these regulatory mechanisms on gene and disease expression. The regulation of gene expression occurs at both the transcription and translation levels:

1. transcription *(expression),* in which DNA molecules give rise to RNA molecules, which are translated into proteins in most cases
2. *translation,* in which RNA directs the synthesis of proteins. Translation occurs in ribosomes, where mRNA induces transfer RNA (tRNA)-mediated recruitment of amino acids to "build" a protein

Transcription factors are proteins that bind to specific DNA sequences and thus control the flow (or transcription) of genetic information from DNA to mRNA. Transcription factors perform this function by promoting or repressing the recruitment of RNA polymerase to specific genes.

In the human genome, approximately 10% of genes code for transcription factors. Transcription factors contain 1 or more DNA-binding domains, which attach to specific DNA sequences adjacent to the genes they regulate. Numerous transcription factor gene

families exist, including the homeobox and paired box genes. *PAX6* acts as a master control gene for the development of the eye, an example of the key role of transcription factors in embryogenesis.

CLINICAL PEARL

Many ophthalmic diseases result from transcription factor pathogenic variants. *PAX2* pathogenic variants may cause colobomas of the optic nerve and renal hypoplasia. *PAX3* pathogenic variants may cause Waardenburg syndrome with dystopia canthorum (types WS1 and WS3). *PAX6* pathogenic variants are the basis of virtually all cases of aniridia, occasional cases of Peters anomaly, and several other rarer phenotypes, specifically autosomal dominant keratitis and dominant foveal hypoplasia.

The 3 stages of mRNA translation by the ribosome are initiation, elongation, and termination. Translation starts with an initiation step, in which mRNA and the small ribosomal subunit bind together. The tRNA molecule carries the amino acid methionine, which binds to a start codon; the initiation complex is formed once the large ribosomal subunit binds. During elongation, each codon is translated by the ribosome, creating a polypeptide chain. After all codons are translated, the polypeptide sequence is released so that another translation process may occur. Translation ends when a stop codon in the mRNA enters the ribosome, a process called termination. The translation process is regulated at many levels, including initiation, phosphorylation of ribosomes, and interference by siRNA. In addition, post-translational modifications, such as acetylation, methylation, phosphorylation, and glycosylation, may take place after termination.

CLINICAL PEARL

siRNA therapies for the management of several ophthalmic diseases, including glaucoma, diabetic retinopathy, age-related macular degeneration, and retinitis pigmentosa, are being evaluated.

Gupta A, Kafetzis KN, Tagalakis AD, Yu-Wai-Man C. RNA therapeutics in ophthalmology—translation to clinical trials. *Exp Eye Res.* 2021;205:108482. doi:10.1016/j.exer.2021.108482

Intron Excision

Before exons can undergo translation in the ribosomes, introns are excised from mRNA via a highly organized process called *splicing,* which leaves only the exons, or coding segments, of the mRNA. Splicing takes place in specialized structures called *spliceosomes,* which are composed of RNA and proteins. Errors in the splicing process can lead to genetic disease. Approximately 15% of single-nucleotide (point) variations that cause human disease do so by generating splicing errors that result in aberrations such as exon skipping, intron retention, or the use of a cryptic splice site. For example, pathogenic variations in proteins involved in splicing can cause RP.

Alternative Splicing and Isoforms

Alternative splicing is the creation of multiple pre-mRNA sequences from the same gene by the action of different promoters. These promoters cause certain exons to be skipped during gene transcription. The protein products of alternative splicing are often called *isoforms.* Because the promoters are usually tissue-specific, different tissues may express different isoforms. The gene for dystrophin is an example of alternative splicing. Full-length dystrophin is the major isoform expressed in muscle; shorter isoforms predominate in the retina, peripheral nerve, and central nervous system.

Alternative splicing also underlies the basis of corneal avascularity. Vascular endothelial growth factor (VEGF) receptor 1 is a key blood vessel receptor that binds and transduces a signal from the primary mediator of angiogenesis, VEGF. In the cornea, high levels of an alternatively spliced isoform, soluble VEGF receptor 1 (sVEGFR-1), are expressed. This soluble isoform is present in the extracellular matrix and serves as an endogenous VEGF trap or decoy receptor. Without sVEGFR-1, free VEGF levels would increase, making the cornea vulnerable to vascular invasion.

Ambati BK, Nozaki M, Singh N, et al. Corneal avascularity is due to soluble VEGF receptor-1. *Nature.* 2006;443(7114):993–997.

Methylation

Regions of DNA undergoing transcription lack 5-methyl cytosine residues, which normally account for 1%–5% of total DNA. There is a close correlation between methylation and gene inactivation, and the regulation of DNA methylation may be responsible for controlling imprinting. Thus, methylation may account for variation in the phenotypic expression of some diseases.

Imprinting

Genomic imprinting is a heritable yet reversible process by which a gene is modified, depending on which parent provides it. The mechanism is unclear but appears to operate at the chromatin-organization level and involve heterochromatization and methylation of CpG (cytosine-phosphate-guanine) sites. Examples of genes that can be imprinted include the Wilms tumor suppressor gene and the human *SNRPN* (small nuclear ribonucleoprotein polypeptide N) gene.

Prader-Willi and Angelman syndromes are examples of diseases resulting from imprinting abnormalities. Approximately 70%–80% of patients with Prader-Willi syndrome harbor a deletion of the paternally derived 15q11–q13, resulting in the loss of this region's normal contribution from the paternal line. About 70%–80% of patients with Angelman syndrome have a deletion of 15q11–q13 from the maternally derived chromosome, resulting in the loss of the maternal contribution. Chromosome 15 uniparental disomy, wherein both copies of chromosome 15 are inherited from the same parent, can also cause these syndromes. The uniparental disomy chromosome 15 copies are maternal in Prader-Willi syndrome and paternal in Angelman syndrome. The *SNRPN* gene maps to 15q11–q13 but appears to be expressed only from the paternally inherited allele.

X-Inactivation

During early human embryo development, the random permanent inactivation of 1 of the 2 X chromosomes in females is a significant event that prevents the expression of the majority of genes on that chromosome. The precise time of X-inactivation is not known, but it is thought to occur within a period of several cell divisions during the blastocyst–gastrula transition. X-inactivation is also called *lyonization* in tribute to its discoverer, Mary Lyon. Lyonization affects the severity of the phenotype of several X-linked retinal conditions, such as RP and incontinentia pigmenti.

DNA Damage and Repair

DNA is constantly sustaining damage from mutagens such as ultraviolet (UV) light, chemicals, and spontaneous deamination. Each cell loses 10,000 bases per day due to spontaneous DNA breakdown related to normal body temperature alone. In the absence of repair, these changes accumulate and result in tumor formation. Damaged DNA is estimated to cause approximately 80%–90% of cancers in humans.

Repair

Damaged DNA sites are repaired by 2 main mechanisms: *excision repair* and *mismatch repair.* The processes of replication, transcription, mismatch repair, excision repair, and gene expression are closely coordinated by cross-acting systems. The enzymes that cut or patch segments of DNA during crossing over at meiosis are also involved in DNA repair, and the molecules that unwind double-stranded DNA (called *helicases*) are involved in replication, transcription, and DNA excision repair.

Tumor protein P53, also called TP53 or p53, appears to play a vital role as the "guardian of the genome" by preventing the proliferation of cells that have irreparably damaged DNA. Levels of p53 increase after UV or ionizing radiation exposure. The p53 protein inhibits DNA replication by interacting with RNA polymerase transcription factor IIH. If the degree of damage is slight, increased p53 production induces reversible cell arrest until DNA repair can take place. If the degree of damage is too great or irreversible, p53 production is massively increased, triggering apoptosis. This process probably occurs through the stimulation of the expression of the *BAX* gene, whose product promotes apoptosis. If *p53* is lost, cells will fail to arrest to allow for DNA damage repair and will not enter apoptosis; thus, *p53* pathogenic variants predispose the individual to tumorigenesis.

The affected gene in ataxia-telangiectasia (Louis-Bar syndrome), a protein kinase called *ATM,* also appears to be integrally involved in DNA repair, possibly by informing the cell of radiation damage. The *ATM* gene product associates with synaptonemal complexes, promotes chromosomal synapsis, and is required for meiosis. Individuals with ataxia-telangiectasia have a threefold greater risk of cancer.

Xeroderma pigmentosum is a severe condition in which the functions of the enzymes that repair UV-damaged DNA are crippled. Patients with this condition typically have diffuse pigmented anomalies on sun-exposed skin and are at high risk for basal cell and squamous

cell carcinoma, as well as melanoma. Ocular surface cancers (squamous cell carcinoma and melanoma) can also develop in affected patients.

Lim R, Sethi M, Morley AMS. Ophthalmic manifestations of xeroderma pigmentosum: a perspective from the United Kingdom. *Ophthalmology*. 2017;124(11):1652–1661.

Apoptosis

Apoptosis is a Greek word describing leaves dropping from trees. (*Ptosis,* drooping of the upper eyelid, comes from the same root.) Apoptosis is the process of programmed cell death that occurs in multicellular organisms, whereas necrosis is a form of traumatic cell death that results from acute cellular injury. Biochemical events in apoptosis result in characteristic cell changes and cell death. Morphological changes include cell shrinkage, nuclear fragmentation, chromatin condensation, and chromosomal DNA fragmentation. Mitochondria are targeted in several key events, including the release of caspase activators, changes in electron transport, loss of mitochondrial transmembrane potential, altered cellular reduction–oxidation (redox) reactions, and activation of pro- and antiapoptotic Bcl-2 family proteins.

Apoptosis also plays a crucial role in the developing human embryo. Scaffolding cells, such as those involved in eyelid opening, are removed by epidermal apoptosis. In later life, excessive apoptosis causes atrophy, such as in RP or glaucoma, whereas insufficient apoptosis results in uncontrolled cell proliferation, such as in cancers, including retinoblastoma.

Pathogenic Variants

A change in the structure or sequence of a gene is called a *pathogenic variant* (or *mutation*). A pathogenic variant can randomly occur anywhere along the DNA sequence of a gene and may result from the substitution of 1 nucleotide for another (single-nucleotide variation). A single-nucleotide variation that changes the amino acid in the sequence is called a missense variant. Variations do not always alter the amino acid sequence because different codons can transcribe the same amino acid. A variation that occurs in a noncoding portion of the gene may or may not be of clinical consequence. Similarly, a variation may structurally alter a protein in a manner that does not notably compromise its function. Single base-pair variations that code for the same amino acid or generate a tolerable change in the amino acid sequence are called *conserved base-pair variants* (see the section Polymorphisms).

More gross variations may involve deletion, translocation, insertion, inversion, or internal duplication of a portion of the DNA sequence. Some pathogenic variants result in the destruction of the offspring or sterility. Other variants are less harmful or potentially beneficial and become established in subsequent generations. Variants can occur spontaneously for reasons that are not understood or may be induced by exposure to an environmental agent called a *mutagen,* such as radiation, viruses, and certain chemicals.

Genetic variants may arise in somatic cells as well as germinal cells. Somatic variants in humans are often difficult to identify. Because germinal cells are not involved, somatic variants are not transmitted to subsequent generations; however, some may contribute to the inception of certain forms of neoplasia (eg, an individual with heritable retinoblastoma manifesting disease after acquiring a second somatic variant).

Deletion, insertion, or duplication of any number of base pairs not divisible by 3 creates a frameshift in the entire DNA sequence downstream, which will eventually result in the formation of a stop codon and the truncation of the message. Variants that result in stop codon formation are known as nonsense variants.

Variants that prevent the production of an active gene product are called *null variants*. Null variants include nonsense or missense variants that (1) either directly produce a stop codon or produce a frameshift that induces premature stop codon formation downstream or (2) cause an alteration at the acceptor splice junction site that results in the loss of exons or the inappropriate incorporation of introns into the spliced mRNA.

Genetic variants can also lead to a gain of function that may be beneficial (leading to evolution) or detrimental (leading to disease). An example of a beneficial gain of function is the emergence of antibiotic resistance among bacteria. An example of a detrimental gain of function is the production of a receptor protein that binds too tightly with its target protein, preventing normal physiologic function. Loss-of-function variants are typically inherited in an autosomal recessive pattern, and autosomal dominant disorders are often of this type.

Polymorphisms

Many base changes have little or no deleterious effect on the organism. A *polymorphism* is any DNA sequence variation that occurs at a frequency greater than 1% in the general population. Single-nucleotide polymorphisms (SNPs; also called *single-nucleotide variation*) are important for gene mapping in genome-wide association studies (GWAS). Examples of key polymorphisms associated with disease are those occurring in the region of the *CFH* gene in age-related macular degeneration and the *LOXL1* gene in pseudoexfoliation syndrome. Many polymorphisms are silent and simply linked to the pathogenic variant, but some may influence disease.

Pathogenic Variants Versus Polymorphisms

Pathogenic variants are changes in DNA that can lead to disease, whereas polymorphisms are variations in DNA that were previously thought to rarely cause disease. Differentiating between pathogenic variants and polymorphisms is not always easy. In general, pathogenic variants change the amino acid sequence or, more dramatically, lead to the shortening or nonproduction of the protein encoded by the gene. Polymorphisms tend to either not change the amino acid sequence (because of the built-in redundancy in the DNA code) or change from 1 amino acid to a similar amino acid. However, synonymous changes that do not alter the amino acid sequence could still affect splicing. Many disease-associated SNPs identified in GWAS occur in the noncoding regions of the genome.

Genome, Genotype, Phenotype

The genome is the sum of the genetic material within a cell or an organism—the total genetic endowment. By contrast, the genotype defines the genetic constitution, and thus biological capability, with regard to a specific locus (eg, individual blood groups or a specific enzyme). Phenotypes are the observable or manifest physical, physiologic, biochemical, or molecular characteristics of an individual, which are determined by the genotype but can be modified by the environment.

A clinical manifestation produced entirely by environmental factors that nevertheless closely resembles or is even identical to a phenotype is known as a *phenocopy.* For example, pigmentary retinopathy induced by congenital rubella has occasionally been confused with a hereditary dystrophic disorder of the retina, RP. Similarly, cornea verticillata, a whorl-like pattern of opacities in the corneal epithelium, is part of the phenotype commonly observed in the X-linked dystrophic disorder Fabry disease, whereas the phenocopy can be induced by drugs such as amiodarone.

Single-Gene Disorders

Approximately 4500 diseases are known to be caused by a defect in a single gene. As a group, these disorders are called *monogenic* or *mendelian* diseases. Monogenic diseases typically follow 1 of 3 patterns of inheritance: autosomal dominant, autosomal recessive, or X-linked. Disorders of mitochondrial DNA are inherited in a fourth manner, termed *maternal inheritance.*

Cancer Genes

Cancer pathogenesis can result from a number of genetic mechanisms, including the activation of oncogenes and the loss of tumor suppressor genes. Proto-oncogene products are often involved in the signal transduction of external messages to the intracellular machinery that governs normal cell growth and differentiation. As such, proto-oncogene DNA sequences are highly conserved in nature between such different organisms as humans and yeast. Proto-oncogenes can be converted to oncogenes via the loss or disruption of normal gene regulation processes.

Oncogenes

Oncogenes were first detected in retroviruses, which acquire them from their host in order to take control of cell growth. The names of such oncogenes often refer to the viral source (eg, *ras*, identified from *ra*t *s*arcoma virus). However, oncogenes are known to be activated in not only virus-induced malignancies but also common nonviral cancers in humans. Oncogenes behave like autosomal dominant traits in that only 1 allelic pathogenic variant is needed for tumor formation, presumably by inducing a dominant-negative effect on the regulation of signal transduction.

Tumor suppressor genes

Tumor suppressor genes, also called *antioncogenes,* must be present in 1 functional copy to prevent uncontrolled cell proliferation. Although some antioncogene products participate in cell cycle checkpoints, a characteristic of tumor suppressor genes is the diversity of their normal functions. Examples of tumor suppressor genes include the genes for retinoblastoma, nephroblastoma (Wilms tumor), neurofibromatosis types 1 and 2, tuberous sclerosis, ataxia-telangiectasia, and retinocerebral angiomatosis (von Hippel–Lindau disease). Excepting ataxia-telangiectasia, these examples behave as autosomal dominant traits; however, the tumor formation mechanisms of tumor suppressor genes and oncogenes are distinct. If 1 allele is defective because of a hereditary pathogenic variant, the other allele must also be lost for tumor formation to occur (also known as the *2-hit hypothesis*). This loss of the second allele is termed *loss of heterozygosity* and can occur from a second variant, gene deletion, chromosomal loss, or mitotic recombination.

Anticipation

Variability is an intrinsic property of human genetic disease that reflects the quantitative and qualitative differences in phenotype among individuals with the "same" allelic variant. Even within a single family with a genetic disease, the disease may manifest to a different degree, with different features, or at a different age in each affected individual. For example, there is wide variation in both the severity and age at detection of features of myotonic dystrophy (also called *Steinert disease*), which include motor myotonia, cataracts, gonadal atrophy, and presenile baldness. Even within a single family, the characteristic cataracts may begin to affect vision at any time from the second to the seventh decade of life.

Such variability in clinical manifestation led to the concept of *anticipation,* the phenomenon of apparently earlier and more severe onset of a disease in successive generations within a family. Before 1990, anticipation was widely accepted to be an artifact of ascertainment rather than a biological phenomenon. However, with the relatively recent discovery of triplet or trinucleotide tandem-repeat expansion diseases, anticipation was found to reflect the increased length of trinucleotide tandem repeats from one generation to the next. Anticipation occurs in autosomal dominant disorders. The discovery and characterization of myotonic dystrophy, fragile X syndrome, Huntington disease, and Kennedy disease (a form of spinobulbar muscular atrophy) contributed to the rejuvenation of the concept of anticipation.

Some human variability is attributable to intrinsic differences in the genetic background of every human being. Other recognizable or presumptive influences on the variable intra- or interfamilial phenotype of the same gene include the following factors:

- sex influences or limitations
- maternal factors, such as the intrauterine environment and even cytoplasmic (eg, mitochondrial) inheritance factors
- modifying loci
- genetic heterogeneity, including both isoalleles and genocopies
- gene alterations induced by either position effects with other genes or somatic variants
- epigenetic factors, methylation, and histone formation

Nongenetic factors (eg, diet, temperature, and drugs) may affect gene expression, either as phenocopies or through ecologic parameters.

Penetrance

The presence or absence of any effect of a gene is described as *penetrance.* If a gene generates any evidence of phenotypic features, no matter how minimal, it is *penetrant;* if it is not expressed at any level of detection, it is *nonpenetrant*. In families with an autosomal dominant genetic variant that has 100% penetrance of the phenotype, an average of 50% of the offspring will inherit the gene and show evidence of the disease.

> Penetrance is an all-or-nothing concept, statistically representing the fraction of individuals carrying a given gene that manifests any evidence of a specific trait.

Although penetrance has an exact statistical definition, its clinical ascertainment is affected by diagnostic awareness and the methods of physical examination. For example, many mild cases of Marfan syndrome would be missed without careful biomicroscopy of the fully dilated pupil and echocardiography of the heart valves and great vessels. Similarly, in families with "dominantly inherited" retinoblastoma, some "nonpenetrant" parents or siblings may have a spontaneously involuted tumor, which clearly identifies them as bearers of the retinoblastoma gene but would only be detected if indirect ophthalmoscopy and scleral depression are included as criteria for identification of the gene. In another example, some family members who have a gene for Best macular dystrophy cannot be identified by clinical ophthalmoscopic examination, and electro-oculographic testing must be performed to detect the gene. Therefore, when examining a potential bearer of a gene, the examiner must carefully search for manifestations of the gene's effects in all susceptible tissues before dismissing someone as from a "skipped generation."

Expressivity

The presence of a defective gene does not necessarily imply a complete expression of every potential manifestation. *Expressivity* describes the variety of ways and levels of severity in which a particular genetic trait manifests among different affected individuals. In neurofibromatosis 1 (NF1), for example, an affected child may have only Lisch nodules of the iris and café-au-lait spots, whereas the affected parent may also have extensive punctiform and pedunculated neurofibromas of the skin, plexiform neurofibroma, and optic nerve glioma.

It is extremely rare that all affected members in the same family have uniform textbook presentations of a given disorder. These differences are a result of variable expressivity.

Differences in the age at onset of clinical manifestations are one way that dominant disorders demonstrate expressivity. Continuing with the example of NF1, an affected individual may experience the following sequence of manifestations: only café-au-lait spots present at birth, Lisch nodules appear at 5–10 years old and gradually increase in number and size, punctiform neurofibromas of the skin develop in early adolescence, subareolar neurofibromas appear after puberty (females), and visual impairment from the effect of an optic glioma occurs in the late teenaged years. Although all of these features are phenotypic components of the pathogenic genetic variant, each feature has a characteristic age at onset and natural history of growth and effect within the umbrella of the total disease. See the section "Genetics of the neurocutaneous syndromes" in Chapter 6 for additional discussion of NF1.

Pleiotropism

Alteration of a single gene may have consequences in various tissues within an individual. The presentation of multiple phenotypic abnormalities in different organ systems influenced by a single gene is termed *pleiotropism*. For example:

- Marfan syndrome: Ectopia lentis occurs with arachnodactyly, aortic aneurysms, and long extremities.

- DIDMOAD (*d*iabetes *i*nsipidus, *d*iabetes *m*ellitus, *o*ptic *a*trophy, and neural *d*eafness) syndrome: Optic atrophy is found in association with juvenile diabetes mellitus, diabetes insipidus, and moderate perceptive hearing impairment.
- Alport syndrome: Neurosensory hearing loss can be associated with hereditary hematuric nephritis, lenticular changes (anterior lenticonus, spherophakia, cataracts), arcus juvenilis, and whitish-yellow retinal lesions.
- Bardet-Biedl syndrome: This syndrome is characterized by pigmentary retinopathy, obesity, genital hypoplasia, mental debility, and polydactyly.

In each of these disorders, pathogenic variants in 1 specific gene can lead to dysfunction in multiple organ systems.

The Search for Genes in Specific Diseases

Various methods have been used to assign individual genes to specific chromosomes, link individual genes to one another, and link diseases to specific genes.

Polymerase Chain Reaction

Polymerase chain reaction (PCR) is a molecular biology technique used to amplify a single copy or a few copies of a segment of DNA or RNA by several orders of magnitude, generating thousands to millions of copies of a particular sequence. PCR is a common and indispensable technique used in clinical and research laboratories for a broad range of applications. Clinically, PCR has been vital in establishing the etiology of ocular infections. For example, PCR can detect numerous members of the herpes virus family in ocular fluids.

PCR methods rely on thermal cycling, which involves exposing the reactants to repeated cycles of heating and cooling, permitting different temperature-dependent reactions of DNA melting and enzyme-driven DNA replication. Primers (short DNA fragments) containing sequences complementary to the target region and a DNA polymerase (usually Taq polymerase) enable selective and repeated amplification. As PCR progresses, the DNA generated is itself used as a template for replication, setting in motion a chain reaction that exponentially amplifies the original DNA template.

Sugita S, Ogawa M, Shimizu N, et al. Use of a comprehensive polymerase chain reaction system for diagnosis of ocular infectious diseases. *Ophthalmology.* 2013;120(9):1761–1768.

Genetic Markers

In cytogenetic studies, a genetic marker such as a large deletion or translocation (eg, 11p13 in aniridia) may occasionally be visible. Other markers used to identify the location of genes include blood groups (eg, as in Duffy blood group and Coppock cataract); restriction fragment length polymorphisms (eg, as in RP); microsatellites of variable number tandem repeats and most recently, SNPs, which are used in many GWAS. Cytogenetic tests are conducted on white blood cells, whereas the other genetic markers test DNA, usually extracted from peripheral blood or saliva.

If a specific chromosomal structure is abnormal, or even normally variant, mapping its transmission through a family with a hereditary disease may support the assumption

that the pathogenic variant and the variant chromosome are comigrating. If this assumption is true, the pathogenic variant is likely to be physically located on the variant chromosome, making the gene a cytogenetic marker for the disease.

Gene Dosage

If a portion of a chromosome containing a specific gene is deleted, the amount of the gene product generated will be determined by the remaining homolog. For example, people with an interstitial deletion of part of the long arm of chromosome 13 may have serum levels of esterase D that are 50% of normal. When several such individuals were found to also have retinoblastoma, it was suggested that the esterase and retinoblastoma genes are located in the missing segment. In contrast to the reduced activity caused by a deletion, a duplication that results in either a chromosomal trisomy or a triplication of a specific chromosomal segment may produce 150% of the normal activity of a given gene product. Gene dosage appears to be a mechanism of disease in anterior segment dysgenesis, which is caused by the duplication or deletion of *FOXC1*; both 50% and 150% of normal transcription factor activity induce this dysgenesis.

Linkage and Disease Association

Even if no information is known about the nature or function of a gene for a disease, linkage studies may be able to localize the gene to a given chromosome or specific marker. In 1937, Bell and Haldane recognized the first linkage between 2 diseases on a human chromosome: congenital color vision deficiency and hemophilia on the X chromosome. Chromosomal mapping of a large number of human ocular diseases has since been achieved.

Gene assignments

Every chromosome has numerous defined genes; approximately 20,000–25,000 genes were identified and mapped in The Human Genome Project. In addition, the OMIM database (www.omim.org) lists information on all known mendelian disorders. Human gene mapping has 2 major applications. The first is identifying the gene for a specific genetic disease by its linkage to a known marker. For example, suppose gene A causes a hereditary disease, and gene B is a known enzyme or polymorphic marker closely linked to A. Tight linkage between A and B would enable a reasonable probability of identifying the disease for prenatal diagnosis and sometimes for carrier detection, even though no biochemical test for A exists. The second application is using mapping as an aid for understanding the cause of the phenotypic malformations observed in specific chromosomal diseases. For example, the phenotype of Down syndrome, which typically arises from chromosome 21 trisomy, may also result from a chromosome rearrangement that triplicates only the distal long arm of chromosome 21.

Linkage can be detected by observing the frequency with which a polymorphic marker is inherited with a disease trait. The physical distance represented by 1 cM corresponds to approximately 1 million bp and a 1% chance that recombination will result from a single meiosis (a 0.01 recombination fraction). When a genetic marker is sufficiently close to a disease gene, they are rarely separated by meiotic recombination. The frequency

of separation by chromosomal exchange during meiosis is termed the *recombination frequency.* To be considered linked, markers should be no more than 20 cM apart. For perspective, the average chromosome contains about 150 cM, and the entire human genome contains approximately 3300 cM (3×10^9 bp).

When determining linkage between a gene and a marker, geneticists compare different models using likelihood ratios. When the likelihood ratio that the odds of one model are greater than those of another is 1000:1, the first is accepted over the second. The base 10 logarithm of the likelihood ratio (*LOD score; l*ogarithm of *od*ds score) is usually reported. An LOD score of 1–2 is of potential interest in terms of linkage, 2–3 is suggestive of linkage, and greater than 3 is generally considered proof of linkage. Although an LOD score of 3 gives a probability ratio of 1000:1 in favor of linkage versus independent assortment, this score does not indicate a type I error as low as 0.001 but, in fact, indicates an error close to 0.05, the standard significance level used in statistics.

Candidate Gene Approaches

Candidate gene screening

Candidate gene screening is the process of screening for variants that are abundantly expressed within a tissue and are either important for function or specifically expressed only in that tissue. Sometimes, the candidate gene is one that recapitulates a human disease in transgenic animals. Examples of candidate gene screening discoveries include the findings of peripherin/*RDS* pathogenic variants in autosomal dominant RP and macular dystrophies and pathogenic variants of the rod cyclic guanosine monophosphate (cGMP) β-subunit of rod phosphodiesterase and the cGMP-gated cation channel in autosomal recessive RP.

Positional candidate gene screening

Whenever a gene is localized to a given chromosomal region through linkage studies, genes already known to reside in the same region become candidate genes for that disease. Some examples of disease localization that resulted from linkage to a given region, which in turn led to the discovery of the disease-causing gene by screening for variants in the region, include autosomal dominant RP from rhodopsin variants (3q), Sorsby macular dystrophy from *TIMP3* variants (22q), and Oguchi disease from point deletions within the arrestin gene (2q).

Pathogenic Variant Screening and Identification

Methods of pathogenic variant detection include Sanger sequencing using radioactive or fluorescent probes, the single-stranded conformational polymorphism technique, denaturing gradient gel electrophoresis, and the use of RFLPs. Whole-exome sequencing may identify many potential pathogenic variants; however, identification of true disease-causing variants requires considerable bioinformatic information. Unique advantages and limitations are associated with each type of genetic test (Table 5-1). Interpreting genetic test results is a complex process that requires expertise and counseling; therefore, both the

Table 5-1 Comparison of Selected Genetic Tests

Test	Resolution	Advantages	Limitations	Estimated Time	Relative Cost
Karyotype	~3.5 Mb	Entire genome, identifies rearrangements, cost-effective	Low resolution, mosaicism, consanguinity, UPD, needs viable cells	~2–6 weeks	$$
Chromosomal microarray	~50–200 kb (deletions) ~100–500 kb (duplications)	Entire genome, copy number, nonviable cells can be used	Balanced rearrangements, mosaicism	~4–8 weeks	$$
FISH	~100 kb	Identifies rearrangements, low cost	Targeted test requiring specific clinical direction, mosaicism, consanguinity, UPD	~3–5 days	$
PCR	Base pair	Low cost, sensitive and specific, fast	Requires knowledge of DNA of interest, contamination susceptibility	~2 weeks	$ per exon
Sequencing	Base pair	Can determine the exact sequence of specific lengths of DNA	Slow, low sensitivity, labor-intensive	~2 weeks	$ per exon
Southern blotting	Tens of base pairs	Detects large duplications, deletions, rearrangements	Small deletions, point variations, labor-intensive	~4 weeks	$
Whole-exome sequencing	Base pair	Entire coding regions of the whole genome, can be used for testing when no specific phenotype is present	Tons of data to be interpreted, high VUS, may reveal things not searching for (also a potential advantage)	~4 months	$$$

FISH = fluorescence in situ hybridization; PCR = polymerase chain reaction; UPD = uniparental disomy; VUS = variant of uncertain significance.

Courtesy of Masood M, Couser NL. Genetic eye disease related terms and resources. *EyeWiki*. American Academy of Ophthalmology. Published December 21, 2014. Accessed February 1, 2023. https://eyewiki.org/Genetic_Eye_Disease_Related_Terms_and_Resources

decision-making to pursue a test and the return of results discussion with families should be done by, or in consultation with, a geneticist or a genetic counselor.

Direct Sequencing

The development of techniques for rapid sequencing of DNA was one of the most significant advances in molecular genetics. Currently, it costs far less to sequence a stretch of DNA than to sequence and characterize the amino acid peptide that the DNA produces.

Although other pathogenic variant screening techniques exist, DNA sequencing is the most direct and conclusive. Sequencing complementary DNA (cDNA) derived from mRNA provides a quick look at the reading frames (exons) of the gene, whereas sequencing genomic DNA, which contains introns and exons, is more time-consuming. The intron–exon boundaries must be known, and multiple PCR assays must be set up to screen for not only the exons and their splice junction sites but also upstream and downstream regions that may be involved in gene activation and regulation.

The 2 main DNA sequencing techniques currently in use are the enzymatic method (or Sanger sequencing), which can be automated (Fig 5-5), and next-generation sequencing (NGS), also known as *massively parallel sequencing*. NGS can be used to sequence the entire genome of an individual. Specific point variations can be detected by some NGS methods using probes: allele-specific oligonucleotide probes are constructed to employ hybridization to recognize a specific DNA sequence (Fig 5-6).

Karyotype

The systematic display of chromosomes from a single somatic cell is called a *karyotype*. Chromosome preparations are usually obtained from peripheral venous blood, although bone marrow, skin fibroblasts, and cells from amniotic fluid or chorionic villi are useful under specific circumstances. Chromosome analysis can be performed directly using neoplastic tissues, as in retinoblastoma and Wilms tumor, for example.

Fluorescence in situ hybridization and chromosome arm painting

For the fluorescence in situ hybridization (FISH) technique, DNA fragments from genes of interest are first tagged with a fluorescent compound and then annealed or hybridized to chromosomes. In the process of chromosome arm painting, the regions of interest are stained to determine whether duplication, deletion, or rearrangement has occurred. Fluorescent molecular probes are useful for detecting and quantifying the presence of specific DNA sequences on a chromosome and identifying microscopic abnormalities that cannot be discerned using conventional cytogenetic methods.

Using microdissections of chromosomal regions and FISH, probes have been developed to label entire arms of chromosomes and each of the individual chromosomes (multicolor spectral karyotyping and combinatorial multifluor FISH). With 2-color FISH, both arms of each chromosome can be simultaneously labeled (Fig 5-7). These probes are valuable for detecting and understanding the mechanisms of complex chromosomal rearrangement.

Genome-Wide Association Studies

Although karyotyping and linkage analysis can still be used to identify disease-associated genes, most research now involves GWAS and NGS. The *International HapMap Project,* which

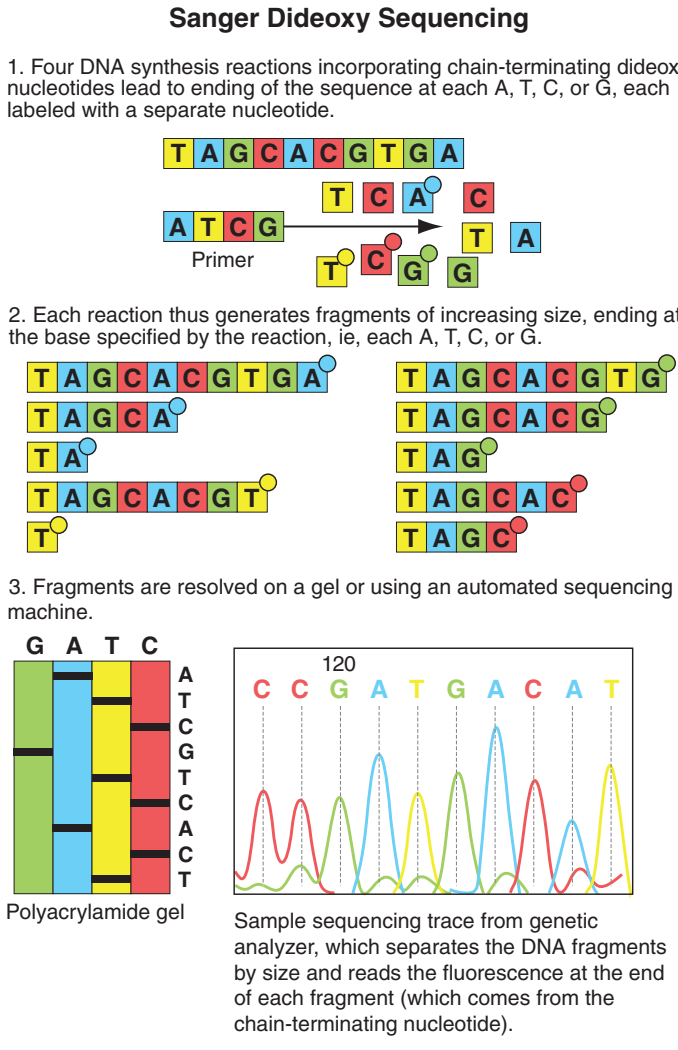


Figure 5-5 Schematic representation of the original Sanger dideoxy chain-termination sequencing method. The results produced are shown in step 3: DNA fragments resolved on a polyacrylamide gel and a sequencing trace from a modern automated sequencing machine. *(Original figure from Oxbridge Biotech Roundtable; redrawn by Mark Miller.)*

followed the creation of the human gene map, compared the DNA sequences of 1184 reference individuals from 11 global populations (creating a catalog called the *HapMap*) to identify regions of variation across individuals and racial groups. By using the HapMap to study individuals from a similar population, researchers have found that many people will share a series of SNPs or a haplotype. Thus, the results of testing only 1 or a few SNPs can be used to infer a large number of adjacent SNPs by imputation. Chip or bead platforms enable the investigation of 100,000 to millions of SNPs across the genome, forming the basis of a GWAS.

GWAS results are usually presented as a *Manhattan plot,* so named because it brings to mind the New York City skyline. In a Manhattan plot, chromosomes are arranged in order

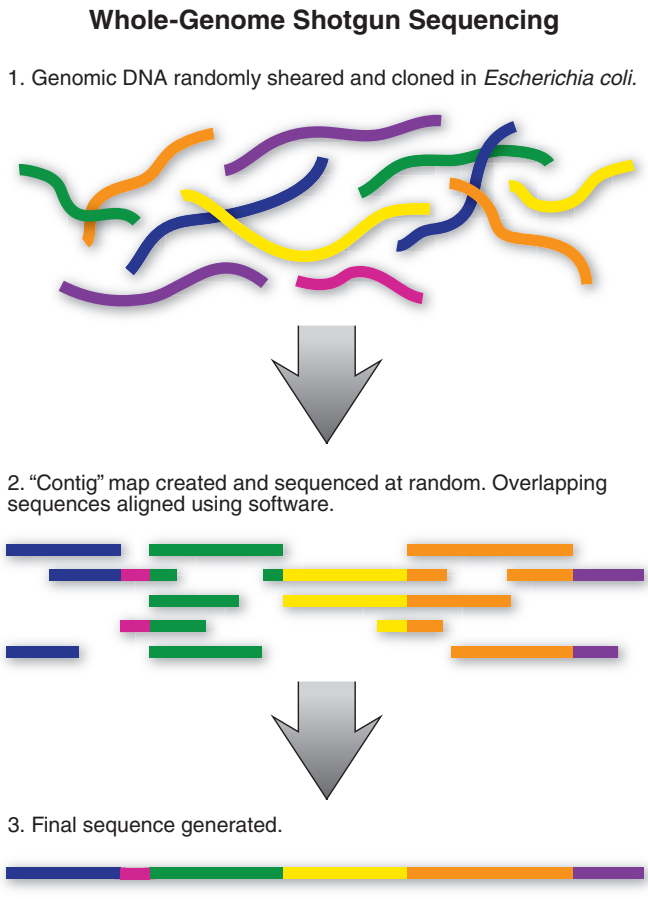


Figure 5-6 Schematic summary of the whole-genome shotgun sequencing method of next-generation sequencing (NGS). All NGS technologies use the same basic principles: fragment the DNA, add primers/adapters, amplify, and sequence. In whole-genome shotgun sequencing, a DNA sample is randomly broken into numerous small fragments that are then sequenced using the chain-termination method. Multiple overlapping DNA fragments produced from numerous repetitions of this process are then assembled into a single continuous sequence using a computer program. The "contig" map depicts overlapping DNA segments that together represent a contiguous genomic region. *(Original figure from Oxbridge Biotech Roundtable; redrawn by Mark Miller.)*

along the x-axis, and the *P* value (as –log *P*) of the association between the disease or trait and the particular SNP at that chromosomal location is given on the y-axis. A significant gene association (threshold $\approx 5 \times 10^{-8}$) will often have multiple adjacent SNPs at high levels of significance, and thus a column of points will appear on the plot. It is rare that the SNPs themselves are the disease-causing variants; usually, they are linked in the haplotype to the pathogenic variant, which is why researchers could then use fine-mapping of the region to identify causal variants associated with the phenotype.

Performing a meta-analysis of numerous studies, usually of multiple ethnic groups, enables the identification of additional associated gene regions. Figure 5-8 is a Manhattan

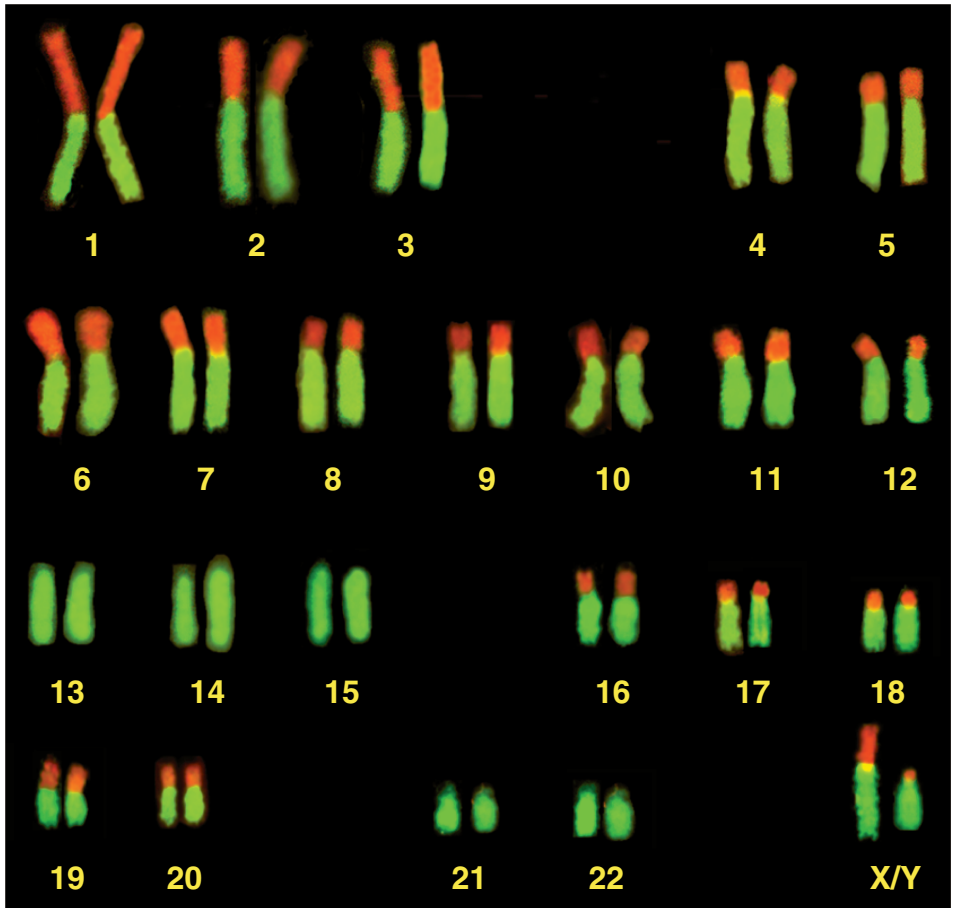


Figure 5-7 Composite karyotype of all human chromosomes hybridized with chromosome arm painting. Metaphase chromosomes were hybridized simultaneously with corresponding short-arm *(red)* and long-arm *(green)* painting probes, and a composite karyotype was generated. *(Reproduced with permission from Guan XY, Zhang H, Bittner M, Jiang Y, Meltzer P, Trent J. Chromosome arm painting probes.* Nat Genet. *1996;12(1):10–11.)*

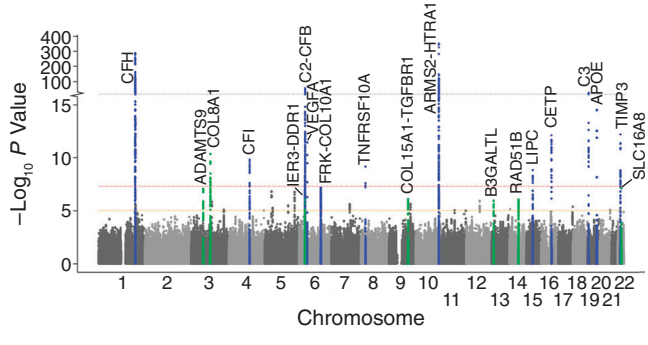


Figure 5-8 Manhattan plot for age-related macular degeneration meta-analysis identifying numerous associated genes. *(Reproduced with permission from Fritsche LG, Chen W, Schu M, et al; AMD Gene Consortium. Seven new loci associated with age-related macular degeneration.* Nat Genet. *2013;45(4):433–439e2:Fig 1.)*

plot presenting the results of a meta-analysis of GWAS for age-related macular degeneration (AMD), with 19 loci identified. The effect size for each of the genes is usually small, but they cumulatively account for approximately 40% of AMD heritability.

Comparison of GWAS of different ethnic groups can help clarify whether the SNP is disease-causing or just linked to the true disease-causing variant(s). An example is the *LOXL1* gene, which is associated with pseudoexfoliation. One SNP was associated with disease in the White population, but disease was associated with the alternate SNP in the Japanese population. Thus, this SNP is unlikely to be disease-causing; instead, different SNPs are likely to be associated with the true pathogenic variant in East Asian and White populations. In contrast, another SNP was equivalently associated with disease in both populations.

For a catalog of GWAS, including ophthalmic studies, see the European Molecular Biology Laboratory–European Bioinformatics Institute catalog at www.ebi.ac.uk/gwas/.

Determining Whether Genetic Change Is a Pathogenic Variant

When considering patient suitability for gene-based therapy, it is important for the clinician to understand how bioinformatics weights the likelihood that a genetic change is a pathogenic variant. With the huge amount of genetic information provided by whole-exome sequencing, whole-genome sequencing, and genome arrays used in GWAS, many variants of unknown significance have been identified. Numerous types of evidence are used to distinguish a benign polymorphism from a pathogenic variant. Evidence can include population data on the frequency of a variant in cases and controls; segregation data in pedigrees; computational and predictive data, including SIFT (sorting intolerant from tolerant) and PolyPhen (polymorphism phenotyping); and functional data from cell and animal models (Table 5-2).

Stone EM, Andorf JL, Whitmore SS, et al. Clinically focused molecular investigation of 1000 consecutive families with inherited retinal disease. *Ophthalmology*. 2017;124(9):1314–1331.

Gene Therapy

Gene therapy holds much promise, but the field remains in its infancy. The potential for cures is not matched by either technology or understanding. Several key challenges that limit gene therapy application remain: characterizing the pathogenic variants of genes for major diseases, understanding the pathogenic relevance of identified genes, and developing proper delivery systems for curative gene constructs (the main long-term gene therapy vehicle—viruses—is currently limited by the size of the gene, inflammatory effects, and the risk of oncogenesis).

Replacement of an Absent Gene Product in X-Linked and Recessive Diseases

For genetic diseases in which the altered allele produces either no message or an ineffective gene product (called a *null allele*), the disorder could potentially be corrected by simply replacing the gene in the deficient cells or tissues. Theoretically, normal genes can be transferred into human cells that harbor either null or pathogenic variants that do not produce a

Table 5-2 Does a Change in a Gene Really Cause Disease?

	Examples of Strong Evidence That a DNA Change is Benign	Examples of Moderate Evidence That a DNA Change is Pathogenic	Examples of Strong Evidence That a DNA Change is Pathogenic
Population data	Frequency of the DNA change is too high in controls	DNA change is absent in population databases	Frequency of the DNA change in affected cases is statistically higher than that in controls
Segregation data	No segregation of DNA change with disease in families	Odds of DNA change and disease occurring together are >1 in 16 in a family	Odds of DNA change and disease occurring together are >1 in 32 in a family
Computational and predictive data	Evidence that a DNA change is silent or that the gene product is unchanged	DNA change affects gene product, such as a missense variant or protein truncation	DNA change produces an amino acid change that is established as pathogenic or as a null variant
Functional data; cell or animal models	Well-established functional data show no deleterious effect	Variant hot spot in well-studied functional domain	Well-established functional studies show a deleterious effect

Note: Bioinformaticians in genetics laboratories use multiple types of data (population, segregation, computational, and functional) to help determine the likelihood that a DNA change is a pathogenic variant. Often, data are incomplete in some domains. The more information there is supporting pathogenicity, the more confident the clinician can be in applying the results of genetic testing to patient management in areas such as predictive DNA testing or gene therapy. Genetic testing for inherited retinal disease can now detect the causative variant in a high percentage of cases.

stable, translated product. Vectors for delivering genetic material into cells include adenoviruses, retroviruses (especially adeno-associated viruses [AAVs]), and plasmid–liposome complexes. AAV vector gene therapy has been successful in curing many disorders in animal models, such as the *RPE65* pathogenic variant that causes RP in the Briard dog.

Human gene therapy trials using *RPE65* suggested no major early adverse effects and some improvement in visual function. In 2017, the US Food and Drug Administration approved the use of voretigene neparvovec-rzyl (AAV2-hRPE65v2) in patients with confirmed biallelic *RPE65*-mediated retinal dystrophy (ie, Leber congenital amaurosis [LCA] and RP). The current cost of treating both eyes is $850,000. In addition, *RPE65* variants account for only a small percentage of LCA; thus, this therapy is not suitable for all patients with LCA. Studies on young children (<3 years) are also underway, and several other retinal dystrophy genes are under investigation for human gene therapy trials.

Carvalho LS, Vandenberghe LH. Promising and delivering gene therapies for vision loss. *Vision Res.* 2015;111(Pt B):124–133.

Russell S, Bennett J, Wellman JA, et al. Efficacy and safety of voretigene neparvovec (AAV2-hRPE65v2) in patients with RPE65-mediated inherited retinal dystrophy: a randomised, controlled, open-label, phase 3 trial. *Lancet*. 2017;390(10097):849–860.

Strategies for Dominant Diseases

Dominant diseases are caused by the production of a gene product that is either insufficient *(haploid insufficiency)* or conducive to disease *(dominant-negative effect)*. Theoretically, haploid insufficiency should be treatable by gene replacement therapy as outlined in the previous section for X-linked and recessive diseases. For dominant disorders produced by defective developmental genes, the gene correction would have to occur in early fetal development.

Disorders resulting from a dominant-negative effect require a different approach. Strategies for the treatment of dominant disease differ depending on whether a functional gene product is produced. Some genes code for RNA molecules that can bind to mRNA from another gene, blocking the translation of the other molecule. Improving our understanding of these genes may facilitate the development of either drugs or gene-encoded RNA molecules that can block the translation of mRNA for defective alleles, thus allowing only the normal allele to be expressed.

Another approach is the use of oligonucleotide or antisense DNA designed to bind with mRNA from allelic pathogenic variants, preventing mRNA translation by ribosomes (Fig 5-9). Although many problems need to be resolved for such therapy to be effective, this approach holds promise for autosomal dominant disorders in which disease is caused by the expression of a gene product pathogenic variant.

The use of ribozymes, RNA molecules that have the ability to cleave certain RNA molecules, provides another approach. A third method utilizes siRNA, which binds to mRNA and leads to the eventual degradation of specific mRNA molecules. The use of

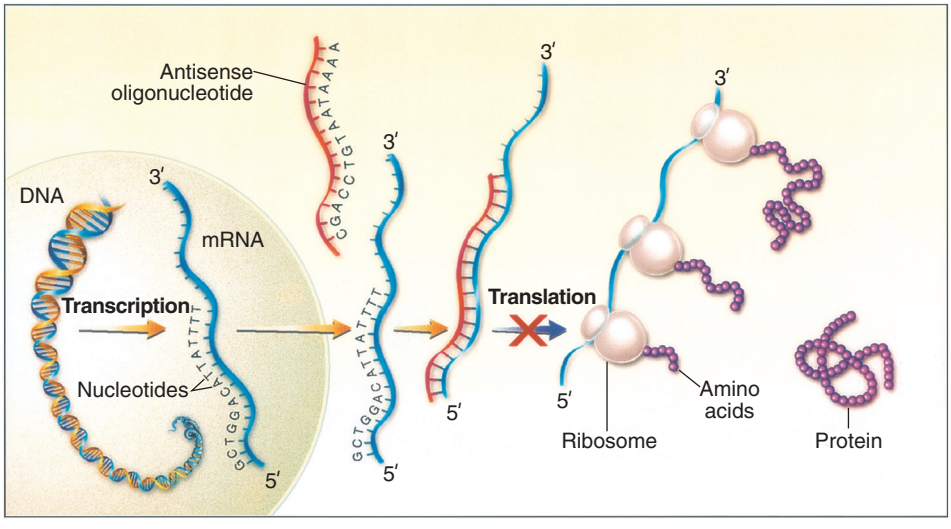


Figure 5-9 Blockade of translation by antisense oligonucleotides. Normal gene transcription of DNA into mRNA is followed by the translation of mRNA into protein. Antisense oligonucleotides bind to a complementary portion of mRNA, preventing translation—either by the steric effect of the binding process itself or (possibly) by inducing degradation of the mRNA by RNase. *(Reproduced with permission from Askari FK, McDonnell WM. Antisense-oligonucleotide therapy.* N Engl J Med. *1996;334(5):316–318.)*

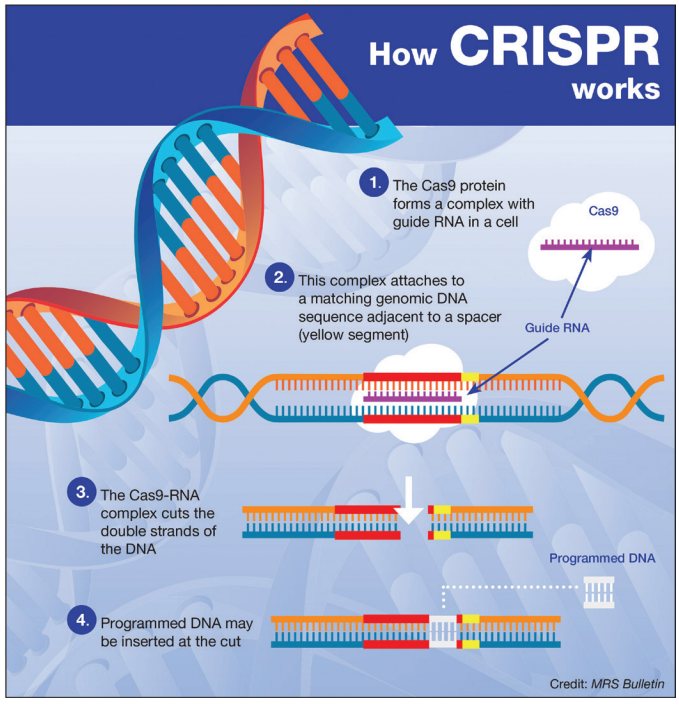


Figure 5-10 CRISPR–Cas9 gene-editing technique. This technology utilizes caspase 9, with the assistance of a guide RNA, to cut areas of variant DNA which can be replaced with the correct/modified copy. The guide RNA targets the specific DNA sequence to be edited. A similar process could be employed to remove variant DNA (not shown). *(Reproduced from Ball P. CRISPR: Implications for materials science.* MRS Bull. *2016;41(11):832–835.)*

siRNA molecules as potential therapeutic agents has become increasingly popular, and this approach has proven to be a powerful means for studying the function of novel gene products. However, one challenge with siRNA therapy is achieving intracellular delivery. Another challenge is cell-surface TLR3 receptor stimulation, which can induce immune or antiangiogenic processes as a generic class property.

A form of genome editing known as *CRISPR–Cas9* (*c*lustered, *r*egularly *i*nterspaced, *s*hort *p*alindromic *r*epeats–CRISPR-*as*sociated protein *9*) has been used to correct point variations in DNA sequences (Fig 5-10). CRISPR–Cas9 technology could potentially be combined with an induced pluripotent stem cell (iPSC) approach to correct pathogenic variants: if a skin biopsy is performed on a patient with an inherited retinal disease, skin cells can then be induced to produce pluripotent stem cells, the causative pathogenic variant can be edited out using CRISPR–Cas9, and the cells could be grown into the appropriate retinal cell line and implanted in the diseased eye. Before clinical trials commence, this personalized therapy, which would be costly, must overcome issues with immunity and the risk of tumor development.

Burnight ER, Giacalone JC, Cooke JA, et al. CRISPR-Cas9 genome engineering: treating inherited retinal degeneration. *Prog Retin Eye Res.* 2018;65:28–49.

Burnight ER, Gupta M, Wiley LA, et al. Using CRISPR-Cas9 to generate gene-corrected autologous iPSCs for the treatment of inherited retinal degeneration. *Mol Ther*. 2017;25(9): 1999–2013.

Hung SSC, McCaughey T, Swann O, Pébay A, Hewitt AW. Genome engineering in ophthalmology: application of CRISPR/Cas to the treatment of eye disease. *Prog Retin Eye Res*. 2016;53:1–20.

CHAPTER 6

Clinical Genetics

Highlights

- To accurately diagnose and manage hereditary eye diseases, it is important to obtain a family history and recognize patterns of inheritance, such as dominant and recessive, X-linked, mitochondrial, and autosomal inheritance. Cytogenetic locations may be found using online databases such as OMIM (Online Mendelian Inheritance of Man).
- Chromosomal abnormalities may be identified through cytogenetics. Two variants relevant to ophthalmologists involve the *RB1* gene on chromosome arm 13q and the *PAX6* gene on chromosome arm 11p, which result in retinoblastoma and aniridia, respectively.
- Neurocutaneous syndromes, or *phakomatoses*, are mostly due to recessive oncogenes, with loss of genes causing germline or somatic tumors in a pattern similar to that in retinoblastoma.
- Mitochondrial DNA (mtDNA) is passed on to children from their mothers. Pathogenic variants in mtDNA are responsible for many diseases with ophthalmic manifestations, including chronic progressive external ophthalmoplegia and Leber hereditary optic neuropathy.
- Appropriate referral for genetic counseling and genetic testing consideration is important in most mendelian diseases. The current American Academy of Ophthalmology guideline does not recommend genetic testing for common eye diseases with multifactorial etiologies, such as age-related macular degeneration and primary open-angle glaucoma, outside the research setting.

Introduction

> The most valuable tool in clinical genetics is the question: "Does anyone else in the family have . . . ?"

At present, an accurate family history carries greater specificity and sensitivity than most laboratory genetic tests. Although numerous pathogenic variants (mutations) have been discovered, the vast majority of disease-causing DNA variants remain to be identified. Genetics is an important factor in every ophthalmic consultation, from those involving rare inborn errors of metabolism or congenital malformations to common eye diseases, such as myopia,

glaucoma, cataract, and age-related macular degeneration (AMD). Even susceptibility to infection and trauma can be genetic. In a clinical context, understanding the genetic basis of a disease may be particularly useful for arriving at a correct diagnosis when another family member has a similar disease. In addition, it is important for clinicians to recognize that a patient presenting with a particular eye problem may be at increased risk for an unrelated disease, such as glaucoma, because of an affected parent.

Ophthalmologists have an obligation to patients with genetic eye diseases—to either provide genetic counseling or arrange for referral to a geneticist or genetic counselor. Clinicians may also encounter patients presenting with DNA test results for themselves or their families. The results may range from the identification of high-risk retinoblastoma gene pathogenic variants (which would significantly influence the management of at-risk children within the family) to genetic associations that are of no more value than iridology (genes have been associated with iris crypts and furrows). It is important to understand the clinical settings in which a genetic test is crucial, useful, or irrelevant to patient management. These distinctions will change in the future as new clinical trials define treatments based on genetic background.

When a patient presents with a DNA result for a disease for which no effective treatment is currently available, the clinician may be asked: "What should we do about this?" The best answer is: "Participate in, or help fund, research so we can find out what the best treatments are." These patients can be referred to the US National Institutes of Health website (www.ClinicalTrials.gov) for information.

The key recommendations of the American Academy of Ophthalmology (AAO) Task Force on Genetic Testing policy are given at the end of this chapter. When faced with the option of ordering genetic tests, clinicians should ask the same question they ask before ordering any tests: "How will the results affect management?" The best use of genetic testing comes from knowledge of the family history. An accurate family history might help an ophthalmologist save not only a patient's sight but also, in cases of retinoblastoma or Marfan syndrome, the patient's life.

Pedigree Analysis

Establishing a pedigree or drawing a family tree is a key tool in clinical genetics. The most useful strategy for establishing a pedigree is to start with broad questions, such as "Are there any eye diseases in the family?" before proceeding to more targeted questions, such as "Did any men on the maternal side of your family lose vision as a young adult?" in cases of potential Leber hereditary optic neuropathy (LHON).

When conducting a pedigree analysis, it is best to convert the patient's family history into a pedigree diagram; however, this can be challenging in some electronic medical records software. An initial, rough outline can be drawn on paper until the information can be entered into a pedigree-drawing software program. The standard protocol for pedigree symbols is outlined in Figure 6-1.

Drawing one's own extended family tree is a useful exercise for clinicians. A basic pedigree should include parents, siblings, and children and note those affected or unaffected by the disorder of interest. Often, asking grandparents, uncles, aunts, and cousins about a specific disorder can help clarify the inheritance pattern.

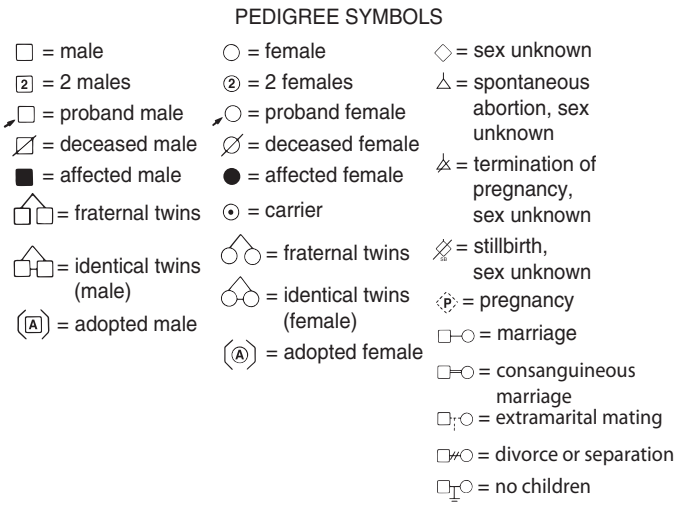


Figure 6-1 Symbols commonly used for pedigree analysis. *(© 2022 American Academy of Ophthalmology.)*

The interviewer should always ascertain whether brothers and sisters are half or full siblings. This procedure not only limits the possible patterns of inheritance but may also identify other individuals at risk for the disorder under consideration. Parentage information must be aggressively pursued (but always privately and confidentially). Although incest and nonpaternity are sensitive social issues, obtaining this information is essential for creating an accurate pedigree. The interviewer should ask specifically about consanguinity when considering rare autosomal recessive diseases. Questions may include: "Are the parents cousins?" "Are there common last names in the families of both parents?" and "Were the parents born in the same area, or do they belong to known ethnic or religious isolates?"

Age at death may be useful in specific situations and can be recorded near the appropriate pedigree symbols. In the case of a child with ectopia lentis and no family history of similar ocular disease, identifying a relative who died from a dissecting thoracic aorta in his fourth decade of life could lead to a tentative consideration of Marfan syndrome in the differential diagnosis. In another example, where atypical tear-shaped congenital hypertrophy of the retinal pigment epithelium (CHRPE) is observed in each eye (Fig 6-2) in a young adult, discovering that a parent died at age 50 from metastatic adenocarcinoma of the colon and a sibling died at age 10 from a brain tumor may lead to a diagnosis of Gardner syndrome and referral to a gastroenterologist for further diagnostic evaluation.

Obtaining a family history does not end at the initial consultation because it may be the first time a patient has heard of the disease. Thus, the patient may discover additional family history when discussing the new diagnosis with their family. Clinicians should encourage patients to talk to their families and update their family history at subsequent consultations. For more complicated genetic diseases, a genetic counselor will be able to assist patients with an extensive pedigree.

Bennett RL, French KS, Resta RG, Doyle DL. Standardized human pedigree nomenclature: update and assessment of the recommendations of the National Society of Genetic Counselors. *J Genet Couns.* 2008;17(5):424–433.

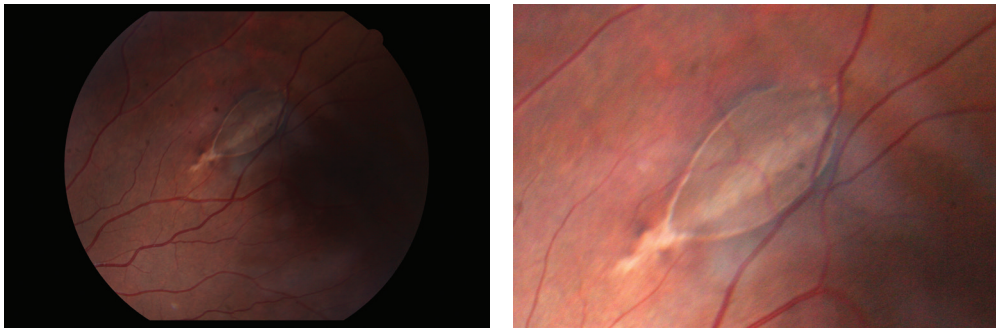


Figure 6-2 Atypical congenital hypertrophy of the retinal pigment epithelium (CHRPE) is found in 70%–80% of individuals with familial adenomatous polyposis (FAP). Patients with FAP and other tumors may have Gardner or Turcot syndrome, depending on the type and location of the tumor. These images demonstrate an atypical tear-shaped CHRPE with depigmentation at 1 margin, usually the apex, which points toward the optic nerve. *(Courtesy of Steven M. Cohen, MD, Retina Gallery.)*

Bennett RL, Steinhaus KA, Uhrich SB, et al; Pedigree Standardization Task Force of the National Society of Genetic Counselors. Recommendations for standardized human pedigree nomenclature. *Am J Hum Genet.* 1995;56(3):745–752.

Patterns of Inheritance

Many of the terms used in this section are defined in the Genetics Glossary in the online appendix (www.aao.org/bcscappendix_section02). See also the section Terminology: Hereditary, Genetic, Congenital, Familial later in this chapter.

Dominant Versus Recessive Inheritance

The terms *dominant* and *recessive* were first used by Gregor Mendel. In classical genetics, an autosomal *dominant* disorder is typically expressed with a similar phenotype, whether the pathogenic gene variant is present in a homozygous or heterozygous state. Stated simply, a dominant gene variant is expressed when only a single copy is present. A genetic disorder is *recessive* if its expression is masked by a normal allele or, more precisely, if it is expressed only in the homozygous (or compound heterozygous) state (ie, when both alleles at a specific locus are variants).

A *trait* is the consequence of the gene's action. It is the trait, or the phenotypic expression of the gene at a clinical level, rather than the gene itself, that is dominant or recessive. A trait is recessive if its expression is suppressed by the presence of a normal gene (as in galactosemia) and dominant if it is apparently unaffected by a single copy of the normal allele (as in Marfan syndrome). If the alleles differ and yet are both manifested in the phenotype, they are said to be *codominant.* Examples of phenotypes with codominant inheritance patterns include the ABO blood types, human leukocyte antigen (HLA) types, and hemoglobin variants (as involved in sickle cell disease).

Epigenetic factors can influence the effect of a gene on an individual or an organ, making the trait more or less apparent. Thus, the dominant or recessive designation of a trait

depends on the testing method used. Although classically a dominant gene has the same phenotype when the allelic variant is present in either the heterozygous or homozygous state, most dominant medical diseases are codominantly expressed—the disease manifestation tends to be more severe in individuals who are homozygous for an allelic variant or who harbor 2 different allelic variants at a particular locus than in those with 1 allelic variant and 1 normal allele at that locus.

The biochemical mechanisms of dominant hereditary diseases appear different from those of recessive disorders. Recessive traits usually result from enzyme deficiencies caused by alterations to the gene specifying the affected enzyme. The altered enzyme may be structurally abnormal or unstable, resulting in altered function or loss of the enzyme itself, respectively. In heterozygotes, normal enzyme activity is usually reduced by approximately 50%, but the trait is clinically unaffected, implying that half of the normal enzyme activity is compatible with near-normal function. If adequate biochemical testing can be performed and the specific enzyme isolated, the heterozygous genetic state may be inferred by quantifying the reduced enzyme activity. Thus, clinically unaffected heterozygotes can be detected for such disorders as homocystinuria (cystathionine β-synthase deficiency), galactosemia (galactose-1-phosphate uridylyltransferase, galactokinase, or epimerase deficiency), gyrate atrophy of the choroid and retina (ornithine aminotransferase deficiency), and Tay-Sachs disease (hexosaminidase A deficiency). Known enzyme disorders with ocular manifestations are listed in Table 6-1.

Rajappa M, Goyal A, Kaur J. Inherited metabolic disorders involving the eye: a clinico-biochemical perspective. *Eye (Lond).* 2010;24(4):507–518.

Autosomal Recessive Inheritance

An autosomal recessive disease is expressed fully when a gene variant is present at the same locus on both homologous chromosomes (ie, homozygosity for a gene variant) or 2 different allelic variants are present at the same locus (compound heterozygosity). A single allelic variant is sufficient to cause a recessive disorder only if the normal allele on the homologous chromosome is deleted. A recessive trait can remain latent through several generations until the mating of 2 individuals heterozygous for an allelic variant gives rise to an affected individual. The frequency of heterozygotes (carriers) for a given disorder will always be considerably greater than that of homozygotes. It is estimated that all humans inherit numerous pathogenic variants for different recessive disorders for which they are heterozygotes. Figure 6-3 shows an example of autosomal recessive inheritance.

Enzyme defects

Autosomal recessive diseases often result from defects in enzymatic proteins. Most so-called inborn errors of metabolism that result from enzyme defects are autosomal recessive traits, although a few are X-linked recessive disorders (eg, Lesch-Nyhan syndrome).

In some other disorders with genetic blocks in metabolism, the phenotypic consequences are related to a lack of a normal product distal to the block. One example is *albinism,* in which the metabolic block prevents melanin synthesis from the amino acid tyrosine. In other inborn errors of metabolism, the phenotypic expression results from excessive

Table 6-1 Known Enzyme Disorders and Corresponding Ocular Signs

Disorder	Defective Enzyme	Ocular Sign
Storage diseases		
Fabry disease	Ceramide trihexosidase (α-galactosidase A)	Corneal epithelial verticillate changes; aneurysmal dilation and tortuosity of retinal and conjunctival vessels
GM_1 gangliosidosis type I (generalized gangliosidosis)	β-Galactosidase-1	Macular cherry-red spot; optic atrophy; corneal clouding (mild)
GM_2 gangliosidosis type I (Tay-Sachs disease)	Hexosaminidase A	Macular cherry-red spot; optic atrophy
GM_2 gangliosidosis type II (Sandhoff disease)	Hexosaminidase A and B	Macular cherry-red spot
Leukodystrophy (Krabbe disease)	Galactosylceramidase (or galactocerebrosidase)	Optic atrophy
Mannosidosis	α-Mannosidase	Lenticular opacities
Metachromatic leukodystrophy	Arylsulfatase A	Retinal discoloration, degeneration
Mucopolysaccharidosis I, severe (Hurler syndrome)	α-L-Iduronidase	Corneal opacity; pigmentary retinal degeneration
Mucopolysaccharidosis I, attenuated (Hurler-Scheie or Scheie syndrome)	α-L-Iduronidase	Corneal opacity; pigmentary retinal degeneration
Mucopolysaccharidosis II (Hunter syndrome)	Iduronate-2-sulfatase	Corneal opacity (mild type); older patients
Mucopolysaccharidosis III, type A (Sanfilippo syndrome)	Heparan *N*-sulfatase	Pigmentary retinal degeneration; optic atrophy
Metabolic disorders		
Albinism	Tyrosinase	Foveal hypoplasia; nystagmus; iris transillumination
Alkaptonuria	Homogentisic acid oxidase	Dark sclera

Disorder	Defective Enzyme	Ocular Sign
Crigler-Najjar syndrome	Bilirubin uridine diphosphate glucuronosyltransferase	Extraocular movement disorder
Ehlers-Danlos syndrome type VI	Lysyl hydroxylase	Microcornea; corneal ectasia; blue sclera; ectopia lentis; angioid streaks; retinal detachment
Familial dysautonomia (Riley-Day syndrome)	Dopamine-β-hydroxylase	Alacrima; corneal hypoesthesia; exodeviation; methacholine-induced miosis
Galactosemia	Galactose-1-phosphate uridyltransferase (classic), galactokinase, or epimerase	Cataracts
Gyrate atrophy of the choroid and retina	Ornithine aminotransferase	Degeneration of the choroid and retina; cataracts; myopia
Homocystinuria	Cystathionine β-synthase	Dislocated lens
Hyperglycinemia	Glycine cell transport	Optic atrophy
Intermittent ataxia	Pyruvate decarboxylase	Nystagmus
Leigh necrotizing encephalopathy	Pyruvate carboxylase	Optic atrophy
Maple syrup urine disease	Branched-chain decarboxylase	Ophthalmoplegia; nystagmus
Niemann-Pick disease	Sphingomyelinase	Macular cherry-red spot
Refsum disease	Phytanoyl-CoA hydroxylase	Retinal degeneration
Sulfite oxidase deficiency	Sulfite oxidase	Ectopia lentis
Tyrosinemia type II	Tyrosine aminotransferase	Pseudodendritic keratitis

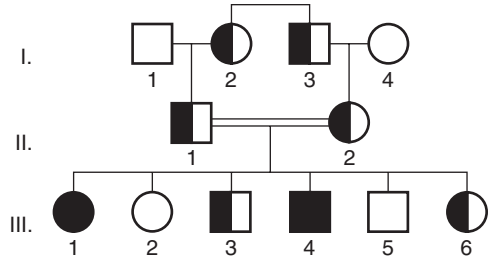


Figure 6-3 Autosomal recessive disease. In the first generation of the pedigree, I-2 is a carrier female, and I-3 is a carrier male. In the second generation, there is a consanguineous marriage between II-1 and II-2, who are both carriers. In the third generation, III-1 and III-4 are affected, and III-3 and III-6 are carriers. *(© 2022 American Academy of Ophthalmology.)*

production of a product proximal to the block or a normally alternative and minor metabolic pathway.

Carrier heterozygotes

The heterozygous carrier of a gene variant for a recessive disorder may show minimal clinical evidence of the gene defect. However, dysfunction may be evident at the biochemical level. Carrier heterozygotes can be detected by a variety of methods:

- identification of abnormal metabolites by electrophoresis (eg, galactokinase deficiency)
- hair bulb assay (eg, oculocutaneous albinism and Fabry disease)
- monitoring leukocyte enzyme activity (eg, galactose-1-phosphate uridyltransferase in galactosemia)
- skin culture for analysis of fibroblast enzyme activity (eg, ornithine aminotransferase deficiency in gyrate atrophy of the retina and choroid)
- assays of serum and tears (eg, hexosaminidase A in Tay-Sachs disease)

In contrast to the transmission of dominant traits, most reproduction resulting in the transmission of recessive disorders involves phenotypically normal heterozygous parents. Among 4 offspring produced by parents carrying the same gene for an autosomal recessive disease, on average, 1 will be affected (homozygote), 2 will be carriers (heterozygotes), and 1 will be genetically and phenotypically unaffected. Thus, clinically unaffected heterozygous parents will produce offspring with a ratio of 1 clinically affected child to 3 clinically normal children. There is no predilection for either sex. Because of this inheritance pattern, a patient with a recessive disease is frequently the only affected family member. For instance, approximately 40%–50% of patients with retinitis pigmentosa (RP) have no family history of the disorder. However, their age at onset, rate of progression, and other phenotypic characteristics may be similar to those of other individuals with defined recessive inheritance patterns.

> When a child is born with a recessive disorder to unaffected parents, the genetic risk for each subsequent child of the same parents is 25%.

The concept of recessive inheritance has specific implications for genetic counseling. All offspring of an affected individual will be carriers; however, they are unlikely to be affected by the disorder unless their clinically unaffected parent is also a carrier of the gene. The statistical risk that a clinically unaffected sibling of a child with a recessive disorder is a genetic carrier is 2 chances in 3. As the genes for recessive diseases are identified, these individuals and their offspring will benefit from predictive DNA testing.

Consanguinity

The mating of close relatives can increase the probability that their children will inherit a homozygous genotype for a recessive trait, particularly if that trait is rare. For example, the probability that the same recessive allele is present in first cousins is 1 in 8. Therefore, 1 in every 16 offspring of a first-cousin sexual union will carry the gene in a homozygous state and manifest that autosomal recessive trait within a given family. An inquiry for consanguinity between parents should be made when gathering a family history, particularly in cases where a rare recessive disease is present or suspected.

In contrast to rare recessive traits, inbreeding is less likely to influence the expression of common recessive traits because most homozygous offspring are the progeny of unrelated parents. This pattern is usually the case with such frequent disorders as sickle cell disease and cystic fibrosis. The characteristics of autosomal recessive inheritance are summarized in Table 6-2.

Pseudodominance

Occasionally, an affected homozygote mates with a heterozygote. Of their offspring, 50% will be carriers, and 50% will be affected homozygotes. Because this segregation pattern mimics that of dominant inheritance, it is called *pseudodominance.* Such matings are rare and are unlikely to affect more than 2 vertical generations.

Autosomal Dominant Inheritance

When an autosomal allele leads to a regular, clearly definable abnormality in the heterozygote, the trait is termed *dominant.* Autosomal dominant traits often represent defects in structural nonenzymatic proteins, such as in fibrillin in Marfan syndrome or collagen in Stickler syndrome (hereditary progressive arthro-ophthalmopathy). A dominant mode of inheritance has also been observed for some malignant neoplastic syndromes, such as retinoblastoma, retinocerebral angiomatosis (von Hippel–Lindau syndrome), tuberous sclerosis, and familial colorectal polyposis (Gardner syndrome). Although the neoplasias in these diseases are inherited as autosomal dominant *traits,* the defect is recessive at the cellular level, and tumors only arise from the loss of function of both alleles. See the section Knudson's 2-Hit Hypothesis and the Genetics of Retinoblastoma and the Neurocutaneous Syndromes later in this chapter.

Table 6-2 Characteristics of Autosomal Recessive Inheritance

The gene variant usually does not cause clinical disease (recessive) in the heterozygote.
Individuals who inherit both defective genes (homozygotes) express the disorder.
Typically, the trait expressed appears only in siblings, not in their parents, offspring, or other relatives.
The ratio of unaffected to affected individuals in a sibship is 3:1.
The sexes are affected in equal proportions.
Parents of the affected person may be genetically related (consanguinity), especially if the trait is rare.
The offspring of affected individuals are carriers (heterozygotes) of the gene but are typically clinically unaffected.

Nearly all bearers of dominant disorders in the human population are heterozygotes.

In dominant inheritance, the heterozygote is clinically affected—a single gene variant interferes with normal function. Occasionally, depending on the frequency of the abnormal gene in the population and the phenotype, 2 parents heterozygous for the same abnormality produce children. The offspring of 2 heterozygous parents have a 25% risk of being an affected homozygote. Figure 6-4 shows an example of autosomal dominant inheritance.

Some dominant diseases are caused by pathogenic variants affecting structural proteins, such as cell receptor growth factors (eg, *FGFR2* in Crouzon syndrome [craniofacial dysostosis]), or functional deficits generated by abnormal polypeptide subunits (eg, unstable hemoglobins). The dominant disorders aniridia and Waardenburg syndrome result from the loss of 1 of the 2 alleles for the developmental transcription factors *PAX6* and *PAX3*, respectively.

In some instances, dominantly inherited traits are not clinically expressed. In other instances—such as in some families with autosomal dominant RP—pedigree analysis may show a defective gene in individuals who do not manifest any discernible clinical or functional impairment. This situation is called *incomplete penetrance* or a *skipped generation*.

Conclusive evidence of autosomal dominant inheritance with complete penetrance requires evidence of the disease in at least 3 successive generations, typical disease expression in both sexes, and transmission from a male to his male offspring. The characteristics of autosomal dominant inheritance with complete (100%) penetrance are summarized in Table 6-3. In the usual clinical situation, the offspring of an affected heterozygote with

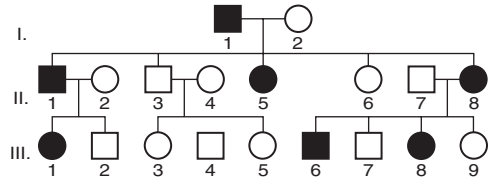


Figure 6-4 Autosomal dominant disease. In the first generation of the pedigree, I-1 is an affected male. In the second generation, II-1, II-5, and II-8 are affected. In the third generation, III-1, III-6, and III-8 are affected. *(© 2022 American Academy of Ophthalmology.)*

Table 6-3 Characteristics of Autosomal Dominant Inheritance With Complete Penetrance

The trait appears in 3 or more successive generations (vertical transmission).
Affected males and females are equally likely to transmit the trait to male and female offspring. Thus, male-to-male transmission occurs.
Each affected individual has an affected parent unless the condition arose from a new pathogenic variant in the given individual.
Males and females are affected in equal proportions.
Unaffected persons do not transmit the trait to their children.
The trait is expressed in the heterozygote but is more severe in the homozygote.
The age of fathers of isolated (new pathogenic variant) cases is usually advanced.
The more severely the trait interferes with survival and reproduction, the greater the proportion of isolated cases.
Variability in trait expression from generation to generation and between individuals in the same generation is expected.
On average, affected persons transmit the trait to 50% of their offspring.

a dominant disorder has a 1 in 2 chance of inheriting the gene variant, regardless of sex, and demonstrates some effect. The degree of variability in the expression of certain traits is usually more pronounced in autosomal dominantly inherited disorders than in genetic disorders with other inheritance patterns. Moreover, in clinical disorders that are inherited in more than 1 mendelian pattern, the clinical expression of the dominantly inherited disorder is generally more severe than that of the recessively inherited disorder.

Counseling for the recurrence risk of autosomal dominant traits must involve a thorough examination of not only the affected person (who may have the full syndrome) but also their parents. If 1 parent is even mildly affected, the risk of additional siblings being genetically affected rises to 50%. Thus, it is crucial that ophthalmologists do not overlook variable expressivity when examining their patient's parents and other family members. In some ocular disorders, family members can inherit a gene for a dominant trait but not show clinically apparent manifestations. In these cases, impairments may be detected via electrophysiological or genetic testing. For example, a relatively inexpensive genetic test can detect the pathogenic variant for Best vitelliform macular dystrophy in clinically unaffected family members.

X-Linked Inheritance

A trait determined by genes on either of the sex chromosomes is properly termed *sex-linked.* This genetic pattern became widely known due to the occurrence of hemophilia in European and Russian royal families.

The rules governing all modes of sex-linked inheritance can be logically derived by considering the chromosomal basis. Individuals assigned female at birth have 2 X chromosomes, 1 of which will go to each ovum. Those assigned male at birth have both an X and a Y chromosome, and the male parent contributes his only X chromosome to all his daughters and his only Y chromosome to all his sons. Traits determined by genes on the Y chromosome are transmitted from a father to 100% of his sons. Among these Y chromosomal genes is the *testis-determining factor* (*TDF;* also called *sex-determining region Y,* or *SRY*). Genes controlling tooth size, stature, spermatogenesis, and hairy pinnae (hypertrichosis pinnae auris) are also on the Y chromosome. All other sex-linked traits or diseases are thought to result from genes on the X chromosome and are properly termed *X-linked.* Some X-linked conditions have considerable frequencies in human populations; congenital color vision defects, such as protan and deutan anomalies, were among the first human traits assigned to a specific chromosome.

> The distinctive feature of X-linked inheritance, both dominant and recessive, is the absence of father-to-son transmission. Because the male X chromosome passes only to daughters, all daughters of an affected male will inherit the X-linked gene variant.

X-linked recessive inheritance

A male has only 1 copy of any X-linked gene and thus is said to be *hemizygous* for the gene rather than homozygous or heterozygous. Because there is no normal gene to balance an X-linked gene variant in the male, its resulting phenotype, whether dominant or recessive, will always be expressed. A female may be heterozygous or homozygous for an X-linked variant. With X-linked *recessive* conditions, traits are typically only fully expressed if the normal

allele is absent, modified, or inactivated. Thus, males (with their single X chromosome) are predominantly affected. All the phenotypically healthy but heterozygous daughters of an affected male are carriers. By contrast, each son of a heterozygous woman has an equal chance of being unaffected or hemizygously affected. Figure 6-5 shows an example of X-linked recessive inheritance.

A female will be affected by an X-linked recessive trait under a limited number of circumstances:

- She is homozygous for the gene variant by inheritance (ie, from an affected father and a heterozygous [or homozygous] mother).
- Her mother is heterozygous, and her father contributes a new pathogenic variant.
- She is missing part or all of 1 X chromosome (Turner syndrome) and therefore is effectively hemizygous.
- She has a highly unusual skewing of inactivation of her normal X chromosome, as explained by the Lyon hypothesis (discussed in the section Lyonization later in this chapter).
- Her disorder is actually an autosomal genocopy of the X-linked condition.

Table 6-4 summarizes the characteristics of X-linked recessive inheritance. X-linked recessive inheritance should be considered when all affected individuals in a family are males, especially when they are related through historically unaffected women (eg, uncle and nephew, or multiple affected half-brothers with different fathers). Many X-linked RP pedigrees have been mislabeled as autosomal dominant because of manifesting female carriers. The key feature of an X-linked pedigree is no male-to-male transmission.

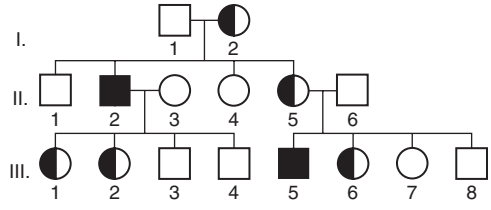


Figure 6-5 X-linked recessive disease. In the first generation of the pedigree, I-2 is a carrier female. In the second generation, II-2 is an affected male, and II-5 is a carrier female. In the third generation, III-1, III-2, and III-6 are carrier females, and III-5 is an affected male. *(© 2022 American Academy of Ophthalmology.)*

Table 6-4 Characteristics of X-Linked Recessive Inheritance

Usually, only males are affected.
An affected male transmits the gene to all of his daughters (obligate carriers) and none of his sons.
All daughters of affected males, even those who are phenotypically normal, are carriers.
Affected males in a family are either brothers or related to one another through carrier females (eg, maternal uncles).
If an affected male has children with a carrier female, 50% of their daughters will be homozygous and affected, and 50% will be heterozygous and carriers, on average.
Heterozygous females may rarely be affected (manifesting heterozygotes) because of lyonization.
Female carriers transmit the gene, on average, to 50% of their sons, who are affected, and 50% of their daughters, who are carriers.
There is no male-to-male transmission.

X-linked dominant inheritance

X-linked dominant traits are caused by gene variants expressed in a single dose and carried on the X chromosome. Thus, both heterozygous women and hemizygous men are clinically affected. Females are affected nearly twice as frequently as males. All daughters of males with the disease are affected, and all sons of affected males are free of the trait unless their mothers are also affected. Because only the children of affected males provide information discriminating X-linked dominance from autosomal dominance, it may be impossible to distinguish these inheritance modes on genetic grounds when the pedigree is small or the available data are scarce. Some X-linked dominant disorders, such as incontinentia pigmenti (Bloch-Sulzberger syndrome), may prove lethal to the hemizygous male. Figure 6-6 presents an example of X-linked dominant inheritance. The characteristics of X-linked dominant inheritance are summarized in Table 6-5.

X-linked disorders

Females with X-linked diseases have milder symptoms than males. Occasionally, males may be so severely affected that they die before the reproductive period, preventing transmission of the gene. Such is the case with Duchenne muscular dystrophy, in which most affected males die before their mid-teens. In other disorders, males are so severely affected that they die before birth, and only females survive. Families with such disorders would include only affected daughters, unaffected daughters, and normal sons at a ratio of 1:1:1. Incontinentia pigmenti is one such lethal genetic disorder. In affected females, an erythematous, vesicular skin eruption perinatally develops and progresses to marbled, curvilinear pigmentation (Fig 6-7). The syndrome may also include dental abnormalities, congenital or secondary cataracts, retinal neovascularization with tractional retinal detachment (Fig 6-8), and pseudogliomas.

Aicardi syndrome Aicardi syndrome is among the most severe X-linked dominant disorders with lethality for hemizygous males. No verified birth of a male with this disorder has ever been reported. Affected females have profound cognitive disabilities and delays; muscular

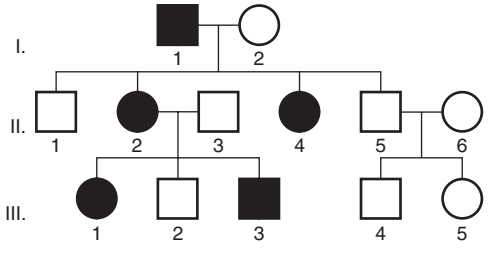


Figure 6-6 X-linked dominant disease. In the first generation of the pedigree, I-1 is an affected male. In the second generation, II-2 and II-4 are affected females. In the third generation, III-1 and III-3 are affected. *(© 2022 American Academy of Ophthalmology.)*

Table 6-5 Characteristics of X-Linked Dominant Inheritance

Both males and females are affected, but the incidence of the trait is approximately twice as high in females as in males (or exclusively occurs in females if the trait is lethal to males).
An affected male transmits the trait to all of his daughters and none of his sons.
Heterozygous affected females transmit the trait to both sexes with equal frequency.
The heterozygous female tends to be less severely affected than the hemizygous male.

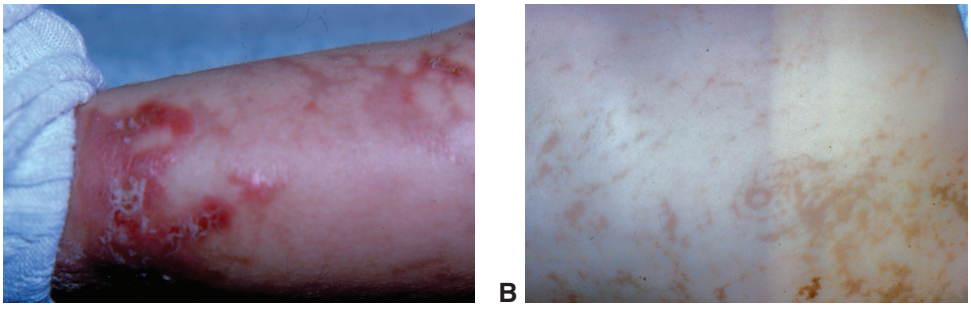


Figure 6-7 Pigmented skin lesions in a patient with incontinentia pigmenti. **A,** Bullous lesions. **B,** Hyperpigmented macules. *(Courtesy of Edward L. Raab, MD.)*

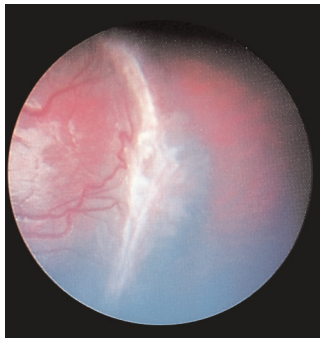


Figure 6-8 Vascular abnormalities of the temporal retina in the right eye of a 2-year-old with incontinentia pigmenti. Note the avascularity peripheral to the circumferential white vasoproliferative lesion, which showed profuse leakage on fluorescein angiography.

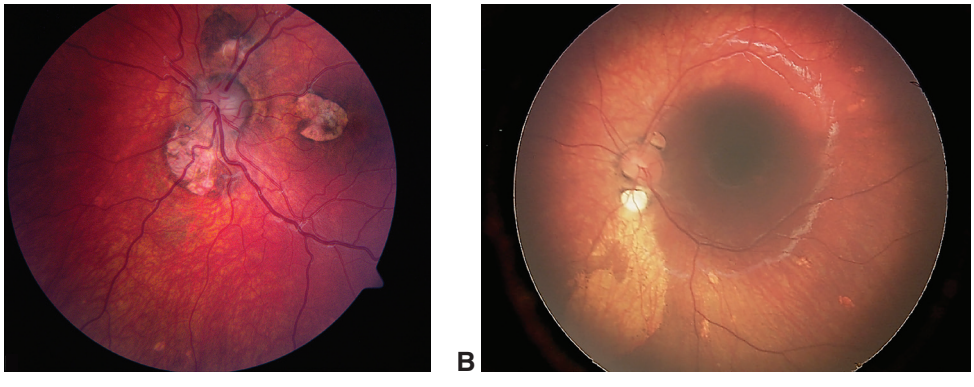


Figure 6-9 Aicardi syndrome. **A,** Fundus photograph demonstrating chorioretinal lacunae circumferential to the optic disc. **B,** Fundus photograph with chorioretinal lacunae adjacent to the optic disc with large and small areas of hypopigmentation resulting from chorioretinal atrophy. *(Courtesy of Elias I. Traboulsi, MD, MEd.)*

hypotonia; blindness, which may be associated with a characteristic lacunar juxtapapillary chorioretinal dysplasia and optic disc anomalies (Fig 6-9); and central nervous system (CNS) abnormalities, the most common characteristic of which is agenesis of the corpus callosum. No recurrence of the disease has been reported among siblings, and parents can be

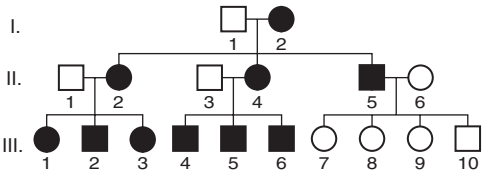


Figure 6-10 Maternally inherited disease. In the first generation of the pedigree, I-2 is an affected female. In the second generation, II-2, II-4, and II-5 are affected. In the third generation, III-1, III-2, III-3, III-4, III-5, and III-6 are affected. *(© 2022 American Academy of Ophthalmology.)*

reassured that the risk in subsequent children is minimal. All instances of the disease appear to arise from a new X-dominant lethal pathogenic variant, and affected females do not survive long enough to reproduce. The pathogenic variant is thought to occur at the distal end of the short arm of the X chromosome because some patients with a deletion in this region have exhibited features of Aicardi syndrome.

Color blindness Most color vision defects involve red–green discrimination relating to the genes coding for the L- and M-cone opsins, which are on the X chromosome. Thus, males are more commonly affected than females. There is 1 copy of the L-cone opsin gene at the centromeric end of the X chromosome, and there are 1–6 copies of the M-cone gene arranged in a head-to-tail tandem array. Normally, only the most proximal of these 2 genes is expressed. Most color vision abnormalities are caused by unequal crossing over between the L- and M-cone opsin genes. This inequality creates hybrid opsins with different spectral absorption functions that are usually less ideal than those of normal opsins.

Maternal Inheritance

When nearly all offspring of an affected woman are at risk for inheriting and expressing a trait, and the daughters are subsequently at risk for passing on the trait to the next generation, the pattern of inheritance is called *maternal inheritance*. The disease stops with all male offspring, whether affected or not. This form of inheritance is highly suggestive of a mitochondrial disorder. Figure 6-10 demonstrates an example of maternal inheritance. See the section Mitochondrial Disease later in this chapter.

Terminology: Hereditary, Genetic, Congenital, Familial

A *hereditary* disease or trait results directly from an individual's particular genetic composition (or *genome*) and can be passed from one generation to another. A *genetic* disorder is caused by a gene defect, whether acquired or inherited. In some instances, such as pathogenic variants in genes related to ocular melanoma, the disease is clearly genetic but is not passed to subsequent generations and therefore is not hereditary. Thus, the terms *hereditary* and *genetic* are not synonymous but are sometimes used to convey similar concepts. Both hereditary and genetic disorders may be congenital or develop later in life.

The term *congenital* refers to characteristics present at birth. These characteristics may be hereditary and/or familial, or they may occur as an isolated event, often as the result of an infection (eg, rubella, toxoplasmosis, or cytomegalovirus) or exposure to a toxic agent (eg, as in thalidomide embryopathy or fetal alcohol syndrome). The presence of such characteristics *at birth* or shortly after (in the first weeks of life) is the defining

factor. Pediatric ophthalmology literature has traditionally used the terms *congenital nystagmus*, *congenital esotropia*, *congenital glaucoma*, and *congenital cataract*; however, in many cases, these disorders are not present at birth and would be more accurately referred to as *infantile*.

A condition is *familial* if it occurs in more than 1 member of a family. It may, of course, be hereditary but need not be. A familial disorder can be caused by common exposure to infectious agents (eg, adenoviral conjunctivitis), excess food intake (eg, obesity), or environmental agents (eg, cigarette smoke). However, genetic factors may contribute to the effects of exposure to these environmental factors, which can make it difficult to determine causality.

Heritability is the proportion of phenotypic variation in a population that is attributable to genetic variation among individuals. Heritability estimations aim to answer the "nature versus nurture" debate and allow researchers to pursue the genetic and/or environmental determinants of disease, although most cases involve a combination of the 2 determinants. Heritability studies compare the phenotypic similarities between genetically closely related individuals with those of less closely related individuals. The best example of this type of study is a comparison of the correlation between the phenotypes of identical twins (monozygotic twins, who share 100% of their DNA sequence) with the correlation between the phenotypes of nonidentical twins (dizygotic twins, who share 50% of their DNA sequence). Because twins are the same age and share similar intrauterine and (usually) early childhood environments, most of the variation between them is thought to be due to genetic factors. An example of a twin study on the highly heritable trait of central corneal thickness is shown in Figure 6-11.

A condition known to be genetic and hereditary (eg, RP) may appear in only 1 individual of a family. Such an individual is said to have a *simplex* (or *isolated*) form of a

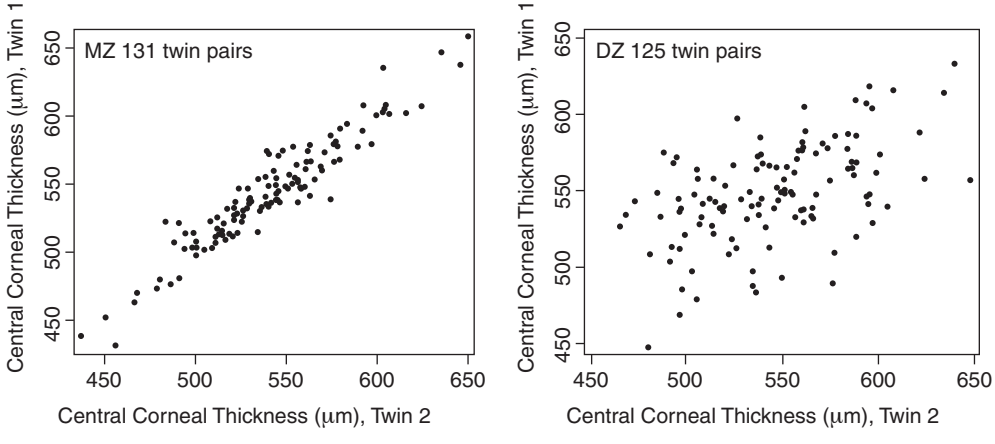


Figure 6-11 Comparison of the correlation levels of central corneal thickness in a set of monozygotic (MZ) twins with that of a set of dizygotic (DZ) twins. *Left,* MZ twins (correlation, 0.95). *Right,* DZ twins (correlation, 0.52). Heritability is calculated based on the difference in the correlation levels of the 2 sets of twins. In this example, the heritability of central corneal thickness is 95%. *(Courtesy of David A. Mackey, MD.)*

genetic disease. A genetically determined trait may be isolated in the pedigree for several reasons:

- The pedigree is small.
- The full expression of the disease has not been sought or has not manifested in other relatives.
- The disorder represents a new genetic variant or chromosomal change.
- The disorder is recessive, and the investigation to determine whether the parents are carriers has been inadequate.
- There is nonpaternity.

Clinically similar disorders may be inherited in several different ways. For example, RP can occur from an autosomal dominant, autosomal recessive, X-linked recessive, or mitochondrial variant. These genetic forms represent distinct gene defects with different alterations in the gene structure and biochemical pathogeneses but similar clinical phenotypic expressions. Clarifying genetic heterogeneity is important because only with the proper diagnosis and correct identification of the inheritance pattern can appropriate genetic counseling and prognosis be offered.

Some genetic disorders originally thought to be a single and unique entity are later found to be 2 or more fundamentally distinct entities. Further clarification of the inheritance pattern or biochemical analysis enables the separation of initially similar disorders. Such has been the case for Marfan syndrome and homocystinuria. Patients with these disorders tend to be tall and thin, with long arms, legs, fingers, and toes; they also have ectopia lentis. However, the presence of dominant inheritance, aortic aneurysms, and valvular heart disease in Marfan syndrome distinguishes it from homocystinuria, which is characterized by recessive inheritance and thromboembolic disease.

Genetic heterogeneity is a general term that applies to the phenotypic similarity that may be produced by 2 or more fundamentally distinct genetic entities; this term implies that the genes are nonallelic. Leber congenital amaurosis, which has more than 14 causative genes, is a good example. Most examples of genetic heterogeneity cease to be a problem for diagnosis or classification once the gene's location on a chromosome and molecular structure are determined. However, clinical, allelic, and locus heterogeneity can remain perplexing issues. For example, pathogenic variants of the Norrie disease gene, *NDP,* usually result in the typical phenotype of pseudoglioma from exudative retinal detachments, but some *NDP* pathogenic variants have been associated with X-linked exudative vitreoretinopathy without any systemic associations.

Sanfilippo PG, Hewitt AW, Hammond CJ, Mackey DA. The heritability of ocular traits. *Surv Ophthalmol.* 2010;55(6):561–583.

Chromosome Analysis

Cytogenetics is the study of chromosomes and their properties. Chromosomal defects are changes in the chromosome number or structure that damage sensitive genetic functions, leading to developmental or reproductive disorders. These defects usually result from (1) a disruption of the mechanisms controlling chromosome movement during cell division or

(2) alterations of the chromosome structure that lead to abnormal chromosomal behavior or changes in the number or arrangement of genes.

In the standardized nomenclature for a specific band, or range of bands, within a stained chromosome, the first letter or numbers refers to the involved chromosome (1-22, or X or Y). Next, the chromosome arm (p for the shorter arm; q for the longer arm) is listed, followed by the specific position on the arm. The number increases as the position on the gene becomes farther from the chromosome centromere. For example, DiGeorge syndrome, also called 22q11.2 deletion syndrome, is caused when a small piece of chromosome 22 is missing. The deleted chromosome material occurs at a specific location on the long arm (q) of chromosome 22, region 1, band 1, sub-band 2.

Major chromosomal abnormalities occur in approximately 0.5%–0.7% of live births, and 1%–2% of all pregnancies involving parents older than 35 years. About 7% of perinatal deaths and some 40%–50% of retrievable spontaneous abortuses are caused by significant chromosomal aberrations. Virtually any change in chromosome number during early development profoundly affects the formation of tissues and organs and the viability of the entire organism. Most major chromosomal disorders are characterized by both developmental delay and cognitive disability, as well as a variety of somatic abnormalities.

Ophthalmologists should be aware of the value of learning the constitutional and tumor karyotypes for infants with retinoblastoma, especially if the tumor represents a new genetic variant. Chromosome analysis (also called *karyotyping*) is suggested in patients with isolated (nonfamilial) aniridia (which is often associated with nephroblastoma [Wilms tumor]) and other systemic malformations.

A chromosomally abnormal state in a previous child warrants consideration of amniocentesis or chorionic villus sampling for prenatal diagnosis in subsequent pregnancies. Preimplantation genetic diagnosis may also be considered (see the section Reproductive Issues).

Aneuploidy of Autosomes

Aneuploidy is an abnormal number of chromosomes in cells. The presence of 3 homologous chromosomes in a cell, rather than the normal pair, is termed *trisomy. Monosomy* is the presence of only 1 member of any pair of autosomes or only 1 sex chromosome. The absence of a single autosome is almost always lethal to the embryo; an extra autosome is often catastrophic to surviving embryos. Aneuploidy of sex chromosomes (eg, X, XXX, XXY, and XYY) is less disastrous. Monosomies and trisomies are generally caused by mechanical accidents that increase or decrease the number of chromosomes in the gametes. Meiotic *nondisjunction,* which results from a disruption of chromosome movement during meiosis, is the most common accident leading to aneuploidy. (See Chapter 5, Figure 5-2.)

Trisomy 21 syndrome (commonly called *Down syndrome*) is the most common chromosomal syndrome in humans, with an overall incidence of 1 in 800 live births. The clinical features of this syndrome have been well known since John Langdon Down originally described them in 1866. Down syndrome is clinically characterized by a number of distinctive, if variable, phenotypic features, whereas the karyotype describes the chromosomal constitution of the cells and tissues of individuals with this disorder.

The most important risk factor for having a child with Down syndrome is maternal age. Per 10,000 live births, the incidence of Down syndrome is as follows:

- age <20: 6.2
- age 20–24: 6.3
- age 25–29: 6.2
- age 30–34: 10.3
- age 35–39: 25.6
- age ≥40: 81.6

In more than 80% of Down syndrome cases, the genetic error occurs in meiosis I (see Chapter 5); and in more than 95% of all cases, the error occurs in maternal rather than paternal meiosis. Approximately 5% of patients with Down syndrome have a *translocation* resulting from the attachment of the long arm of chromosome 21 to the long arm of another acrocentric chromosome, usually 14 or 22. (Acrocentric chromosomes are those with the centromere close to one end of the chromosome.) These translocations cause pairing problems during meiosis, resulting in the generation of a daughter cell containing the translocated fragment of chromosome 21 along with a normal chromosome 21. As in nondisjunction, the fragment becomes trisomic on fertilization. Trisomy of only the distal one-third of chromosome arm 21q is sufficient to cause Down syndrome. Genes within the q22 band of chromosome 21 appear to be specifically responsible for the pathogenesis of Down syndrome.

Individuals with Down syndrome may exhibit the following features:

- cognitive disabilities
- characteristic facies: oblique palpebral fissure, epicanthus, flat nasal bridge, and protruding tongue
- short, broad hands and wide space between first and second toes; characteristic dermatoglyphics
- hypotonia
- congenital heart disease
- immunologic and hematologic anomalies
- gastrointestinal anomalies
- atlantoaxial instability
- epilepsy
- Alzheimer disease
- short stature
- infertility
- dental hypoplasia

The ophthalmic features of Down syndrome are presented in Table 6-6.

Bull MJ, Trotter T, Santoro SL, Christensen C, Grout RW; Council on Genetics. Health supervision for children and adolescents with Down syndrome. *Pediatrics.* 2022;149(5): e2022057010. doi:10.1542/peds.2022-057010

Mosaicism

Occasionally, an individual or a tissue contains 2 or more cell lines with distinctly different chromosomal constitutions. Such persons or tissues are termed *mosaics.* Sometimes the

Table 6-6 Ocular Findings in Down Syndrome (Trisomy 21)

More common
Almond-shaped palpebral fissures
Upward-slanting palpebral fissures
Prominent epicanthal folds
Blepharitis, usually chronic
Nasolacrimal duct obstruction
Strabismus, usually esotropic
Nystagmus (typically horizontal)
Aberrant retinal vessels (at optic nerve head margin)
Iris stromal hypoplasia
Brushfield spots
Cataract (congenital or acquired)
Myopia
Less common
Infantile glaucoma
Keratoconus
Optic nerve head abnormalities

peripheral blood, which is the usual source for chromosomal analysis, contains populations of cells with completely different chromosomal constitutions. If only a few abnormal cells are present in the peripheral blood sample, a second tissue, such as skin fibroblasts, can be analyzed to demonstrate mosaicism.

The clinical effects of mosaicism are difficult to predict because the distribution of abnormal cells in the embryo is determined by the timing of the error and other variables. If mitotic nondisjunction immediately follows conception, the zygote divides into 2 abnormal cells: 1 trisomic and 1 monosomic. The monosomic cells rarely survive and may decrease in number or disappear entirely over time. Mitotic nondisjunction may occur when the embryo comprises a small population of cells, resulting in the establishment of 3 cell populations—1 normal and 2 abnormal—although some abnormal cell lines may be "discarded" or lost during development. If mitotic nondisjunction occurs at a more advanced stage of development, the resulting abnormal populations constitute a minority of the embryo's cells, and mosaicism may have little or no measurable effect on development.

A small population of aneuploid mosaic cells may not directly affect development; however, when such cells occur in the reproductive tissues of otherwise unaffected people, some of their gametes may carry extra chromosomes or lack some chromosomes entirely. Consequently, mosaic parents tend to be at high risk for having chromosomally abnormal children.

The most common example of autosomal mosaicism is *trisomy 21 mosaicism.* Some patients with trisomy 21 mosaicism have the typical features of Down syndrome; others show no abnormalities in appearance or intelligence. The crucial variables affecting clinical manifestation seem to be the frequency and embryologic distribution of the trisomic cells during early development, which do not necessarily correlate with the percentage of trisomic cells in any one tissue, such as peripheral blood.

Several types of sex chromosome mosaicism may occur. Again, the physical effects tend to vary, probably reflecting the quantity and distribution of the abnormal cells during development. For example, a cell population lacking 1 X chromosome can arise in a female

embryo, leading to 45,X/46,XX mosaicism. In some cases, these patients develop normally; in other cases, some or all of the features of Turner syndrome (eg, short stature, ovarian insufficiency, a webbed neck, lymphedema of hands and feet) appear. Similarly, the Y chromosome may be lost in some cells of a developing male embryo, producing 45,X/46,XY mosaicism. An embryo with X/XY mosaicism may develop as a phenotypically unaffected male, a female with the features of Turner syndrome, or an individual with physical characteristics intermediate between the sexes (*intersex* or *pseudohermaphrodite*).

Important Chromosomal Aberrations in Ophthalmology

Short arm 11 deletion (11p13) syndrome: aniridia

Classic aniridia results from a defect in the developmental gene, *PAX6,* located at 11p13. The *PAX6* gene product is a transcription factor required for the normal development of the eye. Classic aniridia is a panophthalmic disorder characterized by the following features:

- iris absence or severe hypoplasia
- cataracts (usually anterior polar)
- keratitis due to limbal stem cell failure
- subnormal visual acuity
- congenital nystagmus
- foveal or macular hypoplasia
- optic nerve hypoplasia
- glaucoma
- strabismus
- ectopia lentis

When working with a new patient with aniridia, the ophthalmologist should, if possible, carefully examine the patient's parents for the variable expression of autosomal dominant aniridia. Although almost all cases of aniridia result from *PAX6* pathogenic variants, a rare autosomal recessive disorder called *Gillespie syndrome* (phenotype OMIM number 206700) also produces partial aniridia, as well as cerebellar ataxia, mental deficiency, and congenital cataracts.

Aniridia (often with cataract and glaucoma) can also occur sporadically in association with Wilms tumor, other genitourinary anomalies, and cognitive disability, the so-called *WAGR syndrome.* This complex of findings is called a *contiguous gene-deletion syndrome* because it results from a deletion affecting multiple adjacent genes. Most patients affected by WAGR syndrome have a karyotypically visible interstitial deletion of a segment of 11p13. Patients with aniridia that is *not* clearly part of an autosomal dominant trait, and those with coincident systemic malformations, should undergo chromosome analysis (karyotyping) and observation for possible Wilms tumor.

Pathogenic variants of *PAX6* have also been reported in Peters anomaly, autosomal dominant keratitis, and dominant foveal hypoplasia. The mechanism that disrupts normal embryology and results in degenerative disease in aniridia and other *PAX6* disorders appears to be *haploinsufficiency,* which, in this case, is the inability of a single active allele to activate transduction of the developmental genes regulated by the *PAX6* gene product. In this way, aniridia is different from retinoblastoma and Wilms tumor, which result from the

absence of both functional alleles at each of the homologous gene loci. (For further discussion of *PAX6*, see the section Homeobox Gene Program in Chapter 4.)

Landsend ES, Utheim ØA, Pedersen HR, Lagali N, Baraas RC, Utheim TP. The genetics of congenital aniridia—a guide for the ophthalmologist. *Surv Ophthalmol.* 2018;63(1): 105–113.

Long arm 13 deletion (13q14) syndrome: retinoblastoma

Retinoblastoma is one of several heritable childhood malignancies. Ocular tumors, which are usually noted before 4 years of age, affect between 1 in 15,000 and 1 in 34,000 live births in the United States. The disease exhibits both hereditary occurrence (approximately 30%–40%), in which tumors tend to be bilateral and multicentric, and sporadic occurrence, in which unilateral and solitary tumors are the rule. On clinical presentation, about 10% of patients have a family history of the disease, and 90% have a negative family history, therefore possessing a new pathogenic variant in their germ cells. Retinoblastoma does not develop in approximately 10% of all obligate carriers of a germline pathogenic variant (ie, incomplete penetrance).

A karyotypically visible deletion of part of the long arm of chromosome 13 occurs in 3%–7% of all cases of retinoblastoma. Large deletions manifest more severe phenotypes, which can include cognitive disabilities and developmental delays, microcephaly, hand and foot anomalies, and ambiguous genitalia.

Although the hereditary pattern in familial retinoblastoma is that of an autosomal dominant pathogenic variant, the defect is recessive at the cellular level. Predisposition to retinoblastoma is caused by hemizygosity of the retinoblastoma gene *(RB1)* within band 13q14. *RB1* is a member of a class of genes called *recessive tumor suppressor genes,* the products of which regulate the cell cycle at the G_1 checkpoint. The alleles normally present at these loci help prevent tumor formation; at least 1 active normal allele is needed to control proliferation. Thus, tumor formation in retinoblastoma is due to the loss of function of both normal alleles. Homozygous deletions within the 13q14 band have been noted in retinoblastomas derived from enucleated eyes. In addition, patients who inherit a defective allele from 1 parent are at greater risk for developing retinoblastoma due to an inactivation of the normal allele through other mechanisms.

The first step in tumorigenesis in retinoblastoma is a recessive pathogenic variant of 1 of the homologous alleles at the retinoblastoma locus by inheritance, germinal pathogenic variant, or somatic pathogenic variant. Hereditary retinoblastomas arise from a single additional somatic event in a cell that carries an inherited pathogenic variant, whereas sporadic cases require 2 somatic events. In approximately 50% of tumors, homozygosity for such a recessive variant results from the mitotic loss of a portion of chromosome 13, including the 13q14 band. The 2 resulting allelic variants at this locus allow tumorigenesis.

Retinoblastoma, therefore, seemingly represents a malignancy caused by defective gene regulation rather than by the presence of a dominant oncogene variant. Those who inherit an allelic variant at this locus have a high incidence of nonocular secondary tumors; almost half of these tumors are osteosarcomas. Other secondary malignancies include soft-tissue sarcoma, pineoblastoma, and melanoma. Unilateral or bilateral retinoblastoma in the presence of an intracranial midline tumor is referred to as trilateral retinoblastoma.

Knudson's 2-Hit Hypothesis and the Genetics of Retinoblastoma and the Neurocutaneous Syndromes

Knudson's hypothesis and the genetics of retinoblastoma

Study of the occurrence of unilateral and bilateral retinoblastoma led to the *2-hit hypothesis,* according to which some tumors arise from a single cell with de novo variations in both copies of a key gene (*RB1* in retinoblastoma or other oncogenes in other diseases). Conversely, in an individual who has a germline variant (first "hit") in every cell of their body, the spontaneous occurrence of a second variant (second "hit") in a somatic cell(s) can result in single or multiple tumors (Fig 6-12). Knudson's hypothesis, now proven, is applicable to many cancers.

RB1 pathogenic variants occurring in a cone precursor cell result in retinoblastoma. In other cell lines, additional variants in other genes (sometimes precipitated by radiation from radiotherapy or computed tomography [CT] scans) can lead to the development of other tumors. A cascade of variations in other genes can also increase the malignancy of a tumor.

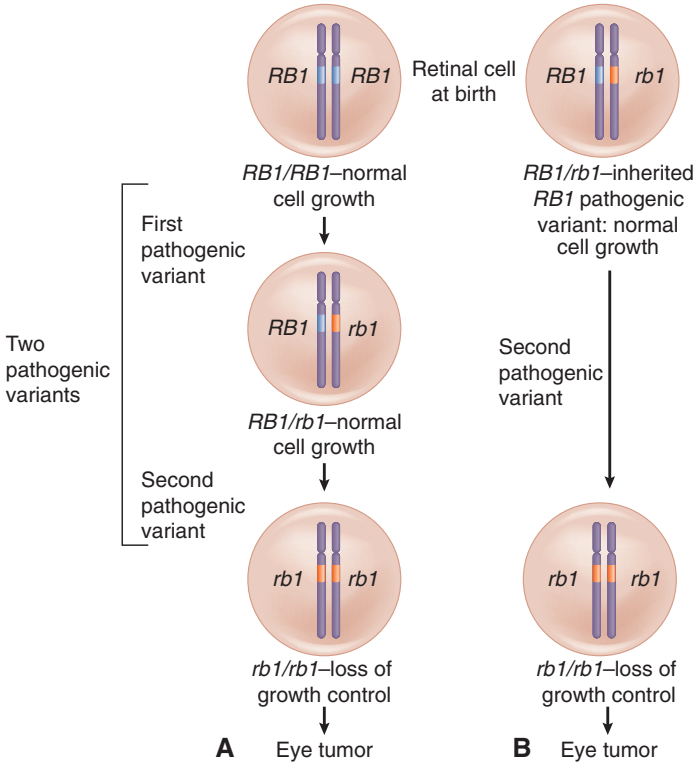


Figure 6-12 Comparison of sporadic retinoblastoma **(A),** where 2 independent pathogenic variants ("hits") in the *RB1* gene occur in a somatic cell, and hereditary retinoblastoma **(B),** where a germline variant is present in every cell and a second pathogenic variant arises in 1 or more cells, leading to tumor formation. *(Illustration by Cyndie C.H. Wooley.)*

CLINICAL PEARL

Although CT scans may be helpful for identifying areas of calcification, their initial use as a diagnostic modality should be avoided due to the radiation exposure and increased risk of secondary malignancies. Ultrasound and magnetic resonance imaging (MRI; orbit/head) should be the initial diagnostic modalities of choice when evaluating individuals with suspected retinoblastoma unless other contraindications are present in the patient.

With an autosomal dominant inheritance pattern, a germline variant may be inherited from either parent. Alternatively, a child may inherit a germline variant from an unaffected parent who has variants in the cells producing eggs or, more often, sperm. The risk of genetic variants in sperm increases with increasing age of the father. Guidelines for clinical screening and DNA testing of children at risk for retinoblastoma were revised in 2018.

Skalet AH, Gombos DS, Gallie BL, et al. Screening children at risk for retinoblastoma: consensus report from the American Association of Ophthalmic Oncologists and Pathologists. *Ophthalmology.* 2018;125(3):453–458.

Genetics of the neurocutaneous syndromes

As mentioned, Knudson's 2-hit hypothesis applies to many tumors, including the neurocutaneous syndromes (phakomatoses). The neurocutaneous syndromes are a group of hereditary disorders characterized by hamartomas of the skin, eye, CNS, and viscera. Some of the more common disorders designated as neurocutaneous syndromes include neurofibromatosis 1 and 2 (NF1 and NF2), retinocerebral angiomatosis, and tuberous sclerosis (Table 6-7).

NF1 (von Recklinghausen disease) occurs with a germline pathogenic variant in the *NF1* gene, which produces neurofibromin. A second "hit," or variant, can result in the development of neurofibromas in nerves, gliomas in the optic nerve, Lisch nodules (iris hamartomas), café-au-lait spots in the skin, and other tumors. Genetic studies of isolated gliomas have found that these can arise from 2 hits in the *NF1* gene.

NF2 occurs with pathogenic variants in the *NF2* gene, which produces merlin (also called *schwannomin*). A second hit can result in acoustic neuromas, meningiomas, gliomas, ependymomas, and schwannomas.

Retinocerebral angiomatosis (also called von Hippel–Lindau syndrome [VHL]) occurs with germline pathogenic variants in the *VHL* tumor suppressor gene. The VHL protein targets *hypoxia-inducible factor,* a regulator of cell division and angiogenesis. The syndrome is characterized by benign and malignant multisystem tumors, including retinal and CNS hemangioblastomas, clear cell renal carcinoma, pheochromocytoma, epididymal cystadenoma, and pancreatic carcinoma.

CLINICAL PEARL

Hypoxia-inducible factors, in particular HIF-1, are activated in cases of ischemia caused by retinal vascular diseases like diabetic retinopathy. Reduced oxygen levels activate HIF-1, which leads to increased expression of vascular endothelial growth factor (VEGF). VEGF inhibitors represent the mainstay of therapy for retinal vascular disease. Absence of the VHL tumor suppressor gene also activates HIF-1, leading to development of vascular tumors.

Table 6-7 Overview and Select Features of Neurocutaneous Syndromes

Disease	Gene Symbol (Chromosome Location)	Inheritance Pattern	Ocular Features	Cutaneous Features	CNS and Other Systemic Features	Incidence and Comments
Neurofibromatosis type 1 (von Recklinghausen disease) (OMIM #162200[a])	*NF1* (17q11.2); tumor suppressor	AD	Orbital or eyelid neurofibroma, glaucoma, prominent corneal nerves, Lisch nodules, iris ectropion, retinal and choroidal hamartomas, optic pathway glioma, refractive error	Café-au-lait spots, neurofibromas, freckling of the axillary or inguinal regions	Sphenoid dysplasia, optic pathway glioma	1/3500 New pathogenic variants common; variable expressivity common; patients with genetic mosaicism should follow same screening guidelines as those with germline pathogenic variants
Neurofibromatosis type 2 (OMIM #101000)	*NF2* (22q12); tumor suppressor	AD	Cataract (PSC most common), combined hamartoma of the RPE and retina, epiretinal membrane, optic nerve sheath meningiomas	Café-au-lait spots	Bilateral acoustic neuromas, spinal cord tumors, meningiomas, cranial nerve palsies	1/33,000 New pathogenic variants common
Tuberous sclerosis complex (Bourneville disease) (OMIM #191100 and #613254)	*TSC1* (9q34), *TSC2* (16p13.3); tumor suppressor	AD	Retinal astrocytic hamartomas, peripheral depigmented or hypopigmented lesions	Angiofibromas, hypopigmented macules, subungual fibromas, shagreen patch	Infantile spasms/seizures, cognitive impairment, SEGA, subependymal nodules, cardiac rhabdomyoma, lymphangiomyomatosis, renal angiomyolipoma	1/10,000 New pathogenic variants very common

(*Continued*)

Table 6-7 *(continued)*

Disease	Gene Symbol (Chromosome Location)	Inheritance Pattern	Ocular Features	Cutaneous Features	CNS and Other Systemic Features	Incidence and Comments
Retinocerebral angiomatosis (von Hippel–Lindau syndrome; VHL) (OMIM #193300)	*VHL* (3p26-p25); tumor suppressor	AD	Retinal capillary hemangioblastoma	Café-au-lait spots, vascular nevi, rare cutaneous manifestations (<5%)	Hemangioblastoma, renal cell carcinoma, pheochromocytoma	1/36,000, de novo in 70%–80% High penetrance; benign and malignant tumors
Encephalofacial angiomatosis (Sturge-Weber syndrome) (OMIM #185300)	*GNAQ* (9q21)	Somatic mosaicism	Diffuse choroidal cavernous angioma, glaucoma	Nevus flammeus	Meningeal angiomas, seizures/infantile spasms	1/50,000 Nevus flammeus alone not pathognomonic
Ataxia-telangiectasia (Louis-Bar syndrome) (OMIM #208900)	*ATM* (11q22.3)	AR	Saccadic initiation failure, conjunctival telangiectasias	Telangiectasias	Cerebellar dysfunction, immunodeficiency, malignancy	1/40,000 *ATM* regulates tumor-suppressor genes and DNA repair
Incontinentia pigmenti (Bloch-Sulzberger syndrome) (OMIM #308300)	*IKBKG* (Xq28)	X-linked dominant	Retinal vasculopathy	Vesicles with evolution to hyperpigmented lesions	Seizures, cognitive impairment	Evolution of skin lesions can occur in utero
Racemose angioma (Wyburn-Mason syndrome)	Nonhereditary	Sporadic	Retinal racemose angioma	Facial lesions (if present)	Intracranial AVMs with bleeding as sequelae	Isolated finding more common than syndrome
Klippel-Trénaunay-Weber syndrome *PIK3CA*-related overgrowth spectrum (PROS)	*PIK3CA* gene	Mosaic	Glaucoma	Nevus flammeus similar to that in encephalofacial angiomatosis; hyperpigmented nevi and streak	Limb anomalies (asymmetric limb hypertrophy, poly-/syn-/oligodactyly), seizures, Kasabach-Merritt syndrome	Capillary and venous malformations with limb overgrowth with or without lymphatic malformation

AD = autosomal dominant; AR = autosomal recessive; AVM = arteriovenous malformation; CNS = central nervous system; PSC = posterior subcapsular cataract; RPE = retinal pigment epithelium; SEGA = subependymal giant cell astrocytoma.

[a] OMIM = Online Mendelian Inheritance in Man; database is online at www.omim.org.

Tuberous sclerosis is caused by pathogenic variants in either of 2 genes: *TSC1,* which produces the protein hamartin, and *TSC2,* which produces the protein tuberin. The 2 proteins interact, forming a heterodimer in the cytoplasm. The *TSC1* and *TCS2* pathogenic variants each account for 50% of cases. Tuberous sclerosis has many clinical features, including optic nerve or retinal tumors (astrocytic hamartoma), which may be flat or mulberry-like in appearance; cerebral tubers; ash-leaf skin lesions; subungual fibromas; and facial angiofibromas. In children, facial angiofibromas are thought to arise from second hits caused by exposure to UV radiation.

These genetic disorders can be inherited (with affected persons usually having multiple tumors) or sporadic (with affected persons having isolated tumors). The latter may occur from 2 hits in a somatic cell. One neurocutaneous syndrome that is not inherited (possibly because germline pathogenic variants are not compatible with life) is *encephalofacial angiomatosis* (also called Sturge-Weber syndrome [SWS]). Encephalofacial angiomatosis is caused by a somatic pathogenic variant in the *GNAQ* gene, which controls the development of blood vessels. This syndrome is characterized by vascular lesions that affect the skin; when the skin lesion is around the eyelids, there can also be vascular lesions of the choroid (hemangioma) and, in many cases, glaucoma. Glaucoma occurs either from trabeculodysgenesis or elevated episcleral venous pressure.

See BCSC Section 5, *Neuro-Ophthalmology*; Section 6, *Pediatric Ophthalmology and Strabismus*; and Section 12, *Retina and Vitreous,* for additional discussion of neurocutaneous syndromes.

Shankar SP, Humberson J, Melvani R, Couser NL. Neurocutaneous Syndromes (Phakomatoses). In: Couser N, ed. *Ophthalmic Genetic Diseases: A Quick Reference Guide to the Eye and External Ocular Adnexa Abnormalities*. Elsevier; 2019:129–135;chap 10.

Racial and Ethnic Concentration of Genetic Disorders

Most genetic diseases exhibit similar prevalence among individuals of different racial or ethnic backgrounds. Some, however, are concentrated in certain population groups and may reflect a previous advantage of the variant (particularly in the carrier state). For example, sickle cell carriers are more resistant to malaria, and the disease is common in people of African descent.

GM_2 gangliosidosis type I (Tay-Sachs disease), with its characteristic macular cherry-red spot, occurs predominantly in persons of Eastern European Jewish (Ashkenazic) ancestry. The estimated carrier rate for this disorder is approximately 1 in 30 in the Ashkenazi Jewish population and 1 in 300 in other populations. Familial dysautonomia *(Riley-Day syndrome*)—characterized by alacrima, corneal hypoesthesia, exodeviation, and methacholine-induced miosis—also occurs more frequently in persons of Ashkenazic ancestry, as do *MAK (male germ cell-associated kinase)-associated RP, Gaucher disease,* and *Niemann-Pick disease.*

Several types of *achromatopsia* (complete color blindness) with *myopia* are common on the South Pacific island of Pingelap, affecting 5% of the Pingelapese population in the Caroline Islands of Micronesia. *Oguchi disease* (stationary night blindness) is observed primarily, though not exclusively, in Japanese people.

The prevalence of *oculocutaneous albinism* is high among the Kuna Indians in Panama. *Hermansky-Pudlak syndrome,* an autosomal recessive disorder characterized by oculocutaneous albinism, pulmonary interstitial fibrosis, easy bruising, and bleeding tendency associated with a prolonged bleeding time and abnormal platelet aggregation, occurs with a higher frequency in persons of Puerto Rican ancestry.

Lyonization

In classical human genetics, females with a gene for a recessive disease or trait on only 1 X chromosome should have no manifestations of the defect. However, there are several ophthalmic examples of structural and functional abnormalities in females heterozygous for supposedly recessive X-linked traits. Such *carrier states,* usually mild but occasionally severe, have been described in carriers of such diseases as

- choroideremia
- X-linked ocular albinism, or ocular albinism type 1 (also called *Nettleship-Falls ocular albinism*)
- X-linked RP
- X-linked sutural cataracts
- Lowe syndrome
- Fabry disease
- color vision defects of the protan and deutan types

See Figure 6-13 and Table 6-8.

Detection of these carrier states of the X-linked traits is clinically relevant, especially for sisters and maternal aunts of affected males. In 1961, geneticist Mary Lyon advanced an explanation for the unanticipated or partial expression of a trait by a heterozygous female. Briefly, every somatic cell of a female has only 1 X chromosome that is actively functioning due to *lyonization* (X-chromosome inactivation). The second X chromosome is inactive and forms a densely staining marginal nuclear structure demonstrated as a Barr body in a buccal smear or "drumsticks," pedunculated lobules of the nucleus identified in about 5% of the leukocytes of the unaffected female. Inactivation of 1 X chromosome occurs randomly in early embryogenesis; the same X chromosome will be irreversibly inactive in every daughter cell of each of these "committed" primordial cells. The active gene is dominant at a cellular level. Thus, a female heterozygous for an X-linked disease will have 2 clonal cell populations (mosaic phenotype), 1 with normal activity for the gene in question and the other with variant activity.

The proportion of variant to normal X chromosomes inactivated usually follows a normal distribution, presumably because inactivation in various cells is a random event. Thus, an average of 50% of paternal X chromosomes and 50% of maternal X chromosomes are inactivated. It is conceivable, however, that in some cases, the X variant is active in almost all cells, and in other cases, the X variant is inactivated in nearly all cells. By this mechanism, a female may express an X-linked disorder; rare cases of women with classic color deficiency or X-linked ocular albinism, X-linked RP, or choroideremia have been reported.

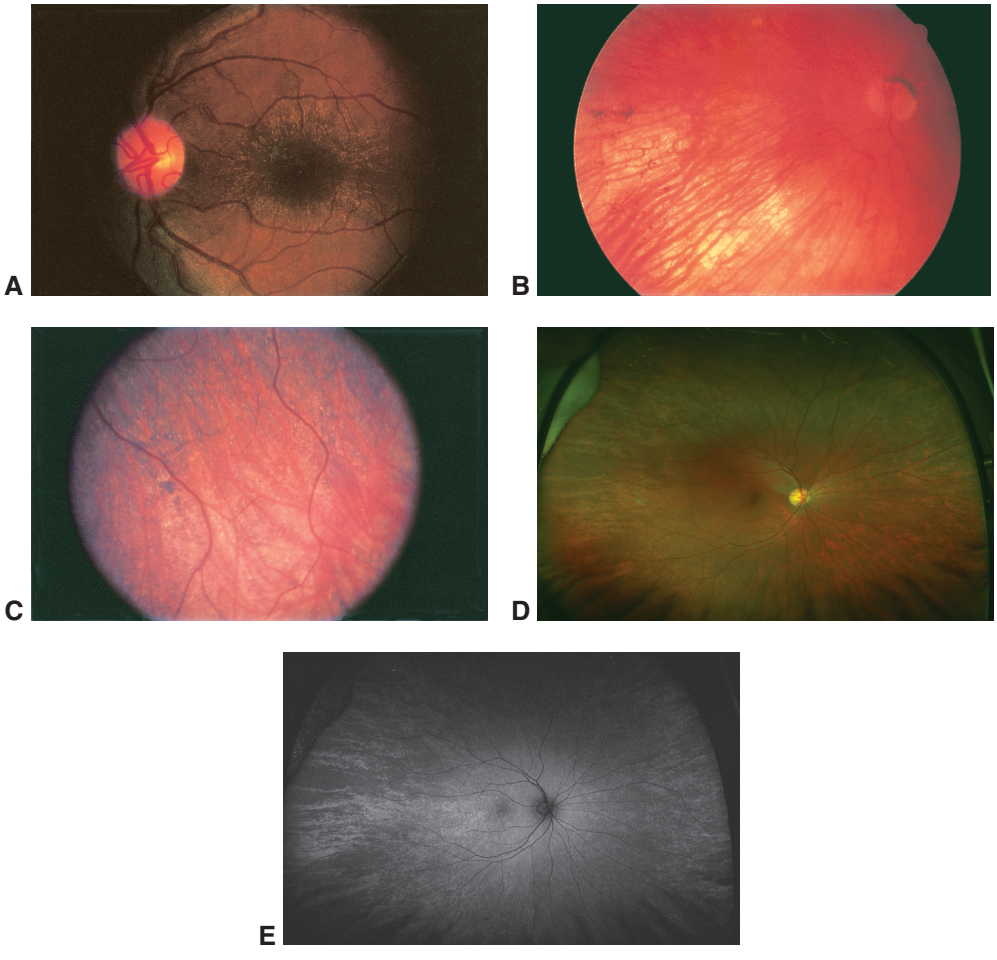


Figure 6-13 Fundus abnormalities in female carriers of "recessive" X-linked diseases. **A,** Yellow, "gold-dust" tapetal-like reflex in the left retina of an X-linked retinitis pigmentosa (RP) carrier. **B,** Nasal midperipheral retina in the left eye of an X-linked RP carrier, showing patchy bone spicule-like pigment clumping. **C,** Peripheral retina in the left eye of a carrier for choroidemia, showing a "moth-eaten" fundus appearance from areas of hypopigmentation and hyperpigmentation. **D,** Wide-field fundus photograph of the right eye of a carrier for ocular albinism, showing chocolate-brown pigmentation from areas of apparently enhanced pigmentation and clusters of hypopigmentation. **E,** Fundus autofluorescence image of the right eye of the same patient as in part D, showing mottled autofluorescence consistent with lyonization. *(Parts D and E courtesy of Elias I. Traboulsi, MD, MEd.)*

Carriers of X-linked ocular albinism may have a mottled mosaic fundus: the normal X chromosome is active in the pigmented retinal epithelial cells, and the X variant is active in the nonpigmented cells. However, these distinguishing features of the carrier state are not always present, and thus the possibility that a female patient is a carrier cannot be definitively ruled out based on the absence of features. In female carriers, the chance inactivation of the X chromosome variant may have occurred in most primordial cells that evolved into the

Table 6-8 Ocular Findings in Carriers of X-Linked Disorders

Disorder	Ocular Findings
S-cone (blue-cone) monochromatism	Abnormalities in cone function on electroretinogram, psychophysical thresholds, and color vision testing
Choroideremia	"Moth-eaten" fundus pigmentary changes, with areas of hypopigmentation, mottling, and pigment clumping in a striated pattern near the equator
Congenital stationary night blindness with myopia	Reductions in electroretinogram oscillatory potentials
Fabry disease	Whorl-like (verticillata) changes within the corneal epithelium
Lowe syndrome	Scattered punctate lens opacities on slit-lamp examination
Ocular albinism	Chocolate-brown clusters of pigment prominent in the midperipheral retina; mottling of macular pigment; iris transillumination
Red–green color vision deficiencies (protan and deutan)	Abnormally wide or displaced color match on a Nagel anomaloscope; decrease in sensitivity to red light in protan carriers (Schmidt sign)
X-linked retinitis pigmentosa	Regional fundus pigmentary changes, "gold-dust" tapetal-like reflex; electroretinogram amplitude and implicit time abnormalities

specific tissue observed, resulting in a phenotypically normal appearance. This subtlety is even more important in the evaluation of family members with X-linked disease if the phenotypic carrier state is age-dependent. Even in obligate carrier females for Lowe syndrome, lenticular cortical opacities are not necessarily present before the third decade of life.

Mitochondrial Disease

A significant number of disorders associated with the eye or visual system involve deletions and variations of mitochondrial DNA (mtDNA). Mitochondrial diseases should be considered whenever the inheritance pattern of a trait suggests maternal transmission. Although the inheritance pattern might superficially resemble that of an X-linked trait, maternal transmission differs in that all offspring of affected females—both daughters and sons—can inherit the trait, but only daughters can pass it on.

The phenotype and severity of mitochondrial diseases appear to depend on the nature of the variation, the presence or degree of heteroplasmy (coexistence of more than 1 species of mtDNA—ie, wild type and variant), and the oxidative needs of the affected tissues. Spontaneous deletions and alterations of mtDNA accumulate with age, decreasing the efficiency and function of the electron transport system and reducing the availability of adenosine triphosphate (ATP). When energy production becomes insufficient to maintain the function of cells or tissue, disease occurs. The expression of inherited mtDNA variants appears to be affected by age and the tissue threshold for oxidative phosphorylation.

Unlike in mendelian inheritance, the number of variant mtDNA copies that are partitioned to a given daughter cell with each cell division is random. After a number of cell

divisions, some cells, purely by chance, receive more normal or more variant copies of mtDNA, resulting in a drift toward homoplasmy (the presence of a single population of mitochondria within a cell, each carrying the same allele at a given locus) in subsequent cell lines. This process is called *replicative segregation*. With mtDNA deletions, preferential replication of the smaller deleted molecules increases their copy numbers over time. The trend toward homoplasmy helps explain why disease worsens with age and why organ systems not previously involved in multisystem mitochondrial disease become involved later in life.

The causes of mitochondrial diseases can be categorized as follows (Table 6-9):

- large rearrangements of mtDNA (deletions or insertions), such as in chronic progressive external ophthalmoplegia (CPEO), Kearns-Sayre syndrome, and Pearson syndrome
- pathogenic variants of mtDNA-encoded ribosomal RNA, such as in maternally inherited sensorineural deafness and aminoglycoside-induced deafness
- pathogenic variants of mtDNA-encoded transfer RNA (tRNA), such as in the syndromes of MELAS (*m*itochondrial *e*ncephalomyopathy, *l*actic *a*cidosis, and *s*trokelike episodes), MERRF (*m*yoclonic *e*pilepsy with *r*agged *r*ed *f*ibers), MIDD (*m*aternally *i*nherited *d*iabetes and *d*eafness), and about 30% of cases of CPEO
- missense and nonsense variants, such as in Leber hereditary optic neuropathy and neuropathy, ataxia, and RP (NARP)

Chronic Progressive External Ophthalmoplegia

CPEO is a disorder involving progressive ptosis and paralysis of eye muscles associated with ragged red myopathy (Fig 6-14), usually as a result of the deletion of a portion of the mitochondrial genome. Patients with CPEO commonly have pigmentary retinopathy that does not create significant visual disability. Infrequently, more marked retinal or other system involvement occurs (the so-called *CPEO-plus syndromes*). In Kearns-Sayre syndrome, CPEO is associated with heart block and severe RP with marked visual impairment. Pearson syndrome results from a large deletion of mtDNA and presents in younger patients with an entirely different phenotype involving sideroblastic anemia and pancreatic exocrine dysfunction. In patients afflicted during their later years, Pearson syndrome can present with a phenotype resembling that of Kearns-Sayre syndrome.

Roughly 50% of patients with CPEO have demonstrable mtDNA deletions, whereas virtually all patients with Kearns-Sayre syndrome have large deletions. Of those patients with CPEO who do not harbor demonstrable mtDNA deletions, up to 30% may have a point variation at nucleotide position 3243, the same tRNA for leucine variant associated with MELAS syndrome. For all syndromes associated with deletions, such as Kearns-Sayre and CPEO, detection of the deletion usually requires muscle tissue examination.

MELAS and MIDD

Two disorders—mitochondrial encephalomyopathy, lactic acidosis, and strokelike episodes (MELAS) and maternally inherited diabetes and deafness (MIDD; also called *type 2 diabetes mellitus with deafness*)—are associated with an mtDNA point variation (A-to-G change at nucleotide position 3243), which affects an mtDNA-encoded tRNA. This variant and macular retinal pigment epithelial atrophy have been described in patients with MELAS.

Table 6-9 Causes and Key Features of Mitochondrial Diseases

Mitochondrial Disease	Primary Clinical Features	Key Genetic Features
Chronic progressive external ophthalmoplegia (CPEO)	Bilateral ptosis, slow progressive extraocular muscle paralysis	Point variation in tRNA $^{Leu(UUR)}$, large deletions
Kearns-Sayre syndrome (KSS)	CPEO, heart block, pigmentary retinopathy	Large deletions in mtDNA
Leber hereditary optic neuropathy (LHON)	Subacute bilateral painless visual acuity and color vision loss typically in second or third decade of life, optic atrophy	Approximately 90% of those affected have an mtDNA variant in either G11778A (most common), T14484C, or G3460A Homoplasmic Male > female predilection
Leigh syndrome	Neurological deterioration with loss of developmental milestones that typically presents in infancy and progresses rapidly	Multiple causes, including nuclear genome variants (*PDHA1*) and mitochondrial DNA variants (*MTATP6*)
Maternally inherited diabetes and deafness (MIDD)	Diabetes and sensorineural hearing loss	Mitochondrial DNA point variation in tRNA $^{Leu(UUR)}$
Mitochondrial encephalomyopathy, lactic acidosis and stroke-like episodes (MELAS)	Encephalomyopathy, stroke-like episodes, lactic acidosis, muscle weakness, recurring headaches, seizures, vomiting	Mitochondrial DNA point variation in tRNA $^{Leu(UUR)}$
Myoclonic epilepsy with ragged red fibers (MERRF)	Myoclonus generalized epilepsy, dementia, ataxia, muscle weakness	Mitochondrial DNA point variation in tRNA ^{Lys}
Neurogenic muscle weakness, ataxia, and retinitis pigmentosa (NARP)	Ataxia, peripheral neuropathy in the arms and legs, pigmentary retinopathy, muscle weakness	Mitochondrial ATPase subunit 6 gene point variation Condition considered to be part of a spectrum with Leigh syndrome, with the latter being more severe and involving a greater percentage of variant mtDNA
Pearson syndrome	Pancytopenia, exocrine pancreatic failure, sideroblastic anemia of childhood, fatigue, difficulties gaining weight, stomach pain, diarrhea	Large deletions in mtDNA

Isashiki Y, Nakagawa M, Ohba N, et al. Retinal manifestations in mitochondrial diseases associated with mitochondrial DNA mutation. *Acta Ophthalmol Scand.* 1998;76(1):6–13.

Yu-Wai-Man P, Griffiths PG, Hudson G, Chinnery PF. Inherited mitochondrial optic neuropathies. *J Med Genet.* 2009;46(3):145–158.

Leber Hereditary Optic Neuropathy

Leber hereditary optic neuropathy (LHON) is more prevalent in males than in females but does not fit a classic X-linked pattern of transmission. The trait is not transmitted to the

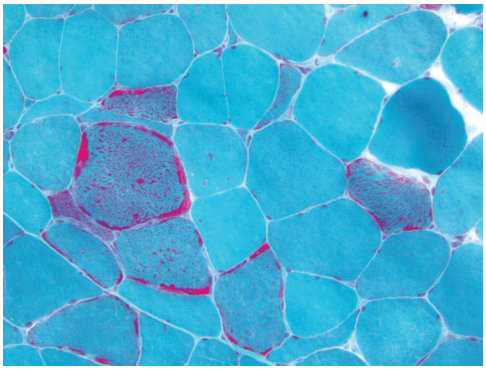


Figure 6-14 Histologic examination of a muscle biopsy specimen shows ragged red fibers (modified Gomori trichrome stain). *(Courtesy of Marjorie R. Grafe, MD.)*

offspring of affected males, but virtually every daughter and son of a female patient with LHON inherits the trait. In approximately 50% of cases, LHON development is associated with a single base change (G to A at nucleotide position 11778 in the *ND-4* gene) in human mtDNA involved in the synthesis of NADH (nicotinamide adenine dinucleotide hydrogen) dehydrogenase. In addition to optic atrophy, patients with LHON can exhibit peripapillary microangiopathy. LHON can also occur from other so-called primary variants at nucleotide positions 3460 of *ND-1* and 14484 of *ND-6,* as well as several other rare variants. At least 12 secondary variants are associated with LHON, often when multiple variants are present in an individual's mitochondria. Some authors have proposed that these secondary variants cause disease via additive detrimental effects on the electron transport system of oxidative phosphorylation. Most of these secondary variants appear in the general population, and debate persists on whether each variant alone is truly pathogenic.

The likelihood of improvement of visual acuity over time appears to differ among patients with the separate variants associated with LHON. A variant at nucleotide position 11778 is associated with the least likelihood of recovery, and a variant at nucleotide position 14484 is associated with the greatest likelihood.

Neuropathy, Ataxia, and Retinitis Pigmentosa

Neuropathy, ataxia, and retinitis pigmentosa (NARP) is associated with a single base-pair variation at nucleotide position 8993 in the *ATPase-6* gene. The NARP phenotype occurs when the percentage of variant mtDNA is less than 80%, whereas higher proportions of the same variant (greater than 95%) can cause Leigh syndrome, a severe neurodegenerative disease of infancy and early childhood. The 8993 pathogenic variant is demonstrable in fibroblasts and lymphoblasts.

Complex Genetic Disease: Polygenic and Multifactorial Inheritance

In chromosomal and mendelian (single-gene) disorders, genetic analysis of phenotypic, biochemical, or molecular parameters is imperative. However, for many common, normal characteristics or disorders for which genetic variability clearly exists, a simple mode of inheritance cannot be assigned, and recurrence risk cannot be predicted. Such traits as stature,

refractive error, intraocular pressure (IOP), central corneal thickness, and iris color are usually distributed as a continuous variation over a wide range without sharp distinction between normal and abnormal phenotypes. This normal distribution contrasts with the bimodal curve (or trimodal curve in codominant models) observed for conditions transmitted by a single gene. Conditions that result from the operation of multiple collaborating genes, each with relatively minor additive effects, are often termed *polygenic*. Many of these common genes with small effects have been identified through GWAS. With the exception of AMD, the discovered genes account for only a small percentage of the genetic effect for the traits and diseases investigated.

The term *multifactorial inheritance* denotes a combination of genetic and environmental factors in the etiology of the disease without specifying the nature of the genetic influence. Examples of disorders involving these factors in humans include refractive error, glaucoma, and AMD.

Counseling for recurrence may be difficult for disorders with multifactorial inheritance patterns. Ideally, empirical data are summarized from exhaustive analyses of similarly affected families in the population. In general, the risk is intermediate between the population risk and the mendelian risk. For example, the population risk for primary open-angle glaucoma (POAG) is 2%–3%, whereas the risk for glaucoma in families with severe myocilin variants is near 50%. The risk for first-degree relatives of POAG patients is approximately 20%. The more severe the abnormality in the index case, the higher the risk of recurrence in relatives, presumably because either a greater number of deleterious genes are at work, or a fixed population of more harmful genes exists. The risk of recurrence in future children increases when more than 1 member of a family is affected, which is not true for mendelian disorders. Such observations have been offered for various forms of strabismus, glaucoma, and significant refractive errors.

Finally, the recurrence risk is distinctly higher if the malformation or disorder has occurred in both paternal and maternal relatives because multiple unspecifiable but potentially harmful genes will be transmitted to their offspring.

Pharmacogenetics

Pharmacogenetics is the study of heritable factors that determine how drugs are chemically metabolized in the body. This field addresses genetic differences responsible for variations in both the therapeutic and adverse effects of drugs among population segments. Investigations in pharmacogenetics are important because they facilitate not only more rational approaches to therapy but also a deeper understanding of drug pharmacology. For further discussion, see Part V, Ocular Pharmacology.

The drug isoniazid provides an example of pharmacogenetic differences. This antituberculosis drug is normally inactivated by the liver enzyme acetyltransferase. A large segment of the population, which varies by geographic distribution, has a reduced amount of this enzyme; these individuals are termed *slow inactivators.* When slow inactivators take isoniazid, the drug reaches higher-than-normal concentrations, causing a greater incidence of adverse effects. Family studies have shown that a reduced acetyltransferase level is inherited as an autosomal recessive trait.

Several other well-documented examples demonstrate the principles of pharmacogenetics. An X-linked recessive trait present in 10% of the African American male population, a high percentage of male Sephardic Jews (originally from around the Mediterranean Sea), and males from a number of other ethnic groups causes a deficiency in the enzyme glucose-6-phosphate dehydrogenase in erythrocytes. Consequently, several drugs (including sulfacetamide, vitamin K, acetylsalicylic acid, quinine, chloroquine, dapsone, and probenecid) may produce acute hemolytic anemia in these individuals. Pharmacogenetic causes have also been ascribed to variations in responses to ophthalmic drugs, such as the increased IOP noted in a segment of the population after prolonged use of topical corticosteroids.

Several drugs have been shown to produce greater reactions in children with Down syndrome than in children without the syndrome. Some children with Down syndrome show hypersensitivity to topical atropine, and some have died after systemic atropine administration. In these patients, atropine exerts a greater-than-normal effect on pupillary dilation. In several children with Down syndrome being treated for strabismus, hyperactivity occurred several hours after local instillation of echothiophate iodide, 0.125%.

One of the earliest examples of an inherited deficit in drug metabolism involved succinylcholine, a strong muscle relaxant commonly used during intubation while administering general anesthesia. Succinylcholine interferes with acetylcholinesterase, the enzyme that catabolizes acetylcholine at neuromuscular junctions. Normally, succinylcholine is rapidly destroyed by plasma cholinesterase (sometimes called *pseudocholinesterase*), so its effect is short-lived—usually no more than a few minutes. However, some individuals are homozygous for a recessive gene that codes for a form of cholinesterase with a considerably lower substrate affinity. Consequently, almost no destruction of succinylcholine occurs at therapeutic doses, and the drug continues to exert its inhibitory effect on acetylcholinesterase, resulting in prolonged periods of apnea.

Clinical Management of Genetic Disease

Genetic diseases may not be curable, but in most cases, the patient benefits considerably from appropriate medical management by the physician. Such care should include all of the steps discussed in this section.

Accurate Diagnosis

Making the appropriate referral to a specialist with training and experience managing patients with ophthalmic genetic disease may be necessary for reaching the correct molecular diagnosis, identifying other current family members or future offspring who may be at risk, connecting the affected family with resources and clinical trials, and obtaining advice for direct management and treatment.

Unfortunately, because health care practitioners may not be as knowledgeable about genetic diagnoses as they are about other areas of medicine, many cases are not precisely diagnosed or, worse, diagnosed incorrectly (Fig 6-15). For example, a patient with deafness and

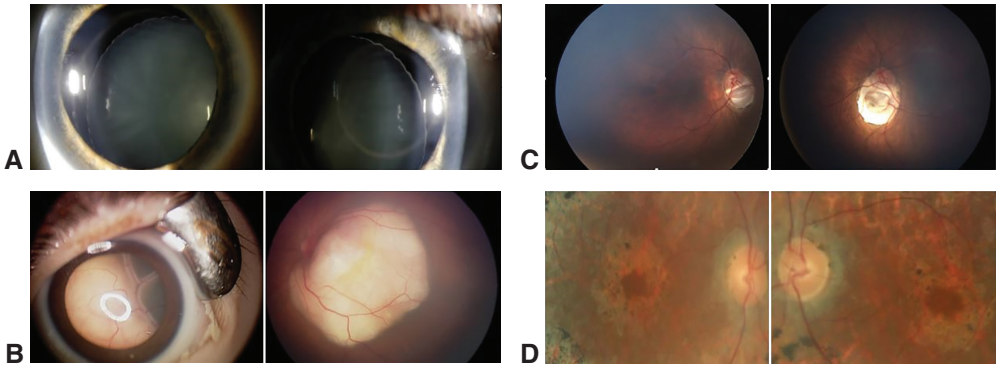


Figure 6-15 Comparison of the suspected initial clinical diagnosis upon referral and the final molecular genetic diagnosis obtained after a comprehensive ophthalmic genetics evaluation. **A,** Referral clinical diagnosis: Marfan syndrome; final molecular diagnosis: homocystinuria. **B,** Referral clinical diagnosis: retinoblastoma; final molecular diagnosis: retinoblastoma with dysmorphic features and intellectual disability due to a large deletion involving the *RB1* gene. **C,** Referral clinical diagnosis: bilateral optic nerve colobomas; final molecular diagnosis: coloboma, heart, atresia of the choanae, retardation of growth and development, genital and urinary anomalies, and ear anomalies (CHARGE syndrome). **D,** Referral clinical diagnosis: age-related macular degeneration; final molecular diagnosis: retinitis pigmentosa. *(Reproduced with permission from Couser NL, Brooks BP, Drack AV, Shankar SP. The evolving role of genetics in ophthalmology.* Ophthalmic Genet. *2021;42(2):110–113.)*

pigmentary retinopathy may receive a diagnosis of rubella syndrome when the correct diagnosis is Usher syndrome. This latter syndrome, of which RP is a symptom, may not be recognized in patients with RP. Similarly, Bardet-Biedl syndrome may not be recognized in patients with RP and congenital polydactyly (surgically corrected in infancy). Establishing the correct diagnosis in such cases is important to ensure that appropriate educational and lifetime support are provided and the needs of both the affected patient and their family are truly met.

Complete Explanation of the Disease

Patients are often very anxious when they do not understand the nature of their disease. Carefully explaining the disorder, as currently understood, will often dispel myths patients may have about their disease and symptoms.

Virtually all genetic disorders confer burdens that may interfere with certain activities later in life. The appropriate time to discuss these burdens with patients and family members is often when they first ask about the consequences of a disease. Such explanations must be tempered with empathy and an understanding of the possible emotional and psychological effects of the information provided.

Treatment of the Disease Process

Definitive cures—that is, reversing or correcting underlying genetic defects—are yet to emerge for most heritable disorders. However, conditions in which metabolic defects have been identified can often be managed through 5 fundamental approaches:

1. dietary control
2. chelation of excessive metabolites

3. enzyme or gene-product replacements
4. vitamin and cofactor therapy
5. drug therapy to reduce the accumulation of harmful products

Dietary control

Some genetic disorders affecting the eye that arise from an inborn error of metabolism can be effectively managed through dietary therapy. These conditions include homocystinuria, Refsum disease, gyrate atrophy, galactokinase deficiency, and galactosemia. Implementing a galactose-free diet can reverse some of the main clinical signs of galactosemia (eg, hepatosplenomegaly, jaundice, and weight loss). In some patients, adhering to a galactose-free diet can halt the progression of cortical cataracts and potentially even regress less extensive lens opacities.

Chelation of excessive metabolites

Disorders that result from enzyme or transport protein deficiencies may lead to the accumulation of a metabolite or metal that harms various tissues. For example, in Wilson disease (hepatolenticular degeneration), low serum ceruloplasmin levels result in poor transport of free copper (Cu^{2+}) ions and the storage of copper in such tissues as the brain, liver, and cornea. Resultant clinical signs can be reversed, at least partially, after the administration of D-penicillamine, a Cu^{2+} chelator. Other copper chelators, such as British anti-Lewisite, can be used in conjunction with a copper-deficient diet to reverse the clinical signs of Wilson disease.

Enzyme replacement therapy

Enzyme replacement therapy via plasma infusions can temporarily decrease plasma levels of the accumulated substrate ceramide trihexoside in patients with Fabry disease. The drugs are expensive (current costs are approximately $250,000 per year), presenting a barrier to successful treatment for many patients around the world. Enzyme replacement therapy for Fabry disease is not a cure, but it improves metabolism, curbs disease progression, and potentially reverses some symptoms.

Organ transplantation can be considered a form of regionalized enzyme replacement. In patients with cystinosis, cystine crystals accumulate in the kidneys and the cornea. When a kidney with normal enzyme function is transplanted into a patient with cystinosis, cystine does not accumulate in the cells of the renal tubules, and renal function tends to remain normal. In a complementary approach, stem cell transplantation is being investigated to treat various diseases, including those of the eye.

Vitamin therapy

Vitamin therapy appears to be of benefit in treating 2 autosomal recessive disorders. In at least some patients with homocystinuria, vitamin B_6 (pyridoxine) administration decreases homocystine accumulation in plasma and reduces the severity of the disorder. Vitamin A and vitamin E therapy benefit some patients with neurologic impairment due to abetalipoproteinemia; such therapy is also likely to slow or lessen the development and progression of retinal degeneration. More long-term therapeutic trials are necessary to better define the efficacy of vitamin therapy for these, and perhaps other, metabolic disorders.

Drug therapy

Various genetically determined disorders can be managed using an appropriate drug. For example, excess uric acid accumulation in primary gout can be prevented or reduced by either blocking the activity of the enzyme xanthine oxidase using the drug allopurinol or increasing uric acid excretion by the kidneys using probenecid. In familial hypercholesterolemia, elevated serum cholesterol levels can often be reduced through the use of various cholesterol-lowering drugs or substances that bind bile acids in the gastrointestinal tract.

Appropriate management of sequelae and complications

Some of the sequelae of genetic diseases, such as glaucoma in Axenfeld-Rieger syndrome or cataracts in RP, can be successfully managed to preserve or partially restore vision. However, it is important to inform patients of how sequelae or management options may differ according to their individual situations.

Gene therapy

Clinical gene therapy trials for a limited number of genes are under way; select viral-mediated gene replacement for inherited retinal disease is available (see discussion of voretigene neparvovec-rzyl in Chapter 5). The ophthalmologist is obliged to carefully search online clinical trial databases and the published literature for treatment trials or refer the patient to another professional who will conduct such a search for treatment trials for which the patient may qualify. (For a database of clinical studies, see www.ClinicalTrials.gov.)

Genetic Counseling

The ophthalmologist who understands the principles of human genetics has a foundation for counseling patients about their diseases. Genetic counseling imparts knowledge of human disease, including a genetic diagnosis and its ocular and systemic implications. The genetic counseling process helps individuals, couples, and families understand the risk of occurrence or recurrence of the disorder within the family. Information about the appropriate use and implications of available genetic testing is provided, along with the interpretation of test results, reproductive options, and facts about therapies, research, and resources. Psychosocial issues are also an integral part of the discussion. Genetic counseling is nondirective and addresses ethical issues as well as ethnic and cultural diversity with sensitivity. All genetic counseling is predicated on the following essential requirements:

- *Accurate diagnosis:* To derive an accurate and specific diagnosis, the physician must be sufficiently aware of the range of human ocular pathology.
  - It is impossible to counsel or refer patients on the basis of "congenital nystagmus," "color blindness," or "macular degeneration;" these are signs, not diagnoses.
- *Complete family history:* A family history will narrow the choices of possible inheritance patterns but may not necessarily exclude new variants, isolated occurrences of recessive diseases, and chromosomal rearrangements in individual circumstances.
  - The ophthalmologist should examine (or arrange to have examined) the parents, siblings, and other family members for mild manifestations of dominant diseases or characteristic carrier states in X-linked disorders.

  - Only an ophthalmologist will be cognizant of, and attentive to, the atypical findings of hereditary ocular disorders. For example, the identification of 1 young adult with the findings of Usher syndrome—prelingual deafness, night blindness, visual field constriction, and ultimately, central vision deterioration—obligates the ophthalmologist to evaluate a younger sibling who is congenitally deaf but "historically" has no eye problems. The probability is very high that the sibling has the same disease.
- *Understanding of the genetic and clinical aspects of the disorder:* The ophthalmologist should appreciate, perhaps more intimately than any other physician, how some clinically similar diseases inherited in the same pattern may be the result of different and even nonallelic defects. For example, the visual implications of, and prognoses for, tyrosinase-positive and tyrosinase-negative albinism are considerably different.
  - Ocular albinism is inherited in an X-linked recessive manner and is very rare in females, whereas oculocutaneous albinism is inherited in an autosomal recessive manner.
  - In another example, pseudoxanthoma elasticum is often a late-onset disease that has serious implications for cardiovascular disease, stroke, gastrointestinal bleeding, and vision. Informed counseling falls short if the ophthalmologist advises an affected patient only about the visual disability associated with angioid streaks without attention to the complete disease and the risks to other family members.

Issues in Genetic Counseling

It is important to remember that an individual affected by a heritable condition may have a homozygous recessive trait. Thus, the ophthalmologist should search for parental consanguinity, ambiguous parentage (nonpaternity, incest, occult adoption), or a new pathogenic variant and inquire about advanced paternal (or maternal grandparental) age. Heterogeneity may complicate the diagnosis. Somatic pathogenic variants underlie some conditions, such as segmental neurofibromatosis or unilateral unifocal retinoblastoma. Nonpenetrance or mild expressivity in other family members should be excluded through diligent examination. However, chromosomal abnormalities and phenocopies caused by infections or drugs may account for the isolated affected person. Nonetheless, the ophthalmologist's obligation to explain the disorder begins with an accurate diagnosis and establishing the mode of heritability.

The genetic counseling process is nondirective; the genetic counselor informs rather than advises. It is inappropriate, perhaps even unethical, for a counselor to tell the patient what to do (eg, not to have any children). Counselors recognize the ability of individuals and families to make appropriate decisions for themselves concerning their health and reproductive choices in accordance with their personal beliefs and opinions—the counselor's role is to support them in the decision-making process.

In some instances, genetic testing for ocular disorders may identify a specific genetic pathogenic variant. Such testing can assist in diagnosis and potentially give patients options to participate in clinical trials. Testing can also identify carrier status and variants in asymptomatic individuals who have known familial pathogenic variants, facilitating early diagnosis and subsequent intervention when available. The implications of these results require careful consideration and counseling because the information often affects other family members in addition to the individual(s) who underwent testing. Genetic testing requests must be

carefully evaluated for compliance with existing guidelines and position statements covering related ethical issues. For example, a parent's request for genetic testing for an adult-onset condition in a child is not indicated when there is no immediate medical benefit for the child.

Reproductive Issues

With a genetic diagnosis, the counseling ophthalmologist should outline the options available for family planning. Some people may choose to have children despite a high statistical risk for a disorder. This decision is based on how they perceive the social and psychological challenges of the disorder. For instance, a female carrier of protanopia may have a considerably different attitude toward reproduction than a female carrier of X-linked RP or choroideremia, even though the statistical risk for an affected son is the same for each carrier. Some may elect to delay childbearing in the hope of future medical advances. For a variety of personal and ethical considerations, others may opt for contraception, termination of pregnancy, sterilization, and/or adoption.

Artificial insemination by a donor is a useful option for family planning when the father has a dominant disease or both parents are carriers of a biochemically detectable recessive disorder. Artificial insemination is clearly not applicable when the mother is affected by an autosomal dominant variant or carries an X-linked or mitochondrial disorder. Finally, donor eggs, donor embryos, and surrogate motherhood—where these options are available—may be alternatives for some families.

In some circumstances, the results of genetic testing may lead an individual or a couple to consider prenatal testing or in vitro fertilization (IVF) technology with preimplantation genetic diagnosis (PGD) to avoid recurrence in their children. Knowledge of these options and the potential ethical, social, and cultural issues they raise is important for clinicians.

Prenatal diagnosis

Prenatal diagnosis (PND) via amniocentesis or chorionic villus sampling (CVS) for biochemically identifiable disorders (eg, Tay-Sachs disease, many mucopolysaccharidoses, and more than 100 other diseases) is useful in the proper genetic scenarios.

Other possible indications for PND include

- advanced maternal age or positive results from prenatal screening, which both carry an increased risk of chromosomal abnormalities
- elevated maternal serum α-fetoprotein, suggesting a neural tube defect
- presence of soft markers or fetal abnormalities that could suggest a chromosomal abnormality or genetic disease
- presence of a familial disease detectable by DNA analysis

Amniocentesis is usually performed at 15–16 weeks of gestation, when enough fluid and cells can be obtained for culture, and the maternal risk of abortion is relatively low. The risk of spontaneous abortion or fetal morbidity from the procedure is approximately 0.5%. CVS can be used for earlier PND of chromosomal abnormalities at about 10 weeks of gestation. In this procedure, tissue from the placenta is obtained under ultrasound visualization. It is then cultured and karyotyped in a manner similar to that used for amniocentesis. CVS

enables diagnosis in the first trimester, which can lead to earlier, and thus safer, pregnancy termination. The rate of spontaneous abortion associated with CVS is estimated at 1%–2%.

Cell-free fetal DNA (cffDNA) testing, sometimes called *noninvasive prenatal screening,* is a new technique that examines fetal DNA in the maternal bloodstream. CffDNA testing is being developed to allow PND without the risks associated with CVS or amniocentesis.

Couples who elect PND via CVS or amniocentesis may face considerable anxiety about complications, such as pregnancy loss, waiting time to obtain the genetic results, and, potentially, the difficult decision of whether to terminate an affected pregnancy—a dilemma that couples are aware they may face repeatedly with each consecutive pregnancy.

Preimplantation genetic diagnosis

PGD enables the selection of unaffected embryos through testing prior to implantation. Embryos are created using *intracytoplasmic sperm injection,* in which a single sperm is injected into each egg in an attempt to achieve fertilization. On day 3 after fertilization, when each embryo consists of 6–8 cells, 1 cell (blastomere) is removed per embryo. DNA is extracted from these cells and amplified using fluorescent polymerase chain reaction to make millions of copies of the relevant DNA region, which is then sequenced to provide a reliable diagnosis of the status of the genetic variant in each embryo. Unaffected embryos are transferred to the uterus on day 4 or 5. Usually, no more than 1 or 2 embryos are transferred to avoid the possibility of multiple births.

PGD is acceptable to many couples and, for some, represents a valuable alternative to PND. For some couples with a moral or religious objection to pregnancy termination who are at risk of having a child with a genetic condition, this technique may provide the opportunity to have an unaffected child. However, similar to the PND methods discussed earlier, PGD may be associated with stress and anxiety for couples. Other concerns include the high cost of IVF and genetic testing (often not covered by insurance) and low IVF pregnancy rates. PGD has raised ethical issues about embryo destruction and sex selection, and the issue of eugenics (selection for perceived favorable nonmedical traits) has also been debated. Just as diseases differ among individuals, so do the concerns and beliefs of different parents; thus, the acceptability of various reproductive technologies should be discussed with each couple.

Referral to Providers of Support for Persons With Disabilities

Referrals to local, regional, or national agencies, support groups, or foundations that provide services for those with a particular disease often provide considerable benefit to individuals and families. These organizations include local and state agencies for the blind or visually impaired, special school education programs, and appropriate consumer groups. Agencies or support groups can greatly aid the individual or family in adjusting to changing visual disabilities, particularly when the disability is chronic and progressive. Such groups also allow individuals or families with a particular genetic disorder to meet others with the same condition who may provide them with support and advice.

National Human Genome Research Institute. Genetic counseling, support and advocacy groups online. Accessed December 20, 2022. www.genome.gov/11510370

Recommendations for Genetic Testing of Inherited Eye Disease

The AAO Task Force on Genetic Testing has stated that when properly performed, interpreted, and acted upon, genetic tests can improve the accuracy of diagnosis, prognosis, and genetic counseling, reduce the risk of disease recurrence in families at risk, and facilitate the delivery of personalized care. Like other forms of medical intervention, genetic testing carries specific risks that vary from patient to patient and family to family. The results of a genetic test may affect plans to have children, create guilt or anxiety, and complicate family relationships. For these reasons, skilled counseling should be provided to all individuals who undergo genetic testing in order to maximize benefits and minimize risks.

The AAO Task Force's recommendations are as follows:

1. Offer genetic testing to patients with clinical findings suggestive of a mendelian disorder whose causative gene(s) have been identified. If unfamiliar with such testing, refer the patient to a physician or counselor who is familiar with it. In all cases, ensure that the patient receives counseling from a physician with expertise in inherited disease or a certified genetic counselor.
2. Use Clinical Laboratories Improvement Amendments–approved laboratories for all clinical testing. When possible, use laboratories that include in their reports estimates of the pathogenicity of observed genetic variants that are based on a review of the medical literature and databases of disease-causing and non–disease-causing variants.
3. Provide a copy of each genetic test report to the patient so that she or he can independently seek mechanism-specific information, such as the availability of gene-specific clinical trials, should the patient wish to do so.
4. Avoid direct-to-consumer genetic testing and discourage patients from obtaining such tests themselves. Encourage the involvement of a trained physician, genetic counselor, or both for all genetic tests so that appropriate interpretation and counseling can be provided.
5. Avoid unnecessary parallel testing; order the most specific test(s) available, given the patient's clinical findings. Restrict massively parallel strategies like whole-exome sequencing and whole-genome sequencing to research studies conducted at tertiary care facilities.
6. Avoid routine genetic testing for genetically complex disorders like age-related macular degeneration and late-onset primary open-angle glaucoma until specific treatment or surveillance strategies have been shown in 1 or more published prospective clinical trials to be of benefit to individuals with specific disease-associated genotypes. In the meantime, confine the genotyping of such patients to research studies.
7. Avoid testing asymptomatic minors with untreatable disorders except in extraordinary circumstances. For the few cases in which such testing is believed to be warranted, the following steps should be taken before the test is performed: (a) the parents and child should undergo formal genetic counseling; (b) the certified counselor or physician performing the counseling should state his or her opinion in writing that the test is in the family's best interest; and (c) all parents with custodial responsibility for the child should agree in writing with the decision to perform the test.

AAO Task Force on Genetic Testing; Stone EM, Aldave AJ, Drack AV, et al. Recommendations for Genetic Testing of Inherited Eye Diseases 2014. *Clinical Statement*. American Academy of Ophthalmology; 2014. Accessed February 3, 2023. www.aao.org/clinical-statement/recommendations-genetic-testing-of-inherited-eye-d

National Center for Biotechnology Information. GTR: Genetic Testing Registry. United States National Library of Medicine. Accessed February 3, 2023. www.ncbi.nlm.nih.gov/gtr

PART IV
Biochemistry and Metabolism

Introduction

Considerable progress has been made in understanding the biochemistry of vision over the past 15 to 20 years, as demonstrated by the numerous reviews, research articles, and books published during this time. Part IV, Biochemistry and Metabolism, was written for practitioners and residents in ophthalmology, as well as for students and researchers seeking a concise picture of the current state of knowledge of the biochemistry of the eye. New information about vision biochemistry has been accompanied by increased specialization among ophthalmic researchers. These chapters cover most areas of research in ocular biochemistry, including tear film; cornea; aqueous humor, iris, and ciliary body; lens; vitreous; retina; retinal pigment epithelium; and free radicals and antioxidants. The text relates basic science to clinical problems that may be encountered during residency training and in subsequent practice.

CHAPTER 7

Tear Film

This chapter includes a related video. Go to www.aao.org/bcscvideo_section02 or scan the QR code in the text to access this content.

Highlights

- The tear film is the first ocular structure that light encounters. Because of the lower refractive index of air relative to that of the tear film, the air–tear film interface at the surface of the cornea constitutes a major refractive element of the eye, directing light toward the cornea.
- Evidence supports a 2-phase model of the tear film, in which a lipid layer overlies a mucoaqueous layer.
- Elevated tear film osmolarity is diagnostic of dry eye syndrome.
- There is mounting evidence that ocular surface inflammation is integral to the pathology of dry eye syndrome.

Overview of Tear Film

Human tears are distributed over the ocular surface, which includes the cornea and the conjunctiva. The tear film is most easily visualized above the lower eyelid, where it forms the tear meniscus (marginal tear strip) (Video 7-1, Fig 7-1).

VIDEO 7-1 Tear film.
Courtesy of Lyndon Jones, PhD, DSc; Jennifer P. Craig, PhD; James Wolffsohn, OD, PhD, Centre for Ocular Research & Education, University of Waterloo. From Tear Film & Ocular Surface Society, TFOS DEWS II.

The primary functions of the tear film are to

- provide a smooth optical surface at the air–cornea interface
- allow diffusion of oxygen and other nutrients
- serve as a medium for removal of debris and protect the ocular surface

The tear film protects the cornea and ultimately the entire eye by carrying tear constituents and debris to the lacrimal puncta, providing a medium for antimicrobial agents (eg, lysozyme and lactoferrin) and immunoglobulins, and preventing desiccation of the ocular surface barrier.

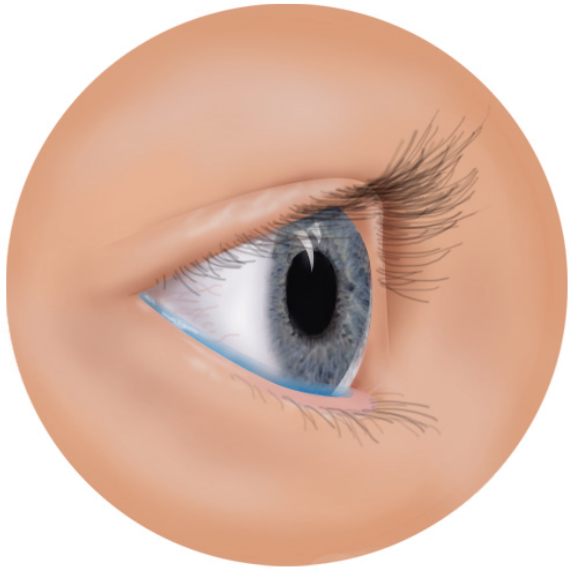


Figure 7-1 Schematic drawing of the tear meniscus (shown in blue). *(Illustration by Cyndie C.H. Wooley.)*

Historically, the tear film was viewed as a 3-layer "sandwich" composed of distinct lipid, aqueous, and mucin layers. Currently, evidence supports a 2-phase model of the tear film, in which a lipid layer overlies a mucoaqueous phase (Fig 7-2). Components of the tear film (lipids, mucins, proteins, and salts) may interact to prevent tear film evaporation and collapse; however, additional studies are needed to confirm this concept.

Measurements of tear film thickness have differed widely, but recent studies using optical coherence tomography (OCT) and reflectometry have found the tear film to be approximately 3.4 μm thick. The steady-state volume of tears is 7.4 μL for the unanesthetized eye and 2.6 μL for the anesthetized eye; this volume decreases with age. Table 7-1 lists properties of the normal human tear film.

CLINICAL PEARL

The maximum amount of fluid that an eye can hold prior to tearing is 25–30 μL. As the average eyedrop is 45 μL, there is never a need to use more than 1 eyedrop at a time.

Bron AJ, de Paiva CS, Chauhan SK, et al. TFOS DEWS II pathophysiology report. *Ocul Surf.* 2017;15(3):438–510. Erratum in: *Ocul Surf.* 2019;17(4):842.

Craig JP, Nelson JD, Azar DT, et al. TFOS DEWS II report executive summary. *Ocul Surf.* 2017;15(4):802–812.

Willcox MDP, Argüeso P, Georgiev GA, et al. TFOS DEWS II Tear Film Report. *Ocul Surf.* 2017;15(3):366–403.

Yokoi N, Georgiev GA. Tear-film–oriented diagnosis for dry eye. *Jpn J Ophthalmol.* 2019; 63(2):127–136.

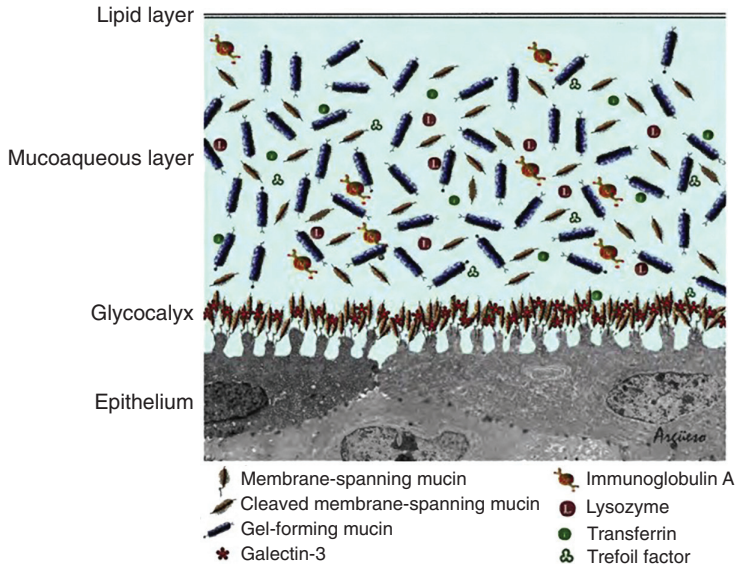


Figure 7-2 Two-phase model of the tear film. Schematic drawing of the structure of the tear film showing the outer lipid layer, the mucoaqueous layer, and the glycocalyx resting on the apical microvilli of the ocular surface epithelium. *(Reproduced with permission from Willcox MDP, Argüeso P, Georgiev GA, et al. TFOS DEWS II tear film report.* Ocul Surf. *2017;15(3):366–403.)*

Table 7-1 Approximate Properties of Normal Human Tear Film

Composition	Water	98.2%
	Solid	1.8%
Thickness	Total	3.4 μm
	Lipid layer	0.015–0.16 μm
Volume	Unanesthetized	7.4 μL
	Anesthetized	2.6 μL
Secretory rate	Unanesthetized	
	Schirmer	3.8 μL/min
	Fluorophotometry	0.9 μL/min
	Anesthetized	
	Schirmer	1.8 μL/min
	Fluorophotometry	0.3 μL/min
Turnover rate	Normal	12%–16%/min
	Stimulated	300%/min
Evaporation rate		0.06 μL/cm^2/min
Osmolarity		296–308 mOsm/L
pH		6.5–7.6
Electrolytes	Na^+	134–170 mmol/L
	K^+	26–42 mmol/L
	Ca^{2+}	0.5 mmol/L
	Mg^{2+}	0.3–0.6 mmol/L
	Cl^-	120–135 mmol/L
	HCO_3^-	26 mmol/L

Lipid Layer

The outermost layer of the tear film, or lipid layer, has the following functions:

- impedes evaporation of the tear film
- contributes to the optical properties of the tear film because of its position at the air–tear film interface
- maintains a hydrophobic barrier *(lipid strip)* that prevents tear overflow by decreasing surface tension
- prevents the tears from damaging the eyelid margin

The lipid layer is approximately 43 nm thick and contains polar and nonpolar lipids in multilayers with a complex lipid composition. Polar amphiphilic phospholipids interact with the mucoaqueous layer, and a thick layer of nonpolar hydrophobic lipids occupies the outermost layer at the air–eye interface. These phospholipids are secreted primarily by the *meibomian (tarsal) glands,* which are located in the tarsal plate of the upper and lower eyelids and are supplied by parasympathetic nerves that are cholinesterase positive and contain vasoactive intestinal polypeptide (VIP). Sympathetic and sensory nerves are present but sparsely distributed. Neuropeptide Y (NPY)–positive nerves are abundant. There are approximately 30–40 meibomian glands in the upper eyelid and 20–30 in the lower eyelid. Each gland orifice opens onto the skin of the eyelid margin, between the tarsal *gray line* and the *mucocutaneous junction* (see Chapter 1, Fig 1-30). The sebaceous glands of Zeis, located at the eyelid margin close to the eyelash roots, also secrete lipid, which is incorporated into the tear film. Clinically, tear film evaporation can be evaluated by assessing the tear breakup time (see BCSC Section 8, *External Disease and Cornea*).

The melting point of meibomian gland secretion ranges from 32°C to 40°C. With meibomian gland inspissation in chronic marginal blepharitis, the melting point is elevated, and the secretions become stagnant. In a study to determine whether tear film lipid layer thickness was altered after therapy with warm, moist compresses, samples of meibomian secretions from subjects without meibomian gland dysfunction (MGD) started to melt at 32°C, whereas secretion samples from subjects with MGD were began melting at 35°C. Five minutes after initiation of compress therapy, the thickness of the tear film lipid layer increased by more than 80%.

Mucoaqueous Layer

The functions of the mucoaqueous layer are as follows:

- transmits oxygen to the avascular corneal epithelium
- maintains a constant electrolyte composition over the ocular surface epithelium
- provides an antibacterial and antiviral defense
- smooths minute irregularities of the anterior corneal surface
- converts the corneal epithelium from a hydrophobic to a hydrophilic layer, which is essential for the even and spontaneous distribution of the tear film
- interacts with the tear lipid layer to reduce surface tension, thereby stabilizing the tear film
- lubricates the eyelids as they pass over the globe

Aqueous Component

The core aqueous stratum is secreted by the main and accessory lacrimal glands (see Chapter 1, Fig 1-40). The main lacrimal gland is divided into 2 anatomical parts, the *orbital* and the *palpebral* lobes, by the lateral horn of the levator aponeurosis. The *glands of Krause,* which constitute two-thirds of the accessory lacrimal glands, are located in the lateral part of the upper fornix. A number of Krause glands are also present in the lower fornix. The *glands of Wolfring* are variably located along the proximal margin of each tarsus. The accessory lacrimal glands are structurally like the main lacrimal gland.

The aqueous stratum consists of electrolytes, water, and proteins. *Electrolytes* and small molecules regulate the osmotic flow of fluids between the corneal epithelial cells and the tear film, buffer tear pH (average 6.5 to 7.6), and serve as enzyme cofactors in controlling membrane permeability. The sodium (Na^+) concentration of tears parallels that of serum; however, the concentration of potassium (K^+) is 5–7 times that of serum. Na^+, K^+, and chloride (Cl^-) regulate the osmotic flow of fluids from the cornea to the tear film and thereby contribute to corneal clarity. Bicarbonate (HCO_3^-) regulates tear pH. Other tear electrolytes (Fe^{2+}, Cu^{2+}, Mg^{2+}, Ca^{2+}, PO_4^{3-}) are enzyme cofactors.

CLINICAL PEARL

In some cases of corneal edema (eg, Fuchs dystrophy), hypertonic saline is used to help dehydrate the cornea.

Tear film solutes include urea, glucose, lactate, citrate, ascorbate, and amino acids. All enter the mucoaqueous layer of the tear film via the systemic circulation, and their concentrations parallel those of serum levels. Fasting tear glucose levels are 3.6–4.1 mg/mL in persons with and without diabetes. However, after a 100-mg oral glucose load, tear glucose levels exceed 11 mg/mL in 96% of diabetic persons tested.

Proteins in the mucoaqueous layer of the tear film include immunoglobulin (Ig) A and secretory IgA (sIgA). IgA is formed by plasma cells in interstitial tissues of the main and accessory lacrimal glands (see Chapter 1, Fig 1-42) and by the substantia propria of the conjunctiva. The secretory component is produced within lacrimal gland acini, and sIgA is secreted into the lumen of the main and accessory lacrimal glands. IgA plays a role in local host-defense mechanisms of the external eye, as shown by increased levels of IgA and IgG in human tears associated with ocular inflammation. Other immunoglobulins in tears are IgM, IgD, and IgE.

Vernal conjunctivitis causes elevated tear and serum levels of IgE, increased numbers of IgE-producing plasma cells in the giant papillae of the superior tarsal conjunctiva, and elevated histamine levels. Increased levels of tear histamine support the concept of conjunctival TC (tryptase and chymotryptic proteinase containing) mast-cell degranulation triggered by IgE–antigen interaction. TC mast cells are unique to the conjunctiva and are specifically sensitive to commercially available topical mast-cell stabilizers.

Levels of matrix metalloproteinase 9 (MMP-9) in the tear film are elevated in patients with severe disorders affecting the ocular surface, including Sjögren syndrome and graft-vs-host disease, as well as in patients after laser in situ keratomileusis (LASIK). MMP-9

cleaves epithelial basement membrane components and tight-junction proteins. MMP-9 levels parallel corneal staining severity and may represent a sign of late-stage dry eye syndrome (DES). In addition, expression of intercellular adhesion molecule 1 (ICAM-1) is upregulated on lymphocytes and/or vascular endothelial cells, resulting in lymphocytic migration to the lacrimal and conjunctival tissues in DES.

CLINICAL PEARL

Lymphocyte adhesion to ICAM is blocked by lifitegrast, a therapeutic agent for DES (see the section Tear Dysfunction, later in this chapter).

Lysozyme, lactoferrin, group II phospholipase A_2, lipocalins, and defensins are important antimicrobial constituents of the mucoaqueous layer. Interferon is also present; it inhibits viral replication and may help limit the severity of herpetic keratitis.

In addition, the mucoaqueous layer of the tear film contains a wide array of cytokines and growth factors, including transforming growth factor βs, epidermal growth factor, fibroblast growth factor β, interleukin 1α and 1β, and tumor necrosis factor α. These constituents may play a role in the proliferation, migration, and differentiation of corneal and conjunctival epithelial cells. They may also regulate wound healing of the ocular surface.

Mucin Component

The mucin component of the mucoaqueous layer coats the microplicae of the superficial corneal epithelial cells and forms a fine network over the conjunctival surface. In addition to mucin, it contains proteins, electrolytes, water, and carbohydrates in a polar *glycocalyx*. Mucins are glycoproteins; they have a protein backbone modified by the covalent addition of multiple long carbohydrate chains composed of repeating sugar molecules strung end to end (see Fig 7-2).

Two main types of mucins are produced within the body: secreted and membrane-spanning. Secreted mucins are

- divided into gel-forming mucins and soluble mucins
- released into the extracellular environment
- secreted principally by the goblet cells of the conjunctiva

Membrane-spanning mucins (also called *membrane-anchored, membrane-bound,* or *membrane-tethered mucins*) are

- embedded in the lipid bilayer of the cells
- expressed by the stratified squamous cells of the conjunctival and corneal epithelia

Some clinicians think that the membrane-spanning mucins help spread the secreted mucins across the ocular surface. Both are minimally secreted by the main lacrimal gland. Goblet cells produce mucin at a rate of 2–3 μL/day in contrast to the 2–3 mL/day of aqueous tear production.

Tear dysfunction may result when tear mucins are deficient in number (eg, in vitamin A deficiency and conjunctival destruction), excessive in number (eg, in hyperthyroidism;

foreign-body stimulation; and allergic, vernal, and giant papillary conjunctivitis), or biochemically altered (eg, in keratoconjunctivitis).

CLINICAL PEARL

Mucous discharge differs in various conditions. For example, stringy, thin, and translucent mucus is characteristic of DES; globular and crusting mucus occurs in infection; and thick, tenacious, and stretchy strands of mucus are present in vernal conjunctivitis. See BCSC Section 8, *External Disease and Cornea,* for further discussion of these conditions.

Tear Secretion

Contrary to earlier belief—which ascribed basic secretion to the accessory lacrimal glands of Krause and Wolfring and reflex secretion to the main lacrimal gland—it is now thought that all lacrimal glands function as a unit in conjunction with the ocular surface and the brain. In addition, the cornea and conjunctiva can respond by secreting electrolytes, water, and mucins.

Although the meibomian glands are innervated, it is not known whether nerves mediate lipid secretion from these glands. Reflex tear secretion is neurally mediated and induced in response to physical irritation (ie, superficial corneal and conjunctival sensory stimulation by mechanical, thermal, or chemical means), psychogenic factors, and bright light. Induction of sensory nerves by a local neural reflex activates the parasympathetic and sympathetic nerves that innervate the tear glands and epithelia, causing secretion (Fig 7-3; also see Chapter 3, Video 3-3). Tear turnover rate is significantly lower in symptomatic patients with dry eye (5%) than in asymptomatic dry eye patients (12%).

A neural feedback mechanism for tear secretion has been widely accepted. The cornea and lacrimal gland are not directly connected; however, corneal damage profoundly affects the lacrimal gland, which, in turn, downregulates tear production. In the *vicious circle theory of DES,* this downregulation is due to the secretion of inflammatory cytokines that block neural signals for tear secretion. The feedback loop, initiated by inflammation on the surface of the eye (caused by various factors, including blepharitis, topical and systemic drugs, allergic and microbial conjunctivitis, contact lens wear, refractive and other ocular surgeries, and autoimmune diseases), further suppresses or downgrades lacrimal gland function, creating a vicious circle that worsens DES (Fig 7-4).

Peptide and steroid hormones constitute another mechanism for stimulating tear secretion (in addition to nerves), as follows:

- Peptide hormones, including α-melanocyte–stimulating hormone (α-MSH) and adrenocorticotropic hormone (ACTH), stimulate protein secretion from the main lacrimal gland.
- Steroid hormones, specifically the androgens, stimulate secretion of sIgA from the main lacrimal gland and lipid from the meibomian glands.

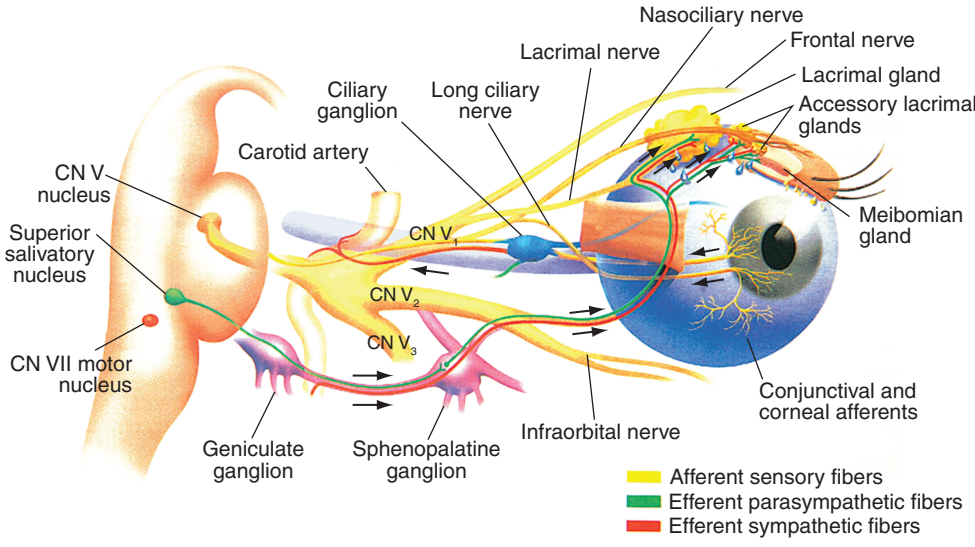


Figure 7-3 Sensory and motor nerves connecting the components of the lacrimal functional unit. Sensation (afferent) from the ocular surface is provided by branches of the long ciliary nerve of the ophthalmic division of cranial nerve V (CN V_1). Efferent fibers from both members of the automatic nervous system stimulate lacrimal secretion at the main and accessory lacrimal glands. *(Modified with permission from Pflugfelder SC, Beuerman RW, Stern ME, eds.* Dry Eye and Ocular Surface Disorders. *Marcel Dekker; 2004:12.)*

Eyelid movement is important in tear film renewal, distribution, turnover, and drainage. As the eyelids close in a complete blink, the superior and inferior fornices are compressed by the force of the preseptal muscles, and the eyelids move toward each other, with the upper eyelid moving over the longer distance and exerting force on the globe. This force clears the anterior surface of debris and any insoluble mucin and expresses secretions from meibomian glands. The lower eyelid moves horizontally in a nasal direction and pushes tear fluid and debris toward the superior and inferior puncta. When the eyelids are opened, the tear film is redistributed. The upper eyelid pulls the mucoaqueous phase of the tear film by capillary action. The lipid layer spreads as fast as the eyelids move, so that no area of the tear film is left uncovered by lipid.

CLINICAL PEARL

Incomplete or infrequent blinks (eg, from Parkinson disease or Bell palsy) can lead to ineffective distribution of the tear film, resulting in DES.

See BCSC Section 7, *Oculofacial Plastic and Orbital Surgery,* which discusses the lacrimal system in depth, with numerous illustrations.

Stern ME, Gao J, Siemasko KF, Beuerman RW, Pflugfelder SC. The role of the lacrimal functional unit in the pathophysiology of dry eye. *Exp Eye Res.* 2004;78(3):409–416.

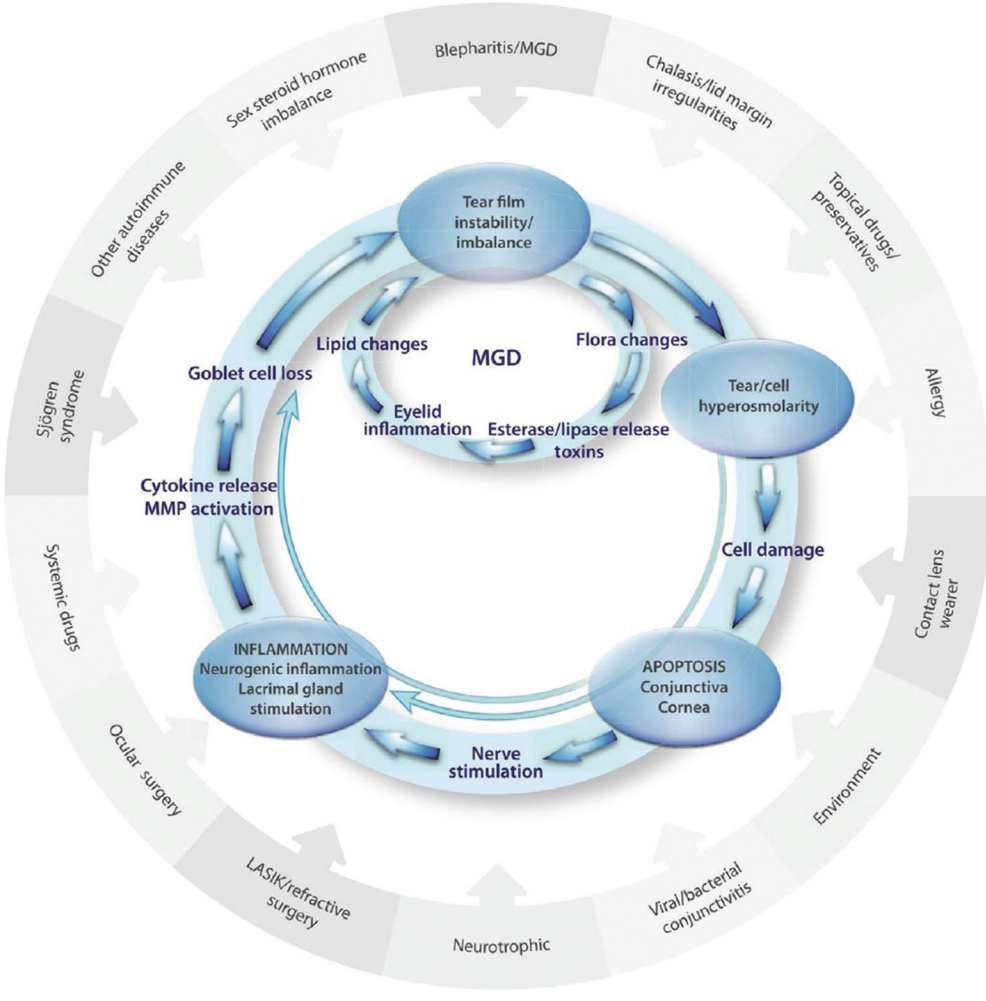


Figure 7-4 The vicious circle theory of DES. Risk factors or causative factors are shown on the outside of the circle; internal pathologic mechanisms are shown on the inside. The external causative factors are independent or interacting processes that may lead to entry into the circle, and any form of DES can interact with and exacerbate other forms. The internal pathologic mechanisms also interact, as activity in 1 area exacerbates another process. LASIK = laser in situ keratomileusis; MGD = meibomian gland dysfunction; MMP = matrix metalloproteinase. *(Reproduced with permission from Baudouin C, Messmer EM, Aragona P, et al. Revisiting the vicious circle of dry eye disease: a focus on the pathophysiology of meibomian gland dysfunction.* Br J Ophthalmol. *2016;100(3):300–306.)*

Tear Dysfunction

A qualitative or quantitative abnormality of the tear film may occur as a result of

- change in the amount of tear film
- change in the composition of the tear film
- uneven dispersion of the tear film because of corneal surface irregularities
- ineffective distribution of the tear film caused by eyelid–globe incongruity

The amount or composition of the tear film can change because of aqueous deficiency, mucin deficiency or excess (with or without associated aqueous deficiency), lipid abnormality (meibomian gland dysfunction), and/or ocular surface exposure. The inciting factors for a dysfunctional tear film are multifactorial (see Fig 7-4).

Increases in tear film osmolarity are diagnostic of DES and can be found in blepharitis and with contact lens use. The tear film is dispersed unevenly with an irregular corneal or limbal surface (inflammation, scarring, dystrophic changes) or poor contact lens fit. Eyelid–globe incongruity results from congenital, traumatic, or neurogenic eyelid dysfunction or absent or dysfunctional blink mechanism and results in ineffective tear film distribution. Also, although overall hormone balance is unique to each person, estrogen and androgen deficiencies—combined with stress, pollution, and poor diet—produce a number of signs and symptoms, including dry eye, especially in postmenopausal women. In addition, the quality and quantity of the tear film diminish with age. Environmental factors such as air conditioning, dry air, and wind may also lead to tear dysfunction. Diagnostic tests for tear dysfunction include tear breakup time, fluorescein staining, lissamine

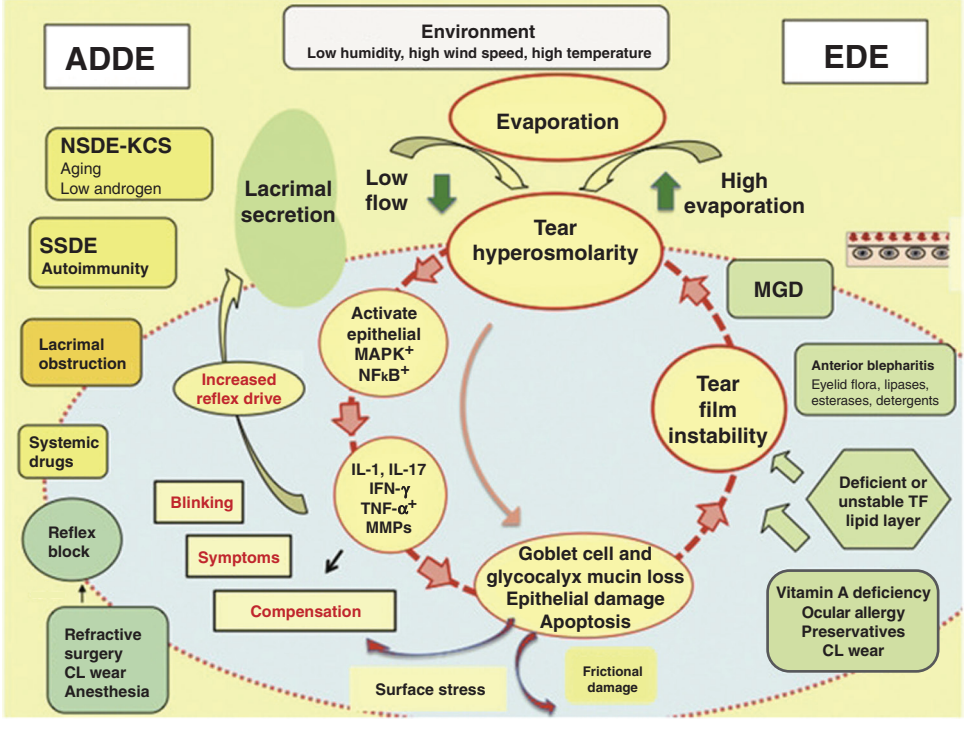


Figure 7-5 Inflammatory mediators in DES. ADDE = aqueous-deficient dry eye; CL = contact lens; EDE = evaporative dry eye; IFN-γ = interferon gamma; IL-1, IL-17 = interleukins 1 and 17; KCS = keratoconjunctivitis sicca; MAPK = mitogen-activated protein kinase; MGD = meibomian gland dysfunction; MMPs = matrix metalloproteinases; NFκB = nuclear factor kappa–light-chain enhancer of activated B cells; NSDE = non-Sjögren dry eye; SSDE = Sjögren syndrome dry eye; TNF-α = tumor necrosis factor alpha; TF = tear film. *(Modified from Bron AJ, de Paiva CS, Chauhan SK, et al. TFOS DEWS II pathophysiology report.* Ocul Surf. *2017;15(3):438–510. With permission from Elsevier.)*

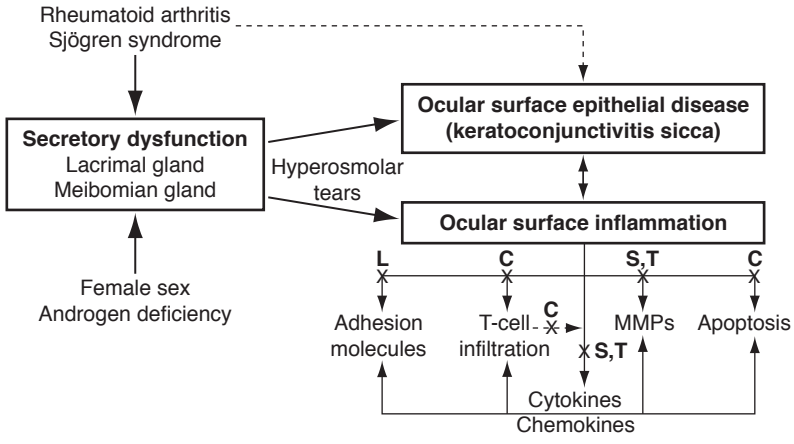


Figure 7-6 Targets of anti-inflammatory therapies for DES. C = cyclosporine A; L = lifitegrast; MMPs = matrix metalloproteinases; S = (cortico)steroids; T = tetracycline. *(Modified with permission from Pflugfelder SC. Antiinflammatory therapy for dry eye.* Am J Ophthalmol. *2004;137(2):400.)*

green staining, rose bengal staining, osmolarity testing, Schirmer test, tear meniscus evaluation, and MMP-9 testing.

There is increasing evidence that DES is associated with ocular surface inflammation (Fig 7-5). Studies have found adhesion molecule expression by conjunctival epithelial cells, T-cell infiltration of the conjunctiva, and increases in soluble mediators (cytokines and proteases) in the tear film of patients with DES. Preliminary clinical studies have shown that using preservative-free tear substitutes to treat patients with DES may reduce tear osmolarity and improve ocular symptoms. Moreover, a variety of anti-inflammatory drugs (including corticosteroids, cyclosporine, lifitegrast, and doxycycline) have been used as therapy for DES and observed to improve the clinical symptoms of these patients (Fig 7-6).

Topical cyclosporine A emulsion and lifitegrast are approved by the US Food and Drug Administration for treating the inflammatory component of DES. Cyclosporine, a fungus-derived peptide emulsion, is effective in stimulating aqueous tear production, especially in patients with autoimmune DES. Lifitegrast, a lymphocyte function–associated antigen 1 (LFA-1) antagonist that inhibits binding of ICAM-1 to LFA-1, reduces inferior corneal staining and provides greater symptom relief in treated patients with DES than in control groups. No significant systemic or ocular adverse events (except for burning symptoms) were observed. Because the average T cell has a life span of 90 days, drugs that interfere with T-cell function may take a long time to achieve their full effect.

See also BCSC Section 8, *External Disease and Cornea,* which discusses DES in greater detail.

Willcox MDP, Argüeso P, Georgiev GA, et al. TFOS DEWS II tear film report. *Ocul Surf.* 2017;15(3):366–403.

CHAPTER 8

Cornea

Highlights

- Corneal avascularity is maintained by soluble vascular endothelial growth factor receptor 1.
- The corneal limbus, where corneal stem cells reside, is characterized by stromal invaginations known in humans as the *palisades of Vogt.*
- Corneal stem cells repopulate the desquamating epithelium. Recent research suggests that corneal stem cells exist in the central cornea as well as at the limbus.
- The corneal epithelium provides a barrier to diffusion of hydrophilic molecules; however, corneal proteoglycans confer hydrophilic properties to the stroma. Thus, when hydrophilic drugs are applied topically, the drug molecules must change their biochemical properties to reach the anterior chamber.
- Collagen fibrils and fibers (fibril bundles) within the corneal stroma maintain a regular arrangement with minimal variation in diameter; this uniformity is critical for corneal clarity.

Biochemistry and Physiology of the Cornea

Corneal avascularity is required in order to maintain optical clarity, and it contributes to the immune privilege of the cornea. Vascular endothelial growth factor A (VEGF-A), which is present in the cornea, is a potent angiogenic agent. Its actions are blocked by a soluble form of VEGF receptor 1 (also known as sFlt-1). Suppression of this molecule leads to increased levels of unbound VEGF-A and blood vessel growth in the cornea.

Because of the lack of blood vessels in the cornea, oxygen is provided to the cornea via the *tear film* (which obtains oxygen from the air and eyelid vasculature) and aqueous humor. Glucose is the primary metabolic substrate for epithelial cells, stromal keratocytes (corneal fibroblasts residing in the stroma), and endothelial cells. The stroma receives glucose primarily from the aqueous humor by carrier-mediated transport through the endothelium; the epithelium receives glucose by passive diffusion through the stroma and from the tear film. The tear film and limbal vessels supply approximately 10% of the glucose used by the cornea. Glucose is metabolized in the cornea by all 3 metabolic pathways:

- hexose monophosphate (HMP) shunt
- tricarboxylic acid (TCA) cycle
- glycolysis

In the epithelium and endothelium, the HMP pathway breaks down 35%–65% of the glucose, but the keratocytes of the stroma metabolize very little glucose via this pathway. The keratocytes lack 6-phosphogluconate dehydrogenase, an important enzyme in the HMP pathway. Pyruvic acid, the end product of glycolysis, is converted either to carbon dioxide and water (via the TCA cycle under aerobic conditions) or to lactic acid (under anaerobic conditions).

NADPH is 1 of the primary products of the HMP pathway. NADPH is a reducing agent and functions in redox reactions that protect the cornea from oxidative stress generated by constant exposure to ultraviolet light.

Production of lactic acid increases in conditions of oxygen deprivation, as in the case of tight-fitting contact lenses with low oxygen permeability. Accumulation of lactic acid in the cornea has detrimental consequences for vision, such as edema (due to an increase in an osmotic solute load) or stromal acidosis, which can change endothelial morphology and function.

CLINICAL PEARL

Accumulation of lactic acid in the cornea is 1 of the factors that lead to complications of contact lens overwear.

Human corneas possess remarkably high levels of aldehyde dehydrogenase and transketolase. Together, these 2 proteins constitute 40%–50% of the soluble proteins in corneal stroma. Similar to enzyme crystallins of the lens, both aldehyde dehydrogenase and transketolase are thought to contribute to the optical properties of the cornea. Both proteins are also thought to protect corneal cells against free radicals and oxidative damage by absorbing ultraviolet-B radiation.

The biomechanical properties of the cornea affect its functional responses. An understanding of these properties can help clinicians to better anticipate or understand the cornea's responses to stress and strain and also aid in diagnosing and treating corneal disease. The following clinically relevant principles have been confirmed:

- The paracentral and peripheral cornea are stiffer than the central cornea because their orientation and the number of their collagen fibrils differ.
- The elastic strength of the corneal stroma is greatest anteriorly and decreases posteriorly; thus, laser in situ keratomileusis (LASIK) flap creation and interruption of the anterior stromal lamellae are thought to disproportionately weaken the cornea and contribute to ectasia.
- The stiffness of the cornea increases with age, apparently as a result of natural collagen crosslinking (Fig 8-1).

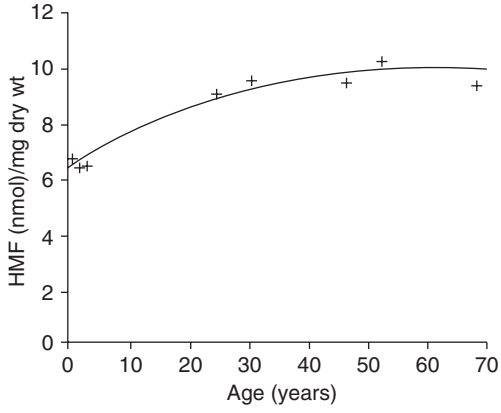


Figure 8-1 Change in glycation of corneal collagen with age, as measured by the thiobarbituric acid assay. Collagen contains both lysyl oxidase and glycation-induced crosslinks. 5-Hydroxymethyl furfural (HMF) is a product of glycation in this assay. An initial increase is observed in corneal glycation, but the curve appears to level off with increasing age (after 40 years). *(Reproduced with permission from Malik NS, Moss SJ, Ahmed N, Furth AJ, Wall RS, Meek KM. Ageing of the human corneal stroma: structural and biochemical changes.* Biochim Biophys Acta. *1992;1138(3):222–228.)*

Ambati BK, Nozaki M, Singh N, et al. Corneal avascularity is due to soluble VEGF receptor-1. *Nature*. 2006;443(7114):993–997.

Hjortdal JØ. Regional elastic performance of the human cornea. *J Biomech*. 1996;29(7): 931–942.

CLINICAL PEARL

The need for collagen crosslinking procedures for patients with ectatic disorders (eg, keratoconus) decreases with age because of the natural collagen crosslinking of the cornea.

Epithelium

The epithelium, approximately 50 μm in thickness, constitutes 5%–10% of the total corneal thickness. Surface projections (microvilli and microplicae) are present on the apical surface of the most superficial cell layer of epithelium. These projections are coated with filamentous material known as *glycocalyx*. Mucin glycoproteins, the major constituents of glycocalyx, are thought to promote both stability of the tear film and wettability of the corneal surface.

Plasma membrane proteins and the lipids of corneal epithelial cells, similar to those of other cell types, are heavily glycosylated and play an important role in cell–cell adhesion as well as in adhesion of the basal cells of the corneal epithelium to the underlying basement membrane. The sugar residues of the plasma membrane glycoproteins and the glycolipids of corneal epithelium also play a role in wound-healing mechanisms; they do so by mediating corneal epithelial sheet migration over the wound surface following ocular injury. These residues also contribute to the pathogenesis of corneal infection by serving as attachment sites for microbes. The normal rate of epithelial cell migration is 2 mm per day and is adversely affected by preservatives in topical eyedrops.

Beginning with the discovery of the centripetal cell migration that occurs in the cornea, early studies on epithelial cell renewal led to the conclusion that the proliferative source of the corneal epithelium resides at the limbus. Interestingly, results of a more recent study suggest that corneal stem cells may also exist in the central cornea. The limbus is characterized by stromal invaginations known in humans as the *palisades of Vogt* (see Chapter 2, Fig 2-11A). These papillae-like projections show a distinctive vasculature with radially oriented arterial and venous components. The palisades of Vogt have been suggested to be the reservoir that

- protects stem cells from traumatic and environmental insults
- allows epithelial–mesenchymal interactions
- provides access to chemical signals that diffuse from the rich underlying vascular network

Normal corneal epithelium remains in a steady state in which cell proliferation is necessary to replace cells lost by terminal differentiation and desquamation (Fig 8-2). While basal cells of the central cornea proliferate actively, basal cells at the limbus consist of a mixture of slow-cycling stem cells and their progeny—transient amplifying (TA) cells—which are affected by growth factors, cytokines, and extracellular matrix. During treatment of corneal wounds with cryopreserved amniotic membrane, TA cells are likely upregulated to enhance wound healing.

Yoon JJ, Ismail S, Sherwin T. Limbal stem cells: central concepts of corneal epithelial homeostasis. *World J Stem Cells.* 2014;6(4):391–403.

Penetration of the Corneal Epithelium

Hydrophilic molecules penetrate the epithelium poorly, but they may pass through tight junctions if the polar molecule has a mass lower than 500 Da. Hydrophilic drugs can also reach very high corneal penetration levels when the corneal epithelium is damaged or

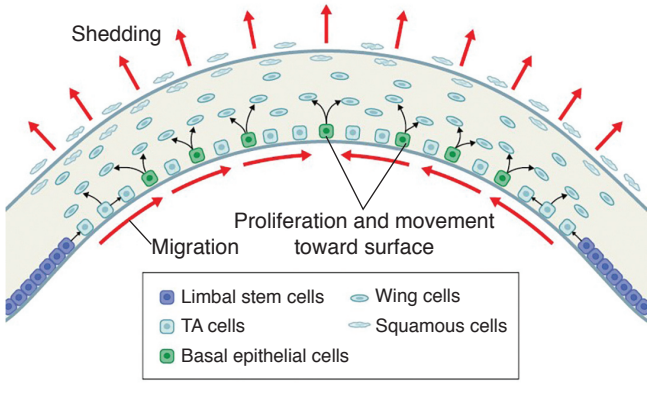


Figure 8-2 Desquamation of corneal epithelial cells. Stem cells migrate centrally from the limbus and give rise to transient amplifying (TA) cells and basal epithelial cells. *Arrows* indicate migration, differentiation, and desquamation pathways. *(Reproduced with permission from Levin LA, Nilsson SFE, Ver Hoeve J, Wu SM.* Adler's Physiology of the Eye. *11th ed. Elsevier/Saunders; 2011:95.)*

inflamed. The dissociation constant (also called the *ionization constant*) is likewise important in determining a molecule's permeability across the cornea. To diffuse across the epithelium, organic molecules should be in an uncharged state. However, a charged molecule can more readily penetrate the stroma. To penetrate the cornea and enter the anterior chamber, therefore, an organic molecule should be able to dissociate at physiologic pH and temperature (ie, within the stroma).

Majo F, Rochat A, Nicolas M, Jaoudé GA, Barrandon Y. Oligopotent stem cells are distributed throughout the mammalian ocular surface. *Nature*. 2008;456(7219):250–254.

Bowman Layer

Bowman layer is immediately beneath the epithelial basal lamina and is composed of randomly packed type I and type V collagen fibers that are 30 nm in diameter. The fibers are enmeshed in a matrix consisting of proteoglycans and glycoproteins. Bowman layer is secreted during embryogenesis by the anterior stromal keratocytes and epithelium. It is acellular and does not regenerate when damaged.

It is thought that this layer, by virtue of its acellularity and packing distribution, prevents exposure of stromal keratocytes to growth factors secreted by epithelial cells, such as transforming growth factor β. This effect is notable because, in excimer laser surgery (photorefractive keratectomy [PRK] or laser subepithelial keratomileusis [LASEK]), Bowman layer is removed, along with anterior corneal stromal tissue. Corneal haze, a potentially significant postoperative complication of these procedures, is presumably due to absence of Bowman layer and consequent keratocyte exposure to growth factors. In laser-assisted in situ keratomileusis (LASIK), by contrast, Bowman layer is transected but retained; therefore, central corneal haze is extremely rare after this procedure.

Stroma

The stroma makes up approximately 90% of the total corneal thickness. Stromal cells, known as *keratocytes,* constitute 10%–40% of corneal volume, depending on age; loss of keratocyte density occurs with age. Usually, these cells reside between the collagen lamellae. The stroma is made up of roughly 200 lamellae, which are 1.5–2.5 μm thick and composed of collagen fibrils enmeshed in a matrix consisting of proteoglycans, proteins, and glycoproteins. The stromal fibrils within each lamella are narrow and uniform in diameter; in humans, the average fibril diameter is 30 nm. The stroma is less compact posteriorly, facilitating deeper placement of intrastromal ring segments for keratoconus.

Collagen fibrils within each lamella run parallel to one another from limbus to limbus. The orientation of the lamellae with respect to one another depends on their location within the stroma. The lamellae are obliquely oriented in the anterior one-third and perpendicular in the posterior two-thirds of the stroma. Also, collagen fibrils in each lamella are regularly spaced, with a center-to-center distance of 55–60 nm. The narrow and uniform diameter of collagen fibrils and their regular arrangement are characteristic of collagen of the corneal stroma and are necessary for the transparency of this tissue (Fig 8-3).

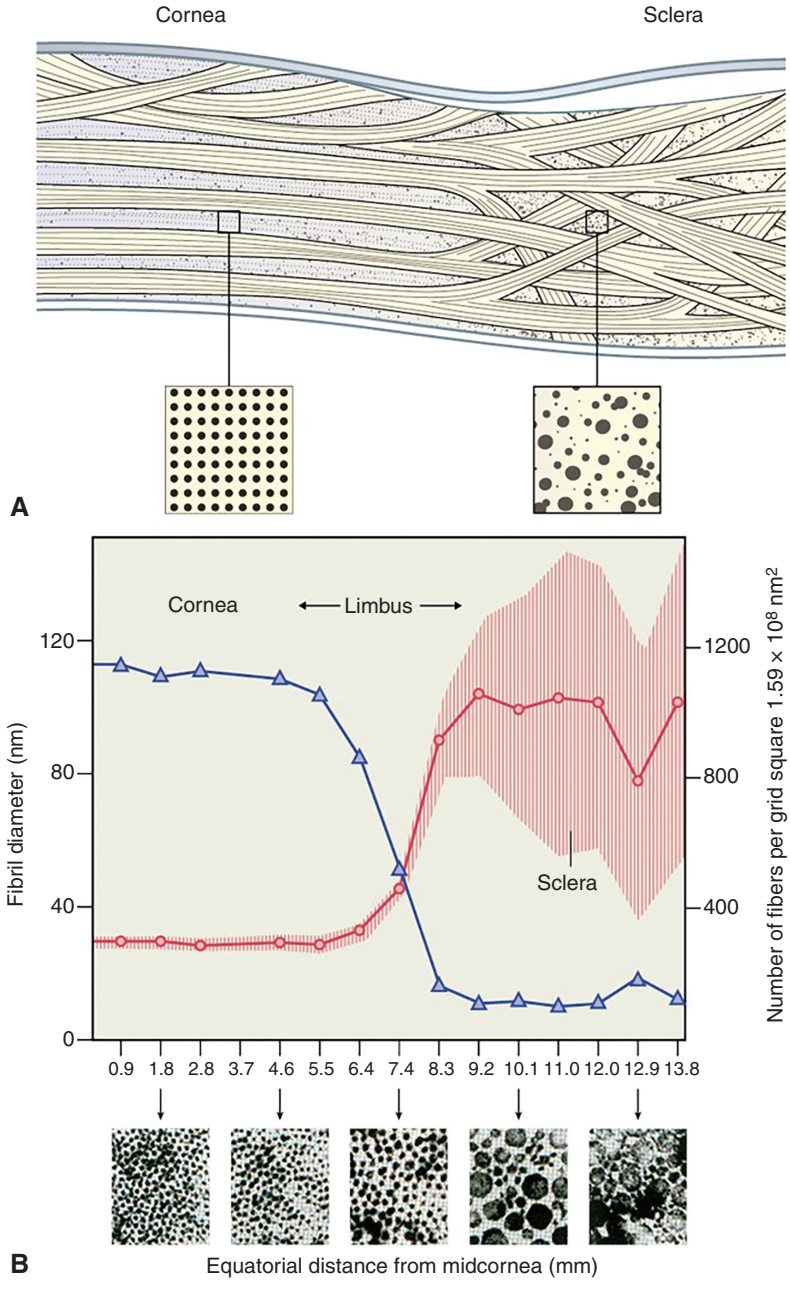


Figure 8-3 Cornea and sclera. **A,** Both are composed of similar collagen fibrils. However, fibril diameter and fiber density are consistent throughout the cornea, whereas in the sclera they are not. **B,** The density of the fibers decreases in the sclera *(blue),* and the variation in fibril diameter increases *(red).* This heterogeneity contributes to the opacity of the sclera, as compared with the cornea, despite their similar collagen fiber composition. *(Modified with permission from Levin LA, Nilsson SFE, Ver Hoeve J, Wu SM.* Adler's Physiology of the Eye. *11th ed. Elsevier/Saunders; 2011:117.)*

Type I is the major collagen component of the corneal stroma; it constitutes approximately 70% of the total stromal dry weight. Immunohistochemical and biochemical studies have demonstrated that normal adult corneal stroma also contains collagen types V, VI, VII, XII, and XIV. Type III collagen production is associated uniquely with stromal wound healing.

After collagen, proteoglycans are the second most abundant biological constituents of the cornea and constitute approximately 10% of its dry weight. Proteoglycans are glycosylated proteins with at least 1 glycosaminoglycan (GAG) chain covalently bound to the protein core. GAGs are composed of repeating disaccharides. GAGs are hygroscopic and thus attract water, generating swelling pressure and conferring hydrophilic properties to the corneal stroma. The GAGs found in corneal stroma include

- keratan sulfate
- chondroitin sulfate
- dermatan sulfate

Matrix metalloproteinases (MMPs) are a family of Zn^{2+}-dependent enzymes responsible for degradation of the components of the extracellular matrix (including proteoglycans and various types of collagens) during normal development as well as in disease processes. Of the dozen-plus known MMPs, only MMP-2 proenzyme has been found in healthy cornea. However, after corneal injury, additional MMPs (including MMP-1, MMP-3, and MMP-9) are synthesized. The proteinase inhibitors of the cornea play a key role in corneal protection by restricting damage during corneal inflammation, ulceration, and wound healing. Many of these inhibitors are synthesized by resident cells of the cornea; some are derived from tears, aqueous humor, and limbal blood vessels.

Randleman JB, Dawson DG, Grossniklaus HE, McCarey BE, Edelhauser HF. Depth-dependent cohesive tensile strength in human donor corneas: implications for refractive surgery. *J Refract Surg*. 2008;24(1):S85–S89.

Descemet Membrane and Endothelium

Descemet Membrane

Descemet membrane is a specialized basement membrane, 10–12 μm thick, between the corneal endothelium and the posterior stroma. It is secreted by endothelium and comprises an anterior banded layer and a posterior nonbanded layer. The latter is secreted throughout life, which is why Descemet membrane is 3–4 times thicker in adulthood than at birth (Fig 8-4). Type IV is the most abundant collagen in Descemet membrane. It has been hypothesized that the posterior-most 15 μm of stroma may represent a distinct, tough acellular layer (Dua layer).

Endothelium

The corneal endothelium, located posterior to Descemet membrane, is a monolayer of hexagonal cells with a diameter of 20 μm. In young adult eyes, the normal endothelial cell

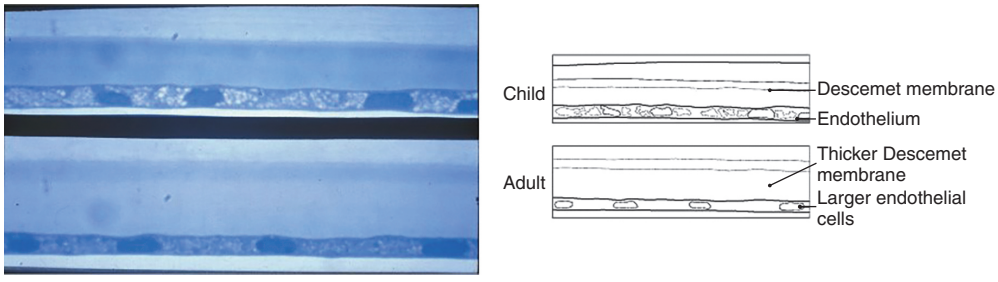


Figure 8-4 Thickening of Descemet membrane with age as the posterior nonbanded layer is continuously produced. *(Courtesy of John Marshall.)*

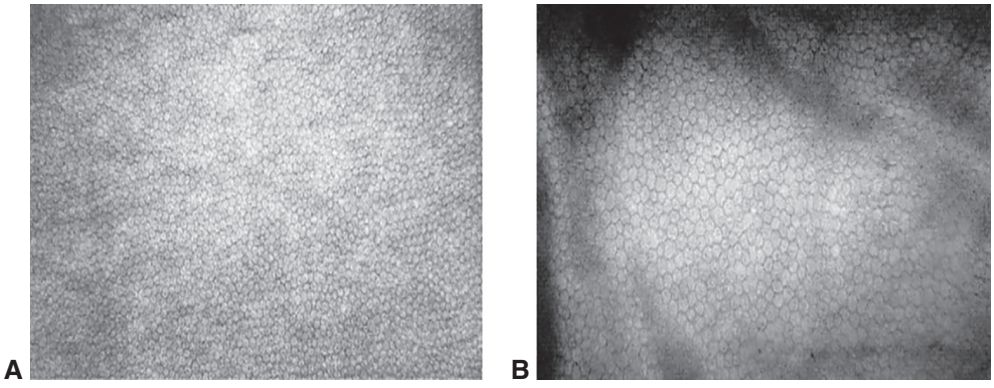


Figure 8-5 Corneal endothelium. Endothelial cells do not replicate. Over time, adjacent cells increase in size to accommodate for age-related endothelial cell loss. **A,** Specular micrograph of the cornea of an 18-month-old infant. **B,** Specular micrograph of the cornea of a healthy 74-year-old man. *(Modified with permission from Spalton DJ, Hitchings RA, Hunter PA, Tan JCH, Harry J.* Atlas of Clinical Ophthalmology. *3rd ed. Mosby; 2005:151.)*

count is approximately 3000/mm^2 centrally. The number of endothelial cells is higher in the periphery and decreases with age, with concomitant spreading and thinning of the remaining cells. The rate of physiologic corneal endothelial cell loss with normal aging has been reported to be 0.6% per year (Fig 8-5, Table 8-1).

Adjacent endothelial cells interdigitate in a complex way and form a variety of tight junctions, serving as a barrier to aqueous humor penetration, but desmosomes are never observed between normal cells. Approximately 20–30 short microvilli per cell extend from the apical plasma membrane into the aqueous humor. The endothelium functions both as a permeability barrier between the aqueous humor and the corneal stroma and as a pump to maintain the cornea in a dehydrated state by generating negative hydrostatic pressure, which also serves to hold free corneal flaps (eg, LASIK flaps) in place. The endothelium utilizes temperature-dependent Na^+,K^+-ATPase to maintain the hydration of the stroma at 78% and sustain corneal clarity. In vivo, the endothelium derives sufficient oxygen from the aqueous humor to maintain normal pump function.

Table 8-1 Corneal Endothelial Cell Density

Parameter	Value
Density during first decade of life	4000 cells/mm^3
Average density at age 40 years	2600 cells/mm^3
Rate of cell loss	0.6% per year
Minimum density required for adequate function	400–700 cells/mm^3

CLINICAL PEARL

GAGs within the corneal stroma have an intrinsic property to absorb water. Subsequent movement of water into the stroma creates the swelling pressure. The pumps in the corneal endothelium use energy-dependent processes to remove water and maintain stromal hydration at 78% to achieve corneal clarity. Breakdown of the epithelial and endothelial barriers, as may occur in trauma or acute hydrops, results in increased stromal hydration and loss of corneal clarity due to unopposed swelling pressure.

If the endothelium is injured, healing occurs mainly via migration, rearrangement, and enlargement of the residual cells. Substantial cell loss or damage results in irreversible edema because human corneal endothelial cells have limited ability to divide after birth. Infiltration of polymorphonuclear leukocytes in response to severe corneal injury can induce endothelial cells to become fibroblastic and to synthesize a *retrocorneal fibrous membrane (RCFM).* An RCFM forms between Descemet membrane and the corneal endothelium and causes a significant decrease in visual acuity. Unlike healthy corneal endothelial cells, which accumulate a limited amount of type I collagen protein, fibroblastic cells isolated from the RCFM express predominantly type I collagen.

Panjwani N. Cornea and sclera. In: Harding JJ, ed. *Biochemistry of the Eye.* Chapman & Hall Medical; 1997:16–51.

CHAPTER 9

Aqueous Humor, Iris, and Ciliary Body

Highlights

- Aqueous humor is secreted by the nonpigmented ciliary epithelium (NPE) from a substrate of blood plasma.
- Aqueous humor is distinct from plasma, as it has low protein content and a high concentration of ascorbate. The antioxidant properties of ascorbate help protect intraocular structures by blocking ultraviolet (UV) light.
- The blood–aqueous barrier is composed of the tight junctions of the NPE, the iris vasculature, and the inner wall endothelium of the Schlemm canal.
- Disruption of the blood–aqueous barrier allows blood and ocular fluids to mix, producing a plasmoid aqueous, as occurs in anterior uveitis.

Physiology of the Iris and Ciliary Body

The iris and ciliary body are the anterior parts of the uvea (also called *uveal tract*), which is continuous with the choroid posteriorly. The iris is a highly pigmented tissue that functions as a movable diaphragm between the anterior and posterior chambers of the eye to regulate the amount of light that reaches the retina. It is a delicate, dynamic structure that can make precise and rapid changes in pupillary diameter in response to light and specific pharmacologic stimuli. The ciliary body produces the aqueous humor, regulates its composition, and contributes to uveoscleral outflow, thereby directly influencing the ionic environment and metabolism of the cornea, lens, and trabecular meshwork.

The ciliary body is a major pharmacologic target in the treatment of glaucoma. Many of the agents used to lower intraocular pressure (IOP) in glaucoma work through receptors and their respective signal transduction pathways. The iris and ciliary body are rich in many types of receptors that bind to various ligands. Chapter 16 discusses these receptors and pharmacologic agents relevant to the treatment of glaucoma.

The ciliary body is a major contributor to the defense against oxidative stress in the anterior and posterior chambers, via molecules secreted into the aqueous humor, as discussed later in this chapter. It has the highest concentration of redox (reduction-oxidation) enzymes in the anterior segment. The ciliary body also contains proteins of

the cytochrome P450 family, though only a small number compared with the liver. These enzymes are involved in detoxification, whereby they convert hydrophobic to hydrophilic compounds via hydroxylation.

See Chapter 2 for further discussion of the structures mentioned in this section.

Dynamics of the Aqueous Humor

Blood–Aqueous Barrier

The aqueous humor *(aqueous)* is a transparent fluid that fills the anterior and posterior chambers of the eye. It is the major nutrient source for the avascular lens and cornea and also serves as a medium for removal of waste products.

Ocular fluids are separated from blood by barriers formed by the tight junctions of epithelial cells and those of endothelial cells. These barriers are called either *blood–aqueous* or *blood–retina barriers,* depending on their location in the eye. These barriers carefully control the composition and amounts of all materials entering and leaving the eye. Perturbations of these *blood–ocular barriers* cause blood constituents to mix with ocular fluids; this mixing leads to plasmoid aqueous, retinal exudates, or retinal edema.

The blood–aqueous barrier is composed of tight junctions of the following:

- nonpigmented ciliary epithelium
- iris vasculature
- inner wall endothelium of the Schlemm canal

This barrier restricts plasma proteins from entering the aqueous. Consequently, aqueous is essentially protein-free, giving it a refractive index of 1.336 and allowing optical clarity for transmission of light along the visual pathway. The blood–aqueous barrier, along with active transport systems, also allows increased levels of ascorbate and some amino acids in aqueous compared with levels in blood plasma. Breakdown of this barrier is discussed later in this chapter.

Aqueous Humor Formation and Secretion

The ciliary epithelium is a bilayer of polarized epithelial cells that line the surface of the ciliary body. The 2 cell layers are the nonpigmented epithelium (NPE), which faces the aqueous humor, and the pigmented epithelium (PE), which faces the ciliary stroma. These 2 layers are connected to each other at their apical membranes; their basal membranes face the aqueous and ciliary stroma. The NPE has tight junctions proximal to the apical plasma membrane that form part of the blood–aqueous barrier, thereby preventing paracellular transport from the ciliary stroma into the posterior chamber. In contrast, the PE cell layer is considered a leaky epithelium because it allows solutes to move through the space between the PE cells.

Aqueous humor is secreted by the NPE from a substrate of blood plasma into the posterior chamber (see Fig 9-1). The NPE expresses aquaporin channels, which, as their name

implies, facilitate the transport of water. Aqueous humor is secreted at a rate of 2–3 μL/min, but this rate fluctuates according to our circadian rhythm and other factors, resulting in variation of IOP over a 24-hour period.

CLINICAL PEARL

Several factors affect IOP, including the circadian rhythm. This is the basis for taking IOP measurements in glaucoma patients at different times of day to assess for fluctuations. In certain instances, the highest or lowest IOP measurement may occur outside of normal clinic hours.

Aqueous enters the posterior chamber from the ciliary processes by means of active and passive physiologic mechanisms:

- *active:* energy-dependent secretion of certain ions and substrates
- *passive:* diffusion and ultrafiltration

The active process of aqueous secretion involves proteins and enzymes present in the NPE, such as sodium-potassium adenosine triphosphatase (Na^+,K^+-ATPase) and carbonic anhydrase (CA). Active secretion of sodium by Na^+,K^+-ATPase and accompanying anions creates high osmolarity on the basolateral (aqueous) side of the NPE, which in turn promotes diffusion of water. In humans, CA is present in both the PE and NPE. Its inhibitors reduce the rate of entry of sodium and bicarbonate into the aqueous, causing a reduction in aqueous flow. See Chapter 16 for further discussion.

Cotransport is the coupled transport of 2 chemical substances across a membrane, with 1 substance transported down its concentration gradient, driving movement of the other substance against its concentration gradient. Symport and antiport are cotransport mechanisms. *Symporters* are membrane proteins that mediate the cotransport of molecules in the same direction, whereas *antiporters* mediate the cotransport of molecules in opposite directions.

These systems' activities and cellular distributions along the membranes of PE and NPE cells determine unidirectional net secretion from the ciliary stroma to the posterior chamber, a process that involves 3 steps (Fig 9-1):

1. uptake of solute and water at the stromal surface by PE cells
2. transfer of solute and water from PE to NPE cells
3. transfer of solute and water by NPE cells into the posterior chamber

Likewise, it is thought that there is a mechanism for transporting solute and water from the posterior chamber back into the stroma. In this unidirectional reabsorption, another set of transporters may be involved in extruding sodium, potassium, and chloride back into the stroma.

Diffusion is the movement of solutes or ions across a membrane down the concentration or ionic gradient. In aqueous formation, ultrafiltration is the nonenzymatic

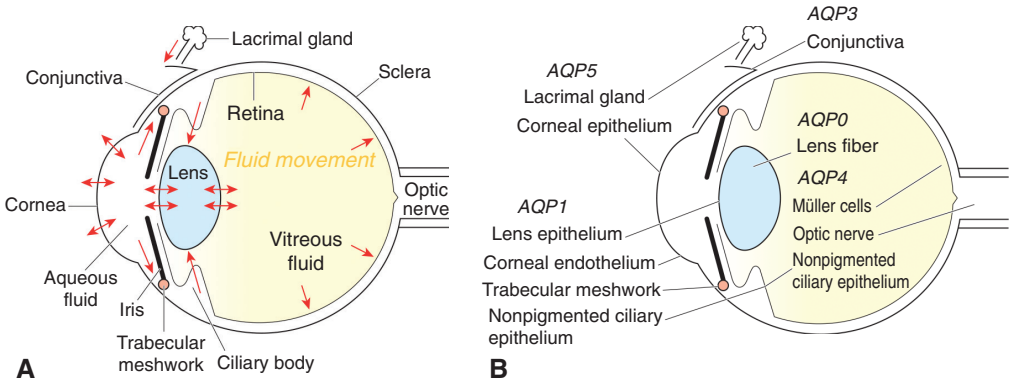


Figure 9-1 Movement of fluid and location of aquaporin (AQP) channels in the eye. **A,** The primary source of intraocular fluid is the ciliary body. The *red arrows* demonstrate secretion of aqueous humor by the ciliary body and the multiple exit routes (trabecular, uveal scleral, and across the retina, where this facilitates retinal adhesion). *Double arrows* note points of fluid exchange between the cornea and lens with surrounding fluid. This transport of fluid is supported by aquaporins, which are water channels found in various tissues throughout the body. **B,** Distribution of aquaporin channels in ocular and adnexal tissues. AQP4 channels in the optic nerve are the target of antibodies in neuromyelitis optica. *(Modified with permission from Forrester JV, Dick AD, McMenamin PG, Roberts F, Pearlman E.* The Eye: Basic Sciences in Practice. *4th ed. Elsevier; 2016:233.)*

component that depends on IOP, blood pressure, and the blood osmotic pressure in the ciliary body. Ultrafiltration decreases with increasing IOP.

IOP is maintained by continuous aqueous formation and drainage, which allow removal of metabolic waste products from the surrounding tissues. The factors determining IOP are represented in the Goldmann equation:

$$IOP = (F - U) / C + EVP$$

In this equation, F represents the rate of aqueous humor production, U represents the rate of aqueous drainage through the uveoscleral (pressure-insensitive) pathway, C represents the outflow facility through the trabecular (pressure-sensitive) pathway, and EVP represents the episcleral venous pressure. See BCSC Section 10, *Glaucoma,* for further discussion of this topic, including a more detailed explanation of the pressure-insensitive and pressure-sensitive pathways.

Mansouri K, Tanna AP, De Moraes CG, Camp AS, Weinreb RN. Review of the measurement and management of 24-hour intraocular pressure in patients with glaucoma. *Surv Ophthalmol.* 2020;65(2):171–186.

Clinical Implications of Breakdown of the Blood–Aqueous Barrier

The blood–aqueous barrier may be disrupted in a number of conditions, including ocular trauma (mechanical, chemical, or physical), infection or inflammation, and ischemia, as well as with use of pharmacologic agents (eg, prostaglandin analogues, cholinesterase

inhibitors). With compromise of this barrier, the levels of inflammatory mediators, immunoglobulins, fibrin, and proteases rise, and the balance among the various growth factors is disrupted. The protein content of the aqueous humor increases, possibly as much as 10–100 times normal levels, especially in high-molecular-weight polypeptides.

The clinical sequelae include fibrinous exudate (with or without a macrophage reaction and formation of cyclitic membranes) and synechiae formation (peripheral and posterior), as well as an abnormal neovascular response, which further exacerbates breakdown of the blood–aqueous barrier. Chronic disruption of this barrier is implicated in the abnormal hyperplastic response of the lens epithelium, corneal endothelium, trabecular meshwork, and iris, as well as in the formation of complicated cataracts. Degenerative and proliferative changes may occur in various ocular structures as well. The use of anti-inflammatory steroidal and nonsteroidal drugs, cycloplegics, protease activators or inhibitors, growth factor and anti–growth factor agents, and even surgical intervention may be necessary to combat these events.

Composition of the Aqueous Humor

Table 9-1 summarizes the composition of the aqueous humor compared with that of plasma and vitreous. Aqueous secretion is not an ultrafiltrate of plasma (as was once speculated), because it is produced by energy-dependent processes in the epithelial layer of the ciliary body. This mode of production allows precise control to be maintained over composition of the fluid that bathes the structures essential for normal vision.

The ionic composition of the aqueous humor is determined by selective active transport systems (eg, Na^+,K^+-$2Cl^-$ symport, Cl^--HCO_3^- and Na^+,H^+ antiports, cation channels, water channels [aquaporins], Na^+,K^+-ATPase, K^+ channels, Cl^- channels, H^+-ATPase) that participate in secretion of aqueous humor by the NPE (Fig 9-2). Active secretion of ions and molecules leads to higher levels of ascorbate and of some amino acids in aqueous than in plasma.

Molecular studies have shown that the secretory properties of the ciliary epithelium are not limited to ions and electrolytes but extend to a wide range of molecules of different sizes. Common features of many of these molecules are their local synthesis in the ciliary epithelium and their secretion by the NPE cells through the regulatory pathway

Table 9-1 Comparison of Components of Plasma, Aqueous Humor, and Vitreous

Components (mmol/kg H_2O)	Plasma	Aqueous	Vitreous
Na^+	146	163	144
Cl^-	109	134	114
HCO_3^-	28	20	20–30
Ascorbate	0.04	1.06	2.21
Glucose	6	3	3.4

Reproduced from Macknight AD, McLaughlin CW, Peart D, Purves RD, Carré DA, Civan MM. Formation of the aqueous humor. *Clin Exp Pharmacol Physiol*. 2000;27(1–2):100–106.

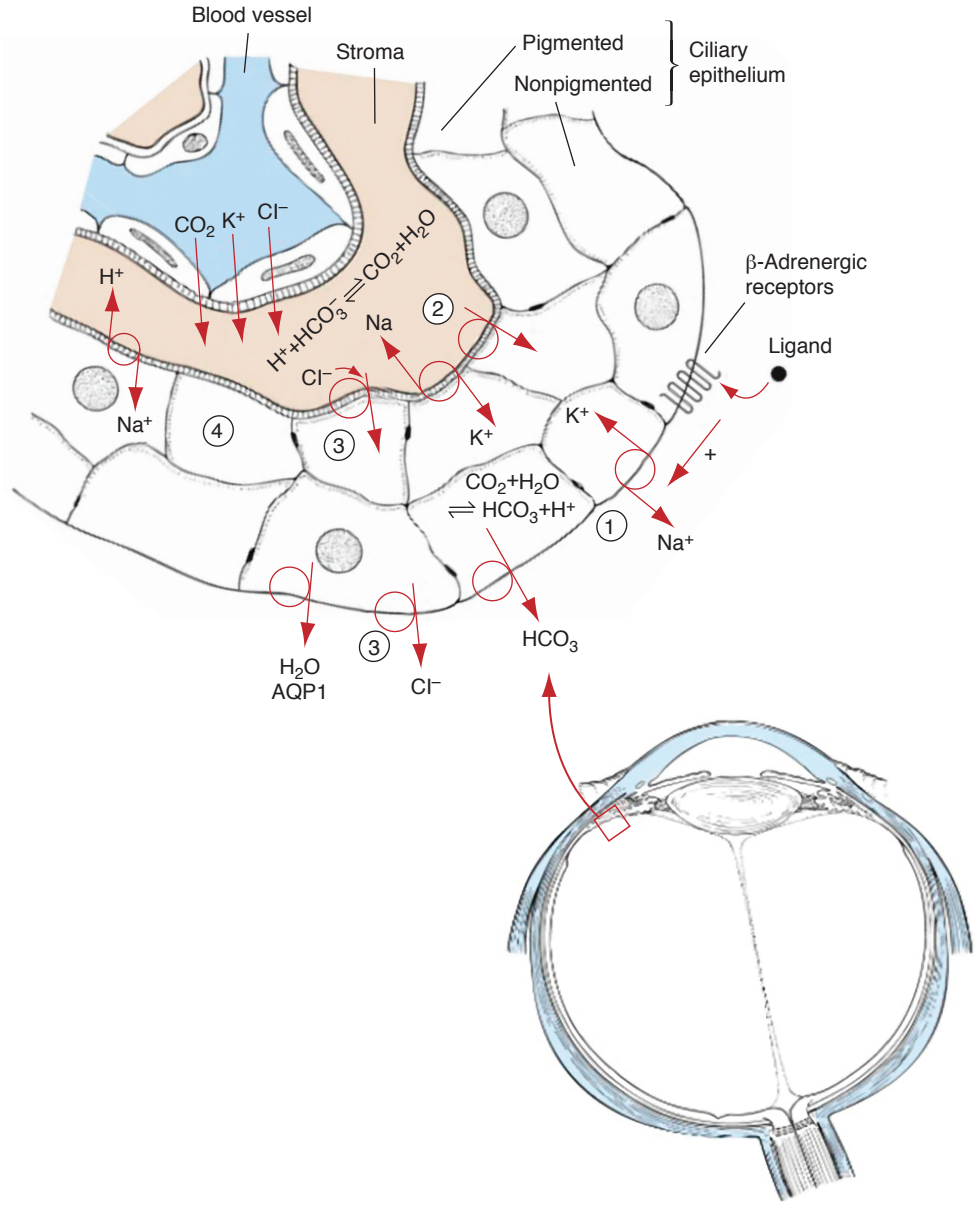


Figure 9-2 Production and secretion of aqueous humor. The oncotic pressure of the ciliary body stroma draws water toward the stroma from the neighboring blood vessel but also away from the posterior chamber. Thus, energy-dependent mechanisms (active transport) are needed to secrete water across the ciliary epithelium. This is accomplished by sodium-potassium adenosine triphosphatase (Na^+,K^+-ATPase), which pumps Na^+ into the posterior chamber. The resultant increase in osmolarity draws water into the posterior chamber via aquaporin channels. Within the epithelial layers, carbonic anhydrase provides hydrogen ions (H^+), which are exchanged with Na^+ to help provide a supply of sodium within the epithelium and drive the flow of water. Adrenergic stimulation has been reported to drive Na^+,K^+-ATPase. 1, Na^+,K^+ antiport; 2, K^+ channel; 3, Cl^- channel; 4, Na^+,H^+ antiport; AQP1 = aquaporin channel 1. *(Modified with permission from Forrester JV, Dick AD, McMenamin PG, Roberts F, Pearlman E.* The Eye: Basic Sciences in Practice. *4th ed. Elsevier; 2016:224.)*

into the aqueous humor. Among the proteins whose messenger RNA expression has been demonstrated are

- plasma proteins (eg, complement component C4, α_2-macroglobulin, selenoprotein P, apolipoprotein D, plasma glutathione peroxidases, angiotensinogen)
- proteinases (eg, cathepsin D, cathepsin O)
- cellular retinaldehyde–binding protein (CRALBP) and other components of the vision cycle
- neurotrophic factor (eg, PE-derived factor)
- neuropeptide-processing enzymes (eg, carboxypeptidase E, peptidylglycine α–amidating monooxygenase)
- neuroendocrine peptides (eg, secretogranin II, neurotensin, galanin)
- bioactive peptides and hormones (eg, atrial natriuretic peptide, brain natriuretic peptide)

These findings support the view that the ciliary epithelium exhibits neuroendocrine properties that are directly related to the makeup of the aqueous humor and its regulation. The aqueous humor composition is in dynamic equilibrium, determined both by its rate of production and outflow and by continuous exchanges with the tissues of the anterior segment. The aqueous contains the following:

- inorganic ions and organic anions
- carbohydrates
- glutathione and urea
- proteins
- growth-modulatory factors
- oxygen and carbon dioxide

Yang W, Bradley JC, Reid TW, McCartney DL. Growth factors in aqueous humor. *Ophthalmology*. 2011;118(5):1003.e1.

Inorganic Ions

The concentrations of sodium, potassium, and magnesium in the aqueous are similar to those in plasma, but the level of calcium in aqueous is only half that in plasma. The 2 major anions are chloride and bicarbonate. Phosphate is also present in the aqueous (aqueous-to-plasma ratio, ~0.5 or lower), but its concentration is too low to have significant buffering capacity. Iron, copper, and zinc are all found in the aqueous humor at essentially the same levels as in plasma: approximately 1 mg/mL.

Organic Anions

Lactate is the most abundant organic anion in the aqueous, and its concentration there is always higher than that in plasma. The high lactate level in aqueous is a result of glycolytic metabolism, upon which the avascular lens depends.

Ascorbate (vitamin C) levels in aqueous are much higher (10–50 times higher) than those in plasma. Ascorbate has antioxidant properties, and its high concentration in the aqueous protects intraocular structures by blocking UV light.

Carbohydrates

Glucose concentration in the aqueous is roughly 50%–70% of that in plasma. The rate of entry of glucose into the posterior chamber is much more rapid than would be expected from its molecular size and lipid solubility, suggesting that the transport of glucose across the ciliary epithelium occurs by facilitated diffusion.

> **CLINICAL PEARL**
>
> In individuals with diabetes, glucose levels in the aqueous humor are increased. As a result, glucose concentrations are higher in the lens, which has short-term refractive and longer-term cataract implications.

Inositol, which is important for phospholipid synthesis in the anterior segment, is found in the aqueous at a concentration approximately 10 times higher than that in plasma.

Glutathione

Glutathione, an important tripeptide with a reactive sulfhydryl group, is also found in the aqueous humor. Its concentration in primates ranges from 1 to 10 μmol/L. Blood contains a high concentration of glutathione; however, virtually all glutathione resides within the erythrocytes, and plasma has a low concentration of only 5 μmol/L or less.

Glutathione stabilizes the redox state of the aqueous by reconverting ascorbate to its functional form after oxidation, as well as by removing excess hydrogen peroxide. Glutathione also serves as a substrate in the enzymatic conjugation by cytosolic enzymes; this process is involved in the cellular detoxification of electrophilic compounds. These enzymes (glutathione S-transferases) are important in protecting ocular tissues from oxidative damage and oxidative stress and are highly concentrated in the ocular ciliary epithelium.

Proteins

As stated earlier, the tight junctions of the NPE, along with other structures, establish the blood–aqueous barrier, which prevents diffusion of plasma proteins from the ciliary stroma into the posterior chamber. Nevertheless, plasma proteins do enter the aqueous humor, possibly through the root and anterior surface of the iris. Normal aqueous contains approximately 0.02 g of protein per 100 mL, as compared with the typical plasma level of 7 g per 100 mL. The most abundant plasma proteins identified in aqueous humor are albumin and transferrin, which together may account for 50% of the total protein content.

In addition to the plasma proteins that enter the aqueous, there is compelling evidence that some proteins may be synthesized within the ciliary body and secreted directly into the aqueous humor. Molecular techniques (such as the screening of complementary DNA [cDNA] libraries constructed from intact human and bovine ciliary bodies) have enabled the isolation and identification of numerous protein-encoding genes. These studies,

therefore, challenge the long-held view that plasma proteins in the aqueous humor are transported into the aqueous from outside the eye. Among the cDNA molecules isolated from the ciliary body are

- C4, a component of the classical complement pathway that participates in immune-mediated inflammatory responses
- α_2-macroglobulin, a carrier protein that is involved in proteinase inhibition, clearance, and targeting, as well as the processing of foreign peptides
- apolipoprotein D, which binds and transports hydrophobic substances, including cholesterol, cholesteryl esters, and arachidonic acid (AA)
- selenoprotein P, which has antioxidant properties

Proteinases and inhibitors

Several proteinases and proteinase inhibitors have also been identified in the aqueous humor. Of the proteinase inhibitors, α_2-macroglobulin and α_1-antitrypsin are perhaps the most extensively studied. An imbalance in equilibrium between proteinases and proteinase inhibitors could alter aqueous humor composition, which may cause disease (eg, glaucoma).

Enzymes

Activators, proenzymes, and fibrinolytic enzymes are present in the aqueous and could play a role in the regulation of outflow resistance. Both plasminogen and plasminogen activator are found in human and monkey aqueous, but only traces of plasmin have been reported.

Neurotrophic and neuroendocrine proteins

The ciliary epithelia, which are derived from neuroectoderm, are functionally similar to neuroendocrine glands elsewhere in the body. The ciliary body has neuroendocrine peptides and neuroendocrine processing enzymes. Bioactive neuroendocrine markers, identified through human ciliary body cDNA subtraction studies, include neurotensin, angiotensin, endothelins, and natriuretic peptides. These markers are known to have systemic vascular hemodynamic effects and, by implication, may have similar roles in IOP regulation or aqueous secretion.

The neuroendocrine properties of the ciliary epithelium may determine the composition of the aqueous humor, the diurnal (circadian) rhythm of aqueous humor secretion and IOP, the ciliary blood flow, and the immune privilege status of intraocular structures.

Coca-Prados M, Escribano J. New perspectives in aqueous humor secretion and in glaucoma: the ciliary body as a multifunctional neuroendocrine gland. *Prog Retin Eye Res.* 2007; 26(3):239–262.

Growth-Modulatory Factors

The physical and chemical properties of the aqueous humor play a substantial role in modulating the proliferation, differentiation, functional viability, and wound healing of ocular tissues. These properties are largely influenced by several growth-promoting and

differentiation factors that have been identified or quantified in aqueous humor, including the following:

- transforming growth factor βs 1 and 2 (TGF-β_1 and -β_2)
- acidic and basic fibroblast growth factors (aFGF and bFGF)
- insulin-like growth factor I (IGF-I)
- insulin-like growth factor binding proteins (IGFBPs)
- vascular endothelial growth factors (VEGFs)
- transferrin

The growth factors in the aqueous humor perform diverse, synergistic, and sometimes opposite biological activities. Normally, the lack of significant mitosis of the corneal endothelium and trabecular meshwork in vivo is probably controlled by the complex coordination of effects and interactions among the different growth-modulatory substances present in the aqueous humor.

Disruption in the balance among various growth factors, which occurs with the production of plasmoid aqueous humor as a result of breakdown of the blood–aqueous barrier, may explain the abnormal hyperplastic response of the lens epithelium and corneal endothelium observed in chronic inflammatory conditions and traumatic insults to the eye.

Growth factor levels in the aqueous humor are altered in several disease states. Levels of IGFBPs are elevated fivefold in patients with diabetes without retinopathy, and IGF-I levels are elevated in patients with diabetic retinopathy. VEGF levels in the aqueous humor are elevated in eyes with retinal vascular disease and acute nonarteritic ischemic optic neuropathy, whereas interleukin 2 concentration is reduced.

Micieli JA, Lam C, Najem K, Margolin EA. Aqueous humor cytokines in patients with acute nonarteritic anterior ischemic optic neuropathy. *Am J Ophthalmol.* 2017;177:175–181.

Vascular endothelial growth factors

Although VEGF-A and its receptors are most studied in relation to the vascular endothelium, they are also present in other tissues and organ systems, a finding that underscores other possible physiological roles, such as retinal leukostasis and neuroprotection. In addition, VEGF-A may play a role in regulating IOP by elevating levels of nitric oxide (NO), which increases aqueous outflow facility. VEGF-A upregulates expression of endothelial NO synthase (eNOS), which produces NO; VEGF-A blockage may cause IOP elevation by decreasing NO production.

VEGF-A levels in ocular fluids, including aqueous humor, are elevated in patients with retinal vascular disease and particularly in eyes with secondary iris neovascularization. The expression of VEGF is increased by hypoxia in retinal endothelial cells, retinal pericytes, Müller cells, retinal pigment epithelium cells, and the NPE cells of the ciliary body. Levels of VEGF-A in the aqueous humor increase in response to anterior segment ischemia in animal models, as well as in response to retinal hypoxia. Aqueous VEGF-A levels fall after intravitreal injection of anti-VEGF agents. See also Chapter 16 for further discussion regarding VEGF and VEGF inhibitors.

Karaman S, Leppänen V-M, Alitalo K. Vascular endothelial growth factor signaling in development and disease. *Development*. 2018;145(14):dev151019.

Penn JS, Madan A, Caldwell RB, Bartoli M, Caldwell RW, Hartnett ME. Vascular endothelial growth factor in eye disease. *Prog Retin Eye Res*. 2008;27(4):331–371.

Oxygen and Carbon Dioxide

Oxygen in the aqueous humor is derived from the blood supply to the ciliary body and iris, as the atmospheric oxygen flux across the cornea is negligible. Indeed, the corneal endothelium depends critically on the aqueous oxygen supply for the active fluid-transport mechanism that maintains corneal transparency. The lens and the endothelial lining of the trabecular meshwork also derive their oxygen supply from the aqueous. Oxygen is present in the aqueous humor at a partial pressure lower than that in arterial blood.

CLINICAL PEARL

Oxygen concentration in the aqueous humor may increase with age-related vitreous degeneration or after surgical removal of vitreous. Elevated oxygen concentration induces oxidative damage in the lens and trabecular meshwork and leads to an increased risk of cataract and open-angle glaucoma after vitrectomy.

The carbon dioxide content of the aqueous ranges from 40 to 60 mm Hg, contributing approximately 3% of the total bicarbonate. The relative proportions of carbon dioxide and bicarbonate determine the pH of the aqueous, which in most species ranges between 7.5 and 7.6. Carbon dioxide is continuously lost from the aqueous by diffusion across the cornea into the tear film and atmosphere.

Gong H, Tripathi RC, Tripathi BJ. Morphology of the aqueous outflow pathway. *Microsc Res Tech*. 1996;33(4):336–367.

CHAPTER 10

Lens

Highlights

- As a result of its high protein content, the lens has an index of refraction that is higher than that of the surrounding media.
- Proteins constitute 33% of the weight of the lens, which is 2–3 times higher than their concentration in other body tissues.
- The lens relies primarily on glycolysis to generate adenosine triphosphate (ATP). Alterations in this metabolic pathway have been implicated in the development of both congenital cataract and diabetic cataract.

Overview

The lens is a transparent, avascular structure that, in concert with the cornea, focuses incident light onto the sensory elements of the retina. To do so, the lens must be transparent and have an index of refraction higher than that of the surrounding fluids. The index of refraction of the lens is 1.41 centrally at the nucleus and 1.39 in the peripheral cortical region. The high refractive index is due to the high concentration of proteins—especially of soluble proteins called *crystallins*—in the lens cells. Furthermore, because there is little if any turnover of protein in the central region of the lens (where the oldest, denucleated cells are found), the proteins of the human lens must be extremely stable to remain functionally viable for a lifetime. Considering the lens's mode of growth and the chronic stresses to which it is exposed, it is remarkable that, in most people, lenses retain good transparency until later in life; visually significant opacities typically develop by the sixth or seventh decade of life.

This chapter discusses the structure and chemical composition of the lens, as well as aspects of membrane function, metabolism, and regulatory processes within the lens. BCSC Section 11, *Lens and Cataract,* provides additional information about the lens, cataractogenesis, and cataract surgery.

Structure of the Lens

Capsule

The lens is enclosed in an elastic basement membrane called the *lens capsule* (Fig 10-1; see also Chapter 2, Fig 2-35). The capsule is acellular and is composed primarily of type IV collagen; it contains smaller amounts of other collagens and extracellular matrix components

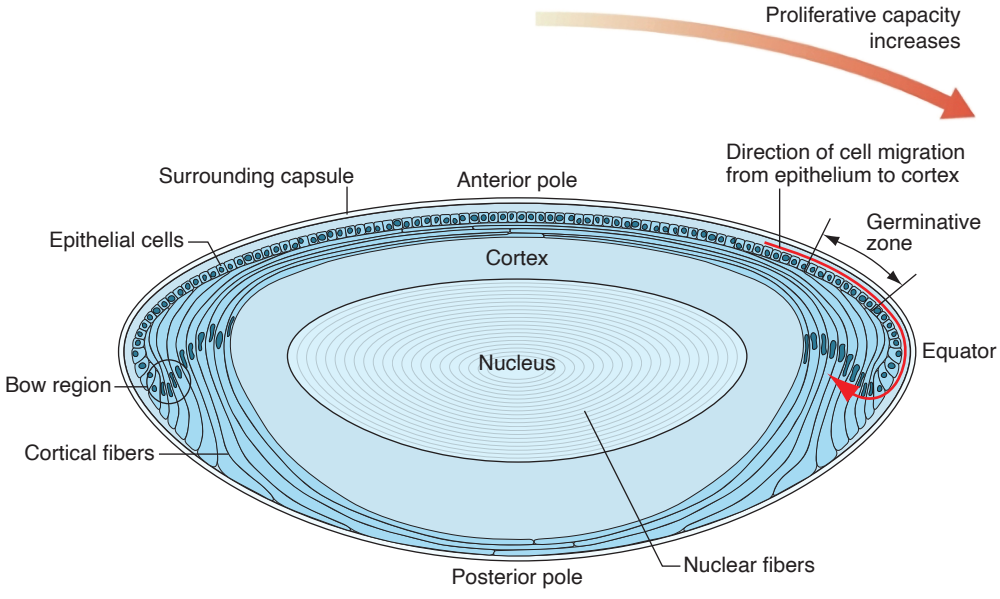


Figure 10-1 Schematic of the mammalian lens in cross section. *Arrow* indicates the direction of cell migration from the epithelium to the cortex. Near the equator is the bow region, where the lens-fiber cells elongate until their 2 ends meet. At this point, they are fully mature. As they are pushed inward by newer fibers, they lose their nuclei and organelles. These fibers do not shed over time. As a result, the lens increases in size throughout life. *(Modified with permission from Friedman NJ, Kaiser PK, Trattler WB.* Review of Ophthalmology. *3rd ed. p. 288. Copyright 2018, Elsevier. Illustration by Mark Miller.)*

(including glycosaminoglycans, laminin, fibronectin, and heparan sulfate proteoglycan). The capsule is thicker (11–15 μm) on the anterior surface of the lens, where the epithelial cells continue to secrete capsular material throughout life. On the posterior surface of the lens, where there is no epithelium, the posterior fiber cells have limited capacity to secrete such material, and the capsule is relatively thinner (2–4 μm). The zonular fibers, from which the lens is suspended, insert into the capsule near the equator on both the anterior and posterior aspects. The capsule is not a barrier to diffusion of water, ions, small molecules, or proteins up to the size of serum albumin.

CLINICAL PEARL

The relative thinness of the posterior capsule compared with the anterior capsule renders it more susceptible to inadvertent tear or rupture during cataract surgery. Early recognition of this intraoperative complication (including the status of the underlying vitreous) is important.

Epithelium

A single layer of epithelial cells covers the anterior surface of the lens. These cells have full metabolic capacity and play the primary role in regulating the water and ion balance of the entire lens. Although the cells of the central epithelium are not mitotically active,

a germinative zone exists as a ring anterior to the equator, where the epithelial cells divide. The new cells migrate toward the equator and begin to differentiate into lens fibers at the bow region (see Fig 10-1). In the adult lens, epithelial cells are not normally found posterior to the equator.

Cortex and Nucleus

Aside from the single layer of epithelial cells on its anterior surface, the lens is composed of lens fibers, which are long, ribbonlike cells. These fibers are formed from epithelial cells at the lens equator; therefore, younger fibers are always exterior to older ones (see Fig 10-1 and Chapter 2, Fig 2-36). The lens structure is analogous to the growth rings of a tree: the oldest fibers are in the center, and the progressively younger layers, or *shells,* of fiber cells are toward the periphery. Unlike the case with many tissues in the body, no cells are sloughed from the lens, and cells produced before birth remain at the center of the lens throughout life. The fiber mass of the adult lens can be divided into the *cortex* (the outer fibers, laid down after approximately age 20 years) and the *nucleus* (the cells produced from embryogenesis through adolescence).

As new fiber cells elongate and differentiate into mature fibers, their cell nuclei form the *bow zone,* or *bow region,* at the lens equator (see Fig 10-1). Elongating fibers substantially increase their volume and surface area and express large amounts of both lens crystallins (discussed later in this chapter) and a lens-fiber–specific membrane protein called *major intrinsic protein (MIP).* As the fibers become fully elongated and make sutures at each end with fibers that have elongated from the opposite side of the lens, they become mature, terminally differentiated fiber cells. The cell nuclei disintegrate, as do mitochondria and other organelles. This process has been proposed to occur via *autophagy,* the degradation of the cell's own unneeded and/or damaged components via a defined intracellular process. See Chapter 13.

In the central portion of the lens, elimination of cellular organelles is necessary because such bodies are sufficiently large to scatter light and thereby degrade visual acuity. Also, with the loss of cell nuclei, the mature fibers lose the machinery required for synthesis of proteins.

Chai P, Ni H, Zhang H, Fan X. The evolving functions of autophagy in ocular health: a double-edged sword. *Int J Biol Sci.* 2016;12(11):1332–1340.

Costello MJ, Brennan LA, Basu S, et al. Autophagy and mitophagy participate in ocular lens organelle degradation. *Exp Eye Res.* 2013;116:141–150.

Chemical Composition of the Lens

Plasma Membranes

The chemical composition of lens-fiber plasma membranes suggests that they are both very stable and very rigid. A high saturated fatty acid content, a high cholesterol-to-phospholipid ratio, and a high concentration of sphingomyelin all contribute to the tight packing and low fluidity of the membrane. Although lipids make up only around 1% of the

total lens mass, they constitute approximately 55% of the plasma membrane's dry weight; cholesterol is the major neutral lipid. As the lens ages, the protein-to-lipid and cholesterol-to-phospholipid ratios increase as a result of phospholipid loss, especially in the nucleus.

Lens Proteins

The lens has the highest protein content of any tissue in the body; proteins constitute 33% of the weight of the lens, which is 2–3 times higher than their concentration in other body tissues. In some animal species, more than 50% of lens weight is protein. Lens crystallins are a diverse group of proteins that are abundantly expressed in the cytoplasm of lens-fiber cells. They are thought to play crucial roles in providing the transparency and refractile properties essential to lens function. Crystallins constitute 90%–95% of total lens protein. In addition to crystallins, the lens has a full complement of enzymes and regulatory proteins that are present primarily in the epithelium and in immature fiber cells, where most metabolic activity occurs.

Crystallins

Crystallins are water-soluble proteins so named for their high abundance in the crystalline lens. Crystallins can be divided into 2 groups. The first group includes α-crystallin and the β,γ-crystallin family, both of which seem to be present in all vertebrate lenses but have also been demonstrated in other ocular tissues. The second group consists of taxon-specific crystallins, which are present only in certain species.

Andley UP. Crystallins in the eye: function and pathology. *Prog Retin Eye Res*. 2007;26(1):78–98.
Slingsby C, Wistow GJ. Functions of crystallins in and out of lens: roles in elongated and post-mitotic cells. *Prog Biophys Mol Biol*. 2014;115(1):52–67.

α-Crystallin α-Crystallin is a member of the small heat shock protein family. Heat shock proteins are molecular chaperones; they stabilize partially folded proteins and prevent them from aggregating. Zinc ions enhance the chaperone function and stability of α-crystallin. Because protein aggregates in the lens scatter light and cause loss of transparency, the antiaggregative function of α-crystallin is crucial to the long-term maintenance of transparency in the fibers of the lens nucleus, where synthesis of new protein is impossible and protein molecules must exist for decades. Knockout models have confirmed that pathogenic variants (mutations) of the α-crystallin gene result in premature cataract development.

Berry V, Francis P, Reddy MA, et al. Alpha-B crystallin gene (*CRYAB*) mutation causes dominant congenital posterior polar cataract in humans. *Am J Hum Genet*. 2001;69(5):1141–1145.
Brady JP, Garland D, Duglas-Tabor Y, Robison WG Jr, Groome A, Wawrousek EF. Targeted disruption of the mouse alpha A-crystallin gene induces cataract and cytoplasmic inclusion bodies containing the small heat shock protein alpha B-crystallin. *Proc Natl Acad Sci USA*. 1997;94(3):884–889.

β- and γ-Crystallins β-Crystallins and γ-crystallins are divided on the basis of molecular mass and isoelectric points. β-Crystallins exist as polymers, and γ-crystallins are monomeric. The specific functions of these crystallins are unknown. Acquired posttranslational

modifications of β-crystallins have been associated with cataract formation. Most expression of γ-crystallins occurs early in development; thus, they tend to be most concentrated in the nuclear region of the lens. Given their compact and symmetric structures (which can be very densely packed), γ-crystallins tend to be highly concentrated in aged, hard lenses, which have little to no accommodative ability.

Cytoskeletal and membrane proteins

Although most proteins in the normal lens are water soluble, several important structural proteins can be solubilized only in the presence of chaotropic agents or detergents. These water-insoluble proteins include the cytoskeletal elements *actin* (actin filaments), *vimentin* (intermediate filaments), and *tubulin* (microtubules), as well as 2 additional proteins called *filensin* and *phakinin.* The last 2 proteins have been found only in lens-fiber cells and compose a cytoskeletal structure, the *beaded filament,* which is unique to the lens. The filamentous structures of the cytoskeleton provide structural support to the cells and play crucial roles in processes such as differentiation, motility and shape change, and organization of the cytoplasm. Pathogenic variants of the beaded filament result in congenital cataract formation.

Lens-fiber membranes have 1 quantitatively dominant protein, MIP, which is expressed only in lens-fiber cells and was earlier thought to be a gap-junction protein. In fact, it is not a connexin but rather an aquaporin—a member of a large, diverse family of proteins involved in regulating water transport. MIP has been reported to function as a water channel and to play a role in cell adhesion. Pathogenic variants of the *MIP* gene lead to cataract formation.

Chepelinsky AB. Structural function of MIP/aquaporin 0 in the eye lens; genetic defects lead to congenital inherited cataracts. *Handb Exp Pharmacol.* 2009;(190):265–297.

Jakobs PM, Hess JF, FitzGerald PG, Kramer P, Weleber RG, Litt M. Autosomal-dominant congenital cataract associated with a deletion mutation in the human beaded filament protein gene BFSP2. *Am J Hum Genet*. 2000;66(4):1432–1436.

Posttranslational modifications to lens proteins

The proteins of the lens are some of the longest-lived in the body; the oldest ones (in the center of the lens nucleus) are synthesized before birth. As would be expected, these proteins become structurally modified in various ways, including oxidation of sulfur and aromatic residue side chains, inter- and intrapolypeptide crosslinking, glycation, racemization, phosphorylation, deamidation, and carbamylation. Many of these modifications occur early in life and are probably part of a programmed modification of the crystallins that is required for their long-term stability and functionality. There is evidence that some of these processes (phosphorylation, thiol oxidation) are reversible and may serve a regulatory function, although this hypothesis remains to be proved.

As the proteins age (particularly in some cataracts), certain oxidative modifications accumulate, contributing to the crosslinking of crystallin polypeptides, alterations in fluorescent properties, and an increase in protein-associated pigmentation. In particular, the formation of disulfide crosslinks in the proteins of the lens nuclear region is associated with the formation of protein aggregates, light scattering, and cataract.

Transparency and Physiologic Aspects of the Lens

Lens Transparency

Transparency of the lens depends on the precise organization and maintenance of its elements. This is accomplished structurally by the orderly spatial distribution of the lens fibers and by the tight connections formed between them via specialized interdigitations (Fig 10-2). Light scatter is reduced by the minimized space between cells. Scatter is also diminished by the loss of nuclei and organelles as the lens fibers elongate and approach the visual axis. Light scatter alters lens transparency, thereby affecting vision. Loss of transparency can have beneficial effects. In the aging lens, accumulation of yellow chromophores protects the retina from shorter wavelengths of light.

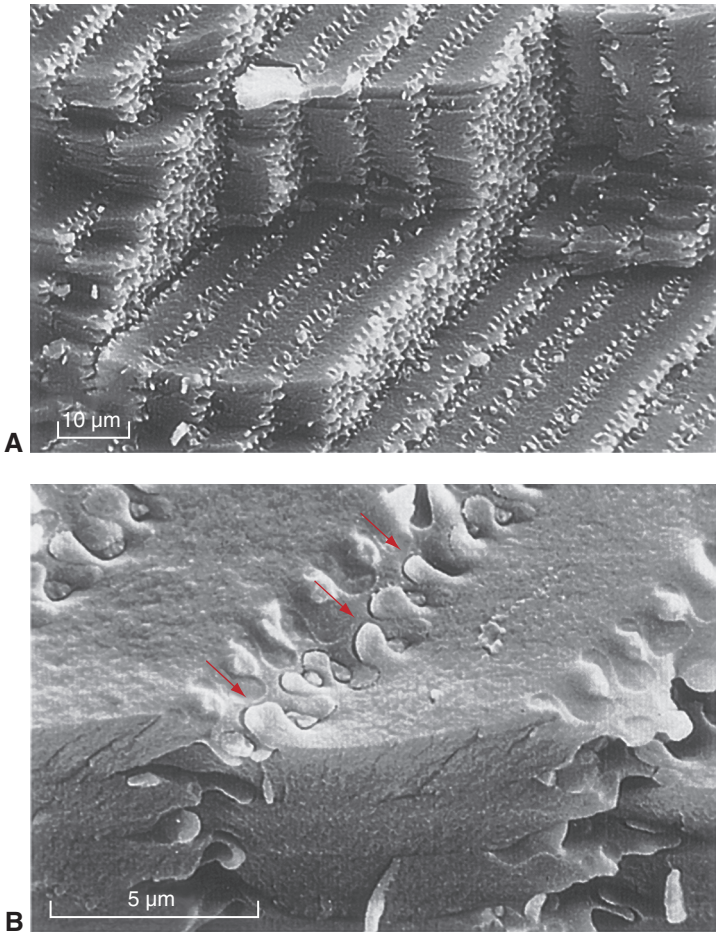


Figure 10-2 Scanning electron micrographs depicting the relationship between **(A)** hexagonal packing of lens fibers and **(B)** interdigitation *(arrows)*. *(Reproduced from Kessel RG, Kardon RH.* Tissues and Organs: A Text-Atlas of Scanning Electron Microscopy. *WH Freeman; 1979.)*

The cornea and aqueous humor protect the retina from wavelengths below the visible spectrum. The visible spectrum refers to the part of the electromagnetic spectrum that is perceived as light, with wavelengths generally ranging from 400 nm to 700 nm. Wavelengths shorter than 400 nm are referred to as *UV light*. Wavelengths of 300 nm or below are blocked by the cornea and by ascorbate (vitamin C), which is present at high levels in the aqueous humor. Wavelengths of 360 nm or below are blocked by the lens (Fig 10-3).

Lens Physiology

Because of its avascularity and mode of growth, the lens faces some unusual physiologic challenges. All nutrients must be obtained from the surrounding fluids. Likewise, all waste products must be released into those fluids. Most of the cells of the adult lens have reduced metabolic activity and lack the membrane machinery to regulate ionic homeostasis independently. Understanding how the lens maintains ionic balance and how solutes move from cell to cell throughout the lens is crucial to comprehending normal biology and the maintenance of lens transparency.

In the normal lens, sodium (Na^+) levels are low (~10 mmol/L), and potassium (K^+) levels are high (~120 mmol/L). In the aqueous humor, Na^+ levels are approximately 150 mmol/L, and K^+ levels are around 5 mmol/L. When normal regulatory mechanisms are abrogated, K^+ leaks out of the lens and Na^+ floods in, followed by chloride (Cl^-). Water then enters in response to the osmotic gradient, causing loss of transparency by altering the organization of lens fibers, as can occur following traumatic violation of the lens capsule.

The ionic balance in the lens is maintained primarily by Na^+,K^+-ATPase (also called *sodium-potassium pump*), an intrinsic membrane protein complex that hydrolyzes adenosine triphosphate (ATP) to transport Na^+ out of and K^+ into the lens; Figure 10-4 demonstrates the location of these pumps as well as the "pump-leak" hypothesis. Functional Na^+,K^+-ATPase is found primarily at the anterior surface of the lens, specifically in the

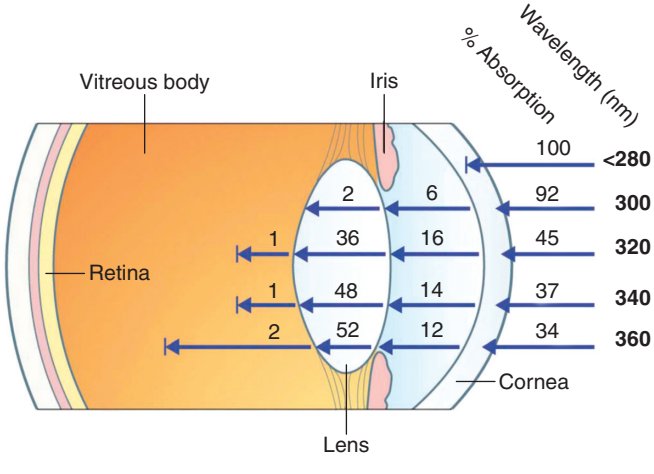


Figure 10-3 Blockage of ultraviolet light by the cornea, aqueous humor, and lens. *(Reproduced with permission from Levin LA, Nilsson SFE, Ver Hoeve J, Wu SM.* Adler's Physiology of the Eye. *11th ed. Elsevier/Saunders; 2011:114. Copyright 2011, Elsevier.)*

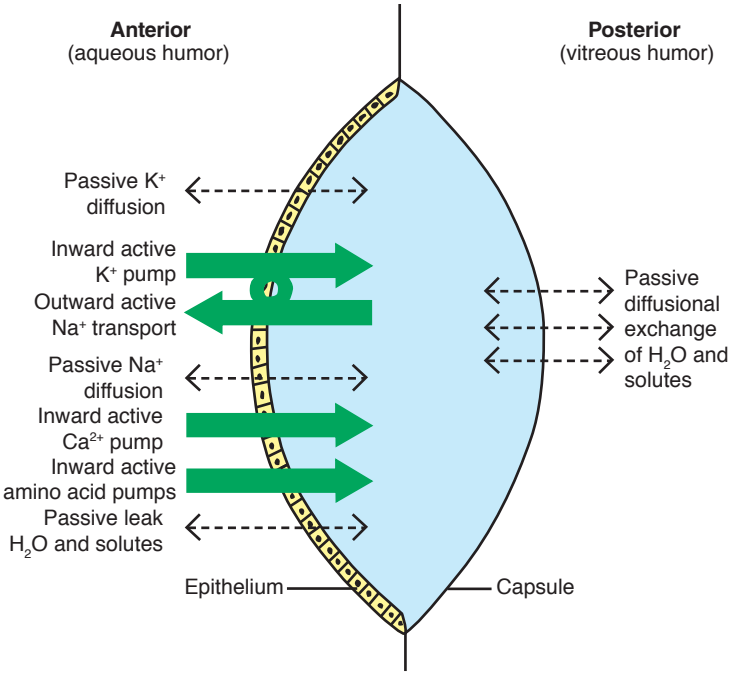


Figure 10-4 The pump–leak hypothesis of pathways of solute movement in the lens. The major site of active-transport mechanisms is the anterior epithelium. Passive diffusion occurs over both surfaces of the lens. *(Modified with permission from Paterson CA, Delamere NA. The lens. In: Hart WM Jr, ed.* Adler's Physiology of the Eye. *9th ed. Mosby; 1992:365.)*

epithelium and the outer, immature fibers. Studies using ouabain, a specific inhibitor of Na^+,K^+-ATPase, have established the pump's role as the primary determinant of the normal ionic state of the lens. Lens cells also contain membrane channels that pass ions; in particular, K^+-selective channels have been studied by patch-clamp techniques and found to be present primarily in the epithelial cells.

Lens cells communicate via gap junctions, which are thought to account for most ion and small-molecule movement between cells. In fact, the density of gap junctions in the lens-fiber cells is greater than that in all other cells in the body.

Lens Metabolism and Formation of Sugar Cataracts

Energy Production

Energy, in the form of ATP, is produced in the lens primarily through *glycolysis* in metabolically active cells in the anterior lens. This process is necessary because the oxygen tension in the lens is much lower than that in other tissues, given that oxygen reaches the avascular lens only via diffusion from the aqueous humor.

Most of the glucose entering the lens is phosphorylated to glucose-6-phosphate by hexokinase, the rate-limiting enzyme of the glycolytic pathway. Under normal conditions, most glucose-6-phosphate passes through glycolysis, wherein 2 molecules of ATP are

formed per original molecule of glucose. A small proportion of glucose-6-phosphate is metabolized through the *pentose phosphate pathway* (also called *hexose monophosphate shunt*). This pathway is activated under conditions of oxidative stress because it is responsible for replenishing the supply of nicotinamide adenine dinucleotide phosphate (NADPH) that becomes oxidized through the increased activity of glutathione reductase under such conditions (Fig 10-5).

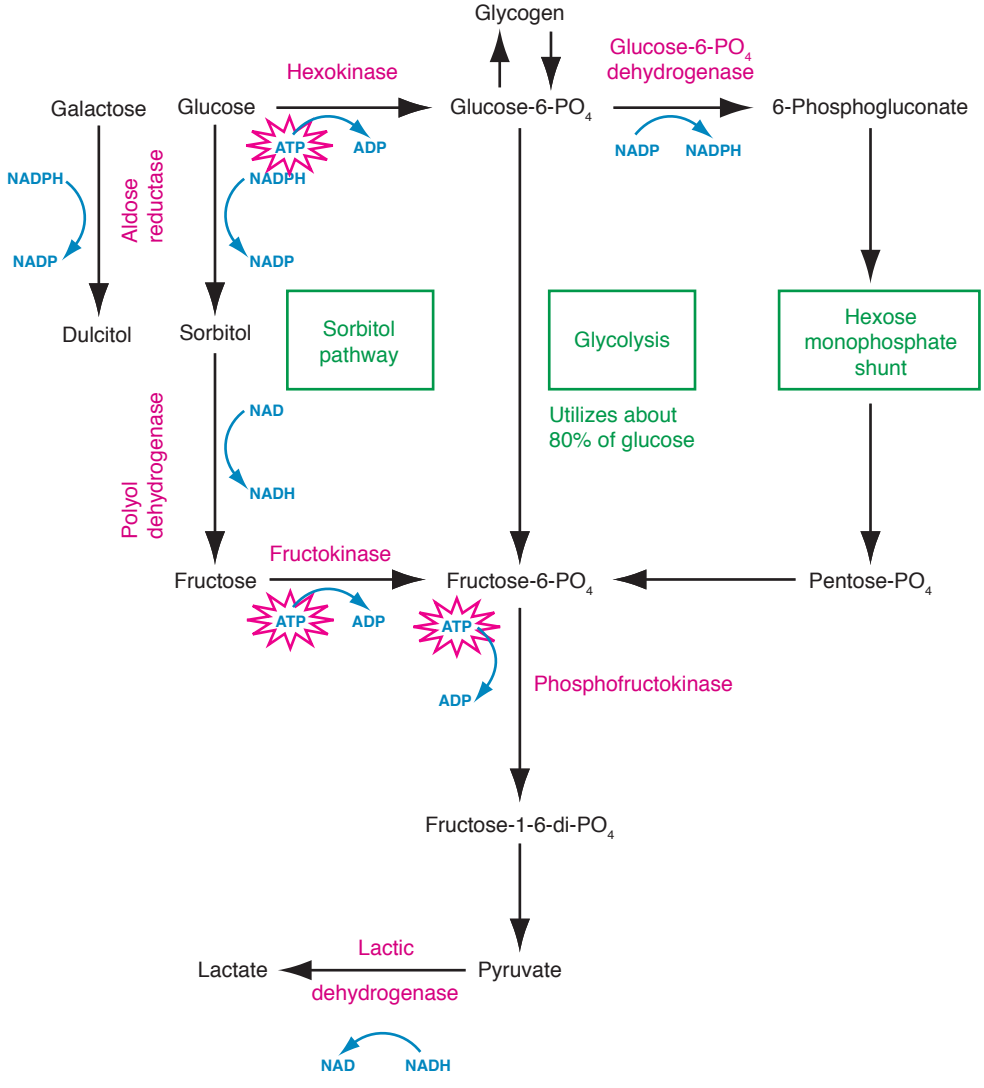


Figure 10-5 Glucose metabolism in the lens. Energy (adenosine triphosphate [ATP]) from glucose is derived primarily through glycolysis. Alternatively, glucose can participate in the hexose monophosphate shunt (also called *pentose phosphate pathway*), generating nicotinamide adenine dinucleotide phosphate (NADPH) for reduction-oxidation (redox) reactions. In cases of hyperglycemia or galactosemia, the polyol pathway (also called *sorbitol pathway*) has been implicated in the formation of cataract. *(Adapted with permission from Hart WM Jr, ed.* Adler's Physiology of the Eye: Clinical Application. *9th ed. Mosby; 1992:362.)*

Carbohydrate Cataracts

Sugar cataracts, which are associated with diabetes and galactosemia, have stimulated most of the research on lens carbohydrate metabolism. True diabetic cataract is a rapidly developing bilateral snowflake cataract (see Fig 5-19 in BCSC Section 11, *Lens and Cataract*) that appears in the lens cortex of persons with poorly controlled type 1 diabetes. Individuals with type 2 diabetes do not typically develop this type of cataract but do have a higher prevalence of age-related cataract with a slightly earlier onset. It is likely that for these patients, the diabetes is simply an additional factor contributing to the development of age-related cataracts.

Defects in galactose metabolism also cause cataracts. Classic galactosemia is caused by a deficiency of galactose-1-phosphate uridyltransferase. Infants with this inborn error of metabolism develop bilateral cataracts within a few weeks of birth unless milk (lactose) is removed from the diet. Cataracts are also associated with a deficiency of galactokinase.

Under certain conditions in which sugar levels are elevated significantly, some glucose (or galactose) is metabolized through the polyol pathway, also known as the sorbitol pathway (see Fig 10-5). Aldose reductase is the key enzyme for this pathway, and it converts the sugars into the corresponding sugar alcohols. Under normal conditions, little or no activity occurs through this pathway because aldose reductase has low affinity for glucose (or galactose). Under hyperglycemic conditions, however, aldose reductase competes with hexokinase for glucose (or galactose).

Studies in animal models have demonstrated the importance of the polyol pathway in experimental sugar cataracts. Animals with diabetes (either natural or induced) develop cataracts that are associated with the presence of sorbitol in the lens and with the influx of water. The *osmotic hypothesis* may account for these findings. According to this hypothesis, aldose reductase plays a central role in the pathology by increasing the sorbitol content of the lens. Sorbitol is largely unable to penetrate cell membranes and thus is trapped inside the cells. Because it is slow to convert to fructose via polyol dehydrogenase, sorbitol builds up in lens cells under conditions of hyperglycemia. As a result, it creates an osmotic pressure that draws water into the lens. This osmotic pressure swells the cells, damages membranes, and causes cataract.

Hejtmancik JF, Riazuddin SA, McGreal R, Liu W, Cvekl A, Shiels A. Lens biology and biochemistry. *Prog Mol Biol Transl Sci*. 2015;134:169–201.

CHAPTER 11

Vitreous

Highlights

- The vitreous represents up to 80% of the volume of the eye.
- The vitreous is most firmly attached to the retina at the vitreous base. Additional adhesion points include the posterior lens capsule (ligament of Weigert), perimacular region, and optic nerve margin, as well as along the retinal vessels.
- Vitreous liquefaction has been associated with loss of vitreous ascorbate and the development of posterior vitreous detachment.
- Pars plana vitrectomy increases the diffusion of oxygen in the posterior segment of the eye. The resultant increase in oxidative stress has been implicated in the acceleration of cataract formation after vitrectomy.

Overview

During formation of the eye, the *primary vitreous* contributes to the hyaloid artery, which nourishes the developing anterior segment and lens. Failure of the vitreous to regress following this stage leads to pathology of the anterior and/or posterior segment. See BCSC Section 6, *Pediatric Ophthalmology and Strabismus,* and Section 12, *Retina and Vitreous,* for further discussion of persistent fetal vasculature (also called *persistent hyperplastic primary vitreous*). The *secondary vitreous* consists of a gel matrix representing the largest structure of the eye and is routinely seen on clinical examination. The *tertiary vitreous* gives rise to the zonular fibers.

The vitreous accounts for four-fifths of the volume of the eye. In the adult eye, where the vitreous is a static structure, one of its main functions is to act as conduit for fluid across the vitreous cavity. It occupies a volume of 4 mL and has an osmotic pressure and index of refraction (1.334) similar to those of the aqueous humor. Its viscosity, however, is almost twice that of water. The basic physical structure of the vitreous is that of a gel composed of a collagen framework interspersed with molecules of hydrated hyaluronan, also known as *hyaluronic acid*. The hyaluronan contributes to the viscosity of the vitreous humor and is thought to help stabilize the collagen network.

The relative amounts of collagen determine whether the vitreous is a liquid or a gel. The rigidity of the gel is greatest in regions of highest collagen concentration: the peripheral (cortical) vitreous and the vitreous base. The collagen fibrils confer resistance to tensile forces and give plasticity to the vitreous; the hyaluronan resists compression and confers viscoelastic properties. Degeneration of these fibrils occurs in most of the population and may lead to retinal pathology.

Composition

The vitreous is composed primarily of water (~99%) and macromolecules (0.15%), including collagen, hyaluronan, and soluble proteins. There are very few resident cells in the vitreous; these are called *hyalocytes* (see Fig 11-3). In addition to the 2 major structural components, collagen and hyaluronan, several noncollagenous structural proteins and glycoproteins have been identified in the vitreous. They include chondroitin sulfate (versican), opticin, VIT1, and fibrillin. The human vitreous also contains hyaluronidase and at least 1 matrix metalloproteinase (MMP-2, or *gelatinase*), suggesting that turnover of vitreous structural macromolecules can occur.

Collagen

At present, more than 20 types of collagen are known, and the genes for several have been identified. Tropocollagen, the smallest molecular unit of the various collagen types, is arranged in a specific pattern to create collagen fibrils. Aggregation of fibrils, sometimes of different types, gives rise to collagen fibers. Vitreous collagen fibers are composed of 3 different collagen types (Fig 11-1):

- Type II fibrils are the major structural components of the fiber and are also found in cartilage.

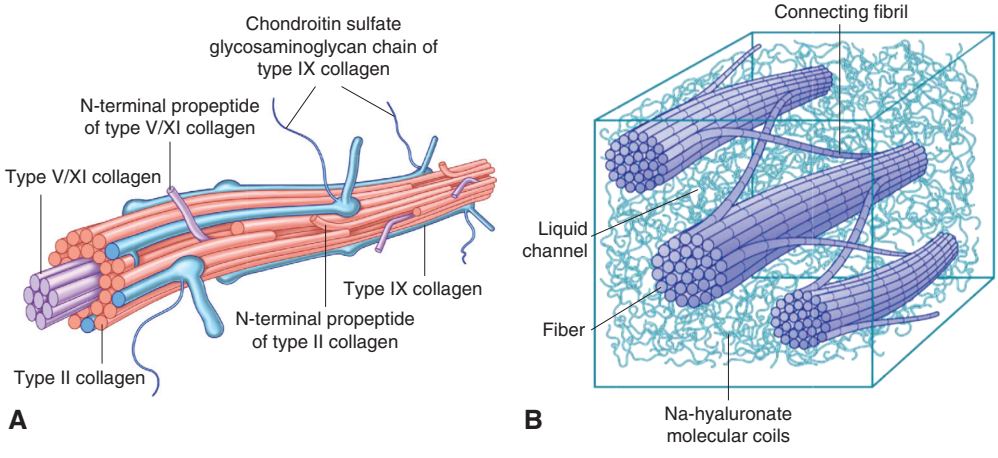


Figure 11-1 Vitreous collagen fiber. Collagen fibrils of different types combine to form the vitreous collagen fiber. **A,** Model for the structure of a collagen fiber from the vitreous. Type II collagen *(red)* forms the major structure of the vitreous, accounting for three-quarters of the total vitreous collagen. Type IX collagen *(blue),* the second most common collagen found in the vitreous, lies on the surface of the fiber. Type IX collagen is thought to protect type II collagen from degeneration. Type V/XI collagen *(purple)* is present in the core of the fibril and functions in fibrillogenesis. **B,** Vitreous collagen fibers are organized into bundles surrounded by sodium hyaluronate. *(Part A modified with permission from Schachat AP, Wilkinson CP, Hinton DR, Sadda SR, Widemann P.* Ryan's Retina. *5th ed. Elsevier; 2013:482. Part B modified with permission from Le Goff MM, Bishop PN. Adult vitreous structure and postnatal changes.* Eye (Lond). *2008;22(10):1214–1222.)*

- Type IX fibrils, found on the surface of the fiber, shield type II collagen fibrils and prevent them from fusing together, which can lead to condensation of vitreous collagen.
- Type V/XI fibrils, located in the core of collagen fibers, likely participate in the initial stages of fiber formation.

The vitreous collagens are closely related to the collagens of hyaline cartilage. They differ from the collagens commonly found in scar tissue and in tissues such as dermis, cornea, and sclera.

Collagen fibers are condensed in the peripheral vitreous, which comprises the cortical vitreous and has a thickness of approximately 100–300 μm. The vitreoretinal interface exists between the cortical vitreous and the internal limiting membrane (ILM). Interaction between the collagen fibers of the cortical vitreous (known as the *posterior hyaloid* over the posterior pole) and the ILM is mediated by laminin, fibronectin, and the proteoglycan chondroitin sulfate, among others (Fig 11-2). The adhesion of cortical vitreous to the ILM is relatively weak in the posterior pole compared with adhesion in the region near the vitreous base, where the fibers are firmly anchored to the peripheral retina and pars plana.

The points of physiologic vitreoretinal adhesion include the following:

- vitreous base
- optic nerve margin
- posterior lens capsule (ligament of Weigert)
- perimacular region
- along retinal vessels

CLINICAL PEARL

Although the posterior pole bolsters relatively weak vitreoretinal adhesion, the cortical vitreous maintains firmer attachment around the optic nerve. The collagen fiber anchors in this area are the last to separate as posterior vitreous detachment (PVD) occurs. A complete or partial ring within the posterior hyaloid is often visualized over the optic nerve as an indicator of PVD and creates a shadow on the retina, manifesting clinically as floaters. Other areas of vitreous adhesion can lead to posterior segment pathology when PVD occurs (see also BCSC Section 12, *Retina and Vitreous*).

Le Goff MM, Bishop PN. Adult vitreous structure and postnatal changes. *Eye (Lond).* 2008; 22(10):1214–1222.

Hyaluronan and Chondroitin Sulfate

Hyaluronan is present in nearly all vertebrate connective tissues and is nonimmunogenic. It is a polysaccharide (glycosaminoglycan, or GAG) that has a repeating unit of glucuronic acid and *N*-acetylglucosamine. At physiologic pH, hyaluronan is a weak polyanion because of the ionization of the carboxyl groups present in each glucuronic acid residue.

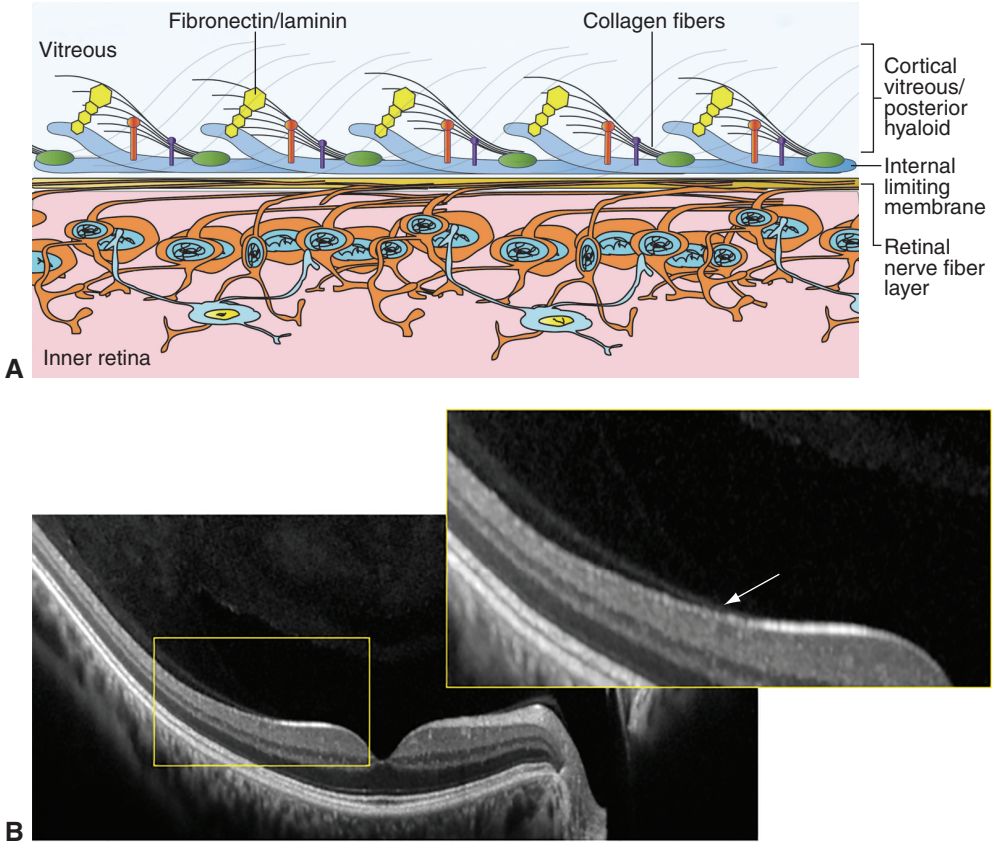


Figure 11-2 Vitreoretinal interface. **A,** Condensed collagen fibers in the peripheral vitreous form the cortical vitreous, which, over the posterior pole, is also known as the *posterior hyaloid.* The vitreoretinal interface lies between the collagen fibers of the posterior hyaloid and the internal limiting membrane (ILM). Interaction between the cortical collagen fibers and the ILM occurs via several macromolecules, including laminin and fibronectin. This interaction has been the target for pharmacologic cleavage facilitating posterior vitreous detachment. **B,** Optical coherence tomography scan of the vitreoretinal interface *(arrow).* *(Part A reproduced with permission from Barak Y, Ihnen MA, Schaal S. Spectral domain optical coherence tomography in the diagnosis and management of vitreoretinal interface pathologies.* J Ophthalmol. *2012;2012:876472. Part B courtesy of Vikram S. Brar, MD.)*

This ionization, together with the GAG residues, confers a negative charge on hyaluronan. The negative charge attracts sodium and thereby water, hydrating the vitreous. Production of hyaluronan begins around the time of birth, when the corresponding hydration is thought to contribute to vitreous transparency and growth of the eye.

In free solution, hyaluronan occupies an extremely high volume relative to its weight and may fill all the space in the vitreous except for that occupied by the collagen fibers (see Fig 11-1B). Hyaluronan molecules of the vitreous may undergo lateral interactions with one another, and such interactions may be stabilized by noncollagenous proteins. Both the concentration and the molecular weight of hyaluronan in the vitreous vary, depending on

the species and on the location in the vitreous body. Higher concentrations are typically found in the posterior pole.

Chondroitin sulfate is also a GAG, but unlike hyaluronan, it is sulfated. Chondroitin sulfate plays an independent role in maintaining the ultrastructure of the vitreous. Versican is the predominant form of chondroitin sulfate in the vitreous, where it interacts with hyaluronan. Versican has been reported to participate in the formation of the vitreous gel.

CLINICAL PEARL

Pathogenic variants (mutations) of the *VCAN* gene, which encodes versican, have been implicated in Wagner syndrome. Affected patients have an optically empty vitreous with peripheral condensation and retinal degeneration (see also BCSC Section 12, *Retina and Vitreous*).

Kloeckener-Gruissem B, Bartholdi D, Abdou M-T, Zimmermann DR, Berger W. Identification of the genetic defect in the original Wagner syndrome family. *Mol Vis*. 2006;12:350–355.

Theocharis DA, Skandalis SS, Noulas AV, Papageorgakopoulou N, Theocharis AD, Karamanos NK. Hyaluronan and chondroitin sulfate proteoglycans in the supramolecular organization of the mammalian vitreous body. *Connect Tissue Res*. 2008;49(3):124–128.

Soluble and Collagen Fiber–Associated Proteins

Many proteins remain in solution after the collagen fibers and other insoluble elements present in the vitreous gel are removed by filtration or centrifugation. Serum albumin is the major soluble vitreous protein, followed by transferrin. Other proteins include neutrophil elastase inhibitor (which may play a role in resisting neovascularization) and tissue plasminogen activator (which may have a fibrinolytic role in the event of vitreous hemorrhage). The concentration of serum proteins in the vitreous gel depends on the integrity of the retinal vasculature and the degree of intraocular inflammation. Consequently, if the blood–ocular barrier is compromised, the concentration of soluble proteins within the vitreous cavity can rise dramatically.

Some structural proteins are specifically associated with the collagen fibers. These include a leucine-rich repeat glycoprotein called *opticin,* which is produced in the nonpigmented epithelium (NPE) of the ciliary body, and another glycoprotein called VIT1. Both opticin and VIT1 are thought to play key roles in the structure of collagen fibers and to interact with proteoglycans within the vitreous.

Zonular Fibers

Some zonular fibers are present in the anterior vitreous and can be observed by electron microscopy. However, most of these fibers form the zonular apparatus, which is the structural connection between the lens and the ciliary body. The major structural protein of these fibers is a large linear protein named *fibrillin,* which has an unusually high cysteine content.

CLINICAL PEARL

Defects in fibrillin-1 are present in individuals with Marfan syndrome, some of whom experience spontaneous lens subluxation and premature vitreous liquefaction, which can lead to retinal detachment.

Low-Molecular-Weight Solutes

Ions and organic solutes in the vitreous originate from adjacent ocular tissues and blood plasma. The barriers that control their entry into the vitreous include the following:

- vascular endothelium of iris vessels
- NPE of the ciliary body
- inner wall endothelium of Schlemm canal
- vascular endothelium of retinal vessels
- retinal pigment epithelium (RPE)

Together, these structures constitute the blood–ocular barrier. The concentrations of sodium (Na^+) and chloride (Cl^-) in the vitreous are similar to those in plasma, but the concentration of potassium (K^+) is higher than that in plasma, as is that of ascorbate.

Bishop PN. Structural macromolecules and supramolecular organisation of the vitreous gel. *Prog Retin Eye Res.* 2000;19(3):323–344.

Mayne R, Brewton RG, Ren Z-X. Vitreous body and zonular apparatus. In: Harding JJ, ed. *Biochemistry of the Eye.* Chapman & Hall Medical; 1997:135–143.

Hyalocytes

Under normal physiologic conditions, the vitreous cavity has very few cells. The predominant cell type is the hyalocyte (Fig 11-3). The highest concentration of these cells exists at the vitreous base and in the posterior cortical vitreous. Hyalocytes possess phagocytic properties, process antigens, and thereby regulate the immunologic response within the vitreous cavity. A process similar to anterior chamber–associated immune deviation (ACAID) occurs in the vitreous cavity (VCAID) and is likely mediated by hyalocytes.

CLINICAL PEARL

In specimens obtained after PVD, hyalocytes have been found on the surface of the retina, where they contribute to formation of idiopathic epiretinal membranes (also known as *macular pucker* or *cellophane maculopathy*).

Sakamoto T, Ishibashi T. Hyalocytes: essential cells of the vitreous cavity in vitreoretinal pathophysiology? *Retina.* 2011;31(2):222–228.



Figure 11-3 Hyalocyte within the cortical vitreous. *Arrows* indicate granules. C = chromatin; CF = collagen fibril; M = mitochondrion; Mi = microvillus; N = nucleus; V = vacuole. *(Modified with permission from Schachat AP, Wilkinson CP, Hinton DR, Sadda SR, Widemann P.* Ryan's Retina. *4th ed. Elsevier; 2001:1923.)*

Biochemical Changes With Aging and Disease

Vitreous Liquefaction and Posterior Vitreous Detachment

The human vitreous gel undergoes progressive liquefaction beginning around 40 years of age, so that typically by age 80–90 years, more than half of the vitreous is liquid. A crucial step in the process of vitreous liquefaction is the breakdown of the thin (12–15-nm) collagen fibrils into smaller fragments. Implicated in this process is reduced shielding of type II collagen fibrils due to the age-related exponential loss of type IX collagen. Some proteolytic enzymes, such as plasminogen, may have elevated vitreous concentrations with increasing age, but others, such as MMP-2, do not.

The fragments aggregate into thicker fibers, or *fibrillar opacities,* which are visible with low-power slit-lamp microscopy. As liquefaction proceeds, the collagen fibers condense into the residual gel phase and are absent from (or in low concentration in) the liquid phase. In terms of hyaluronan concentration or molecular weight, there are no differences between the gel and liquid phases. With increasing age, a weakening of adhesion occurs at the vitreoretinal interface, which lies between the cortical vitreous gel and the ILM. These combined processes eventually result in PVD in approximately 50% of individuals after 50 years of age.

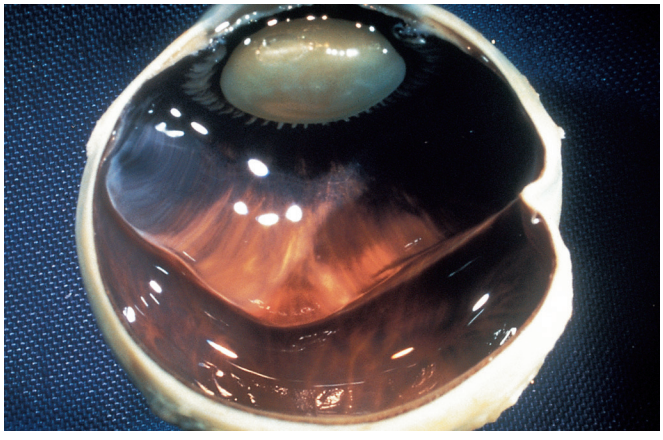


Figure 11-4 Posterior vitreous detachment (PVD). Gross photograph of an eye with PVD. The vitreous gel remains anchored anteriorly at the vitreous base, having separated from the posterior pole. *(Courtesy of Hans E. Grossniklaus, MD.)*

PVD is a separation of the cortical vitreous gel from the ILM as far anteriorly as the posterior border of the vitreous base; the separation does not extend into the vitreous base owing to the unbreakable adhesion between the vitreous and retina in that zone (Fig 11-4). PVD is often a sudden event, during which liquefied vitreous from the center of the vitreous body passes through a hole in the posterior vitreous cortex, at its attachment to the optic nerve, and then dissects the residual cortical vitreous away from the ILM. As the residual vitreous gel collapses anteriorly within the vitreous cavity, retinal tears sometimes occur in areas where the retina is more strongly attached to the vitreous than the surrounding retina can withstand, which subsequently can result in rhegmatogenous retinal detachment. Anomalous PVD can lead to the formation of epiretinal membranes and macular holes (see BCSC Section 12, *Retina and Vitreous*).

Bishop PN, Holmes DF, Kadler KE, McLeod D, Bos KJ. Age-related changes on the surface of vitreous collagen fibrils. *Invest Ophthalmol Vis Sci*. 2004;45(4):1041–1046.

Fincham GS, James S, Spickett C, et al. Posterior vitreous detachment and the posterior hyaloid membrane. *Ophthalmology*. 2018;125(2):227–236.

Myopia

Myopia is associated with faster liquefaction and earlier development of PVD. Vitreous samples taken from myopic eyes exhibit a higher concentration of MMP-2. MMPs are proteases involved in remodeling extracellular matrices, such as the vitreous. Physiologically, MMPs can facilitate cell differentiation, proliferation, and migration. Pathologically, they participate in inflammatory responses and promote angiogenesis. Premature vitreous liquefaction may be a result of increased MMP activity, leading to vitreoretinal pathologies in myopic individuals.

Zhuang H, Zhang R, Shu Q, et al. Changes of TGF-β2, MMP-2, and TIMP-2 levels in the vitreous of patients with high myopia. *Graefes Arch Clin Exp Ophthalmol*. 2014;252(11):1763–1767.

Vitreous as an Inhibitor of Angiogenesis

Numerous studies have shown that the normal vitreous is an inhibitor of angiogenesis. This inhibitory activity is decreased in proliferative diabetic retinopathy. However, the molecular basis of the phenomenon remains poorly understood. Known inhibitors of angiogenesis, such as thrombospondin 1 and pigment epithelium–derived factor, are present within the mammalian vitreous and may inhibit angiogenesis in healthy eyes. The vitreous protein opticin also suppresses angiogenesis in mouse models of retinal neovascularization. In contrast, the level of vascular endothelial growth factor (VEGF), a promoter of angiogenesis, is markedly elevated in the vitreous of patients with proliferative diabetic retinopathy, a condition in which the vitreous also acts as a scaffold for retinal neovascularization.

Le Goff MM, Lu H, Ugarte M, et al. The vitreous glycoprotein opticin inhibits preretinal neovascularization. *Invest Ophthalmol Vis Sci.* 2012;53(1):228–234.

Physiologic Changes After Vitrectomy

Most of the changes in ocular physiology that occur after vitrectomy result from altered viscosity in the vitreous cavity; when the vitreous is removed, the viscosity decreases between 300- and 2000-fold. Consequently, growth factors and other compounds, such as antibiotics, transfer between the posterior and anterior segments more easily and are also cleared more quickly from the eye. This effect is proportional to the change in diffusion coefficient, which is of the same magnitude as the change in viscosity.

Fluid currents that move solutes even more rapidly may be present. In particular, oxygen movement is accelerated. The oxygen gradient that exists between the well-oxygenated anterior segment and the posterior segment under normal physiologic conditions is abolished, increasing oxygen tension in the vitreous cavity. Under physiologic conditions, vitreous ascorbate combines with oxygen, forming dehydroascorbate and water. However, after pars plana vitrectomy, oxygen levels exceed the capacity of ascorbate, leading to increased oxidative stress at the posterior pole of the lens and the development of cataract (Fig 11-5).

Holekamp NM, Shui Y-B, Beebe DC. Vitrectomy surgery increases oxygen exposure to the lens: a possible mechanism for nuclear cataract formation. *Am J Ophthalmol.* 2005;139(2):302–310.

Shui Y-B, Holekamp NM, Kramer BC, et al. The gel state of the vitreous and ascorbate-dependent oxygen consumption: relationship to the etiology of nuclear cataracts. *Arch Ophthalmol*. 2009;127(4):475–482.

Injury With Hemorrhage and Inflammation

Injury to the eye can cause inflammation and, in many cases, intraocular hemorrhage. If blood penetrates the vitreous cortex, platelets come into contact with vitreous collagen, aggregate, and initiate clot formation. The clot then stimulates a phagocytic inflammatory reaction, and the vitreous liquefies in the area of a hemorrhage. The subsequent inflammatory reaction varies in degree for unknown reasons and may result in proliferative vitreoretinopathy (see also BCSC Section 12, *Retina and Vitreous*).

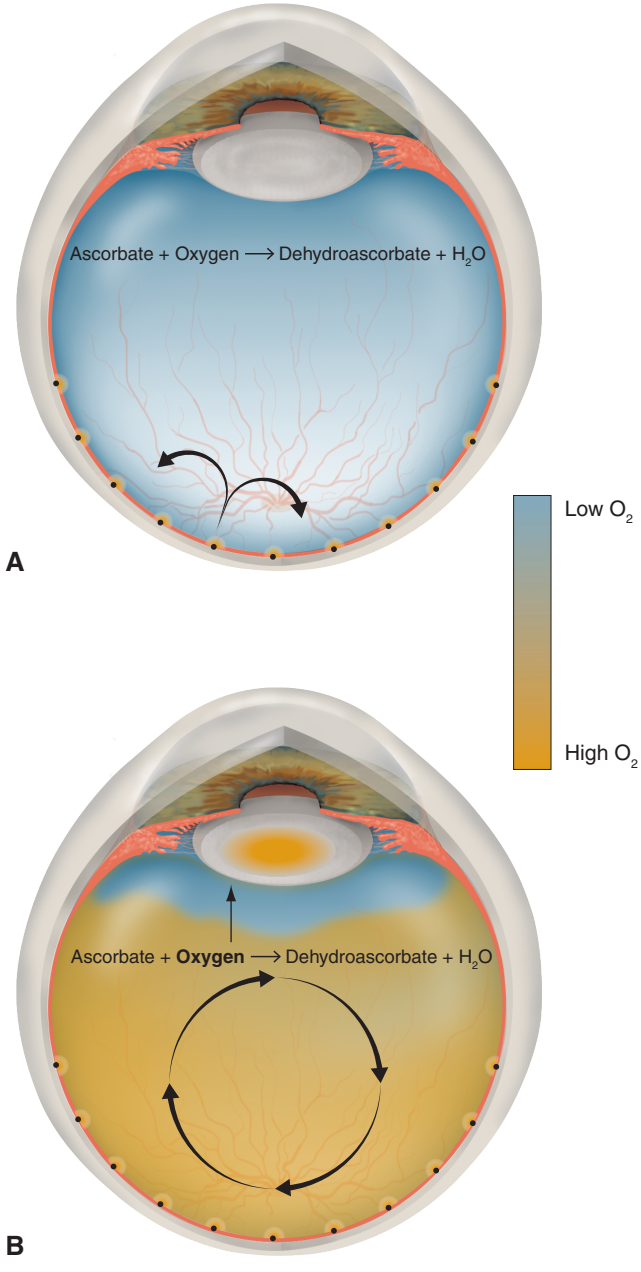


Figure 11-5 The role of ascorbate in the vitreous cavity. **A,** The vitreous acts as a barrier to the diffusion of oxygen within the posterior segment. The available ascorbate binds with oxygen, forming dehydroascorbate, which is taken up by surrounding cells. **B,** In postvitrectomized eyes, the amount of oxygen exceeds the capacity for clearance, leading to the production of reactive compounds that create oxidative stress in the lens, which in turn accelerates cataract formation. *(Illustration by Cyndie C.H. Wooley.)*

Genetic Disease Involving the Vitreous

Stickler syndrome is most commonly due to a pathogenic variant of the gene *COL2A1,* which codes for type II collagen, a major component of vitreous collagen fibers. Affected patients have an optically empty vitreous due to premature liquefaction with peripheral condensation, which may induce retinal detachment (see also BCSC Section 12, *Retina and Vitreous*). Pathogenic variants of both the α_1(II) and α_1(XI) collagen chains are responsible for this syndrome.

Wagner syndrome is another condition in which patients present with an optically empty vitreous and have an increased risk of retinal detachment. As mentioned earlier in this chapter, this condition is caused by pathogenic variants of the *VCAN* gene, encoding versican, which participates in formation of the vitreous gel.

Robin NH, Moran RT, Ala-Kokko L. Stickler syndrome. In: Adam MP, Everman DB, Mirzaa GB, et al, eds. *GeneReviews* [Internet]. University of Washington, Seattle; 1993–2019. Accessed February 2, 2023. www.ncbi.nlm.nih.gov/books/NBK1302

Enzymatic Vitreolysis

Considerable interest exists in enzyme preparations that can be injected into the vitreous cavity to help clear blood from the vitreous and induce PVD. Enzymes that have been proposed for injection include hyaluronidase, plasmin, dispase, and chondroitinase. Clinical trials with hyaluronidase and collagenase failed to induce PVD. However, ocriplasmin, which cleaves fibronectin and laminin (see Fig 11-3), was better able to induce PVD than placebo and demonstrated efficacy in nonsurgical management of vitreomacular traction and macular holes. Because of subsequent reports describing retinal changes on optical coherence tomography and altered electroretinogram following administration of ocriplasmin, the use of this agent is limited (see also BCSC Section 12, *Retina and Vitreous*).

Fahim AT, Khan NW, Johnson MW. Acute panretinal structural and functional abnormalities after intravitreous ocriplasmin injection. *JAMA Ophthalmol.* 2014;132(4):484–486.

Gandorfer A. Enzymatic vitreous disruption. *Eye (Lond).* 2008;22(10):1273–1277.

Stalmans P, Benz MS, Gandorfer A, et al; MIVI-TRUST Study Group. Enzymatic vitreolysis with ocriplasmin for vitreomacular traction and macular holes. *N Engl J Med.* 2012;367(7):606–615.

Tibbetts MD, Reichel E, Witkin AJ. Vision loss after intravitreal ocriplasmin: correlation of spectral-domain optical coherence tomography and electroretinography. *JAMA Ophthalmol.* 2014;132(4):487–490.

CHAPTER 12

Retina

This chapter includes a related video. Go to www.aao.org/bcscvideo_section02 or scan the QR code in the text to access this content.

Highlights

- Because of its high metabolic activity, the retina has the highest rate of oxygen consumption of any tissue in the human body.
- Retinal neurons (photoreceptor, bipolar, horizontal, amacrine, and ganglion cells), glial cells (Müller cells, astrocytes, and microglia), and vascular cells (endothelial cells and pericytes) together form a functional neurovascular unit that converts light into a neural signal.
- Light induces hyperpolarization, leading to a cascade of reactions in the photoreceptor outer segments called phototransduction, which in turn converts light energy into an electrical impulse.
- Rods are highly sensitive and can be stimulated by a single photon, whereas cone photoreceptors can adapt to a wider range of light intensities.
- Pathogenic gene variants (mutations) that affect components of the phototransduction pathway may lead to inherited retinal dystrophies with varying clinical phenotypes.

Overview

Two laminar structures line the back of the eye: the retinal pigment epithelium (RPE) and the neurosensory retina. This chapter discusses the neurosensory retina; the RPE is discussed in Chapter 13. These laminar structures arise from an invagination of the embryonic optic cup that folds the neuroectodermal layer into apex-to-apex contact with itself, creating the subretinal space. The 2 layers form a hemispheric shell on which the visual image is focused by the anterior segment of the eye. The retina comprises neural, glial, and vascular components.

The neural retina contains multiple types of cells (see also Chapter 2):

- photoreceptors (rods and 3 types of cones)
- bipolar cells (rod on-bipolar cells and cone on- and off-bipolar cells)
- interneurons (horizontal and amacrine cells)
- ganglion cells and their axons, which form the retinal nerve fiber layer (NFL) and the optic nerve

- glial cells, including astrocytes, Müller cells, and microglia
- endothelial cells and supporting cells

Retinal Oxygen Consumption

The retina consumes oxygen at a higher rate than other tissues in the body and requires a continuous supply of oxygen. Oxygen tension is highest in the choroid and adjacent RPE and varies in the inner and outer retina, based on location within the retina and light versus dark adaptation. Retinal oxygenation maintains the following:

- dual circulation
- autoregulation of retinal vasculature
- concentration of mitochondria in the photoreceptor inner segments
- lack of metabolic regulation of choroidal vasculature

Perfusion via dual circulation ensures that the high metabolic demands of the retina are met under physiologic conditions. The vascular elements responsible for supplying oxygen to the retina are described in Chapter 2 of this volume and in BCSC Section 12, *Retina and Vitreous*. Although there is no autonomic regulation of the retina vessels, local oxygen levels maintain flow through autoregulation to ensure stable oxygen tension in the inner retina despite changes in systemic oxygen levels. The high oxygen tension in the choroid supplies the photoreceptors and their respective nuclei. Photoreceptor mitochondria, which generate adenosine triphosphate (ATP), are concentrated in the ellipsoid layer of the inner segments. This layer is easily identified on optical coherence tomography (see Chapter 2, Fig 2-40). The choroidal vasculature does not possess an autoregulatory mechanism and is thus susceptible to changes in systemic oxygenation.

Wangsa-Wirawan ND, Linsenmeier RA. Retinal oxygen: fundamental and clinical aspects. *Arch Ophthalmol.* 2003;121(4):547–557.

Photoreceptors and Phototransduction

Phototransduction is the process by which photosensitive cells in the retina convert light energy into an electrical impulse that is transmitted to the brain. Rods and cones are highly polarized photoreceptor cells that capture energy from photons and generate a neural response. Rods are highly sensitive and can be stimulated by a single photon. Cones are less sensitive than rods, but they can adapt to a wider range of light intensities and respond more rapidly to repetitive stimulation.

Rod Phototransduction

Most of our knowledge of phototransduction comes from information about rods, which are sensitive nocturnal light detectors. Considerably more biochemical material can be obtained from rods than from cones because rods are much more numerous in most

retinas. In addition, rods contain far more membrane (ie, surface area) than do cones, contributing to the rods' greater sensitivity to detect light.

The outer segment of photoreceptors contains all the components required for phototransduction. It is composed primarily of plasma-membrane material organized into discs flattened perpendicular to the long axis of the outer segment (see Chapter 2, Fig 2-39). There are approximately 1000 discs within a rod outer segment and 1 million membrane-bound rhodopsin molecules in each disc. The discs float within the cytoplasm of the outer segment like a stack of coins disconnected from the plasma membrane. The discs contain the protein machinery to capture and amplify light energy. This abundance of outer-segment membrane increases the number of rhodopsin molecules, which can absorb light. Some deep-sea fish, which need considerable sensitivity to detect small amounts of light, rely on longer rod segments than those found in humans.

Rhodopsin is a freely diffusible membrane protein with 7 helical loops that is embedded in the lipid membrane (Fig 12-1). Rhodopsin absorbs green light best at wavelengths

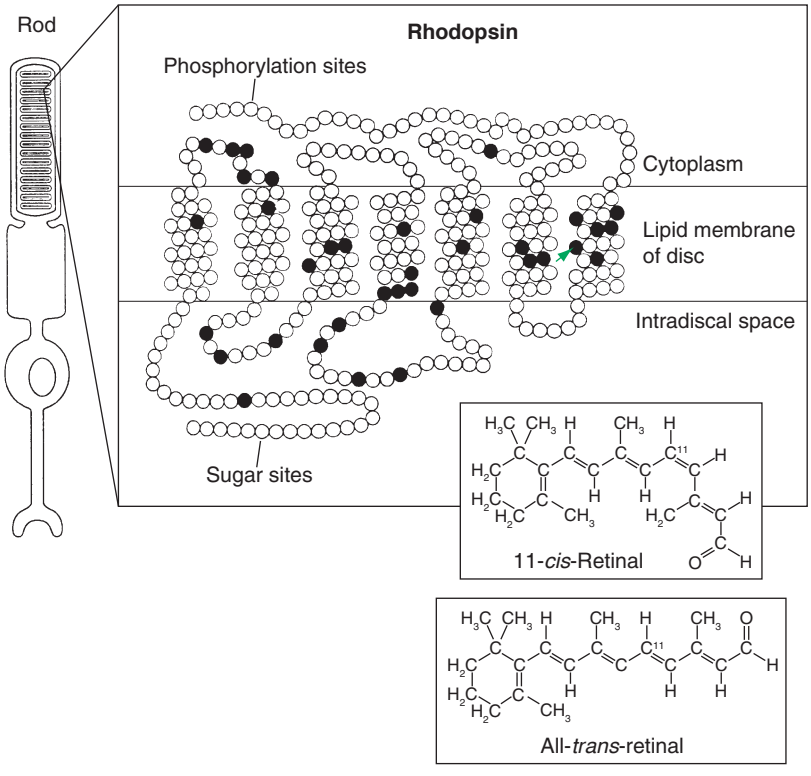


Figure 12-1 The rhodopsin molecule is embedded in the lipid membrane of the outer segment with 7 helical loops. Each circle represents an amino acid, and the highly conserved ones are shown in *black*. The *green arrow* represents the lysine to which the vitamin A chromophore is linked. Phosphorylation sites occur on the cytoplasmic and sugar attachment sites on the intradiscal (extracellular) ends of the rhodopsin molecule. Insets show the structures of 11-*cis*-retinal and all-*trans*-retinal. *(Courtesy of Peter Gouras, MD.)*

of approximately 510 nm. It absorbs blue and yellow light less well and is insensitive to longer wavelengths (ie, red light). Rhodopsin is tuned to this part of the electromagnetic spectrum by its amino-acid sequence and by the binding of its chromophore 11-*cis*-retinal (also called 11-*cis*-retinaldehyde), which creates a molecular antenna.

The plasma membrane of the outer segment contains cationic cyclic nucleotide–gated (CNG) channels, which are gated by cyclic guanosine monophosphate (cGMP). This channel controls the flow of sodium (Na^+) and calcium (Ca^{2+}) ions into the outer segment. In the dark, Na^+ and Ca^{2+} flow in through the channel, which is kept open by cGMP. Ionic balance is maintained by Na^+,K^+-ATPase (also called the *sodium-potassium pump*) in the inner segment and an Na^+,K^+-Ca^{2+} exchanger in the outer-segment membrane, both of which require metabolic energy.

This flow of ions sets up the circulating dark current that keeps the photoreceptor's membrane potential in a relatively depolarized state. The depolarized state of the photoreceptors causes a steady release of the inhibitory transmitter glutamate from its synaptic terminal in the dark (Fig 12-2). Bipolar cells are thereby held in an inactive state as long as the rhodopsin molecule is not exposed to light.

Light activation of rhodopsin starts a series of reactions that lead to hyperpolarization of the photoreceptor's membrane potential (Fig 12-3). Once rhodopsin absorbs a quantum of light, the 11-*cis* double bond of retinal is reconfigured (creating all-*trans*-retinal, also called all-*trans*-retinaldehyde), and the opsin molecule undergoes a series of rapid configurational changes to an activated state known as *metarhodopsin II,* initiating a signal transduction cascade.

Light-activated rhodopsin triggers a second molecule, transducin, by causing an exchange of guanosine diphosphate (GDP) for guanosine triphosphate (GTP) (see Fig 12-3A). One rhodopsin molecule can activate 100 transducin molecules, amplifying the reaction. Activated transducin excites a third protein, cGMP phosphodiesterase (PDE), which hydrolyzes cGMP to 5′-noncyclic GMP. The decrease in cGMP closes the CNG channels, which stops entry of Na^+ and Ca^{2+} and hyperpolarizes the rod. Hyperpolarization stops the release of glutamate from the synaptic terminal.

With the suppression of glutamate removed, the bipolar cells depolarize. The ensuing signal is conveyed to the ganglion cell and then to the lateral geniculate body. The change in polarization of the cells in the retina following exposure to light can be measured and used to study the retina. See the section Retinal Electrophysiology later in this chapter.

Recovery of the dark current requires that the catalytically active components of the phototransduction cascade (Video 12-1) be fully quenched and cGMP resynthesized to allow opening of the CNG channels. With the CNG channels closed, hyperpolarization of the photoreceptor cell occurs due to sequestration of Na^+ and Ca^{2+} outside the disc membrane. Ca^{2+} regulates the function of many proteins within the cell, including recoverin and retinal guanylate cyclase (also called *guanylyl cyclase*). A decrease in intracellular Ca^{2+} levels releases recoverin from rhodopsin kinase (RK) (see Fig 12-3B). RK phosphorylates rhodopsin to facilitate binding with arrestin, thereby arresting or deactivating rhodopsin (see Fig 12-3B). Subsequently, transducin and PDE activity diminishes. In the absence of PDE, hydrolysis of cGMP ceases to provide cGMP to open the CNG channels. This

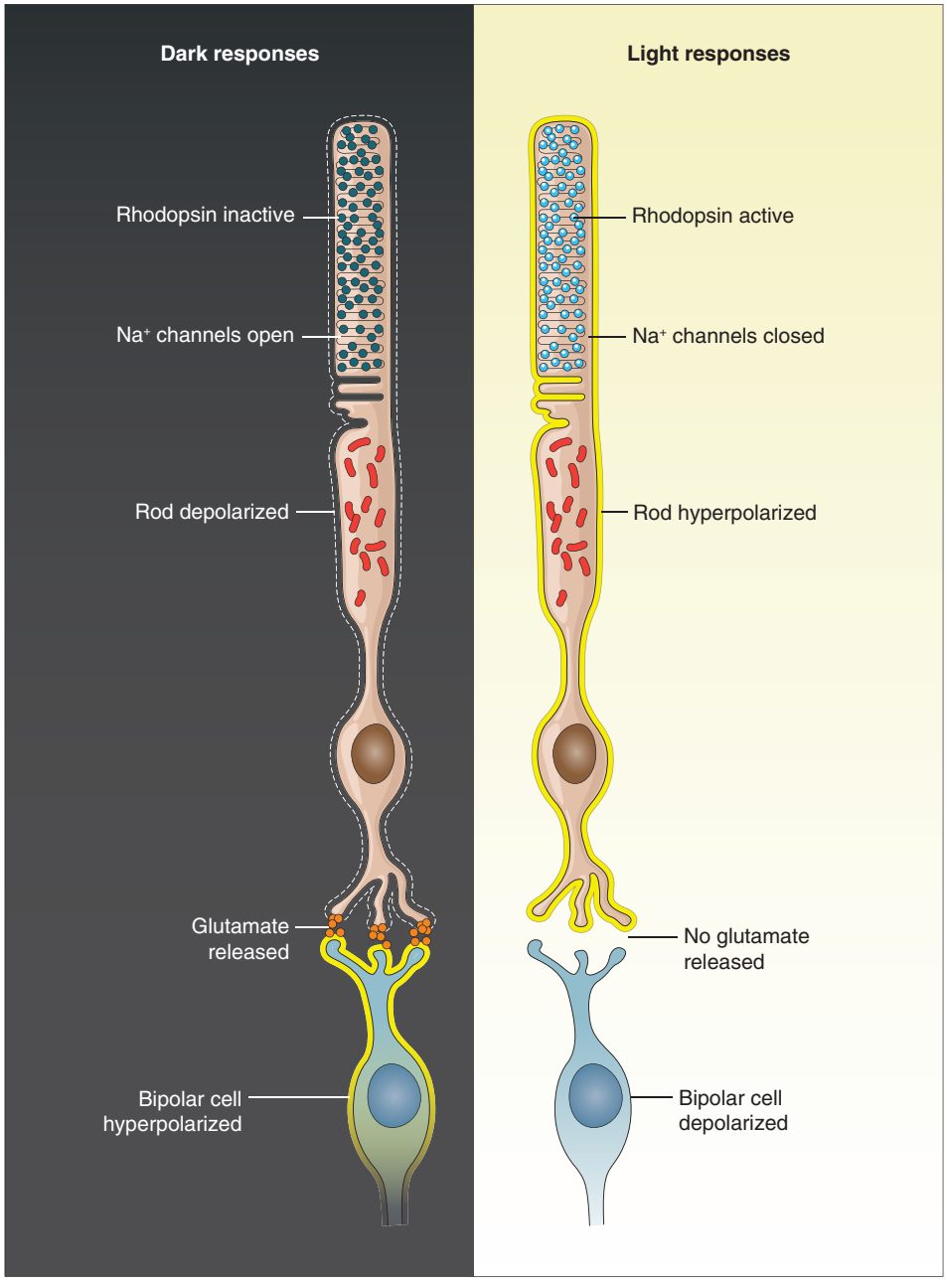


Figure 12-2 Dark current and light response. *(Left)* In the dark, rhodopsin is inactive; the cyclic nucleotide–gated (CNG) channels in the outer segment are open; and the rod is depolarized with a steady release of glutamate from its axonal terminal. The inhibitory neurotransmitter glutamate maintains the bipolar cell in a hyperpolarized or off state. *(Right)* Rhodopsin is activated by light, which leads to closing of the CNG channels, rod membrane hyperpolarization, and inhibition of glutamate release from the axon terminal. The bipolar cell then depolarizes, sending a signal to the ganglion cell and eventually the lateral geniculate nucleus. *(Illustration by Mark Miller.)*

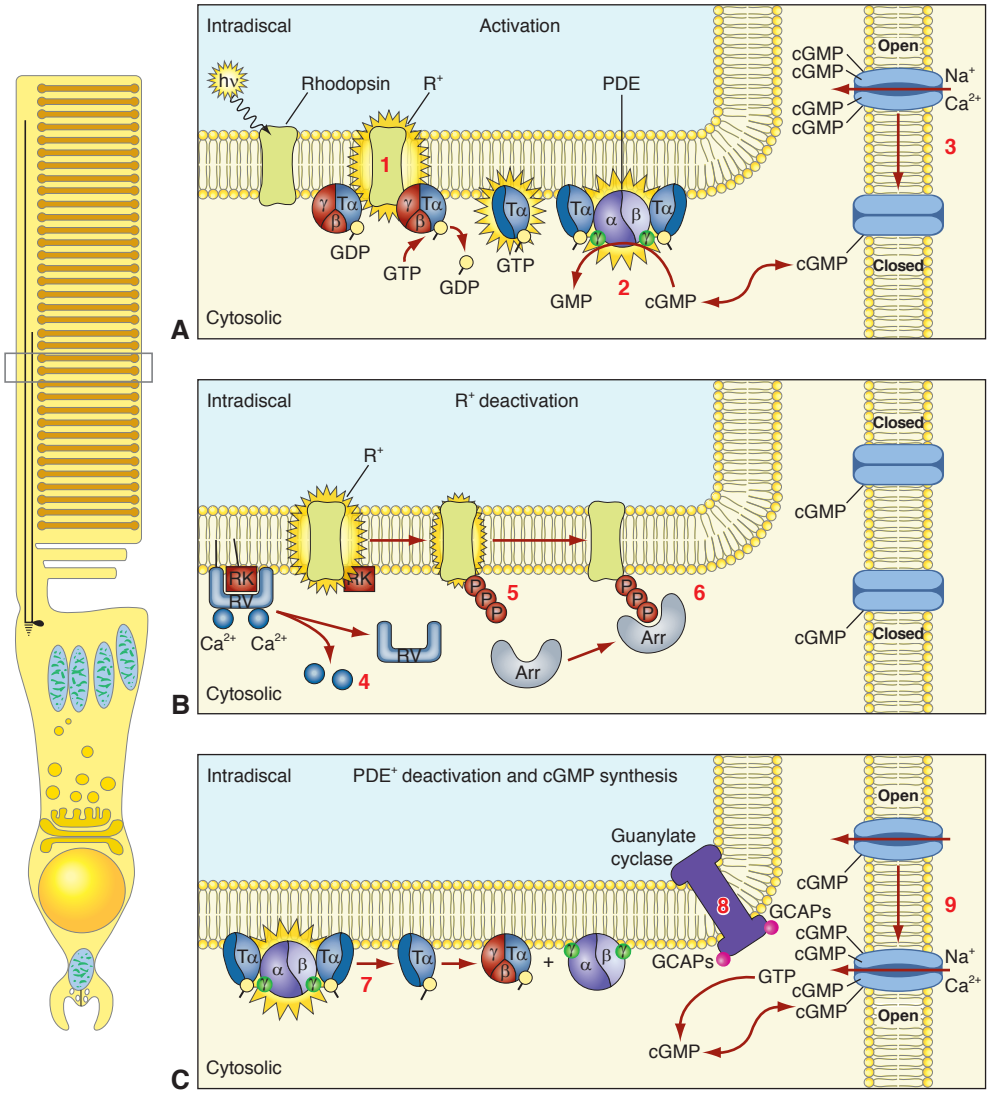


Figure 12-3 Schematic representation of the phototransduction cycle in photoreceptor outer segments. **A, (1)** Light-activated rhodopsin (R^*) causes levels of cGMP to be reduced via **(2)** transducin-disinhibited phosphodiesterase (PDE), leading to **(3)** closure of cGMP voltage-gated channels (CNG) and subsequent hyperpolarization of the photoreceptor cell. **B, (4)** As calcium levels decrease following closure of cGMP voltage-gated channels, recoverin (RV) dissociates from rhodopsin kinase (RK). Phosphorylation is mediated by rhodopsin kinase (RK), which is regulated by recoverin (RV). **(5)** R^* is deactivated through phosphorylation (indicated by Ps) and the binding of the protein arrestin (Arr). **(6)** Arrestin binds to phosphorylated R^*, completing the process. **C, (7)** cGMP levels are restored through deactivation of transducin (T) via its intrinsic GTPase activity. **(8)** PDE activity then decreases and guanylate cyclase activity increases, allowing **(9)** cGMP levels to rise and open the voltage-gated channels. cGMP = cyclic guanine monophosphate; GCAP = guanylate cyclase–activating protein; GDP = guanosine diphosphate; GTP = guanosine triphosphate; Tα, Tβ, Tγ = subunits of transducin. *(Modified with permission from Ryan SJ, Schachat AP, Wilkinson CP, Hinton DR, Sadda SR, Wiedemann P.* Retina. *5th ed. Saunders/Elsevier; 2013:Fig 14-4.)*

process is further supported by increased guanylate cyclase activity in the absence of Ca^{2+}, providing additional cGMP to help restore the resting state.



VIDEO 12-1 Phototransduction cascade in photoreceptor outer segments.

Animation developed by Mandeep Singh Dhalla, MD. Illustration modified with permission from Ryan SJ, Schachat AP, Wilkinson CP, Hinton DR, Sadda SR, Wiedemann P. Retina. *5th ed. Saunders/Elsevier; 2013:Fig 14-4.*



Although the phototransduction cascade has been most extensively studied in rods, a similar process occurs in cone outer segments; see the section Cone Phototransduction later in this chapter.

"Rim" proteins

The discs of rod outer segments differ from those of cones in that they are disconnected from the outer plasma membrane. The rim of each rod disc has a collection of proteins, including peripherin and rod outer segment protein 1 (ROM1), which play a role in the development and maintenance of the disc's curvature. Peripherin and ROM1 are also found in cone outer segments. Another protein in rod discs is ABCA4, an ATP-binding cassette (ABC) transporter. It is a transmembrane protein involved in the energy-dependent transport of substrates from the disc lumen to the rod cytosol. ABCA4 is unique to rod discs and is not found in cones. It functions as a transporter of all-*trans*-retinal.

CLINICAL PEARL

Pathogenic variants of the *ABCA4* gene cause Stargardt disease. This progressive disease is the most common juvenile maculopathy.

Tsybovsky Y, Molday RS, Palczewski K. The ATP-binding cassette transporter ABCA4: structural and functional properties and role in retinal disease. *Adv Exp Med Biol.* 2010;703:105–125.

Energy Metabolism of Photoreceptor Outer Segments

Adenosine triphosphate is necessary to drive the reactions that control the ionic current generators as well as the transporters in the outer segment. Because only the inner, and not the outer, segment contains mitochondria, oxidative metabolism is confined to the former. The outer segment is responsible for glycolysis, including the hexose monophosphate pathway and the phosphocreatine shuttle, which produces ATP and GTP and modulates nicotinamide adenine dinucleotide phosphate (NADPH). NADPH reduces retinal to retinol before it is returned to the RPE for isomerization, and it reduces glutathione, which protects against oxidative stress.

Cone Phototransduction

Qualitatively, the phototransduction of cones resembles that of rods. Light-activated cone opsins initiate an enzymatic cascade that hydrolyzes cGMP and closes cone-specific cGMP–gated cationic channels on the outer-segment membrane. Cone phototransduction

is comparatively insensitive but fast and capable of adapting significantly to ambient levels of illumination. The greater the ambient light level is, the faster and more temporally accurate the response of a cone will be.

Speed and temporal fidelity are important for all aspects of cone vision. This is one reason visual acuity improves progressively with increased illumination. Because of their ability to adapt, cones are indispensable to good vision. A person without cones loses the ability to read and identify colors and may be considered legally blind. In comparison, lost rod function is a less severe visual problem, except under scotopic (dark) conditions.

Several factors contribute to light adaptation. For example, higher levels of illumination bleach away photopigments, making the outer segment less sensitive to light. As light levels increase, so does the noise level, which reduces sensitivity. Biochemical and neural feedback speed up the cone response. This feedback must be increased as light intensity increases and the cone absorbs more and more light. All the processes that turn off the rod response are probably stronger in cones.

Visual Cycle

Once the phototransduction cycle is complete, all of the proteins within the discs of the photoreceptor outer segments are prepared to receive another photon of light. However, this process is not fully reset until the vitamin A moiety is returned to its original configuration. Once rhodopsin is activated, all-*trans*-retinal is shed. A complex series of steps, involving shuttles and enzymes, is required to restore this molecule to its native 11-*cis*-retinal state. This process of vitamin A regeneration, known as the *visual cycle,* occurs between the photoreceptors and the RPE. Thus, for the vision system to be fully restored and resume sensing another photon of light, both the phototransduction cascade and the visual cycle must complete their course. Chapter 13 in this volume discusses the visual cycle in detail.

Trivariant Color Vision

To be able to see colors, mammals must have at least 2 different spectral classes of cones. Most humans have 3 types of cones and, consequently, a 3-variable color vision (3-cone-opsin) system:

- short-wavelength-sensitive cones (termed *S cones*), which detect only color by comparing their signals with those of the M cones; this mechanism creates blue-yellow color vision
- middle-wavelength-sensitive cones (termed *M cones*), which detect high-resolution achromatic (black-and-white) contrast
- long-wavelength-sensitive cones (termed *L cones*), which evolved in primates to enhance color vision; this mechanism creates red-green color vision

Both L and M cones contribute to achromatic and chromatic contrast. Therefore, both are more numerous than S cones in the human retina. Most color vision defects involve red-green discrimination and the genes coding for the L- and M-cone opsins. See Chapter 6 for further discussion.

Photoreceptor Gene Alterations Causing Retinal Degeneration

Pathogenic gene variants involving the phototransduction pathway may lead to inherited retinal dystrophies with varying degrees of visual impairment. These variants can disrupt physiology in different ways: They can alter the transduction cascade, protein folding, or localization of the affected protein. Retinitis pigmentosa (RP), Leber congenital amaurosis (LCA), and Stargardt disease are among the most prevalent inherited retinal dystrophies.

Autosomal dominant RP (ADRP) can be caused by more than 100 different pathogenic variants of the rhodopsin gene *(RHO).* The most common *RHO* variant is P23H (responsible for 10% of RP cases in the United States), which causes the rhodopsin protein to not fold properly but instead accumulate in the rough endoplasmic reticulum. Generally, *RHO* variants affecting the intradiscal area and the amino-terminal end of rhodopsin result in less severe defects than do variants affecting the cytoplasmic region and the carboxyl tail. Alterations in the middle of the gene, coding for the transmembrane regions of rhodopsin, result in moderately severe defects. Relatively uncommon alterations have been reported in the rhodopsin gene that cause autosomal recessive RP (ARRP) and a stationary form of nyctalopia. Tables 12-1 through 12-4 list other gene variants that cause inherited retinal dystrophies. See also BCSC Section 12, *Retina and Vitreous,* for further discussion.

Molday RS. Photoreceptor membrane proteins, phototransduction, and retinal degenerative diseases. The Friedenwald Lecture. *Invest Ophthalmol Vis Sci.* 1998;39(13):2491–2513.

Table 12-1 Rod-Specific Pathogenic Gene Variants

Proteins Affected	Corresponding Retinal Disease
Rod transducin	A dominant pathogenic variant in the *GNAT1* gene causes congenital stationary night blindness, Nougaret type, the oldest known form of AD stationary nyctalopia. Transducin becomes continuously activated, an example of constitutively active rods that do not degenerate.
Rod cGMP phosphodiesterase	Alterations in either the α-subunit (PDEA) or the β-subunit (PDEB) of cGMP phosphodiesterase (rod PDE) cause ARRP. These are nonsense variants that truncate the catalytic domain of the protein. An H258D variant in PDEB also causes dominant stationary nyctalopia.
Rod cGMP–gated channel	Null variants of the rod cGMP–gated channel β-subunit cause ARRP.
Arrestin, rhodopsin kinase	A pathogenic variant of either the gene *SAG* (2q37), which encodes arrestin, or the gene *GRK1* (13q34), which encodes rhodopsin kinase, causes Oguchi disease, a form of stationary nyctalopia.
Guanylate cyclase	Null variants of the guanylate cyclase gene cause LCA, a childhood AR form of RP. LCA shows genetic heterogeneity.
Rod ABC transporter	Alterations in the *ABCA4* gene cause recessive defects of ABC transporter proteins, which cause Stargardt disease.

ABC = adenosine triphosphate–binding cassette; AD = autosomal dominant; AR = autosomal recessive; ARRP = autosomal recessive retinitis pigmentosa; cGMP = cyclic guanosine monophosphate; LCA = Leber congenital amaurosis; RP = retinitis pigmentosa.

Table 12-2 Cone- and Rod-Specific Gene Variants

Proteins Affected	Corresponding Retinal Disease or Condition
Peripherin/RDS (PRPH2)	There is substantial allelic heterogeneity in the *PRPH2* gene. Pathogenic variants cause several dominantly inherited retinal degenerations that range from ADRP to macular degeneration, pattern macular dystrophy, vitelliform macular dystrophy, butterfly macular dystrophy, and fundus flavimaculatus.
Rod outer segment protein 1 (ROM1)	Double-heterozygotic pathogenic variants in both the *ROM1* and the peripherin genes cause digenic RP. A *ROM1* gene variant alone has been reported in a patient with vitelliform macular dystrophy.
Myosin VIIA	Myosin VIIA is a protein found in cochlear hair cells and in the cilium connecting the rod inner and outer segments. A heterozygous null pathogenic variant in a form of myosin VIIA causes Usher syndrome type 1. Affected patients have early and profound deafness, vestibular areflexia at birth, and ARRP.

ADRP = autosomal dominant retinitis pigmentosa; ARRP = autosomal recessive retinitis pigmentosa; RP = retinitis pigmentosa.

Table 12-3 Cone-Specific Gene Variants

Proteins Affected	Corresponding Retinal Disease
Cone cGMP–gated channel	A homozygous variant of the cone cGMP–gated channel α-subunit causes achromatopsia, loss of all cone function.
L- and M-cone opsins	Pathogenic variants of the genes coding for L- and M-cone opsins cause alterations that lead to S-cone (or blue-cone) monochromatism. These alterations occur only in males because of the gene's location on the X chromosome. Variants in all 3 cone opsins lead to achromatopsia, also known as *rod monochromatism.*
L- or M-cone opsins	Variants in one or the other of the X-linked L- or M-cone opsin genes cause red-green color deficiencies, almost exclusively in males.

cGMP = cyclic guanosine monophosphate; L cone = long-wavelength–sensitive cone; M cone = middle-wavelength–sensitive cone; S cone = short-wavelength–sensitive cone.

Classes of Retinal Cells

The retina contains 3 broad classes of cells (Fig 12-4):

1. neurons (photoreceptor, bipolar, horizontal, amacrine, and ganglion cells)
2. glial cells (Müller cells, astrocytes, and microglia)
3. vascular cells (endothelial cells and pericytes)

The major route of information flow from photoreceptors to the optic nerve consists of a 3-neuron chain—photoreceptor cell to bipolar cell to ganglion cell. Horizontal cells and

Table 12-4 Ubiquitously Expressed Genes That Cause Retinal Degeneration

Proteins Affected	Corresponding Retinal Disease
Rab escort protein 1 (REP-1)	Pathogenic variants of *CHM,* the gene encoding REP-1, cause choroideremia, an X-linked disease. The protein is involved in prenylating Rab proteins, a process that facilitates their binding to cytoplasmic membranes and promotes vesicle fusion. Photoreceptors, the RPE, and/or the choroid must be uniquely vulnerable for this process to occur.
Ornithine aminotransferase (OAT)	Homozygous pathogenic variants of the *OAT* gene cause gyrate atrophy. The OAT enzyme breaks down ornithine, which, in high concentrations, seems to be toxic to the RPE.
Microsomal triglyceride transfer protein (MTTP)	Homozygous variants of the *MTTP* gene cause abetalipoproteinemia, or Bassen–Kornzweig syndrome, characterized by ARRP and an inability to absorb fat. The condition is treatable with fat-soluble vitamins.
Peroxins	Homozygous variants in *PEX1* cause infantile Refsum disease with RP, cerebellar ataxia, polyneuropathy, anosmia, hearing loss, and cardiomyopathy. Infantile Refsum disease represents the least severe disease in a spectrum of familial disorders involving pathogenic variants of the *PEX* genes, which code for peroxins, proteins necessary for peroxisome biogenesis.
Phytanoyl-CoA hydroxylase (PHYH)	Homozygous variants of the *PHYH* gene cause Refsum disease, characterized by RP, cerebellar ataxia, and peripheral polyneuropathy. The enzyme, located in peroxisomes, degrades phytanic acid. Elevated levels of phytanic acid are toxic to the RPE. Patients with Refsum disease may be treated with a phytanic acid–restricted diet.

ARRP = autosomal recessive retinitis pigmentosa; RP = retinitis pigmentosa; RPE = retinal pigment epithelium.

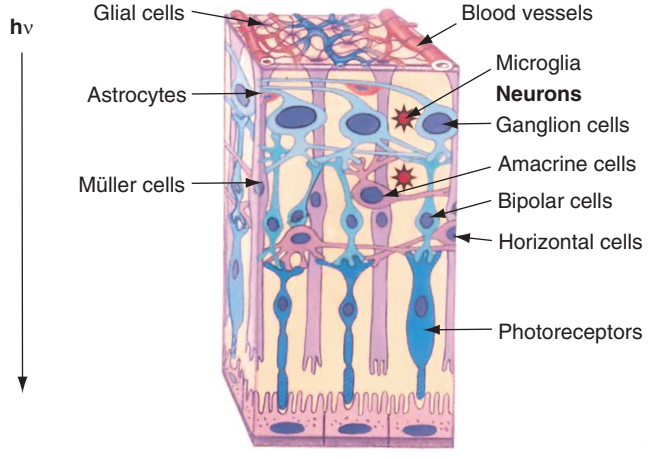


Figure 12-4 Schematic of the 3 major classes of retinal cells: glial cells (Müller cells, astrocytes, and microglia); neurons (photoreceptor, bipolar, horizontal, amacrine, and ganglion cells); and vascular cells (pericytes and endothelial cells, not shown). *(Reproduced with permission from Gardner TW, Antonetti DA, Barber AJ, LaNoue KF, Levison SW. Diabetic retinopathy: more than meets the eye.* Surv Ophthalmol. *2002;47(Suppl 2):S253–S262. Fig 1. Copyright 2002, Elsevier.)*

amacrine cells are interneurons that regulate the flow of information. Glial cells and vascular elements support the neuronal components.

Neurons

Bipolar cells

Retinal bipolar cells receive neural signals from photoreceptors (discussed earlier in this chapter) and convey them to the inner retina. Separate bipolar cells exist for cones and rods. Morphologically, there are 9–12 different kinds of cone bipolar cells but only 1 type of rod bipolar cell. Functionally, in the cone pathway there are *on-bipolar* and *off-bipolar* cells (Fig 12-5). On-bipolar cells are optimized to detect increases in light intensity, and off-bipolar cells detect decreases in light intensity. When light hyperpolarizes a cone, the on-bipolar cell is excited (turned on), and the off-bipolar cell is inhibited (turned off). When a shadow depolarizes the cones, the opposite occurs.

Some cone bipolar cells synapse only with L cones and others only with M cones (see the section Trivariant Color Vision, earlier in this chapter), a differentiation that is necessary for color vision. In the fovea, some cone bipolar cells (midget bipolar cells) synapse with a single L or M cone, which allows the highest spatial acuity. This cone selectivity is preserved throughout the ganglion cell layer. Separate L- and M-cone on-bipolar cells and off-bipolar cells transmit a faster, phasic signal to a parallel system of larger ganglion cells. Rods and probably S cones have only on-bipolar cells. Thus, neither rods nor S cones are involved in high spatial resolution. S cones are involved in color vision; rods, in dim light (night vision).

Horizontal cells

Horizontal cells are antagonistic interneurons that provide negative feedback to photoreceptors (see Figs 12-4, 12-5). The dendrites of horizontal cells synapse with cones. One type of horizontal cell modulates L and M cones; another type modulates mainly S cones.

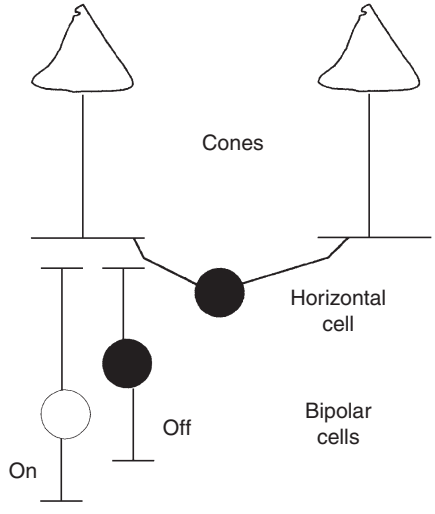


Figure 12-5 Basic circuitry of the cones. Separate on- and off-bipolar cells contact each cone. In the fovea, a cone has midget bipolar cells contacting only a single cone, and usually a single ganglion cell, for high spatial acuity. Horizontal cells are antagonistic neurons between cones. Absorbing light hyperpolarizes the cone; this, in turn, hyperpolarizes the horizontal cell, which resembles an off-bipolar cell. *(Courtesy of Peter Gouras, MD.)*

The dendrites of horizontal cells receive glutamate from cones and rods and release γ-aminobutyric acid (GABA) back onto them. This process provides negative feedback. When light causes the cone to hyperpolarize and stop its transmitter release, the neighboring horizontal cells are also hyperpolarized (turned off). This effect stops the release of GABA from the horizontal cell onto the cone, consequently depolarizing the cone. This feedback inhibition allows visualization of low-contrast details against background luminance.

CLINICAL PEARL

Horizontal cell feedback also turns off the cone response more quickly, enabling the cone to respond rapidly to a new stimulus. The *flicker fusion threshold* is the frequency of a repetitive stimulus at which it appears to be a completely steady light stimulus. This threshold is much higher in cones (approximately 100 Hz) than in rods (approximately 20 Hz). Thus, a 30 Hz flicker stimulus is used to selectively elicit a cone response during electrophysiologic testing.

Amacrine cells

Like horizontal cells, amacrine cells are inhibitory interneurons. Cone amacrine cells mediate antagonistic interactions among on-bipolar, off-bipolar, and ganglion cells. Rod bipolar cells do not usually synapse directly with ganglion cells but rather send their signal to amacrine cells, which then deliver the signal to on- and off-bipolar ganglion cells. Thus, rod signals undergo additional synaptic delays before they reach the ganglion cell output.

Ganglion cells

The functional division of the cone pathway into on and off channels begins at the first synapse (between the cones and the on-bipolar or off-bipolar cells). This division is preserved across the pathway to the higher visual centers. On-bipolar cells synapse with on-ganglion cells and off-bipolar cells with off-ganglion cells. Midget ganglion cells, a special type of ganglion cell with small dendritic trees, are dominant in the central macula. They have a 1:1:1 ratio with cones and midget bipolar cells, allowing high spatial resolution.

Ganglion cells can be divided into 3 subgroups: (1) tonic cells driven by L or M cones, (2) tonic cells driven by S cones, and (3) phasic cells. The tonic system transmits signals from the cones that are relatively well maintained for the duration of the light or dark stimulus. The phasic system transmits signals at the beginning or end of a light stimulus, producing a brief or transient response.

Tonic cells driven by either L or M cones include small cells concentrated in the fovea (responsible for high acuity) and other cells located extrafoveally. They mediate both high spatial resolution and color vision. Tonic cells driven by S cones are designed to detect successive color contrast, for example, blue-yellow or gray-brown borders. These ganglion cells are excited by short waves entering and long waves leaving their receptive fields.

Phasic cells are larger, less concentrated in the fovea, and faster conducting than the other ganglion cells. Phasic cells may be important in movement detection.

Glial Cells

Müller cells are glial in origin and form a supporting element in the neural retina extending from the inner segments of the photoreceptors to the internal limiting membrane (ILM), which is formed by their end feet. They buffer the ionic concentrations in the extracellular space, enclose the subretinal space by helping to form the external limiting membrane (ELM), and may play a role in vitamin A metabolism of cones.

The other nonneural, or neuroglial, cells of the retina are *macroglia* (mainly astrocytes) and *microglia.* Macroglia perform the following functions:

- providing physical support to neuronal and vascular cells
- regulating the ionic and chemical composition of the extracellular milieu
- participating in the inner blood–retina barrier
- forming the myelin sheath of the optic nerve (This function is performed by oligodendrocytes, which are macroglia that are similar to Schwann cells in the peripheral nervous system. Because the myelination does not usually extend into the retina, these glial cells are not found in the retina.)
- guiding neuronal migration during development
- exchanging metabolites with neurons

Microglia are related to tissue macrophages and are activated when retinal homeostasis is disturbed. These cells mediate immune responses in the central nervous system.

Vascular Cells

In addition to neural and glial cells, the retina contains blood vessels with endothelial cells and pericytes. Pericytes surround the endothelial cells and are modified smooth muscle cells that play a role in autoregulation of retinal blood vessels. Endothelial cells form the inner blood–retina barrier; pericytes structurally support the endothelium and suppress proliferation, loss of which leads to increased permeability and development of microaneurysms.

Together, the neuronal, glial, and vascular components of the retina form a functional neurovascular unit. Ophthalmoscopically, the vascular components are the only visible part of the retina. The neural retina lacks pigment (except for foveal xanthophyll) and is transparent, thus allowing the passage of light through the inner retinal layers. Conditions such as diabetic retinopathy are categorized on the basis of clinically evident vascular changes. Despite the clinical emphasis on vascular changes, there is strong evidence of neuronal dysfunction early in the disease process, even prior to the detection of clinically evident disease.

Gardner TW, Antonetti DA, Barber AJ, LaNoue KF, Levison SW. Diabetic retinopathy: more than meets the eye. *Surv Ophthalmol.* 2002;47(Suppl 2):S253–S262.

Retinal Electrophysiology

Changes in the light flux on the retina produce electrical changes in all retinal cells, including the RPE and Müller cells, as well as in neurons. These electrical changes result from ionic currents that flow when ion-specific channels are opened or closed. These currents reach the vitreous and the cornea, where they can be detected noninvasively and form the basis of the electroretinogram (ERG) (Fig 12-6). Figure 12-7 depicts the different electrophysiological tests used to study different parts of the retina.

The currents are initiated by the ionic response started in the rods and cones. This response influences the ionic current *directly* by changes in Na^+, K^+, and Ca^{2+} fluxes and *indirectly* by synaptic modification of second-order retinal neurons. The ionic changes are due to shifts in the photoreceptors' conductivity of Na^+, K^+, and Ca^{2+}; this conductivity is facilitated by the CNG channels (see Fig 12-3).

See BCSC Section 12, *Retina and Vitreous,* for detailed discussion of ERGs and retinal responses.

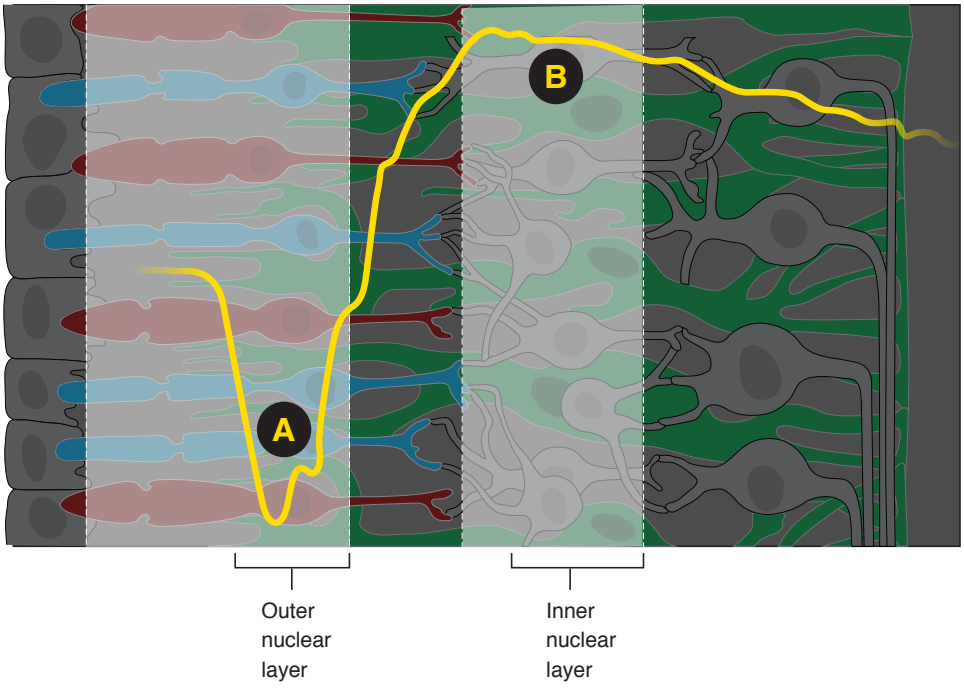


Figure 12-6 Electroretinogram (ERG). Diagram of ERG demonstrating the combined response of rods and cones after bright flash stimulus. The electrical tracing of the ERG *(yellow)* overlies the retina and the respective cells of origin. The A wave is a negative deflection reflecting the initial hyperpolarization of the photoreceptors as a result of the phototransduction cascade. The B wave is positive deflection reflecting the depolarization of the bipolar cells resulting from the absence of the inhibitory neurotransmitter glutamate. Müller cells also contribute to the B wave. The contribution of ganglion cells is lost in the large B wave and requires different testing conditions. *(Illustration by Mark Miller.)*

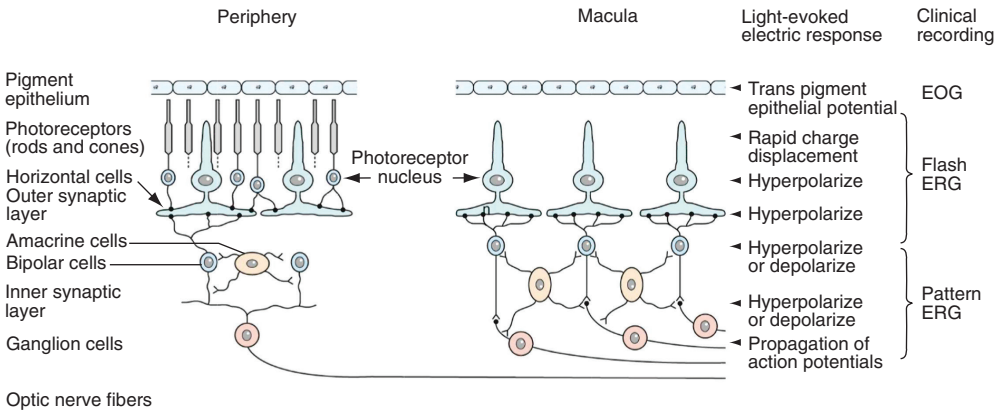


Figure 12-7 Origins of measurable electrical signals from the retina. EOG = electro-oculogram; ERG = electroretinogram. *(Modified with permission from Forrester JV, Dick AD, McMenamin PG, Roberts F, Pearlman E.* The Eye: Basic Sciences in Practice. *4th ed. Elsevier/Saunders; 2016:297.)*

CHAPTER 13

Retinal Pigment Epithelium

Highlights

- The retinal pigment epithelium (RPE) is derived embryologically from the same neural anlage as the neurosensory retina.
- Although it has no photoreceptive or neural function, the RPE is essential for the viability of photoreceptor cells and the choriocapillaris and plays a critical role in the regeneration of 11-*cis*-retinal and the phototransduction cycle.
- The gene *RPE65,* which encodes the enzyme RPE65 isomerohydrolase, converts all-*trans*-retinyl ester to 11-*cis*-retinal. Pathogenic variants of *RPE65* are the target of a treatment approved by the US Food and Drug Administration, in which an adeno-associated virus vector delivers human RPE65 complementary DNA to the RPE of a small subset of patients with Leber congenital amaurosis or retinitis pigmentosa.
- Autophagy is a homeostatic process whereby the cell degrades its own damaged components and recycles the products. In the RPE, autophagy is essential for management of phagocytosed outer segments as well as for turnover of its components.

Overview of RPE Structure

The RPE is a monolayer of neuroectoderm-derived epithelial cells, located between the highly vascular choriocapillaris and the photoreceptor outer segments (Figs 13-1, 13-2). Embryologically, it is derived from the same neural anlage as the neurosensory retina. The retina and RPE develop as an invagination of the embryonic optic cup, folding the neuroectodermal layer into apex-to-apex contact with itself. The outer layer forms the RPE, and the inner layer forms the neurosensory retina. The intervening area remains throughout life as a potential space and is the plane of separation for retinal detachment.

The human eye contains approximately 4–6 million RPE cells. On the apical surface of RPE cells are long microvilli that interdigitate with the outer segments of photoreceptor cells (see Figs 13-1, 13-2). These cells are joined near their apical side by tight junctions that establish polarity, block the passage of water and ions, and constitute the outer blood–retina barrier. The RPE basal surface, which is adjacent to Bruch membrane (an extracellular matrix between the RPE and the choriocapillaris), has many infoldings that increase the surface area available for the exchange of solutes (see Fig 13-1).

In addition to the organelles found in most cells (eg, the nucleus, Golgi apparatus, smooth and rough endoplasmic reticulum, and mitochondria), RPE cells contain melanin

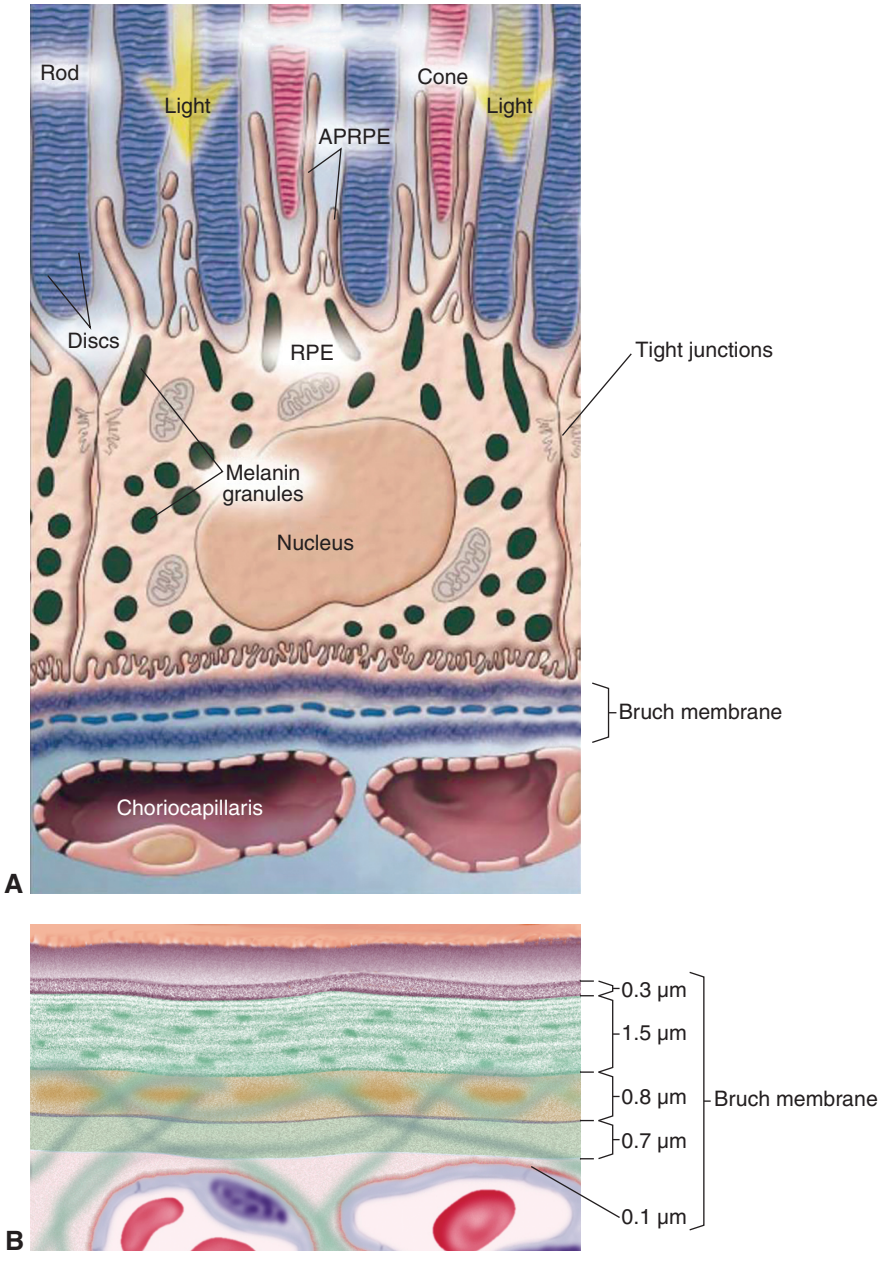


Figure 13-1 The retinal pigment epithelium (RPE) and Bruch membrane. **A,** Bruch membrane separates the RPE from the choriocapillaris. Note the interdigitation of the apical processes of the RPE (APRPE) with the photoreceptor outer segments as well as the infoldings of the basal surface. **B,** The thickness of the different layers of Bruch membrane is demonstrated (starting from the top): basement membrane of the RPE, inner collagenous layer, elastic layer, outer collagenous layer, and basement membrane of the choriocapillaris. *(Part A modified from David Williams, University of Rochester; part B illustration by Daniel Casper, MD, PhD.)*

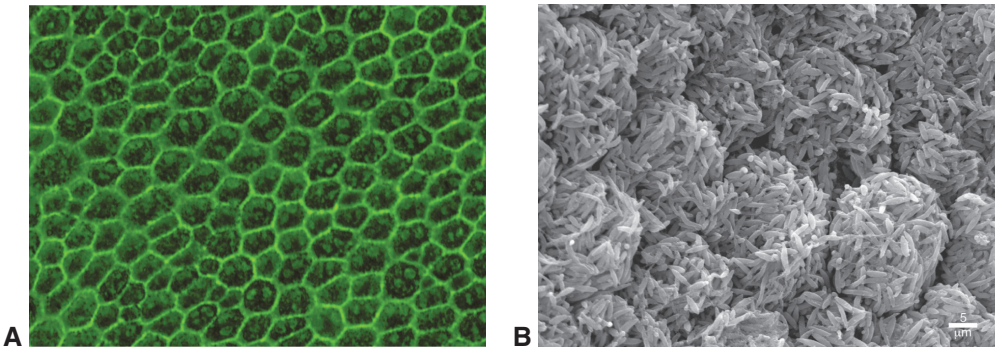


Figure 13-2 RPE. **A,** Monolayer of cultured RPE cells grown to confluence shows the polygonal appearance of the RPE cells (phase microscopy, 25×). **B,** Scanning electron micrograph of RPE cells demonstrates the apical microvilli. *(Reproduced with permission from Thumann G, Dou G, Wang Y, Hinton DR. Cell biology of the retinal pigment epithelium. In: Schachat AP, ed.* Ryan's Retina. *5th ed. Elsevier; 2013:402–403.)*

granules and phagosomes, reflecting their role in light absorption and phagocytosis (discussed later in this chapter). The RPE is particularly rich in microperoxisomes, suggesting that it is active in detoxifying the many free radicals and oxidized lipids generated in this highly oxidative and light-rich environment.

Biochemical Composition of the RPE

Biochemically, the RPE is dynamic and complex. It must meet demands for its own active metabolism, its extraordinary phagocytic function, and its role as a biological filter for the neurosensory retina. These processes impose a very high energy requirement on the RPE; not surprisingly, RPE cells contain the enzymes of the 3 major biochemical pathways: (1) glycolysis, (2) Krebs cycle, and (3) the pentose phosphate pathway. Glucose is the primary carbon source used for energy metabolism and for conversion to protein. Although the RPE makes a minor contribution to the glycosaminoglycan- and proteoglycan-containing interphotoreceptor matrix, glucose is not converted to glycogen in the RPE. Glucosamine, fucose, galactose, and mannose are all metabolized to some extent in the RPE, although mannose seems to be passed on almost directly to the photoreceptors.

Proteins

Nearly 850 proteins have been identified in the RPE. Many proteins found in other cells are also present in the RPE. These include hydrolytic enzymes such as glutathione, peroxidase, catalase, and superoxide dismutase, which are important for detoxification. The cytoskeletal proteins actin, myosin, α-actinin, fodrin, and vinculin are also present in both the RPE and other cells.

Some proteins are localized differently in the RPE than in other cells. A well-known example is Na^+,K^+-ATPase (also called the *sodium-potassium pump*), which has a unique location in RPE cells. In most polarized epithelial cells, Na^+,K^+-ATPase is localized to the basolateral membrane, but in the RPE, this enzyme is found on the apical membrane. The sodium-potassium pump uses energy derived from adenosine triphosphate (ATP) hydrolysis to transport sodium (Na^+) and potassium (K^+) against their electrochemical gradients. It is thought that the apical location of Na^+,K^+-ATPase in the RPE maintains the balance of Na^+ and K^+ in the subretinal space. RPE cells also contain proteins whose polarity is reversed in comparison to the polarity of other epithelial cells; examples include an isoform of neural cell adhesion molecule (NCAM-140) and folate receptor α.

Some proteins are expressed only in the RPE. One such protein, RPE-specific protein 65 kDa (RPE65), is an obligate component of the isomerization and hydrolysis of vitamin A, which is required for regeneration of visual pigment (described later in the section Vitamin A Regeneration).

Lipids

Lipids account for approximately 3% of the wet weight of the RPE; about half are phospholipids. Phosphatidylcholine and phosphatidylethanolamine make up more than 80% of the total phospholipid content. In general, levels of saturated fatty acids are higher in the RPE than in the adjacent outer segments. The saturated fatty acids palmitic acid and stearic acid are used for retinol esterification and for energy metabolism by the RPE mitochondria. The RPE also acquires phospholipids from phagocytosis of photoreceptor discs (see the following sections), in particular docosahexaenoic acid (22:6, n-3), which is recycled back to the photoreceptors. The RPE actively conserves and efficiently reuses fatty acids, thus preventing their loss as waste products.

Fu Z, Kern TS, Hellström A, Smith LEH. Fatty acid oxidation and photoreceptor metabolic needs. *J Lipid Res.* 2021;62:100035. doi:10.1194/jlr.TR120000618

Nucleic Acids

RNA is synthesized continually by the RPE. This process is required to produce the numerous enzymes that are necessary for cell metabolism, phagocytosis of shed discs, and maintenance of the retinoid pathway and transport functions.

Major Physiologic Roles of the RPE

The RPE has various physiologic roles (Fig 13-3). Its crucial functions include

- vitamin A regeneration, which is integral to sustaining vision
- phagocytosis of shed photoreceptor outer-segment discs
- biological filtration for the neurosensory retina via transport of necessary nutrients and ions to photoreceptor cells and removal of waste products from photoreceptors

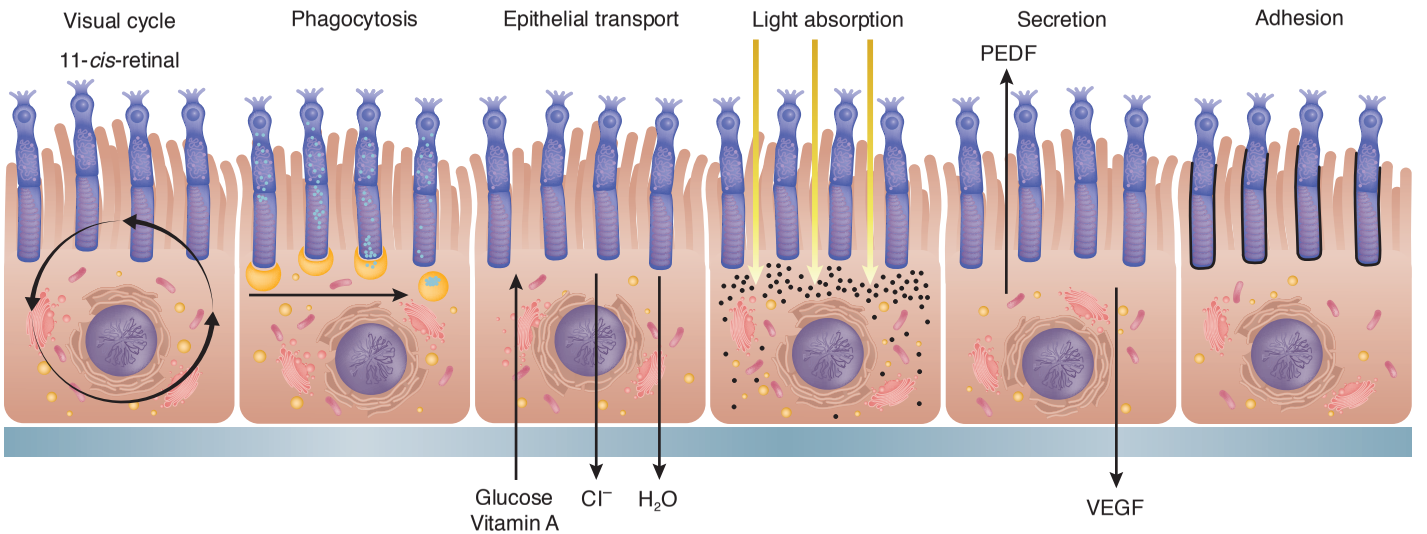


Figure 13-3 Physiologic functions of the RPE. Additional functions (not shown) include its role in synthesis and remodeling of the interphotoreceptor matrix, formation of the outer blood–retina barrier, and formation of the basal lamina of Bruch membrane. PEDF = pigment epithelium–derived factor; VEGF = vascular endothelial growth factor. *(Illustration by Cyndie C.H. Wooley.)*

- absorption of scattered and out-of-focus light via pigmentation
- adhesion of the retina
- secretion of humoral and growth factors

These functions are discussed briefly in the following sections. Other important functions subserved by the RPE include its role in synthesis and remodeling of the interphotoreceptor matrix, formation of the outer blood–retina barrier, and formation of the basal lamina of Bruch membrane.

Vitamin A Regeneration

The RPE, second only to the liver in its concentration of vitamin A, plays a major role in the uptake, storage, and mobilization of vitamin A. The RPE supplies the photoreceptor outer segments with vitamin A, which is tethered to rhodopsin in rods and to the 3 different cone opsins (red, green, and blue). Although the different opsins have specific absorption spectra, vitamin A changes its configuration identically in response to the particular wavelength of light (see Chapter 12).

The basic function of the RPE cell is to generate 11-*cis*-retinal (also called 11-*cis*-retinaldehyde) (Fig 13-4). Light-induced activation of rhodopsin leads to isomerization of 11-*cis*-retinal to all-*trans*-retinal and initiates the phototransduction cascade. Light-activated rhodopsin releases all-*trans*-retinal and must bind with another 11-*cis*-retinal to be ready for activation by the next photon of light. The free all-*trans*-retinal isomer undergoes a series of enzymatic reactions, called the *visual cycle* or *retinoid cycle,* to regenerate 11-*cis*-retinal. The visual cycle ensures a steady supply of 11-*cis*-retinal for the opsins in order to maintain vision and requires close interaction between the RPE and photoreceptor outer segments. Similar processes occur in all photoreceptors; the process specific to rods is discussed next.

Free all-*trans*-retinal is cleared from the rod discs by ABCA4, an ATP-binding cassette (ABC) transporter protein. After transport from the rod discs to the cytosol of the outer segments, all-*trans*-retinal is enzymatically reduced to all-*trans*-retinol by retinol dehydrogenase. All-*trans*-retinol is rapidly released by photoreceptor cells to the interphotoreceptor matrix, where it binds to interphotoreceptor retinoid-binding protein (IRBP). RPE cells contain cellular retinol-binding protein 1 (CRBP1), which promotes the uptake of all-*trans*-retinol into the RPE. The RPE also obtains vitamin A from the blood, where it is complexed with retinol-binding protein (RBP) and transthyretin. Phagocytosis of shed photoreceptor outer-segment discs (see the following section) by the RPE also allows recycling of vitamin A.

Within RPE cells, CRBP1-bound all-*trans*-retinol is enzymatically esterified by lecithin retinol acyltransferase (LRAT). The resultant retinyl ester is hydrolyzed and isomerized to the 11-*cis* configuration by the retinoid isomerohydrolase RPE65. 11-*cis*-Retinol is then oxidized to 11-*cis*-retinal by 11-*cis*-retinol dehydrogenase. The newly formed 11-*cis*-retinal is released from RPE cells to the interphotoreceptor matrix. From there it is transported by IRBP (which binds both retinol and retinal forms) to the photoreceptor outer-segment discs to generate another visual transduction cycle.

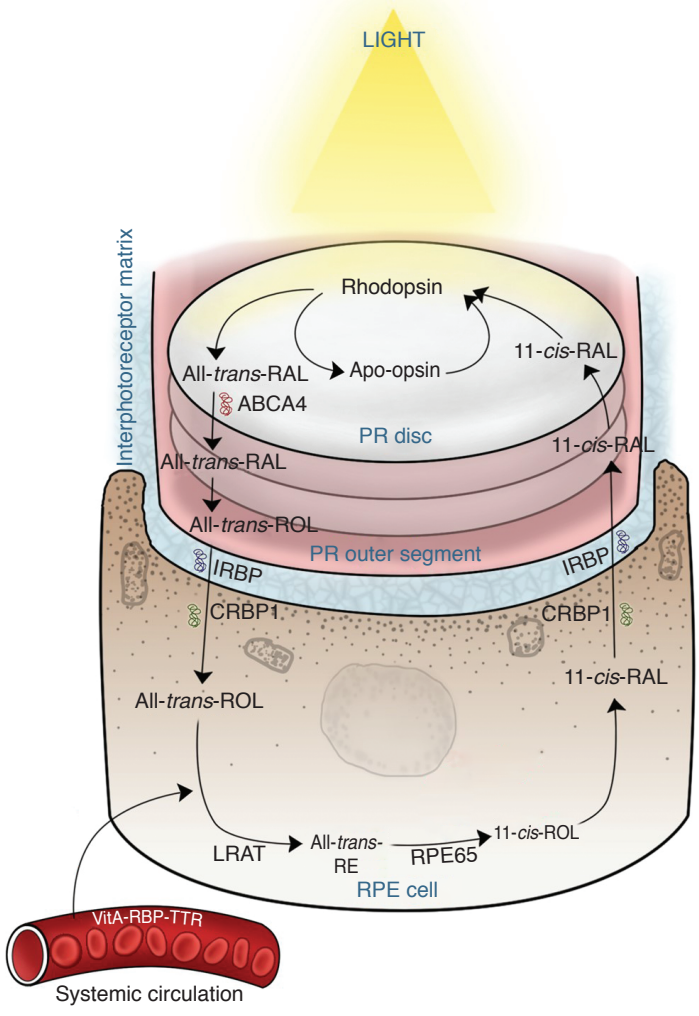


Figure 13-4 In the visual cycle (also known as the *retinoid cycle*), a series of reactions in the photoreceptor outer segments and retinal pigment epithelium (RPE) regenerate 11-*cis*-retinal (also known as 11-*cis*-retinaldehyde). 11-*cis*-Retinal attaches to a lysine residue on rhodopsin. When the complex absorbs light, 11-*cis*-retinal transforms into all-*trans*-retinal via a process known as *photoisomerization*. This process induces a conformational change in the attached rhodopsin molecule, activating the second-messenger system and initiating the phototransduction cascade within the photoreceptor (PR). The all-*trans*-retinal is shed from rhodopsin and transported by ABCA4 from the rod disc to the cytosol, where it is converted to all-*trans*-retinol. Then, all-*trans*-retinol is delivered to the RPE via interphotoreceptor retinoid-binding protein (IRBP), which acts as a shuttle and also shields the cell membranes from the membranolytic retinoid molecules. Once in the RPE, this molecule is esterified by lecithin retinol acyltransferase (LRAT). The resultant retinyl ester is converted to 11-*cis*-retinol by the isomerohydrolase RPE65. 11-*cis*-Retinol is then oxidized to 11-*cis*-retinal by retinol dehydrogenase (RDH) and shuttled back to the photoreceptor outer-segment discs by IRBP to participate in another visual cycle. ABCA4 = ATP-binding cassette transporter protein; Apo-opsin = apo-rhodopsin; CRBP1 = cellular retinol-binding protein 1; RAL = retinal; RBP = retinol-binding protein; RE = retinyl ester; ROL = retinol; TTR = transthyretin; VitA = vitamin A. *(Modified with permission from Singh RSJ, Kim JE. Visual cycle modulation. In: Lim J, ed.* Age-Related Macular Degeneration. *3rd ed. CRC Press; 2012:330.)*

CLINICAL PEARL

Because vitamin A intermediaries are membranolytic, they require shuttles or are esterified to protect the plasma membranes of the photoreceptors and RPE. Pathogenic variants of the genes that encode the corresponding shuttles and enzymes have been identified in many inherited retinal diseases. Pathogenic variants of the retinoid isomerohydrolase *RPE65* gene, which encodes the RPE65 protein, causes a subset of LCA and retinitis pigmentosa (see Table 13-1). RPE65 isomerohydrolase is the target of a treatment approved by the US Food and Drug Administration (FDA) that uses an adeno-associated virus vector to deliver human RPE65 complementary DNA to the RPE of patients with some forms of LCA and retinitis pigmentosa.

Testa F, Maguire AM, Rossi S, et al. Three-year follow-up after unilateral subretinal delivery of adeno-associated virus in patients with Leber congenital amaurosis type 2. *Ophthalmology*. 2013;120(6):1283–1291.

Phagocytosis of Shed Photoreceptor Outer-Segment Discs

The RPE plays a crucial role in turnover of the photosensitive membrane of rod and cone photoreceptors (Fig 13-5). Each photoreceptor cell sheds approximately 100 outer-segment discs per day. Because many photoreceptors interdigitate with a single RPE cell, each RPE cell ingests and digests more than 4000 discs daily. The shedding event follows a circadian rhythm: in rods, shedding is most vigorous at dawn; in cones, shedding occurs most vigorously at dusk.

The shed outer-segment discs are encapsulated in phagosomes (see Fig 13-5C), which in turn fuse with lysosomes and are digested. During degradation of the discs, building blocks are recycled into photoreceptors for use in the synthesis and assembly of new discs. The lipofuscin characteristic of the RPE is derived from the photosensitive membranes and is responsible for generating the signal detected in fundus autofluorescence imaging (Fig 13-6).

As described earlier in this chapter, phototransduction causes release of free all-*trans*-retinal, which is transported from the outer-segment discs into the outer-segment cytosol by ABCA4. In certain disease states (eg, Stargardt disease), the free all-*trans*-retinal is not readily cleared from the outer-segment discs by ABCA4. The excess all-*trans*-retinal combines with phosphatidylethanolamine (PE) in the disc lipid bilayer, forming *N*-retinylidene-PE (*N*-ret-PE). Elevated *N*-ret-PE and all-*trans*-retinal undergo a secondary nonenzymatic condensation in the outer segments to yield A2PE-H2. The distal outer segments containing A2PE-H2 and elevated all-*trans*-retinal and *N*-ret-PE are phagocytosed by the RPE as part of the normal disc-renewal process, but the RPE is unable to fully degrade the nonphysiologic load. As a result, toxic retinal fluorophores like A2E (derived from A2PE-H2) accumulate, damaging the RPE.

Transport

The health and integrity of retinal neurons depend on a well-regulated extracellular environment. A crucial function of the RPE that contributes to this regulation is control of the volume and composition of fluid in the subretinal space through transport of ions, fluid,

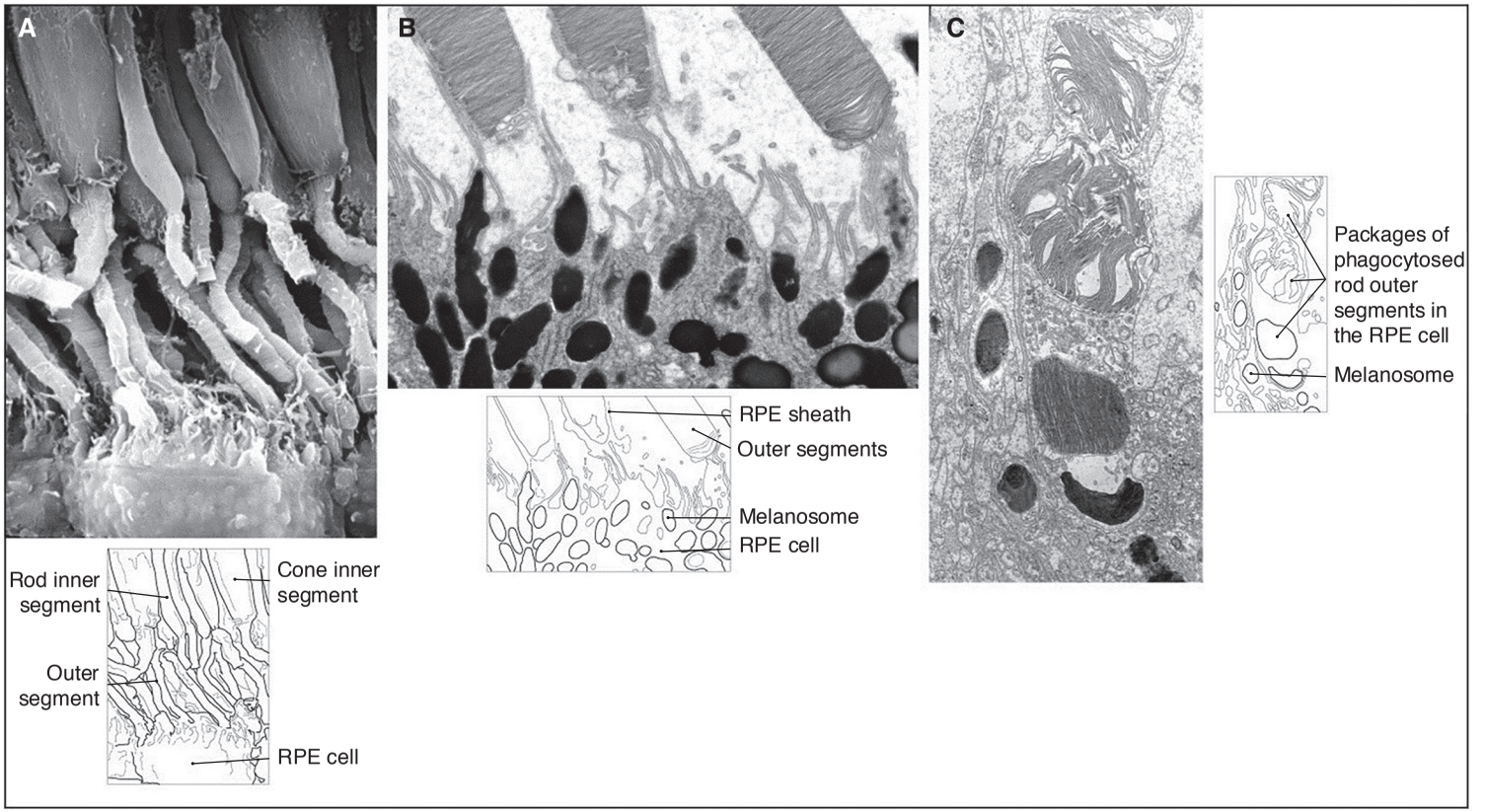


Figure 13-5 RPE. **A,** Interdigitization of the apical processes of the RPE with photoreceptors in the subretinal space. **B,** RPE apical microvilli surround photoreceptor outer segments. Cytosolic melanin granules are also shown. **C,** Phagocytosed photoreceptor outer segments within the RPE. *(Reproduced with permission from Spalton D, Hitchings R, Hunter P.* Atlas of Clinical Ophthalmology. *3rd ed. Elsevier/Mosby; 2005:403.)*

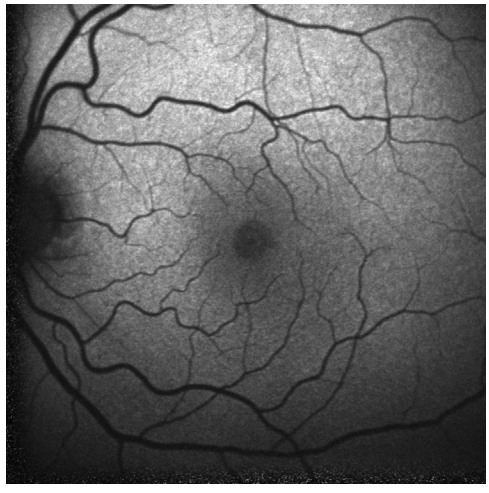


Figure 13-6 Example of fundus autofluorescence imaging, which is facilitated by lipofuscin molecules present within the RPE. Changes in fundus autofluorescence patterns reflect disorders of the RPE in the presence of hyperfluorescence and atrophic RPE in the presence of hypofluorescence (see BCSC Section 12, *Retina and Vitreous*). *(Courtesy of Vikram S. Brar, MD.)*

and metabolites. The distribution of transport proteins residing in the apical and basolateral membrane domains of the cell is asymmetric, and this segregation allows the epithelium to carry out vectorial transport. The membrane proteins remain in their proper location because of tight junction proteins. The polarity of the cell is maintained because of the intracellular molecular machinery that synthesizes new proteins and delivers them preferentially to the apical or basolateral cell membranes. Cytoskeletal proteins are fundamental in determining cell polarity and regulating transport.

The aqueous environment of the subretinal space is actively maintained by the ion-transport systems of the RPE, which regulate transport of a variety of ions (K^+, Ca^{2+}, Na^+, Cl^-, and HCO_3^-). This transport is vectorial in most cases; for example, Na^+ is actively transported from the choriocapillaris toward the subretinal space, whereas K^+ is transported in the opposite direction. The apical membrane of the RPE appears to be the major locus of this transport. As mentioned earlier, ouabain-sensitive Na^+,K^+-ATPase is present at the apical (but not the basal) side. Similarly, an active bicarbonate-transport system appears to be located in the apical RPE membrane. High carbonic anhydrase activity seems to be associated with both the apical and basal sides of the cell.

Net ionic fluxes in the RPE are responsible for the transepithelial electrical potential that can be measured across the RPE apical membrane—a potential that is rapidly modified in the presence of a variety of metabolic inhibitors (eg, ouabain and dinitrophenol). Ion gradients across the RPE drive the transport of water from the subretinal space to the choriocapillaris. The RPE also transports lactic acid produced by metabolic activity in the retina away from the subretinal space. Active vectorial transport systems for other retinal metabolites (eg, taurine, methionine, and folate) have also been demonstrated. The RPE, therefore, appears to be important for maintaining the ionic environment of the subretinal space, which in turn is responsible for maintaining the integrity of the RPE–photoreceptor interface. The trans-RPE potential is the basis for the electro-oculogram (EOG), which is the most common electrophysiologic test for evaluating the RPE (see Chapter 12, Fig 12-7).

Pigmentation

A characteristic feature of the RPE is the presence of melanin pigment. Pigment granules are abundant in the cytoplasm of the adult RPE cell, predominantly in the apical and midportions (see Fig 13-5B). During development, activation of the tyrosinase promoter triggers the onset of melanogenesis in this cell and marks the commitment of the neuroectoderm to become RPE. Although most melanogenesis occurs before birth, melanin production in the RPE occurs throughout life, albeit at a slow rate. As humans age, the melanin granules fuse with lysosomes; thus, the fundus of an older person is less pigmented than that of a young person. Clinically, this is most evident in the peripheral fundus.

The exact role of melanin within cells remains speculative. A universally recognized function of melanin is to act as a neutral-density filter in scattering light. In so doing, melanin may have a protective role. But even in the minimally pigmented fundus, visual acuity can be 20/20. Vision problems in persons with albinism are attributable to foveal hypoplasia, not optical scatter. When melanin levels are below a critical level, as in oculocutaneous albinism, there is aberrant neuronal migration in the visual pathway (more contralateral projections of ganglion cells), incomplete foveal development, low vision, nystagmus, and strabismus.

Melanin is also a free-radical stabilizer and can bind many toxins and drugs (such as chloroquine and hydroxychloroquine). Some clinicians regard this feature as protective; others think that it contributes to tissue toxicity.

CLINICAL PEARL

In addition to its functions as a neutral-density filter in scattering light and as a free-radical stabilizer, melanin within the RPE absorbs the light delivered to the eye during laser photocoagulation of the retina. The absorbed energy is transferred to the surrounding tissues as heat. The outer retina is damaged, and the ensuing inflammatory reaction creates an adhesion between the retina and the RPE. Because of the high blood flow of the choroid, the heat typically dissipates, with minimal or no damage to the choroid.

Retinal Adhesion

The subretinal space is never bridged by tissue, and yet the neural retina remains firmly attached to the RPE throughout life. The RPE is crucial for maintaining retinal adhesion. Detachment of the photoreceptors from the RPE can lead to permanent morphologic and functional changes in the retina.

Numerous factors keep the retina in place, including passive hydrostatic forces, interdigitation of outer segments and RPE microvilli, active transport of subretinal fluid, and the complex structure of the interphotoreceptor matrix and its binding properties (van der Waals forces). In pathologic conditions, retinal adhesion can diminish, and detachment of the retina occurs. Detachment does not occur simply because there is a hole in the retina or a leak in the RPE; there must be either positive traction pulling the neural retina or positive forces pushing fluid into the subretinal space that overwhelms the removal capacity of the RPE.

CLINICAL PEARL

In select cases of rhegmatogenous retinal detachment, pneumatic retinopexy can be used to repair the detached retina. This technique involves injection of a gas bubble into the vitreous cavity. The patient's head is positioned so that the gas bubble lies over the retinal break. The RPE pumps out the subretinal fluid while the gas bubble occludes the retinal break and prevents additional fluid from entering the subretinal space. As a result, the retina can reattach, allowing laser retinopexy to be performed.

Secretion

Various growth factors, cytokines, and immune modulators are secreted by the RPE and are essential for maintaining the physiologic function of the photoreceptors and the choriocapillaris. Examples include PEDF (pigment epithelium–derived factor) and CNTF (ciliary neurotrophic factor), which prevent photoreceptor cell death; VEGF (vascular endothelial growth factor), which maintains choroidal vascular endothelium; and TIMP (tissue inhibitor of metalloproteinases), which maintains the extracellular matrix.

The Role of Autophagy in the RPE

Autophagy is a normal homeostatic mechanism whereby the cell degrades its own damaged components and recycles the degradation products for continued cell survival. There are several types of autophagy, and in each, the degradation is directed toward certain intracellular components, including

- *microautophagy:* cytoplasmic material
- *chaperone-mediated autophagy:* proteins that can be recognized by a heat shock protein complex
- *macroautophagy:* cell organelles
- *mitophagy (a type of macroautophagy):* mitochondria

In RPE cells, autophagic machinery, which includes phagosomes and lysosomes, is abundant. Autophagy is essential to the RPE for management of phagocytosed outer segments and for turnover of its own components. Because RPE cells do not divide under normal conditions, autophagy is also important for quality control of intracellular components.

CLINICAL PEARL

Dysregulated autophagy is involved in the pathophysiology of diseases such as age-related macular degeneration, glaucoma, and photoreceptor loss in retinal detachment. Drugs that inhibit autophagy (eg, chloroquine) lead to RPE and photoreceptor damage.

Frost LS, Mitchell CH, Boesze-Battaglia K. Autophagy in the eye: implications for ocular cell health. *Exp Eye Res.* 2014;124:56–66.

Table 13-1 RPE-Specific Gene Defects

Protein Affected	Corresponding Retinal Degenerations and Disorders
RPE65 isomerohydrolase	Homozygous variants of the *RPE65* gene, which encodes the RPE65 isomerohydrolase, cause LCA. LCA usually has an autosomal recessive pattern. Null variants of the guanylate cyclase gene (see Chapter 12) also cause LCA. The protein is the target of an FDA-approved treatment using an adeno-associated virus to deliver the gene to the RPE of patients with LCA and some cases of retinitis pigmentosa.
Bestrophin	Heterozygous variants of the bestrophin gene *(BEST1)* cause Best disease. The encoded protein bestrophin functions as a chloride channel, found on the basolateral surface of the RPE.
TIMP3	Heterozygous point variations of the *TIMP3* gene lead to Sorsby macular dystrophy. The TIMP3 protein is an inhibitor of a metalloproteinase that regulates the extracellular matrix, where it acts as an antiangiogenesis factor.
CRALBP	Homozygous variations of the gene *RLBP1,* which encodes cellular retinaldehyde-binding protein, cause retinitis punctata albescens. This protein facilitates 11-*cis*-retinal formation and shields the plasma membrane from the potential lytic effects of its aldehyde moiety.
11-*cis*-Retinol dehydrogenase	A pathogenic variant of *RDH5,* the gene encoding 11-*cis*-retinol dehydrogenase, causes fundus albipunctatus, a form of stationary nyctalopia. This enzyme forms 11-*cis*-retinal from 11-*cis*-retinol.
EFEMP1	A single heterozygous, nonconservative variant of the gene *EFEMP1* (EGF-containing fibrillin-like extracellular matrix protein) causes Malattia Leventinese (Doyne honeycomb dystrophy), a dominant form of macular degeneration. It is uncertain whether the protein is unique to the RPE.

EGF = epidermal growth factor; FDA = US Food and Drug Administration; LCA = Leber congenital amaurosis; RPE = retinal pigment epithelium.

The RPE in Disease

The RPE is vital for normal visual function. Genetic defects unique to the RPE may produce retinal degenerations and disorders. Table 13-1 presents some of these conditions.

RPE cells play a role in nongenetic ophthalmic conditions as well. Defects in the pump mechanism of the RPE have been proposed as the cause of central serous chorioretinopathy. In certain pathologic conditions, RPE cells, which normally do not divide, detach from the basement membrane and become migratory. On contact with the vitreous and/or transforming growth factor β (TGF-β), these cells undergo metaplasia, acquiring myofibroblast qualities. Proliferative vitreoretinopathy (PVR) is an example of such a condition. In PVR, the metaplastic RPE cells form contractile membranes on the surface of the retina, leading to retinal detachment. PVR is the most common cause of recurrent retinal detachment after surgery. See BCSC Section 12, *Retina and Vitreous,* for further discussion.

Marmor MF, Wolfensberger TJ, eds. *The Retinal Pigment Epithelium: Function and Disease.* Oxford University Press; 1998:103–134.

Parapuram SK, Chang B, Li L, et al. Differential effects of TGFbeta and vitreous on the transformation of retinal pigment epithelial cells. *Invest Ophthalmol Vis Sci.* 2009;50(12): 5965–5974.

CHAPTER 14

Reactive Oxygen Species and Antioxidants

Highlights

- Oxidative stress can cause many vision-threatening diseases, including cataract, glaucoma, diabetic retinopathy, and age-related macular degeneration.
- Oxidative processes play a central role in the development of nuclear sclerosis. The lens utilizes glutathione, among other antioxidant mechanisms, to combat oxidative stress.
- The Age-Related Eye Disease Study confirmed the role of antioxidants in slowing the progression of macular degeneration.
- Targeting oxidative pathways affords new therapeutic interventions for some of the most common ophthalmic diseases.

Overview

Under physiologic conditions, reactive oxygen species (ROS) participate in normal biochemical processes, where they either act as intermediaries or function as second messengers. ROS can also be generated exogenously, such as through exposure to ultraviolet (UV) light or cigarette smoking. Oxidative stress occurs when the production of ROS exceeds their degradation.

Unchecked, ROS injure cell membranes and DNA, leading to tissue damage and cell death. ROS, like free radicals, react with unsaturated fatty acids that are present within cells and cell membranes, forming lipid peroxides. The oxidation of membrane phospholipids has been hypothesized to increase the permeability of cell membranes and/or inhibit membrane ion pumps. This loss of barrier function is thought to lead to edema, disturbances in electrolyte balance, and elevation of intracellular calcium levels, all of which contribute to cell malfunction and, potentially, to cell death. Free radical–mediated DNA damage can also cause cell death through induction of apoptosis.

The resultant loss of cells leads to dysfunction in the eye, whether at the level of the trabecular meshwork and retinal ganglion cells (RGCs) in glaucoma, the inner retina in diabetic retinopathy, or the outer retina in age-related macular degeneration (AMD).

Reactive Oxygen Species

Sources of Reactive Oxygen Species

ROS are generated from metabolic processes, inflammatory responses, and exposure to UV light. ROS include hydrogen peroxide (H_2O_2) and singlet oxygen ($^1O_2$), as well as lipid peroxides and reactive carbohydrates such as ketoamine and ketoaldehyde groups. Free radicals, another group of ROS, possess an unpaired electron that makes them highly reactive toward other molecular species.

Exogenous sources of ROS include UV light and tobacco smoke. Endogenous sources include the *electron transport chain* in mitochondria and as part of *respiratory burst,* our innate immune response, in which superoxide anion ($O_2^{\bullet -}$) and the hydroxyl radical (OH•) form to attack pathogens (Fig 14-1). The nicotinamide adenine dinucleotide phosphate oxidases (Nox) constitute an enzyme family that functions primarily to produce ROS and is expressed in many cells. Table 14-1 presents some important ROS.

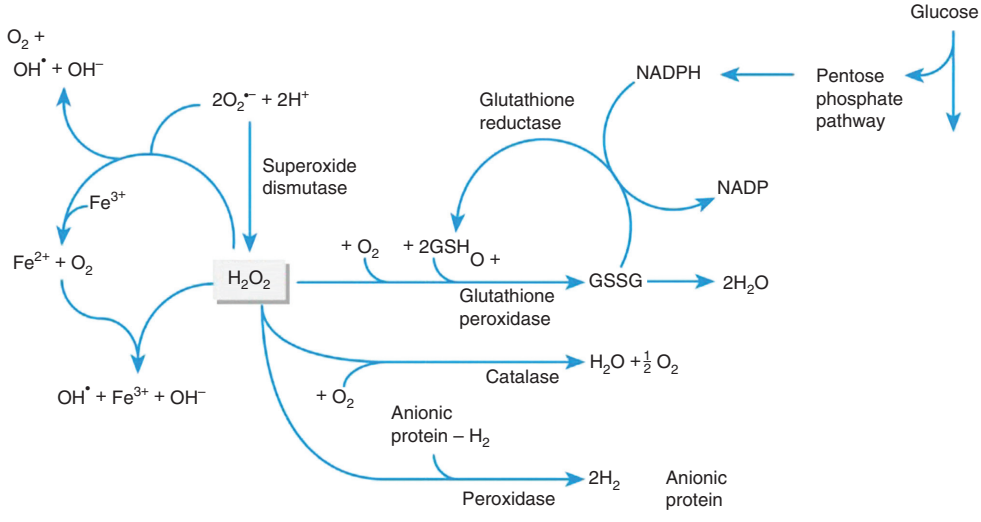


Figure 14-1 Generation and detoxification of reactive oxygen species. *Left,* Generation of hydroxyl radicals (OH•) through the reaction of iron with the superoxide anion ($O_2^{\bullet -}$) and hydrogen peroxide (H_2O_2). *Center,* Conversion of $O_2^{\bullet -}$ into H_2O_2 and the 3 subsequent pathways involved in eliminating it via (1) glutathione peroxidase; (2) catalase; and (3) peroxidase. *Right,* The role of the glucose-initiated pentose phosphate pathway in providing reduced glutathione (GSH) for redox reactions. GSSG = oxidized glutathione; $NADP^+$ = nicotinamide adenine dinucleotide phosphate; NADPH = reduced $NADP^+$. *(Modified with permission from Forrester JV, Dick AD, McMenamin PG, Roberts F, Pearlman E.* The Eye: Basic Sciences in Practice. *4th ed. Elsevier/Saunders; 2016:194.)*

Table 14-1 ROS and Antioxidant Pathways

ROS	ROS Sources	Antioxidants Involved in Detoxification
Superoxide anion ($O_2^{\bullet-}$)	Electron transport chain (mitochondria), respiratory burst (neutrophils), xanthine oxidase	Superoxide dismutase
Hydroxyl radical (OH•)	Electron transport chain (mitochondria), respiratory burst (neutrophils)	Catalase and peroxidase
Hydrogen peroxide (H_2O_2)	Electron transport chain (mitochondria), respiratory burst (neutrophils), superoxide dismutase	Catalase and peroxidase, glutathione peroxidase
Singlet oxygen ($^1O_2$)	Photo-oxidation	Carotenoids (quenching)

ROS = reactive oxygen species.

CLINICAL PEARL

Leber hereditary optic neuropathy (LHON) arises from RGC loss secondary to pathogenic variants (mutations) in the mitochondrial DNA affecting the electron transport chain. This process leads to reduced ATP production, accumulation of free radicals, and subsequent apoptosis. Ubiquinone, also known as coenzyme Q_{10} (CoQ), is an electron carrier within the transport chain. The oral drug idebenone is a short-chain benzoquinone whose function is similar to that of CoQ. Administration of this medication supplies mitochondria with an alternative electron carrier, which improves function through increased ATP and decreased oxidative stress. Idebenone has been evaluated in the treatment of patients with LHON. See BCSC Section 5, *Neuro-Ophthalmology,* for further discussion of LHON.

Lipid Peroxidation

Lipid peroxidation occurs via auto-oxidation and photo-oxidation. Random oxidation of lipids occurs via *auto-oxidation,* a free radical chain reaction usually described as a series of 3 steps:

1. initiation
2. propagation
3. termination

During initiation, fatty acids are converted to an intermediate radical following removal of an allylic hydrogen. During propagation, which follows immediately, the fatty acid radical intermediate reacts with oxygen at both ends to produce fatty acid peroxy radicals (ROO•); this process is known as *lipid peroxidation.* Thus, a new fatty acid radical is formed, which again can react with oxygen. As long as oxygen is available, a single free radical can cause oxidation of thousands of unsaturated fatty acids. A termination reaction, in which 2 radicals

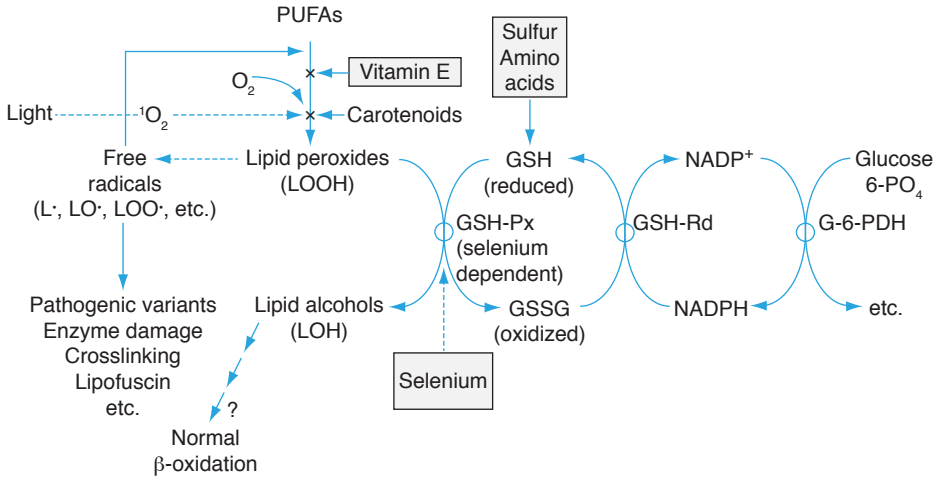


Figure 14-2 Mechanisms by which several antioxidants protect against oxidative damage. *Upper left,* Free radicals lead to the formation of lipid peroxides. Vitamin E inhibits this auto-oxidation process by scavenging free radical intermediates. Carotenoids inhibit photo-oxidation by quenching singlet oxygen ($^1O_2$). *Center,* If lipid hydroperoxides are formed, they can be reduced by glutathione peroxidase (GSH-Px), which requires selenium as a cofactor. If these protective enzymes are not fully active, more free radicals are formed by the breakdown of lipid peroxides, which in turn leads to additional oxidation of polyunsaturated fatty acids (PUFAs). G-6-PDH = glucose-6-phosphate dehydrogenase; GSH = glutathione; GSH-Rd = glutathione reductase; GSSG = oxidized glutathione; $NADP^+$ = nicotinamide adenine dinucleotide phosphate; NADPH = reduced $NADP^+$. *(Courtesy of F.J.G.M. van Kuijk, MD, PhD.)*

form a nonradical product, can interrupt the chain reaction. Auto-oxidation is also inhibited by free radical scavengers such as vitamin E, which cause termination reactions (Fig 14-2).

Polyunsaturated fatty acids (PUFAs) are susceptible to auto-oxidation because of their double bonds, whose allylic hydrogen atoms are easily removed by several types of initiating radicals. The primary products of auto-oxidation formed during the propagation step are hydroperoxides (ROOH), which may decompose, especially in the presence of trace amounts of transition metal ions (eg, ferrous ions [reduced iron, Fe^{2+}] or cupric ions [reduced copper, Cu^{1+}]), to create ROO•, OH•, and oxy radicals (RO•).

PUFAs that are particularly susceptible to peroxidation include arachidonic acid and docosahexaenoic acid. Docosahexaenoic acid is found in photoreceptor outer segments and accounts for up to 40% of total lipid content in rod photoreceptor cells. See the section Vulnerability of the Retina to Reactive Oxygen Species later in this chapter.

In *photo-oxidation,* by contrast, oxygen is activated by light to form $^1O_2$, which in turn reacts with unsaturated fatty acids or other cellular constituents. The most widely accepted mechanism of $^1O_2$ generation involves exposure of a photosensitizer to light in the presence of normal triplet oxygen ($^3O_2$). Photo-oxidation can be inhibited by $^1O_2$ quenchers such as carotenoids (see the section Carotenoids) (see Fig 14-2).

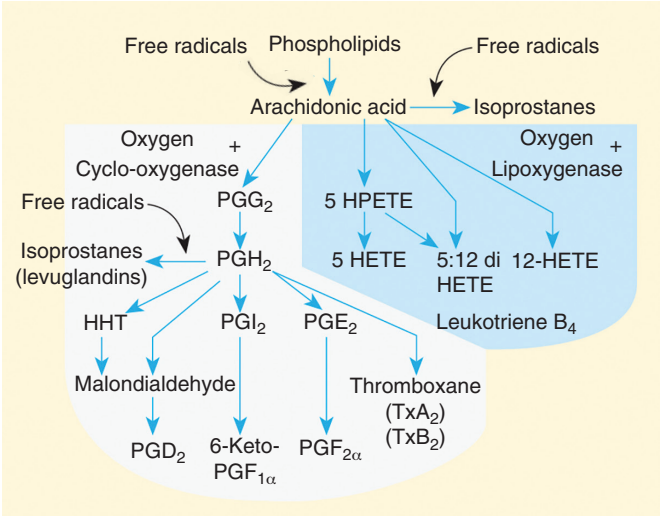


Figure 14-3 Consequences of lipid peroxidation. Large quantities of arachidonic acid are released following peroxidation of the phospholipid bilayer. Subsequently, arachidonic acid acts as a substrate for the production of several inflammatory mediators shown in this figure. In addition, free radicals directly contribute to the production of isoprostanes, which are markers and mediators of oxidative stress. HETE = hydroxyeicosatetraenoic acid; HHT = hydroxyheptadecatrenoic acid; HPETE = hydroperoxyeicosatetraenoic acid; PGD= prostaglandin D; PGE = prostaglandin E; PGF = prostaglandin F; PGG = prostaglandin G; PGH = prostaglandin H; PGI = prostaglandin I. *(Modified with permission from Forrester JV, Dick AD, McMenamin PG, Roberts F, Pearlman E.* The Eye: Basic Sciences in Practice. *4th ed. Elsevier; 2016:205.)*

Lipid peroxidation causes not only direct damage to the cell membrane but also secondary damage to cells through its breakdown products (Fig 14-3). Lipid peroxides are unstable, and they break down to form many aldehydes, such as malondialdehyde and 4-hydroxyalkenals. These aldehydes can quickly react with proteins, inhibiting the proteins' normal functions. Both the lens and the retina are susceptible to such oxidative damage.

Reactive Oxygen Species and Defense Mechanisms

Although the eye is constantly exposed to light, it is protected from the consequences of UV-light exposure via various mechanisms employed by different ocular structures. The cornea and the lens prevent different wavelengths of UV light from reaching the retina (see Chapter 10, Fig 10-3). The high concentration of ascorbate (vitamin C) in the aqueous and vitreous also acts to block UV light and participates in cellular antioxidant pathways.

Cellular components are protected from ROS by antioxidant mechanisms. Cells contain enzymes that neutralize ROS and the toxic metabolites formed by the interaction between ROS and cellular components (see Fig 14-1). These enzymes include superoxide dismutase (SOD), catalase, glutathione reductase, and glutathione peroxidase (GSH-Px); they are discussed later in this chapter. The transcription factor *nuclear factor erythroid 2–related factor 2 (Nrf2)* regulates expression of numerous antioxidant genes and is

upregulated under oxidative stress. Nrf2 is a potential therapeutic target, and induction of Nrf2 enhanced RGC survival in experimental models of oxidative stress generated by ischemia–reperfusion injury.

The cell is also protected from ROS through the compartmentalization of these species, which prevents their contact with intracellular components. An example is the electron transport chain, which is contained within the walls of the mitochondria. However, some reactive species may leak out of their enzyme-binding sites or escape antioxidant enzymes, causing damage to cellular components such as proteins, membrane lipids, and DNA. In addition, any free iron (Fe^{2+}) present may catalyze the formation of OH• from superoxide anion ($O_2^{\bullet -}$) and H_2O_2 (see Fig 14-1).

CLINICAL PEARL

Formation of H_2O_2 by Fe^{2+} is the mechanism underlying damage to structures in the eye in siderosis bulbi and hemosiderosis bulbi. The former is due to iron released into the eye from a retained intraocular foreign body, the latter, from the breakdown of hemoglobin molecules in cases of intraocular hemorrhage. In both conditions, excess Fe^{2+} can accumulate in the trabecular meshwork, neurosensory retina, and retinal pigment epithelium (RPE), leading to secondary dysfunction. See BCSC Section 11, *Lens and Cataract,* and Section 12, *Retina and Vitreous,* for additional discussion of siderosis bulbi.

Oxidative Damage to the Lens and Protective Mechanisms

As stated earlier, ROS are generated by metabolic processes, inflammatory responses, and exposure to UV light. The lens relies almost entirely on anaerobic metabolism and is shielded from the immune system. Thus, the major source of ROS in the lens is exposure to UV light. Although most UVB radiation (<320-nm wavelength) that strikes the human eye is absorbed either by the cornea or by the ascorbate present at high levels in the aqueous humor, a certain amount reaches the lens epithelium, where it can cause damage. UVA light (320–400-nm wavelength) can penetrate more deeply into the lens, where it can react with various chromophores to generate H_2O_2, $O_2^{\bullet -}$, and $^1O_2$.

Although repair and regeneration mechanisms are active in the lens epithelium and superficial cortex, no such mechanisms exist in the deep cortex and the nucleus, where any damage to lens proteins and membrane lipids is irreversible. One result of this damage can be crosslinking and insolubilization of proteins, leading to loss of transparency (see Chapter 10 in this volume and BCSC Section 11, *Lens and Cataract*). The lens contains unusually high levels of protein sulfhydryl groups that must exist almost entirely in the reduced state for the tissue to remain transparent. The young, healthy lens possesses a variety of effective antioxidant systems to protect against oxidative stress. These defenses include the enzymes glutathione reductase, GSH-Px, catalase, and SOD (see Fig 14-1).

Glutathione (GSH), concentrated at the lens epithelium, acts as a major scavenger of ROS in the lens. With age, levels of GSH decline significantly in the human lens, particularly

in the nucleus. Studies have indicated that a cortical–nuclear barrier may exist in the mature human lens, which inhibits the free flow of GSH to the nucleus. As a result, the human lens nucleus becomes more susceptible to oxidative damage and cataract formation with age.

The free radical scavengers ascorbate and vitamin E, also present in the lens, work in conjunction with GSH and the GSH reduction-oxidation (redox) cycle to protect against oxidative damage (see Fig 14-2). Carotenoids that can quench $^1O_2$ also exist in the lens. Epidemiologic (observational) studies have shown that individuals with higher levels of plasma antioxidants, particularly vitamin E, have a reduced risk of cataract, especially nuclear cataract. However, 3 prospective, randomized, placebo-controlled clinical trials—the Age-Related Eye Disease Study (AREDS); the Age-Related Eye Disease Study 2 (AREDS2); and the Vitamin E, Cataract, and Age-Related Maculopathy Trial (VECAT)—found that high-dose formulations of antioxidants neither prevented the development nor slowed the progression of age-related cataracts.

Age-Related Eye Disease Study Research Group. A randomized, placebo-controlled clinical trial of high-dose supplementation with vitamins C and E and beta carotene for age-related cataract and vision loss: AREDS report no. 9. *Arch Ophthalmol.* 2001;119(10):1439–1452. [Erratum appears in *Arch Ophthalmol.* 2008;126(9):1251.]

Age-Related Eye Disease Study 2 (AREDS2) Research Group; Chew EY, SanGiovanni JP, Ferris FL, et al. Lutein/zeaxanthin for the treatment of age-related cataract: AREDS2 randomized trial report no. 4. *JAMA Ophthalmol.* 2013;131(7):843–850.

Cetinel S, Semenchenko V, Cho J-Y, et al. UV-B induced fibrillization of crystallin protein mixtures. *PLoS One*. 2017;12(5):e0177991. doi:10.1371/journal.pone.0177991

McNeil JJ, Robman L, Tikellis G, Sinclair MI, McCarty CA, Taylor HR. Vitamin E supplementation and cataract: randomized controlled trial. *Ophthalmology.* 2004;111(1): 75–84.

Vulnerability of the Retina to Reactive Oxygen Species

Experimental data have shown that retinal photoreceptors degenerate when exposed to oxidative challenges such as hyperbaric oxygen, iron overload, or injection of lipid peroxide into the vitreous humor. In addition, the retina degenerates when antioxidant defenses are reduced, presumably increasing lipid peroxidation even in the absence of unusual oxidative stress. The retina has several distinctive characteristics that make it vulnerable to damage from lipid peroxidation, including the following:

- Vertebrate rod outer segments are susceptible to damage by oxygen because of their high levels of PUFAs. Their phospholipids contain docosahexaenoic acid, the most highly polyunsaturated fatty acid occurring in nature. It is well established that PUFAs are sensitive to peroxidation in proportion to their number of double bonds.
- Rod inner segments are very rich in mitochondria. Most endogenous ROS are produced by the mitochondrial electron transport chain, which may leak activated oxygen species.
- The abundant oxygen supply through the choroid and the retinal vessels elevates the risk of oxidative damage. Vertebrate retinas maintained in vitro showed at least a sevenfold-higher rate of oxygen consumption per milligram of protein than all

other tissues tested (except the adrenal gland). The oxygen tension is highest at the choroid and decreases toward the inner segments of the retina.
- There are many chromophores in the outer retina. Light exposure may trigger photo-oxidative processes mediated by $^1O_2$.

Intense light at levels that may be encountered in daily life is phototoxic to the retina. Even though the cornea absorbs UV radiation, the retinas of eyes without nuclear sclerotic cataract are exposed to UV light in the range of 350–400 nm. As the lens yellows with age, it can block wavelengths of up to 430 nm. Because the adult lens absorbs nearly 100% of light below 400 nm, little or no UV light reaches the retina in older people.

Antioxidants in the Retina and Retinal Pigment Epithelium

As mentioned earlier, several antioxidant mechanisms have been established in biological systems, including free radical scavenging, quenching of $^1O_2$, and enzymatic reduction of ROOH. Antioxidants found in vertebrate retinas and RPE include the following:

- selenium
- GSH
- selenium-dependent GSH-Px
- non–selenium-dependent GSH-Px (glutathione-*S*-transferase)
- vitamin E
- SOD
- catalase
- carotenoids

Figure 14-2 depicts the relation between some of these antioxidants and the protective mechanisms.

Yu BP. Cellular defenses against damage from reactive oxygen species. *Physiol Rev.* 1994;74(1): 139–162.

Selenium, Glutathione, and Glutathione Peroxidase

Figures 14-1 and 14-2 illustrate the role of GSH (discussed earlier in this chapter). The primary enzyme involved in GSH-mediated detoxification of peroxides is GSH-Px, which is selenium dependent. The RPE contains the highest concentration of selenium in the human eye: RPE cells may contain 100–400 ng, up to 10 times as many as in the retina (40 ng). In the human eye, the selenium level in the retina remains constant with age; in the RPE, however, the level increases with age.

González de Vega R, García M, Fernández-Sánchez ML, González-Iglesias H, Sanz-Medel A. Protective effect of selenium supplementation following oxidative stress mediated by glucose on retinal pigment epithelium. *Metallomics*. 2018;10(1):83–92.

Vitamin E

Vitamin E scavenges free radicals, thus terminating the propagation step (described earlier) and leading to interruption of the auto-oxidation reaction. A detailed study of the vitamin E

content of microdissected parts of vertebrate eyes showed that the RPE is rich in vitamin E relative to photoreceptors and that photoreceptors are rich in vitamin E relative to most other cells in the eye. Furthermore, vitamin E levels in human retinal tissues increase with age until the sixth decade of life, after which they decrease. This decrease coincides with the age at which the incidence of AMD increases in the population.

Friedrichson T, Kalbach HL, Buck P, van Kuijk FJ. Vitamin E in macular and peripheral tissues of the human eye. *Curr Eye Res.* 1995;14(8):693–701.

Superoxide Dismutase and Catalase

SOD catalyzes the dismutation of superoxide to H_2O_2, which is further reduced to water by catalase or peroxidase. Two types of SOD are isolated from mammalian tissues: (1) copper-zinc SOD (CuZnSOD), the cytoplasmic enzyme, which is inhibited by cyanide; and (2) manganese SOD (MnSOD), the mitochondrial enzyme, which is not inhibited by cyanide. SOD activity and polymorphisms have been implicated in AMD in certain populations.

Catalase catalyzes the reduction of H_2O_2 to water. At present, information on catalase activity in the retina is limited. Total retinal catalase activity has been found to be very low but detectable in rabbits. A protective role for catalase has been reported in rats with retinal ischemia–reperfusion injury, where it prevented RGC loss and preserved function as shown by electroretinography. In addition, treatment with catalase was shown to be protective against hyperglycemia-induced oxidative stress in cell culture and animal models.

Anand A, Sharma NK, Gupta A, Prabhakar S, Sharma SK, Singh R. Superoxide dismutase1 levels in North Indian population with age-related macular degeneration. *Oxid Med Cell Longev*. 2013;2013:365046.

Chen B, Tang L. Protective effects of catalase on retinal ischemia/reperfusion injury in rats. *Exp Eye Res*. 2011;93(5):599–606.

Kowalski M, Bielecka-Kowalska A, Oszajca K, et al. Manganese superoxide dismutase (MnSOD) gene (Ala-9Val, Ile58Thr) polymorphism in patients with age-related macular degeneration (AMD). *Med Sci Monit.* 2010;16(4):CR190–CR196.

Ohta Y, Yamasaki T, Niwa T, Niimi K, Majima Y, Ishiguro I. Role of catalase in retinal antioxidant defence system: its comparative study among rabbits, guinea pigs, and rats. *Ophthalmic Res*. 1996;28(6):336–342.

Ascorbate

In many species, ascorbate (vitamin C) is found throughout the eye in concentrations that are high relative to those in other tissues. In addition to blocking UV light in the aqueous humor, ascorbate is thought to function synergistically with vitamin E to terminate free radical reactions. Vitamin C functions as an electron donor, reducing oxidized elements and molecules. It has been proposed that vitamin C can react with the vitamin E radicals formed when vitamin E scavenges free radicals. Vitamin E radicals are then regenerated to form native vitamin E. The vitamin C radicals resulting from this regeneration can be reduced by nicotinamide adenine dinucleotide (NADH) reductase, with NADH as the electron acceptor. Ascorbate is found at high levels in the aqueous humor as well as in the vitreous, where it also functions to reduce oxygen levels (see Chapter 11, Fig 11-5).

Buettner GR. The pecking order of free radicals and antioxidants: lipid peroxidation, α-tocopherol, and ascorbate. *Arch Biochem Biophys*. 1993;300(2):535–543.
Reddy VN, Giblin FJ, Lin LR, Chakrapani B. The effect of aqueous humor ascorbate on ultraviolet-B-induced DNA damage in lens epithelium. *Invest Ophthalmol Vis Sci*. 1998;39(2):344–350.
Rose RC, Bode AM. Ocular ascorbate transport and metabolism. *Comp Biochem Physiol A Comp Physiol*. 1991;100(2):273–285.

Carotenoids

Carotenoids (xanthophylls) are thought to play various roles in biological systems, including limiting chromatic aberration at the fovea of the retina and quenching of $^1O_2$. Beta carotene, the precursor of vitamin A, can act as a free radical trap at low oxygen tension. Studies of postmortem human retinas have shown that carotenoids make up the yellow pigment in the macula. Two carotenoids, *lutein* and *zeaxanthin,* are present in the macula and located in Henle fiber layer. In humans, zeaxanthin is concentrated primarily in the fovea, whereas lutein is dispersed throughout the retina. Interestingly, little beta carotene is present in the human eye. Furthermore, carotenoids are present only in the retina and are absent from the RPE. In the peripheral retina, lutein and zeaxanthin are concentrated in rod outer segments and may act as antioxidants to protect against short-wavelength visible light. Figure 14-4A shows the localization of antioxidants in the human macula and peripheral retina, and Figure 14-4B shows their localization in a cross section of the peripheral retina.

Chew EY, Clemons TE, Agrón E, et al; Age-Related Eye Disease Study Research Group. Long-term effects of vitamins C and E, β-carotene, and zinc on age-related macular degeneration. AREDS report no. 35. *Ophthalmology.* 2013;120(8):1604–1611.e4.
Khachik F, Bernstein PS, Garland DL. Identification of lutein and zeaxanthin oxidation products in human and monkey retinas. *Invest Ophthalmol Vis Sci.* 1997;38(9):1802–1811.

The Role of Oxidative Stress in Vision-Threatening Ophthalmic Diseases

ROS and oxidative stress have been directly implicated in the pathogenesis of several diseases that are the leading causes of blindness, including glaucoma, diabetic retinopathy, and AMD (Table 14-2). In many cases, the onset of oxidative damage may precede the clinical manifestation of these conditions.

In addition to their role in the diseases discussed in the following sections, oxidative mechanisms are involved in numerous diseases of the anterior and posterior segments and are central to many inherited diseases of the eye. Future research and treatment will target these mechanisms, directly and indirectly, to aid in the management of their related conditions. Figure 14-5 outlines these mechanisms and describes areas for therapeutic intervention.

Ung L, Pattamatta U, Carnt N, Wilkinson-Berka JL, Liew G, White AJR. Oxidative stress and reactive oxygen species: a review of their role in ocular disease. *Clin Sci (Lond).* 2017;131(24):2865–2883.

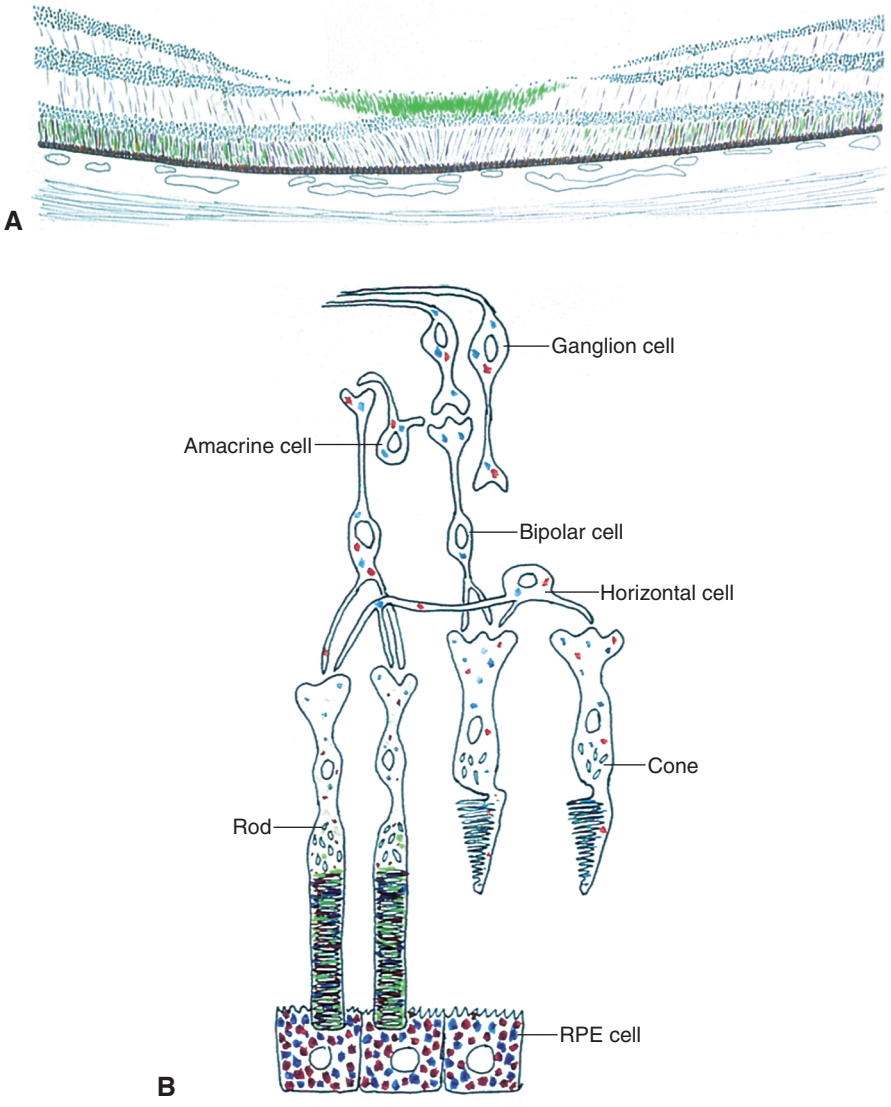


Figure 14-4 Localization of antioxidants in the retina. **A,** Localization of antioxidants in the human macula. Vitamin E *(blue)* and selenium *(red)* are concentrated primarily in the retinal pigment epithelium (RPE). In the macula, carotenoids *(green)* are present in Henle fiber layer; in the peripheral retina, they are also present in the rods. **B,** Localization of antioxidants in a cross section of the peripheral retina. Vitamin E and selenium remain concentrated mainly in the RPE but are also enriched in the rod outer segments. Carotenoids have been found in rod outer segments in the peripheral retina. *(Illustrations by J. Woodward, MD; courtesy of F.J.G.M. van Kuijk, MD, PhD.)*

Glaucoma

The involvement of ROS in glaucoma may pertain to their effect on the trabecular meshwork and RGCs. An increasing body of evidence suggests that trabecular dysfunction occurs following exposure of the trabecular meshwork to ROS. In addition, several reports have demonstrated the development of oxidative stress and cell loss when RGCs in culture are exposed to increased pressure.

Table 14-2 Oxidative Mechanism in the Pathophysiology of Common Retinal Diseases

Disease	Mechanism
AMD	AMD risk factors (eg, aging, smoking) linked to increased systemic oxidative stress Oxidative modifications to proteins and DNA in Bruch membrane, drusen, and RPE cells Light exposure associated with increased generation of ROS and AGEs and with increased risk of AMD Colocalization of RAGE with AGE deposits and macular disease in AMD retinas RAGE-induced secretion of VEGF in RPE cells Low macular pigment associated with AMD Dietary or supplemental intake of antioxidants (eg, vitamins, carotenoids) and zinc linked to lower risk of AMD progression Decreased viability and increased proliferation in cultured RPE and choroidal endothelial cells exposed to the oxidant *t*-BHP Increased proliferation and VEGF upregulation in choroidal endothelial cells exposed to AGEs
Diabetic retinopathy	Mitochondrial overproduction of superoxide potentially disruptive to multiple pathways implicated in diabetes (eg, polyol, AGE, protein kinase C, hexosamine) Prevention of early retinal cell death by superoxide inhibition Involvement of oxidative stress–activated caspases and NF-κB in retinal cell death Increased expression of oxidative stress markers in endothelial cells and pericytes in a high-glucose environment Impaired glucose transport in H_2O_2-exposed retinal endothelial cells Link between the oxidant peroxynitrite and upregulated VEGF expression in endothelial cells
Inherited retinal degenerations	Increased oxygen concentration in outer retina of multiple animal models of retinal degeneration Cone damage due to increased retinal oxygen levels Link between thioredoxin antioxidant defense and a rod-derived cone survival factor Increased ROS and decreased GSH in an in vitro model of photoreceptor apoptosis Downregulation of DNA repair mediators in the *rd1* mouse retina Reduction in cone cell loss and preservation of cone ERGs observed in *rd1* mice treated with antioxidants Decreased antioxidant defense (eg, GST and GSH-Px) in *rd1* mice

AGE = advanced glycation end product; AMD = age-related macular degeneration; ERG = electroretinogram; GSH = glutathione; GSH-Px = glutathione peroxidase; GST = glutathione-*S*-transferase; NF-κB = nuclear factor κB; RAGE = receptor of AGEs; ROS = reactive oxygen species; RPE = retinal pigment epithelium; *t*-BHP = *tert*-butyl hydroperoxide; VEGF = vascular endothelial growth factor.

Modified with permission from Schachat AP, ed. *Ryan's Retina*. 5th ed. Elsevier; 2013:Table 22.1.

Population-based studies on the effect of dietary antioxidants have shown conflicting results in glaucoma, and earlier studies failed to show a benefit of these antioxidants. However, a subsequent study, with longer follow-up, demonstrated that the risk of developing primary open-angle glaucoma (POAG) was 20% lower in participants who consumed more foods high in antioxidants. Furthermore, in patients with POAG, a similar diet reduced the risk of development of paracentral visual field defects by 44%. The mechanism of such an effect has been suggested to involve aberrant nitric oxide pathways.

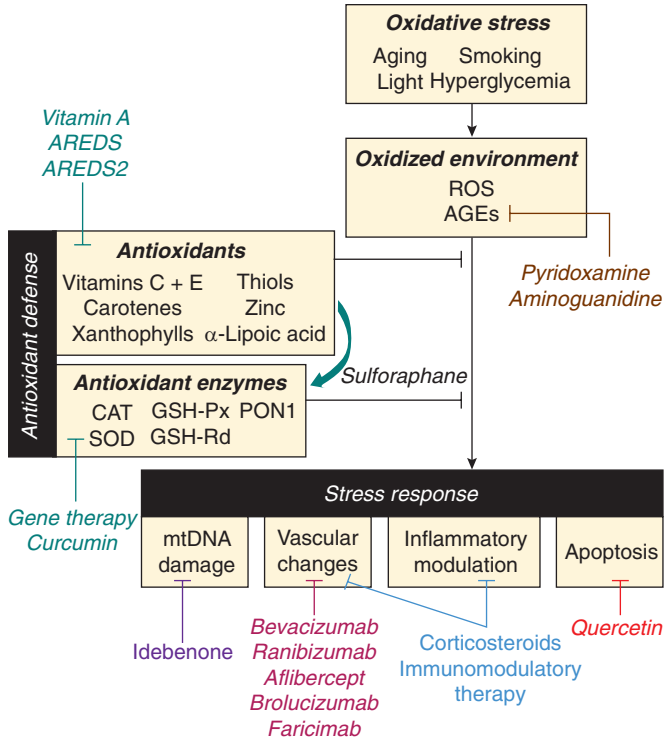


Figure 14-5 Oxidative mechanisms and areas of current and potential therapeutic intervention in retinal diseases. Pathways indicated in *green* describe supportive interventions, while those in all other colors represent inhibition. AGEs = advanced glycation end products; AREDS = Age-Related Eye Disease Study; AREDS2 = Age-Related Eye Disease Study 2; CAT = catalase; GSH-Px = glutathione peroxidase; GSH-Rd = glutathione reductase; mtDNA= mitochondrial DNA; PON1 = paraoxonase 1; ROS = reactive oxygen species; SOD = superoxide dismutase. *(Modified with permission from Schachat AP, ed.* Ryan's Retina. *5th ed. Elsevier; 2013:Fig 22.1.)*

Benoist d'Azy C, Pereira B, Chiambaretta F, Dutheil F. Oxidative and anti-oxidative stress markers in chronic glaucoma: a systematic review and meta-analysis. *PLoS One*. 2016;11(12):e0166915. doi:10.1371/journal.pone.0166915

Kang JH, Willett WC, Rosner BA, Buys E, Wiggs JL, Pasquale LR. Association of dietary nitrate intake with primary open-angle glaucoma: a prospective analysis from the Nurses' Health Study and Health Professionals Follow-up Study. *JAMA Ophthalmol*. 2016;134(3):294–303.

Diabetic Retinopathy

Diabetic retinopathy is the leading cause of blindness worldwide in adults aged 20 to 64 years. Several metabolic pathways, initiated by hyperglycemia and lack of insulin signaling, generate oxidative stress and are implicated in the development of diabetic retinopathy:

- polyol pathway
- protein kinase C (PKC) pathway
- hexosamine pathway

Advanced glycation end products (AGEs) result from nonenzymatic glycation of various molecules (proteins, lipids, nucleic acids) and exist in foods prepared at very high temperatures. AGEs interact with specific cell-surface receptors, which then signal intracellular inflammatory pathways, leading to generation of ROS.

ROS can lead to long-term changes via epigenetic modification, especially in mitochondrial DNA. This may partly explain the phenomenon of metabolic memory, wherein beneficial effects of past tight metabolic control persist for a period, reducing the progression of retinopathy, as demonstrated by the Diabetes Control and Complications Trial (DCCT). Conversely, in patients with poor metabolic control, epigenetic modifications may allow diabetic retinopathy to progress even after intensive control has been achieved. Most data supporting a role for antioxidants in diabetic retinopathy have come from cell culture or animal models. One clinical trial evaluated the role of the PKC inhibitor ruboxistaurin, which reduced vision loss and the need for macular laser therapy in comparison to controls in patients with diabetic retinopathy.

CLINICAL PEARL

Radiation retinopathy is an example of retinal damage from ROS. Clinically, the retinal findings in this condition are comparable to those of diabetic retinopathy. Diabetic retinopathy and complications of radiation retinopathy, such as macular edema and retinal neovascularization, are therefore managed similarly.

Aiello LP, Vignati L, Sheetz MJ, et al; PKC-DRS and PKC-DRS2 Study Groups. Oral protein kinase C β inhibition using ruboxistaurin: efficacy, safety, and causes of vision loss among 813 patients (1,392 eyes) with diabetic retinopathy in the Protein Kinase C β Inhibitor-Diabetic Retinopathy Study and the Protein Kinase C β Inhibitor-Diabetic Retinopathy Study 2. *Retina*. 2011;31(10):2084–2094.

Behl T, Kaur I, Kotwani A. Implication of oxidative stress in progression of diabetic retinopathy. *Surv Ophthalmol*. 2016;61(2):187–196.

Calderon GD, Juarez OH, Hernandez GE, Punzo SM, De la Cruz ZD. Oxidative stress and diabetic retinopathy: development and treatment. *Eye (Lond)*. 2017;31(8):1122–1130.

Li C, Miao X, Li F, et al. Oxidative stress-related mechanisms and antioxidant therapy in diabetic retinopathy. *Oxid Med Cell Longev*. 2017;2017:9702820. doi:10.1155/2017/9702820

Van Puyvelde K, Mets T, Njemini R, Beyer I, Bautmans I. Effect of advanced glycation end product intake on inflammation and aging: a systematic review. *Nutr Rev*. 2014;72(10):638–650.

Age-Related Macular Degeneration

AMD represents the leading cause of blindness in the Western world. Risk factors related to oxidative mechanisms include sunlight exposure, smoking, and, to some extent, genetics. Several models demonstrate the protective effect of antioxidants in this condition. AREDS and AREDS2 represent 2 of the largest prospective randomized clinical trials studying the effects of antioxidants on the eye, especially the development of lenticular opacity and the development and progression of AMD. No data confirmed oral supplements had a role

in the development of cataract; however, both trials supported the role of antioxidants in limiting the progression of AMD in high-risk patients. See BCSC Section 12, *Retina and Vitreous,* for further discussion of AREDS.

Age-Related Eye Disease Study 2 Research Group. Lutein + zeaxanthin and omega-3 fatty acids for age-related macular degeneration: the Age-Related Eye Disease Study 2 (AREDS2) randomized clinical trial. *JAMA*. 2013;309(19):2005–2015.

Shaw PX, Stiles T, Douglas C, et al. Oxidative stress, innate immunity, and age-related macular degeneration. *AIMS Mol Sci*. 2016;3(2):196–221.

PART V
Ocular Pharmacology

CHAPTER 15

Pharmacologic Principles

Highlights

- Topical medications that are absorbed by the nasal mucosa bypass first-pass metabolism by the liver and can attain significant levels in the blood. Systemic effects can be reduced by having patients gently close their eyes or apply digital nasolacrimal compression for 5 minutes after instilling an eyedrop.
- To protect internal ocular structures from medication-related toxicity when intraocular drugs are used, preserved medication must be avoided and the drug's concentration carefully controlled.
- For systemically administered medications, lipophilic compounds are more likely than hydrophilic compounds to penetrate the blood–ocular and blood–brain barriers.
- Strict adherence to standard aseptic technique is necessary for preparation and injection of intraocular medication so that infection can be prevented.
- Genetic polymorphisms can alter the way that patients respond to drug therapies. These variations are under evaluation in patients with age-related macular degeneration and in those with glaucoma.

Amphipathic Containing both hydrophilic and lipophilic properties.

Bioavailability The rate at which an active drug reaches the site of action and the extent to which it is available to the target tissue.

Biologic agent A product made from living organisms or containing components of living organisms and used in the prevention, diagnosis, or treatment of disease.

Emulsion A mixture of 2 immiscible components.

Hydrophilic (lipophobic) Tendency of a molecule to dissolve in water.

Lipophilic (hydrophobic) Tendency of a molecule to dissolve in lipids.

Pharmacodynamics The study of the biochemical and physiological effects of drugs/agents on a biological system, including the mechanisms of their actions.

Pharmacokinetics The study of the absorption, distribution, metabolism, and excretion of drugs/agents in a biological system.

Pharmacology The study of drug action and the interactions of living organisms with therapeutic substances through biochemical processes.

(Continued)

Pharmacotherapeutics The study of how to achieve the desired effects, or prevent/minimize the adverse effects or toxicity, of a drug or agent.

Suspension A mixture of a substance with poor solubility and a dispersion medium in which the substance is evenly distributed.

Introduction to Pharmacologic Principles

This chapter reviews the general principles of pharmacology and includes discussion of special features of the eye that facilitate or impede ocular therapy.

Pharmacokinetics

Pharmacokinetics concerns the movement of a drug through the body, including the absorption, distribution, metabolism, and excretion of that drug. To achieve a therapeutic effect, a drug must reach its site of action in sufficient concentration. The concentration at the site of action is a result of the following:

- route of administration
- amount administered
- extent and rate of absorption at the administration site
- distribution and binding of the drug in tissues
- movement by bulk flow in circulating fluids
- transport between body compartments
- biotransformation
- excretion

Together, pharmacokinetics and dose determine *bioavailability,* or the concentration of the active drug at the therapeutic site.

Pharmacodynamics

Pharmacodynamics concerns the biological activity and clinical effects of a drug—the drug's action after distribution (pharmacokinetics) of the active agent to the therapeutic site. Pharmacodynamics includes the tissue receptor for the drug and the intracellular changes initiated by the active drug binding with the receptor. Thus, the pharmacodynamic action of a drug is often described using the receptor for that drug; for example, a drug may be categorized as an α-adrenergic agonist or a β-adrenergic antagonist.

Mechanism of action

Most drugs act by binding to and altering the function of regulatory macromolecules, usually neurotransmitter receptors, hormone receptors, or enzymes. Binding may be a reversible association mediated by electrostatic and/or van der Waals forces, or it may involve formation of a covalent intermediate. If the drug–receptor interaction stimulates the receptor's natural function, the drug is termed an *agonist.* Stimulation of an opposing effect characterizes an

antagonist. Corresponding effectors of enzymes are termed *activators* and *inhibitors*. This terminology is crucial to understanding Chapter 16.

The relationship between the initial drug–receptor interaction and the drug's clinical dose-response curve may be simple or complex. In some cases, the drug's clinical effect closely reflects the degree of receptor occupancy on a moment-to-moment basis. Such is usually the case for drugs that affect neural transmission or for drugs that are enzyme inhibitors. In contrast, some drug effects lag hours behind receptor occupancy or persist long after the drug is gone. Such is the case with many drugs acting on hormone receptors because their effects are often mediated through a series of biochemical events.

In addition to differences in timing of receptor occupancy and drug effects, the degree of receptor occupancy can differ considerably from the corresponding drug effect. For example, because the amount of carbonic anhydrase present in the ciliary processes is 100 times that required to support aqueous secretion, more than 99% of the enzyme must be inhibited before secretion is reduced. On the other hand, some maximal hormone responses occur at concentrations well below those required for receptor saturation, indicating the presence of "unbound receptors."

Pharmacotherapeutics

Pharmacotherapeutics is the study of the uses of drugs in reaching a given clinical endpoint, such as the prevention or treatment of disease. The therapeutic dose may vary for any patient and is related to the patient's age, sex, race, other currently prescribed medications, and preexisting medical conditions. Ocular pharmacotherapeutics is covered in Chapter 16 of this volume.

Toxicity

Toxicity refers to the adverse effects of either medications or environmental chemicals, including poisoning. Toxicity may be influenced by pharmacokinetics and/or pharmacodynamics (the biochemical and physiological effects of a drug/agent). For example, topically applied ophthalmic medications are readily absorbed through the mucous membranes of the eye and nasopharynx, as well as through the iris and ciliary body. Topical absorption avoids the first-pass metabolism of the liver and increases systemic bioavailability. Therefore, the systemic toxicity of these medications may be greater than expected relative to the total topical dose.

The importance of pharmacokinetics and its influence on potential toxicity is illustrated in the pediatric population. Drug metabolism and excretion are less developed in neonates and infants than in adults. For example, in early neonatal life, the drug-metabolizing activities of the cytochrome P450–dependent, mixed-function oxidases and the conjugating enzymes are approximately 50%–70% of those in adults. A second example is the formation of glucuronide, which does not reach adult levels until the third or fourth year of life. Similarly, the glomerular filtration rate is low in young infants, reaching the adult value by 6–12 months of life. Therefore, drug doses and dosing schedules must be adjusted appropriately in pediatric populations to avoid toxicity.

Local toxicity of topical drugs is more common than is systemic toxicity. Local toxicity may be a type I immunoglobulin E (IgE)–mediated hypersensitivity reaction, or it may represent a delayed hypersensitivity reaction to either the medication itself or its associated preservatives.

Preservatives and toxicity

Preservatives commonly used in ophthalmic preparations include quaternary cationic surfactants such as benzalkonium chloride and benzododecinium bromide; mercurial agents such as thimerosal, chlorobutanol, and parahydroxybenzoates; and aromatic alcohols (Table 15-1). Preservatives used in ophthalmic solutions can be toxic to the ocular surface following topical administration; they can also enhance the corneal permeability of various drugs (Table 15-2).

Some preservatives use different methods to reduce the toxic effect on the ocular surface. In one such method, the preservative dissipates upon exposure to light or to the ions in the tear film. Examples of preservatives using this method include stabilized oxychloro complex, which breaks down to sodium chloride and water, and sodium perborate, which breaks down to hydrogen peroxide before becoming oxygen and hydrogen. Theoretically, these "disappearing preservatives" have no toxic effect on the corneal surface.

Other preservative systems may be less toxic to the ocular surface than quaternary cationic surfactants such as benzalkonium chloride. One such system is an ionic buffer containing borate, sorbitol, propylene glycol, and zinc that breaks down into innate elements upon encountering the cations in the tear film. Polyquaternium-1, another preservative system, is a cationic polymer of quaternary ammonium structures that lacks a hydrophobic region. Although polyquaternium-1 is a detergent, human corneal epithelial cells tend to repel the compound.

Table 15-1 Commonly Used Preservatives in Eyedrops

Compound	Class	Antimicrobial Action	Trade Name	Example
Benzalkonium chloride	Quaternary ammonium	Detergent action dissolves cell walls and membranes	NA	Common in many topical ophthalmic solutions
Polyquartenium 1	Detergent	Acts on cell membranes	Polyquad	Tears Naturale II
Stabilized oxychloro complex	Oxidizing	Oxidizes intracellular lipids and glutathione	Purite	Alphagan P
Sodium perborate	Oxidizing	Forms hydrogen peroxide; has oxidizing action similar to the above	GenAqua	Genteal
Borate, sorbitol, propylene glycol, and zinc	Ionic buffer	Multiple	SofZia	Travatan Z

NA = not applicable.

Adapted from Steven DW, Alaghband P, Lim KS. Preservatives in glaucoma medication. *Br J Ophthalmol.* 2018;102(11):1498.

Table 15-2 Ocular Side Effects of Preservatives

Eyelids and Conjunctiva	Cornea
Allergic reactions	Punctate keratitis
Hyperemia	Edema
Erythema	Pseudomembrane formation
Blepharitis	Decreased epithelial microvilli
Conjunctiva (papillary conjunctivitis)	Vascularization
Edema	Scarring
Pemphigoid lesion with squamous metaplasia	Delayed wound-healing symblepharon
Contact lens intolerance	Increased transcorneal permeability
	Decreased stability of tear film
	Squamous metaplasia

Courtesy of Fraunfelder FT, Fraunfelder FW. *Drug-Induced Ocular Side Effects.* 8th ed. Elsevier; 2021:4.

To completely eliminate toxicity from preservatives, some topical ophthalmic products are available preservative-free, in single-use containers.

CLINICAL PEARL

Benzalkonium chloride, the most commonly used ophthalmic preservative, can cause toxicity to the ocular surface as well as to intraocular structures. In addition to inducing apoptosis on corneal and conjunctival epithelial cells, it has also been shown to affect the trabecular meshwork and lens epithelial cells. Patients with glaucoma, who are continually exposed to benzalkonium chloride, need to be monitored for toxicity. Combination medications, medications containing alternative preservatives, or preservative-free eyedrops should be considered for use in these patients. See BCSC Section 10, *Glaucoma*, for further discussion on long-term medical management of glaucoma.

Rasmussen CA, Kaufman PL, Kiland JA. Benzalkonium chloride and glaucoma. *J Ocul Pharmacol Ther.* 2014;30(2–3):163–169.

Steven DW, Alaghband P, Lim KS. Preservatives in glaucoma medication. *Br J Ophthalmol.* 2018;102(11):1497–1503.

Pharmacologic Principles and Aging

Pharmacologic principles apply differently in children and older individuals. Renal blood flow is lower in infants and toddlers compared with older children and adults. Children attain adult level glomerular filtration rates by age 2. In addition, the total body water percentage is higher in infants under age 1 than in adults. This affects the volume over which medications, particularly water-soluble compounds, distribute. Thus, in neonates, lower drug doses can achieve equivalent efficacy. Although a complete discussion of the variation in drug distribution and absorption in children, particularly those under age 2, is beyond the scope of this text, it is important for physicians to consult the US Food and Drug Administration (FDA) package insert when prescribing medications to children. An example of this is weight-based dosing.

Compared with younger patients, older patients have less lean body mass because of a decrease in muscle bulk, less body water and albumin, and an increased relative percentage of adipose tissue. These physiologic differences also alter the tissue binding and distribution of a drug. Eventually, human renal function declines with age; both hepatic perfusion and enzymatic activity are variably affected as well. Older patients tend to take more medications for chronic conditions than do younger patients, and many of the drugs they use are processed simultaneously by their already-compromised metabolic systems.

According to the National Kidney Foundation, the average estimated glomerular filtration rate (GFR) in different age groups is as follows:

- 20–29 years: 116 mL/min/1.73 m^2
- 30–39 years: 107 mL/min/1.73 m^2
- 40–49 years: 99 mL/min/1.73 m^2
- 50–59 years: 93 mL/min/1.73 m^2
- 60–69 years: 85 mL/min/1.73 m^2
- 70 years and older: 75 mL/min/1.73 m^2

Thus, the pharmacokinetic processing of drugs is significantly altered in older individuals, extending the effective half-life of most systemically administered medications. The pharmacodynamic action of a drug is often independently potentiated in these patients. The increase in both drug effect and adverse effects can occur even when the dose is decreased in consideration of these pharmacokinetic differences. Therefore, the pharmacotherapeutic effects and toxicity of a medication may be altered simply by the aging process, independent of drug dosage. Accordingly, the selection of a specific therapeutic agent should be guided by the general health and age of the individual, as well as by concomitant medication used by the patient.

Awwad S, Mohamed Ahmed AHA, Sharma G, et al. Principles of pharmacology in the eye. *Br J Pharmacol.* 2017;174(23):4205–4223.

Myers TM, Wallace DK, Johnson SM. Ophthalmic medications in pediatric patients. *Medscape Compr Ophthalmol Update.* 2005;6(2):85–101. Accessed February 3, 2023. www.medscape.com/viewarticle/504199

National Kidney Foundation. Estimated glomerular filtration rate (eGFR). Accessed February 3, 2023. www.kidney.org/atoz/content/gfr

Pharmacokinetics: The Route of Drug Delivery

Several different approaches are employed for ophthalmic drug delivery; these are summarized in Table 15-3 and discussed in the following sections.

Topical Administration: Eyedrops

Most ocular medications are administered topically as eyedrops. This route of administration maximizes the anterior segment concentrations while minimizing systemic toxicity. The drug gradient, from the concentrated tear reservoir to the relatively barren corneal

Table 15-3 Routes of Ophthalmic Drug Delivery

Route	Benefits	Challenges	Application in the Treatment of Disease
Topical	High patient adherence, self-administrable, noninvasive	Higher tear dilution and turnover rate, corneal barrier, efflux pumps, BA <5%	Keratitis, uveitis, conjunctivitis, scleritis, episcleritis, blepharitis, glaucoma
Oral/systemic	High patient adherence, noninvasive	BAB, BRB, high doses cause toxicity, BA <2%	Scleritis, episcleritis, CMV retinitis, PU
Intravitreal	Direct delivery to vitreous and retina, sustains drug levels, evades BRB	Retinal detachment, hemorrhage, cataract, endophthalmitis	AMD, PU, BRVO, CRVO, DME, CME, UME, CMV retinitis
Intracameral	Bypasses corneal epithelial barrier, provides higher drug levels in the anterior chamber, eliminates use of topical eyedrops, reduces corneal and systemic adverse effects associated with topical therapy	TASS, TECDS	Anesthesia, prevention of endophthalmitis, inflammation, pupil dilation, glaucoma
Subconjunctival	Bypasses conjunctival epithelial barrier, direct delivery to anterior and posterior segment, site for depot formulations	Conjunctival and choroidal circulation	Glaucoma surgery, uveitis
Sub-Tenon	Bypasses conjunctival epithelial barrier, high vitreal drug levels, relatively noninvasive, fewer complications when compared to intravitreal delivery	RPE barrier, chemosis, subconjunctival hemorrhage, inadvertent intraocular delivery	DME, AMD, RVO, uveitis
Retrobulbar	Can be used to administer high local doses of anesthetics, more effective than peribulbar delivery, minimal influence on IOP	Retrobulbar hemorrhage, globe perforation, respiratory arrest	Anesthesia
Posterior juxtascleral	Safe delivery of depot formulations, sustains drug levels to the macula for up to 6 months, avoids risk of endophthalmitis and intraocular damage	Surgery required, RPE barrier	AMD

AMD = age-related macular degeneration; BA = bioavailability; BAB = blood–aqueous barrier; BRB = blood–retinal barrier; BRVO = branch retinal vein occlusion; CME = cystoid macular edema; CMV = cytomegalovirus; CRVO = central retinal vein occlusion; DME = diabetic macular edema, IOP = intraocular pressure; PU = posterior uveitis; RPE = retinal pigmented epithelium; RVO = retinal vein occlusion; TASS = toxic anterior segment syndrome; TECDS = toxic endothelial cell destruction syndrome; UME = uveitic macular edema.

Adapted from Gaudana R, Ananthula HK, Parenky A, Mitra AK. Ocular drug delivery. *AAPS J.* 2010;12(3):348–360.

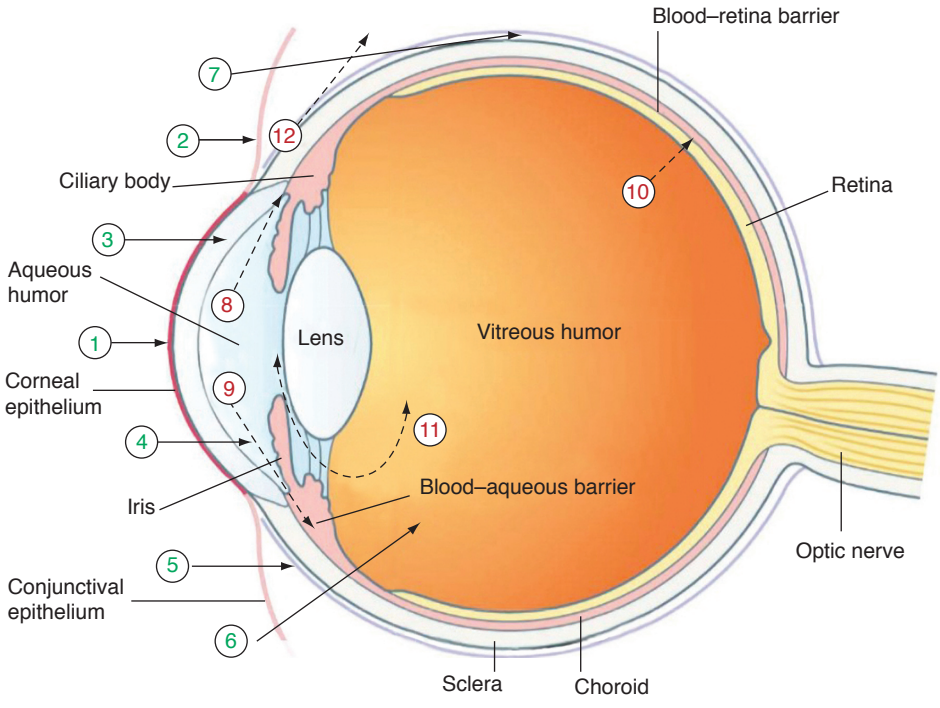


Figure 15-1 Diagram of the eye with common drug delivery routes and elimination pathways. *Delivery routes:* (1) Transcorneal route from the tear film across the cornea into the anterior chamber; (2) transconjunctival route across the conjunctiva, sclera, and anterior uvea into the posterior chamber; (3) intrastromal route directly into corneal stroma; (4) intracameral route directly into the anterior chamber; (5) subconjunctival route from the anterior subconjunctival space across the sclera and anterior uvea into the posterior chamber or across the sclera, choroid, retinal pigment epithelium (RPE), and retina into the anterior vitreous; (6) intravitreal drug injection directly into the vitreous; (7) sub-Tenon route from the posterior sub-Tenon space across the sclera, choroid, RPE, and retina into the posterior vitreous. *Absorption pathways:* (8) elimination of drug in the aqueous humor across the trabecular meshwork and Schlemm canal into the systemic vascular circulation; (9) elimination of drug in the aqueous humor across the uvea into the systemic vascular circulation; (10) elimination of drug in the vitreous humor across the blood–retina barrier to the systemic vascular circulation; (11) drug elimination from the vitreous across the anterior hyaloid to the posterior chamber or vice versa; (12) drug elimination from the subconjunctival and/or episcleral space to systemic lymphatic or vascular circulation. *(Modified with permission from Levin LA, Nilsson SFE, Ver Hoeve J, Wu SM.* Adler's Physiology of the Eye. *11th ed. Elsevier/Saunders; 2011:113.)*

and conjunctival epithelia, forces a passive route of absorption (Fig 15-1). The transcorneal route is the primary pathway for medications to achieve intraocular concentrations. After a medication has been applied topically, various factors (eg, aqueous dynamics, structural barriers provided by the iris and ciliary body epithelium) limit its diffusion

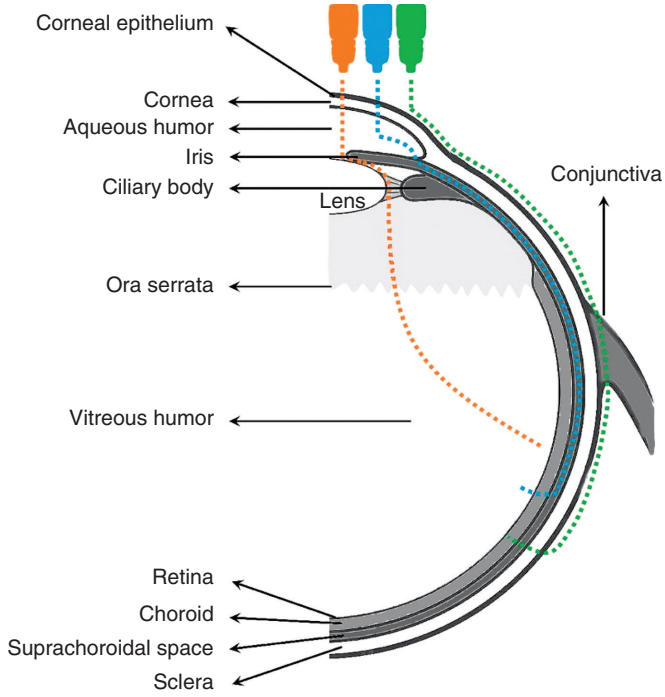


Figure 15-2 Diagram of pathways for topical medications to reach the posterior segment. The cornea is the primary site of absorption for topically administered medications; the 2 subsequent pathways to the posterior segment are (1) transvitreal *(orange)* and (2) uveal-scleral *(blue).* A third route, periocular *(green),* relies on a transconjunctival/transscleral pathway to reach the posterior segment. Even though the conjunctival surface area is 17 times larger than the corneal surface area, this pathway does not contribute significantly to intraocular drug concentrations due to rapid clearance by the conjunctival and choroidal vessels. The RPE provides an additional barrier to penetration. Similar limitations apply to the uveal-scleral pathway. *(Reproduced with permission from Varela-Fernández R, Díaz-Tomé V, Luaces-Rodríguez A, et al. Drug delivery to the posterior segment of the eye: biopharmaceutic and pharmacokinetic considerations.* Pharmaceutics. *2020;12(3):269:Fig 7.)*

past the lens. Figure 15-2 illustrates various potential pathways whereby topically applied medications can reach the posterior segment.

Retention of topical agents

Some features of topical ocular therapy limit treatment effectiveness. Very little of an administered eyedrop is retained by the eye. When a 50-μL drop is delivered from a conventional commercial dispenser, the volume of the tear lake rises from 7 μL to only 10 μL in the blinking eye of an upright patient. As a result, at most only 20% of the administered drug is retained (10 μL/50 μL). Thus, in the absence of misapplication, there is no benefit to consecutively administering 2 eyedrops of the same medication at the same time. Further, rapid turnover of fluid also occurs in the tear lake—16% per minute in the undisturbed eye—with even faster turnover if the eyedrop elicits reflex tearing. Consequently, for slowly absorbed drugs, at most only 50% of the drug that was initially retained in the tear reservoir, or 10% of the original dose (50% of the 20% of the delivered medication), remains 4 minutes after instillation, and only 17%, or 3.4% of the original dose, remains after 10 minutes.

The amount of time that a drug remains in the tear reservoir and tear film is called the *residence time* of a medication. This time is affected not only by drug formulation but also by the timing of the administration of any subsequent medications, tear production, and drainage.

Some simple measures can be implemented to improve ocular absorption of materials that do not rapidly traverse the cornea:

- Patients using more than 1 topical ocular medication should be instructed to allow 5 minutes between instillation of drops; otherwise, the second drop may simply wash out the first.
- Blinking also diminishes a drug's effect by activating the nasolacrimal pump mechanism, forcing fluid from the lacrimal sac into the nasopharynx, and creating a negative sac pressure that empties the tear lake (see BCSC Section 7, *Oculofacial Plastic and Orbital Surgery*). Patients can circumvent this loss of drug reservoir either by compressing the nasolacrimal duct through application of digital pressure at the medial canthus (nasolacrimal occlusion) or by closing their eyes for 5 minutes after instillation of each drop. These 2 measures will prevent emptying of the tear lake, thereby increasing the residence time while decreasing absorption through the nasal mucosa. Either method will increase corneal absorption of topically applied medications and decrease systemic absorption and potential toxicity (Fig 15-3).
- Tear reservoir retention and drug contact time can also be extended either by increasing the viscosity of the vehicle or by using drug delivery objects such as contact lenses, collagen shields, and inserts.

Topical medications that are absorbed by the nasal mucosa avoid first-pass metabolism by the liver and can reach significant levels in the blood; 1 or 2 drops of a topical medication may provide a significant systemic dose of that drug. For example, a 1% solution of atropine has 1 g/100 mL, or 10 mg/1 mL. A simpler way of remembering this conversion is to add a 0 to the drug percentage to change the value to milligrams per milliliter. For example, there are

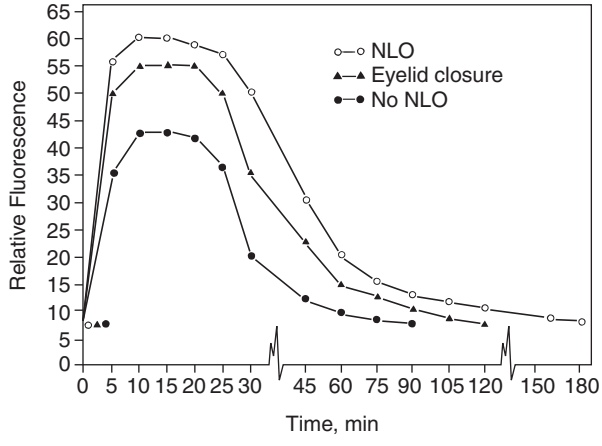


Figure 15-3 Relative fluorescence in the anterior chamber at various times after application: with nasolacrimal occlusion (NLO), with 5 minutes of eyelid closure, or with no intervention (no NLO). NLO increases contact time by limiting clearance of topically applied medication via the nasal lacrimal system. Eyelid closure accomplishes a similar effect by apposing the lacrimal puncta to each other, effectively blocking access to the nasal lacrimal system.

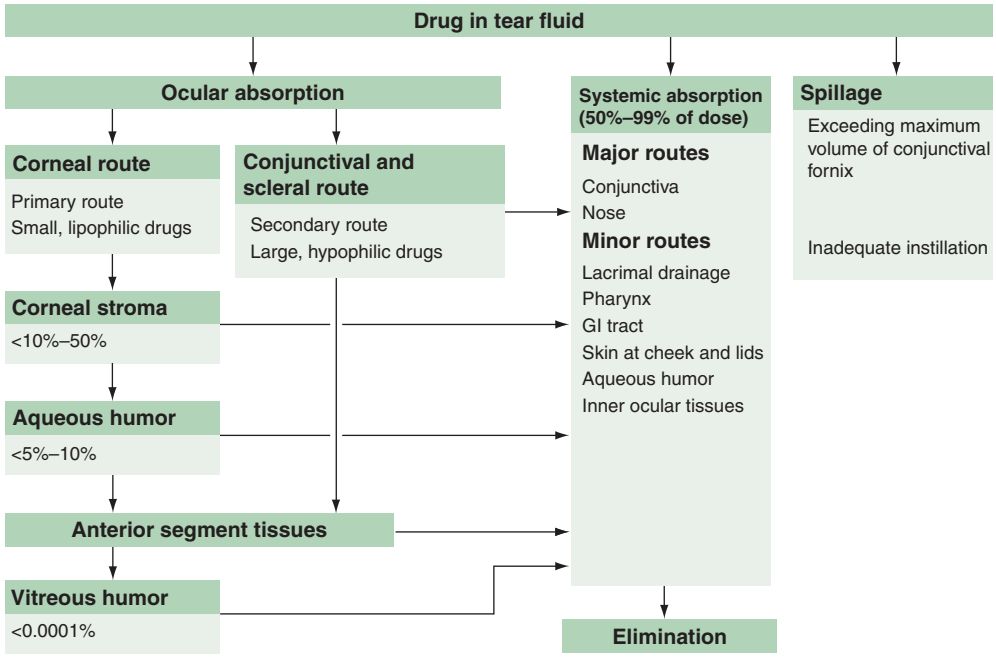


Figure 15-4 Pharmacokinetics of topical eyedrop drug delivery. GI tract = gastrointestinal tract. *(Modified with permission from Levin LA, Nilsson SFE, Ver Hoeve J, Wu SM.* Adler's Physiology of the Eye. *11th ed. Elsevier/Saunders; 2011:113.)*

20 drops per milliliter (up to 40 in some newer, small-tip dispensers), so there is ¼–½ mg of 1% atropine per drop. If this drop is given bilaterally, up to 1 mg of active agent is available for systemic absorption, although the actual amount absorbed is limited by dilution and the washout effect of tears (Fig 15-4).

Absorption of topical agents

The nasolacrimal system can remove topically applied medications 100 times faster than the ocular surface can absorb it. Because the contact time of topical medication is short, the rate of transfer from the tear fluid into the cornea is crucial for intraocular penetration. Ocular tissues absorb only 1%–10% of topically applied medications.

The factors determining the amount of medication that can penetrate the cornea are

- concentration and solubility in the delivery vehicle
- viscosity of the delivery vehicle
- lipid solubility
- pH
- ionic and steric forms
- molecular size
- surfactants (also called *surface-active agents*)
- reflex tearing
- binding of medications

Drug concentration, solubility, and vehicles

In order for a sufficient amount of a drug to pass through the corneal barriers, it may be necessary to load the tear reservoir with concentrated solutions (eg, by selecting pilocarpine, 4%, instead of pilocarpine, 1%). A practical limit to exploiting these high concentrations is reached when the high tonicity of the resulting solutions elicits reflex tearing or when drugs that are poorly water-soluble reach their solubility limits and precipitate. A drug with adequate solubility in an aqueous solution can be formulated as a solution, whereas a drug with poor solubility may need to be provided in a suspension.

A *suspension* is a mixture of a substance with poor solubility and a dispersion medium in which the substance is evenly distributed. A suspension requires agitation (ie, shaking the bottle) so that the active medication is redistributed before administration. Suspensions may be more irritating to the ocular surface than are solutions, a factor that may affect the choice of drug formulation. Prednisolone acetate and brinzolamide are 2 examples of topical suspensions.

An *emulsion* is similar to a suspension in that it is also a mixture of 2 components; however, these components are immiscible (not susceptible to being mixed) liquids. External force or an emulsifying agent is required to maintain the stability of the emulsion. Compared with solutions, emulsions have the advantages of increased contact time and greater bioavailability. An emulsion typically has a cloudy appearance, but in contrast with a suspension, shaking the container before instillation is not necessary. Because emulsions are more viscous than solutions, patients may experience foreign-body sensation after instillation. Difluprednate and cyclosporine are examples of topical emulsions.

Because the units of concentration or dilution of solution are not standardized, students of pharmacology need to familiarize themselves with conversions between different units. The solution's labeled percentage (%) represents the amount of active ingredient in the number of grams per 100 mL of solution (eg, 1% = 1 g/100 mL, or 1000 mg/100 mL, or 10 mg/1 mL). The solution concentration may also be presented in a dilution ratio. For example, a 1:1000 solution has 1 g of active ingredient per 1000 mL solution, or 1000 mg/1000 mL, or 1 mg/1 mL. Converting this ratio to a percentage, a 1:1000 solution equals a concentration of 0.1 g/100 mL, or 0.1%.

Vehicles are inactive substances added to the active ingredient to facilitate its administration. These include the solutions into which medications are dissolved or suspended in or are combined with, as described in the preceding paragraphs. Additional technologies employ slow-release mechanisms, liposomes, and nanotechnology; see the section Ocular Drug Design and Methods of Delivery later in this chapter. Vehicles can also affect the viscosity of the solution (see the section "Viscosity").

CLINICAL PEARL

Vehicle selection can significantly affect the duration of efficacy for a given medication. For example, when administered intravitreally as a solution, 0.4 mg of dexamethasone phosphate clears the vitreous within a few days. In contrast, the 0.7-mg biodegradable polymer slow-release implant delivers dexamethasone over a period of 1–3 months.

Viscosity

When added to a drug, high-viscosity substances such as methylcellulose and polyvinyl alcohol (PVA) increase drug retention in the inferior cul-de-sac, aiding drug penetration. For example, when timolol maleate is formulated in gellan gum or xanthan gum, which are high-molecular-weight, water-soluble, anionic polysaccharides that thicken on contact with the tear film, dosing can be decreased to once daily while still maintaining therapeutic levels of the drug.

Improvement in ocular drug delivery is observed when drug viscosity is in the range of 1–15 cP (1 cP = 1 millipascal-second [mPas]); the optimal viscosity is 12–15 cP. Viscosity values above 15 cP do not seem to proportionally increase a drug's concentration in aqueous humor; in fact, formulations with higher viscosity levels tend to cause ocular surface irritation, resulting in reflex blinking, lacrimation, and increased drainage of the applied formulation. They may also inhibit product–tear mixing and distort the ocular surface. Finally, products with viscosity levels that are too high may be uncomfortable for patients to use because they may impart a sticky feeling and cause blurring of vision.

Lipid solubility

The corneal epithelium and endothelium have tight junctions that limit paracellular passage of molecules. Further, desmosomes between epithelial cells act as an additional barrier. To enter the anterior segment, topically applied medications must first pass through lipophilic/hydrophobic cell membranes in the corneal epithelium, then through the hydrophilic/lipophobic stroma, and finally through the lipophilic/hydrophobic cell membranes in the endothelium. Thus, in theory, topical ophthalmic drug formulations should be amphipathic (ie, possessing both lipophilic and hydrophilic properties). However, studies of the permeability of isolated corneas to families of chemical compounds show that lipid solubility is more important than water solubility in promoting penetration.

Similar considerations apply to the conjunctiva. However, the permeability of the conjunctiva to small water-soluble molecules is thought to be 20 times that of the cornea. Table 15-4 outlines the lipid solubility of ocular structures.

pH and ionic charge

Because nonionic particles are more lipophilic than are ionic particles, they pass through cellular phospholipid membranes more readily. The pH of the medication can be manipulated to adjust the percentage of the drug that is in the ionized form and the nonionized form to optimize the rate of drug penetration. Many ophthalmic medications are alkaloids, or weak bases, and are most stable at an acidic pH. The capacity of the buffer system used should be adequate to maintain pH within the stability range for the duration of the product's shelf life.

The pH range that a patient can tolerate is narrow. A large difference between the pH of a topical solution and that of tears may result in ocular irritation and stimulate reflex tearing that dilutes or washes away the topical eyedrops. Thus, the buffer capacity should be adequate for stability but minimized to allow the overall pH of the tear fluid to be disrupted only momentarily upon instillation. Drugs such as tropicamide, cyclopentolate, atropine, and epinephrine exist in both charged and uncharged forms at the slightly alkaline pH of tears (pH 7.4). The partition coefficients, and therefore drug penetration, can be increased by raising the pH of the water phase, thereby increasing the proportion of drug molecules in the more lipid-soluble, uncharged form.

Table 15-4 Lipid Solubility of Ocular Structures

Structure	Solubility
Tear film	
Mucoaqueous layer	Hydrophilic
Mucin layer	Hydrophilic
Cornea	
Epithelium	Lipophilic
Stroma	Hydrophilic
Endothelium	Lipophilic
Conjunctiva	Hydrophilic
Tenon capsule	Lipophilic
Sclera	Hydrophilic
Uvea	Lipophilic
Blood–aqueous barrier	Lipophilic
Blood–retina barrier	Lipophilic

Note: The aforementioned attest only to the relative lipid solubility of the ocular structures listed. Several additional factors ultimately determine the permeability of a compound across a particular tissue.

A solution's ionic charge can also independently affect penetration when it traverses a structure of opposite charge. Both the corneal stroma and the sclera are hydrophilic. However, the extracellular matrix of the sclera is negatively charged, which limits the passage of positively charged molecules.

Molecular size

The molecular size of a topically applied medication will affect its penetration into the anterior chamber. For traversing an epithelium, smaller (<450 Dalton [Da]) lipophilic molecules are better suited for the transcellular pathways, while larger hydrophilic molecules diffuse better via paracellular pathways. Although the sclera is a hydrophilic structure, transscleral absorption is affected more by molecular size than it is by lipophilicity.

Surfactants

To prevent bacterial contamination, many topical eyedrops contain preservatives called surfactants (also called *surface-active agents*) that alter cell membranes in the cornea as well as in bacteria, reducing the barrier effect of the corneal epithelium and increasing drug penetration. For example, a 0.1% carbachol solution containing 0.03% benzalkonium chloride can elicit the same miotic response as a 2% solution without this preservative. Mechanical disruption of the epithelial barrier in corneal abrasion also increases the rate of intraocular drug penetration.

Reflex tearing

As previously mentioned, ocular irritation and secondary tearing wash out the drug reservoir in the tear lake and reduce the contact time of the drug with the cornea. Reflex tearing occurs when topical medications are not isotonic and when they have a nonphysiologic pH or contain irritants.

Binding of medication

Tear and ocular surface proteins, as well as ocular melanin, may bind topical or systemic medications, making the drug unavailable or creating a slow-release reservoir. This binding may alter the lag time, or onset, of a medication as well as the peak effect and duration of action, and it can cause local toxicity that occurs after discontinuation of the medication. One example of this effect is the retinal toxicity that progresses even after discontinuation of the aminoquinoline antimalarial drugs chloroquine and hydroxychloroquine. The latter is also often used in the management of autoimmune diseases such as lupus and rheumatoid arthritis.

Topical Administration: Ointments

Another strategy for increasing the contact time of ocular medications is through the use of ointments. Commercial oil-based ointments usually consist of petrolatum and mineral oil. The mineral oil allows the ointment to melt at body temperature. Both ingredients are also effective lipid solvents. However, most water-soluble medications are insoluble in the ointment and are present as microcrystals. Only those microcrystals on the surface of the ointment dissolve in the tears; the rest are trapped until the ointment melts. This protracted slow release may prevent the drug from reaching a therapeutic level in the tears. Only when the drug achieves high lipid solubility (allowing it to diffuse through the ointment) and some water solubility can it escape from the ointment into both the corneal epithelium and the tears. Fluorometholone, chloramphenicol, and tetracycline are examples of drugs that achieve higher aqueous levels when administered as ointment than as drops.

Local Administration: Injections

Periocular injections

Injection of medication beneath the conjunctiva or the Tenon capsule allows drugs to bypass the conjunctival and corneal epithelial barriers (see Fig 15-1). Periocular administered medications can reach the posterior segment through various routes:

- transscleral pathway into the uvea
- systemic circulation via absorption into periocular vessels
- transcorneal pathway into the anterior segment

Because the paracellular pathways are large, the conjunctival epithelium is relatively permeable to hydrophilic substances. Subconjunctival injections can create a reservoir of a drug that is released into the tear film. Transscleral absorption is limited due to rapid clearance by conjunctival vasculature and lymphatics.

Sub-Tenon injections bypass the conjunctiva and allow medications to absorb passively down a concentration gradient across the sclera and into intraocular tissues. The Tenon capsule is a lipophilic barrier; if a hydrophilic drug is injected into the sub-Tenon space, it can penetrate intraocular tissue more quickly than a topical application can. This approach is especially useful for drugs with low lipid solubility (such as penicillin), which do not penetrate the eye adequately when given topically. Sub-Tenon injection can also be utilized to deliver an anesthetic prior to or during intraocular surgery.

Periocular injections can also be helpful in delivering medication closer to the local site of action—for example, posterior sub-Tenon injections of steroids for cystoid macular edema (CME) or subconjunctival injection of fluorouracil (5-FU) after trabeculectomy. See BCSC Section 10, *Glaucoma,* for further discussion of local application of antifibrotic agents in filtering surgery.

Other injections

Retrobulbar and peribulbar injections also act directly at the site of delivery but are not used to deliver intraocular therapy. These techniques are typically used for delivery of ophthalmic anesthesia and are covered in BCSC Section 11, *Lens and Cataract.* Other examples of local, injectable medications are botulinum toxin, used in the treatment of benign essential blepharospasm and hemifacial spasm, as well as for strabismus; and retrobulbar alcohol, used as therapy for chronic pain in blind eyes.

Intraocular injections

Intraocular injection of drugs instantly delivers effective concentrations at the target site. Although this route of administration may reduce systemic adverse effects, ocular adverse effects, which can include transient ocular hypertension and inflammation/infection, may be more pronounced. Clinicians must take great care to avoid the use of medications with preservatives and to control the concentration of intraocular drugs so that the delicate internal structures of the eye are protected from toxicity. Also, clinicians should strictly adhere to standard aseptic technique for the preparation and injection of intraocular medication so that infection is prevented. There are 2 types of intraocular injections: intracameral, or injection into the anterior chamber; and intravitreal, or injection into the vitreous cavity. Examples of substances and medications delivered via intraocular routes are presented in Table 15-5.

Intracameral Intracameral injections of an antibiotic may be administered at the end of cataract surgery to prevent endophthalmitis. These injections can reduce the need for postoperative dosing of medications. Cefuroxime, a broad-spectrum cephalosporin, is commonly used for this purpose. However, single-dose solution of cefuroxime is unavailable in the United States, and strict aseptic compounding protocol for reconstitution and dilution needs to be followed. Vancomycin also needs to be diluted before intracameral injection but is effective against methicillin-resistant *Staphylococcus aureus* (MRSA). However, the risk of inducing drug resistance with indiscriminate use of vancomycin is a concern, as is the rare complication of vancomycin-associated hemorrhagic occlusive retinal vasculitis. Another option is diluting preservative-free topical moxifloxacin—a broad-spectrum, fourth-generation fluoroquinolone—for intracameral use. It is important that antibiotic solutions prepared for intracameral injection be free of preservatives or other additives.

CLINICAL PEARL

Intracameral lidocaine is used to supplement anesthesia during cataract surgery. It is critical that the surgeon verify the dose and use only preservative-free preparations to avoid secondary intraocular inflammatory response. Cases of toxic anterior segment syndrome (TASS) have been reported after the use of any intracameral medication with preservatives and/or dosing errors.

Table 15-5 Examples of Medications Delivered by Intracameral and Intravitreal Routes

Route of Administration	Clinical Application
Intracameral	
Antibiotics (eg, cefuroxime, moxifloxacin, vancomycin)	Preventing endophthalmitis following cataract surgery
Acetylcholine	Constricting pupil in intraocular surgery
Carbachol	Same as above
Balanced salt solution	Intraocular surgery, re-forming anterior chamber
Ophthalmic viscosurgical devices (OVDs)	Same as above
Epinephrine (preservative- and bisulfite-free[a])	Dilating pupil in intraocular surgery
Phenylephrine 1%/ketorolac 0.3%	Maintaining pupil dilatation in intraocular surgery (added to irrigation solution)
Lidocaine (preservative-free)	Intraocular surgery, anesthesia
Trypan blue	Staining anterior capsule in cataract surgery
Tissue plasminogen activator (tPA) (off-label use)	Assisting fibrinolysis of fibrin in anterior chamber and subretinal hemorrhage
Intravitreal	
Anti–vascular endothelial growth factor agents	Choroidal neovascularization, diabetic retinopathy, diabetic macular edema, retinal vein occlusion
Corticosteroids (eg, triamcinolone acetonide; sustained-release intraocular implants such as dexamethasone in poly(lactic-*co*-glycolic acid) matrix and fluocinolone acetonide in a polyvinyl acetate/silicone laminate)	Cystoid macular edema, diabetic macular edema, retinal vein occlusion, posterior uveitis, postoperative inflammation
Foscarnet	Cytomegalovirus retinitis and acute retinal necrosis
Ganciclovir	Cytomegalovirus retinitis
Silicone oil	Vitreoretinal surgery
Intraocular gases	Same as above
Perfluorocarbon	Same as above
Various antibiotics	Preventing/treating intraocular infection

[a] Preservative-free epinephrine with 0.1% bisulfite ampules of 1:1000 epinephrine can be safely injected intracamerally if it is diluted 1:4 with either a balanced salt solution (BSS) or a fortified BSS (BSS Plus).

Intravitreal Intravitreal injection is the most common form of intraocular drug delivery. These injections are most often used to manage patients with complications of diabetic retinopathy (diabetic macular edema, retinal neovascularization), age-related macular degeneration (choroidal neovascularization), and retinal vein occlusions (cystoid macular edema, retinal neovascularization). They are also used in the treatment of uveitis, endophthalmitis, and other conditions. For example, for retinal vascular diseases, various agents are available that target vascular endothelial growth factor (VEGF). Intravitreal delivery can result in a relevant systemic concentration, as evidenced by the effects noted in fellow eyes in clinical trials. For discussion of individual agents used for intravitreal injection, see Chapter 16 in this volume and BCSC Section 12, *Retina and Vitreous*.

Medications administered intravitreally are cleared from the eye via anterior and/or posterior routes (see elimination pathways in Fig 15-1). Hydrophilic, high-molecular-weight compounds exit anteriorly following the aqueous humor outflow, while lipophilic, low-molecular-weight compounds progress across the retina and retinal pigment epithelium to exit into the choroid. Medications cleared via the anterior pathway exhibit longer half-lives than those exiting the posterior pathway. This is likely due to the smaller size of molecules able to traverse the retina and the larger surface area of the posterior segment.

Ho AC, Scott IU, Kim SJ, et al. Anti-vascular endothelial growth factor pharmacotherapy for diabetic macular edema: a report by the American Academy of Ophthalmology. *Ophthalmology.* 2012;119(10):2179–2188.

Wen JC, McCannel CA, Mochon AB, Garner OB. Bacterial dispersal associated with speech in the setting of intravitreous injections. *Arch Ophthalmol.* 2011;129(12):1551–1554.

Witkin AJ, Chang DF, Jumper JM, et al. Vancomycin-associated hemorrhagic occlusive retinal vasculitis: clinical characteristics of 36 eyes. *Ophthalmology.* 2017;124(5):583–595.

Yeh S, Albini TA, Moshfeghi AA, Nussenblatt RB. Uveitis, the Comparison of Age-Related Macular Degeneration Treatments Trials (CATT), and intravitreal biologics for ocular inflammation. *Am J Ophthalmol.* 2012;154(3):429–435.

Systemic Administration

Medications administered systemically may address intraocular diseases or systemic conditions with ophthalmic manifestations. They are delivered via oral and/or intravenous (parenteral) routes. Although there are clear distinctions between the 2 delivery routes in regard to clinical use, both face similar barriers to intraocular penetration.

Just as the tight junctions of the corneal epithelium and endothelium limit anterior access to the interior of the eye, similar barriers limit access of systemically administered medications through vascular channels. The vascular endothelium of the retina, like that of the brain, is nonfenestrated and knitted together by tight junctions. Although both the choroid and the ciliary body have fenestrated vascular endothelia, the choroid is effectively sequestered by the retinal pigment epithelium (tight junctions); and the ciliary body, by its nonpigmented epithelium (tight junctions).

Compared with medications with lower lipid solubility, drugs with higher lipid solubility more readily penetrate the blood–ocular barrier. For example, chloramphenicol, which is highly lipid-soluble, penetrates 20 times better than does penicillin, which has poor lipid solubility.

The ability of systemically administered drugs to gain access to the eye is also influenced by the degree to which they are bound to plasma proteins. Only the unbound form can cross the blood–ocular barrier. Sulfonamides are lipid-soluble but penetrate poorly because, at therapeutic levels, more than 90% of the medication is bound to plasma proteins. Similarly, compared with methicillin, oxacillin has reduced penetration because of its increased binding of plasma protein.

Bolus administration of a drug exceeds the binding capacity of plasma proteins and leads to higher intraocular drug levels than can be achieved by a slow intravenous drip. This approach is used for the administration of antibiotics in order to attain high peak intraocular levels.

Oral administration

The benefit of oral administration is its ease of delivery; patients can easily take their medication at home instead of needing to have it delivered via intravenous access, which requires hospitalization or placement of a peripherally inserted central catheter (also known as a PICC line). The effectiveness of orally administered medication relies on bioavailability and its ability to achieve clinically relevant concentrations without toxicity.

> **CLINICAL PEARL**
>
> Fluconazole and voriconazole have high bioavailability and achieve clinically relevant intraocular concentration when taken orally. Their use has limited the need for/duration of intravenous therapy in the management of endogenous fungal endophthalmitis.

Sustained-release oral preparations The practical value of sustained-release preparations is substantial. For example, a single dose of acetazolamide reduces intraocular pressure for up to 10 hours, whereas a single dose of sustained-release acetazolamide produces a comparable effect that lasts 20 hours. A sustained-release medication offers a steadier blood level of the drug, avoiding marked peak concentrations and low concentrations, and reduces the frequency of administration.

Intravenous injections

Intravenously injected agents can be administered for diagnosis of ophthalmic conditions. For example, sodium fluorescein and indocyanine green are 2 agents used during retinal angiography to aid in the diagnosis of retinal and choroidal diseases.

Intravenous agents are also used therapeutically in ophthalmology. Although intravitreal injections have replaced intravenous therapy for postoperative endophthalmitis, continuous intravenous administration of an antibiotic is an effective way of maintaining therapeutic intraocular levels in patients with endogenous infection (see BCSC Section 12, *Retina and Vitreous*).

Although intravenous medications have better bioavailability and bypass first-pass metabolism by the liver, they still face similar barriers to achieving intraocular penetration as orally administered medications. The intraocular penetration of a drug may be better in the inflamed eye than in the healthy eye because of the disruption of the blood–aqueous and blood–retina barriers that occurs with inflammation. This disruption is demonstrated by the leakage of fluorescein from inflamed retinal vessels into the vitreous during angiography.

Intramuscular and subcutaneous injections

In ophthalmology, intramuscular and subcutaneous injections are used less frequently than topical, oral, or intravenous administration of medications. Notable exceptions include intramuscular injection of botulinum toxin, given for local effect (eg, in facial dystonias and in some cases of strabismus), and subcutaneous injection of adalimumab for treatment of noninfectious uveitis.

Cholkar K, Patel SP, Vadlapudi AD, Mitra AK. Novel strategies for anterior segment ocular drug delivery. *J Ocul Pharmacol Ther.* 2013;29(2):106–123.

Gote V, Sikder S, Sicotte J, Pal D. Ocular drug delivery: present innovations and future challenges. *J Pharmacol Exp Ther.* 2019;370(3):602–624.
Patel A, Cholkar K, Agrahari V, Mitra AK. Ocular drug delivery systems: an overview. *World J Pharmacol.* 2013;2(2):47–64.

Ocular Drug Design and Methods of Delivery

New ocular drugs are designed with a focus on specificity of action and safety, with delivery systems aimed at improving convenience and therefore patient adherence to a medication regimen. Each of the following approaches is a response to a specific challenge in ocular pharmacokinetics.

Prodrugs

Ophthalmic prodrugs are therapeutically inactive derivatives of drug molecules that are designed to be activated by enzymatic systems within the eye in order to improve ocular penetration. These derivatives are usually synthesized by conjugation of a specific promoiety to the parent drug via ester or amide. The ester and amide ophthalmic prodrugs are hydrolyzed by esterase and amidases to the active molecules as they permeate through the cornea or conjunctiva. Permeability across the cornea is also improved by the increased lipid solubility of the prodrug. Prostaglandin analogues are successful examples of this drug delivery strategy. Latanoprost, travoprost, and tafluprost are prostaglandin analogues that interact with the prostaglandin FP receptor. They require hydrolyzation prior to becoming active compounds in the eye.

Valacyclovir hydrochloride is an antiviral prodrug that, when taken orally, is easily absorbed through the gastrointestinal tract and quickly converted to the active form of acyclovir. Likewise, famciclovir is a prodrug of the active antiviral penciclovir.

Sustained-Release and Alternative Methods of Drug Delivery

As previously mentioned, eyedrop therapy involves periodic delivery of relatively large quantities of a drug to overcome low ocular bioavailability due to various factors, such as tearing and blinking, nasolacrimal drainage, conjunctival blood and lymph flow, metabolic degradation, and corneal and blood–aqueous barriers. The high peak drug levels attained with bolus dosing can cause local and systemic side effects, such as induced accommodation producing brow ache, which can occur after pilocarpine use. In addition, drug concentration in the eye can vary significantly because of variations in application technique and patient adherence to dosing amounts and schedules. Thus, there is a need for an efficient delivery system that can provide controlled release of a drug with a reduced dosing frequency.

Ocular inserts

Ocular inserts are sterile, thin, multilayered, drug-impregnated, solid or semisolid devices placed into the fornix of the conjunctiva, sized and shaped for ophthalmic application. These devices deliver an adequate supply of medication at a steady-state level, achieving

beneficial effects with fewer adverse effects. The first steady-state drug delivery system, a nonbiodegradable insert designed to deliver pilocarpine at a steady rate of 40 μg/hr, became available in the 1970s. This device was discontinued as the use of pilocarpine decreased. Ocular inserts are cylindrical in shape and are placed in the fornix of the conjunctiva for prolonged drug release.

Ocular inserts can be categorized as soluble or insoluble:

- *Soluble* inserts release the drug via interaction between the polymeric matrix of the device and the tear film. Removal of these inserts is unnecessary.
- *Insoluble* inserts may achieve a more constant rate of drug release than soluble inserts, but removal of the device is required once the medication is depleted.

Ocular inserts have the advantages of prolonged and steady delivery of drugs, which can improve patient adherence. However, they have the potential for patient discomfort including foreign-body sensation and misalignment of the implant.

Intraocular implants

To circumvent the need for repeated intraocular injections, various implantable devices have been developed for sustained drug delivery. The first sustained-release implant to become available was the ganciclovir intravitreal implant for treatment of cytomegalovirus (CMV) retinitis. An ethylene vinyl acetate disc with a PVA coating served as the drug reservoir. The thickness of the PVA lid regulated the delivery of ganciclovir to the target tissue. After surgical implantation, the device delivered a steady source of ganciclovir for 5–8 months. The ganciclovir intravitreal implant was discontinued after the patent expired in 2015.

Current intraocular sustained-release products approved by the US FDA include 3 nonbiodegradable fluocinolone acetonide intravitreal implants (0.59 mg, 0.19 mg, and 0.18 mg), a biodegradable 0.7-mg dexamethasone intravitreal implant (Fig 15-5), and a biodegradable 15-μg bimatoprost intracameral implant.

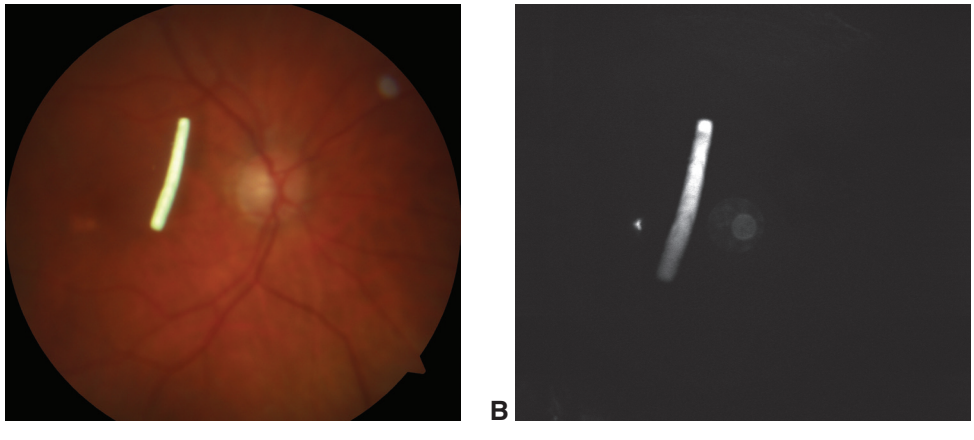


Figure 15-5 Intravitreal biodegradable 0.7-mg dexamethasone implant. **A,** Color fundus photograph shows implant over the posterior pole. **B,** Near-infrared image demonstrates early cavitation on the surface of the implant consistent with degradation. *(Courtesy of Vikram S. Brar, MD.)*

Intraocular lenses and other sustained-release systems

Sustained-release systems that use biodegradable polymers entrapped with triamcinolone acetonide or antibiotics to prevent intraocular infection and control postoperative intraocular inflammation and are attached to the periphery or haptics of an artificial intraocular lens are under investigation. Other research efforts include development of an intraocular lens prepared with biomaterials that not only allow high transmittance at visible wavelengths but also can be loaded with dexamethasone to achieve sustained release of this drug after cataract surgery.

Intraocular sustained-release devices are being studied as alternatives to glaucoma medical therapy, which has demonstrated poor patient adherence. Products under investigation include injectable sustained-release biodegradable implants through which various hypotensive medications can be delivered into the supraciliary space or beneath the conjunctiva to achieve a sustained reduction of intraocular pressure for months.

Contact lenses

Ongoing research approaches for contact lens (CL) drug delivery systems focus on improving the residence time of the drug at the surface of the eye to enhance bioavailability and to provide more convenient and efficacious therapy. Various techniques are used to incorporate the drug into the CL body, including

- soaking the CL in drug solution
- incorporating monomers able to interact with target drugs into the CL hydrogels
- incorporating drug-loaded colloidal nanoparticles into the matrix of the CL
- using a molecular imprinting technique in which the components of the hydrogel network are organized so that high-affinity binding sites for the drug are created

These CL delivery systems need to be designed so that they also preserve the transparency required for vision and the oxygen permeability necessary for corneal health. One way to maintain transparency is by lathing the encapsulated drug-polymer film in the periphery of the CL hydrogel. CLs embedded with timolol, latanoprost, timolol/dorzolamide, and timolol/latanoprost are under evaluation.

Guzman-Aranguez A, Colligris B, Pintor J. Contact lenses: promising devices for ocular drug delivery. *J Ocul Pharmacol Ther.* 2013;29(2):189–199.

Punctal plug–mediated delivery

Various punctal plug–mediated drug delivery systems are currently under clinical investigation. The design of these delivery systems generally includes a cylindrical polymeric core loaded with the drug compound, an impermeable shell, and a cap (or head portion of the plug exposed to the tear film) with pores from which the drug is released by diffusion. Most examples of punctal plug systems show nearly constant drug-release rates for drug molecules. Delivery of drugs by punctal plug has several potential advantages over administration via eyedrops, including lack of exposure to preservatives, dose reduction, controlled release of the drug at an optimum rate, and improved patient adherence. Limitations of these delivery systems include the low doses of medication that can be delivered and the potential adverse effects, including ocular irritation, itching, discomfort, increased lacrimation, and spontaneous extrusion of the plug.

The only US FDA-approved punctal plug system is a resorbable intracanalicular implant designed to release 0.4 mg dexamethasone over 30 days for treatment of postoperative inflammation and pain. A similar system for the release of travoprost is under investigation.

Hydrogels

Gel-forming drops are an example of hydrogels that use pentablock copolymers as a vehicle for topical drug delivery. The drug is added to a nonviscous polymer drop. Once the drop is in contact with the surface of the eye, the drop transforms into a gel upon exposure to body temperature. Gellan and xanthan gum are examples of gel-forming vehicles that carry timolol products designed for extended release. Other examples include artificial tears and viscous lidocaine preparations. Newer applications of ophthalmic gels/hydrogels include lens and vitreous replacement, intravitreal drug delivery, and stem cell delivery/tissue engineering.

Al-Kinani AA, Zidan G, Elsaid N, Seyfoddin A, Alani AWG, Alany RG. Ophthalmic gels: past, present, and future. *Adv Drug Deliv Rev*. 2018;126:113–126.

Kirchhof S, Goepferich AM, Brandl FP. Hydrogels in ophthalmic applications. *Eur J Pharm Biopharm*. 2015;95(Pt B):227–238.

Liposomes

Liposomes are synthetic lipid microspheres that serve as multipurpose vehicles for the topical delivery of drugs, genetic material, and cosmetics. They are produced when phospholipid molecules interact to form a bilayer lipid membrane in an aqueous environment. The interior of the bilayer consists of the hydrophobic fatty-acid tails of the phospholipid molecule, whereas the outer layer is composed of hydrophilic polar-head groups of the molecule. A water-soluble drug can be dissolved in the aqueous phase of the interior compartment; a hydrophobic drug can be intercalated into the lipid bilayer itself. However, the routine use of liposome formulation for topical ocular drug delivery is limited by the short shelf life of these products, their limited drug-loading capacity, and how difficult it is to stabilize the preparation.

Bhattacharjee A, Das PJ, Adhikari P, et al. Novel drug delivery systems for ocular therapy: with special reference to liposomal ocular delivery. *Eur J Ophthalmol.* 2019;29(1):113–126.

Nanotechnology

Nanotechnology has been increasingly applied in medication design to protect active molecules and provide sustained drug delivery. Methods for transporting hydrophilic and lipophilic drugs and genes include the use of biodegradable nanoparticles such as nanospheres, nanocapsules, and nanomicelles; the colloidal dispersion of nanoparticles as nanosuspension; and the use of nanoemulsion. These methods are modeled after the molecular structure of viruses.

A system of 0.09% cyclosporine drops that use nanomicelle technology has been developed for the treatment of dry eye syndrome. This system utilizes an encapsulated cyclosporine, which has the potential to deliver therapeutic concentrations of cyclosporine with less discomfort than the currently available formulation.

The physical process of moving charged molecules via an electrical current is called *iontophoresis.* This procedure places a relatively high concentration of a drug locally, where

it can achieve maximum benefit with little waste or systemic absorption. Animal studies have demonstrated that iontophoresis increases penetration of various antibiotics and antiviral drugs across ocular surfaces into the cornea and the interior of the eye. However, patient discomfort, ocular tissue damage, and necrosis restrict the widespread use of this mode of drug delivery.

Kompella UB, Hartman RR, Patil MA. Extraocular, periocular, and intraocular routes for sustained drug delivery for glaucoma. *Prog Retin Eye Res.* 2021;82:100901.

Singh RB, Ichhpujani P, Thakur S, Jindal S. Promising therapeutic drug delivery systems for glaucoma: a comprehensive review. *Ther Adv Ophthalmol.* 2020;12:2515841420905740. doi:10.1177/2515841420905740

Pharmacogenetics: The Influence of Genetic Variation on Drug Efficacy and Toxicity

Genetic polymorphisms in genes that encode drug-metabolizing enzymes, drug transporters, and receptors contribute, at least in part, to the wide interindividual variability in drug response and adverse drug reactions. *Pharmacogenetics* is the study of the influence of genetic variation on drug efficacy or toxicity, focusing on single genes. The term is often used interchangeably with *pharmacogenomics,* which is the study of how genetic makeup affects an individual's response to drugs; in other words, the focus is on many genes. Pharmacogenetics can be broadly divided into (1) the study of genetic variations that affect drug metabolism (pharmacokinetics); and (2) the study of genetic variations that affect drug targets (pharmacodynamics).

Thus far, some small-scale studies have demonstrated an association between various genotypes or haplotypes and response to drug therapies for 2 major eye disorders—age-related macular degeneration and glaucoma—but the results are conflicting. One example is the relationship between single nucleotide polymorphisms (SNPs; also called *single-nucleotide variations*) in genes and the response to latanoprost, specifically, SNPs in the genes coding for matrix metalloproteinases and SNPs in the prostaglandin F2α receptor gene *(PTGFR).* Another example is the pharmacogenetic relationship between polymorphisms in specific genes and the different levels of drug efficacy achieved in the treatment of exudative age-related macular degeneration.

Although translation of pharmacogenetic and pharmacogenomic data into clinical practice would provide significant opportunities to increase the safety and efficacy of pharmacotherapy, consensus (social, ethical, and economical) on issues such as genetic discrimination needs to be reached and such issues addressed by regulatory agencies. Clinicians must be aware of the ethical, legal, and social issues associated with genetic testing.

Arslan J, Baird PN. Changing vision: a review of pharmacogenetic studies for treatment response in age-related macular degeneration patients. *Pharmacogenomics.* 2018;19(5): 435–461.

Shastry BS. Genetic diversity and medicinal drug response in eye care. *Graefes Arch Clin Exp Ophthalmol.* 2010;248(8):1057–1061.

CHAPTER 16

Ocular Pharmacotherapeutics[1]

This chapter includes a related video. Go to www.aao.org/bcscvideo_section02 or scan the QR code in the text to access this content.

Highlights

- Off-label drug use is common in ophthalmology. Certain off-label uses are even the predominant treatment options for some conditions.
- Compounded pharmaceuticals are used to treat numerous ophthalmic diseases. Practicing ophthalmologists should be up to date with current state and federal pharmacy regulations concerning compounded pharmaceuticals.
- When applied to skin, topical povidone-iodine solution should be allowed to dry completely for maximal antiseptic effect.
- Unsupervised and/or prolonged use of topical anesthetic drops can lead to significant ocular complications.
- When administering systemic medications to pediatric patients, it is important to note that these medications typically require weight-based dosing.

The reader is encouraged to consult the resources given in the following reference list for more information on many of the topics covered in this chapter.

Brunton LL, Hilal-Dandan R, Knollmann BC, eds. *Goodman & Gilman's The Pharmacological Basis of Therapeutics.* 14th ed. McGraw-Hill; 2023.

Fraunfelder FT, Fraunfelder FW. *Drug-Induced Ocular Side Effects.* 8th ed. Elsevier; 2020.

Physicians' Desk Reference for Ophthalmic Medicines. Thomson PDR; 2012.

[1] This chapter may include information on pharmaceutical applications that are not considered community standard, that are approved for use only in restricted research settings (ie, investigational drugs), or that reflect indications not approved in US Food and Drug Administration (FDA) labeling (ie, off-label use). For example, many medications are used off-label in opthalmology, including most antibiotics and antifungal drugs compounded for systemic treatment of ocular infections such as keratitis and endophthalmitis. Many antifungal drugs are used off-label on the basis of in vitro and animal data because human data for unusual infectious agents are often limited. **The US FDA has stated that it is the responsibility of the physician to determine the FDA status of each drug or device he or she wishes to use and to use it with appropriate, informed patient consent in compliance with applicable law. (The legal aspect of medical therapy varies by country and region. For example, the General Medical Council [GMC] in the United Kingdom recognizes that a physician has a moral duty toward all of his or her patients that may affect the choice of appropriate medical therapy under tight budgetary restrictions.)**

PDR Network. *Prescriber's Digital Reference.* Accessed January 26, 2023. www.pdr.net
US Food and Drug Administration. Drugs@FDA: FDA-approved drugs. Accessed January 26, 2023. www.accessdata.fda.gov/scripts/cder/daf/

Legal Aspects of Medical Therapy

The US Food and Drug Administration (FDA) has statutory authority to approve the marketing of prescription drugs and to specify the uses of these drugs. The US FDA's Office of Prescription Drug Promotion reviews and regulates prescription drug advertising and promotion through surveillance activities and issuance of enforcement letters to pharmaceutical manufacturers, whereas the Federal Trade Commission regulates advertising and promotion for over-the-counter drugs. The FDA has created a 3-step process for human testing of new drugs before they are approved for marketing:

- *Phase 1:* After animal and in vitro studies have been completed, human testing begins in clinical trials with a limited number of participants for collection of toxicology data and pharmacokinetic data on dosage range, absorption, and metabolism.
- *Phase 2:* Clinical trials involving up to hundreds of affected people are conducted to determine safety and effectiveness of the drug. Researchers use information from phase 2 studies to refine their research questions and/or protocols and to design phase 3 trials.
- *Phase 3:* These trials are aimed at determining efficacy and monitoring for adverse events and typically include randomized clinical trials, often prospective, double-blind, multicenter trials. Phase 3 trials involve a much larger cohort of affected participants with matched controls over longer period (1–4 years) than do phase 2 trials. They evaluate the overall risk–benefit relationship of the drug and provide an adequate basis for physician labeling. The data gathered from these studies are then submitted as part of a new drug application for marketing.
- *Phase 4:* Once the drug or device has been approved by the FDA, these trials are carried out; they typically occur during postmarket safety monitoring and are aimed at reporting data not discovered in the previous phases.

The American Academy of Ophthalmology's IRIS (Intelligent Research Into Sight) Registry may play an important role in phase 4 or postmarket surveillance studies. IRIS is an electronic health record–based repository of patient data that can be used to uncover unrecognized safety issues related to the use of a drug or device that were not discovered during phase 1–3 clinical trials. Such analysis is an example of a phase 4 study. For more information on the IRIS Registry, see Chapter 18 in this volume and www.aao.org/iris-registry.

Chiang MF, Sommer A, Rich WL, Lum F, Parke DW II. The 2016 American Academy of Ophthalmology IRIS Registry (Intelligent Research in Sight) Database: characteristics and methods. *Ophthalmology.* 2018;125(8):1143–1148.

The FDA's approval of each drug and its specific uses ("on-label" prescribing) are based on documentation submitted by manufacturers that details the safety and efficacy of the drug. Although the FDA is committed to making drugs available as rapidly as possible, the process of bringing a new product to market requires extensive research and development and millions of dollars.

Once approved for a specific use(s), a drug may be prescribed by individual physicians for other indications and/or patient populations. For example, doxycycline, typically prescribed to treat infection, can also be used to treat ocular rosacea (based on its inhibition of matrix metalloproteinases). Such off-label drug use, defined as prescribing a drug for an indication or employing a dosage or dose form that has not been approved through the FDA process, is common. An off-label use may even be the predominant treatment option for a given clinical condition. However, even though an off-label use of a drug may be the primary treatment option for a particular medical condition, drug proprietors may decide not to seek FDA approval for the new indication for financial reasons.

Off-label use of medications is common practice in ophthalmology. Some examples are listed in Table 16-1.

Table 16-1 Common Drugs Used Off-label in Ophthalmology

Drug	Indications
Bevacizumab, an antiangiogenic drug	Used as an intravitreal injection for numerous neovascular ocular diseases
Acetylcysteine (10% or 20%)	Used as a mucolytic drug in filamentary keratopathy and as an anticollagenase drug in severe alkali injuries
Tissue plasminogen activator (tPA)	Used as an intravitreal injection for thrombolysis and fibrinolysis
5-Fluorouracil (5-FU)	Improves the outcomes of glaucoma filtering surgery
Mitomycin C (MMC)	Improves the outcomes of glaucoma filtering surgery and treats ocular surface neoplasia
Cyclosporine A 2% compounded solution	Used in high-risk corneal transplants and in severe vernal, ligneous, and autoimmune keratopathies
Doxycycline	Used in ocular rosacea
Edetate disodium (salt of EDTA)	Used in band keratopathy
Fibrin sealant	Used to adhere the conjunctival graft to the scleral bed in pterygium resection
Triamcinolone acetonide[a]	The preparation Kenalog is used in intravitreal and sub-Tenon injections of triamcinolone acetonide for a variety of conditions, including macular edema, anterior/intermediate uveitis, and retinal vein occlusions

[a] The preservative-free formulation of triamcinolone acetonide (Triesence) is FDA-approved for intraocular use.

One of the most commonly used ophthalmic medications, topical prednisolone acetate, has not been approved by the FDA for postoperative care. Use of this medication after cataract surgery is thus considered an off-label application, though it is widely used in this regard.

Although off-label drug use is a commonly accepted practice, prescribing physicians must always adhere to the *standard of care* to limit malpractice risk. Unapproved use of a drug that does not adhere to an applicable standard of care can place a practitioner at higher risk for legal claims. In contrast, practicing within the scope of standard of care (ie, exercising the degree of knowledge and care ordinarily possessed and exercised by other members of the profession acting under similar conditions and circumstances) mitigates and lowers that risk. In other words, if other physicians, similarly situated, would have prescribed off-label in the same manner, a standard of care can be met in most jurisdictions. In equivocal cases where the standard of care is uncertain, detailed and well-documented informed consent should be obtained.

Expanded access refers to the clinical use of investigational new drugs (INDs) prior to their approval by the FDA. Clinical use of INDs in this setting is typically requested for patients with terminal conditions who either do not qualify for a clinical trial or who may succumb to their illness before the drug obtains approval. The treating physician must ensure that the drug manufacturer is willing to provide the drug/device and agrees with the physician's proposed treatment plan.

US Food and Drug Administration. The drug development process: Step 3: Clinical research. US FDA website. Updated January 4, 2018. Accessed January 26, 2023. www.fda.gov/patients/drug-development-process/step-3-clinical-research

Compounded Pharmaceuticals

Compounded pharmaceuticals are used to treat numerous ophthalmic diseases during both surgical and diagnostic procedures. Compounding is defined by the US Pharmacopeia (USP) as "the preparation, mixing, assembling, altering, packaging, and labeling of a drug, drug-delivery device, or device in accordance with a licensed practitioner's prescription, medication order, or initiative based on the practitioner/patient/pharmacist/compounder relationship in the course of professional practice."

The Pharmacy Compounding Accreditation Board (PCAB) accredits pharmacies that provide evidence of adherence to quality standards for pharmacy compounding. The PCAB requires proper licensure with state and federal regulatory authorities, appropriate training of personnel, and facilities and methods that permit aseptic compounding of sterile preparations and that meet the USP guidelines. Compounding pharmacies are also regulated by the FDA and by state pharmacy boards.

The 2013 Drug Quality and Security Act created a new 2-tiered regulatory structure for compounding pharmacies and the products they distribute. The law defines government oversight authority over large-volume compounding facilities, preserving a

pathway for ophthalmologists to access certain compounded drugs for office use. Under the law:

- In accordance with section 503A of the Food, Drug, and Cosmetic Act (FDCA), traditional compounding pharmacies require a patient-specific prescription for all drugs compounded. Oversight of these pharmacies remains primarily a state function unless the FDA receives a complaint.
- According to section 503B of the FDCA, new outsourcing facilities do not require a prescription, but they must meet higher federal safety, sterility, and quality control standards than conventional drug manufacturing plants, while being subject to similar regular federal inspections.

Although ensuring the safety and sterility of compounded products is important, maintaining practitioner access to essential compounded products for office use is crucial. Unfortunately, the implementation of the new system and its regulation have been uncertain and costly. State rules for 503A compounding pharmacies still prevent some small, local compounders (including hospital pharmacies) from providing ophthalmologists with supplies of fortified antibiotics and other commonly compounded drugs for urgent cases. Shipment of compounded medications across state lines is more difficult because the compounder must have an in-state pharmacy license. In addition, costly, extensive baseline testing required for each of the compounded products shortens the compendium list. Finally, although the FDA has dropped its 5-day expiration rule and allows 503B pharmacies to determine the expiration dates on biologic drugs, additional expensive testing regimens are required on the part of compounders to substantiate a longer shelf life on the label.

The American Academy of Ophthalmology (AAO) has issued the following recommendations for the sourcing of compounded drugs used in intravitreal injection:

1. Select a compounding pharmacy that is accredited by the PCAB and adheres to quality of aseptic compounding of sterile medications set forth by USP General Chapter 797. (For further information regarding PCAB accreditation, see www.achc.org/compounding-pharmacy; for information regarding USP General Chapter 797, see www.usp.org/compounding/general-chapter-797.)
2. Record the lot numbers of the medication vial and the syringes used on each patient in the patient's record or another type of log, in case they need to be tracked.

These recommendations were made after the 2011 outbreaks of infectious endophthalmitis associated with compounded bevacizumab. Practicing ophthalmologists should stay up to date with current state and federal pharmacy regulations concerning compounding pharmaceuticals. The AAO and many subspecialty societies send e-mail alerts and provide updates on regulations and legislation to their members.

Adherence

Nonadherence with a physician's prescribed therapeutic regimen is a serious obstacle to patient care. Although much of the research on nonadherence in ophthalmology has been

Table 16-2 Factors Contributing to Nonadherence to Therapy

Advanced age
Lower economic status
High medication cost
Limited health insurance
Patient's forgetfulness
Patient's anxiety about disease and treatment
Patient's poor understanding of the disease
Patient's misunderstanding of the physician's instructions
Patient's fear of becoming dependent on medication
Complexity and length of treatment
Patient's concurrent medical conditions or disabilities
Adverse effects

conducted in patients who required medical therapy for glaucoma, the findings can be applied to medical therapy for other ophthalmic conditions.

Generally, the degree of adherence reported by patients is lower than their actual adherence. The degree of adherence to treatment is generally poor in patients with chronic ophthalmic diseases, similar to that of adherence in those with other chronic diseases. Concurrent medical conditions or disabilities may also impact adherence. The list of factors that contribute to nonadherence is long. Selected examples are presented in Table 16-2.

Depending on the factors identified, reasonable options for improving adherence include educating the patient about the disease or medical therapy in a language and context the patient understands, simplifying the medical regimen, using sustained drug delivery systems where applicable, maximizing cost reduction, and recruiting support from family members. Although positive effects of these interventions have not been proven, nonadherence can lead to unnecessary disease progression, additional medical costs and physician visits, and unneeded change or escalation of therapy. Clinicians can play an active role in improving adherence and preventing these outcomes. See also Chapter 1 in BCSC Section 1, *Update on General Medicine*.

Hahn SR. Patient-centered communication to assess and enhance patient adherence to glaucoma medication. *Ophthalmology*. 2009;116(11 Suppl):S37–S42.

Tsai JC. A comprehensive perspective on patient adherence to topical glaucoma therapy. *Ophthalmology*. 2009;116(11 Suppl):S30–S36.

Cholinergic Drugs

Several commonly used ophthalmic medications affect the activity of acetylcholine receptors in synapses of the somatic and autonomic nervous systems (Fig 16-1). These receptors are found in

- the motor end plates of the extraocular and levator palpebrae superioris muscles (supplied by somatic motor nerves)

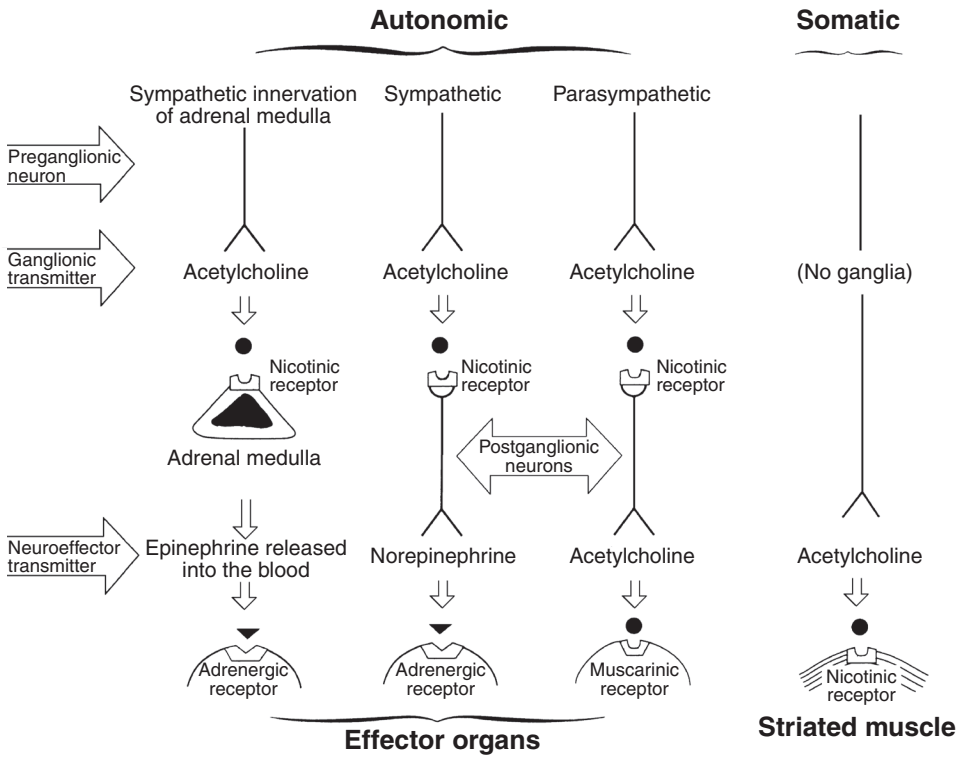


Figure 16-1 Summary of the neurotransmitters released and the types of receptors found within the autonomic and somatic nervous systems. *(Reproduced with permission from Mycek MJ, Harvey RA, Champe PC, eds.* Pharmacology. *2nd ed. Lippincott's Illustrated Reviews. Lippincott-Raven; 1997:32.)*

- the cells of the superior cervical (sympathetic) ganglion and the ciliary and sphenopalatine (parasympathetic) ganglia (supplied by preganglionic autonomic nerves)
- parasympathetic effector sites in the iris sphincter and ciliary body as well as in the lacrimal, accessory lacrimal, and meibomian glands (supplied by postganglionic parasympathetic nerves)

Although all cholinergic receptors are by definition responsive to acetylcholine, they are not homogeneous and can be classified by their responses to 2 drugs: muscarine and nicotine (Table 16-3). *Muscarinic receptors* are found in the end organs of the parasympathetic autonomic system. *Nicotinic receptors* are found in the postganglionic neurons of both the sympathetic and parasympathetic systems, in striated muscle (the end organ of the somatic system), and in the adrenal medulla. Cholinergic drugs may be further divided into the following groups (Fig 16-2):

- *direct-acting agonists,* which act on the receptor to elicit an excitatory postsynaptic potential
- *indirect-acting agonists,* which increase endogenous acetylcholine levels at the synaptic cleft by inhibiting acetylcholinesterase
- *antagonists,* which block the action of acetylcholine on the receptor

Table 16-3 Cholinergic and Adrenergic Receptors[a]

Receptors	Agonists	Blocking Agents
Cholinergic (sphincter)	Acetylcholine	
Muscarinic	Muscarine	Atropine
Nicotinic	Nicotine	D-Tubocurarine
Adrenergic (dilator)	Norepinephrine	
Alpha[b]	Phenylephrine	Phentolamine and phenoxybenzamine
α_1	Phenylephrine	Prazosin, thymoxamine, dapiprazole
α_2	Apraclonidine	Yohimbine
Beta	Isoproterenol	Propranolol and timolol
β_1	Tazolol	Betaxolol
β_2	Albuterol	Butoxamine

[a] The cholinergic agonists and the adrenergic blockers listed cause miosis; the adrenergic agonists and the cholinergic blockers listed cause dilation.
[b] The prefixes α_1 and α_2 have been proposed for postsynaptic and presynaptic α-adrenoceptors, respectively. According to the present view, the classification into α_1 and α_2 subtypes is based exclusively on the relative potencies and affinities of agonists and antagonists, regardless of their function and localization.

Muscarinic Drugs

Direct-acting agonists

Topically applied, direct-acting agonists have 3 actions:

1. They cause contraction of the iris sphincter, which not only constricts the pupil *(miosis)* but also changes the anatomical relationship of the iris to both the lens and the chamber angle.
2. They cause contraction of the circular fibers of the ciliary muscle, relaxing zonular tension on the lens equator and allowing the lens to shift forward and assume a more spherical shape *(accommodation)*.
3. They cause contraction of the longitudinal fibers of the ciliary muscle, producing tension on the scleral spur (opening the trabecular meshwork) and facilitating aqueous outflow (see Chapter 2, Video 2-2). Contraction of the ciliary musculature also produces tension on the peripheral retina, occasionally resulting in a retinal tear or even rhegmatogenous detachment.

Because acetylcholine does not penetrate the corneal epithelium well and is rapidly degraded by acetylcholinesterase (Fig 16-3), it is not used topically. Acetylcholine, 1%, and carbachol, 0.01%, are available for intracameral use in anterior segment surgery. These drugs produce prompt and marked miosis.

Although the onset of intracameral acetylcholine, 1%, is more rapid than that of intracameral carbachol (acetylcholine acts within seconds of instillation), its effect is short-lived. It is not stable in aqueous form and, as mentioned previously, is rapidly broken down by acetylcholinesterase in the anterior chamber. When administered similarly, intracameral carbachol, 0.01%, is 100 times more effective and longer lasting than acetylcholine, 1%. Maximal miosis is achieved within 5 minutes and lasts for 24 hours. In addition, carbachol, 0.01%, is an effective hypotensive drug that lowers intraocular pressure (IOP) during the crucial 24-hour period after surgery.

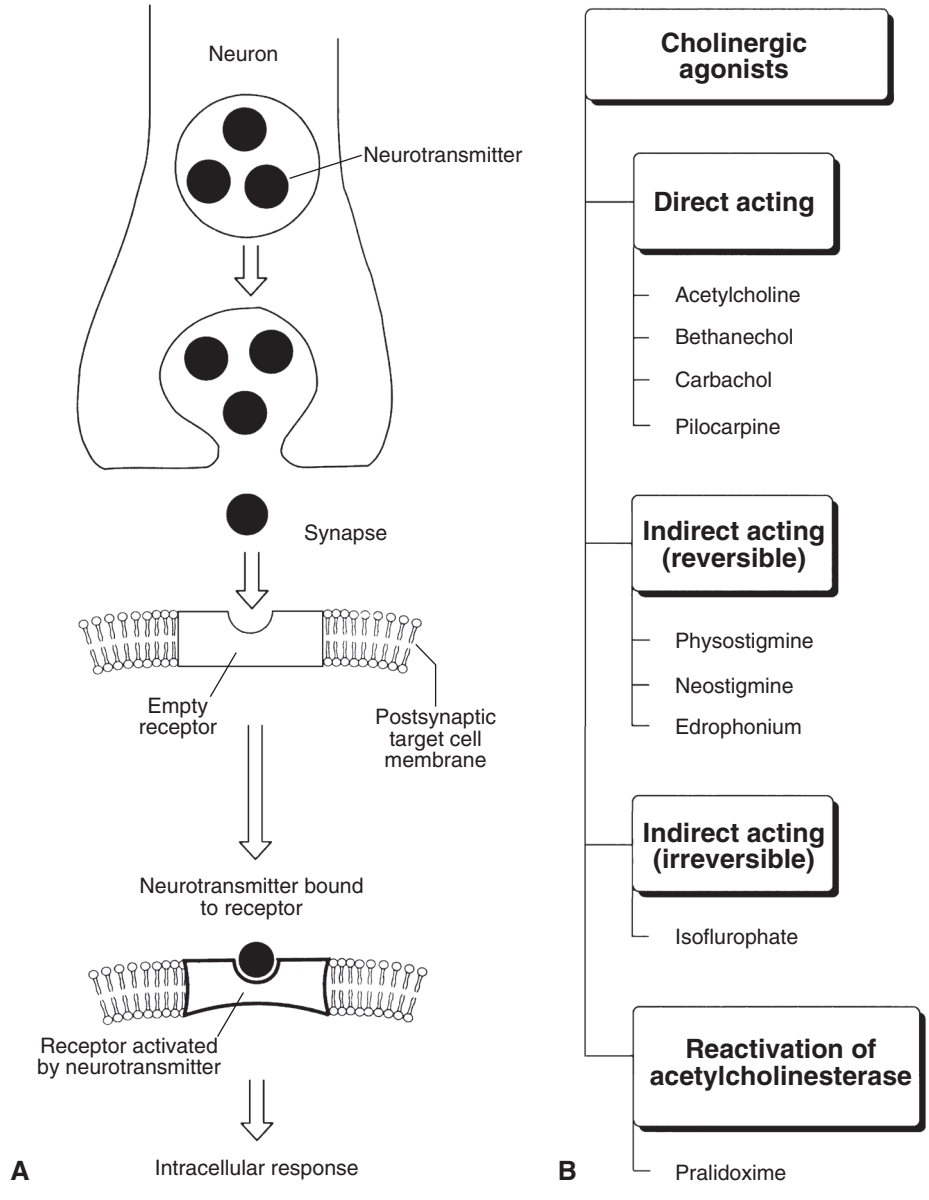


Figure 16-2 Cholinergic synapses. **A,** Neurotransmitter binding triggers an intracellular response. **B,** Summary of cholinergic agonists. *(Reproduced with permission from Harvey RA, Champe PC, eds.* Pharmacology. *Lippincott's Illustrated Reviews. Lippincott; 1992:30, 35.)*

Pilocarpine, 0.12%, is used diagnostically to confirm an Adie (tonic) pupil, a condition in which the parasympathetic innervation of the iris sphincter and ciliary muscle is defective because of the loss of postganglionic fibers. Denervated muscarinic smooth muscle fibers in the affected segments of the iris exhibit supersensitivity and respond well to this weak miotic, whereas the normal iris does not.

Pilocarpine and carbachol can be used in the treatment of primary open-angle glaucoma (POAG) because they lower intraocular pressure (IOP) by facilitating outflow (Table 16-4).

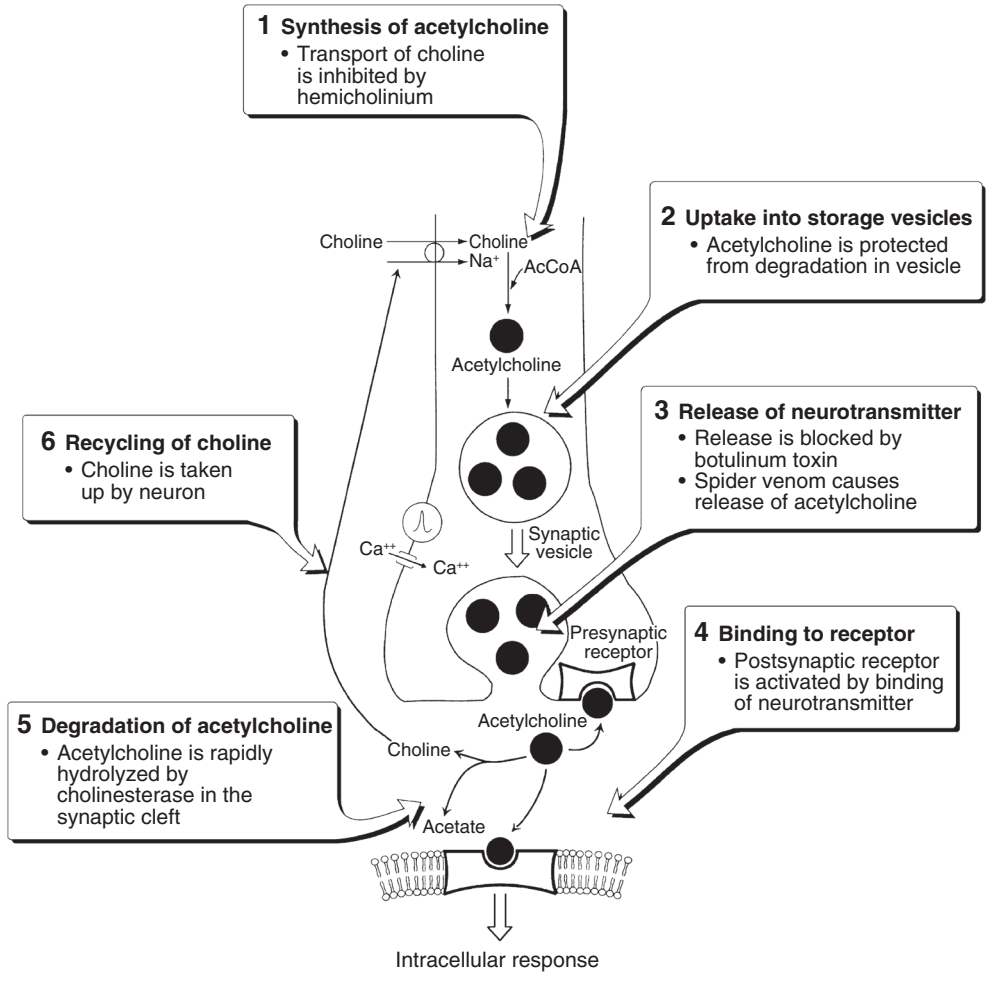


Figure 16-3 Synthesis and release of acetylcholine from the cholinergic neuron. AcCoA = acetyl coenzyme A. *(Reproduced with permission from Mycek MJ, Harvey RA, Champe PC, eds.* Pharmacology. *2nd ed. Lippincott's Illustrated Reviews. Lippincott-Raven; 1997:37.)*

Use of pilocarpine at a dosage beyond 2% is not more effective and may even cause a paradoxical increase in IOP in some individuals with angle-closure glaucoma because this strong miotic may induce anterior movement of the lens–iris diaphragm. This is a concern particularly in cases of secondary angle closure attributed to anterior rotation of the ciliary body and choroidal edema (eg, malignant glaucoma [also referred to as *aqueous misdirection* or *ciliary block glaucoma*] and topiramate-induced angle closure, respectively).

Miotic therapy can also be used (1) to treat elevated IOP in patients with POAG in which the anterior chamber angle remains occludable despite laser iridotomy; and (2) as prophylaxis for angle closure before iridotomy, but not as a long-term substitute for laser iridotomy (see BCSC Section 10, *Glaucoma,* for additional information).

Table 16-4 Miotic Drugs

Generic Name	Trade Name	Strengths
Cholinergic drugs		
Acetylcholine	Miochol-E	1%
Carbachol	Miostat	0.01%
Pilocarpine HCl	Isopto Carpine	1%, 2%, 4%
	Vuity	1.25%
	Available generically	0.5%, 1%, 2%, 3%, 4%
Pilocarpine HCl ointment	Pilopine HS gel	4%
Cholinesterase inhibitors		
Physostigmine	Available generically	1 mg/mL ampule
Echothiophate iodide[a]	Phospholine Iodide	0.125%

[a] Not available for ophthalmic use in the United States.

CLINICAL PEARL

Pilocarpine 1.25% has been approved by the FDA for the treatment of presbyopia in adults. Dosed once daily, this medication induces miosis and ciliary muscle contraction to produce a relative myopic state.

Ocular adverse effects of muscarinic therapy include miosis, cataractogenesis and induced myopia. Although the broad range of retinal dark adaptation usually compensates sufficiently for the effect of miosis on vision during daylight hours, patients taking these drugs may be visually incapacitated in dim light. In addition, miosis often compounds the effect of axial lenticular opacities; thus, many patients with cataracts are unable to tolerate miotics. Furthermore, older patients with early cataracts have visual difficulty in scotopic conditions, and the miosis induced by cholinergic drugs may increase the risk of falls in these individuals. Younger patients may also experience difficulty with miotic agents. For example, patients younger than 50 years may manifest disabling myopia and induced accommodation because of drug-induced contraction of the ciliary body, which increases the convexity of the lens and shifts the lens forward. Other complications observed with use of higher concentrations of miotics include iris cysts and retinal detachment caused by ciliary body contraction and traction on the pars plana.

Systemic adverse effects of muscarinic agonists include salivation, diarrhea, urinary urgency, vomiting, bronchial spasm, bradycardia, and diaphoresis. However, systemic adverse effects are rare following topical use of direct-acting agonists. For example, application of a slowly dissolving pilocarpine gel at bedtime minimizes the adverse effects of the agent and is useful for younger patients, patients with symptoms of variable myopia or intense miosis, older patients with lens opacities, and patients who have difficulty adhering to more frequent dosing regimens.

Ciliary muscle stimulation can help manage accommodative esotropia. The near response is a synkinesis of accommodation, miosis, and convergence. As discussed previously, muscarinic agonists contract the ciliary body and induce accommodation. Therefore, the patient does not need to accommodate at near, which decreases not only the synkinetic convergence response but also the degree of accommodative esotropia.

Indirect-acting agonists

Indirect-acting muscarinic agonists (cholinesterase inhibitors) have the same actions as direct-acting muscarinic agonists; however, they have a longer duration of action and are frequently more potent. These medications react with the active serine hydroxyl site of cholinesterases, forming an enzyme–inhibitor complex that renders the enzyme unavailable for hydrolyzing acetylcholine.

Cholinesterase inhibitors are divided into 2 classes:

1. *reversible inhibitors,* such as physostigmine (available as a powder for compounding and as a solution for injection), neostigmine, and edrophonium
2. *irreversible inhibitors,* such as echothiophate (Phospholine Iodide, no longer available for ophthalmic use in the United States); diisopropyl phosphorofluoridate (no longer available for ophthalmic use in the United States), which phosphorylates both the acetylcholinesterase of the synaptic cleft and the butyrylcholinesterase (pseudocholinesterase) of plasma; and demecarium bromide (no longer available for ophthalmic use in the United States)

The duration of inhibitory action of these medications is determined by the strength of the bond between the inhibitor and the enzyme. Inhibitors that are organic derivatives of phosphoric acid (eg, organophosphates such as echothiophate) undergo initial binding and hydrolysis by the enzyme, forming a phosphorylated active site. Such a covalent phosphorus–enzyme bond is extremely stable and hydrolyzes very slowly. Because of the marked differences in their duration of action, organophosphate inhibitors are irreversible inhibitors.

The action of phosphorylating cholinesterase inhibitors can be reversed by treatment with oxime-containing compounds. Oxime pralidoxime—though useful in the treatment of acute organophosphate poisoning (eg, insecticide exposure)—is of little value in reversing the marked reduction of plasma butyrylcholinesterase activity that occurs with long-term irreversible cholinesterase-inhibitor therapy.

Patients receiving long-term irreversible cholinesterase-inhibitor therapy such as echothiophate may experience toxicity from systemic absorption of local anesthetics containing ester groups (eg, procaine), which are normally inactivated by plasma cholinesterase. Administration of the muscle relaxant succinylcholine during induction of general anesthesia is also hazardous in these patients because the drug will not be metabolized and will prolong respiratory paralysis.

Phosphorylating cholinesterase inhibitors may also cause local ocular toxicity. In children, cystlike proliferations of the iris pigment epithelium may develop at the pupil margin, which can block the pupil. For unknown reasons, cyst development can be minimized by concomitant use of phenylephrine (2.5%) drops. In adults, cataracts may develop,

or preexisting opacities may progress. Interestingly, such cataracts are rare in children, and significant epithelial cysts are rare, if they occur at all, in adults.

Antagonists

Topically applied muscarinic antagonists, such as atropine, react with postsynaptic muscarinic receptors to block the action of acetylcholine. Paralysis of the iris sphincter, coupled with the unopposed action of the dilator muscle, causes pupillary dilation, or *mydriasis* (Table 16-5). Mydriasis facilitates examination of the peripheral lens, ciliary body, and retina. Muscarinic antagonists are approved for therapeutic use in the treatment of anterior uveitis in adults because they reduce contact between the posterior iris surface and the anterior lens capsule, thereby preventing the formation of iris–lens adhesions, or *posterior synechiae*. Topically applied muscarinic antagonists also reduce the permeability of the blood–aqueous barrier and are useful for treating ocular inflammatory disease. Atropine

Table 16-5 Mydriatics and Cycloplegics

Generic Name	Trade Name	Strengths	Onset of Action	Duration of Action
Phenylephrine HCl	AK-Dilate	Solution, 2.5%, 10%	30–60 min	3–5 h
	Altafrin	Solution, 2.5%, 10%		
	Mydfrin	Solution, 2.5%		
	Neofrin	Solution, 2.5%		
	Neo-Synephrine	Solution, 2.5%		
	Available generically	Solution, 2.5%, 10%		
Hydroxyamphetamine hydrobromide, 1%	Available generically	Available as powder for compounding	30–60 min	3–5 h
Atropine sulfate	Atropine-Care	Solution, 1%	45–120 min	7–14 d
	Isopto Atropine	Solution, 1%		
	Available generically	Solution, 1% Ointment, 1%		
Cyclopentolate HCl	AK-Pentolate	Solution, 1%	30–60 min	1–2 d
	Cyclogyl	Solution, 0.5%–2%		
	Cylate	Solution, 1%		
	Available generically	Solution, 1%, 2%		
Homatropine hydrobromide	Isopto Homatropine	Solution, 2%, 5%	30–60 min	3 d
	Homatropaire	Solution, 5%		
Scopolamine hydrobromide	Isopto Hyoscine	Solution, 0.25%	30–60 min	4–7 d
Tropicamide	Mydral	Solution, 0.5%, 1%	20–40 min	4–6 h
	Mydriacyl	Solution, 1%		
	Tropicacyl	Solution, 0.5%, 1%		
	Available generically	Solution, 0.5%, 1%		
Cyclopentolate HCl/ phenylephrine HCl[a]	Cyclomydril	Solution, 0.2%/1%	30–60 min	1–2 d
Hydroxyamphetamine hydrobromide/ tropicamide[b]	Paremyd	Solution, 1%/0.25%	20–40 min	4–6 h

[a] A dilute combination agent for infant examinations.

[b] Used for dilating the pupil; cannot be used to test for Horner syndrome.

and cyclopentolate have been approved by the FDA for use in pediatric patients but not for all indications.

Muscarinic antagonists also paralyze the ciliary muscles, which helps relieve pain associated with iridocyclitis; inhibit accommodation for accurate refraction in children (cyclopentolate, atropine); and treat ciliary block (malignant) glaucoma. However, use of cycloplegic drugs to dilate the pupils of patients with POAG may elevate IOP, especially in patients who require miotics for pressure control. Therefore, it is advisable to use short-acting medications and monitor IOP in patients with severe optic nerve damage.

CLINICAL PEARL

Glycopyrronium bromide is a competitive inhibitor of muscarinic receptors. When applied topically, this medication is used to reduce sweating in patients with hyperhidrosis. Glycopyrronium, 2.4%, is available commercially in medicated pads, which patients use to apply the medication to their axillae. In addition to anticholinergic adverse effects including dry eye syndrome; occasionally, this medication may inadvertently get into the eye and thus should be considered in the differential diagnosis of acute acquired mydriasis.

In situations requiring complete cycloplegia, such as the treatment of iridocyclitis (scopolamine, homatropine, or atropine for adults) or the full refractive correction of accommodative esotropia, more potent drugs are preferred. Although a single drop of atropine has some cycloplegic effect that lasts for days, 2 or 3 instillations a day may be required to maintain full cycloplegia for pain relief from iridocyclitis. In addition, inflamed eyes have rapid turnover of aqueous fluid, necessitating more frequent dosing of cycloplegic agents. It may become necessary to change medications if atropine elicits a characteristic local irritation with swelling and maceration of the eyelids and conjunctival injection (hyperemia). When mydriasis alone is necessary to facilitate examination or refraction, drugs with a shorter residual effect are preferred because they allow faster return of pupil response and reading ability.

Systemic absorption of topical muscarinic antagonists can cause dose-related toxicity, especially in children, for whom the dose is distributed within a smaller body mass. A combination of central and peripheral effects, including flushing, fever, tachycardia, constipation, urinary retention, and even delirium, can result. Mild cases may require only discontinuation of the drug, but severe cases can be treated with intravenous (IV) physostigmine (approved for adults and children), slowly titrated until the symptoms subside. Physostigmine is used because it is a tertiary amine (uncharged) and can cross the blood–brain barrier.

Systemic administration of atropine blocks the oculocardiac reflex, a reflex bradycardia that is sometimes elicited during ocular surgery by manipulation of the conjunctiva, the globe, or the extraocular muscles. The reflex can also be prevented at the afferent aspect by retrobulbar anesthesia, although it can occur during administration of the retrobulbar block.

Nicotinic Drugs

Indirect-acting agonists

Edrophonium is the only cholinesterase inhibitor that is administered in a dose high enough so that it works as an indirect-acting nicotinic agonist. Edrophonium is a short-acting competitive inhibitor of acetylcholinesterase that binds to the enzyme's active site but does not form a covalent link with it. It is used in the diagnosis of myasthenia gravis, a neuromuscular disease caused by autoimmunity to acetylcholine receptors (nicotinic receptors) in the neuromuscular junction and characterized by muscle weakness and marked fatigability of skeletal muscles. This disease may manifest primarily as ptosis and diplopia. In patients with myasthenia gravis, the inhibition of acetylcholinesterase by edrophonium allows acetylcholine released into the synaptic cleft to accumulate to levels that can act through the reduced number of acetylcholine receptors. Because edrophonium also augments muscarinic transmission, muscarinic adverse effects (vomiting, diarrhea, urination, and bradycardia) may occur unless 0.4–0.6 mg of atropine is coadministered intravenously (see BCSC Section 5, *Neuro-Ophthalmology*).

Another drug used in the diagnosis of myasthenia gravis is neostigmine methylsulfate, a longer-acting intramuscular drug. Its longer duration of activity allows the examiner to assess specific complex endpoints, such as orthoptic measurements.

Antagonists

Nicotinic antagonists are neuromuscular blocking agents that facilitate intubation for general anesthesia (Table 16-6). There are 2 types of nicotinic antagonists:

- *nondepolarizing agents,* including curare-like drugs such as rocuronium, vecuronium, gallamine, and pancuronium, bind competitively to nicotinic receptors on striated muscle but do not cause contraction
- *depolarizing agents,* such as succinylcholine and decamethonium, bind competitively to nicotinic receptors and cause initial receptor depolarization and muscle contraction

In singly innervated (en plaque) muscle fibers, depolarization and contraction are followed by prolonged unresponsiveness and flaccidity. However, depolarizing agents produce sustained contractions of multiply innervated fibers, which make up one-fifth of the muscle

Table 16-6 Cholinergic Antagonists

Category	Generic Names	Trade Names
Muscarinic receptor–blocking drugs	Atropine sulfate	Isopto Atropine, Atropine-Care
	Scopolamine hydrobromide	Isopto Hyoscine, Transderm-Scop, Scopace, Maldemar
Ganglion-blocking drugs	Mecamylamine HCl	Inversine, Vecamyl
	Nicotine	Commit, Habitrol NicoDerm CQ, Nicorette, Nicotrol Inhaler, Nicotrol ProStep, Nicotrol NS
Neuromuscular blocking drugs	Pancuronium bromide	Pavulon
	Rocuronium bromide	Zemuron, Esmeron
	Succinylcholine chloride	Anectine, Quelicin
	Vecuronium bromide	Norcuron

fibers of extraocular muscles. Such contractions of extraocular muscles (a nicotinic agonist action) exert force on the globe.

CLINICAL PEARL

Depolarizing agents should not be used to induce general anesthesia for operations on open globes because the force of extraocular muscle contractions on the eye that occurs with use of these drugs could expel intraocular contents. In addition, these agents can increase IOP via a similar mechanism and thus should be used with caution for examinations under anesthesia.

Adrenergic Drugs

Several ophthalmic medications target the activity of adrenergic receptors (also called *adrenoceptors*) in synapses of the peripheral nervous system. These receptors are found in

- the cell membranes of the iris dilator muscle, the superior palpebral smooth muscle of Müller, the ciliary epithelium and processes, the trabecular meshwork (TM), and the smooth muscle of ocular blood vessels (supplied by postganglionic autonomic fibers from the superior cervical ganglion)
- the presynaptic terminals of some sympathetic and parasympathetic nerves, where the receptors have feedback-inhibitory actions

Although adrenergic receptors were originally defined by their response to epinephrine (adrenaline), the transmitter of most sympathetic postganglionic fibers is actually norepinephrine. Adrenergic receptors are subclassified into 5 categories on the basis of their profile of responses to natural and synthetic catecholamines (Fig 16-4):

- *α_1-Receptors* generally mediate smooth muscle contraction.
- *α_2-Receptors* mediate feedback inhibition of presynaptic sympathetic (and sometimes parasympathetic) nerve terminals.
- *β_1-Receptors* are found predominantly in the heart, where they mediate stimulatory effects.
- *β_2-Receptors* mediate relaxation of smooth muscle in most blood vessels and in the bronchi.
- *β_3-Receptors* are found on fat cells and mediate lipolysis.

Adrenergic drugs may be direct-acting agonists, indirect-acting agonists, or antagonists at 1 or more of the 5 types of receptors. Systemic absorption of ocular adrenergic drugs is frequently sufficient to cause systemic effects, which manifest in the cardiovascular system, the bronchial airways, and the brain.

α-Adrenergic Drugs

Direct-acting α_1-adrenergic agonists

The primary clinical use of direct-acting α_1-adrenergic agonists, such as phenylephrine, is stimulation of the iris dilator muscle to produce mydriasis. Systemic absorption of

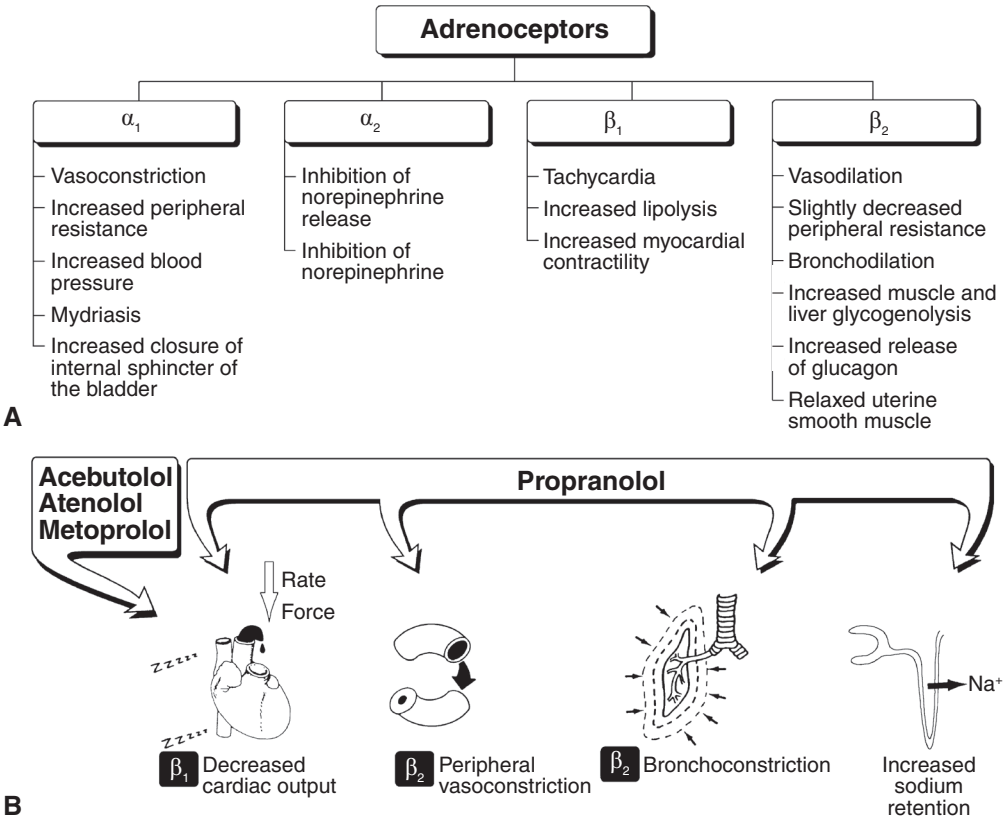


Figure 16-4 Adrenergic receptors. **A,** Major effects mediated by α- and β-adrenoceptors. **B,** Actions of propranolol and β_1-blockers. *(Reproduced with permission from Mycek MJ, Harvey RA, Champe PC, eds.* Pharmacology. *2nd ed. Lippincott's Illustrated Reviews. Lippincott-Raven; 1997:60, 75.)*

phenylephrine may elevate systemic blood pressure. This effect is clinically significant if the patient is an infant or has an abnormally increased sensitivity to α-agonists, which occurs with orthostatic hypotension and in association with the use of drugs that accentuate adrenergic effects (eg, reserpine, tricyclic antidepressants, cocaine, monoamine oxidase [MAO] inhibitors—discussed later). Even with lower doses of phenylephrine (2.5%), infants may exhibit a transient rise in blood pressure because the dose received in an eyedrop is high for their weight.

Because the parasympathetically innervated iris sphincter muscle is much stronger than the dilator muscle, the dilation achieved with phenylephrine alone is largely overcome by the pupillary light reflex during ophthalmoscopy. Coadministration of a cycloplegic drug allows sustained dilatation.

Phenylephrine, 10%, should be used cautiously, particularly in pledget application and in patients with vasculopathic risk factors. A 10% solution contains 5 mg of drug per drop, and ocular medications that pass through the canalicular system are available

for systemic absorption through the vascular nasal mucosa (see Chapter 15). In contrast, the typical systemic dose of phenylephrine for hypotension is 50–100 μg, administered all at once. The ophthalmic use of phenylephrine, 10%, has been associated with stroke, myocardial infarction, and cardiac arrest. Vascular baroreceptors are particularly sensitive to phenylephrine. An increase in blood pressure after topical application may therefore cause a significant drop in pulse rate that can be particularly dangerous in an individual with vasculopathy who is already taking a β-blocking medication for systemic effect.

The compound Omidria (phenylephrine, 1%/ketorolac, 0.3%) is added to irrigating solutions and has been approved by the FDA to prevent miosis during cataract surgery and prevent postoperative pain. One study demonstrated the efficacy of this compound for management of intraoperative floppy iris syndrome (IFIS) in patients taking tamsulosin.

Hovanesian JA, Sheppard JD, Trattler WB, et al. Intracameral phenylephrine and ketorolac during cataract surgery to maintain intraoperative mydriasis and reduce postoperative ocular pain: integrated results from 2 pivotal phase 3 studies. *J Cataract Refract Surg*. 2015;41(10):2060–2068.

Silverstein SM, Rana VK, Stephens R, et al. Effect of phenylephrine 1.0%-ketorolac 0.3% injection on tamsulosin-associated intraoperative floppy-iris syndrome. *J Cataract Refract Surg*. 2018;44(9):1103–1108.

α_2-Adrenergic agonists

Apraclonidine hydrochloride (*para*-aminoclonidine) is a selective α_2-adrenergic agonist and a clonidine derivative that prevents release of norepinephrine at nerve terminals (Tables 16-7, 16-8). It decreases aqueous production as well as episcleral venous pressure and improves trabecular outflow. However, its true ocular hypotensive mechanism is not fully understood. When administered preoperatively and postoperatively, the drug effectively diminishes the acute increase in IOP that follows laser iridotomy, selective laser trabeculoplasty, Nd:YAG laser capsulotomy, and cataract extraction (see BCSC Section 10, *Glaucoma,* for additional information on apraclonidine). Although apraclonidine hydrochloride may be effective for

Table 16-7 Adrenergic Agonists

Generic Name	Trade Name	Strengths
β_2-Adrenergic agonists		
Dipivefrin HCl	Propine	0.1%
	Available generically	0.1%
Epinephrine HCl	Not available in the United States	0.5%, 1%, 2%
α_2-Selective agonists		
Apraclonidine HCl	Iopidine	0.5%, 1% (single-use container)
Brimonidine tartrate	Alphagan P	0.1%, 0.15%
	Available generically	0.2%
Brimonidine tartrate/timolol maleate	Combigan	Brimonidine tartrate 0.2%/ timolol maleate 0.5%

Table 16-8 Mode of Action of Antiglaucoma Drugs

Primary Mechanism of Action	Drug Class	Examples
Decrease aqueous humor production	1. β-Adrenergic antagonists	Timolol, betaxolol, carteolol, levobunolol
	2. α_2-Adrenergic agonists	Apraclonidine, brimonidine
	3. Rho kinase inhibitors	Netarsudil
Increase trabecular outflow	1. Miotics	Pilocarpine
	2. Adrenergic agonists	Epinephrine, dipivalyl epinephrine
	3. Rho kinase inhibitors	Ripasudil, netarsudil
	4. Prostaglandins	Latanoprostene bunod
Increase uveoscleral outflow	1. Prostaglandins	Latanoprost, bimatoprost, travoprost, tafluprost, latanoprostene bunod
	2. α_2-Adrenergic agonists	Apraclonidine, brimonidine
Decrease episcleral venous pressure	1. Rho kinase inhibitors	Ripasudil, netarsudil

the short-term reduction of IOP, the potential for topical sensitivity and tachyphylaxis often limits its long-term use.

Ligand binding to α_2-receptors in other systems mediates inhibition of the enzyme adenylate cyclase. Adenylate cyclase is present in the ciliary epithelium and is thought to have a role in aqueous production.

Apraclonidine can also be used to diagnose Horner syndrome, which is characterized by denervation hypersensitivity of the α_1-receptors in the iris. Under normal conditions, as a weak α_1-adrenergic agonist, apraclonidine has no effect on pupil dilation; however, in individuals with Horner syndrome, instillation of the drug results in dilation of the affected pupil (see BCSC Section 5, *Neuro-Ophthalmology*, for additional information on the role of apraclonidine in the diagnosis of Horner syndrome).

CLINICAL PEARL

Oxymetazoline is a combined α_1- and α_2-adrenergic agonist. A 0.1% solution has been approved for the treatment of acquired ptosis in adults. Dosed once daily, this medication improves ptosis through stimulation of Müller muscle.

Brimonidine tartrate is another selective α_2-adrenergic agonist. Compared with apraclonidine, brimonidine tartrate is more α_2 selective, is more lipophilic, and causes less tachyphylaxis with long-term use. The rate of toxicity reactions, such as follicular conjunctivitis and contact blepharodermatitis, is also lower (less than 15% for brimonidine but up to 40% for apraclonidine). Cross-sensitivity to brimonidine in patients with known hypersensitivity to apraclonidine is minimal.

Brimonidine's mechanism of action to lower IOP is thought to involve both decreased aqueous production and increased uveoscleral outflow. As with β-blockers, a central mechanism of brimonidine, 0.2%, may account for some IOP reduction: A 1-week trial of treatment in a single eye caused a statistically significant IOP reduction of 1.2 mm Hg in the fellow eye.

The peak IOP reduction achieved with brimonidine is approximately 26%. At peak concentration (2 hours postdose), its IOP reduction is comparable to that of a nonselective β-blocker and superior to that of the selective β-blocker betaxolol; however, at trough (12 hours postdose), the reduction is only 14%–15%, which makes brimonidine at trough less effective than the nonselective β-blockers but comparable to betaxolol.

In addition to brimonidine, 0.2%, preserved with benzalkonium chloride, available solutions include a 0.15% solution preserved with polyquaternium-1 and 0.15% and 0.1% solutions preserved with sodium chlorite. When given 3 times daily, brimonidine tartrate, 0.15%, is comparable to brimonidine, 0.2%.

Ophthalmologists should exercise caution when using apraclonidine or brimonidine in patients with severe cardiovascular disease and in patients taking MAO inhibitors or tricyclic antidepressants. Use of these drugs concomitantly with β-blockers (ophthalmic and systemic), antihypertensives, and cardiac glycosides also requires prudence.

Though effective for rapid lowering of IOP in individuals with angle-closure glaucoma, these drugs may also induce vasoconstriction that can prolong iris sphincter ischemia and reduce the efficacy of concurrent miotics. Apraclonidine has a much greater affinity for α_1-receptors than does brimonidine and is therefore more likely to produce vasoconstriction in the eye. Brimonidine does not induce vasoconstriction in the posterior segment or the optic nerve.

Because brimonidine is more lipophilic than apraclonidine, its penetration of the blood–brain barrier is presumably higher. Central nervous system (CNS) adverse effects include fatigue and drowsiness.

CLINICAL PEARL

Severe systemic toxicity, with hypotension, hypothermia, and bradycardia, has been reported in infants treated with topical ocular brimonidine and/or apraclonidine. As a result, these drugs are contraindicated in infants and should be used with caution in young children.

Indirect-acting adrenergic agonists

Indirect-acting adrenergic agonists (cocaine, 4% or 10%, and hydroxyamphetamine, 1%, currently available only through compounding pharmacies) are used to test for and localize defects in sympathetic innervation to the iris dilator muscle. Typically, pupil response fibers originating in the hypothalamus pass down the spinal cord to synapse with cells in the intermediolateral columns. In turn, preganglionic fibers exit the cord through the anterior spinal roots in the upper thorax to synapse in the superior cervical ganglion in the neck. Finally, postganglionic adrenergic fibers terminate in a neuroeffector junction with the iris dilator

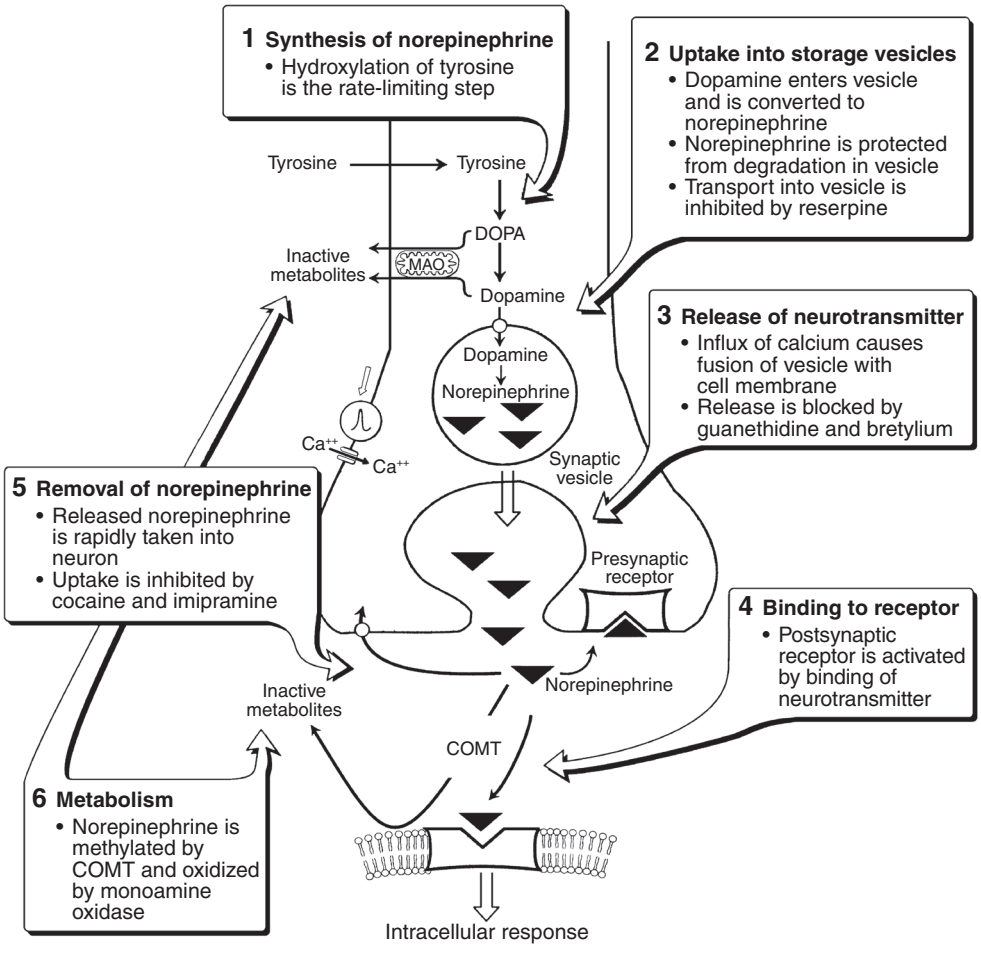


Figure 16-5 Synthesis and release of norepinephrine from the adrenergic neuron. COMT = catechol-O-methyltransferase; DOPA = dihydroxyphenylalanine; MAO = monoamine oxidase inhibitor. *(Reproduced with permission from Mycek MJ, Harvey RA, Champe PC, eds.* Pharmacology. *2nd ed. Lippincott's Illustrated Reviews. Lippincott-Raven; 1997:57.)*

muscle. The norepinephrine released is inactivated primarily by reuptake into secretory granules in the nerve terminal (Fig 16-5). Approximately 70% of released norepinephrine is recaptured (see the discussion of Horner syndrome in BCSC Section 5, *Neuro-Ophthalmology*).

Antagonists

Thymoxamine hydrochloride (moxisylyte), an α_1-adrenergic blocking agent, acts by competitively inhibiting norepinephrine at the receptor site. Thymoxamine inhibits α-adrenergic receptors of the dilator muscle of the iris and causes pupil constriction; however, it has no significant effect on ciliary muscle contraction and therefore does not induce substantial changes in anterior chamber depth, facility of outflow, IOP, or accommodation in eyes with POAG. In patients with an increase in IOP secondary to primary angle closure, thymoxamine

may widen the peripheral angle and reduce IOP. Thymoxamine is useful in differentiating angle-closure glaucoma from POAG with narrow angles and in reversing the pupil dilation caused by phenylephrine. This drug is not commercially available in the United States, although it has been widely used in Europe for years.

Dapiprazole hydrochloride (no longer available in the United States) is an α-adrenergic blocking agent that reverses, in 30 minutes, the mydriasis produced by phenylephrine and tropicamide but not by cycloplegics. It affects the dilator muscle but not ciliary muscle contraction (anterior chamber depth, facility of outflow, or accommodation are also unaffected).

β-Adrenergic Drugs

β_2-Adrenergic agonists

β_2-Adrenergic agonists lower IOP by increasing trabecular outflow and possibly by increasing uveoscleral outflow. The beneficial effect on outflow more than compensates for a small increase in aqueous inflow as detected by fluorophotometry. The effect on outflow facility seems to be mediated by β_2-receptors.

β_2-Receptors linked to adenylate cyclase are present in the ciliary epithelium and processes as well as in the TM. Treatment with L-epinephrine, a nonselective mixed α- and β-agonist, increases intracellular levels of cyclic adenosine monophosphate (cAMP) in these tissues and in the aqueous humor. In other tissues, β-receptor–mediated generation of cAMP in turn activates cAMP-dependent enzymes, which results in reactions such as glycogenolysis and gluconeogenesis in the liver and lipolysis in adipose tissue. However, the biochemical mechanisms responsible for lowering IOP remain to be determined.

Topical L-epinephrine is no longer commercially available in the United States, nor is it used in most countries (see Table 16-7). Local and systemic adverse effects are common (see BCSC Section 10, *Glaucoma*). Clinically, nonselective adrenergic drugs have been replaced by the selective α_2-adrenergic agonists because of their improved efficacy and favorable adverse effect profiles. In an animal model, long-term therapy with epinephrine was shown to downregulate the number of β-receptors. This phenomenon may underlie the loss of some of the drug's therapeutic effectiveness over time (tachyphylaxis).

β-Adrenergic antagonists

β-Adrenergic antagonists, also known as β-*blockers,* lower IOP by reducing aqueous humor production by as much as 50% (Table 16-9). Six β-blockers are approved for use in the treatment of glaucoma: betaxolol, carteolol, levobunolol, metipranolol, timolol hemihydrate, and timolol maleate. Although it is likely that the ciliary body is the site of action for these medications, it is not known whether it is the vasculature of the ciliary processes or the pumping mechanism of the ciliary epithelium that is primarily affected. A possible mechanism may be an effect on the β-adrenergic receptor–coupled adenylate cyclase of the ciliary epithelium.

Although systemic administration of β-blockers has been reported to elevate blood lipid levels, such elevation has not been demonstrated with topical β-blockers such as timolol. All β-blockers can inhibit the increase in pulse and blood pressure that is exhibited in response to exertion. For this reason, they may be poorly tolerated in older adults during routine activities, as well as in young, physically active individuals. Nonselective β-blockers inhibit

Table 16-9 β-Adrenergic Antagonists

Generic Name	Trade Name	Strengths
Betaxolol HCl	Betoptic S	0.25%
	Available generically	0.5%
Carteolol HCl	Ocupress	1%
	Available generically	1%
Levobunolol HCl	Betagan	0.25%, 0.5%
	Available generically	0.25%, 0.5%
Metipranolol HCl	OptiPranolol	0.3%
	Available generically	0.3%
Timolol hemihydrate	Betimol	0.25%, 0.5%
Timolol maleate	Istalol	0.5%
Solution	Timoptic in Ocumeter or Ocumeter Plus container	0.25%, 0.5%
	Available generically	0.25%, 0.5%
Gel	Timoptic-XE in Ocumeter or Ocumeter Plus container	0.25%, 0.5%
	Available generically as Timolol gel-forming solution	0.25%, 0.5%
Timolol maleate (preservative-free)	Timoptic in OcuDose	0.25%, 0.5%
Brimonidine tartrate/ timolol maleate	Combigan	Brimonidine tartrate, 0.2%/ timolol maleate, 0.5%
Dorzolamide HCl/ timolol maleate	Cosopt Ocumeter Plus	Dorzolamide, 2%/timolol, 0.5%
	Available generically	Dorzolamide, 2%/timolol, 0.5%
Dorzolamide HCl/ timolol maleate (preservative-free)	Cosopt in OcuDose	Dorzolamide, 2%/timolol, 0.5%
	Available generically	Dorzolamide, 2%/timolol, 0.5%

the pulmonary β_2-receptors that dilate the respiratory tree. The induced bronchospasm may be significant in patients with asthma or chronic obstructive lung disease. In patients with bradycardia and second- or third-degree atrioventricular block, the underlying cardiac condition may be exacerbated with use of these drugs.

The traditional teaching that topical β-blockers are contraindicated in patients with congestive heart failure is no longer accurate. Indeed, current cardiologic evidence strongly demonstrates that β-blockage is an important component of treatment for heart failure, *except in advanced cases*. It is important for ophthalmologists to maintain continuous communication with patients' internists or cardiologists regarding the possible systemic effects of ophthalmic therapy.

Timolol maleate and levobunolol are mixed β_1-/β_2-antagonists. Tests of more specific β-blockers suggest that β_2-antagonists have a greater effect on aqueous secretion than do

β_1-antagonists. For example, comparative studies have shown that the specific β_1-antagonist betaxolol, 0.5%, is approximately 85% as effective as timolol, 0.5%, in lowering IOP.

Metipranolol hydrochloride is a nonselective β_1- and β_2-adrenergic receptor–blocking drug. In a 0.3% topical solution, it is similar in effect to other topical nonselective β-blockers, in addition to reducing IOP.

Carteolol hydrochloride demonstrates intrinsic sympathomimetic activity; in other words, in addition to acting as a competitive antagonist, it also causes a slight to moderate activation of receptors. Thus, even though carteolol has β-blocking activity, it may be tempered, reducing its effects on cardiovascular and respiratory systems. Carteolol is also less likely than other β-blockers to adversely affect the systemic lipid profile.

Betaxolol is a selective β_1-antagonist that is substantially safer than the nonselective β-blockers for use in patients with pulmonary, cardiac, CNS, or other systemic conditions. Betaxolol may be useful in patients with a history of bronchospastic disorders, although other therapies should be tried first because betaxolol's β selectivity is relative and not absolute, and some β_2 effects can therefore remain. In general, the IOP-lowering effect of betaxolol is less than that of the nonselective β-adrenergic antagonists.

Betaxolol is available as a generic 0.5% solution and as a 0.25% suspension. The 0.25% suspension causes less irritation on instillation yet maintains its clinical efficacy compared with the brand-name 0.5% solution (now discontinued), a finding that is generally extrapolated to the currently available generic 0.5% solution.

Prodrugs of nonselective β-blockers are being developed. They may offer higher potency of β_1-/β_2-blocking medications while reducing their systemic adverse effects.

Curiously, both β-agonist and β-antagonist drugs can lower IOP. This paradox is compounded by the observation that β-agonist and β-antagonist drugs have slightly additive effects in lowering IOP.

Carbonic Anhydrase Inhibitors

Systemic carbonic anhydrase inhibitors (CAIs) such as acetazolamide and methazolamide are approved for the treatment of glaucoma and idiopathic intracranial hypertension (IIH, also known as *pseudotumor cerebri*), in addition to other systemic conditions (Table 16-10). They may also be effective in treating cystoid macular edema (CME).

Systemic CAIs can be administered orally and/or parenterally. The longer half-life of methazolamide allows it to be used twice daily; acetazolamide is also available in a 500-mg sustained-release form used twice daily. Neither of these compounds has the ideal combination of high potency (low binding affinity, K_i), good ocular penetration (high penetration percentage in the nonionized form and high lipid solubility to facilitate passage through the blood–ocular barrier), high proportion of the drug present in the blood in unbound form, and long plasma half-life.

The mechanism of action of this class of medications is via inhibition of carbonic anhydrase. The amount of carbonic anhydrase present in tissues is much higher than that needed to supply the amount of bicarbonate (HCO_3^-) required. Calculations based on the K_{cat} (catalysis constant) and K_m (apparent affinity constant) of the enzyme and on the concentrations of substrates and product indicate that the amount of enzyme present in the

Table 16-10 Carbonic Anhydrase Inhibitors

Generic Name	Trade Name	Strengths	Onset of Action	Duration of Action
Systemic				
Acetazolamide (oral)	Diamox Sequels	500 mg (extended-release)	1–1.5 h, 2 h	8–12 h, 18–24 h
	Available generically	125 mg, 250 mg, 500 mg (extended-release)	1–1.5 h	8–12 h
Acetazolamide sodium (parenteral)	Available generically	500 mg, 5–10 mg/kg[3]	2 min	4–5 h
Methazolamide (oral)	Available generically	25 mg, 50 mg	2–4 h	10–18 h
Topical				
Brinzolamide	Azopt	1% suspension	2–3 h	8–12 h
Dorzolamide HCl	Trusopt Ocumeter Plus	2% solution	2 h	8 h
	Available generically	2% solution	2 h	8 h
Combination drugs				
Dorzolamide HCl/ timolol maleate	Cosopt Ocumeter Plus	Dorzolamide HCl, 2%/timolol, 0.5%	2 h	8–12 h
	Available generically	Dorzolamide HCl, 2%/timolol, 0.5%	2 h	1 h
Dorzolamide HCl/ timolol maleate (preservative-free)	Cosopt in OcuDose	Dorzolamide HCl, 2%/timolol, 0.5%	2 h	1 h
	Available generically	Dorzolamide HCl, 2%/timolol, 0.5%	2 h	1 h
Brinzolamide/ brimonidine tartrate	Simbrinza	Brinzolamide 1%/brimonidine 0.2%	2–3h	8–12 h

ciliary body is 100 times greater than needed. Correspondingly, in clinical use, the enzyme must be more than 99% inhibited to significantly reduce aqueous flow. In contrast, the amount of enzyme in the kidney, which is 1000-fold greater than needed, must be more than 99.9% inhibited to affect the usual pathway for HCO_3^- reabsorption.

In addition to lowering IOP by inhibiting ciliary body carbonic anhydrase, at high doses, each drug further lowers IOP by causing renal metabolic acidosis. The mechanism by which acidosis lowers secretion is uncertain, but it probably involves reduction in HCO_3^- formation and activity of Na^+,K^+-ATPase.

At the onset of acidosis, renal effects cause alkaline diuresis, with loss of Na^+, K^+, and HCO_3^-. In patients receiving CAI therapy concurrently with diuretics, steroids, or adrenocorticotropic hormone (ACTH), severe hypokalemia can result. This situation may be dangerous for patients using digitalis, in whom hypokalemia may elicit arrhythmias. When such patients are receiving long-term CAI therapy, they should have their potassium levels checked at regular intervals, preferably by their primary care physician.

Over time, the acidosis prompts a renal mechanism for HCO_3^- reabsorption unrelated to carbonic anhydrase; this mechanism limits the degree of acidosis and halts both the diuresis and K^+ loss after the first few days of treatment.

In individuals with certain systemic conditions, CAI therapy may cause or contribute to additional adverse effects. Alkalinization of the urine, present during initial CAI treatment, prevents excretion of ammonium (NH_4^+), a factor to consider in patients with cirrhosis. Metabolic acidosis may exacerbate diabetic ketoacidosis or precipitate sickle cell crisis. In patients with severe chronic obstructive pulmonary disease, impairment of CO_2 transfer from the pulmonary vasculature to the alveoli may cause respiratory acidosis. Older adults are predisposed to severe metabolic acidosis with the use of systemic CAIs because of their physiologically reduced renal function.

CLINICAL PEARL

With the inhibitor methazolamide, the difference between the concentrations of carbonic anhydrase in the ciliary body and in the kidney can be exploited to lower IOP without incurring renal HCO_3^- loss, and metabolic acidosis can be limited, resulting in fewer adverse effects. Although renal stone formation has been reported with use of methazolamide, the incidence is substantially lower than with other drugs because methazolamide is metabolized in the liver. In contrast, acetazolamide is actively secreted into the renal tubules, and renal effects are unavoidable.

The use of acetazolamide has been linked to the formation of stones in the urinary tract. A retrospective case-control series showed that the incidence of stones was 11 times higher in patients using this drug than in those not using it. The increased risk occurred primarily during the first year of therapy. Continued use after occurrence of a stone was associated with a high risk of recurrent stone formation. However, a history of spontaneous stone formation more than 5 years prior to acetazolamide therapy did not appear to increase risk. The mechanisms responsible for stone formation may be related to metabolic acidosis and associated pH changes, as well as to decreased excretion of citrate.

Nearly 50% of patients taking systemic CAIs experience CNS or gastrointestinal adverse effects. These adverse effects include numbness and tingling of the hands, feet, and lips; malaise; metallic taste when drinking carbonated beverages; anorexia and weight loss; nausea; somnolence; impotence and loss of libido; and depression. When the clinical situation allows, it is wise to begin therapy at low dosages (eg, 125 mg of acetazolamide 4 times daily or 25–50 mg methazolamide twice daily) to reduce the incidence and severity of adverse effects. It is important to inform patients of the potential adverse effects of these drugs; otherwise, they may fail to associate their systemic symptoms with the medication prescribed by their ophthalmologists.

Rare adverse effects from this class of drugs include those common to other members of the sulfonamide family, such as transient myopia, hypersensitive nephropathy, skin rash, Stevens-Johnson syndrome, and thrombocytopenia. One potential adverse effect, aplastic anemia, is idiosyncratic. Blood cell counts do not identify susceptible patients. CAIs have also been associated with teratogenic effects (forelimb deformity) in rodents, and their use is not advised during pregnancy. However, these systemic adverse effects are rare with topical CAIs (see the section "Sulfonamides" later in the chapter for discussion of allergies to sulfonamides).

The topical CAIs—dorzolamide and brinzolamide—are also available for long-term treatment of glaucoma. They penetrate the cornea easily and are water soluble. When administered as solution 3 times per day, these drugs effectively inhibit carbonic anhydrase II while avoiding the systemic adverse effects associated with oral administration. The 2 medications are equally effective and reduce IOP by 14%–17%. Adverse effects of topical CAIs include burning on instillation, punctate keratitis, local allergy, and bitter taste. The hypotensive effects of topical and oral CAIs are probably not additive when adequate doses of each are used. Both topical CAIs are also available in combination drops (see Table 16-10).

Prostaglandin Analogues

Currently, 5 prostaglandin (PG) analogues have been approved by the FDA for clinical use (Table 16-11). Latanoprost, bimatoprost, travoprost, and tafluprost are administered once daily, with nighttime dosing preferred. Tafluprost is available preservative-free in single-use containers. Latanoprost, travoprost, and tafluprostare prodrugs that require hydrolyzation before becoming active compounds in the eye. These prodrugs interact with the prostaglandin FP receptor. In contrast, bimatoprost is not a prodrug, and it acts on the prostamide receptor.

PG analogues appear to lower IOP by enhancing uveoscleral outflow and may reduce the pressure by 6–9 mm Hg (25%–33%). In addition to once-daily dosing (except for unoprostone), other advantages of this class of medications include a lack of cardiopulmonary adverse effects and additivity to other antiglaucoma medications.

Table 16-11 Prostaglandin Analogues

Generic Name	Trade Name	Strengths
Bimatoprost	Lumigan	0.01%, 0.03%
Bimatoprost intracameral implant	Durysta	10 μg
Latanoprost	Xalatan	0.005%
	Xelpros (benzalkonium chloride–free)	0.005%
	Available generically	0.005%
Tafluprost	Zioptan in single-use containers (preservative-free)	0.0015%
Travoprost	Travatan	0.004%
	Travatan Z	0.004%
Bimatoprost/timolol maleate	Ganfort[a]	Bimatoprost, 0.03%/timolol, 0.5%
Latanoprost/timolol maleate	Xalacom[a]	Latanoprost, 0.005%/timolol, 0.5%
Travoprost/timolol maleate	DuoTrav[a]	Travoprost, 0.004%/timolol, 0.5%
Latanoprostene bunod	Vyzulta	0.024%

[a] Not available in the United States.

A unique ocular adverse effect associated with this class of drugs is the darkening of the iris and periocular skin as a result of increased numbers of melanosomes (increased melanin content, or melanogenesis) within the melanocytes. The risk of increased iris pigmentation correlates with baseline iris pigmentation. In 10%–20% of light-colored irides, increased pigmentation may occur in the initial 18–24 months of therapy, whereas nearly 60% of eyes that are light brown or 2-toned may experience increased pigmentation over the same period. The long-term sequelae of this adverse effect, if any, are unknown. Other adverse effects associated with topical PG analogues include conjunctival injection, hypertrichosis of the eyelashes, CME, and uveitis. CME and uveitis are more common in eyes with preexisting risk factors for either condition.

Reported systemic reactions include flulike symptoms, rash, and possible uterine bleeding in postmenopausal women. Reactivation of herpetic keratitis has been reported with use of latanoprost. Although their elimination from human plasma is rapid, PGs are known to cause contraction of the uterus. Thus, topical PGs should be used with caution in pregnant patients.

In 2020, the FDA approved a sustained-release intracameral bimatoprost implant. This biodegradable implant is injected into the anterior chamber via a 28-gauge needle. After the injection, the patient is instructed to sit upright for an hour to allow the device to settle into the inferior angle and out of the visual axis. The IOP lowering effects of the implant last 3–4 months, and it is typically dosed every 16 weeks. In the phase 3 trial, it was observed that after receiving 3 consecutive implants at 16-week intervals, approximately 80% of participants did not require additional IOP lowering therapy. This effect of the medication lasting past its clearance from the aqueous humor is thought to result from upregulation of matrix metalloproteinase (MMP) expression and/or activity in the ciliary body and TM. The implant is contraindicated in patients with intraocular inflammation, corneal endothelial cell dystrophy, corneal transplant, and/or absent or ruptured posterior capsules. Adverse reactions include implant migration, corneal endothelial cell loss, macular edema, intraocular inflammation, iris pigmentation, and endophthalmitis.

Nitric Oxide Donors

Nitric oxide (NO) is a ubiquitous, versatile, endogenous signaling molecule with diverse biological effects. As a gaseous molecule, NO is highly lipophilic and volatile, able to readily diffuse across cell membranes and function as a paracrine messenger that induces changes in adjacent cells. NO is also a highly reactive free radical. Excessive NO, particularly in individuals with ischemia, can result in tissue damage.

Endogenous NO is derived from the amino acid L-arginine by the action of NO synthase (NOS). The enzyme has 3 isoforms: endothelial NOS (eNOS or NOS-3), found mainly in endothelial cells; neuronal NOS (nNOS or NOS-1), expressed in central and peripheral neurons; and inducible NOS (iNOS or NOS-2), expressed primarily in macrophages but potentially in any cell type and induced by inflammatory cytokines or bacterial endotoxins.

In physiologic conditions, eNOS is present in the endothelium of ciliary and retinal vessels, ciliary muscle, and Schlemm canal cells, whereas nNOS is found in the nonpigmented

ciliary epithelium and optic nerve head. Under stimulated conditions, iNOS can be detected in the iris, ciliary body, vessels, and optic nerve head. NO generated in the TM is most likely mediated by iNOS.

Significant clinical and experimental evidence indicates that an endogenous insufficiency of NO bioavailability is linked to POAG, although the exact relationship between the two is unclear. NO is thought to lower IOP by increasing trabecular outflow. Evidence suggests that NO affects trabecular outflow by relaxing the juxtacanalicular TM, altering contractility and cell volume of the TM and Schlemm canal cells. NO may be involved in aqueous secretion through regulation of blood flow, uveoscleral outflow via relaxation of the smooth muscle fibers, and autoregulation of optic nerve head circulation during changes in IOP. Exogenous NO delivered to the anterior eye can facilitate outflow and lower IOP.

Latanoprostene bunod (LBN) ophthalmic solution, 0.024%, is a NO-donating PG analogue that chemically combines a NO-donating moiety with latanoprost. The molecular structure of LBN is nearly identical to that of latanoprost. However, LBN is distinguished by the integration of a NO-donating moiety (a terminal butyl nitrate ester functional group) in lieu of an isopropyl ester. Upon topical administration, LBN is hydrolyzed by endogenous corneal esterases into latanoprost acid and butanediol mononitrate, which is further metabolized to NO and the inactive 1,4-butanediol. The molecule is thought to exert pharmacologic effects, with latanoprost increasing uveoscleral outflow and NO enhancing trabecular outflow.

LBN is dosed once daily at bedtime and has an adverse effect profile similar to that of other PGs in clinical settings. In phase 3 clinical trials, LBN produced a mean IOP reduction of 7.5–9.1 mm Hg and was superior to twice-daily timolol 0.5%; in addition, LBN's IOP-lowering efficacy lasted for 12 months. Notably, in the phase 2 study, reduction in IOP was 1.2 mm Hg greater with LBN treatment for 28 days than with latanoprost.

NO-donating moieties combined with other ocular hypotensive agents are under development. They include introduction of NO-donating moieties to bimatoprost (another PG analogue), to a nonselective β-blocker, and to the CAIs dorzolamide and brinzolamide.

Aliancy J, Stamer WD, Wirostko B. A review of nitric oxide for the treatment of glaucomatous disease. *Ophthalmol Ther*. 2017;6(2):221–232.

Rho Kinase Inhibitors

Rho kinase (ROCK) is a serine/threonine kinase that serves as an important downstream effector of Rho guanosine triphosphate hydrolase (Rho GTPase). The Rho family of GTPases is composed of small (≈21 kDa) signaling G proteins (also known as *guanine nucleotide-binding proteins*) found in the cytosol and has 3 main classes: Rho, Rac, and Cdc42.

The Rho class has 3 isoforms: RhoA, RhoB, and RhoC. RhoA is activated by guanine nucleotide exchange factors. Upon binding to GTP, RhoA activates ROCK, which phosphorylates several downstream substrates involved in a wide variety of cellular functions. Two isoforms—ROCK-I and ROCK-II—have been isolated.

ROCK plays a critical role in regulating the tone of smooth muscle tissues. Animal studies of the effects of ROCK inhibitors have demonstrated increased ocular blood flow presumably through the relaxation of vascular endothelial smooth muscle, as well as the neuroprotective promotion of retinal ganglion cell survival and axon regeneration. ROCK inhibitors may also reduce scarring after glaucoma filtering surgery by blocking the assembly and contraction of transforming growth factor β–induced stress fibers and inhibiting fibroproliferation and collagen deposition postoperatively.

ROCK inhibitors have also been proposed for the treatment of corneal endothelial decompensation. Topical ROCK inhibitors have promoted cell proliferation in animal models, and pilot clinical research suggests a similar response in humans. ROCK inhibitors are being studied for wound healing in the corneal endothelium, Fuchs endothelial corneal dystrophy, and corneal decompensation after cataract surgery, as well as for enhancing engraftment of corneal endothelial cells onto recipient tissues in tissue engineering therapy.

Selective ROCK inhibitors are thought to increase aqueous humor drainage through the TM, subsequently decreasing IOP. The exact molecular mechanism is not fully understood. ROCK inhibitors appear to have several actin cytoskeletal–related targets that directly affect the contractile properties of TM outflow tissue.

In 2014, the ROCK inhibitor ripasudil, 0.4%, twice-daily ophthalmic solution was approved in Japan for the treatment of glaucoma and ocular hypertension when other therapeutic drugs are not effective or cannot be administered. Another agent, netarsudil, is an inhibitor of both ROCK and the norepinephrine transporter. Netarsudil is thought to work via 3 mechanisms:

1. increase of trabecular outflow
2. reduction of episcleral venous pressure
3. reduction of aqueous production by norepinephrine transporter inhibition

In a phase 3 clinical trial, netarsudil was associated with a 3.3- to 4.6-mm Hg reduction in IOP. In another study, netarsudil, 0.02%, dosed once daily was noninferior to timolol, 0.5%, dosed twice daily. The drug is currently FDA-approved for the reduction of IOP. Common adverse effects include hyperemia (up to 53% of study eyes), cornea verticillata (20% of study eyes), irritation, and blurred vision.

Fixed-combination therapy with netarsudil, 0.02%, and latanoprost, 0.005%, is also available.

Okumura N, Okazaki Y, Inoue R, et al. Effect of the Rho-associated kinase inhibitor eyedrop (ripasudil) on corneal endothelial wound healing. *Invest Ophthalmol Vis Sci*. 2016; 57(3): 1284–1292.

Serle JB, Katz LJ, McLaurin E, et al; ROCKET-1 and ROCKET-2 Study Groups. Two phase 3 clinical trials comparing the safety and efficacy of netarsudil to timolol in patients with elevated intraocular pressure: Rho Kinase Elevated IOP Treatment Trial 1 and 2 (ROCKET-1 and ROCKET-2). *Am J Ophthalmol*. 2018;186:116–127.

Tanna AP, Johnson M. Rho kinase inhibitors as a novel treatment for glaucoma and ocular hypertension. *Ophthalmology*. 2018;125(11):1741–1756.

Table 16-12 Fixed-Combination Glaucoma Medications

Generic Name	Trade Name	Strengths	Dosing Schedule
Dorzolamide HCl/timolol maleate solution	Cosopt	Dorzolamide, 2%/timolol, 0.5%	2 times daily
Brimonidine tartrate/timolol maleate solution	Combigan	Brimonidine, 2%/timolol, 0.5%	2 times daily
Brinzolamide/brimonidine tartrate suspension	Simbrinza	Brinzolamide, 1%/brimonidine, 0.2%	3 times daily
Latanoprost/timolol maleate solution	Xalacom[a]	Latanoprost, 0.005%/timolol, 0.5%	Once daily
Travoprost/timolol maleate solution	DuoTrav[a]	Travoprost, 0.004%/timolol, 0.5%	Once daily
Bimatoprost/timolol maleate solution	Ganfort[a]	Bimatoprost, 0.03%/timolol, 0.5%	Once daily
Netarsudil/latanoprost solution	Rocklatan	Netarsudil, 0.02%/latanoprost, 0.005%	Once daily

[a] Not available in the United States.

Fixed-Combination Medications

Medications that are combined in a single bottle have the potential benefits of improved efficacy, convenience, and patient adherence as well as reduced cost. FDA guidelines require the fixed combination to be more efficacious than either drug given alone.

Table 16-12 lists the currently available fixed-combination medications for glaucoma (some are not available in the United States). Before a patient uses the combination drug, each component should be checked for its effect on that patient's IOP (see BCSC Section 10, *Glaucoma*).

Osmotic Drugs

Actions and Uses

Increased serum osmolarity reduces IOP and vitreous volume by drawing fluid across vascular barriers and out of the eye. The osmotic activity of a drug depends on the number of particles in the solution and the maintenance of an osmotic gradient between the plasma and the intraocular fluids. This activity is independent of molecular weight. Low-molecular-weight agents such as urea, which penetrate the blood–ocular barrier, produce a small increase in IOP after an initial reduction because of a reversal of the osmotic gradient when the kidneys clear the blood of excess urea.

Osmotic drugs are FDA-approved for the short-term management of acute glaucoma in adults and may be used to reduce vitreous volume before intraocular surgery.

The hyperosmotic drugs glycerin, mannitol, and urea are currently available for ophthalmic use in the United States (Table 16-13). Osmotic drugs should be used with care in patients in whom cardiovascular overload can occur with moderate vascular volume

Table 16-13 Hyperosmotic Drugs

Generic Name	Trade Name	Strengths	Dose	Route	Onset of Action	Duration of Action
Glycerin[a]	Available generically	50%	1–1.5 g/kg	Oral	10–30 min	5 h
Mannitol[b]	Osmitrol	5%–20%	0.25–2 g/kg	Intravenous	30–60 min	4–8 h
	Available generically	5%–25%	0.25–2 g/kg	Intravenous	30–60 min	4–8 h
Urea	Available generically	Powder	0.5–2 g/kg	Intravenous	30–45 min	5–6 h

[a] Commercially unavailable, but available from compounding pharmacies.
[b] A single mannitol dose of 0.25–0.5 g/kg is often enough to reduce intraocular pressure (IOP).

expansion; this includes patients with a history of congestive heart failure, angina, and systemic hypertension or recent myocardial infarction.

Lichter PR. Glaucoma clinical trials and what they mean for our patients. *Am J Ophthalmol.* 2003;136(1):136–145.

Netland PA. *Glaucoma Medical Therapy: Principles and Management.* 2nd ed. Ophthalmology Monograph 13. American Academy of Ophthalmology; 2008.

Intravenous Drugs

Mannitol must be administered intravenously because it cannot be absorbed from the gastrointestinal tract. This drug may be given as either an IV infusion or an IV push. For an IV infusion, mannitol may be given as a 20% premixed solution (concentration, 200 mg/mL) over 30–60 minutes. For an IV push, a 25% solution may be injected over 3–5 minutes. A too-rapid infusion of mannitol may shift intracellular water into the extracellular space, causing cellular dehydration with a high risk of hyponatremia, cardiovascular overload, congestive heart failure, pulmonary edema, and intracranial bleeding.

Mannitol has been associated with subarachnoid hemorrhage attributed to rapid volume overload of the blood vessels and/or rapid shrinkage of the brain with traction of the subarachnoid vessels. This shrinkage is of particular concern in older adults, who may already have brain shrinkage from microischemic disease and are therefore at increased risk of bleeding.

These drugs are cleared by the kidneys and produce marked osmotic diuresis that may be troublesome during surgery. Conscious patients should void shortly before surgery, and a urinal or bedpan should be available. If general anesthesia is used, an indwelling urethral catheter may be required to prevent bladder distension.

Oral Drugs

Glycerin, 50%, was discontinued in the United States in 2004; however, it can be compounded by diluting the 100% solution. This frequently used oral osmotic drug is given over cracked ice to minimize its nauseatingly sweet taste. Glycerin is chiefly converted to glucose, glycogen, and other carbohydrates in the liver. Hyperglycemia and glycosuria can result from the oral

administration of the agent. The nonmetabolized sugar isosorbide was previously preferred in patients with diabetes, but it has been discontinued in the United States.

Anti-inflammatory Drugs

Ocular inflammation can be treated with medications administered topically, by local injection, by ocular implantation, or systemically. Anti-inflammatory agents are classified as glucocorticoids, nonsteroidal anti-inflammatory drugs (NSAIDs), mast-cell stabilizers, antihistamines, or antifibrotics.

Glucocorticoids

Corticosteroids, or steroids, are applied topically to prevent or suppress ocular inflammation in trauma and uveitis, as well as after most ocular surgical procedures (Table 16-14). Subconjunctival, sub-Tenon, and intravitreal injections/implantation of steroids are used to treat more severe cases of ocular inflammation (Table 16-15). Systemic steroid therapy is used to treat systemic immune diseases, such as giant cell arteritis, vision-threatening capillary hemangiomas in childhood, and severe ocular inflammation that is resistant to topical therapy. Intravenous methylprednisolone is sometimes used in short-term management of various orbital and neuro-ophthalmic conditions (see BCSC Section 5, *Neuro-Ophthalmology,* and Section 7, *Oculofacial Plastic and Orbital Surgery*). Corticosteroids are divided into 2 major groups, glucocorticoids and mineralocorticoids, on the basis of their predominant biological activities.

Glucocorticoids induce cell-specific effects on lymphocytes, macrophages, polymorphonuclear leukocytes, vascular endothelial cells, fibroblasts, and other cells. In each of these cells, glucocorticoids must

- penetrate the cell membrane
- bind to soluble receptors in the cytosol
- allow the translocation of the glucocorticoid receptor complex to nuclear-binding sites for gene transcription
- induce or suppress the transcription of specific messenger RNA (mRNA)

The proteins produced in the eye under the control of these mRNAs are not known; only resultant effects have been described.

At the tissue level, glucocorticoids prevent or suppress local hyperthermia, vascular congestion, edema, and the pain of initial inflammatory responses, whether the cause is traumatic (radiant, mechanical, or chemical), infectious, or immunologic. They also suppress the late inflammatory responses of capillary proliferation, fibroblast proliferation, collagen deposition, and scarring.

At the biochemical level, the most important effect of anti-inflammatory drugs may be the inhibition of arachidonic acid release from phospholipids (see the section Nonsteroidal Anti-inflammatory Drugs). Liberated arachidonic acid is otherwise converted into PGs, PG endoperoxides, leukotrienes, and thromboxanes, which are potent mediators of inflammation. Glucocorticoids also suppress the liberation of lytic enzymes from lysozymes.

Table 16-14 Topical Anti-inflammatory Drugs

Generic Name	Trade Name	Strengths
Corticosteroids		
Dexamethasone sodium phosphate	Maxidex	Suspension, 0.1%
	Maxidex, Ocu-Dex[a]	Ointment, 0.05%
	Available generically	Solution, 0.1%
Difluprednate	Durezol	Emulsion, 0.05%
Fluorometholone	FML S.O.P.	Ointment, 0.1%
	FML Liquifilm	Suspension, 0.1%
	FML Forte Liquifilm	Suspension, 0.25%
	Fluor-Op	Suspension, 0.1%
	Available generically	Suspension, 0.1%
Fluorometholone acetate	Flarex	Suspension, 0.1%
Loteprednol etabonate	Alrex	Suspension, 0.2%
	Eysuvis	Suspension, 0.25%
	Lotemax	Suspension, 0.5%
	Lotemax	Ointment, 0.5%
Medrysone	HMS	Suspension, 1%
Prednisolone acetate	Econopred Plus	Suspension, 1%
	Omnipred	Suspension, 1%
	Pred Forte	Suspension, 1%
	Available generically	Suspension, 1%
	Pred Mild	Suspension, 0.12%
Prednisolone sodium phosphate	Inflamase Forte	Solution, 1%
	Available generically	Solution, 1%, 0.125%
Nonsteroidal anti-inflammatory drugs		
Bromfenac sodium	Bromday	Solution, 0.09%
	Prolensa	Solution, 0.07%
	Available generically	Solution, 0.09%
Diclofenac sodium	Voltaren	Solution, 0.1%
	Available generically	Solution, 0.1%
Flurbiprofen sodium	Ocufen	Solution, 0.03%
	Available generically	Solution, 0.03%
Ketorolac tromethamine	Acular, Acular PF	Solution, 0.5%
	Acular LS	Solution, 0.4%
	Acuvail	Solution, 0.45%
	Available generically	Solution, 0.5%
Nepafenac	Nevanac	Suspension, 0.1%
	Ilevro	Suspension, 0.3%

[a] Not available in the United States.

The effects of glucocorticoids on immune-mediated inflammation are complicated. Glucocorticoids do not affect the titers of either immunoglobulin E (IgE), which mediates allergic mechanisms, or immunoglobulin G (IgG), which mediates autoimmune mechanisms. Also, glucocorticoids do not appear to interfere with normal processes in the afferent limb of cell-mediated immunity, as in graft rejection. Instead, they interfere with the subsequent efferent limb of the immune response. For example, glucocorticoids prevent macrophages from being attracted to sites of inflammation by interfering with the cells'

Table 16-15 Intravitreal Corticosteroids

Generic Name	Brand Name	Dose	Formulation	Ophthalmic Indications
Triamcinolone acetonide	Kenalog-40	4 mg/100 μl	40 mg/ml suspension	Off-label use: CME, CNV, DME, macular edema secondary to retinal vein occlusion, uveitis, ocular inflammatory conditions unresponsive to topical corticosteroids, visualization of vitreous during intraocular surgery
Triamcinolone acetonide (preservative-free)	Triesence	4 mg/100 μl: elimination half-life was 18.7 ± 5.7 days in nonvitrectomized eyes, 3.2 days in vitrectomized eyes	40 mg/ml suspension	Sympathetic ophthalmia, temporal arteritis, uveitis, ocular inflammatory conditions unresponsive to topical corticosteroids, visualization of vitreous during intraocular surgery
Dexamethasone phosphate	Decadron	0.4 mg/100 μl	4mg/ml solution	Off-label use: CME, CNV, uveitis, and ocular inflammatory conditions unresponsive to topical corticosteroids
Dexamethasone implant	Ozurdex	0.7 mg: clinical efficacy ~ 3m	Biodegradable implant	Macular edema secondary to retinal vein occlusion, noninfectious posterior uveitis, and DME
Fluocinolone acetonide implants	Retisert (scleral fixated)	0.59 mg: 0.6 μg/d for 1 mo, 0.3 to 0.4g/d for next 30 mo	Nonbiodegradable implant	Chronic noninfectious posterior uveitis
	Illuvien	0.19 mg: 0.25 μg/d over 36 mo	Nonbiodegradable implant	DME
	Yutiq	0.18 mg: 0.25 μg/d over 36 mo	Nonbiodegradable implant	Chronic noninfectious posterior uveitis

CME = cystoid macular edema; CNV = choroidal neovascularization; DME = diabetic macular edema.

response to lymphocyte-released migration-inhibiting factor. Glucocorticoids administered for systemic effect cause sequestration of lymphocytes, especially the T lymphocytes that mediate cellular immunity. However, the posttranscriptional molecular mechanisms of these responses remain unknown. BCSC Section 9, *Uveitis and Ocular Inflammation,* discusses immune responses in detail.

Adverse effects

Glucocorticoids may cause several adverse effects in the eye and elsewhere in the body. Possible complications in the eye include

- glaucoma
- posterior subcapsular cataracts
- exacerbation of bacterial and viral (especially herpetic) infections through suppression of protective immune mechanisms
- fungal infection
- ptosis
- mydriasis
- scleral melting
- eyelid skin atrophy
- pseudohypopyon from intraocular injection
- central serous chorioretinopathy

In the body, oral doses can cause

- suppression of the pituitary–adrenal axis
- gluconeogenesis resulting in hyperglycemia, muscle wasting, and osteoporosis
- redistribution of fat from the periphery to the trunk
- CNS effects, such as euphoria
- insomnia
- aseptic necrosis of the hip
- peptic ulcer
- diabetes
- psychosis

Patients older than 65 years face challenges when taking long-term systemic steroids. For example, the adverse effect of proximal muscle wasting may make it difficult for these patients to climb stairs. Osteoporosis, another adverse effect of glucocorticoids, exacerbates the risk of falls and fractures for these patients, who are generally at an increased risk of both. Thus, older adults with inflammatory diseases may require a steroid-sparing regimen.

Steroid-induced IOP elevation may occur with topical, intraocular, periocular, nasal, and systemic glucocorticoid therapies. The exact mechanism by which steroids diminish aqueous outflow through the TM remains unknown but may be related to deposition of glycosaminoglycans in the TM.

Individual response to steroids is dependent on the duration, potency, and frequency of therapy and the route of administration of the drug used. Steroid-induced IOP elevation

almost never occurs in durations less than 5 days and is infrequent in less than 2 weeks of use. However, failure of IOP to rise after 6 weeks of therapy does not ensure that a patient will maintain normal IOP after several months of therapy. For this reason, monitoring of IOP at periodic intervals is required throughout the course of long-term steroid therapy to prevent iatrogenic glaucomatous nerve damage. Steroid-induced elevation in IOP is usually reversible by discontinuing therapy; however, permanent elevation of pressure is not uncommon and may require medical and/or surgical interventions.

Table 16-16 lists the anti-inflammatory and IOP-elevating potencies of 6 steroids used in ophthalmic therapy. The anti-inflammatory potencies were determined by an in vitro assay of inhibition of lymphocyte transformation, and the IOP effects were determined by tests in individuals already known to be highly responsive to topical dexamethasone. However, until all these drugs are compared in a model of ocular inflammation relevant to human disease, no conclusion can be reached about the observed dissociation of effects. The lower-than-expected effect on pressure with some of these drugs may be explained by more rapid metabolism of fluorometholone in the eye compared with dexamethasone and by the relatively poor penetration of medrysone. The efficacy of these drugs for intraocular inflammation may be similarly reduced.

CLINICAL PEARL

The rates of IOP spikes for various steroids differ and depend on the potency, formulation, and delivery of the particular drug. When patients are treated with steroids, it is important that ophthalmologists consult the literature for information on individual agents and their effects on IOP.

Table 16-16 Comparison of Anti-inflammatory [a] and IOP-Elevating [b] Potencies

Glucocorticoid	Relative Potency	Rise in IOP (mm Hg)
Dexamethasone, 0.1% (equivalent to betamethasone, 0.1%; less than or equivalent to difluprednate, 0.05%)	24.0	22
Fluorometholone, 0.1% [c]	21.0	6
Prednisolone acetate, 1%	2.3	10
Medrysone, 1% [d]	1.7	1
Tetrahydrotriamcinolone, 0.25%	1.4	2
Hydrocortisone, 0.5%	1.0	3

[a] Anti-inflammatory potency determined by in vitro assay of inhibition of lymphocyte transformation. Anti-inflammatory potency of difluprednate, 0.05%, is equal to or stronger than betamethasone, 0.1%, which has a 6-fold anti-inflammatory potency compared with that of prednisolone or equivalent to that of dexamethasone. In clinical trials on uveitis, a significant increase in IOP occurred in 6% of patients treated with difluprednate, 0.05%, emulsion compared with 5% of those treated with prednisolone acetate, 1%.

[b] IOP effects determined in topical dexamethasone responders.

[c] Rapid metabolism of fluorometholone in the eye compared with dexamethasone.

[d] Relatively poor ocular penetration.

When a steroid-induced pressure rise is suspected but continued steroid therapy is warranted, the physician faces the following choices:

- continue the same treatment and closely monitor the status of the optic nerve
- attempt to offset the pressure rise with other drugs or treatments
- reduce the potency, concentration, or frequency of the steroid used while monitoring both pressure and inflammation
- consider a steroid-sparing alternative

Immunomodulatory therapy (IMT) is an important component in the management of ocular inflammation and avoids the toxicity associated with long-term corticosteroid therapy. IMT drugs are classified as antimetabolites, inhibitors of T-cell signaling, alkylating agents, and biologic response modifiers. Biologic response modifiers inhibit various cytokines and pathways, which are active in inflammation. See Table 16-17 for a summary of this class of medications and also BCSC Section 9, *Uveitis and Ocular Inflammation*.

Jabs DA. Immunosuppression for the uveitides. *Ophthalmology*. 2018;125(2):193–202.

Dick AD, Rosenbaum JT, Al-Dhibi HA, et al; Fundamentals of Care for Uveitis International Consensus Group. Guidance on noncorticosteroid systemic immunomodulatory therapy in noninfectious uveitis: Fundamentals Of Care for UveitiS (FOCUS) initiative. *Ophthalmology*. 2018;125(5):757–773.

Mehta NS, Emami-Naeini P. A review of systemic biologics and local immunosuppressive medications in uveitis. J *Ophthalmic Vis Res*. 2022;17(2):276–289.

Specific drugs and regimens

Appropriate selection from the available corticosteroid drugs, formulations, and dosage regimens are contingent on the clinical situation. Steroids can be administered topically, periocularly, intravitreally, orally, and intravenously (Table 16-18). All corticosteroids may exacerbate infections or lead to ocular adverse effects. Recent research in corticosteroids has focused on medications that can be used intraocularly and periocularly as well as developing drugs with decreased effect on IOP. As a general rule, however, the more potent the steroid, the more prevalent and severe are the adverse events.

Loteprednol etabonate is structurally similar to other steroids but lacks a ketone group at position 20. Loteprednol etabonate, 0.2%, is approved for the temporary treatment of allergic conjunctivitis; the 0.5% strength is indicated in patients with postoperative inflammation and pain. Loteprednol, 0.25%, has been approved for the short-term treatment of dry eye syndrome. The combination drug loteprednol etabonate (0.5%)/tobramycin (0.3%) is approved for use in patients with superficial bacterial infections of the eye with inflammation. Studies have shown that in corticosteroid responders treated with loteprednol, the incidence of clinically significant IOP elevation is low.

Difluprednate is a difluorinated derivative of prednisolone. Its glucocorticoid receptor-binding affinity and corneal penetration are greatly enhanced by modification of the glucocorticoid molecule with the addition of fluorine atoms and ester groups at several carbon positions. Difluprednate is formulated as a stable oil-in-water emulsion to achieve consistent dose uniformity compared with suspensions, regardless of bottle storage position or whether it is shaken before use. Although the strong therapeutic potency of difluprednate emulsion is

Table 16-17 Immunomodulatory Medications in the Treatment of Uveitis

Class	Medication	Mechanism of Action	Dosage	Potential Complications
Conventional immunosuppressive drugs				
Antimetabolites				
	Methotrexate	Folate analogue; inhibits dihydrofolate reductase	Initial dose: 15 mg/wk by mouth, SQ, or IM Maximum dose: 25 mg/kg by mouth, SQ, or IM	Hepatitis, cytopenias, fatigue/malaise, nausea
	Azathioprine	Purine nucleoside analogue, interferes with DNA replication and RNA	Initial dose: 2 mg/kg/d by mouth Maximum dose: 3 mg/kg/d by mouth	Gastrointestinal upset, cytopenias, hepatitis
	Mycophenolate mofetil	Reversible IMPDH inhibitor; inhibits the de novo pathway of guanosine nucleotide synthesis	Initial dose: 1 g twice daily by mouth Maximum dose: 1.5 g twice daily by mouth	Diarrhea, cytopenias, hepatitis
Alkylating agents				
	Cyclophosphamide	Cross-links DNA	Initial dose: 2 mg/kg/d by mouth Maximum dose: 250 mg/d by mouth	Cytopenias, bladder toxicity, alopecia, sterility, teratogenicity, malignancy
	Chlorambucil	Cross-links DNA	Initial dose: 0.1 mg/kg/d by mouth Maximum dose: 0.2 mg/kg/d by mouth	Cytopenias, sterility, teratogenicity, malignancy
T-cell inhibitors				
	Cyclosporine	Calcineurin inhibitor; inhibits T-lymphocyte activation	Microemulsion dose (Neoral): 2.0 mg/kg/d by mouth, then adjusted to 1–5 mg/kg/d Standard preparation (Sandimmune): 2.5–5 mg/kg/d, given twice daily. Maximum dose: 7.0 mg/kg/d	Nephrotoxicity, hypertension, anemia, hirsutism

(Continued)

Table 16-17 *(continued)*

Class	Medication	Mechanism of Action	Dosage	Potential Complications
	Tacrolimus	Calcineurin inhibitor; inhibits T-lymphocyte activation	0.10–0.15 mg/kg/d	Nephrotoxicity, neurotoxicity (tremors)
	Sirolimus	Inhibits T-lymphocyte activation in G1; blunts T- and B-lymphocyte responses to lymphokines	6-mg loading dose, 2-mg maintenance dose; intravitreal dose in phase 3 study for noninfectious uveitis: 440 μg in 20 μL, repeated in 60 d and 120 d	Diabetes-like symptoms, lung toxicity, immunosuppression, malignancy, impaired wound healing
Biologic response modifiers				
TNF inhibitors				
	Infliximab [a]	TNF-α inhibitor	3 mg/kg IV at wk 0, 2, and 4 and then every 4–8 wk	Susceptibility to infection; reactivation of tuberculosis, histoplasmosis, hepatitis B, and fungal infection; hypersensitivity reactions; demyelinating disease; lupuslike syndrome; malignancy; thromboembolic events; congestive heart failure
	Adalimumab [a, b]	TNF-α inhibitor	Initial dose: 80 mg SQ Maintenance dose: 40 mg SQ every other wk	Same as for infliximab
	Golimumab [c]	TNF-α inhibitor	50 mg SQ every 4 wk	Same as for infliximab
	Certolizumab [c,d]	TNF-α inhibitor	200 mg SQ every 2 wk	Same as for infliximab

Class	Medication	Mechanism of Action	Dosage	Potential Complications
Lymphocyte inhibitors				
	Abatacept	Binds to CD80 or CD86 molecule and prevents antigen presentation to T cell for T-cell activation	500–1000 mg IV loading, then 125 mg SQ weekly	Susceptibility to infections, allergic reactions, headache, nausea, malignancy
	Rituximab	Binds to CD20 on B cells, triggering cell death	500–1000 mg IV at wk 0 and 2; may repeat at 6–12 mo thereafter	Susceptibility to infections, infusion reactions, gastrointestinal disturbance, cardiovascular events, muscle spasm, headache
Anti-interleukins				
	Anakinra[e]	IL-1 receptor inhibitor	100 mg SQ daily	Serious infections, hypersensitivity, gastrointestinal symptoms
	Canakinumab[e]	IL-1β antibody	2–4 mg/kg SQ every 4–8 wk Maximum dose: 300 mg	Serious infections, hypersensitivity, immunosupression, gastrointestinal symptoms
	Gevokizumab[f]	IL-1β antibody	60 mg SQ every 4 wk	FDA package insert not available. In small trials, adverse effect profile was similar to placebo
	Tocilizumab	IL-6 receptor inhibitor	8 mg/kg IV every 4 wk	Serious infections, hypersensitivity reactions, gastrointestinal perforation
	Secukinumab	IL-17A antibody	150–300 mg SQ weekly for 5 doses, then every 4 wk 10 mg/kg IV every 2 wk or 30 mg/kg IV every 4 wk	Serious infections, hypersensitivity, gastrointestinal symptoms
	Ustekinumab[g]	IL-12 and IL-23 antibody	Initial dose: ≤55 kg: 260 mg IV 55–85 kg: 390 mg IV >85 kg: 520 mg IV Maintenance dose: 90 mg SQ every 8 wk	Serious infections, hypersensitivity, malignancies, posterior reversible encephalopathy syndrome

(Continued)

Table 16-17 *(continued)*

Class	Medication	Mechanism of Action	Dosage	Potential Complications
Interferons				
	IFN-α2a and -α2b		3.0 MIU up to 9.0 MIU SQ 3 times weekly	Flulike symptoms, depression
	Pegylated IFN-α2b		1.5 μg/kg/wk	Fatigue, headache, rigors, fevers, nausea, myalgia, anxiety, emotional lability, irritability
JAK inhibitors				
	Tofacitinib	JAK inhibitor	5 mg twice daily or 11 mg once daily (XR) by mouth	Serious infections, gastroinestinal perforation, hematopoetic abnormalities, risk of malignancy and lymphoproliferative disorders
	Baricitinib	JAK1 and JAK2 inhbitor	2 mg once daily by mouth	Serious infections, gastroinestinal perforation, hematopoetic abnormalities, thrombosis, risk of malignancy and lymphoproliferative disorders

IFN = interferon; IL = interleukin; IM = intramuscularly; IMPDH = inosine monophosphate dehydrogenase; IV = intravenous; JAK = Janus kinase; MIU = million international units; NF-AT = nuclear factor of activated T-cell lymphocyte; SQ = subcutaneously; TNF = tumor necrosis factor; XR = extended release.

[a] In uveitis, most of the data on biologic agents are related to use of agents directed against TNF-α and involve infliximab and adalimumab.

[b] Adalimumab is FDA-approved for the treatment of uveitis.

[c] Golimumab and certolizumab have limited data regarding their use in treatment of uveitis. Both have been shown to demonstrate efficacy in refractory uveitis, including in patients taking other TNF-α inhibitors.

[d] This agent does not cross the placenta.

[e] These agents were administered together in studies for treatment of uveitis.

[f] This medication is still under investigation and is not yet FDA-approved. Dosing varies per study protocol. Dosing listed was used in a Phase 3 trial.

[g] Dosing based on inflammatory bowel disease regimen. This regimen was also reported in case studies using this medication to treat uveitis in patients already on other immunomodulatory therapy.

Table 16-18 Usual Route of Corticosteroid Administration in Ocular Inflammation

Condition	Route
Blepharitis	Topical
Conjunctivitis	Topical
Endophthalmitis	Periocular, systemic, intravitreal
Keratitis	Topical
Macular edema, cystoid	Topical, periocular, intravitreal injection or implant
Macular edema, diabetic	Periocular, intravitreal
Optic neuritis	Systemic
Scleritis	Topical, periocular, systemic
Scleritis-Epi (episcleritis)	Topical
Sympathetic ophthalmia	Topical, periocular, systemic, intravitreal
Temporal arteritis	Systemic
Uveitis, anterior	Topical, periocular, systemic
Uveitis, posterior	Periocular, systemic, intravitreal injection or implant

desirable, IOP increase has been reported both anecdotally and clinically to be greater than that of other moderate to strong topical steroids.

Rimexolone, 1%, is a synthetic topical steroid designed to minimize IOP elevations, similar to fluorinated steroids. Elevated IOP has been reported with this medication, but it is rare. Ocular adverse effects include secondary glaucoma and posterior subcapsular cataracts. Systemic adverse effects—including headache, hypotension, rhinitis, pharyngitis, and altered taste—occur in fewer than 2% of patients.

Fluocinolone acetonide (FA) is available in 3 intraocular devices (see Table 16-15). A nonbiodegradable 0.59-mg FA implant, surgically placed in the pars plana region, is approved by the FDA for the treatment of chronic noninfectious posterior uveitis. It is designed to release FA at a nominal initial rate of 0.6 μg/day, decreasing over the first month to a steady state between 0.3 and 0.4 μg/d over approximately 30 months. A 0.19-mg nonbiodegradable FA implant, delivered by intravitreal injection, is FDA-approved for the treatment of diabetic macular edema in patients who are not steroid responders. It releases fluocinolone acetonide at an average rate of 0.25 μg/d for 36 months. In 2018, the FDA approved another intravitreal 0.18-mg nonbiodegradable FA implant for the treatment of chronic noninfectious posterior uveitis. It is designed to provide 0.25 μg/d for 36 months.

A 0.7-mg dexamethasone biodegradable polymer matrix for injection into the vitreous cavity is approved for the treatment of macular edema secondary to retinal vein occlusion, noninfectious posterior uveitis, and diabetic macular edema. The polymer dissolves, and dexamethasone is slowly released for up to 6 months, with clinical efficacy lasting at least 3 months.

A 40-mg/mL preservative-free triamcinolone acetonide injectable suspension is approved by the FDA for intraocular use. Its indications include visualization during vitrectomy and treatment of sympathetic ophthalmia, temporal arteritis, uveitis, and ocular inflammatory conditions that do not respond to topical corticosteroids.

Armaly MF. Effect of corticosteroids on intraocular pressure and fluid dynamics, I: the effect of dexamethasone in the normal eye. *Arch Ophthalmol.* 1963;70(4):482–491.
Armaly MF. Effect of corticosteroids on intraocular pressure and fluid dynamics, II: the effect of dexamethasone in the glaucomatous eye. *Arch Ophthalmol.* 1963;70(4):492–499.

Nonsteroidal Anti-inflammatory Drugs

Derivatives

Derivatives of arachidonic acid, a 20-carbon chain essential fatty acid, mediate a wide variety of biological functions, including regulation of smooth muscle tone (in the blood vessels, bronchi, uterus, and gut), platelet aggregation, hormone release (growth hormone, ACTH, insulin, renin, and progesterone), and inflammation. The synthetic cascade that produces a wide variety of arachidonic acid derivatives (depending on the stimulus and tissue) begins with stimulation of phospholipase A_2. Phospholipase A_2 liberates arachidonic acid from phospholipids of the cell membrane and is a target of steroid therapy (Fig 16-6).

Arachidonic acid is then converted either into hydroperoxides by lipoxygenase or into cyclic endoperoxides by cyclooxygenase (COX, also called *prostaglandin-endoperoxide synthase*). The hydroperoxides form a chemotactic agent and the leukotrienes C_4, D_4, and E_4, a series of compounds previously known as the slow-reacting substance of anaphylaxis. Like oral antihistamines, oral leukotriene inhibitors are used in the management of seasonal allergies.

Subsequent products of endoperoxides include the PGs, which mediate inflammation and other responses; prostacyclin, a vasodilator and platelet antiaggregant; and thromboxane, a vasoconstrictor and platelet aggregant. PGs have profound effects on inflammation in the eye, aqueous humor dynamics, and blood–ocular barrier functions. When administered intracamerally or topically at high concentrations, arachidonic acid and PGs of the E and F subtypes cause miosis, an elevation of IOP, an increase in aqueous protein content, and the entry of white cells into the aqueous and tear fluid.

COX has 2 isoforms (ie, COX-2 and COX-1):

- COX-2 is the relevant enzyme in inflammation (it is expressed at low levels under normal physiologic conditions and is regulated only in response to pro-inflammatory signals).
- Constitutively expressed COX-1 (but not COX-2) is present in various tissues (including the inner lining of the stomach).

Previously developed NSAIDs (eg, ibuprofen, naproxen) inhibit both COX-1 and COX-2 and compete with arachidonate in binding to the COX active site. Although these compounds are effective anti-inflammatory drugs, all of them can produce gastric ulcers when administered systemically. In contrast, COX-2 inhibitors, which are still anti-inflammatory and analgesic, lack gastrointestinal toxicity. Moreover, they provide time-dependent, reversible inhibition of the COX-2 enzyme. However, oral COX-2 inhibitors, including rofecoxib, celecoxib, and valdecoxib, increase risks of cardiovascular toxicity and complications (eg, myocardial infarction).

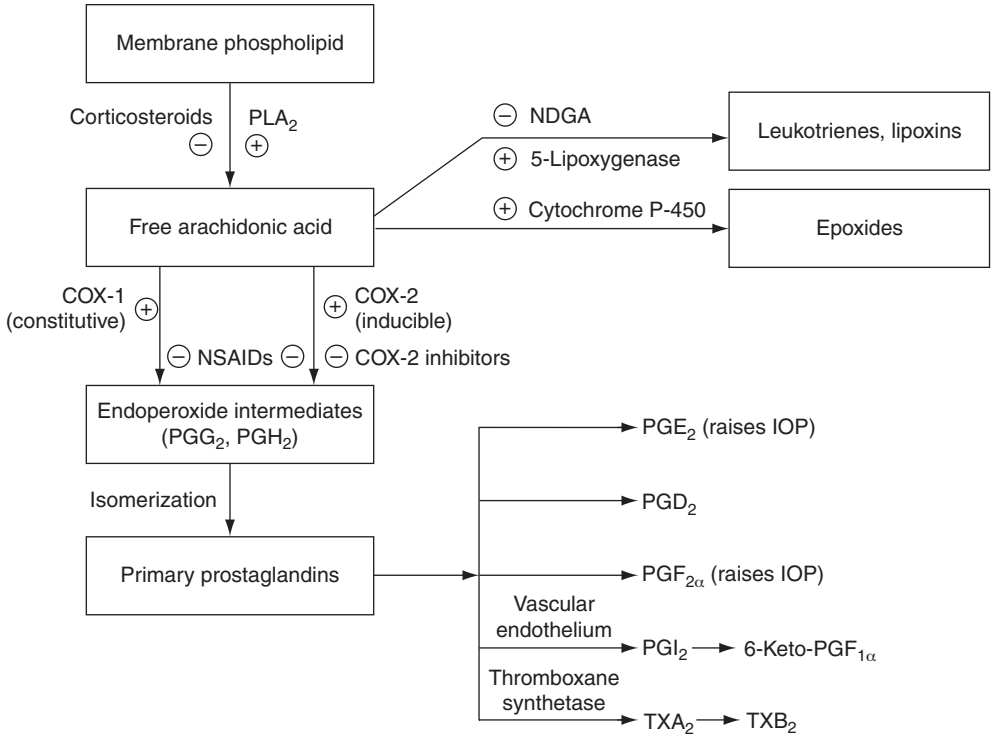


Figure 16-6 An outline of the synthesis of prostaglandins (PGs) and leukotrienes from arachidonic acid. In response to stimulation of a target cell with a relevant stimulus (eg, a cytokine, a neurotransmitter, various pharmacologic agents), phospholipase A_2 (PLA_2) is activated, and arachidonic acid is released from the sn-2 position of membrane phospholipids. Arachidonic acid is then converted by cyclooxygenase-1 (COX-1) or cyclooxygenase-2 (COX-2) to prostaglandin H_2 (PGH_2), and then PGH_2 is isomerized to biologically active prostanoid products. Arachidonic acid can also be metabolized through the 5-lipoxygenase and cytochrome P-450 pathways to generate leukotrienes and epoxides, respectively. PLA_2 can be inhibited by corticosteroids such as dexamethasone; COX-1, by nonsteroidal anti-inflammatory drugs (NSAIDs) such as indomethacin and aspirin; COX-2, by DUP697, SC58125, L-745-337, and NS398; and the 5-lipoxygenase pathway, by nordihydroguaiaretic acid (NDGA). IOP = intraocular pressure; PGD_2 = prostaglandin D_2; PGE_2 = prostaglandin E_2; $PGF_{1\alpha}$ = prostaglandin $F_{1\alpha}$; $PGF_{2\alpha}$ = prostaglandin $F_{2\alpha}$; PGG_2 = prostaglandin G_2; PGI_2 = prostaglandin I_2; TXA_2 = thromboxane A_2; TXB_2 = thromboxane B_2. *(Courtesy of Ata Abdel-Latif, PhD.)*

Specific drugs

Table 16-19 lists several NSAIDs along with their initial adult oral dosages. Table 16-20 lists the relative analgesic efficacy of selected NSAIDs. Aspirin and other NSAIDs inhibit the local signs of inflammation (heat, vasodilation, edema, swelling), as well as pain and fever. However, they have complex effects on clotting. At low doses (300 mg every other day), aspirin permanently inhibits the COX in platelets, which is essential for the conversion of arachidonic acid to prostaglandin G_2 and thromboxane. Inhibition of thromboxane production, in turn, prevents coagulation. Although nucleated cells can replenish their COX, anucleate platelets cannot. After aspirin is stopped, COX activity recovers by 10% per day in parallel with platelet

Table 16-19 Nonsteroidal Anti-inflammatory Drugs (Systemic)

Drug (Generic Name)	Trade Name	Starting Oral Dosage (Adult)
Aspirin	Ascriptin, Ecotrin	650 mg, 4 times daily
Celecoxib	Celebrex	100 mg, 2 times daily
Diclofenac	Cataflam, Voltaren-XR	50 mg, 3 times daily
Diflunisal	Dolobid	500 mg, 2 times daily
Etodolac	Lodine	300 mg, 2 times daily
Fenoprofen	Nalfon	200 mg, 4 times daily
Flurbiprofen	Ansaid	300 mg, 3 times daily
Ibuprofen	Advil, Motrin	400 mg, 4 times daily
Indomethacin	Indocin	25 mg, 3 times daily
Ketoprofen	Orudis	75 mg, 3 times daily
Ketorolac	Toradol	10 mg, 4 times daily
Meloxicam	Mobic	7.5 mg, 4 times daily
Nabumetone	Relafen	1000 mg, 4 times daily
Naproxen	Aleve, Aflaxen	250 mg, 2 times daily
Oxaprozin	Daypro	1200 mg, 4 times daily
Piroxicam	Feldene	20 mg, 4 times daily
Sulindac	Clinoril, Sulin	150 mg, 2 times daily
Tolmetin	Tolectin	400 mg, 3 times daily

Table 16-20 Relative Analgesic Efficacy for Selected NSAIDs

Drug (Generic Name)	Numbers Needed to Treat[a]
Aspirin, 650 mg	4.4
Celecoxib, 200 mg	3.5
Naproxen, 200 mg	3.4
Piroxicam, 20 mg	2.7
Ibuprofen, 200 mg	2.7
Ketorolac, 10 mg	2.6
Diclofenac, 25 mg	2.6

[a] Numbers needed to treat are calculated for the proportion of patients with at least 50% pain relief over 4–6 hours compared with placebo in randomized, double-blind, single-dose studies in patients with moderate to severe pain.

Excerpted with permission from the Oxford League Table of Analgesic Efficacy. Bandolier website. Accessed January 26, 2023. www.bandolier.org.uk/booth/painpag/Acutrev/Analgesics/lftab.html

turnover. The anticoagulant effect of aspirin therefore lasts for at least 48–72 hours despite discontinuation of aspirin therapy. Other NSAIDs inhibit clotting in a reversible fashion, and their use does not need to be discontinued so far in advance of elective surgery.

When used during febrile viral infections in children, aspirin has been associated with Reye syndrome, although no causal link has been proven. The National Reye's Syndrome Foundation, the US Surgeon General, the FDA, the Centers for Disease Control and Prevention, and the American Academy of Pediatrics recommend that aspirin and combination products containing aspirin not be taken by anyone younger than 19 years during episodes of fever-causing

or viral illnesses. The British Medicines and Healthcare Products Regulatory Agency recommends that aspirin labels state that the drug is not intended for use in children younger than 16 years unless recommended by a physician. Other NSAIDs are effective antipyretics and are not associated with the constellation of symptoms observed in Reye syndrome.

The relative risks and benefits of aspirin therapy should be assessed for each patient. Aspirin therapy for postoperative pain or for pain associated with traumatic hyphema may increase the risk of hemorrhage because of aspirin's antiaggregant effect on platelets. The same side effect may benefit patients with platelet emboli, as in some cases of amaurosis fugax. Diversion of arachidonic acid to the lipoxygenase pathway by inhibition of COX may explain why aspirin is associated with asthma attacks and hypersensitivity reactions (mediated by the leukotrienes C_4, D_4, and E_4) in susceptible people. Systemic acidosis associated with concomitant use of CAIs may shift a higher proportion of aspirin molecules into the more lipid-soluble nonionized form, which penetrates the blood–brain barrier more readily and potentiates CNS toxicity from aspirin. Aspirin and other COX inhibitors are less effective than steroids in the treatment of scleritis and uveitis.

NSAIDs such as indomethacin can be effective for orbital inflammatory diseases. The prophylactic use of indomethacin in patients undergoing cataract surgery has reduced the incidence of angiographically detected CME, but its effect on visually significant CME has yet to be determined. Flurbiprofen sodium, 0.03% (generic available), was the first commercially available topical ocular NSAID. When applied preoperatively, it reduces PG-mediated intraoperative miosis.

In addition to treating ocular inflammation, topical NSAIDs as a class have been reported to prevent and treat CME related to cataract surgery. Topical diclofenac sodium, 0.1% (generic available), is approved by the FDA for treatment of inflammation and pain following cataract surgery, and ketorolac tromethamine (0.4%, 0.45%, and 0.5%) has been approved to treat postoperative pain and irritation. Additional topical NSAIDs with various dosages have been approved by the FDA for the treatment of inflammation and reduction of pain after cataract extraction, with dosing initiated 1 day before surgery and continued through the first 2 weeks postoperatively. These agents include nepafenac, 0.1%, 3 times daily, and 0.3%, once daily; and bromfenac sodium, 0.09%, once daily or twice daily, and 0.07%, once daily (see Table 16-14).

NSAIDs have been associated with corneal complications, including melting and corneal perforation. These complications have been observed both in postoperative patients and in cases of uveitis, usually in patients with preexisting diabetes and ocular surface disorders.

Congdon NG, Schein OD, von Kulajta P, Lubomski LH, Gilbert D, Katz J. Corneal complications associated with topical ophthalmic use of nonsteroidal anti-inflammatory drugs. *J Cataract Refract Surg.* 2001;27(4):622–631.

Flach AJ. Corneal melts associated with topically applied nonsteroidal anti-inflammatory drugs. *Trans Am Ophthalmol Soc.* 2001;99:205–210.

Kim SJ, Flach AJ, Jampol LM. Nonsteroidal anti-inflammatory drugs in ophthalmology. *Surv Ophthalmol.* 2010;55(2):108–133.

Antiallergic Drugs: Mast-Cell Stabilizers and Antihistamines

The human eye has approximately 50 million mast cells. Each cell contains several hundred granules that in turn contain preformed chemical mediators. Allergic conjunctivitis is an immediate hypersensitivity reaction in which triggering antigens couple to antibodies (IgE) on the cell surface of mast cells and basophils, causing the release of histamine, PG, leukotrienes, and chemotactic factors from secretory granules. The released histamine causes capillary dilatation and increased permeability and, therefore, conjunctival injection and swelling. It also stimulates nerve endings, causing pain and itching.

Drugs treat ocular allergies by interfering at different points along this pathway. Corticosteroids are very effective, but associated adverse effects limit their application for this chronic condition. Mast-cell stabilizers and antihistamines (which block histamine receptor-1 [H_1]) are associated with fewer and less dangerous adverse effects and can be used singly or in combination. Table 16-21 lists drugs that relieve allergic conjunctivitis.

Table 16-21 Drugs for Allergic Conjunctivitis

Generic Name	Trade Name	Class
Alcaftadine	Lastacaft	H_1-antagonist/mast-cell stabilizer
Azelastine HCl	Optivar, also available generically	H_1-antagonist/mast-cell stabilizer
Bepotastine besilate	Bepreve	H_1-antagonist/mast-cell stabilizer
Cetirizine	Zerviate	H_1-antagonist
Cromolyn sodium	Crolom, also available generically	Mast-cell stabilizer
Emedastine difumarate	Emadine	H_1-antagonist
Epinastine HCl	Elestat, also available generically	H_1-antagonist/mast-cell stabilizer
Ketotifen fumarate	Zaditor (OTC), Alaway (OTC), also available generically	H_1-antagonist/mast-cell stabilizer
Levocabastine HCl	Discontinued in the United States	H_1-antagonist
Lodoxamide tromethamine	Alomide	Mast-cell stabilizer
Loteprednol etabonate	Alrex	Corticosteroid
Naphazoline HCl	Ak-Con, Albalon, also available generically	Decongestant
Naphazoline HCl/antazoline phosphate	Vasocon-A (OTC)	Antihistamine/decongestant
Naphazoline HCl/pheniramine maleate	Naphcon-A (OTC), Opcon-A (OTC), Visine-A (OTC)	Antihistamine/decongestant
Nedocromil sodium	Alocril	Mast-cell stabilizer
Olopatadine HCl	Pataday 0.1%, 0.2%, 0.7% (OTC)	H_1-antagonist/mast-cell stabilizer
Pemirolast potassium	Alamast	Mast-cell stabilizer

OTC = over-the-counter.

Corticosteroids

Corticosteroids are very effective for treating ocular allergies, especially in the acute phase, but they are prone to overuse and have a more dangerous adverse effect profile than other antiallergic drugs (see the section "Adverse effects" under Glucocorticoids). Loteprednol etabonate, 0.2%, a steroid designed to cause less IOP elevation, can be used for temporary treatment of ocular allergies. Recalcitrant cases of severe allergic, vernal, and atopic conjunctivitis may require the short-term use of stronger topical steroids, but these cases should be carefully monitored and patients switched to an antihistamine and/or a mast-cell stabilizer as soon as clinically prudent.

Antihistamines

Patients may achieve short-term relief of mild allergic symptoms with over-the-counter topical antihistamines such as antazoline and pheniramine, which are usually combined with the decongestant naphazoline. Specific H_1-antagonists include emedastine, levocabastine, and cetirizine.

Emedastine difumarate, 0.05%, is a relatively selective H_1-receptor antagonist indicated for temporary relief of signs and symptoms of allergic conjunctivitis. Dosing is 1 drop up to 4 times daily. The most common adverse effect reported is headache (11% of patients). Other adverse effects are altered taste, blurred vision, burning or stinging, corneal infiltrates, dry eye syndrome, rhinitis, and sinusitis.

Levocabastine hydrochloride, another H_1-receptor antagonist, has an onset of action in minutes and lasts for at least 4 hours. It is as effective as cromolyn sodium for treating allergic conjunctivitis. The usual dosage of levocabastine, 0.05%, is 1 drop 4 times daily for up to 2 weeks. This drug has been discontinued in the United States.

Cetirizine, 0.24%, is also a selective H_1-receptor antagonist. It has similar onset within minutes of application; however, it is dosed twice daily and lasts 8 hours. Adverse reactions occurred in less than 10% of study patients and included red eye, pain, and blurred vision.

> **CLINICAL PEARL**
>
> Systemic use of antihistamines for allergies may cause dry eye syndrome and dry mouth and can lead to pupillary dilation in patients due to their anticholinergic effects.

Mast-cell stabilizers

Mast-cell stabilizers are thought to prevent calcium influx across mast-cell membranes, thereby preventing mast-cell degranulation and mediator release. Traditional mast-cell stabilizers such as cromolyn sodium, lodoxamide, and pemirolast prevent mast-cell degranulation but take days to weeks to reach peak efficacy. They have little or no antihistamine effect and do not provide immediate relief from allergic symptoms. Therefore, topical steroids or H_1-antagonists may have to be used concurrently with mast-cell stabilizers for the first several weeks, until these drugs are fully effective.

Lodoxamide stabilizes the mast-cell membrane 2500 times more effectively than does cromolyn sodium. In the treatment of allergic conjunctivitis, its onset of action is also more

rapid, with less stinging, when compared to that of cromolyn sodium. In addition, a multicenter double-blind study showed that lodoxamide was superior to cromolyn sodium in treating vernal keratoconjunctivitis. The usual dose of lodoxamide, 0.1%, for adults and children older than 2 years is 1 drop in the affected eye 4 times daily for up to 3 months. The most frequently reported adverse reactions are burning, stinging, and discomfort upon instillation (15% of patients).

Combined antihistamine and mast-cell stabilizers

Some drugs, including olopatadine, ketotifen, epinastine, azelastine, and alcaftadine, have a mast cell–stabilizing effect as well as H_1-antagonism. These drugs provide immediate relief against released histamine and prevent the future degranulation of mast cells. Olopatadine hydrochloride, 0.1%, has a rapid onset, and its duration of action is at least 8 hours. Recommended dosing is 1 drop in the affected eye 2 times daily at an interval of 6–8 hours. This drug is now also available for once-a-day dosing as olopatadine, 0.2% or 0.7%. Adverse reactions including ocular burning, stinging, dry eye syndrome, foreign-body sensation, hyperemia, keratitis, eyelid edema, pruritus, asthenia, cold syndrome, pharyngitis, rhinitis, sinusitis, and taste disturbance were all reported at an incidence of less than 5% (for each adverse effect). For ketotifen fumarate, 0.025%, the recommended dosing is 1 drop every 8–12 hours. Conjunctival injection, headaches, and rhinitis were reported at an incidence of 10%–25%.

Abelson MB, Shetty S, Korchak M, Butrus SI, Smith LM. Advances in pharmacotherapy for allergic conjunctivitis. *Expert Opin Pharmacother*. 2015;16(8):1219–1231.

La Rosa M, Lionetti E, Reibaldi M, et al. Allergic conjunctivitis: a comprehensive review of the literature. *Ital J Pediatr.* 2013;39:18.

Antifibrotic Drugs

Antiproliferative medications, also known as *antimetabolites,* are used to treat severe ocular inflammatory diseases. They can also be used locally as antiproliferative agents in patients with ocular surface neoplasia and as antifibrotic agents to limit scarring related to ophthalmic procedures, particularly of the ocular surface, as in glaucoma filtering procedures and pterygium surgery. Additional applications include alleviation of recalcitrant scarring of the ocular adnexa and increasing the success rate of dacryocystorhinostomies. Use of 5-fluorouracil (5-FU) and mitomycin C (MMC) for these purposes, though common, is considered off-label.

Fluorouracil is a fluorinated pyrimidine nucleoside analogue that blocks production of thymidylate synthase and interrupts normal cellular DNA and RNA synthesis. Its primary action may be to cause cellular thymine deficiency and resultant cell death. The effect of 5-FU is most pronounced on rapidly growing cells, and its use as an antiviral drug is related primarily to the destruction of infected cells (eg, warts) by topical application. This drug is also thought to inhibit cellular proliferation that may otherwise occur in response to inflammation.

In a study involving high-risk patients, including young patients (≤40 years of age) with glaucoma, the success rate for initial trabeculectomy with adjunctive 5-FU was higher than the rate with surgery without the adjunct. 5-FU was used postoperatively as a subconjunctival injection and intraoperatively as a topical application to the trabeculectomy site.

MMC, another antiproliferative compound, is isolated from the fungus *Streptomyces caespitosus.* The parent compound becomes a bifunctional alkylating agent after enzymatic

alteration within the cell; it then inhibits DNA synthesis by DNA cross-linkage. Although mitomycin's immunosuppressive properties are fairly weak, it is a potent inhibitor of fibroblast proliferation. During glaucoma filtering operations, MMC is used topically in a single application to impede scarring and prevent surgical failure (see BCSC Section 10, *Glaucoma*). Complications associated with this therapy include wound leakage, hypotony, and localized scleral melting. In an animal model, severe toxicity was reported with intraocular instillation of MMC, resulting in irreversible progressive bullous keratopathy.

Both MMC and 5-FU are used to treat ocular surface tumors. For example, both are used to treat ocular surface squamous neoplasia; MMC is also effective when used to treat ocular surface melanomas. The recommended dosage for 5-FU is 1%, 4 times daily; for MMC it is 0.02%–0.04%, 4 times daily. MMC is also commonly used to reduce haze in patients undergoing phototherapeutic keratectomy and has been recommended both as single-dose topical therapy and as postoperative eyedrops to prevent recurrence of pterygia after pterygium excision. The reported recurrence rate with this therapy has been as low as 0%–11%. However, MMC is more toxic in comparison to 5-FU. Several adverse effects, such as corneal edema, corneal and scleral perforation, corectopia, anterior uveitis, cataract, and intractable pain, have been reported with MMC. For additional information on uses of MMC and 5-FU, see BCSC Section 8, *External Disease and Cornea*.

Medications for Dry Eye Syndrome

Artificial tear preparations (demulcents and emollients) form an occlusive film over the corneal surface to lubricate and protect the eye from drying. The active ingredients in demulcent preparations are polyvinyl alcohol, cellulose, and methylcellulose as well as their derivatives: hydroxypropyl cellulose, hydroxyethylcellulose, hydroxypropyl methylcellulose, and carboxymethylcellulose. Other ingredients used include glycerin, polysorbate 80, polyethylene glycol 400, dextran 70, povidone, and propylene glycol.

The viscosity of artificial tears varies in part because of the concentration of the wetting agent. For example, carboxymethylcellulose is available in 0.25%, 0.5%, and 1% solutions; higher-viscosity solutions are used to treat increasingly severe dry eye symptoms.

Ocular emollients are ointments prepared with sterile petrolatum, liquid lanolin, mineral oil, methylparaben, and polyparaben. Ophthalmic lubricating ointments help ease the symptoms of dry eye syndrome and exposure keratopathy and are suitable for nighttime use in patients with dry eye and nocturnal lagophthalmos.

Some data support the hypothesis that changes in tear osmolality trigger corneal and conjunctival epithelial damage and initiation of dry eye syndrome. Artificial tear products with lower osmolality may relieve dry eye symptoms to a greater extent, but clinical results thus far have not been conclusive.

The pH of commercially available artificial tear products also varies widely. A patient may experience a stinging sensation after eyedrop use because of a mismatch between the pH of the instilled eyedrops and that of the patient's own tear film. Patients who report a stinging sensation following eyedrop use can try another product with a different pH.

Multidose preparations also contain preservatives, including benzalkonium chloride, EDTA (ethylenediaminetetraacetic acid), methylparaben, polyquad (polyquaternium 1),

potassium sorbate, propylparaben, sodium chlorite, sodium perborate, and sorbic acid. Newer preservatives, including SofZia, an ionic-buffered preservative, and Purite, a preservative that breaks down upon contact with the air, can oxidize microbial cellular components but have no significant effect on human cells and are thus less toxic to the ocular surface. Nonpreserved unit-dose preparations eliminate the cytotoxic effects of preservatives.

Topical cyclosporine emulsion, originally only in a formulation of 0.05%, targets the inflammatory etiology of dry eye syndrome. Because cyclosporine is poorly water soluble, it is prepared in an emulsion composed of glycerin, castor oil, and polysorbate 80. It is available in a multidose bottle and a preservative-free single-use package. The oily vector is marketed separately as a tear supplement. Studies have shown that twice-daily dosing with this drug has negligible systemic absorption and adverse effects. Biopsies have demonstrated a measurable repopulation of goblet cells and a decrease in both conjunctival epithelial cell turnover and the number of lymphocytes. Cyclosporine emulsions in formulations of 0.09% and 0.1% have recently become available.

Lifitegrast, 5%, preservative-free topical solution, is a lymphocyte function–associated antigen 1 (LFA-1) antagonist administered twice daily. It inhibits binding of intercellular adhesion molecule-1 (ICAM-1) to LFA-1 and has been effective in reducing ocular surface inflammation and symptoms of dry eye syndrome.

Some principles can help guide the selection of artificial tear preparation for a particular patient from among the wide variety of commercially available products. Generally, the viscosity of the tear lubricant increases as the severity of the dry eye increases. A trial-and-error approach that involves titration of the frequency of instillation according to the patient's daily activities, the use of tear substitutes with different mechanisms of action or properties, and even a combination of different lubricants may be necessary. Preservative-free products should be utilized if frequent instillation is required, such as in cases of severe dry eye syndrome. Nonpreserved preparations are at risk of microbial contamination.

For the treatment of ocular surface diseases such as persistent epithelial defects, superior limbic keratoconjunctivitis, keratoconjunctivitis sicca, and neurotrophic keratopathy, autologous serum eyedrops are beneficial. They are formulated by compounding a 20%–80% solution packaged into sterile dropper bottles. Reported complications include peripheral corneal infiltrate and ulcer, eyelid eczema, microbial keratitis, ocular discomfort or epitheliopathy, bacterial conjunctivitis, scleral vasculitis and melting in patients with rheumatoid arthritis, and immune complex deposition with 100% serum.

Topical N-acetylcysteine, 10% (trade name Mucomyst), which can be made by a compounding pharmacy for ophthalmic use, can help to dissolve cornea-bound mucus. This agent can be helpful in treating patients with filamentary keratitis.

Varenicline, 0.03 mg, nasal spray, which was approved by the FDA in 2021, is a highly selective nicotinic acetylcholine receptor agonist that stimulates the nasolacrimal reflex pathway by binding to receptors of the ethmoid branch of the trigeminal nerve found within the nasal mucosa. This medication has been shown to increase basal tear production in patients with dry eye syndrome.

Two dry eye products currently under investigation are diquafosol tetrasodium and rebamipide. Diquafosol tetrasodium is a $P2Y_2$ purinergic receptor agonist that activates $P2Y_2$ receptors on the ocular surface, causing rehydration through activation of the fluid pump

mechanism of the accessory lacrimal glands on the conjunctival surface. It was approved for use in Japan in 2010 for treating dry eye syndrome. Rebamipide is a derivative of quinolone-class antibiotics that enhances the secretion of mucin to support tear film adhesion and slow tear film breakup time (also see BCSC Section 8, *External Disease and Cornea*).

Tong L, Petznick A, Lee S, Tan J. Choice of artificial tear formulation for patients with dry eye: where do we start? *Cornea*. 2012;31(suppl 1):S32–S36.

Ocular Decongestants

Common drugs such as naphazoline, oxymetazoline, tetrahydrozoline, and phenylephrine hydrochloride are used as topical drops to cause temporary vasoconstriction of conjunctival vessels. This effect is mediated by α_1-receptors. Other than providing temporal relief of hyperemia, they have no clear therapeutic benefit. Possible adverse effects include rebound vasodilation and conjunctival injection. The mechanisms of the adverse effects are unclear; possibilities include preservative toxicity and receptor desensitization and damage to the ocular surface as a result of vasoconstriction of arteries, which may involve activation of α_2-receptors. These medications can be abused by patients and may cause ocular surface toxicity. Systemic absorption of ocular adrenergic drugs is frequently sufficient to cause systemic effects, which are manifested in the cardiovascular system, the bronchial airways, and the brain (see the earlier section Adrenergic Drugs).

Although ocular decongestants are available as over-the-counter preparations, patients should be instructed not to use them on a long-term basis. Further, all efforts should be made to determine the etiology of the patient's hyperemia and to target the source before use of these medications is considered.

CLINICAL PEARL

Patients predisposed to angle closure should be cautioned on the use of topical decongestants as these drugs may lead to mydriasis and precipitate acute angle-closure glaucoma.

Antimicrobial Drugs

Penicillins and Cephalosporins

The penicillins and cephalosporins are β-lactam–containing antibacterial drugs that react with and inactivate a particular bacterial transpeptidase that is essential for bacterial cell-wall synthesis (Table 16-22). Some bacteria are resistant to the action of penicillins and cephalosporins. The lipopolysaccharide outer coat of many gram-negative bacteria may prevent certain hydrophilic antibiotics from reaching their cytoplasmic membrane sites of action. Furthermore, some bacteria produce β-lactamases (penicillinase), enzymes capable of cleaving the critical amide bond within these antibiotics. The different penicillins and cephalosporins vary in susceptibility to the β-lactamases produced by different bacterial species.

Table 16-22 Principal Antibiotics and Their Administration [a]

Drug Name	Topical	Subconjunctival	Intravitreal	Intravenous (Adult)
Amikacin sulfate	10 mg/mL	25 mg	400 μg	15 mg/kg daily in 2 or 3 doses
Ampicillin sodium	50 mg/mL	50–150 mg	500 μg	4–12 g daily in 4 doses
Bacitracin zinc	10,000 units/mL	5000 units	NA	NA
Carbenicillin disodium	4–6 mg/mL	100 mg	250–2000 μg	8–24 g daily in 4–6 doses
Cefazolin sodium	50 mg/mL	100 mg	2250 μg	2–4 g daily in 3 or 4 doses
Ceftazidime	50 mg/mL	200 mg	2000 μg	1 g daily in 2 or 3 doses
Ceftriaxone sodium	50 mg/mL	125 mg	2000 μg	1–2 g daily
Clindamycin	50 mg/mL	15–50 mg	1000 μg	900–1800 mg daily in 2 doses
Colistimethate sodium	10 mg/mL	15–25 mg	100 μg	2.5–5.0 mg/kg daily in 2–4 doses
Erythromycin	50 mg/mL	100 mg	500 μg	NA
Gentamicin sulfate	8–15 mg/mL	10–20 mg	100–200 μg	3–5 mg/kg daily in 2 or 3 doses
Imipenem/cilastatin sodium	5 mg/mL	NA	NA	2 g daily in 3 or 4 doses
Kanamycin sulfate	30–50 mg/mL	30 mg	500 μg	15 mg/kg daily in 2 or 3 doses
Methicillin sodium	50 mg/mL	50–100 mg	1000–2000 μg	6–10 g daily in 4 doses
Neomycin sulfate	5–8 mg/mL	125–250 mg	NA	NA
Penicillin G	100,000 units/mL	0.5–1.0 million units	300 units	12–24 million units daily in 4 doses
Polymyxin B sulfate	10,000 units/mL	100,000 units	NA	NA
Ticarcillin disodium	6 mg/mL	100 mg	NA	200–300 mg/kg daily
Tobramycin sulfate	8–15 mg/mL	10–20 mg	100–200 μg	3–5 mg/kg daily in 2 or 3 doses
Vancomycin HCl	10–50 mg/mL	25 mg	1000 μg	500 mg every 6 h or 1 g every 12 h

NA = not applicable.

[a] Most penicillins and cephalosporins are physically incompatible when combined with aminoglycosides in the same bottle or syringe.

The penicillins and cephalosporins penetrate the blood–ocular and blood–brain barriers poorly and are actively transported out of the eye by the organic-acid transport system of the ciliary body. However, their penetration into the eye increases with inflammation and with coadministration of probenecid.

Serious and occasionally fatal hypersensitivity (anaphylactoid) reactions can occur in association with penicillin and cephalosporin therapy. A history of immediate allergic response (anaphylaxis or rapid onset of hives) to any penicillin is a strong contraindication to the use of any other penicillin. Approximately 10% of people who are allergic to a penicillin will have cross-reactivity to cephalosporins.

Kelkar PS, Li JT. Cephalosporin allergy. *N Engl J Med.* 2001;345(11):804–809.

Penicillins

Penicillins are divided into 5 classes, which differ in their spectrum of antibiotic activity and in their resistance to penicillinase:

1. Penicillin G, penicillin V, and phenethicillin are highly effective against most gram-positive and gram-negative cocci; many anaerobes; and *Listeria, Actinomyces, Leptospira,* and *Treponema* organisms. However, most strains of *Staphylococcus aureus* and many strains of *Staphylococcus epidermidis,* anaerobes, and *Neisseria gonorrhoeae* are now resistant, often through production of penicillinase. Resistance by enterococci often arises from altered penicillin-binding proteins. Penicillin V and phenethicillin are absorbed well orally, whereas penicillin G is inactivated by stomach acid and is thus better absorbed when administered intravenously. These penicillins are excreted rapidly by the kidneys and have short half-lives unless they are given in depot form (ie, procaine penicillin G) or administered with probenecid, which competitively inhibits excretion by the kidneys.
2. The penicillinase-resistant penicillins include methicillin sodium, nafcillin, oxacillin sodium, cloxacillin sodium, dicloxacillin sodium, and floxacillin. They are less potent than penicillin G against susceptible organisms but are the drugs of choice for infections that are caused by penicillinase-producing *S aureus* and that are not methicillin resistant. Methicillin and nafcillin are acid labile; therefore, they are administered either parenterally or by subconjunctival injection. The other medications in this group have reasonable oral absorption. When they are given systemically, coadministration of probenecid reduces renal excretion and outward transport from the eye.
3. The broad-spectrum penicillins such as ampicillin, amoxicillin, and bacampicillin hydrochloride have antibacterial activity that extends to such gram-negative organisms as *Haemophilus influenzae, Escherichia coli, Salmonella* and *Shigella* species, and *Proteus mirabilis.* Resistant strains of *H influenzae* are common. These drugs are stable in acid and may be given orally. They are not resistant to penicillinase or to the broader-spectrum β-lactamases that are increasingly common among gram-negative bacteria.
4. Carbenicillin and ticarcillin have antimicrobial activity that extends to *Pseudomonas* and *Enterobacter* species and indole-positive strains of *Proteus.* These drugs are given parenterally or subconjunctivally, although the indanyl ester of carbenicillin may be given orally. They are not resistant to penicillinase and are less active against gram-positive bacteria and *Listeria* species.
5. Piperacillin sodium, mezlocillin sodium, and azlocillin are particularly potent against *Pseudomonas* and *Klebsiella* species and retain strong gram-positive coverage and activity against *Listeria* species. They are administered parenterally or subconjunctivally, and they are not resistant to penicillinase.

Cephalosporins

Bacterial susceptibility patterns and resistance to β-lactamases dictate the classification of the cephalosporins as first, second, third, fourth, or fifth generation, although sixth-generation drugs are under development.

1. *First generation.* Cephalothin, cefazolin, cephalexin, cefadroxil, and cephradine have strong antimicrobial activity against gram-positive organisms, especially *Streptococcus* species and *S aureus.* They retain moderate activity against gram-negative organisms. Of these drugs, cephalothin is the most resistant to staphylococcal β-lactamase and is used in severe staphylococcal infections. Because cephalothin is painful when given intramuscularly, it is used only intravenously. In contrast, cefazolin is more sensitive to β-lactamase but has somewhat greater activity against *Klebsiella* species and *E coli.* Cefazolin also has a longer half-life and is tolerated both intramuscularly and intravenously; thus, it is used more frequently than the other first-generation cephalosporins. Cephalexin, cefadroxil, and cephradine are stable in gastric acid and are available in oral forms.
2. *Second generation.* These medications were developed to expand activity against gram-negative organisms while retaining much of their gram-positive spectrum of activity. Compared with first-generation medications, cefamandole, cefoxitin, and cefuroxime display greater activity against *H influenzae, Enterobacter aerogenes,* and *Neisseria* species. Cefamandole has increased activity against *Enterobacter* and indole-positive *Proteus* species, *H influenzae,* and *Bacteroides* species. Cefoxitin is active against indole-positive *Proteus* and *Serratia* organisms, as well as against *Bacteroides fragilis.* Cefuroxime is valuable in the treatment of penicillinase-producing *N gonorrhoeae* and ampicillin-resistant *H influenzae,* and its penetration of the blood–brain barrier is adequate for initial treatment of suspected pneumococcal, meningococcal, or *H influenzae* meningitis.
3. *Third generation.* The third-generation cephalosporins have further enhanced activity against gram-negative bacilli, specifically the β-lactamase–producing members of the Enterobacteriaceae family, but they are inferior to first-generation cephalosporins with regard to their activity against gram-positive cocci. Commonly used drugs include cefotaxime, cefoperazone sodium, ceftriaxone sodium, ceftazidime, and ceftizoxime sodium. These drugs have a similar spectrum of activity against gram-positive and gram-negative organisms; anaerobes; *Neisseria, Serratia,* and *Proteus* species; and some *Pseudomonas* isolates. Cefoperazone and ceftazidime are particularly effective against *Pseudomonas* but lose more coverage of the gram-positive cocci. Cefotaxime penetrates the blood–brain barrier better than do the other cephalosporins, and it presumably also penetrates the blood–ocular barrier.
4. *Fourth generation.* Cefepime hydrochloride and cefpirome have a spectrum of gram-negative coverage similar to that of the third-generation cephalosporins, but these drugs are more resistant to some β-lactamases.
5. *Fifth generation*. Ceftaroline and ceftobiprole (not available in the United States) are fifth-generation drugs. Ceftraloine has similar coverage as ceftriaxone, with increased activity against gram-negative species, excepting *Pseudomonas aeruginosa*. In addition, it has coverage against methicillin-resistant *S aureus* (MRSA) and vancomycin-intermediate *S aureus* (VISA).

No cephalosporin, alone, provides coverage for enterococci, *Listeria* and *Legionella* species. Combination therapy with ampicillin and ceftriaxone has demonstrated efficacy in treating some enterococcal infections.

Other Antibacterial Drugs

Tables 16-23 and 16-24 list ophthalmic antibacterial drugs and ophthalmic combination anti-inflammatory/antibiotic drugs, respectively.

Fluoroquinolones

Fluoroquinolones are synthetic fluorinated derivatives of nalidixic acid. These drugs are highly effective broad-spectrum antimicrobials with potent activity against common gram-positive and gram-negative ocular pathogens. Their mechanism of action targets bacterial DNA supercoiling through the inhibition of bacterial topoisomerase II (DNA gyrase) and topoisomerase IV, 2 of the enzymes responsible for replication, genetic recombination, and DNA repair. Pathogenic variations (mutations) in the bacterial genes for these enzymes allow for the development of resistance to fluoroquinolone drugs, an incidence that is increasing, as is evidence of cross-resistance among them. Fluoroquinolone resistance has been reported in *Mycobacterium chelonae, S aureus,* coagulase-negative *Staphylococcus* species, *P aeruginosa, Clostridium difficile, Salmonella enterica, E coli,* and *Helicobacter pylori.*

The efficacy of fluroquinolones against gram-positive bacteria varies depending on the fluroquinolone considered. The older generations of fluoroquinolones have good potency against gram-negative bacteria; the newer generations were designed to broaden the spectrum of coverage and increase potency against gram-positive bacteria. For example, the second-generation fluoroquinolone ciprofloxacin may be more effective against *P aeruginosa* than the newer drugs.

In vitro studies have demonstrated that the fluoroquinolones, especially ciprofloxacin and temafloxacin, inhibit 90% of common corneal bacterial pathogens and have a lower minimum inhibitory concentration than that of the aminoglycosides gentamicin and tobramycin and the cephalosporin cefazolin. They are also less toxic to the corneal epithelium than are the aminoglycosides. Methicillin-susceptible strains of *S aureus* are generally susceptible to fluoroquinolones, but methicillin-resistant strains of staphylococci are often resistant to them.

The 7 currently available topical fluoroquinolones are ofloxacin ophthalmic solution, 0.3%; ciprofloxacin, 0.3%; levofloxacin, 0.5%; gatifloxacin, 0.3% and 0.5%; moxifloxacin, 0.5%; norfloxacin, 0.3%; and besifloxacin, 0.6%. They are used to treat corneal ulcers caused by susceptible strains of *S aureus, S epidermidis, Streptococcus pneumoniae, P aeruginosa, Serratia marcescens* (efficacy studied in fewer than 10 infections), and *Propionibacterium acnes.* They are also indicated for bacterial conjunctivitis due to susceptible strains of *S aureus, S epidermidis, S pneumoniae, Enterobacter cloacae, H influenzae, P mirabilis,* and *P aeruginosa.* These fluoroquinolones have a high rate of penetration into ocular tissue. Their sustained tear concentration levels exceed the minimum inhibitory concentrations of key ocular pathogens for 12 hours or more after 1 dose. They also deliver excellent susceptibility kill rates; 1 in vitro study confirmed eradication of 87%–100% of indicated pathogenic bacteria, including *P aeruginosa.* Ofloxacin has a high intrinsic solubility that enables formulation at a near-neutral pH of 6.4. Ciprofloxacin is formulated at a pH of 4.5, gatifloxacin at a pH of 6.0, and moxifloxacin at a pH of 6.8.

The most frequently reported drug-related adverse reaction with fluoroquinolones is transient ocular burning or discomfort. Other reported reactions are stinging, redness, itching, chemical conjunctivitis/keratitis, periocular/facial edema, foreign-body sensation,

Table 16-23 Selected Ophthalmic Antibacterial Drugs

Generic Name	Trade Name	Strength
Individual drugs		
Azithromycin	AzaSite	Solution, 1%
Bacitracin zinc	Ak-Tracin, also available generically	Ointment (500 units/g)
Besifloxacin	Besivance	Suspension, 0.6%
Chloramphenicol	Powder available for compounding	Solution, 0.5%; ointment, 1%
Ciprofloxacin HCl	Ciloxan, also available generically	Solution, 0.3%; ointment, 0.3%
Erythromycin	Romycin, also available generically	Ointment, 0.5%
Gatifloxacin	Zymar, Zymaxid	Solution, 0.3%; solution, 0.5%
Gentamicin sulfate	Garamycin, Gentak Genoptic, Gentasol Available generically	Solution, 0.3%; ointment, 0.3% Solution, 0.3% Solution, 0.3%; ointment, 0.3%
Levofloxacin	Quixin	Solution, 0.5%
Moxifloxacin HCl	Vigamox, Moxeza, also available generically	Solution, 0.5%
Norfloxacin	Norflox	Solution, 0.3%
Ofloxacin	Ocuflox, also available generically	Solution, 0.3%
Sulfacetamide sodium	Bleph-10, also available generically	Solution, 10%; ointment, 10%
Tobramycin sulfate	AK-Tob, Tobrasol Tobrex Available generically	Solution, 0.3% Solution, 0.3%; ointment, 0.3% Solution, 0.3%
Combination drugs		
Polymyxin B sulfate/ bacitracin zinc	AK-Poly-Bac, Polycin-B, also available generically	Ointment (10,000 units/g, 500 units/g)
Polymyxin B sulfate/ neomycin sulfate/ bacitracin zinc	Available generically	Solution (10,000 units, 1.75 mg, 0.025 mg/mL), ointment (10,000 units/g, 3.5 mg/base, 400 units/g)
Polymyxin B sulfate/ neomycin sulfate/ gramicidin	Neosporin, also available generically	Solution (10,000 units/mL, 1.75 mg base/mL, 0.025 mg/mL)
Polymyxin B sulfate/ oxytetracycline	Terak	Ointment (10,000 units/g, equivalent to 5 mg base/g)
Polymyxin B sulfate/ trimethoprim sulfate	Polytrim, also available generically	Solution (10,000 units/mL, equivalent to 1 mg base/mL)

photophobia, blurred vision, tearing, dry eye, and eye pain. Though rare, dizziness has also been reported. Both norfloxacin and ciprofloxacin have caused white, crystalline corneal deposits of medication, which have resolved after discontinuation of the drug.

Case reports of tendonitis and tendon rupture have been associated with systemic fluoroquinolone use. The possibility of damage to growth-plate cartilage poses a safety concern for the use of fluoroquinolones in children. However, larger cohorts and comparative studies

Table 16-24 Combination Ocular Anti-inflammatory and Antibiotic Drugs

Generic Name	Trade Name	Preparation and Concentration
Dexamethasone/neomycin sulfate/polymyxin B sulfate	AK-Trol, Poly-Dex, Dexacidin, Dexasporin, Maxitrol, also available generically	Suspension, 0.1%; equivalent to 3.5 mg base/mL; 10,000 units/mL
	Maxitrol, AK-Trol, Poly-Dex, also available generically	Ointment, 0.1%; equivalent to 3.5 mg base/g; 10,000 units/g
Dexamethasone/tobramycin	Tobradex, also available generically	Suspension, 0.1%, 0.3%
	Tobradex ST	Suspension (in xanthan gum), 0.3%, 0.05%
	Tobradex	Ointment, 0.1%, 0.3%
Fluorometholone/ sulfacetamide	FML-S	Suspension, 0.1%, 10%
Hydrocortisone/neomycin sulfate/polymyxin B sulfate	Cortisporin, also available generically	Suspension, 1%; equivalent to 3.5 mg base/mL; 10,000 units/mL
Hydrocortisone/neomycin sulfate/polymyxin B sulfate/bacitracin zinc	AK-Spore, Cortisporin, also available generically	Ointment, 1%; equivalent to 3.5 mg base/g; 5000 units/g; 400 units/g
Loteprednol etabonate/ tobramycin	Zylet	Suspension, 0.5%, 0.3%
Neomycin sulfate/polymyxin B sulfate/prednisolone acetate	Poly-Pred, also available generically	Suspension; equivalent to 0.35% base; 10,000 units/ mL; 0.5%
Prednisolone acetate/ gentamicin sulfate	Pred-G	Suspension; equivalent to 0.3% base; 1%
	Pred-G S.O.P.	Ointment; equivalent to 0.3% base; 0.6%
Prednisolone acetate/ sulfacetamide sodium	Blephamide, also available generically	Suspension, 0.2%, 10%
	Blephamide S.O.P.	Ointment, 0.2%, 10%
Prednisolone sodium phosphate/sulfacetamide sodium	Vasocidin, also available generically	Solution, 0.25%, 10%
	AK-Cide	Ointment, 0.5%, 10%

did not show an increased risk of musculoskeletal disorders in children treated with systemic fluoroquinolones.

CLINICAL PEARL

There is no evidence that the ophthalmic administration of fluoroquinolones has any effect on weight-bearing joints in the pediatric population.

Sulfonamides

Sulfonamides are derivatives of para-aminobenzenesulfonamide. They are structural analogues of para-aminobenzoic acid (PABA) and competitive antagonists of dihydropteroate

synthase for the bacterial synthesis of folic acid. Unlike mammals, bacteria cannot use exogenous folic acid but must synthesize it from PABA. Sulfonamides are bacteriostatic only and are more effective when administered with trimethoprim or pyrimethamine, each of which is a potent inhibitor of bacterial dihydrofolate reductase; together, they block successive steps in the synthesis of folic acid. For example, sulfadiazine, systemic pyrimethamine, and folinic acid are used in the treatment of toxoplasmosis, with the folinic acid coadministered to minimize bone marrow suppression. A 3-week course of systemic sulfonamide therapy is also useful for the treatment of chlamydial infection.

Sulfacetamide ophthalmic solution (10%–30%) and ointment (10%) penetrate the cornea well but may sensitize the patient to sulfonamide medications. Susceptible organisms include *S pneumoniae, Corynebacterium diphtheriae, H influenzae, Actinomyces* species, and *Chlamydia trachomatis.* Common adverse effects from topical administration include local irritation, itching, periorbital edema, and transient stinging. As for all sulfonamide preparations, severe sensitivity reactions such as toxic epidermal necrolysis and Stevens-Johnson syndrome have been reported. The incidence of adverse reactions to all sulfonamides is approximately 5%.

The cross-allergenicity between sulfonamide antibiotics and nonantibiotic sulfonamide-containing drugs complicates drug therapy. The immunologic determinant of type I immediate hypersensitivity reaction to sulfonamide antibiotics is the N1 heterocyclic ring. Nonantibiotic sulfonamides do not contain this structural feature. Non–type I hypersensitivity responses to sulfonamide antibiotics are largely attributable to reactive metabolites formed at the N4 amino nitrogen of the sulfonamide antibiotics, a structure that is also absent from nonantibiotic sulfonamide drugs. Therefore, cross-reactivity between sulfonamide antibiotics and nonantibiotic sulfonamide-containing drugs is unlikely. However, a T-cell–mediated immune response to the parent sulfonamide structure appears to be responsible for hypersensitivity that occurs in a small subset of patients. Thus, cross-reactivity remains possible, at least theoretically. There is no cross-allergenicity between sulfonamide and the sulfate group (*sulfate* refers to the bivalent SO_4 group of a compound).

Brackett CC, Singh H, Block JH. Likelihood and mechanisms of cross-allergenicity between sulfonamide antibiotics and other drugs containing a sulfonamide functional group. *Pharmacotherapy.* 2004;24(7):856–870.

Lehmann DF. The metabolic rationale for a lack of cross-reactivity between sulfonamide antimicrobials and other sulfonamide-containing drugs. *Drug Metab Lett.* 2012;6(2):129–133.

Strom BL, Schinnar R, Apter AJ, et al. Absence of cross-reactivity between sulfonamide antibiotics and sulfonamide nonantibiotics. *N Engl J Med.* 2003;349(17):1628–1635.

Tetracyclines

The tetracycline family includes agents produced by *Streptomyces* species (chlortetracycline, oxytetracycline, demeclocycline), as well as the semisynthetically produced medications tetracycline, doxycycline, and minocycline. Tetracyclines enter bacteria by active transport across the cytoplasmic membrane. They inhibit protein synthesis by binding to the ribosomal subunit 30S, thereby preventing access of aminoacyl transfer RNA to the acceptor site on the mRNA–ribosome complex. Host cells are less affected because they lack an active transport system. Doxycycline and minocycline are more lipophilic and are thus more active by weight.

Tetracyclines are broad-spectrum bacteriostatic antibiotics that are active against many gram-positive and gram-negative bacteria and against *Rickettsia* species, *Mycoplasma pneumoniae,* and *Chlamydia* species. However, many strains of *Klebsiella* and *H influenzae* and nearly all strains of *Proteus vulgaris* and *P aeruginosa* are resistant. These medications demonstrate cross-resistance. Tetracycline is poorly water soluble but is soluble in eyedrops containing mineral oil; it readily penetrates the corneal epithelium. Chlortetracycline was previously used in ophthalmic preparations, but neither chlortetracycline nor tetracycline is currently available for ophthalmic use in the United States. Oxytetracycline is available in combination with polymyxin as an ophthalmic ointment.

Systemic therapy with the tetracyclines is used to treat chlamydial infections. Because these drugs are excreted into oil glands, they are also used to treat staphylococcal infections of the meibomian glands. Tetracyclines have anti-inflammatory properties that include suppression of leukocyte migration, reduced production of NO and reactive oxygen species, inhibition of MMPs, and inhibition of phospholipase A_2. In the management of meibomian gland dysfunction and rosacea, they are used mainly for their anti-inflammatory and lipid-regulating properties rather than for their antimicrobial effects (see BCSC Section 8, *External Disease and Cornea*).

As bacteriostatic drugs, tetracyclines may inhibit bactericidal medications such as the penicillins; therefore, these drugs should not be used concurrently. Tetracyclines also depress plasma prothrombin activity and thereby potentiate warfarin. In addition, the use of tetracyclines may decrease the efficacy of oral contraceptives. Patients should be instructed to use an additional form of birth control during administration of tetracyclines and for 1 month after discontinuation of their use.

Tetracyclines chelate to calcium in milk and antacids and are best taken on an empty stomach. Because tetracyclines may cause gastric irritation, they may be taken with nondairy foods to improve patient adherence. Tetracyclines should be used with caution in children under 8 years old and should not be given to pregnant women because they may be deposited in growing teeth, causing permanent discoloration of the enamel, and they may deposit in bone, inhibiting bone growth. They can also cause photosensitivity; consequently, patients taking tetracycline should avoid extended exposure to sunlight. Degraded or expired tetracyclines may cause renal toxicity, also called *Fanconi syndrome.* Tetracyclines have been implicated as a cause of IIH, a condition discussed in BCSC Section 5, *Neuro-Ophthalmology.*

Geerling G, Tauber J, Baudouin C, et al. The international workshop on meibomian gland dysfunction: report of the Subcommittee on Management and Treatment of Meibomian Gland Dysfunction. *Invest Ophthalmol Vis Sci*. 2011;52(4):2050–2064.

Chloramphenicol

Chloramphenicol, a broad-spectrum bacteriostatic drug, inhibits bacterial protein synthesis by binding reversibly to the ribosomal subunit 50S, preventing aminoacyl transfer RNA from binding to the ribosome. Chloramphenicol is effective against *H influenzae, Neisseria meningitidis,* and *N gonorrhoeae,* as well as all anaerobic bacteria. It has some activity against *S pneumoniae, S aureus, Klebsiella pneumoniae, Enterobacter* and *Serratia* species, and *P mirabilis. P aeruginosa* is resistant.

Chloramphenicol penetrates the corneal epithelium well when applied topically and penetrates the blood–ocular barrier readily when given systemically. However, the use of this medication is limited because it has been implicated in an idiosyncratic and potentially lethal aplastic anemia. Although most cases of this type of anemia have occurred after oral administration, some have been associated with parenteral and even topical ocular therapy. Chloramphenicol is available as a powder for compounding, but it should not be used if an alternative drug with less potential toxicity is available.

Aminoglycosides

The aminoglycosides consist of amino sugars in glycosidic linkage. These bactericidal agents are transported across the cell membrane into bacteria, where they bind to ribosomal subunits 30S and 50S, interfering with initiation of protein synthesis. The antibacterial spectrum of these drugs is determined primarily by the efficiency of their transport into bacterial cells. Such transport is energy dependent and may be reduced in the anaerobic environment of an abscess. Resistance to aminoglycosides may be caused by failure of transport, low affinity for the ribosome, or a plasmid-transmitted ability to enzymatically inactivate the drug. The coadministration of drugs such as penicillin that alter bacterial cell-wall structure can markedly increase aminoglycoside penetration, resulting in a synergism of antibiotic activity against gram-positive cocci, especially enterococci. One such aminoglycoside, amikacin, is remarkably resistant to enzymatic inactivation.

Gentamicin, tobramycin, kanamycin, and amikacin have antibacterial activity against aerobic, gram-negative bacilli such as *P mirabilis; P aeruginosa;* and *Klebsiella, Enterobacter,* and *Serratia* species. Gentamicin and tobramycin are also active against gram-positive *S aureus* and *S epidermidis.* Kanamycin is generally less effective than the others against gram-negative bacilli. Resistance to gentamicin and tobramycin has gradually increased as a result of the plasmid-transmitted ability to synthesize inactivating enzymes, as described earlier. Amikacin, which is generally impervious to these enzymes, is particularly valuable in treating these resistant organisms. It is effective against tuberculosis, as well as atypical mycobacteria, and can be compounded for topical use against mycobacterial infection.

Aminoglycosides are not absorbed well orally but may still be given systemically, either intramuscularly or intravenously. They do not readily penetrate the blood–ocular barrier but may be administered as eyedrops, ointments, or periocular injections. Gentamicin and carbenicillin should not be mixed for IV administration because carbenicillin inactivates gentamicin over several hours. Similar incompatibilities exist in vitro between gentamicin and other penicillins and cephalosporins.

The use of streptomycin is now limited to *Streptococcus viridans* bacterial endocarditis, tularemia, plague, and brucellosis. Neomycin is a broad-spectrum antibiotic that is effective against *Enterobacter* species, *K pneumoniae, H influenzae, N meningitidis, C diphtheriae,* and *S aureus.* It is given topically in ophthalmology and orally as a bowel preparation for surgery. Topical allergy to ocular use of neomycin occurs in approximately 8% of cases. Neomycin can cause punctate epitheliopathy and retard re-epithelialization of abrasions.

All aminoglycosides can cause dose-related vestibular and auditory dysfunction and nephrotoxicity when they are given systemically. Dosage adjustments must be made to prevent accumulation of drugs and toxicity in patients with renal insufficiency.

Miscellaneous antibiotics

Vancomycin is a tricyclic glycopeptide produced by *Streptococcus orientalis.* It is bactericidal for most gram-positive organisms through the inhibition of glycopeptide polymerization in the cell wall. Vancomycin is useful in the treatment of staphylococcal infections in patients who are allergic to or have not responded to the penicillins and cephalosporins. It can also be used in combination with aminoglycosides to treat *S viridans* or *Streptococcus bovis* endocarditis. Oral vancomycin is poorly absorbed but is effective in the treatment of pseudomembranous colitis caused by *C difficile.* Vancomycin resistance has increased in isolates of *Enterococcus* and *Staphylococcus,* and antibiotic resistance is transmitted between pathogens by a conjugative plasmid.

Vancomycin may be used topically or intraocularly to treat sight-threatening infections of the eye, including infectious keratitis and endophthalmitis caused by MRSA or multidrug-resistant streptococci. It has been used within the irrigating fluid of balanced salt solution during intraocular surgery; however, the contribution of this prophylactic use of vancomycin to the emergence of resistant bacteria, as well as to an increased risk of postoperative CME, is controversial. In the empirical treatment of endophthalmitis, vancomycin is a preferred substitute for a cephalosporin used in combination with an aminoglycoside. See BCSC Section 8, *External Disease and Cornea,* and Section 9, *Uveitis and Ocular Inflammation,* for further discussion.

Topical vancomycin may be compounded and given in a concentration of 10–50 mg/mL in the treatment of infectious keratitis. Intravitreal vancomycin combined with amikacin has been used for initial empirical therapy for exogenous bacterial endophthalmitis. Ceftazidime has largely replaced amikacin in clinical practice, primarily because of concerns about potential aminoglycoside retinal toxicity. A vancomycin dose of 1 mg/0.1 mL establishes intraocular levels that are significantly higher than the minimum inhibitory concentration for most gram-positive organisms. The IV dosage of vancomycin in adults with normal renal function is 500 mg every 6 hours or 1 g every 12 hours. Dosing must be adjusted in patients with renal impairment.

Unlike systemic treatment with vancomycin, topical and intraocular vancomycin has not been associated with ototoxicity or nephrotoxicity. Hourly use of topical 50 mg of vancomycin per milliliter delivers a dose of 36 mg per day, which is well below the recommended systemic dose. In addition to the ototoxicity and nephrotoxicity associated with systemic therapy, possible complications include chills, rash, fever, and anaphylaxis. Furthermore, rapid IV infusion may cause vancomycin flushing syndrome.

Erythromycin is a macrolide (many-membered lactone ring attached to deoxy sugars) antibiotic that binds to subunit 50S of bacterial ribosomes and interferes with protein synthesis. The drug is bacteriostatic against gram-positive cocci such as *Streptococcus pyogenes* and *S pneumoniae,* gram-positive bacilli such as *C diphtheriae* and *Listeria monocytogenes,* and a few gram-negative organisms such as *N gonorrhoeae* and *C trachomatis.* In sufficient dosing, it may be bactericidal against susceptible organisms.

Drug resistance to erythromycin is rising and is as high as 40% among *Streptococcus* isolates. There are 4 mechanisms of resistance:

1. esterases from the Enterobacteriaceae family
2. pathogenic variations that alter the ribosomal subunit 50S

3. enzyme modification of the ribosomal binding site
4. active pumping to extrude the drug

Macrolide antibiotics such as erythromycin are the treatment of choice for *Legionella pneumophila,* the agent of Legionnaires' disease, as well as for *M pneumoniae.* Erythromycin is administered orally as enteric-coated tablets or in esterified forms to avoid inactivation by stomach acid. It can also be administered parenterally or topically as an ophthalmic ointment. The drug penetrates the blood–ocular and blood–brain barriers poorly.

Clarithromycin and azithromycin are semisynthetic macrolides with a spectrum of activity similar to that of erythromycin. Clarithromycin is more effective against staphylococci, streptococci, and *Mycobacterium leprae,* whereas azithromycin is more active against *H influenzae, N gonorrhoeae,* and *Chlamydia* species. Both drugs have enhanced activity against *Mycobacterium avium-intracellulare,* atypical mycobacteria, and *Toxoplasma gondii.* Azithromycin, 1%, has been approved by the FDA for bacterial conjunctivitis caused by coryneform group G, *H influenzae, S aureus,* the *Streptococcus mitis* group, and *S pneumoniae.*

Polymyxin B sulfate is a mixture of basic peptides that function as cationic detergents to dissolve phospholipids of bacterial cell membranes, thereby disrupting cells. It is used topically or by local injection to treat corneal ulcers. Gram-negative bacteria including *Enterobacter* and *Klebsiella* species and *P aeruginosa* are susceptible; bacterial sensitivity is related to the phospholipid content of the cell membrane, and resistance may occur if a cell wall prevents access to the pathogen cell membrane. Systemic use of this medication has been abandoned because of severe nephrotoxicity. One commercially available topical antibiotic contains polymyxin B sulfate and trimethoprim sulfate. Sulfonamide allergy does not preclude the use of products with trimethoprim or with a sulfate group.

Bacitracin zinc is a mixture of polypeptides that inhibits bacterial cell-wall synthesis. It is active against *Neisseria* and *Actinomyces* species, *H influenzae,* most gram-positive bacilli and cocci, and most but not all strains of MRSA. It is available as an ophthalmic ointment either alone or in various combinations with polymyxin, neomycin, and hydrocortisone. The primary adverse effect is local hypersensitivity, although it is not common.

Topical povidone-iodine solution, 5%, exhibits broad-spectrum antimicrobial activity when used to prepare the surgical field and to rinse the ocular surface; it is approved by the FDA for this purpose. To be fully effective, it should be allowed to dry on the skin. Povidone-iodine scrub may be used periocularly, but it is contraindicated in the eye because it is damaging to the corneal epithelium.

Topical povidone-iodine solution has been incorrectly considered contraindicated in patients with hypersensitivity to iodine or to IV contrast dye. Reported allergies to seafood or contrast media are not a contraindication to the use of topical povidone-iodine solution. Iodine is not thought to be the eliciting factor in iodinated contrast media reactions or in those related to shellfish, for which tropomyosin has been implicated. Iodine, a ubiquitous element (eg, iodized salt), is a simple molecule that is widely believed to lack the complexity required for antigenicity. Instead, patients probably develop hypersensitivity reactions to specific proteins of the food itself (eg, seafood) or to the contrast medium, rather than to the iodine in the compound. Cases of hypersensitivity to povidone, another common substance, have been reported. It is important to carefully discuss the ramifications of not using

povidone-iodine with patients before intraocular procedures. The ophthalmologist can also ask, "Have you ever had a reaction to Betadine?" or refer patients for allergy testing. This is especially important in patients who may need repeated procedures, such as intravitreal injections.

Isenberg SJ, Apt L, Yoshimori R, Khwarg S. Chemical preparation of the eye in ophthalmic surgery, IV: comparison of povidone-iodine on the conjunctiva with a prophylactic antibiotic. *Arch Ophthalmol.* 1985;103(9):1340–1342.

Modjtahedi BS, van Zyl T, Pandya HK, Leonard RE II, Eliott D. Endophthalmitis after intravitreal injections in patients with self-reported iodine allergy. *Am J Ophthalmol.* 2016;170:68–74.

Schabelman E, Witting M. The relationship of radiocontrast, iodine, and seafood allergies: a medical myth exposed. *J Emerg Med.* 2010;39(5):701–707.

Scoper SV. Review of third- and fourth-generation fluoroquinolones in ophthalmology: in-vitro and in-vivo efficacy. *Adv Ther.* 2008;25(10):979–994.

Wykoff CC, Flynn HW Jr, Han DP. Allergy to povidone-iodine and cephalosporins: the clinical dilemma in ophthalmic use. *Am J Ophthalmol.* 2011;151(1):4–6.

Antifungal Drugs

Table 16-25 lists common antifungal drugs encountered in ophthalmology practice.

Polyenes

The polyene antibiotics are named for a component sequence of 4–7 conjugated double bonds. That lipophilic region allows these antibiotics to bind to sterols in the cell membrane of susceptible fungi, an interaction that results in damage to the membrane and leakage of essential nutrients. Other antifungals (such as flucytosine and the imidazoles) and even other antibiotics (such as tetracycline and rifampin) can enter through the damaged membrane, yielding synergistic effects.

Natamycin and amphotericin B are 2 examples of polyene macrolide antibiotics. Natamycin is available as a 5% suspension for topical ophthalmic use (once per hour). Local hypersensitivity reactions of the conjunctiva and eyelid and/or corneal epithelial toxicity may occur. Amphotericin B may be reconstituted at 0.25%–0.5% in sterile water (with deoxycholate to improve solubility) for topical use (every 30 minutes). It may also be administered systemically for disseminated disease, although careful monitoring for renal and other toxicities is required. Both drugs penetrate the cornea poorly. They have been used topically against various filamentous fungi, including species of *Aspergillus, Cephalosporium, Curvularia, Fusarium,* and *Penicillium,* as well as the yeast *Candida albicans.* Systemic amphotericin B has been reported as useful in treating systemic *Aspergillus, Blastomyces, Candida, Coccidioides, Cryptococcus,* and *Histoplasma* infections. Amphotericin can also be administered intravitreally; however, it has been associated with retinal toxicity.

Imidazoles and triazoles

The imidazole- and triazole-derived antifungal drugs also increase fungal cell-membrane permeability and interrupt membrane-bound enzyme systems. These antifungals act against various species of *Aspergillus, Coccidioides, Cryptococcus,* and *Candida,* among others. The

Table 16-25 Antifungal Drugs

Generic (Trade) Name	Route	Dosage	Indication (Additional Reports of Use)
Polyenes			
Amphotericin B (Fungizone)	Topical	0.1%–0.5% solution; dilute with water for injection or dextrose 5% in water	*Aspergillus* *Candida* *Cryptococcus* *(Blastomyces)* *(Coccidioides)* *(Colletotrichum)* *(Histoplasma)* *(Mucormycosis)*
	Subconjunctival	1.5 mg	
	Intravitreal	5 μg/100 μL	
	Intravenous	Because of possible adverse effects and toxicity, dose needs to be carefully adjusted	
Natamycin (Natacyn)	Topical	5% suspension	*Fusarium* *(Aspergillus)* *(Candida)* *(Cephalosporium)* *(Curvularia)* *(Penicillium)*
Imidazoles			
Ketoconazole (Nizoral)	Oral	200 mg daily, up to 400 mg for severe or incomplete response	*Blastomyces* *Candida* *Coccidioides* *Histoplasma*
Miconazole nitrate (available as powder for compounding)	Topical	1% solution	*Aspergillus* *Candida* *Cryptococcus*
	Subconjunctival	5 mg/0.5 mL	
	Intravitreal	10–40 μg	
Triazoles			
Fluconazole (Diflucan)	Oral	200 mg daily	*Candida* *Cryptococcus* *(Acremonium)*
	Subconjunctival	10 mg/0.5 mL	
	Intravenous	Same as oral dose	
Itraconazole (Sporanox)	Oral	200 mg daily	*Aspergillus* *Blastomyces* *Histoplasma* *(Candida)* *(Curvularia)* (nonsevere *Fusarium*)
	Intravenous	200 mg twice daily for 4 doses, then once daily	
Voriconazole (Vfend)	Topical	1% (made from intravenous solution)	*Aspergillus* *Blastomyces* *Candida* *Cryptococcus* *Fusarium* *Histoplasma* *Penicillium* *Scedosporium*
	Oral	200 mg orally twice daily	
	Intravenous	3–6 mg/kg intravenously every 12 h	
	Intravitreal	100 μg/100 μL	

Table 16-25 *(continued)*

Generic (Trade) Name	Route	Dosage	Indication (Additional Reports of Use)
Fluorinated pyrimidine			
Flucytosine (Ancobon)	Oral	50–150 mg/kg daily divided every 6 h	*Candida Cryptococcus (Aspergillus)*
	Topical	1% solution	
Echinocandins			
Caspofungin	Intravenous	Loading dose: 50–70 mg; Maintenance dose: 50 mg	*Candida Aspergillus*
Micafungin	Intravenous	100–150 mg	*Candida Aspergillus*
Anidulafungin	Intravenous	Loading dose: 100–200 mg; Maintenance dose: 50–100 mg	*Candida Aspergillus*

triazoles have less effect on human sterol synthesis, as well as a longer half-life, than do the imidazoles, and they are being more actively developed. The imidazole miconazole is available in a 1% solution that may be injected subconjunctivally (5 mg/0.5 mL, once or twice daily) or applied topically. Miconazole penetrates the cornea poorly.

Ketoconazole is available in 200-mg tablets for oral therapy (once or twice daily). Ketoconazole typically penetrates the blood–brain barrier and, presumably, the blood–ocular barrier poorly, but therapeutic levels can be achieved in inflamed eyes. The triazole itraconazole, which has an expanded antifungal spectrum and less systemic toxicity, has largely replaced ketoconazole. However, there is an extensive and growing list of potentially dangerous drug interactions with itraconazole that should be consulted before instituting systemic therapy. Fluconazole, another triazole, has good bioavailability but limited spectrum and may also increase the plasma concentrations of other medications. Oral voriconazole is rapidly replacing other antifungals because of its excellent bioavailability, intraocular penetration, and broad-spectrum coverage. However, resistance to this agent is increasing.

Echinocandins

This class of antifungals inhibits a component (glucan) of the fungal cell wall. Caspofungin and micafungin are the 2 most commonly used agents. Their primary activity is against *Candida* and *Aspergillus* species, and they are used prophylactically in stem cell recipients and in patients with candidemia.

Patil A, Majumdar S. Echinocandins in antifungal pharmacotherapy. *J Pharm Pharmacol*. 2017;69(12):1635–1660.

Fluorinated pyrimidine

Flucytosine (5-fluorocytosine), a fluorinated pyrimidine like 5-fluorouracil (5-FU), is converted by some species of fungal cells to 5-FU by cytosine deaminase and then to 5-fluorodeoxyuridylate. This last compound inhibits thymidylate synthase, an important

enzyme in DNA synthesis. Host cells lack cytosine deaminase activity and are less affected. Only fungi that have both a permease to facilitate flucytosine penetration and a cytosine deaminase are sensitive to flucytosine. Flucytosine is taken orally at 50–150 mg/kg daily, divided every 6 hours. Although the drug is well absorbed and penetrates the blood–ocular barrier well, most *Aspergillus* and half of *Candida* isolates are resistant to it. Flucytosine is used primarily as an adjunct to systemic amphotericin B therapy.

Antiviral Drugs

Table 16-26 summarizes information on common antiviral drugs.

Topical antiviral drugs

Idoxuridine, ganciclovir, trifluridine, and vidarabine compete with natural nucleotides for incorporation into viral and mammalian DNA and have been used to treat herpes simplex virus (HSV) keratitis. Idoxuridine (5-iodo-2′-deoxyuridine) and trifluridine are structural analogues of thymidine and work in a similar manner; vidarabine is an analogue of adenine. Vidarabine is used when a drug with a different mechanism of action is required. Trifluridine (1% drops, every 2–4 hours) is more water-soluble than the other drugs and can be used in drop form, providing adequate penetration of diseased corneas to treat herpetic epithelial keratitis. Trifluridine is currently marketed in the United States, but vidarabine ophthalmic ointment (3%) is not. Idoxuridine and vidarabine powder are available for compounding. Cross-resistance does not seem to occur among these medications.

Acyclovir is activated by HSV thymidine kinase to inhibit viral DNA polymerase. The 3% ophthalmic ointment is not commercially available in the United States, and the 5% dermatologic ointment is not approved for ophthalmic use. Ganciclovir is activated by triphosphorylation to inhibit viral DNA polymerase. It is available as 0.15% ophthalmic gel approved for treatment of HSV keratitis. It is moderately effective in treating cytomegalovirus (CMV) corneal endotheliitis and anterior uveitis.

Systemic antiviral drugs

Acyclovir is a synthetic guanosine analogue. Because the viral thymidine kinase in HSV types 1 and 2 has much more affinity to acyclovir than does host thymidine kinase, high concentrations of acyclovir monophosphate accumulate in infected cells. Acyclovir monophosphate is then further phosphorylated to the active compound acyclovir triphosphate, which cannot cross cell membranes and accumulates further.

Acyclovir-resistant thymidine kinase HSVs have evolved. These resistant viruses occur primarily in patients receiving multiple courses of therapy or in patients with HIV infection. Thymidine kinase variants are susceptible to vidarabine and foscarnet. Changes in viral DNA polymerase structures can also mediate resistance to acyclovir.

Oral acyclovir is only 15%–30% bioavailable, and food does not affect absorption. For unknown reasons, bioavailability is lower in patients with transplants. The drug is well distributed; cerebrospinal fluid (CSF) and brain concentrations equal approximately 50% of serum values. Concentrations of acyclovir in zoster vesicle fluid are equivalent to those in plasma. Aqueous humor concentrations are 35% of those of plasma, and salivary concentrations are 15%. Vaginal concentrations are equivalent to those of plasma, and breast milk concentrations exceed them.

Table 16-26 Common Antiviral Drugs

Generic Name	Trade Name	Topical Concentration/ Ophthalmic Solution	Systemic Dosage/Intravitreal Dosage
Trifluridine	Viroptic, also available generically	1%	NA
Idoxuridine	Available as powder for compounding	0.1%	NA
Vidarabine monohydrate	Vira-A, available as powder for compounding	3% (ointment[a])	NA
Acyclovir sodium[b]	Zovirax, also available generically	NA	Oral: HSV keratitis 200–400 mg 5 times daily for 7–10 d Oral: HZO 600–800 mg 5 times daily for 10 d; intravenous if patient is immunocompromised Intravenous for necrotizing herpetic retinopathy or in immunocompromised adults: 10 mg/kg every 8 h for 7 d, followed by oral therapy
	Zovirax ointment[a]	3% (ointment)	NA
Zidovudine	Retrovir, also available generically	NA	Dosage variable per source consulted; dosing per internal medicine consultation recommended
Cidofovir[b,c]	Vistide	NA	Intravenous: Induction: 5 mg/kg constant infusion over 1 h once weekly for 2 consecutive wk Maintenance: 5 mg/kg constant infusion over 1 h administered every 2 wk
Famciclovir[b,c]	Available generically	NA	500 mg 3 times daily for 7 d
Foscarnet sodium	Foscavir, also available generically	NA	Intravenous: Induction: By controlled infusion only, either by central vein or by peripheral vein induction: 60 mg/kg (adjusted for renal function) given over 1 h every 8 h for 14–21 d; Maintenance: 90–120 mg/kg given over 2 h once daily Intravitreal injection: 2.4 mg/0.1 mL or 1.2 mg in 0.05 mL
Ganciclovir	Vitrasert (discontinued)	NA	Intravitreal: 4.5 mg sterile intravitreal insert designed to release the drug over a 5- to 8-mo period

(Continued)

Table 16-26 *(continued)*

Generic Name	Trade Name	Topical Concentration/ Ophthalmic Solution	Systemic Dosage/Intravitreal Dosage
Ganciclovir sodium [b,c]	Cytovene IV	NA	Intravenous: Induction: 5 mg/kg every 12 h for 14–21 d; Maintenance: 5 mg/kg daily (7 d per wk) or 6 mg/kg once daily (5 d per wk) Intravitreal: Induction: 2 mg/0.1 mL, 0.1-mL injection 2 times per wk for 3 wk; Maintenance: 0.1 mL once per wk
	Zirgan	0.15% gel	NA
Valacyclovir HCl [b,d]	Valtrex	NA	Oral: 1 g 3 times daily for 7–14 d
Valganciclovir	Valcyte	NA	Oral: Induction: 900 mg every 12 h for 21 d; Maintenance: 900 mg once daily

HSV = herpes simplex virus; HZO = herpes zoster ophthalmicus; NA = not applicable.
[a] Not available in the United States.
[b] Dose adjustment is needed for older adults and in those with renal disease or with concomitant nephrotoxic medications.
[c] Because of potential adverse and toxic effects with systemic dosage, the possible dosage adjustments and warnings should be followed properly.
[d] At high doses, valacyclovir has been associated with thrombotic thrombocytopenic purpura/hemolytic uremic syndrome in immunocompromised patients.

For adults and neonates with normal renal function, the plasma half-lives of acyclovir are 3.3 and 3.8 hours, respectively. The half-life increases to 20 hours in patients who are anuric. Acyclovir may interfere with the renal excretion of drugs that are eliminated through the renal tubules (eg, methotrexate); probenecid significantly decreases the renal excretion of acyclovir. This drug is effectively removed by hemodialysis (60% decrease in plasma concentrations following a 6-hour dialysis period) but only minimally removed by peritoneal dialysis.

Acyclovir is used off-label for ocular HSV and herpes zoster virus (HZV) but has proven effective in preventing the recurrence of HSV epithelial and stromal keratitis with twice-daily oral doses of 400 mg. Although this prophylactic dosage was originally studied over a 1-year treatment period, clinicians now use this dosage indefinitely to decrease the likelihood of disease recurrence. Similar dosing of acyclovir has proven beneficial in reducing the likelihood of recurrent herpetic eye disease after corneal transplantation. However, oral acyclovir was not beneficial when used with topical steroids and trifluridine in the treatment of active HSV stromal keratitis. The addition of oral acyclovir to a regimen of topical antiviral drugs may be considered for patients with HSV iridocyclitis. Although the benefit of this drug did not reach statistical significance in 1 study, participant enrollment had been halted because of inadequate numbers of patients.

Acyclovir is well tolerated in oral form, but parenteral acyclovir can cause renal toxicity due to crystalline nephropathy. Neurotoxicity may also occur with IV use. IV dosages vary depending on the patient's age, diagnosis, and renal function.

Valacyclovir is currently approved for management of HZV infections in immunocompetent persons but not for HSV. It is an amino-acid ester prodrug of acyclovir; its bioavailability is much higher than that of acyclovir (54% vs 20%, respectively). Valacyclovir has been associated with nephrotoxicity and thrombocytopenia in immunocompromised patients.

Famciclovir is the oral prodrug of penciclovir and is currently approved for the management of uncomplicated acute HSV. Penciclovir, like acyclovir, requires phosphorylation by viral thymidine kinase to become active. It has demonstrated efficacy in relieving acute zoster signs and symptoms and reducing the duration of postherpetic neuralgia when administered in patients with acute HZV.

Ganciclovir (9-2-hydroxypropoxymethylguanine) is a synthetic guanosine analogue active against many herpesviruses. It is approved for treatment of CMV retinitis and for CMV prophylaxis in patients with advanced HIV infection and in patients undergoing a transplant. Like acyclovir, it must be phosphorylated to become active. Infection-induced kinases, viral thymidine kinase, or deoxyguanosine kinase of various herpesviruses can catalyze this reaction. After monophosphorylation, cellular enzymes convert ganciclovir to the triphosphorylated form, and the triphosphate inhibits viral DNA polymerase rather than cellular DNA polymerase. Because of ganciclovir's potential for toxicity and the availability of acyclovir for treatment of many herpesvirus infections, the use of ganciclovir is currently restricted to treatment of CMV.

Systemic ganciclovir is used primarily intravenously because less than 5% of an oral dose is absorbed. CSF concentrations are approximately 50% of plasma concentrations; peak plasma concentrations reach 4–6 μg/mL. The plasma half-life is 3–4 hours in people with normal renal function, increasing to more than 24 hours in patients with severe renal insufficiency. More than 90% of systemic ganciclovir is eliminated unchanged in urine, and dose modifications are necessary for individuals with compromised renal function. Approximately 50% of ganciclovir is removed by hemodialysis. Bone marrow suppression is the primary adverse effect of systemic therapy. Periodic complete blood counts and platelet counts are required during the course of treatment. Ganciclovir can also be administered intravitreally.

Valganciclovir is a prodrug for ganciclovir that offers significantly higher bioavailability (60%) than ganciclovir (9%) when taken orally. After oral administration, it is rapidly converted to ganciclovir by intestinal and hepatic esterases. It can be used during the induction and/or maintenance phase of treatment in patients with CMV retinitis, affording them an outpatient alternative to ganciclovir.

CLINICAL PEARL

Oral administration of the prodrugs valacyclovir and valganciclovir has greatly improved the bioavailability of acyclovir and ganciclovir, respectively. In many cases, this has facilitated outpatient management of ophthalmic conditions that previously required hospital admission for induction therapy and placement of peripherally inserted central catheters (PICCs) (ie, acute retinal necrosis and CMV retinitis).

Foscarnet (phosphonoformic acid) inhibits DNA polymerases, RNA polymerases, and reverse transcriptases. In vitro, it is active against herpesviruses, the influenza virus, and HIV. Foscarnet is approved for the treatment of CMV retinitis in patients with HIV infection and for acyclovir-resistant mucocutaneous HSV infections in patients who are immunocompromised. It also inhibits CMVs that are resistant to acyclovir and ganciclovir. Foscarnet acts by blocking the pyrophosphate receptor site of CMV DNA polymerase. Viral resistance is attributable to structural alterations in this enzyme.

Foscarnet bioavailability is approximately 20%. Because it can bind with calcium and other divalent cations, foscarnet becomes deposited in bone and may be detectable for many months; 80%–90% of the administered dose appears unchanged in the urine. It is administered intravenously in doses adjusted for renal function and with hydration to establish sufficient diuresis. Treatment may be limited by nephrotoxicity in up to 50% of patients; other adverse effects include hypocalcemia and neurotoxicity. To limit systemic adverse effects, foscarnet can also be administered intravitreally.

Cidofovir is the third medication approved by the FDA for the treatment of CMV retinitis, and it is approved only for that use. Cidofovir is a cytidine nucleoside analogue that is active against herpesviruses, poxviruses, polyomaviruses, papillomaviruses, and adenoviruses. The drug is the second-line therapy for complications after smallpox vaccination (vaccinia virus) and has been used in selected studies for varicella-zoster retinitis, as well as adenoviral keratoconjunctivitis.

Cidofovir's mechanism of action is inhibition of DNA synthesis, and resistance is achieved through pathogenic variations in DNA polymerase. The prolonged intracellular half-life of an active metabolite allows once-weekly dosing during induction, with dosing every 2 weeks thereafter. Cidofovir does not have direct cross-resistance with acyclovir, ganciclovir, or foscarnet, although some virus isolates may have multiple resistances and may even develop triple resistance. In a small series of patients, cidofovir inhibited CMV replication when administered intravitreally. Long-lasting suppression of CMV retinitis was observed; the average time to progression was 55 days.

The primary adverse effect of cidofovir is renal toxicity, which can be decreased by IV prehydration and by both pretreatment and posttreatment with high-dose probenecid. Ocular adverse effects include uveitis and irreversible hypotony.

Zidovudine is a thymidine nucleoside analogue with activity against HIV. Zidovudine becomes phosphorylated to monophosphate, diphosphate, and triphosphate forms by cellular kinases in infected and uninfected cells. It has 2 primary mechanisms of action:

1. The triphosphate acts as a competitive inhibitor of viral reverse transcriptase.
2. The azido group prevents further chain elongation and acts as a DNA chain terminator.

Zidovudine inhibits HIV reverse transcriptase at much lower concentrations than needed to inhibit cellular DNA polymerases.

Since the introduction of zidovudine in the 1980s, numerous antiretroviral drugs have been approved for the treatment of HIV infection. They are divided into 6 classes: nucleoside reverse transcriptase inhibitors, non-nucleoside reverse transcriptase inhibitors, protease inhibitors, fusion inhibitors, entry inhibitors, and integrase strand transfer inhibitors. The current standard antiretroviral therapy (ART) consists of a combination of antiretroviral drugs.

Herpetic Eye Disease Study Group. Acyclovir for the prevention of recurrent herpes simplex virus eye disease. *N Engl J Med.* 1998;339(5):300–306.

Herpetic Eye Disease Study Group. Oral acyclovir for herpes simplex virus eye disease: effect on prevention of epithelial keratitis and stromal keratitis. *Arch Ophthalmol.* 2000;118(8):1030–1036.

Martin DF, Sierra-Madero J, Walmsley S, et al; Valganciclovir Study Group. A controlled trial of valganciclovir as induction therapy for cytomegalovirus retinitis. *N Engl J Med.* 2002;346(15):1119–1126.

Schoenberger SD, Kim SJ, Thorne JE, et al. Diagnosis and treatment of acute retinal necrosis: a report by the American Academy of Ophthalmology. *Ophthalmology*. 2017; 124(3):382–392.

Medications for *Acanthamoeba* Infections

Acanthamoeba is a genus of ubiquitous, free-living amoebae that inhabit soil, water, and air. Their appearance as corneal pathogens has increased because of several factors, including increased use of contact lenses. The species responsible for corneal infections—which include *Acanthamoeba polyphaga, Acanthamoeba castellanii, Acanthamoeba hatchetti,* and *Acanthamoeba culbertsoni*—exist as both trophozoites and double-walled cysts. Because of variations among species of *Acanthamoeba,* no single drug is effective in treating all cases of *Acanthamoeba* keratitis, and combination therapy is commonly required. Polyhexamethylene biguanide (0.02% solution) is a non–FDA-approved disinfectant and is the first-line agent with the lowest minimal amebicidal concentration. Other effective medications include chlorhexidine, 0.02%; neomycin; polymyxin B/neomycin/gramicidin mixtures; natamycin, 5%, topical suspension; imidazoles such as miconazole (powder compounded to 1% topical solution); systemic imidazoles and triazoles; propamidine isethionate, 0.1%, drops (not approved in the United States); and topical dibromopropamidine, 0.15%, ointment (not approved in the United States). In addition, oral miltefosine, which is an alkylphosphocholine anti-amoebic drug that was initially FDA-approved for the treatment of visceral leishmaniasis, has been found to be effective in the treatment of recalcitrant *Acanthamoeba* keratitis. See BCSC Section 8, *External Disease and Cornea,* for further discussion of treatment for *Acanthamoeba* infection.

Dart JKG, Saw VPJ, Kilvington S. Acanthamoeba keratitis: diagnosis and treatment update 2009. *Am J Ophthalmol.* 2009;148(4):487–499.

Seal DV. *Acanthamoeba* keratitis update: incidence, molecular epidemiology, and new drugs for treatment. *Eye (Lond)*. 2003;17(8):893–905.

Thulasi P, Saeed HN, Rapuano CJ, et al. Oral miltefosine as salvage therapy for refractory *Acanthamoeba* keratitis. *Am J Ophthalmol.* 2021;223:75–82.

Ocular Penetration of Systemically Administered Antimicrobial Agents

Various systemically administered antimicrobial agents achieve adequate ocular penetration (Table 16-27). The penetration of antimicrobial agents into the posterior segment of the eye after systemic administration is limited by the blood–retinal barrier. Entry into the anterior segment is limited by the blood–aqueous barrier.

The agents that have been best documented as achieving therapeutic levels in the vitreous are meropenem, linezolid, and moxifloxacin. Vancomycin, cefazoline, ceftriaxone,

Table 16-27 Systemic Antimicrobial Agents With Adequate Ocular Penetration

Antibacterial Agents	Antifungal Agents	Antiviral Agents
Meropenem	Fluconazole	Valacyclovir
Linezolid	Voriconazole	Valganciclovir
Moxifloxacin		Famciclovir
Vancomycin		Ganciclovir
Cefazoline		Foscarnet
Ceftriaxone		Cidofovir
Ceftazidime		
Imipenem		
Trimethoprim-sulfamethoxazole		

ceftazidime, imipenem, and trimethoprim-sulfamethoxazole are able to reach therapeutic levels that justify their use in specific situations. Available data do not support the use of systemically administered ciprofloxacin, levofloxacin, aminoglycosides, aminopenicillins, piperacillin, cefepime, or clarithromycin.

Various antifungal agents also achieve adequate intraocular concentration when administered systemically. Studies showed that fluconazole and voriconazole achieve good ocular penetration and clinical efficacy when administered systemically. However, amphotericin, echinocandins, micafungin, caspofungin, and anidulafungin penetrate ocular compartments poorly. Very few data are available regarding posaconazole.

Several antiviral agents are efficacious for treatment of intraocular viral infections. Orally administered valacyclovir, valganciclovir, and famciclovir can result in substantial vitreous penetration. Several other intravenously administered antiviral agents are efficacious in treating viral retinitis, including ganciclovir, foscarnet, and cidofovir.

CLINICAL PEARL

Systemically administered antimicrobial agents are helpful in the management of potential endophthalmitis, especially in patients with open globe injuries.

Brockhaus L, Goldblum D, Eggenschwiler L, Zimmerli S, Marzolini C. Revisiting systemic treatment of bacterial endophthalmitis: a review of intravitreal penetration of systemic antibiotics. *Clin Microbiol Infect.* 2019;25(11):1364–1369.

Local Anesthetics

Overview

Local anesthetics are used extensively in ophthalmology. Topical preparations yield corneal and conjunctival anesthesia that allows comfortable performance of examination techniques, such as tonometry, gonioscopy, removal of superficial foreign bodies, corneal scraping for bacteriologic studies, and paracentesis, as well as for use of contact lenses

associated with fundus examination and laser procedures. Topical and intracameral anesthesia has also gained increasing acceptance in cataract, pterygium, and glaucoma surgery. Local sub-Tenon, retrobulbar, peribulbar, and eyelid blocks yield excellent anesthesia and akinesia for intraocular and orbital surgery (Tables 16-28, 16-29).

The local anesthetic drugs used in ophthalmology are tertiary amines linked by either ester or amide bonds to an aromatic residue. Because the protonated form is far more soluble and these compounds undergo hydrolysis more slowly in acidic solutions, local anesthetic drugs are supplied in the form of their hydrochloride salts. When exposed to tissue fluids at pH 7.4, approximately 5%–20% of the anesthetic agent's molecules will be in the unprotonated form, as determined by the pK_a value (8.0–9.0) of the individual drug. The more lipid-soluble unprotonated form penetrates the lipid-rich myelin sheath and cell membrane of axons. Once inside, most of the molecules are again protonated. The protonated form gains access to and blocks the sodium channels on the inner wall of the cell membrane and increases the threshold for electrical excitability. As increasing numbers of sodium channels are blocked, nerve conduction is impeded and finally blocked.

After administration of a local anesthetic, small or unmyelinated nerve fibers are blocked the most quickly because their higher discharge rates open sodium channel gates more frequently and because conduction can be prevented by the disruption of a shorter axon. In unmyelinated fibers, the action potential spreads continuously along the axon. In myelinated fibers, the action potential spreads by saltation. Thus, only a short length of an unmyelinated fiber needs to be functionally interrupted, whereas 1 or more nodes must be blocked in a myelinated fiber. In larger myelinated fibers, the nodes are farther apart.

Table 16-28 Regional Anesthetic Drugs

Generic Name (Trade Name)	Concentration (Maximum Dose[a])	Onset of Action	Duration of Action	Major Advantages/ Disadvantages
Bupivacaine[b] (Marcaine, Sensorcaine)	0.25%–0.75% (175 mg)	5–11 min	480–720 min (with epinephrine) 480 min (without epinephrine)	Long duration of action/increased toxicity to the extraocular muscles
Lidocaine[b] (Anestacaine, Xylocaine)	0.5%–2%, 4% (300 mg/ 4.5 mg/kg)	4–6 min	40–60 min; 120 min (with epinephrine)	Spreads readily without hyaluronidase
Mepivacaine[b] (Carbocaine)	1%–2% (400 mg)	3–5 min	120 min	Duration of action greater without epinephrine
Procaine[c] (Novocain)	1%–2% (1000 mg)	7–8 min	30–45 min; 60 min (with epinephrine)	Short duration of action; poor absorption from mucous membranes

[a] Maximum dose stated for single dose without epinephrine. The maximum dose is contingent on whether a vasoconstrictor (epinephrine) was also used. Please consult the package insert.
[b] Amide-type compound.
[c] Ester-type compound.

Table 16-29 Topical Anesthetic Drugs

Generic Name	Trade Name	Strength
Cocaine		1%–4%
Fluorescein sodium/benoxinate HCl (oxybuprocaine)	Fluress	0.25%/0.4%
	Flurox	0.25%
	Available generically	0.25%
Lidocaine HCl	Xylocaine	4%
	Akten	3.5%
Proparacaine HCl	Alcaine	0.5%
	Parcaine	0.5%
	Ophthetic	0.5%
	Available generically	0.5%
Tetracaine HCl	Altacaine	0.5%
	TetraVisc	0.5%
	Available generically	0.5%

Clinically, local anesthetics first block the poorly myelinated and narrow parasympathetic fibers (as evidenced by pupil dilation) and sympathetic fibers (vasodilation), followed by the sensory fibers (pain and temperature), and finally the larger and more myelinated motor fibers (akinesia). The optic nerve, which is enclosed in a meningeal lining, is often not blocked by retrobulbar injections.

For retrobulbar blocks, amide local anesthetics are preferred to ester drugs because the amides have a longer duration of action and less systemic toxicity. Amide local anesthetics are not metabolized locally but are inactivated in the liver primarily by dealkylation; thus, their duration of action is partly determined by diffusion from the site of injection.

Ester anesthetics are susceptible to hydrolysis by serum cholinesterases in ocular vessels as well as by metabolism in the liver. When serum cholinesterase levels are low because of treatment with echothiophate eyedrops or a hereditary serum cholinesterase deficiency, toxicity may occur at lower doses of ester anesthetics.

The toxic manifestations of local anesthetics are generally related to the dose. However, patients with severe hepatic insufficiency may have symptoms of toxicity even at lower doses of either amide or ester local anesthetics. These manifestations include restlessness and tremor that may proceed to convulsions and respiratory and myocardial depression. CNS stimulation can be counteracted by intravenous diazepam; respiratory depression calls for ventilatory support.

Because local anesthetics block sympathetic vascular tone and dilate vessels, a 1:200,000 concentration of epinephrine is frequently added to shorter-acting drugs to retard vascular absorption. Such use of epinephrine raises circulating catecholamine levels and may cause systemic hypertension and cardiac arrhythmias.

Topically applied anesthetics disrupt intercellular tight junctions, increasing corneal epithelial permeability to subsequently administered drugs (ie, dilating drops). They also interfere with corneal epithelial metabolism and repair and thus cannot be used for long-term pain relief. Because topical anesthetics can become drugs of abuse that can eventually lead to chronic pain syndromes and vision loss, they should not be dispensed to patients.

Specific Drugs

Lidocaine is an amide local anesthetic used in strengths of 0.5%, 1%, and 2% (with or without epinephrine) for injection; 2% and 3.5% as a gel; and 4% as a solution for topical mucosal anesthesia. It yields a rapid (4–6-minute) retrobulbar or eyelid block that lasts about an hour (2 hours with epinephrine). The topical solution, applied to the conjunctiva with a cotton swab for 1–2 minutes, can reduce the discomfort of subconjunctival injections. Topical lidocaine is preferable to cocaine or proparacaine for conjunctival biopsy because it has less effect on epithelial morphology. Lidocaine is also extremely useful for cough suppression during ocular surgery. For local injection in adults, the maximum safe dose of the 2% solution is 15 mL. A common adverse effect is drowsiness.

Mepivacaine is an amide drug used in strengths of 1%–3% (with or without a vasoconstrictor). It has a rapid onset and lasts approximately 2 hours; 2% is the most commonly used strength and has a maximum safe dose of 25 mL.

Bupivacaine is an amide anesthetic with a slower onset of action than lidocaine. It may yield relatively poor akinesia but has the advantage of a long duration of action, up to 8 hours without epinephrine. It is available in 0.25%–0.75% solutions (with or without epinephrine) and is frequently administered in a mixture with lidocaine or mepivacaine to achieve a rapid, complete, and long-lasting effect. The maximum safe dose of a 0.75% solution is 25 mL.

Hyaluronidase can be combined with local injection of anesthetics to increase the dispersion of anesthetic drugs for intraocular, adnexal, or orbital surgery. Hyaluronidase catalyzes the hydrolysis of hyaluronic acid, a constituent of the extracellular matrix; it temporarily lowers the viscosity of the extracellular matrix and increases tissue permeability. Increased dispersion of the anesthetic drug may reduce the IOP rise in the limited orbital space, minimize distortion of the surgical site, decrease the risks of postoperative strabismus and myotoxicity, and increase akinesia of the globe and eyelid. In addition, lower volumes of anesthetic may be used.

Hyaluronidase products approved by the FDA include those derived from bovine and ovine sources, as well as a recombinant human product. Because of a lack of reliable animal sources and a shortage of supply from manufacturers, compounded formulations of hyaluronidase from animal-derived active pharmaceutical ingredients are only occasionally used. FDA regulations for compounding pharmacies are not as stringent as are regulations for pharmaceutical products, and concerns have been raised about the potency and purity of compounded hyaluronidase products from animal sources. There have been reports of hypersensitivity reactions to retrobulbar or peribulbar blocks associated with use of animal-derived hyaluronidase. For retrobulbar or peribulbar injection, 1 mL of hyaluronidase (150 USP U/mL; single-dose vial of recombinant human product) can be added to a syringe of the anesthetic to be administered.

Several other drugs are commonly used for topical anesthesia of the ocular surface. Because of their higher lipid solubilities, these medications have a more rapid onset than other topical anesthetics; thus, the initial discomfort caused by the drops is reduced. Proparacaine is an ester anesthetic available as a 0.5% solution. The least irritating of the topical anesthetics, it has a rapid onset of approximately 15 seconds and a duration of approximately 20 minutes. Its structure is different enough from that of other local anesthetics that cross-sensitization apparently does not occur.

CLINICAL PEARL

Used without a preservative, proparacaine reportedly does not inhibit the growth of *Staphylococcus, Candida,* or *Pseudomonas,* so it may be preferred to other drugs for corneal anesthesia before obtaining a scraping for culture from a corneal ulcer.

Benoxinate (also known as *oxybuprocaine*) is an ester anesthetic available in a 0.4% solution with fluorescein for use in tonometry. Its onset and duration are similar to those of proparacaine. Benoxinate is also available alone as a topical anesthetic in Europe.

Tetracaine is an ester anesthetic available in 0.5% solution and approved for short-duration ocular surface procedures. Its onset of action and duration of action are longer than those of proparacaine, and it causes more extensive corneal epithelial toxicity.

Anesthetics in Intraocular Surgery

Topical

The first modern application of topical anesthetics in ophthalmology was Koller's use of cocaine in 1884. Since then, synthetic drugs have become available; cocaine is no longer used because of the potential risk of adverse effects and drug abuse. Tetracaine, 0.5%, and proparacaine, 0.5%, are short-acting (20 minutes) drugs and are the least toxic of the regional and topical anesthetics to the corneal epithelium. Lidocaine, 4%, for injection can be used topically, as can lidocaine jelly, 2% (off-label) and 3.5% (Akten: FDA-approved, preservative-free).

The aim of topical anesthetics is to block the nerves that supply the superficial cornea and conjunctiva—namely, the long and short ciliary nerves. Patients should be warned that they will experience some stinging upon application of the drops onto the surface of the cornea.

Topical anesthetics may be combined with subconjunctival anesthetics. Such combinations are well tolerated by patients and allow subconjunctival and scleral manipulations to be carried out. Alternatively, if topical anesthesia is not sufficient, it can be supplemented intraoperatively with a sub-Tenon infusion of anesthetic using a blunt cannula. Sub-Tenon injection can also be used as a primary method of achieving anesthesia; see the section "Sub-Tenon anesthesia."

In a retrospective series involving a large sample size, one of the potential risk factors for acute-onset endophthalmitis after temporal clear cornea incision phacoemulsification was application of lidocaine gel, 2%, before povidone-iodine preparation. It did not, however, significantly alter rates of endophthalmitis after intravitreal injection.

Intraocular lidocaine

Intraocular lidocaine has been used to provide analgesia during surgery. The solution used is 0.3 mL of 1% isotonic nonpreserved lidocaine administered intracamerally. No adverse effects have been reported, except for possible transient retinal toxicity when lidocaine was injected posteriorly in the absence of a posterior capsule. Intracameral lidocaine obviates the need for intravenous and regional anesthetic supplementation in most patients. Adequate anesthesia is obtained in approximately 10 seconds. As with topical techniques, patient cooperation during surgery is desirable. Contrasting studies have shown no difference in the degree of cooperation regardless of whether intracameral lidocaine was used as a supplement

to topical anesthetics. Because of unreliable patient cooperation, topical and intracameral anesthetics should be used cautiously, if at all, in patients with deafness, dementia, and severe photophobia.

Peribulbar and retrobulbar anesthesia

As stated previously, a mixture of lidocaine and bupivacaine in equal ratio is commonly used for peribulbar or retrobulbar anesthesia. This can be supplemented with hyaluronidase depending on technique and surgeon preference. Before injecting, it is important to pull back on the plunger to ensure that no blood or clear fluid is aspirated into the needle hub. The presence of blood indicates possible intravascular entry, where injection could lead to cardiac arrhythmia. Aspiration of clear fluid suggests the presence of CSF, meaning injection could lead to respiratory depression and seizures. The latter is more likely with the retrobulbar technique. For further discussion of peribulbar and retrobulbar anesthesia and other techniques, see BCSC Section 11, *Lens and Cataract.*

Peribulbar and retrobulbar injections of anesthetics frequently consist of mixtures of lidocaine, bupivacaine, and hyaluronidase. The lidocaine provides rapid onset, and the bupivacaine provides sustained anesthesia. The hyaluronidase promotes diffusion of the block and may reduce the volume of anesthetic delivered into the orbit.

Sub-Tenon anesthesia

Sub-Tenon anesthesia can used as a supplement to the primary methods, discussed previously, or as a primary method in itself for intraocular surgery (Video 16-1). Primary sub-Tenon block has been reported to have lower rates of intraoperative complications than do peribulbar or retrobublar anesthesia during cataract surgery and is employed as a primary method of anesthesia by some surgeons. After creating a localized conjunctival peritomy, usually in the infranasal quadrant, sub-Tenon anesthesia is delivered using a curved blunt-tip canula. Overall, complications from sub-Tenon delivery are similar to those in peri- and retrobulbar techniques. Needle delivery resulted in higher rates of complications than with blunt-tip cannulas. The relative limitations of sub-Tenon anesthesia include prior injections in that quadrant, a history of ocular trauma, and prior vitreoretinal, strabismus, or glaucoma surgery. These conditions may be associated with scarring, which may limit diffusion of the block.

VIDEO 16-1 New technique for administering a sub-Tenon block.
Courtesy of Samir A. Nazarali, MD.

Crandall AS. Anesthesia modalities for cataract surgery. *Curr Opin Ophthalmol.* 2001;12(1):9–11.

Kansal S, Moster MR, Gomes MC, Schmidt CM Jr, Wilson RP. Patient comfort with combined anterior sub-Tenon's, topical, and intracameral anesthesia versus retrobulbar anesthesia in trabeculectomy, phacotrabeculectomy, and aqueous shunt surgery. *Ophthalmic Surg Lasers.* 2002;33(6):456–462.

Retrobulbar alcohol/chlorpromazine

Retrobulbar injection of absolute alcholol (ethanol 80%–100%) is used to achieve pain relief in patients with blind, painful eyes. The first step is to pretreat with retrobulbar anesthesia, as previously described. A recent study used 1.5 mL of the anesthetic mixture followed by 1.5 mL of absolute alcohol; another study used 2 mL of alcohol. The reported success rate of this procedure varied from 20%–87% in patients. The duration of action following injection is also variable. A study comparing retrobulbar alcohol (1.5 mL, 100% ethanol) to chlorpromazine (1.5 ml, 25 mg/mL) revealed similar efficacy between the 2 medications.

Galindo-Ferreiro A, Akaishi P, Cruz A, et al. Retrobulbar injections for blind painful eyes: a comparative study of retrobulbar alcohol versus chlorpromazine. *J Glaucoma.* 2016;25(11):886–890.

Purified Neurotoxin Complex

Botulinum toxin type A is produced from cultures of the Hall strain of *Clostridium botulinum*. It blocks neuromuscular conduction by binding to receptor sites on motor nerve terminals, entering the nerve terminals and inhibiting the release of acetylcholine. Botulinum toxin type A injections provide effective relief of the excessive, abnormal contractions associated with benign essential blepharospasm and hemifacial spasm. Cosmetic use of botulinum toxin, specifically in the treatment of glabellar folds, is popular as well. Botulinum is FDA-approved for the treatment of strabismus; it may function by inducing atrophic lengthening of the injected muscle and corresponding shortening of the muscle's antagonist (see also BCSC Section 6, *Pediatric Ophthalmology and Strabismus,* and Section 7, *Oculofacial Plastic and Orbital Surgery*).

Issaho DC, Carvalho FRS, Tabuse MKU, Carrijo-Carvalho LC, de Freitas D. The use of botulinum toxin to treat infantile esotropia: a systematic review with meta-analysis. *Invest Ophthalmol Vis Sci*. 2017;58(12):5468–5476.

Khan JA, Steinsapir KD, McCracken M. Facial fillers, botulinum toxin, and facial rejuvenation. *Focal Points: Clinical Modules for Ophthalmologists.* American Academy of Ophthalmology; 2011: module 4.

Hyperosmolar Drugs

Topical hyperosmolar drugs are used to decrease corneal and epithelial edema. One such drug is sodium chloride, which is available without a prescription in a 2% or 5% solution or as an ointment. These products are used to treat corneal edema from Fuchs endothelial corneal dystrophy, other causes of endothelial dysfunction, postoperative prolonged edema, and recurrent erosion syndrome.

Irrigating Solutions

Sterile isotonic solutions are available for general ophthalmic use. Depending on the solution, nonprescription ocular irrigating solutions may contain sodium chloride, potassium chloride, calcium chloride, magnesium chloride, sodium acetate, sodium citrate, boric acid, sodium

borate, and sodium phosphate. They are preserved with EDTA, benzalkonium chloride, and sorbic acid. Sterile, physiologically balanced, preservative-free salt solutions are isotonic to eye tissues and are used for intraocular irrigation during surgical procedures. Postoperatively, a solution of glucose, glutathione, and bicarbonate causes the least change in the corneal endothelial morphology and augments endothelial pump function. It is not routinely used because of cost concerns, but it may be used preoperatively in patients who have compromised corneas.

Diagnostic Agents and Surgical Adjuvants

Solutions commonly used in the examination and diagnosis of external ocular diseases include fluorescein, 2%; lissamine green, 1%; and rose bengal staining as impregnated paper strips. The first 2 stains outline defects of the conjunctival and corneal epithelium, whereas rose bengal staining indicates abnormal devitalized epithelial cells. A stinging sensation with instillation of these eyedrops is common.

Rose bengal has significant antiviral activity. Therefore, diagnostic use of rose bengal before viral culture may preclude a positive result, and its use to grade keratitis in the study of new antiviral drugs is discouraged.

For the study of retinal and choroidal circulation as well as abnormalities in the retinal pigment epithelium (RPE), sodium fluorescein solution in a concentration of 5%, 10%, or 25% is injected intravenously. Fundus fluorescein angiography is helpful in diagnosing various vascular diseases and neoplastic disorders. Adverse effects range from localized skin reactions to hypersensitivity and allergic reactions. The most common adverse effect is nausea, occurring in up to 10% of patients.

Indocyanine green (ICG), a tricarbocyanine dye, is approved for the study of choroidal vasculature in a variety of choroidal and retinal disorders. ICG angiography is particularly helpful in identifying and delineating poorly defined choroidal neovascular membranes in eyes with age-related macular degeneration (AMD). ICG angiography can also be used to evaluate patients with anterior scleritis. Typically, 25 mg of dye is injected as an IV solution. ICG is mildly toxic; adverse effects include localized skin reactions, sore throat, and hot flushes. Individual cases of severe adverse effects, such as anaphylactic shock, hypotension, tachycardia, dyspnea, and urticaria, have been reported.

ICG and trypan blue dye are useful for delineating the anterior capsule during phacoemulsification of mature cataracts. Although the FDA has approved trypan blue as an anterior capsule stain during surgery, administration of ICG for this purpose constitutes an off-label use.

ICG, trypan blue, and triamcinolone acetonide are also utilized off-label to facilitate internal membrane (ILM) peeling in macular-hole repair. The preservative-free formulation of triamcinolone acetonide is FDA-approved for intraoperative visualization of the vitreous. Although literature has raised concerns about the toxicity of ICG dye in the retina and RPE, good surgical and visual results have been reported. The toxicity of ICG on cultured RPE cells may be related to the hypoosmolarity of the solvent. Short exposure to trypan blue has not had a toxic effect on cultured RPE cells. However, trypan blue does not appear to stain the ILM as effectively as ICG does. Exposure of the retina to the dye and pooling at the macular hole should be minimized to reduce concerns about retinal toxicity.

Brilliant Blue G (BBG) is the only dye that is FDA-approved to stain the ILM. This premixed solution is injected onto the ILM. It is recommended to allow the dye to remain for 60 seconds prior to removal. The preparation of the solution allows it to stain the ILM, even in the fluid-filled vitreous cavity. In addition, BBG selectively stains the ILM, not an epiretinal membrane or the retina. No adverse effects from the dye itself have been reported.

Azuma K, Noda Y, Hirasawa K, Ueta T. Brilliant Blue G–assisted internal limiting membrane peeling for macular hole: a systematic review of literature and meta-analysis. *Retina.* 2016;36(5):851–858.

Haritoglou C, Gandorfer A, Gass CA, Schaumberger M, Ulbig MW, Kampik A. The effect of indocyanine-green on functional outcome of macular pucker surgery. *Am J Ophthalmol.* 2003;135(3):328–337.

Korb DR, Herman JP, Finnemore VM, Exford JM, Blackie CA. An evaluation of the efficacy of fluorescein, rose bengal, lissamine green, and a new dye mixture for ocular surface staining. *Eye Contact Lens.* 2008;34(1):61–64.

Saini JS, Jain AK, Sukhija J, Gupta P, Saroha V. Anterior and posterior capsulorhexis in pediatric cataract surgery with or without trypan blue dye: randomized prospective clinical study. *J Cataract Refract Surg.* 2003;29(9):1733–1737.

Werner L, Pandey SK, Escobar-Gomez M, Hoddinott DS, Apple DJ. Dye-enhanced cataract surgery. Part 2: learning critical steps of phacoemulsification. *J Cataract Refract Surg.* 2000;26(7):1060–1065.

Ophthalmic Viscosurgical Devices

Ophthalmic viscosurgical devices (OVDs) protect ocular tissues, such as the corneal endothelium and epithelium, from surgical trauma; help maintain the intraocular space; and facilitate tissue manipulation. Thus, they are indispensable tools in cataract and glaucoma surgery, penetrating keratoplasty, anterior segment reconstruction, and retinal surgery. Chemical and physical properties of OVDs include the capacity to resist flow and deformation. OVDs for ophthalmic use must also be inert, isosmotic, sterile, nonpyrogenic, nonantigenic, and optically clear. In addition, they must be sufficiently hydrophilic to allow easy dilution and irrigation from the eye. Naturally occurring and synthetic compounds available in various concentrations include sodium hyaluronate, chondroitin sulfate, hydroxypropyl methylcellulose, and polyacrylamide. Combined chondroitin sulfate/sodium hyaluronate materials are also available.

The 2 basic categories of OVDs are cohesive and dispersive. A cohesive OVD has a higher molecular weight and surface tension and tends to cohere to itself. A dispersive OVD has a lower molecular weight and surface tension and tends to coat intraocular structures. Available OVDs form a continuum on the basis of their cohesive and dispersive properties. The Healon, Healon GV, and Healon5 products are mostly cohesive, and Ocucoat and Viscoat are mostly dispersive. There are also single agents with both cohesive and dispersive properties. (See also BCSC Section 11, *Lens and Cataract.*)

Riedel PJ. Ophthalmic viscosurgical devices. *Focal Points: Clinical Modules for Ophthalmologists.* American Academy of Ophthalmology; 2012: module 7.

Fibrinolytic Agents

Fibrinolytic agents include tissue plasminogen activator (tPA), urokinase, and streptokinase. tPA is a naturally occurring serine protease with a molecular mass of 68 kD. Because tPA is normally present at a higher concentration in the aqueous humor of the human eye than in blood, it is less toxic to ocular tissues than other fibrinolytic agents and is specific for dissolution of fibrin clots. tPA has been used successfully to resolve fibrin clots after intraocular surgery, vitrectomy, keratoplasty, glaucoma filtering procedures, and subretinal hemorrhage due to choroidal neovascularization. These drugs are not approved by the FDA for ocular use and are therefore used off-label.

Chang W, Garg SJ, Maturi R, et al. Management of thick submacular hemorrhage with subretinal tissue plasminogen activator and pneumatic displacement for age-related macular degeneration. *Am J Ophthalmol.* 2014;157(6):1250–1257.

Dotan A, Kaiserman I, Kremer I, Ehrlich R, Bahar I. Intracameral recombinant tissue plasminogen activator (r-tPA) for refractory toxic anterior segment syndrome. *Br J Ophthalmol.* 2014;98(2):252–255.

Zalta AH, Sweeney CP, Zalta AK, Kaufman AH. Intracameral tissue plasminogen activator use in a large series of eyes with valved glaucoma drainage implants. *Arch Ophthalmol.* 2002;120(11):1487–1493.

Thrombin

Thrombin, a sterile protein substance, is approved for the control of hemorrhage from accessible capillaries and small venules, as observed with standard surface incisions. Its use in maintaining hemostasis during complicated intraocular surgery is off-label because such use requires injection. Intravitreal thrombin has been used to control intraocular hemorrhage during vitrectomy. The addition of thrombin (100 U/mL) to the vitrectomy infusate significantly shortens intraocular bleeding time, and thrombin produced by DNA recombinant techniques minimizes the degree of postoperative inflammation. Thrombin causes significant ultrastructural corneal endothelial changes in human corneas when they are exposed to 1000 U/mL.

Fibrin sealant is a biological tissue adhesive that includes a fibrinogen component and a thrombin component, both of which are prepared from pooled human plasma. When activated by thrombin, a solution of human fibrinogen imitates the final stages of the coagulation cascade. Fibrin sealant has been used widely in ophthalmic surgeries, including as a substitute for suturing in conjunctival or corneal wound closures, in fixing conjunctival autografts during pterygium surgery, for closing or preventing corneal perforation, during amniotic membrane transplantation, and in a variety of oculoplastic surgeries. It also has the advantage of reducing the total surgical time. However, the use of fibrin sealant in ophthalmic surgery is off-label.

The tissue sealant is applied as a thin layer to ensure that it covers the entire intended application area. Preparation of this product for application must adhere to the manufacturer's instructions. The incidence of allergic reactions is low, but anaphylactic reactions have been reported after its application.

Antifibrinolytic Agents

Antifibrinolytic drugs, such as ε-aminocaproic acid and tranexamic acid, inhibit the activation of plasminogen. These medications may be used systemically to treat patients with hemorrhage secondary to excessive fibrinolysis and to prevent recurrent hyphema, which most commonly occurs 2–6 days after the original hemorrhage. These agents are contraindicated in the presence of active intravascular clotting, such as diffuse intravascular coagulation, because they can increase the risk of thrombosis. They should not be used in pregnant patients, in patients with coagulopathies or who are receiving platelet inhibition therapy, or in patients with renal or hepatic disease. Patients with larger hyphemas and those with delayed presentation are at high risk of rebleeding, but patients with early presentation and those with smaller hyphemas are at low risk of rebleeding. ε-Aminocaproic acid is usually reserved for patients at higher risk of rebleeding.

ε-Aminocaproic acid is used in a dosage of 50–100 mg/kg every 4 hours, up to 30 g daily. Possible adverse reactions include nausea, vomiting, myopathy, hematologic dyscrasia, epiphora, nasal congestion, headache, rash, pruritus, dyspnea, confusion, cardiac arrhythmias, and systemic hypotension. Gastrointestinal adverse effects are similar with doses of either 50 or 100 mg/kg. The drug should be continued for a full 5–6 days to achieve maximal clinical effectiveness. Topical ε-aminocaproic acid may be an attractive alternative to systemic delivery in the treatment of traumatic hyphema, but the efficacy of topical use has been questioned. Optimal topical concentration to maximize aqueous levels and minimize corneal epithelial toxicity is 30% ε-aminocaproic acid in 2% carboxypolymethylene.

Tranexamic acid is used off-label to reduce the incidence of rebleeding after traumatic hyphema. It is 10 times more potent in vitro than ε-aminocaproic acid. The usual dosage is 25 mg/kg of tranexamic acid 3 times daily for 3–5 days. Gastrointestinal adverse effects are rare.

Vitamin Supplements and Antioxidants

Nonprescription vitamin supplements have had increased popularity because of their antioxidant properties and are used for intermediate to severe AMD. The Age-Related Eye Disease Studies 1 and 2 are discussed in depth in BCSC Section 12, *Retina and Vitreous.* In addition, omega-3 fatty acid supplements may have some benefit in treating meibomian gland dysfunction (see BCSC Section 8, *External Disease and Cornea*).

Interferon

A naturally occurring species-specific defense against viruses, interferon is synthesized intracellularly and increases resistance to viral infection. Synthetic analogues such as polyinosinic acid–polycytidylic acid have induced patients to form their own interferon.

Topically administered interferon (off-label) is ineffective in the treatment of epidemic keratoconjunctivitis caused by adenovirus. Likewise, interferon alone has little effect on herpes simplex keratitis. In combination, however, it seems to act as a topical adjuvant to

traditional antiviral therapy in resistant herpes simplex keratitis. In a study of patients with herpes simplex keratitis, interferon used in conjunction with acyclovir yielded significantly faster healing time than did treatment with acyclovir alone (5.8 vs 9.0 days, respectively). Interferon also speeds the healing of epithelial defects when used in combination with trifluridine. The dosage of interferon (30 million IU/mL) is 2 drops per day for the first 3 days of treatment.

Interferon also has been shown to inhibit vascular endothelial cell proliferation and differentiation. It is particularly effective in the treatment of juvenile pulmonary hemangiomatosis, which was fatal before the development of interferon. Interferon alfa-2b (off-label), administered subconjunctivally, intralesionally, and/or topically, is a treatment option for conjunctival intraepithelial neoplasia and invasive squamous cell carcinoma (see BCSC Section 8, *External Disease and Cornea*). Intralesional administration of interferon is reported to be especially effective in patients with ocular Kaposi sarcoma.

Interferons also exhibit immunomodulatory characteristics. Their off-label use in the management of uveitis has been evaluated in several studies (see Table 16-17 and BCSC Section 9, *Uveitis and Ocular Inflamation*).

Growth Factors and Growth Factor Inhibitors

Growth Factors

Growth factors are a diverse group of proteins that act at autocrine and paracrine levels to affect various cellular processes, including metabolic regulation, tissue differentiation, cell growth and proliferation, maintenance of viability, and changes in cell morphology. Growth factors are synthesized in a variety of cells and have a spectrum of target cells and tissues. The following growth factors have been found in retinal tissues, vitreous humor, aqueous humor, and corneal tissues:

- epidermal growth factor
- fibroblast growth factors
- transforming growth factor βs
- vascular endothelial growth factor (VEGF)
- insulin-like growth factors
- platelet-derived growth factor

These growth factors are capable of diverse, synergistic, and sometimes antagonistic biological activities.

Under normal physiologic conditions, the complex and delicate coordination of both the effects of and the interactions among growth factors maintains the homeostasis of intraocular tissues. The net effect of a growth factor depends on its bioavailability, which is determined by its concentration, its binding to carrier proteins, the level of its receptor in the target tissue, and the presence of complementary or antagonistic regulatory factors.

Pathologically, the breakdown of the blood–ocular barrier disrupts the balance among growth factors in the ocular media and tissues and may result in various abnormalities. Disruption in the balance among isoforms of transforming growth factor βs, basic

fibroblast growth factor, VEGF, and insulin-like growth factors is thought to cause ocular neovascularization. Transforming growth factor βs and platelet-derived growth factor are also implicated in the pathogenesis of proliferative vitreoretinopathy and in the excessive proliferation of Tenon capsule fibroblasts, which can result in scarring of the glaucoma filtration bleb. Increased concentrations of insulin-like growth factors in plasmoid aqueous humor may be responsible for the abnormal hyperplastic response of the lens epithelium and corneal endothelium observed in eyes with inflammatory conditions and in those with ocular trauma.

Identifying growth factors and understanding their mechanisms of action in the eye can provide the ophthalmologist with new methods for manipulation of and intervention in ocular disorders. Epidermal and fibroblast growth factors can accelerate corneal wound repair after surgery, chemical burns, or ulcers and can increase the number of corneal endothelial cells. Fibroblast growth factor also was shown to delay the process of retinal dystrophy in Royal College of Surgeons rats.

Historically, ophthalmic interventions have targeted growth factor inhibition (see the section Growth Factor Inhibitors later in this chapter). Cenegermin (20 μg/mL of recombinant human nerve growth factor [NGF]) is the first drug approved by the FDA for the management of neurotrophic keratopathy. NGF is a neurotrophin that supports epithelial integrity through high-affinity receptors found in the cornea and conjunctiva. When administered topically 6 times daily at 2-hour intervals for an 8-week course, cenegermin demonstrated a greater than twofold higher rate of corneal healing as well as shorter healing times compared with its vehicle alone. However, despite its effects on healing, no improvement in anethesiometry was observed in the treatment group compared with the control group. See BCSC Section 8*, External Disease and Cornea,* for further discussion on neurotrophic keratopathy.

Vascular endothelial growth factor

VEGF, also known as vasculotropin, deserves special mention. It is a dimeric, heparin-binding, polypeptide mitogen with 4 isoforms that are generated from alternative splicing of mRNA. The *VEGF* gene is widely expressed in actively proliferating vascular tissue and is implicated in the pathogenesis of various retinovascular conditions. Through various receptors, VEGF promotes vascular permeability and drives the development of neovascularization.

The VEGF family of glycoproteins includes VEGF-A, -B, -C, and -D, as well as placental growth factor (PlGF). Currently the most thoroughly studied, VEGF-A has 9 isoforms and is the only VEGF family member induced by hypoxia. VEGF-A promotes blood vessel growth and is a potent inducer of vascular permeability. VEGF-C and VEGF-D regulate lymphangiogenesis.

VEGF receptors (VEGFRs) are tyrosine kinases. Three VEGFRs have been identified:

- VEGFR-1 has high affinity for VEGF-A, VEGF-B, and PlGF and acts as a negative regulator of VEGF-A signaling by limiting the amount of ligand available to VEGFR-2.
- VEGFR-2 is the primary mediator of the mitogenic, angiogenic, and vascular permeability effects of VEGF-A.
- VEGFR-3 mediates the angiogenic effects of VEGF-C and VEGF-D on lymphatic vessels.

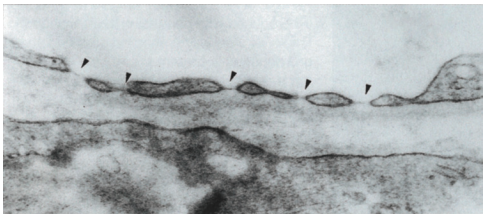


Figure 16-7 Transmission electron micrograph demonstrating vascular endothelial growth factor (VEGF)–mediated breakdown of the blood–retinal barrier where fenestrations develop *(arrowheads)*. VEGF is significantly more potent than histamine in inducing vascular permeability and is a major factor leading to macular edema in retinal vascular disease. *(Courtesy of Wallow IH, Geldner PS. Endothelial fenestrae in proliferative diabetic retinopathy.* Invest Ophthalmol Vis Sci. *1980;19(10):1181:Fig 6.)*

In the developing retina, new blood vessel growth occurs via 2 VEGF-driven processes: vasculogenesis and angiogenesis. Vasculogenesis refers to development of blood vessels from mesenchymal precursors; angiogenesis is the growth of new blood vessels from existing vessels. In the mature retina, new blood vessel growth occurs via angiogenesis as a result of a pathologic process. The mature retina cannot support the remodeling of the extracellular matrix required for angiogenesis; thus, retinal neovascularization extends into the vitreous as long as the vitreous is attached to the retina at that location. Secondary vitreous hemorrhage and tractional retinal detachment can ensue.

VEGF also drives angiogenesis at the level of the choroid, leading to the development of choroidal neovascular membranes and secondary sight threatening complications. Finally, and equally important, VEGF-mediated breakdown of the inner blood–retinal barrier can lead to macular edema and vision loss in a variety of retinal vascular conditions (Fig 16-7).

Growth Factor Inhibitors

VEGF inhibitors

Intravitreal injections of VEGF inhibitors (Table 16-30) are typically used to treat complications resulting from diabetes, retinal vein occlusion, and neovascular ("wet") AMD. Patients with choroidal neovascularization who were treated with anti-VEGF agents showed a slower loss of vision than occurred in those in the control group, especially moderate (>3 lines of vision lost) to severe (>6 lines lost) vision loss, and in many cases, an improvement in vision (≥3 lines of visual acuity). Pegaptanib, which specifically blocks the VEGF-A165 isoform, was the first drug approved for the treatment of choroidal neovascularization. It requires intravitreal injections every 6 weeks for up to 2 years. Newer drugs have largely supplanted pegaptanib.

Bevacizumab and ranibizumab block all isoforms of VEGF-A. Bevacizumab, a full-length antibody against VEGF approved for the IV treatment of advanced carcinomas, has been used extensively in ophthalmology for treatment of neovascular AMD, diabetic retinopathy, retinal vein occlusion, retinopathy of prematurity, and other chorioretinal vascular disorders. Ranibizumab is a monoclonal antibody fragment (Fab) derived from the same parent mouse antibody as bevacizumab and demonstrates similar efficacy. Pegaptanib and ranibizumab were developed for intraocular use, for which they are approved by the FDA, whereas the use of bevacizumab remains off-label. Although these drugs exhibit

Table 16-30 Intravitreal VEGF Inhibitors

Inhibitor (Target)	Brand Name	Dose/Interval	Indiciations
Pegaptinib sodium (VEGF-A165)	Macugen	0.3 mg/90 μl: every 6 wk	Neovascular AMD
Bevacizumab (VEGF-A)	Avastin	1.25 mg/50 μl: every 4–6 wk	Off-label use: Neovascular AMD and all other causes of CNV, CME, macular edema from RVO, DME, diabetic retinopathy, ROP
Ranibizumab (VEGF-A)	Lucentis	0.5 mg/50 μl: every 4 wk	Neovascular AMD, macular edema from RVO, myopic CNV
		0.3 mg/50 μl: every 4 wk	DME, diabetic retinopathy
Aflibercept (VEGF-A and PlGF)	Eylea	2 mg/50 μl: AMD: every 4 wk for 3 doses, then every 8 wk RVO: every 4 wk DME: every 4 wk for 5 doses, then every 8 wk	Neovascular AMD, macular edema from RVO, DME, diabetic retinopathy
Brolucizumab (VEGF-A)	Beovu	6 mg/50 μl: every 4 wk for 3 doses, then every 8–12 wk	Neovascular AMD
Faricimab (VEGF-A and Ang-2)	Vabysmo	6 mg/50 μl: every 4 wk for 4 doses, then every 8–16 wk	Neovascular AMD, DME

AMD = age related macular degeneration; Ang-2 = angiopoietin-2; CME = cystoid macular edema; CNV = choroidal neovascularization; DME = diabetic macular edema; PlGF = placental growth factor; ROP = retinopathy of prematurity; RVO = retinal vein occlusion; VEGF = vascular endothelial growth factor.

excellent safety profiles, ocular and systemic complications, particularly thromboembolic events, remain a concern for patients receiving therapy.

Aflibercept is a novel recombinant fusion protein engineered to bind all isoforms of VEGF-A and PlGF. PlGF inhibition enhances the total VEGF blockade by providing additional free Flt-1 receptors, which neutralize VEGF. Aflibercept has been approved for the treatment of neovascular AMD, retinal vein occlusions, and diabetic macular edema. It may have a longer duration of action than other anti-VEGF therapies; a monthly loading dose is administered for 3 months, after which the drug can be given every 2 months depending on the condition.

Brolucizumab is another anti-VEGF agent approved for the treatment of neovascular AMD. It is a humanized single-chain variable antibody fragment that has demonstrated efficacy in the treatment of neovascular AMD when dosed at 12-week intervals following a monthly loading dose. Although this medication offers a longer duration of action, it is associated with higher rates of noninfectious intraocular inflammation than are other anti-VEGF agents. Approval for use in additional conditions is pending with the FDA.

In January 2022, the FDA approved faricimab for the treatment of neovascular AMD and diabetic macular edema. Faricimab is a humanized immunoglobulin G molecule whose Fc

portion was modified to limit receptor interaction. In addition to binding VEGF-A, faricimab also blocks angiopoietin-2 (Ang-2). Interruption of the Ang-2 pathway provides an additional mechanism to support vascular stability. Both brolucizumab and faricimab obtained FDA approval through phase 3 trials in which they were compared to aflibercept, and both offer the possibility of longer treatment intervals after the initial loading dose period. In clinical trials, the rate of intraocular inflammation of faricimab was comparable to aflibercept (see BCSC Section 12, *Retina and Vitreous,* for additional information on VEGF inhibitors).

Insulin-like growth factor 1 receptor inhibitors

Teprotumumab is an insulin-like growth factor-1 receptor (IGF-1R) inhibitor approved for the management of active thyroid eye disease (TED). IGF-1R has been implicated in inflammatory pathways through stimulation of orbital fibrocytes in patients with TED. In clinical trials, teprotumumab demonstrated greater reduction in proptosis and improvement in diplopia compared with placebo at 24 weeks. In addition, more than half of the responders maintained this improvement at 51 weeks after the last treatment. Teprotumumab is administered intravenously at an initial dose of 10 mg/kg followed by 20 mg/kg given every 3 weeks for a total of 8 doses. Exacerbation of preexisting inflammatory bowel disease and hyperglycemia, particularly in patients with diabetes, needs to be considered when monitoring patients receiving this therapy (see BCSC Section 7, *Oculofacial Plastic and Orbital Surgery,* for additional information on the management of TED).

Biosimilar Drugs

In 2010, the Biologics Price Competition and Innovation Act was signed into law in the United States. It established a shortened FDA-regulated pathway for approval of biological products that are demonstrated to be biosimilar to or interchangeable with an existing FDA-approved product. The FDA defines a biosimilar as "a biological product that is highly similar to and has no clinically meaningful differences from an existing FDA-approved reference product." The FDA adds: "A manufacturer must also demonstrate that its proposed biosimilar product has no clinically meaningful differences from the reference product in terms of safety, purity, and potency (safety and effectiveness)."

Biosimilars are not generic medications (Table 16-31). Generic medications are copies of medications with simple chemical structures, whereas biosimilars require reengineering of a complex molecule that has more stringent regulatory standards.

As successful applications of biologic drugs increase in all fields of medicine, providing access to these treatments is paramount. The primary advantage of biosimilar drugs is cost. With biosimilar drugs, clinicians can use a clinically equivalent product at three-quarters of the cost. Biosimilars have numerous potential applications in ophthalmology where antibodies are currently being employed. The FDA has approved the following biosimilars for ophthalmic use:

- Alymsys (bevacizumab-maly)
- Byooviz (ranibizumab-nuna)
- Cimerli (ranibizumab-eqrn)
- Vegzelma (bevacizumab-abcd)

Table 16-31 Differences Between Generic and Biosmiliar Medications

	Generic Drugs	Biosimilar Drugs
Structure	Simple and identical to original molecule	Same amino acid sequence with different post-translation modifications and inactive components
Analysis	Current technology can fully demonstrate the structural similarity to the original molecule.	At present, only the similarity to the innovator molecule can be proven; full structural identification is not yet possible.
Manufacturing complexity	Simpler, organic pharmacologic chemical reactions	More complex and involves reverse engineering the innovator molecule; applies a biotechnological process
Approval	Demonstration of chemical similarity and purity can lead to marketing approval	Requires pharmacokinetic, pharmacodynamic studies and pharmacovigilance
Interchangeability and substitution	Can be easily substituted or interchanged	Law is still uncertain; depends on case-to-case scenario

Modified with permission from Sharma A, Kumar N, Kuppermann BD, Bandello F, Loewenstein A. Understanding biosimilars and its regulatory aspects across the globe: an ophthalmology perspective. *Br J Ophthalmol.* 2020;104(1):2–7.

Sharma A, Kumar N, Kuppermann BD, Bandello F, Loewenstein A. Understanding biosimilars and its regulatory aspects across the globe: an ophthalmology perspective. *Br J Ophthalmol.* 2020;104(1):2–7.

United States Food and Drug Administration. Biosimilar Product Information. Updated December 19, 2022. Accessed January 26, 2023. www.fda.gov/drugs/biosimilars/biosimilar-product-information

PART VI

Imaging and Digital Ophthalmology

CHAPTER 17

Principles of Radiology for the Comprehensive Ophthalmologist

This chapter includes a related video. Go to www.aao.org/bcscvideo_section02 or scan the QR code in the text to access this content.

This chapter includes related activities. Go to www.aao.org/bcscactivity_section02 or scan the QR codes in the text to access this content.

Highlights

- Computed tomography (CT) is the modality of choice when patients are being evaluated for acute hemorrhage, calcification, and diseases of the bone and orbit as well as in patients for whom magnetic resonance imaging (MRI) is contraindicated.
- MRI is the modality of choice for assessing the central nervous system.
- Administration of contrast material improves the sensitivity and specificity of both CT and MRI in diagnosing a disease and should be requested unless there is a contraindication to contrast agents or they are not required.
- Vascular lesions can be evaluated by CT angiography and/or magnetic resonance angiography. The sensitivity of these studies varies by institution and should be compared with that of cerebral angiography.
- Ophthalmic ultrasonography uses high-frequency sound waves for evaluation of structures in the eye and orbit. The frequency of the ultrasound is directly proportional to its resolution and inversely proportional to its depth of penetration.

Overview

Computed tomography (CT) and magnetic resonance imaging (MRI) are the most common imaging studies ordered by an ophthalmologist to evaluate the orbit, brain, and eye. The ophthalmologist also relies on ultrasonography to provide biometrics, facilitate diagnoses, and evaluate the extent of ocular and orbital diseases. This chapter focuses on the basic principles of these imaging modalities, the use of imaging to identify normal anatomical structures, and recognition of the modality that is best suited to evaluate a certain clinical condition. For more specific indications for radiographic studies in particular diseases, consult the BCSC volumes covering those entities.

Computed Tomography

Computed tomography technology is widely available and provides rapid acquisition of images. CT scanners generate cross-sectional images of the body as an x-ray tube continuously rotates around the patient. Current-generation scanners can image body slices as thin as 0.5 mm, which may be reformatted in multiple anatomical planes. In addition, the acquired sections can be reconstructed in varying thicknesses from the source data, depending on the study and anatomical region examined. Studies are conducted with or without intravenous contrast material enhancement depending on the clinical situation. Although contrast-enhanced studies can increase the sensitivity and specificity of CT scans in disease diagnosis, contrast is not always required. Contrast is beneficial when there is a concern for infection, inflammation, neoplasm, or vascular anomalies. A discussion with a radiologist can help confirm that the correct scan is ordered for the disease in question. Table 17-1 presents some of the advantages and disadvantages of CT, as well as contraindications, in comparison with MRI. CT scans are very useful for identifying acute intracranial/orbital hemorrhage and osseous abnormalities, where the ease of CT and rapidity in obtaining images make it the method of choice for evaluating trauma involving the face and orbit.

Generally, for evaluation of orbital conditions, thin-section (ie, high-resolution) studies are critical to delineate the small anatomical structures of the orbit (Fig 17-1):

- lacrimal gland
- extraocular muscles
- globe
- paranasal sinuses around the orbit

Axial scans are always performed during orbital studies. However, coronal reformations, which provide optimal evaluation of the orbital roof and floor, should also be a standard part of these examinations. Sagittal reformations may be added to help further characterize and localize lesions.

CT is also an excellent modality for evaluating the vascular system. CT angiography (CTA) combines intravenous contrast enhancement with high-resolution imaging to produce high-quality, noninvasive scans of arterial and venous pathologies. Three-dimensional reformations that mimic catheter angiography are routinely produced and can detect cerebral aneurysms measuring 3–5 mm with high sensitivity and specificity. Additional series acquired at later times (CT venography) can be used to evaluate the cerebral venous system, especially in suspected cases of venous thrombosis or obstruction.

When additional diagnostic information is needed, CT scans can be combined with nuclear medicine imaging modalities, as in single-photon emission computed tomography (SPECT) and positron emission tomography (PET-CT). These modalities use radiolabeled molecules to help evaluate metabolic activity in a wide range of diseases. SPECT is commonly used to evaluate myocardial perfusion and brain function, whereas PET-CT scans are typically used to diagnose and stage tumors, as well as to diagnose degenerative diseases of the brain. In ophthalmology, PET-CT has been used to assess ocular adnexal lymphoma and cortical blindness. In addition, PET-CT scans of the body are utilized in evaluation of patients with sarcoidosis and for metastatic screening of patients with uveal melanoma.

Table 17-1 Comparison of Magnetic Resonance Imaging and Computed Tomography

	Advantages	Disadvantages	Contraindications
MRI	Better able to distinguish white matter from gray matter Better visualization of posterior fossa pathology Better visualization of soft tissue Better resolution of optic nerve and orbital apex Ability to establish evolution of intraparenchymal hemorrhage No ionizing radiation	Potential for patient reaction to the contrast dye and systemic nephrogenic fibrosis Greater cost Susceptibility artifacts from metal (eg, braces) or air–tissue interfaces Longer acquisition time	Cochlear implants Ferromagnetic implants/foreign bodies Metallic cardiac valves Non–MRI-compatible intracranial aneurysm clips Pacemakers Pregnancy (gadolinium contrast agent is contraindicated in pregnant patients) Renal insufficiency Other considerations: claustrophobia/patient too large for the bore
CT	Better able to assess bony abnormalities Better able to assess orbital and hyperacute intracranial hemorrhage Better visualization of calcification in lesions Easier evaluation of globe and orbital trauma (includes high-resolution bone algorithms)	Exposure to ionizing radiation (CT head radiation dose = 1.5 mGy [a]) Potential for patient reaction to the iodine-based contrast agents Lack of direct sagittal imaging Limited resolution in the posterior fossa Poor resolution of the orbital apex	Renal insufficiency (ie, if estimated GFR is <30 mL/min/1.73 m^2)
MRA/MRV	Less invasive than catheter angiography	Limited resolution (in aneurysms ≤ 3 mm) Possible overestimation of carotid stenosis or venous sinus stenosis	Same as for MRI
CTA/CTV	Less invasive than catheter angiography	Artifacts from superimposed bone and adjacent vessels, especially where aneurysms lie within or close to bone Limited resolution (in aneurysms ≤ 3 mm)	Same as for CT

CT = computed tomography; CTA = computed tomography angiography; CTV = computed tomography venography; GFR = glomerular filtration rate; MRA = magnetic resonance angiography; MRI = magnetic resonance imaging; MRV = magnetic resonance venography.

[a] *Milligray (mGy)* refers to the total dose of ionizing radiation delivered to a tissue and is not the same as millisievert (mSv), the SI unit that takes into account the type of imaging study and the biological effects of the radiation dose. The biological effect of the total mGy delivered varies depending on the tissue being examined. Some tissues (eg, gonads, eye) are more radiosensitive than others (eg, the skin), and the differing effects of a similar mGy dose on these organ systems are taken into account by reporting radiation doses in the unit mSv.

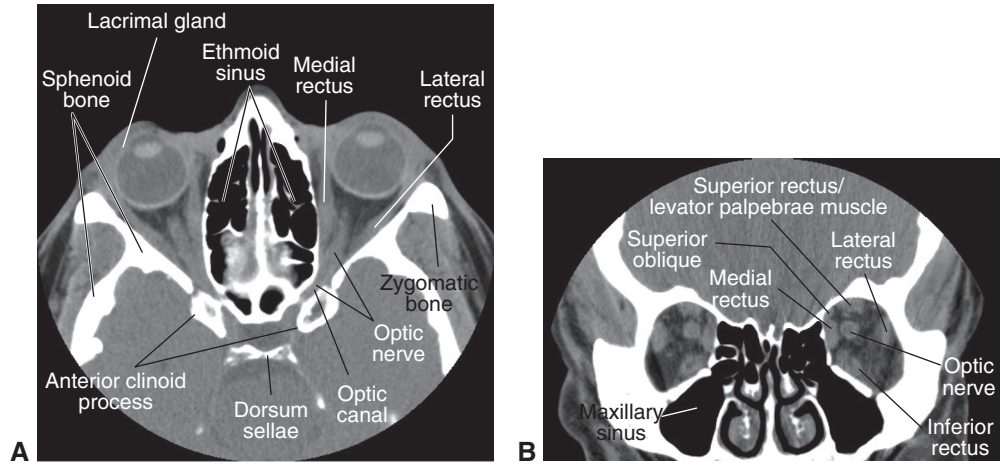


Figure 17-1 Computed tomography (CT) scans. **A,** Axial orbital view of a healthy subject. Note the orbital and intracanalicular portions of the optic nerve. **B,** Coronal orbital view of a healthy subject. *(Courtesy of Rod Foroozan, MD.)*

Betts AM, O'Brien WT, Davies BW, Youssef OH. A systematic approach to CT evaluation of orbital trauma. *Emerg Radiol.* 2014;21(5):511–531.

Yang ZL, Ni QQ, Schoepf UJ, et al. Small intracranial aneurysms: diagnostic accuracy of CT angiography. *Radiology.* 2017;285(3):941–952.

Disadvantages

Although CT is an effective noninvasive technology for evaluating orbital and central nervous system diseases, this imaging modality has limitations and safety concerns. The ionizing radiation employed in CT scans is one potential concern, especially in pediatric cases and pregnant patients. In general, CT scans expose the patient to higher doses of radiation than conventional x-ray studies do. CT scans of the brain are typically oriented to avoid imaging of the globe, which is a more radiosensitive organ. In the International System of Units, millisievert (mSv) is the unit used to determine the amount of tissue damage expected from the absorbed dose of ionizing radiation. Millisievert is technically different from milligray (mGy), which refers to the total dose of ionizing radiation delivered to a tissue during a particular scan sequence. The National Science Foundation has estimated that 10 mSv of radiation may cause an additional case of cancer in 1/1000 patients. However, the impact of a single (or even serial) CT scan(s) of the brain in relation to the risk of cancer development is typically outweighed by the clinical need for diagnostic information; nonetheless, it is important to be aware of this safety consideration when ordering a CT scan, particularly in children, to reduce the risk of future malignancy.

Although CT scans are very useful in studying bony structures, visibility of the posterior fossa may be reduced because of a streak artifact from the skull base. Further, in evaluation of the central nervous system, CT scans provide lower spatial resolution than do MRI scans, although the intravenous administration of iodinated contrast material improves the soft-tissue imaging capabilities of CT.

Iodinated contrast agents pose another potential safety concern for patients undergoing CT, mostly related to the potential for allergic reactions and for nephrotoxicity in those with underlying renal insufficiency. Allergic reactions have been recorded in 1%–12% of patients, depending on the type of contrast material used, with symptoms ranging from relatively mild (eg, pruritus, nausea, and vomiting) to severe (eg, anaphylaxis). The rate of severe allergic reactions has been reduced to less than 0.1% with the use of newer low-osmolar contrast agents. Nephrotoxicity has been reported in 2%–7% of patients receiving contrast media, with higher rates in those with preexisting kidney disease and/or diabetes. The American College of Radiology (ACR) recommends limiting intravenous contrast agent administration in patients with an estimated glomerular filtration rate less than 30 mL/min/1.73 m^2, as well as considering alternative imaging methods (eg, MRI) in these patients or hydrating before the examination. Because recommendations for the use of contrast agents vary by institution, consultation with a diagnostic radiologist is advised before ordering contrast-enhanced CT examinations in at-risk patients.

American College of Radiology, ACR Committee on Drugs and Contrast Media. ACR Manual on Contrast Media. 2022. Accessed January 17, 2023. www.acr.org/-/media/ACR/Files/Clinical-Resources/Contrast_Media.pdf

Meinel FG, De Cecco CN, Schoepf UJ, Katzberg R. Contrast-induced acute kidney injury: definition, epidemiology, and outcome. *Biomed Res Int.* 2014;2014:859328. doi:10.1155/2014/859328

Magnetic Resonance Imaging

Because of its superior contrast resolution, MRI is the imaging modality of choice for evaluation of the central nervous system (see Table 17-1). In addition, because this technology does not use ionizing radiation, it has a relative advantage when compared with CT. Instead, MRI uses a strong magnetic field that causes hydrogen atoms found in water and fat to align themselves with the field. Once the atoms are aligned, protons within a selected imaging section/volume are exposed to a series of radiofrequency (RF) and/or magnetic gradient pulses and become excited. As the protons relax again to a steady state, they emit radio waves, which are detected by a receiver coil in the MRI system. The time it takes for the signal to reach the MRI machine following the applied RF (or gradient) pulse is known as the *echo time (TE),* which varies by type of tissue. The time between RF pulses is known as the *repetition time (TR).* The TE and TR can be adjusted to modify the contrast between images and thus enhance visualization of different tissues.

The energy given off by the rotating protons is expressed by 2 aspects: the longitudinal relaxation constant, or T1, and the transverse relaxation constant, or T2. T1-weighted images (T1WIs), which are generated with shorter TEs and TRs, are typically used for contrast-enhanced studies. In a T1WI, water appears dark (hypointense) and fat appears bright (hyperintense). Melanin shows an intrinsically elevated T1 signal, which can be helpful in providing a diagnosis in patients with uveal melanoma. Sometimes, however, fat suppression is required in T1WIs to improve contrast enhancement and characterization of tissues, such as the optic nerve and other orbital structures. In comparison, T2-weighted images (T2WIs) use a longer TE to depict differences in water content, thus revealing inflammatory,

ischemic, and neoplastic-related edematous changes. On T2WIs, vitreous, cerebrospinal, and other fluids are bright.

On both T1WIs and T2WIs, gray matter is hypointense compared with white matter (Table 17-2, Fig 17-2). In fluid-attenuated inversion recovery (FLAIR) images, the fluid signal is suppressed on T2WIs, facilitating visualization of signal abnormalities associated with changes in the periventricular white matter (eg, as in patients with multiple sclerosis).

Gadolinium-based contrast medium, administered intravenously, is used to enhance T1WIs, especially for assessment of inflammatory and neoplastic lesions. Gadolinium may also be administered during high spatial and temporal resolution MRI sequences of large and medium-sized vessels (ie, MR angiography [MRA]), when dynamic contrast enhancement can be assessed more practically than with CTA. The decision to use MRA versus CTA for evaluation of intracranial and orbital blood vessels is often complex and varies depending on the patient and clinical question being asked; consultation with a neuroradiologist may be required in complex cases. The sensitivity of these studies varies by institution and should be compared with that of cerebral angiography.

Diffusion-weighted imaging (DWI) is another form of MRI used in ophthalmology; this sequence is the most sensitive for the detection of acute ischemic changes (eg, cerebrovascular accident). DWI can detect changes within minutes compared with potentially hours via other MRI methods. A quantitative metric of DWI sequences, the apparent diffusion coefficient (ADC), can be used to further characterize edema as cytotoxic versus vasogenic (eg, as in posterior reversible encephalopathy syndrome). Cytotoxic edema appears bright on DWI signal with dark or low ADC. Vasogenic edema appears dark on DWI signal with a normal ADC.

Functional MRI (fMRI) is a technique that detects changes in blood flow to measure neuronal activity of the brain. It can locate the brain's functional anatomy. fMRI is utilized in patients with blepharospasm, strabismus, visual impairment, and other ocular responses.

Disadvantages

Adverse effects are occasionally associated with the gadolinium chelates used for contrast-enhanced imaging in MRI, though at a lower frequency than with the iodinated contrast agents in CT. Common symptoms are sweating, pruritus, and rash. Although gadolinium agents do not adversely affect renal function at the doses administered for clinical imaging, use of certain gadolinium chelates may be restricted in patients with severe end-stage renal disease because of the risk of nephrogenic systemic fibrosis, a rare and potentially fatal multiorgan fibrosing disorder. In addition, gadolinium has been shown to collect in certain neurologic structures after repeated administration; however, no clinical features have been attributed to this deposition. Recommendations for the use of gadolinium-based contrast agents vary by institution; thus, the ophthalmologist is advised to consult with a diagnostic radiologist before ordering such studies in at-risk patients.

Because MRI uses strong magnetic fields to generate pictures, patients with metallic foreign bodies or implants should also be carefully screened before undergoing imaging. Ophthalmologists may be consulted to assess patients for foreign bodies on the ocular surface, within the eye, and/or in the orbit. The incidence of damage from undetected ocular foreign bodies during MRI is low, restricted to a few case reports; however, it is

Table 17-2 Signal Characteristics of Normal Ocular Structures in Different Imaging Sequences

Ocular Structure	Signal Intensity on T1-Weighted Images[a]	Signal Intensity on T2-Weighted Images[a]	Enhancement on Postcontrast Images[a]	Additional Comments
Sclera, choroid, retina (seen as a single coat)	Hyperintense (bright/white)	Hypointense (dark/black)	None	The 3 coats cannot be distinguished separately on routine imaging
Aqueous	Hypointense (dark/black)	Hyperintense (bright/white)	None	
Lens	Hyperintense (bright/white)	Low (gray)	None	Typically has a biconvex appearance
Vitreous	Hypointense (dark/black)	Hyperintense (bright/white)	None	
Extraocular muscles	Intermediate (gray)	Intermediate (gray)	Enhances brightly	
Orbital fat	Hyperintense (bright/white)	Intermediate (gray)	None	Typically has a homogeneous appearance
Optic nerve	Isointense to cerebral white matter (gray)	Isointense to cerebral white matter (gray)	Does not typically enhance; it can be compared with the extraocular muscles	
Optic nerve sheath with cerebral spinal fluid around the optic nerve	Hypointense (dark/black)	Hyperintense (bright/white)	None	
Lacrimal gland	Isointense with gray matter (gray)	Isointense with gray matter (gray)	Enhances brightly	
Bone	Signal void (dark)	Signal void (dark)	None	Better studied with computed tomography
Cerebral spinal fluid	Hypointense (dark/black)	Hyperintense (bright/white)	None	

[a] Signal intensity (hypointense/hyperintense) is described in comparison with the reference tissue. Intracranially, the reference tissue is the gray matter of the brain; extracranially, it is the skeletal muscle.

Modified with permission from Simha A, Irodi A, David S. Magnetic resonance imaging for the ophthalmologist: a primer. *Indian J Ophthalmol.* 2012;60(4):308.

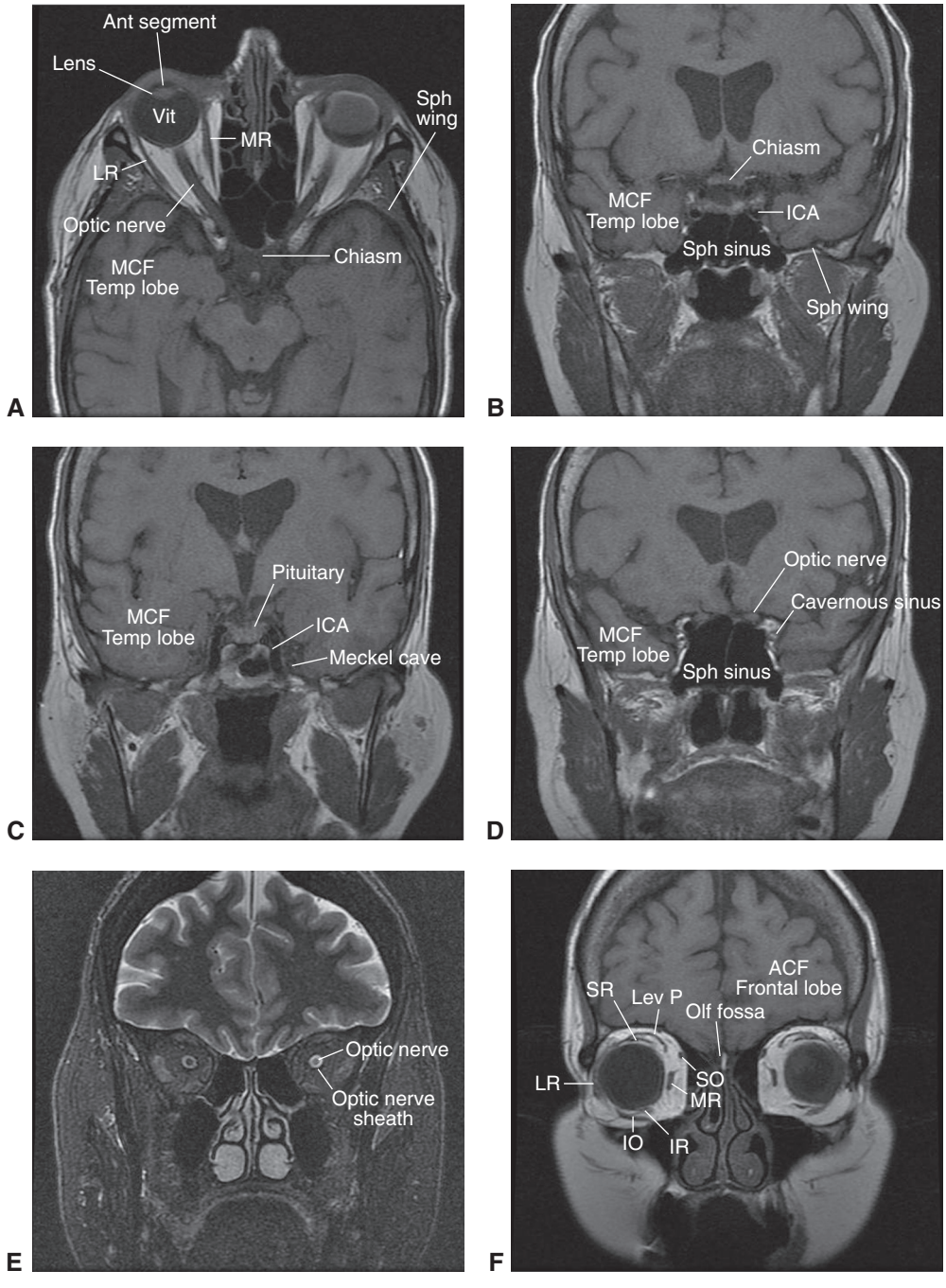


Figure 17-2 Magnetic resonance imaging (MRI) scans of the brain and orbit show the anatomy of visual and orbital structures from the chiasm to the anterior orbit. (*Note:* The left-globe abnormality is not pertinent to this figure's objective.) **A,** T1-weighted axial image. **B–D,** T1-weighted coronal images. **E,** T2-weighted coronal image with fat suppression. **F,** T1-weighted coronal image. ACF = anterior cranial fossa; Ant segment = anterior segment; ICA = internal carotid artery; IO = inferior oblique muscle; IR = inferior rectus muscle; LR = lateral rectus muscle; Lev P = levator palpebrae superioris muscle; MCF = middle cranial fossa; MR = medial rectus muscle; Olf fossa = olfactory fossa; SO = superior oblique muscle; Sph sinus = sphenoid sinus; Sph wing = sphenoid wing; SR = superior rectus muscle; Temp lobe = temporal lobe; Vit = vitreous. *(Courtesy of M. Tariq Bhatti, MD.)*

not zero. This is an important consideration when counseling patients before their scans. Patients are also screened at the imaging center before MRI. Stents used in microinvasive glaucoma surgery (MIGS) are MR-conditional, and a review of the specific device directions for use is recommended. These stents are safe to use in 3 Tesla (3T) MRI.

The following box highlights general and ophthalmic concerns in patients scheduled to undergo MRI. The reader is also directed to the ACR safety guidelines (see the reference list at the end of this section) for further details.

Considerations When Ordering an MRI

- Metal in the body, including metallic intraocular or orbital foreign bodies
  - Screening radiography or CT may be helpful in detecting intraocular and orbital foreign bodies.
  - Consultation with a diagnostic radiologist is advised regarding the safety of some metals (eg, MRI-compatible aneurysm clips).
  - Gold weight and titanium mesh orbital floor implants have shown no movement when placed in a magnetic field. Some clinicians prefer to wait for fibrosis to secure the implant before obtaining an MRI.
- Cardiac pacemaker or defibrillator
  - Consultation with a diagnostic radiologist regarding all implantable devices is advised.
- Allergy to gadolinium-based contrast media
- Consideration and risk-analysis of sedation in children, depending on age and length of scan

Activities 17-1 and 17-2 demonstrate normal structures identified on axial and coronal orbital imaging, respectively, with CT and MRI.



ACTIVITY 17-1 Axial imaging of the normal orbit with computed tomography and magnetic resonance imaging.
Developed by Vikram S. Brar, MD. Figures reproduced with permission from Dutton JJ. Atlas of Clinical and Surgical Orbital Anatomy. *2nd ed. Elsevier/Saunders; 2011:Figs 11-1 to 11-6.*





ACTIVITY 17-2 Coronal imaging of the normal orbit with computed tomography and magnetic resonance imaging.
Developed by Vikram S. Brar, MD. Figures reproduced with permission from Dutton JJ. Atlas of Clinical and Surgical Orbital Anatomy. *2nd ed. Elsevier/Saunders; 2011:Figs 11-7 to 11-12.*



Expert Panel on MR Safety; Kanal E, Barkovich AJ, Bell C, et al. ACR guidance document on MR safe practices: 2013. *J Magn Reson Imaging.* 2013;37(3):501–530.

Lawrence DA, Lipman AT, Gupta SK, Nacey NC. Undetected intraocular metallic foreign body causing hyphema in a patient undergoing MRI: a rare occurrence demonstrating the limitations of pre-MRI safety screening. *Magn Reson Imaging.* 2015;33(3): 358–361.

Marra S, Leonetti JP, Konior RJ, Raslan W. Effect of magnetic resonance imaging on implantable eyelid weights. *Ann Otol Rhinol Laryngol.* 1995;104(6):448–452.
Modjtahedi BS, Rong A, Bobinski M, McGahan J, Morse LS. Imaging characteristics of intraocular foreign bodies: a comparative study of plain film x-ray, computed tomography, ultrasound, and magnetic resonance imaging. *Retina.* 2015;35(1):95–104.
Seidenwurm DJ, McDonnell CH III, Raghavan N, Breslau J. Cost utility analysis of radiographic screening for an orbital foreign body before MR imaging. *AJNR Am J Neuroradiol.* 2000;21(2):426–433.
Sullivan PK, Smith JF, Rozzelle AA. Cranio-orbital reconstruction: safety and image quality of metallic implants on CT and MRI scanning. *Plast Reconstr Surg.* 1994;94(5):589–596.
Williamson MR, Espinosa MC, Boutin RD, Orrison WW Jr, Hart BL, Kelsey CA. Metallic foreign bodies in the orbits of patients undergoing MR imaging: prevalence and value of radiography and CT before MR. *AJR Am J Roentgenol.* 1994;162(4):981–983.

Ultrasonography

Ultrasound refers to sound waves with frequencies above the audible range. Ultrasonography uses echo to image and differentiate tissues. During ultrasonography, electrical energy is converted into sound waves by means of a piezoelectric crystal. The resultant waves are emitted by the ultrasound probe, which is placed as close as possible to the tissue being studied. When the sound waves encounter tissues, their speed changes depending on the density of the surface/interface, and some of the waves bounce back to the probe. Based on their amplitude, frequency, and travel time, these echoes are then converted into a signal. For example, during ultrasonography, a sound wave traversing the cornea encounters the aqueous of the anterior chamber and then the lens–iris diaphragm. As the tissue density changes at the posterior cornea and then again at the lens–iris diaphragm, signals are generated.

The frequency of the ultrasound determines the depth of penetration and the resolution. These 2 variables are inversely related. High-frequency ultrasound, which provides greater detail, is used to evaluate smaller objects such as the eye. Low-frequency ultrasound provides less resolution but offers deeper penetration; for example, low-frequency ultrasound is useful in obstetrics to traverse through the abdominal wall and uterus to image a fetus.

Ophthalmic ultrasonography utilizes high-frequency sound waves (8–80 MHz) for safe, effective, noninvasive imaging of the anterior and posterior segments of the eye and orbit using equipment routinely found in most practices. Indications for ophthalmic ultrasonography include biometry and evaluation of the following structures and conditions:

- intraocular structures with media opacities
- posterior sclera
- extraocular muscles and the surrounding orbit
- intraocular tumors

Three main ultrasound devices are used to evaluate the eye: the A-scan probe, the B-scan probe, and the ultrasound biomicroscopy (UBM) probe (Fig 17-3).

Singh AD, Hayden BC. *Ophthalmic Ultrasonography.* Elsevier/Saunders; 2011.

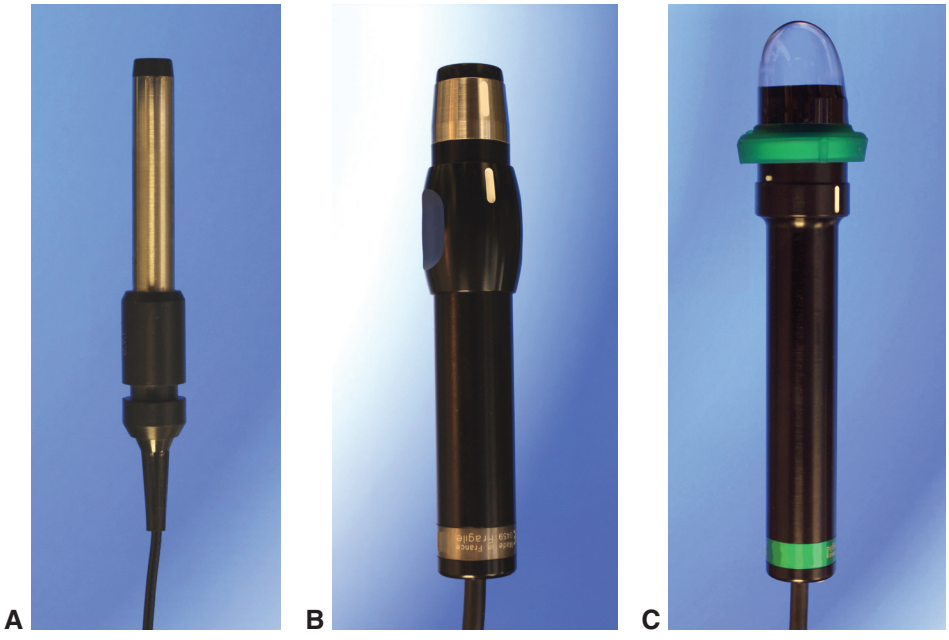


Figure 17-3 Ophthalmic ultrasound probes. **A,** A-scan probe. **B,** B-scan probe. **C,** Ultrasound biomicroscopy (UBM) probe. *(Courtesy of Vikram S. Brar, MD.)*

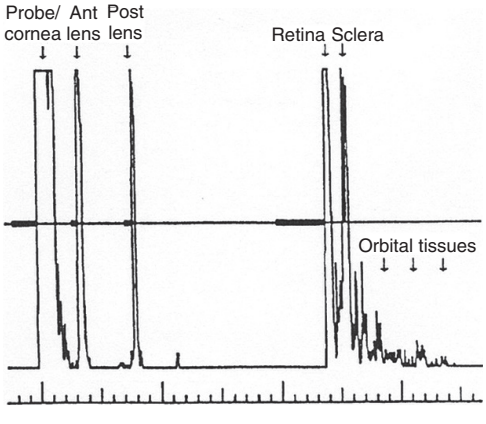


Figure 17-4 A normal A-scan from a healthy eye. *(Reproduced with permission from Waldron RG. A-scan biometry. Medscape Drugs and Diseases: Clinical Procedures. Updated August 10, 2022. Accessed January 17, 2023. https://emedicine.medscape.com/article/1228447)*

A-Scan Ultrasonography

Biometry of the eye with an A-scan probe (eg, for measuring axial length) uses frequencies between 8 and 12 MHz. After a topical anesthetic agent is applied, the probe can either make direct contact with the cornea or may be applied via immersion. The latter method eliminates the possibility of altering the measurement due to compression of the cornea. Figure 17-4 shows a normal A-scan.

When operating at 8 MHz, the A-scan probe can also enable demonstration of intralesional characteristics within the eye and orbit, known as *internal reflectivity.* Reflectivity

Table 17-3 Quantification of Reflectivity in A-Scan Ultrasonography

Grade	A-Scan Spike Height, %
Low	0–33
Medium	34–66
High	67–100

Reproduced with permission from Singh AD, Hayden BC. *Ophthalmic Ultrasonography.* Elsevier/Saunders; 2011:20.

within a lesion may be low, medium, or high depending on the relative percentage of the internal spike compared with that of the initial spike of the lesion (Table 17-3). The reflectivity within a tissue is inversely proportional to its homogeneity. Less-organized tissue, as in a vascular lesion (ie, a choroidal hemangioma), will demonstrate high internal reflectivity compared with homogenous tissue (ie, a choroidal melanoma), which will have low internal reflectivity.

B-Scan Ultrasonography

B-scan ultrasonography commonly uses a 10 MHz frequency, with axial resolution of 100 μm, to provide 2-dimensional images of the eye and orbit. Combining data from 2 orthogonal scans at a given point yields 3-dimensional information: shape, location, and extent. Three types of B-scans—axial, transverse, and longitudinal—are obtained depending on the position of the probe on the eye and the orientation of the linear white marker on its surface (Fig 17-5). These scans are best performed with direct contact on an anesthetized ocular surface, facilitated by a coupling agent safe to use on the ocular surface, such as methylcellulose. Direct contact improves image resolution and allows the examiner to monitor the position of the patient's eyes. The probe marker indicates the direction of the scan and corresponds to the top of the 2-dimensional B-scan image.

Axial scans

In axial scans, the probe is placed directly on the cornea with the patient looking straight ahead and the probe marker oriented vertically at 12 o'clock or horizontally with the probe marker oriented nasally (Fig 17-6). This allows visualization of the posterior pole and the optic nerve. The posterior sclera and underlying Tenon space can also be examined, as in cases of posterior scleritis. Attenuation of the signal by the cornea and lens limits the resolution of these scans.

Transverse scans

Transverse scans cover the greatest area of the posterior segment of the eye. The probe is placed on the sclera, avoiding image degradation from the anterior segment, and is oriented parallel to the limbus, providing a circumferential scan of the opposing retina (ie, when imaging the nasal quadrant, the probe is placed on the temporal sclera with the patient adducting his or her eye; Fig 17-7). The farther the probe traverses posteriorly from the limbus, the

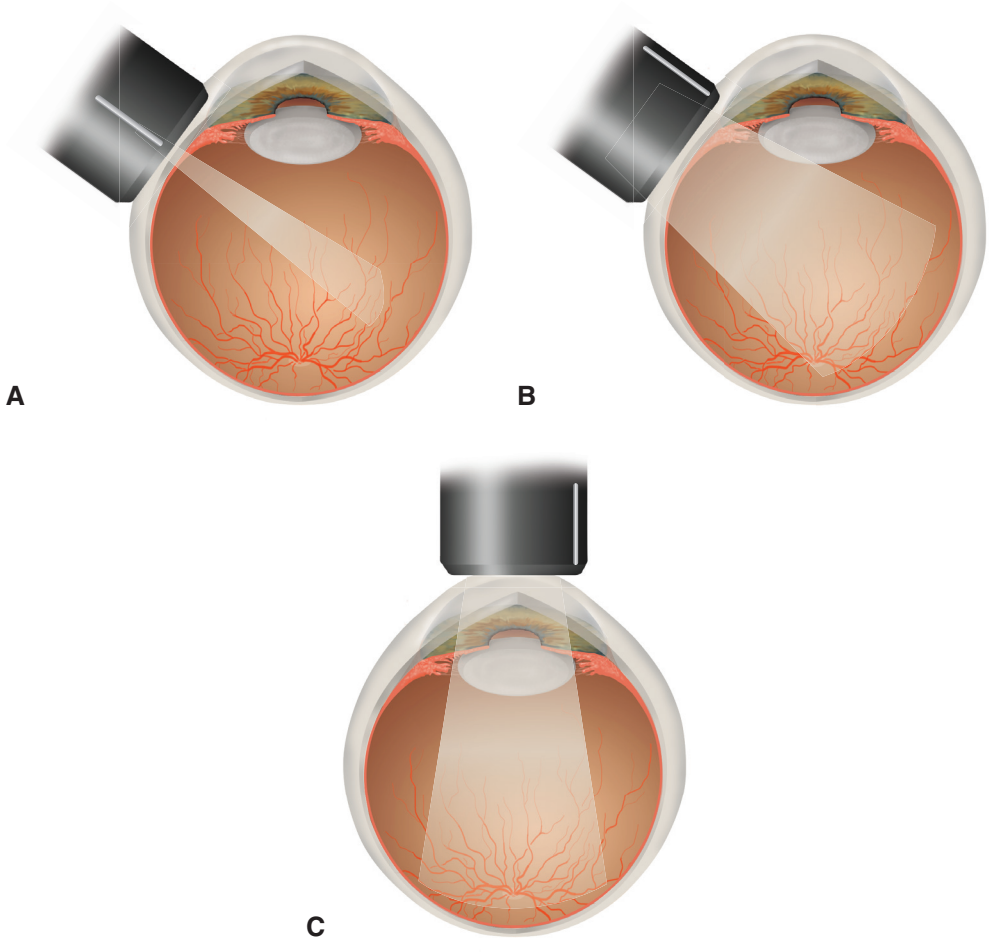


Figure 17-5 Three primary scans used in B-scan ultrasonography. **A,** Transverse scan. **B,** Longitudinal scan. **C,** Axial scan. *(Illustration by Cyndie C.H. Wooley.)*

more the anterior part of the eye is imaged (ie, with the patient looking just nasal to midline, the probe is touching the edge of the limbus, and the back of the 2-dimensional image is posterior to the equator). As the patient looks farther nasally, the probe slides posteriorly on the surface of the globe and the scan is directed more anteriorly (Fig 17-8). This maximizes visualization of that quadrant.

When the posterior segment cannot be visualized, 4 transverse scans (ie, superior, inferior, nasal, and temporal) in addition to the axial scan are typically performed as part of the screening B-scan. The nasal and temporal scans are known as the *lateral transverse scans* (see Fig 17-7). By convention, when the superior or inferior eye is imaged, the probe marker is oriented nasally. In all other positions, the probe marker is oriented superiorly. Figure 17-9 demonstrates the appropriate positioning of the probe and the orientation of the marker for the 4 primary transverse scans.

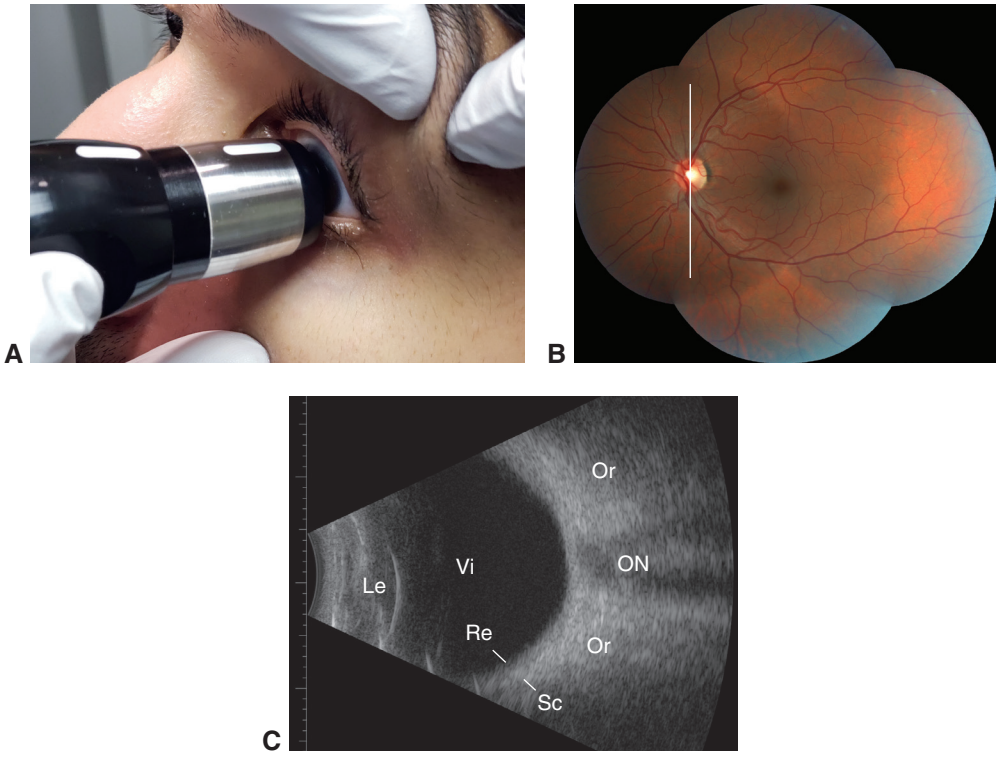


Figure 17-6 Vertical axial B-scan ultrasonography of the left eye. **A,** The probe is placed directly on the cornea and oriented vertically. **B,** Corresponding fundus photograph. The *white line* indicates the corresponding section of the fundus being imaged at the posterior aspect of the scan. **C,** Two-dimensional B-scan image. Based on the orientation of the probe, the top of the scan is the superior retina. Le = lens; ON = optic nerve; Or = orbit; Re = retina; Sc = sclera; Vi = vitreous. *(Courtesy of Vikram S. Brar, MD.)*

Longitudinal scans

Similar to transverse scans, longitudinal scans are performed with the probe placed on the sclera, with the marker oriented perpendicular to the limbus. These scans are performed when a lesion is identified on a screening B-scan and describe the anterior-posterior extent. The optic nerve should be visualized below the center on longitudinal scans (Fig 17-10). Longitudinal scans can also be used to visualize the macula (Fig 17-11).

Dynamic B-scan

B-scan ultrasonography is not a static process. Previous sections discussed the anterior-to-posterior excursion of the ultrasound probe to increase the area imaged during transverse scans. In addition, the patient can be asked to look up and down during lateral transverse scans and right and left during superior/inferior transverse scans to study movement of the vitreous/posterior hyaloid face and a detached retina (Video 17-1). Furthermore, the gain of the scan can be adjusted to enhance visualization of particular structures (Table 17-4).

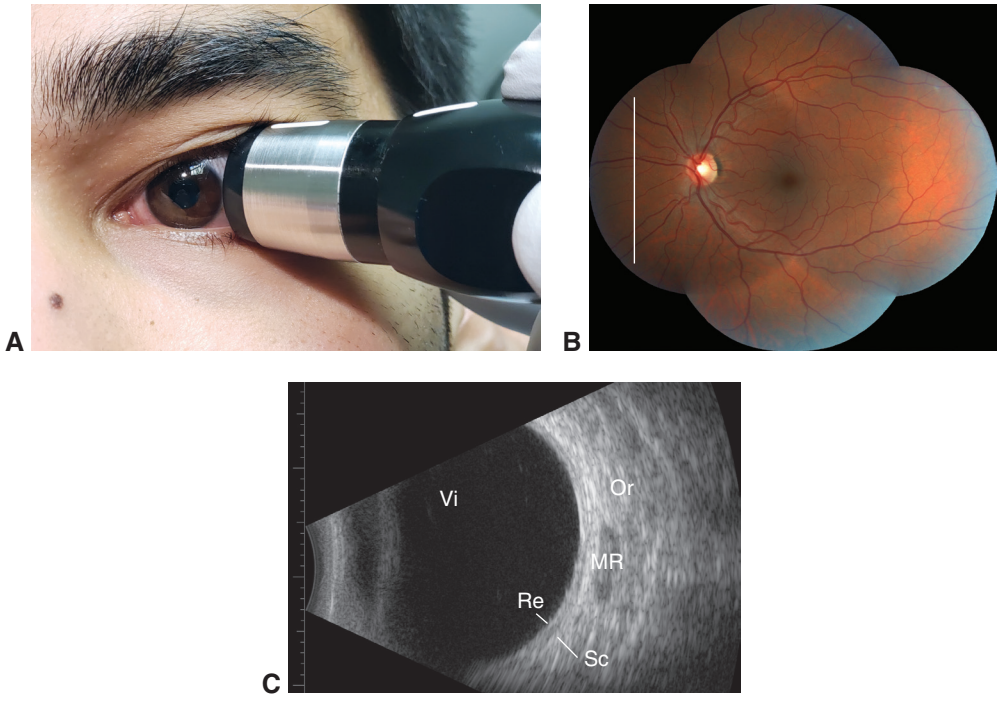


Figure 17-7 Lateral transverse B-scan ultrasonography of the left eye. **A,** The probe is on the temporal sclera (left eye) with the patient looking to his right and the marker oriented up. **B,** Corresponding fundus photograph. The *white line* indicates the corresponding section of the fundus being imaged at the posterior aspect of the scan. **C,** The back of the scan is the nasal retina, and the top is the superior retina. MR = medial rectus muscle; Or = orbit; Re = retina, Sc = sclera; Vi = vitreous. *(Courtesy of Vikram S. Brar, MD.)*

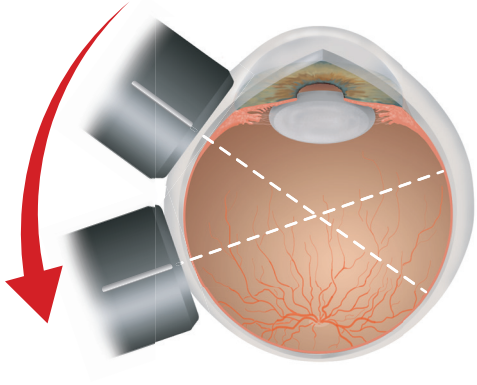


Figure 17-8 When transverse scans are performed, anterior-to-posterior excursion of the B-scan probe maximizes visualization of the desired quadrant. *(Illustration by Cyndie C.H. Wooley.)*

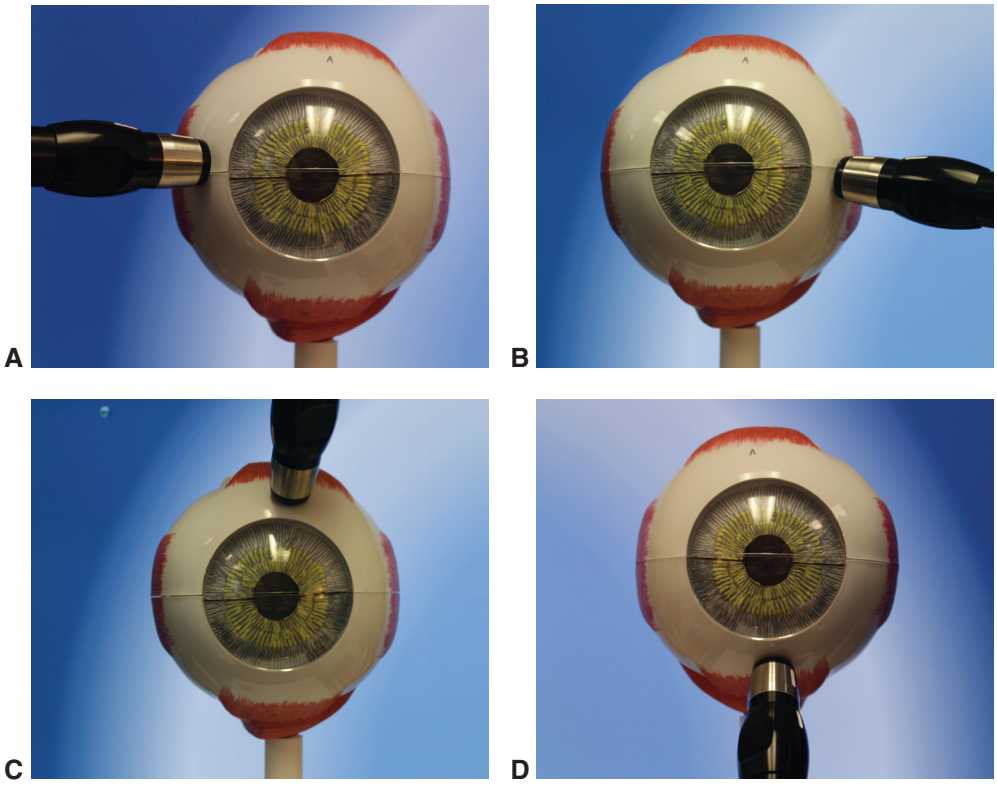


Figure 17-9 Model of the left eye, showing positioning of the probe and orientation of the probe marker in the 4 primary transverse scans performed in a screening B-scan. The probe marker is oriented up for lateral transverse scans (**A,** temporal; **B,** nasal) and nasally for inferior **(C)** and superior **(D)** scans. *(Courtesy of Vikram S. Brar, MD.)*

VIDEO 17-1 Dynamic B-scan of hemorrhagic posterior vitreous detachment.
Courtesy of Vikram S. Brar, MD.

Figures 17-12, 17-13, and 17-14 highlight some of the differential diagnoses requiring ophthalmic ultrasonography and their diagnostic features.

Ultrasound Biomicroscopy

Ultrasound biomicroscopy (UBM) utilizes the highest frequency available in ophthalmic ultrasonography, usually 50 MHz, with axial resolution of 37 μm, to evaluate the anterior segment of the eye. It requires topical anesthesia and a fluid reservoir, which is placed in direct contact with the cornea and/or anterior sclera depending on which structures need to be evaluated. Two types of scans can be obtained with UBM depending on the orientation of the probe. *Axial* UBM scans are generated by placing the probe on the cornea positioned horizontally (Fig 17-15). This allows visualization of the cornea, the anterior chamber, the

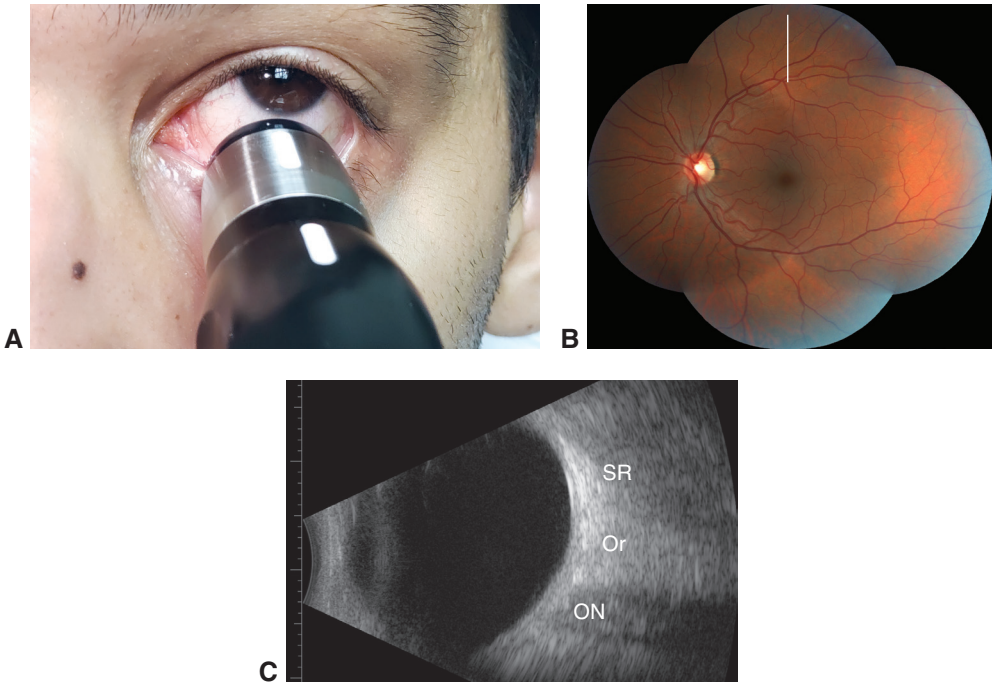


Figure 17-10 Superior longitudinal B-scan ultrasonography of the left eye. **A,** The probe is placed directly on the sclera with the patient looking up and the marker oriented vertically, perpendicular to the limbus. **B,** Corresponding fundus photograph. The *white line* indicates the corresponding section of the fundus being imaged at the posterior aspect of the scan. These scans demonstrate the anterior-posterior extent of a lesion. **C,** In the 2-dimensional B-scan image, the back of the scan represents the superior fundus. Note the positioning of the optic nerve, which is found toward the bottom of longitudinal scans. ON = optic nerve; Or = orbit; SR = superior rectus muscle. *(Courtesy of Vikram S. Brar, MD.)*

iris with the pupil in the center of the iris plane, and the lens. *Radial* UBM scans are generated by centering the probe at the limbus, with the marker oriented perpendicular to the limbus. The anterior chamber angle, the iris, and the ciliary body can be evaluated with this scan (Fig 17-16).

Kendall CJ, Prager TC, Cheng H, Gombos D, Tang RA, Schiffman JS. Diagnostic ophthalmic ultrasound for radiologists. *Neuroimaging Clin N Am.* 2015;25(3):327–365.

Silverman RH. High-resolution ultrasound imaging of the eye: a review. *Clin Exp Ophthalmol.* 2009;37(1):54–67.

Ordering Imaging Studies

Requesting the correct study is imperative for arriving at the correct diagnosis. Imaging orders should include clinical information regarding the patient, the location or perceived location of the pathology to be studied, use of a contrast agent, and urgency. The more detail

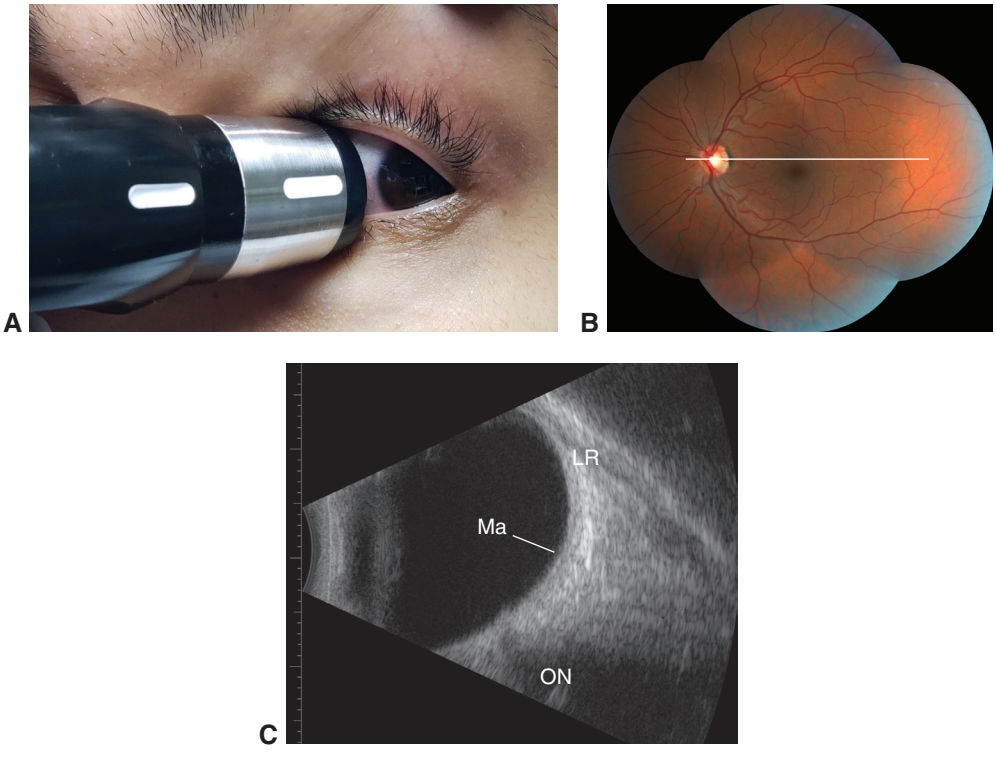


Figure 17-11 Longitudinal B-scan ultrasonography demonstrates the macula in the left eye. **A,** The patient is asked to abduct the eye. The probe is placed directly on the nasal sclera with the marker oriented perpendicular to the limbus. **B,** Corresponding fundus photograph. The *white line* indicates the corresponding section of the fundus being imaged at the posterior aspect of the scan. **C,** In this 2-dimensional image, the top of the scan demonstrates the lateral rectus muscle; the optic nerve is toward the bottom of longitudinal scans. The intervening retina includes the macula. LR = lateral rectus muscle; Ma = macula; ON = optic nerve. *(Courtesy of Vikram S. Brar, MD.)*

Table 17-4 Tissue-Specific Gain Settings in B-Scan Ultrasonography

Tissue	Decibel Value, dB	Gain Setting
Vitreous	75–100	High
Retina/choroid	55–75	Medium
Sclera/orbit/calcification	35–55	Low

Modified with permission from Singh AD, Hayden BC. *Ophthalmic Ultrasonography.* Elsevier/Saunders; 2011:18.

Diagnosis		Ultrasonographic Findings
Myositis Graves orbitopathy	1	Thickened extraocular muscles
Periorbital space-occupying lesions	2	Change in the relief of the orbital wall, sound propagation into perinasal sinuses
Orbital neoplasm	3	Directly evident (it may be difficult to demonstrate a small cavernous hemangioma because of its high acoustic reflectivity)
Inflammatory orbital pseudotumor	4	Widening of normal orbital structures, low acoustic reflectivity, Tenon space may be demonstrated
Disc edema	5	Widened dural diameter of the optic nerve
Axial hyperopia	6	Axial length below 22 mm, ocular walls concentrically thickened
Ocular hypotony	7	Ocular walls concentrically thickened
Macular degeneration		Thickening of the ocular walls in the area of the macula, high acoustic reflectivity
Scleritis	8	Circumscribed widening of the ocular walls, Tenon space apparent

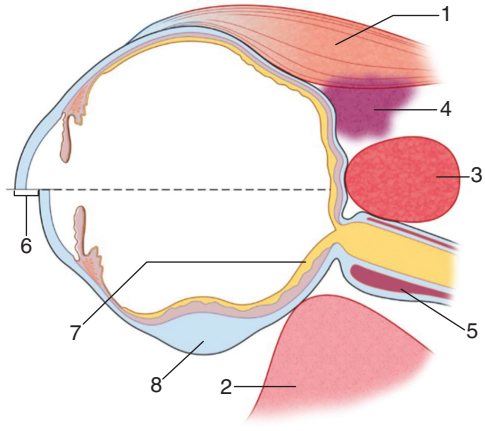


Figure 17-12 Schematic of ultrasonographic findings. The *dotted line* separates the top half of the eye from the bottom half, which is shorter (demonstrating hyperopia) and where different disease processes are depicted. *Inset:* Differential diagnosis for choroidal folds. *(Adapted with permission from Schachat AP, Wilkinson CP, Hinton DR, Sadda SR, Wiedemann P, eds.* Ryan's Retina. *5th ed. Elsevier; 2013:282.)*

Diagnosis		Ultrasonographic Findings
Normal axial length for the patient's age		
Retinoblastoma	1	Widening of the ocular walls, extremely high acoustic reflectivity, shadowing effect, atypical findings possible
Congenital cataract	2	Increased reflectivity from the posterior lens surface, vitreous space empty, ocular walls normal
Shortened axial length		
Retinopathy of prematurity	3	In stages IV and V, beginning or complete traction detachment (normal findings in stages I–III)
PFV	4	Dense strand of tissue between optic nerve head and posterior lens pole; formes frustes may occur (posterior or anterior PFV)
Retinal anomalies		Membranes in the vitreous, atypical detachment, which in part appears solid (no typical echogram)
Fundus coloboma	5	Directly demonstrable protrusion of ocular wall, sometimes with orbital cyst (microphthalmos with cyst)
Coats disease	6	Floating crystals in the vitreous and subretinal space (fast-flickering spikes on A-mode)

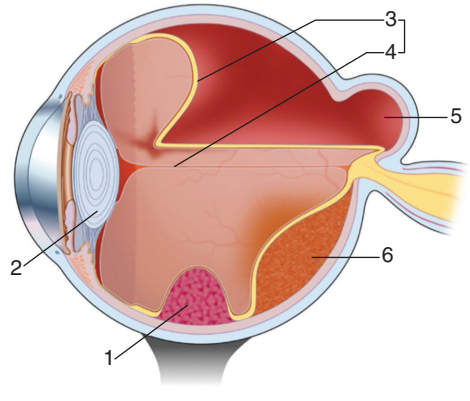


Figure 17-13 Schematic of ultrasonographic findings. *Inset:* Differential diagnosis for leukocoria. PFV = persistent fetal vasculature. *(Adapted with permission from Schachat AP, Wilkinson CP, Hinton DR, Sadda SR, Wiedemann P, eds.* Ryan's Retina. *5th ed. Elsevier; 2013:281.)*

Diagnosis		Ultrasonographic Findings
Symptomatic posterior vitreous detachment	1	Thickened detached posterior hyaloid membrane, occasionally early retinal detachment
Recently formed retinal break with torn vessel	2	Blood-covered vitreous strands converge toward the retinal break; occasionally a high-floating operculum may be detected
Proliferative retinopathy	3	Strands or membranes extending from the optic nerve head or the posterior pole, high acoustic reflectivity
Terson syndrome (vitreous hemorrhage after subchoroidal bleeding	4	Vitreous opacities in front of the optic nerve head or behind the detached vitreous
Disciform macular degeneration	5	Widening of the ocular walls in the macular area, high acoustic reflectivity, vitreous strands extending from the macula
Choroidal melanoma	6	Biconvex thickening of the ocular wall, low acoustic reflectivity, sometimes mushroom-shaped; accompanying retinal detachment distant from the tumor

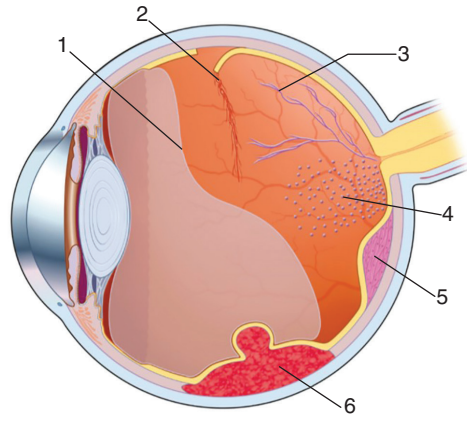


Figure 17-14 Schematic of ultrasonographic findings. *Inset:* Differential diagnosis for vitreous hemorrhage. *(Adapted with permission from Schachat AP, Wilkinson CP, Hinton DR, Sadda SR, Wiedemann P, eds.* Ryan's Retina. *5th ed. Elsevier; 2013:282.)*

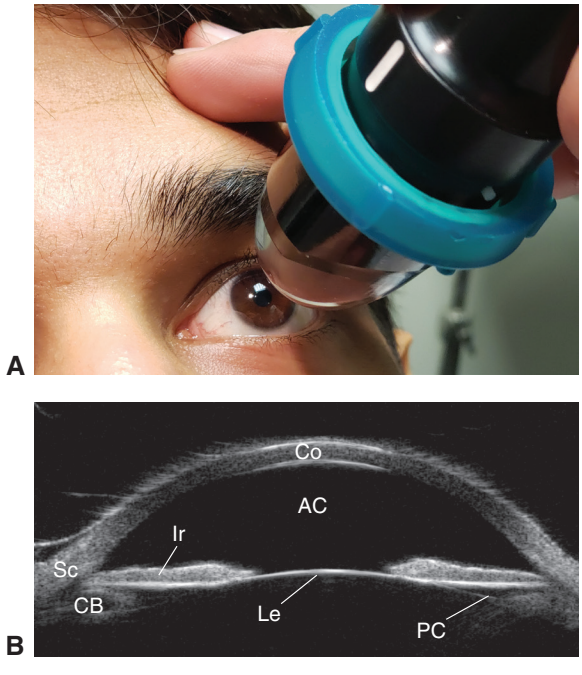


Figure 17-15 Axial UBM. **A,** After the eye is anesthetized, the probe is placed directly on the cornea, in this case, oriented horizontally. **B,** Axial scan of the anterior segment. AC = anterior chamber; CB = ciliary body; Co = cornea; Ir = iris; Le = lens anterior capsule; PC = posterior chamber; Sc = sclera. *(Courtesy of Vikram S. Brar, MD.)*

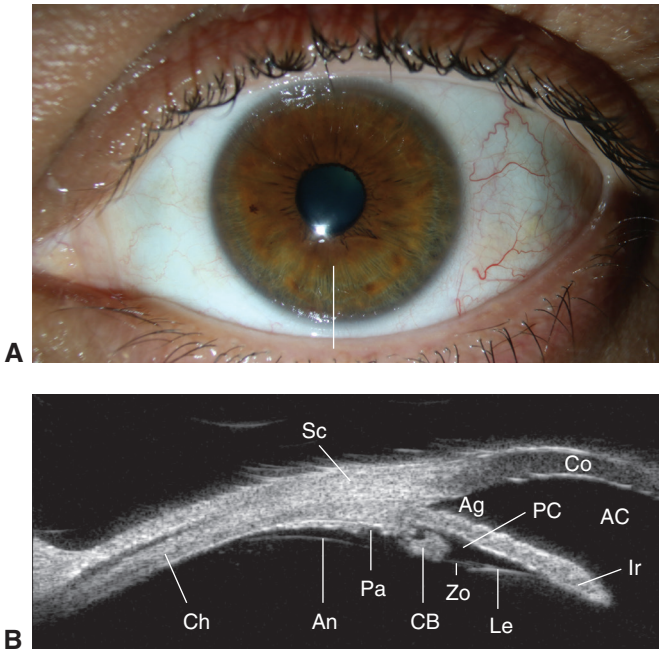


Figure 17-16 Radial UBM. **A,** Slit-lamp photograph. The *white line* demonstrates the location and orientation of the probe. **B,** Radial scan demonstrates the structures. AC = anterior chamber; Ag = angle; An = anterior hyaloid face; CB = ciliary body; Ch = choroid; Co = cornea; Ir = iris; Le = lens anterior capsule; Pa = pars plicata; PC = posterior chamber; Sc = sclera; Zo = zonular fibers. *(Courtesy of Vikram S. Brar, MD.)*

provided with the order, the higher the likelihood of obtaining the desired information. Communication with the diagnostic radiologist can facilitate this process and increase the yield. The following box provides recommendations for ordering a study. Tables 17-5 and 17-6 cover specific disease entities, recommended imaging modality, and use of contrast material for common neuro-ophthalmic and orbital conditions, respectively.

Recommendations for Ordering Imaging Studies in Ophthalmology

- Decide whether a CT or MR scan is indicated. In most cases, MRI is superior to CT for neuro-ophthalmic indications. CT is superior to MRI for visualizing calcifications, bone, and acute hemorrhage and when an emergent scan is needed. CT may also be used when the patient cannot undergo MRI.
- Decide whether contrast-material enhancement is needed. In most cases, contrast material should be ordered for all studies. Contrast enhancement may not be necessary in acute hemorrhage, thyroid ophthalmopathy, and trauma cases.

(Continued)

(continued)

- Localize the lesion clinically ("Where is the lesion?"), and then order a study tailored to that location (eg, head, orbit, neck). To obtain the correct study, take the time to fill out the radiographic order form personally with sufficient clinical details for the radiologist. Do not simply order a "brain MRI" for every case.
- Depending on the clinical indication, consider ordering special imaging sequences (eg, fat suppression for an orbital postcontrast study, FLAIR for white-matter lesions, gradient echo for hemorrhage).
- Tell the radiologist the differential diagnosis ("What is the lesion?") and the location ("Where is the lesion?").
- If the imaging shows either no abnormality or an abnormality that does not match the clinical location, call the radiologist or, better yet, review the films directly with him or her. Ask the radiologist if the area of interest has been adequately imaged, if artifacts might be obscuring the lesion, or if additional studies might show the lesion.
- If the clinical picture suggests a specific lesion or location and initial imaging is "normal," consider repeating the imaging study with thinner sections and higher magnification of the area of interest, especially if the clinical signs and symptoms are progressive.
- Recognize that the lack of an abnormality on imaging does not exclude pathology.

Modified with permission from Lee AG, Brazis PW, Garrity JA, White M. Imaging for neuro-ophthalmic and orbital disease. *Am J Ophthalmol.* 2004;138(5):855.

Kruger JM, Lessell S, Cestari DM. Neuro-imaging: a review for the general ophthalmologist. *Semin Ophthalmol.* 2012;27(5–6):192–196.

Lee AG, Johnson MC, Policeni BA, Smoker WRK. Imaging for neuro-ophthalmic and orbital disease: a review. *Clin Exp Ophthalmol.* 2009;37(1):30–53.

Simha A, Irodi A, David S. Magnetic resonance imaging for the ophthalmologist: a primer. *Indian J Ophthalmol.* 2012;60(4):301–310.

Table 17-5 Neuro-Ophthalmic Indications and Recommended Imaging Study

Indication	Imaging Study	Contrast Material	Comment
Optic nerve drusen	CT scan of the orbit (may show calcification) B-scan ultrasonography (axial) OCT scan	Not necessary	OCT and ultrasonography scans are less costly and more sensitive for drusen than is a CT scan.
Papilledema	MRI of the head (with MRV)	Yes	Consider contrast MRV to exclude venous sinus thrombosis, especially in atypical patients with idiopathic intracranial hypertension (IIH, formerly known as *pseudotumor cerebri*) and in older patients or in those who are thin or male.
Transient visual loss (amaurosis fugax)	MRA or CTA of the neck for carotid stenosis or dissection	Depends on clinical situation	An adjunctive carotid Doppler study or catheter angiography may be required.
Demyelination optic neuritis	MRI of the head and orbit	Yes	Consider FLAIR to look for demyelinating white matter lesions; MRI has prognostic significance for the development of multiple sclerosis.
Inflammatory, infiltrative, or compressive optic neuropathy	MRI of the head and orbit	Yes	Fat suppression will exclude intraorbital optic nerve enhancement; CT is superior in cases of traumatic optic neuropathy for canal fractures.
Junctional scotoma (ie, optic neuropathy in 1 eye and superotemporal visual field loss in fellow eye)	MRI of the head (attention to the sella)	Yes	
Bitemporal hemianopia	MRI of the head (attention to the chiasm and sella)	Yes	Consider CT of the sella if an emergent scan is needed (eg, pituitary or chiasmal apoplexy) or when imaging for calcification (eg, meningioma, craniopharyngioma, or aneurysm).
Homonymous hemianopia	MRI of the head	Yes	Examine the retrochiasmal pathway. DWI may be useful in patients with acute ischemic infarct. If results of structural imaging are negative and there is organic vision loss, consider functional imaging (eg, PET, SPECT, MRS).

(Continued)

Table 17-5 *(continued)*

Indication	Imaging Study	Contrast Material	Comment
Cortical vision loss or possible damage to the visual association cortex (eg, as in cerebral achromatopsia, alexia, prosopagnosia, simultagnosia, optic ataxia, Balint syndrome)	MRI of the head	Yes	Examine the retrochiasmal pathway. DWI may be useful in patients with acute ischemic infarct. If results of structural imaging are negative and there is organic vision loss, consider functional imaging (eg, PET, SPECT, MRS).
Third, fourth, or sixth cranial nerve palsy or cavernous sinus syndrome	MRI of the head with attention to the skull base; isolated vasculopathic cranial neuropathies may not require initial imaging	Yes	Rim calcification in aneurysm, calcification in tumors, and hyperostosis may be better seen on CT.
INO, supranuclear or nuclear gaze palsies, dorsal midbrain syndrome, skew deviation	MRI of the head (brainstem)	Yes	Rule out demyelinating or other brainstem lesion; include a FLAIR sequence.
Nystagmus	MRI of the brainstem	Yes	Localize the nystagmus.
Hemifacial spasm	MRI of the brainstem (with or without MRA)	Yes	Rule out compression of the facial nerve root near its exit from the brainstem by adjacent artery; eg, anterior/posterior inferior cerebellar artery.
Horner syndrome: preganglionic	MRI of the head and neck to the second thoracic vertebra (T2) in the chest with neck MRA	Yes	Rule out lateral medullary infarct, apical lung neoplasm, carotid dissection, etc.
Horner syndrome: postganglionic	MRI of the head and neck to the level of the superior cervical ganglion (C4 level) with MRA of the neck	Yes	Rule out carotid dissection; isolated postganglionic lesions are often benign.

CT = computed tomography; CTA = CT angiography; DWI = diffusion-weighted imaging; FLAIR = fluid attenuation inversion recovery; INO = internuclear ophthalmoplegia; MRA = magnetic resonance angiography; MRI = magnetic resonance imaging; MRS = magnetic resonance spectroscopy; MRV = magnetic resonance venography; PET = positron emission tomography; SPECT = single-photon emission computed tomography.

Modified with permission from Lee AG, Brazis PW, Garrity JA, White M. Imaging for neuro-ophthalmic and orbital disease. *Am J Ophthalmol*. 2004;138(5):854.

Table 17-6 Orbital Indications and Recommendations for Imaging

Indication	Imaging Study	Contrast Enhancement	Comment
Thyroid eye disease	CT or MRI of the orbit	Iodinated contrast medium may interfere with evaluation and treatment of systemic thyroid disease	Bone anatomy is better seen on a CT scan, especially if orbital decompression is being considered.
Orbital cellulitis and orbital disease secondary to sinus disease (eg, silent sinus syndrome, sinusitis)	CT of the orbit and sinuses	Depends on clinical situation	MRI may be a useful adjunct, especially if concomitant cavernous sinus thrombosis is present.
Nonspecific orbital inflammation	CT or MRI of the orbit (with fat suppression)	Yes	Beware of fat suppression artifact.
Orbital tumor (eg, proptosis or enophthalmos, gaze-evoked vision loss)	CT or MRI of the orbit	Yes	Include head imaging if lesion could extend intracranially (eg, optic nerve sheath meningioma); CT scan may be superior if looking for hyperostosis or calcification (eg, sheath meningioma).
Orbital trauma (eg, fracture, subperiosteal hematoma, orbital foreign body, orbital emphysema)	CT scan of the orbit with axial and direct coronal imaging	Not generally necessary	CT is superior for visualizing a fracture or bone fragment; MRI may be superior for optic nerve sheath hemorrhage.
Carotid cavernous sinus or dural fistula (eg, orbital bruit, arterialization of conjunctival and episcleral vessels, glaucoma)	CT or MRI of the head and orbit (with contrast-enhanced MRA)	Yes	CT or MRI may show an enlarged superior ophthalmic vein and may require a catheter angiogram for final diagnosis and therapy. Color flow Doppler studies may be useful for detecting reversal of orbital venous flow.

CT = computed tomography; MRA = magnetic resonance angiography; MRI = magnetic resonance imaging.

Modified with permission from Lee AG, Brazis PW, Garrity JA, White M. Imaging for neuro-ophthalmic and orbital disease. *Am J Ophthalmol*. 2004;138(5):857.

CHAPTER 18

Digital Ophthalmology

Highlights

- Digital ophthalmology, including electronic health record systems and large data repositories, like the American Academy of Ophthalmology's Intelligent Research in Sight Registry, can facilitate quality improvement measures for both clinicians and patients.
- As part of maintenance of certification, the American Board of Ophthalmology requires an element of quality improvement.
- The ubiquitous use of images in ophthalmology facilitates the application of artificial intelligence (AI) to clinical care and research.
- Incorporating AI and/or teleophthalmology into health care delivery systems can expand access for underserved populations and reduce health disparities.

Introduction

Digital ophthalmology applies health information technology to ophthalmology with the aim of improving the quality of care. The Institute of Medicine defines the 6 aims of quality as *safe, effective, efficient, equitable, patient-centered,* and *timely,* expanding the meaning of quality beyond clinical effectiveness to include key concepts such as equity and physician/patient satisfaction. The American Board of Ophthalmology (ABO) requires that ophthalmologists document efforts aimed at improving quality for maintenance of certification (MOC).

Health information technology has the potential to reduce error, improve efficiency, augment skills and knowledge, and provide novel insights into pathology or treatment while offloading cognitive and administrative tasks from clinicians. Ophthalmology is particularly well positioned to benefit from digital health due to the wealth of images, numerous discrete data, and high-quality evidence undergirding the standard of care of the diseases with the highest burden.

In the following sections, we discuss the constituent components of digital ophthalmology: data (including electronic health records, standards, and big data) and analysis (including telemedicine and AI).

American Board of Ophthalmology. Create Your Own Improvement Project. Accessed January 13, 2023. https://abop.org/maintain-certification/improvement-in-medical-practice/create-your-own-improvement-project/

American Academy of Ophthalmology. Medical Information Technology Guideline. Accessed January 13, 2023. www.aao.org/medical-information-technology-guidelines

Institute of Medicine (US) Committee on Quality of Health Care in America. *Crossing the Quality Chasm: A New Health System for the 21st Century*. The National Academies Press; 2001.

Data

Electronic Health Records

According to the Institute of Medicine, the purpose of the medical record is to "recall observations, inform others, instruct students, gain knowledge, monitor performance, and justify interventions." Secondary uses include its function as a medicolegal document and to inform billing. The characteristics of electronic health records (EHRs) offer several advantages over traditional paper-based records. EHRs solve the legibility problem of hand-written notes and address the issues of access and archiving related to bulky paper charts. When information is captured in a structured manner—not as free text, but as discrete data points with specific meaning—EHRs can be used to organize, analyze, search, and present information in a way that is meaningful for the clinician and/or investigator.

Furthermore, EHR data can be used to provide clinical decision support, such as providing alerts related to medication interactions, allergies, duplicate orders, and best practice interventions. EHR systems support communication and notification functions to facilitate order transmission, result reporting, coordination of care, and communication between clinicians and patients.

The practice of ophthalmology requires real-time access to patient images. Picture archiving and communications systems (PACS) store and display images and facilitate image analysis. The integration of PACS with EHRs can help prevent errors and improve the efficiency of clinical practice.

Although EHR systems have the potential to improve care, efficiency, quality, and physician satisfaction, this has not yet been realized. A number of external factors (eg, billing and regulatory requirements) and internal behaviors (eg, copy forwarding and templated charting) have contributed to the frequent use of long and unstructured notes, a phenomenon known as *note bloat* that makes relevant information harder to find. In theory, EHR adoption could improve the quality of documentation and care; in practice, it has been associated with lower efficiency, increased physician burnout, and medical errors. Ongoing quality improvement and research efforts are needed to realize the potential benefits of EHR systems in ophthalmic practice.

Melton GB, McDonald CJ, Tang PC, Hripcsak G. Electronic Health Records. In: Shortliffe EH, Cimino JJ, eds. *Biomedical Informatics*. Springer; 2021:467–509.

Digital Ophthalmology Standards

Digital ophthalmology requires standards for how data are organized and communicated in order to maximize transparency, efficiency, and accuracy. In health care, including ophthalmology, many such standards exist, including the International Classification of Diseases, Tenth Revision (ICD-10) for disease classification and diagnosis; Current Procedural Terminology (CPT) for precise specification of medical procedures; and Digital

Table 18-1 Data Standards in Digital Ophthalmology

Standard	Domain
International Classification of Diseases (ICD)	Terminology for diagnoses
Current Procedural Terminology (CPT)	Procedures and services
Standard Nomenclature of Medicine Clinical Terms (SNOMED CT)	Concepts in medicine, including diagnoses, symptoms, observations, anatomical structures, and medications, as well as their relationships
Logical Observations, Identifiers, Names, and Codes (LOINC)	Laboratory results, clinical observations, and measurements
RxNorm	Medications
Digital Imaging and Communications in Medicine (DICOM)	Diagnostic images and measurements, including visual fields and biometry
HL7 Fast Healthcare Interoperability Resources (FHIR)	Communication of health data and mapping to existing standards, connecting the data in EHRs, PACS, devices, applications, and web services

EHR = electronic health record; PACS = picture archiving and communications systems.

Imaging and Communications in Medicine (DICOM) for precise specification of image and imagelike data. Other important standards for health data are listed in Table 18-1.

The adoption of standards by EHR systems and ophthalmic device vendors is essential for realizing the benefits of digital ophthalmology. Clinicians and patients can benefit from the ability to send and receive clinical notes, full-resolution images, and visual fields across different systems. The integration of clinical and imaging data from multiple systems using data standards would facilitate efficient clinical care and the development of useful datasets for research.

Big Data

The term *big data* is used to describe large datasets comprising data from thousands or more patients. Examples include EHR data, claims databases, genetic repositories, and clinical and imaging data registries such as the American Academy of Ophthalmology's (AAO's) IRIS (Intelligent Research in Sight) Registry.

The *IRIS Registry*, established in 2014, is the most compelling example of big data. It contains structured records of patient encounters shared by participating ophthalmologists. Containing data from more than 70 million patients, IRIS is currently the largest clinical registry of any medical specialty. These large datasets can be powerful tools for clinical research, the characterization of rare diseases, and quality improvement by comparing outcomes across populations. They can also be leveraged to identify novel associations, such as the recently discovered association between cataract surgery and reduced risk of dementia. However, the power of these big datasets is offset at times by the quality and integration of clinical data, the lack of consistent data documentation, and the risk of loss of privacy or of bias from the underrepresentation of certain populations in clinical data.

American Academy of Ophthalmology. IRIS Registry. Accessed January 13, 2023. www.aao.org/iris-registry

Mott M. Deciphering big data studies. *Eyenet.* 2021;25(8):44–49.

Wang SY, Pershing S, Lee AY; AAO Taskforce on AI and AAO Medical Information Technology Committee. Big data requirements for artificial intelligence. *Curr Opin Ophthalmol.* 2020;31(5):318–323.

Teleophthalmology

Teleophthalmology is a form of digital ophthalmology used to care for patients who are separated from the ophthalmologist by distance, time, or both. There are 2 types: synchronous (occurring at the same time but separated by distance) and asynchronous (separated by both space and time). Telemedicine can help improve patient and population outcomes by increasing access to care for patients and populations that may span large geographic areas, live in underserved regions, or, such as in the era of COVID-19, are otherwise unable to participate in the standard in-person ophthalmic visit.

The majority of teleophthalmology is done using the asynchronous or "store-and-forward" telemedicine (SFT) model. In SFT, a *telepresenter*, usually a nonphysician such as a nurse or a technician, gathers clinical information from the patient and transmits it to be reviewed by the provider at a different time. The classic example is diabetic tele–retinal screening, where fundus photos of diabetic patients are obtained in 1 location (eg, primary care) and interpreted elsewhere in a reading center.

There are many other teleophthalmology programs: retinopathy-of-prematurity screening, comprehensive eye exams, teleglaucoma, and telemacula. Teleconsultations are an important use case in teleophthalmology, where a referring provider sends the patient's clinical information in advance or real-time to a specialist who then provides recommendations. In these cases, the referring provider acts as the telepresenter.

Teleophthalmology implementation requires a systems-based approach that includes a robust and secure information technology (IT) infrastructure, the use of data standards such as DICOM, and the interconnectability of devices. To achieve the goals of teleophthalmology, it is essential to implement an effective system for notifying patients of results and to ensure availability of accessible intervention for those patients determined to receive in-person care. An emerging frontier of teleophthalmology is *remote patient monitoring.* An ocular self-monitoring device or mobile application can be used to send data to an ophthalmologist or an AI model to help patients determine if their clinical status has changed and advise them on the need and urgency for intervention.

Horton MB, Brady CJ, Cavallerano J, et al. Practice Guidelines for Ocular Telehealth—Diabetic Retinopathy, Third Edition. *Telemed J E Health.* 2020;26(4):495–543.

Artificial Intelligence

Artificial intelligence (AI) describes systems that perform tasks mimicking human cognitive capabilities using machine learning or other optimization techniques. AI leverages imaging

and clinical data to perform highly cognitive tasks, such as imaging interpretation and clinical decision-making. In ophthalmology, AI has been applied to the diagnosis and staging of many diseases, including diabetic retinopathy, retinopathy of prematurity, age-related macular degeneration, glaucoma, keratoconus, and ocular cancers. AI enables the analysis of large amounts of data for a single patient, thus improving ophthalmologists' effectiveness in using this information. AI also enables large-scale analysis of many patients' data, thus improving ophthalmologists' productivity. Ophthalmology is particularly well suited to AI because of the widespread use of objective imaging data and widely accepted evidence-based clinical standards. Integrating AI-based disease screening into clinical workflows may improve access to care, adherence to screening guidelines, care quality, and outcomes while reducing health disparities and costs, especially for patients in under-resourced and/or geographically isolated locations.

Abràmoff MD, Cunningham B, Patel B, et al; Collaborative Community on Ophthalmic Imaging Executive Committee and Foundational Principles of Ophthalmic Imaging and Algorithmic Interpretation Working Group. Foundational considerations for artificial intelligence using ophthalmic images. *Ophthalmology.* 2022;129(2):e14–e32. doi:10.1016/j.ophtha.2021.08.023

American Academy of Ophthalmology. Artificial Intelligence. Accessed January 13, 2023. www.aao.org/artificial-intelligence

Clinical Example

Consider the development of an autonomous AI system for diagnosing diabetic retinopathy and diabetic macular edema from retinal images. There is substantial evidence that annually examining a patient with diabetes for diabetic retinopathy before symptoms occur helps prevent vision loss. However, for various reasons—including the social determinants of health—many people with diabetes do not undergo consistent eye examinations. The goal of such an AI system would be to improve visual outcomes for people with diabetes by making diabetic eye screening efficient and accessible. In this case, the AI system would identify patients at risk for vision loss, which, at the very least, would reduce the number of images that require reviewing at reading centers.

Based on established guidelines (in this case, the AAO *Diabetic Retinopathy Preferred Practice Pattern* guideline), the outputs of this proposed AI system would be "disease present" when the patient has at least a defined level of disease and "disease absent" otherwise. The outputs must be accurate for the AI to be safe. Because the US population of patients with diabetes is diverse, AI bias—such as differing levels of accuracy in assessing different races, ethnicities, and genders—must be avoided (see the section Design, Bias, and Reference Standards).

Such an AI system would use digital retinal images as inputs. Each pixel in these images measures the property of a small region of the retina, such as color reflectance in fundus images. Reflectance characterizes physiologic and pathologic processes, such as the local hemoglobin level. Blood vessels, hemorrhages, and exudates determine the color of multiple adjoining pixels in different ways. For example, groups of pixels representing a hemorrhage are more likely to have a similar (reddish) color than the rest of the retina. Such similarities can be measured and are described as *spatial coherence*. In addition, similarities in data points

over time (*temporal coherence*) can be harnessed to predict progression. An AI system can be designed to associate such characteristics with a diagnosis using machine learning, as explained in the following section.

Machine Learning

The highest AI accuracy is typically achieved via machine learning algorithms. Without machine learning, explicitly programming an algorithm to mimic human cognitive abilities requires a mathematical definition, which remains elusive. Instead, machine learning algorithms typically have thousands or more parameters that are not explicitly programmed but adjusted step-by-step during a training phase.

Deep learning algorithms are advanced machine learning algorithms that incorporate millions of parameters grouped in complex ways. During the training phase, the algorithm learns to associate coherences in a set of examples with the desired output. For example, in a deep learning algorithm for diagnosing diabetic retinopathy, the *training set* would be a set of retinal images of patients with diabetes along with labels of the disease state, or diagnosis, for each image—called the reference standard or the *ground truth*.

Machine learning uses the power of probabilistic training to differentiate between relevant and irrelevant spatial and temporal coherences in the training images. The process is performed step-by-step, image-by-image. To start, the first image of the training set is input into an algorithm that is initially not very accurate, and the algorithm uses its parameters to calculate the output. If the output is different from the ground truth or reference standard for that image, the algorithm is incorrect, and some of its parameters are adjusted. If the output is accurate, the parameters are typically left unchanged. Over many iterations, the accuracy improves, and the process continues until a desired level of accuracy has been achieved (Fig 18-1). Images from a separate set of patients, known as the test set, can be used to assess the algorithm's performance after the training process.

A key outcome of the machine learning process is that the resulting algorithm systematically generalizes from the training set; it does not memorize each training example. This enables the algorithm to give a correct output for a previously unseen image. This process also demonstrates the importance of accurate labels in the training set: if an algorithm is trained with incorrect reference standard labels, the model will be less accurate.

Thus, larger and more diverse training sets with accurate truths lead to more accurate algorithms with less AI bias. The relevant coherences will dominate the irrelevant, spurious coherences. Unfortunately, in ophthalmology, obtaining such large training sets is an expensive, laborious process within narrow ethical and legal constraints. Such fundamental data scarcity limits the direct translation of AI algorithms widely used outside ophthalmology.

Design, Bias, and Reference Standards

The distribution of the training set explains how various biases, such as racial bias, can be incorporated into the learning process. Some machine learning algorithms, so-called *black box AI,* have no built-in prior knowledge. Black box algorithms can learn to associate any information in the image with the desired output, even information that is irrelevant to the disease. This characteristic can be an advantage when the goal of AI is to discover new, previously

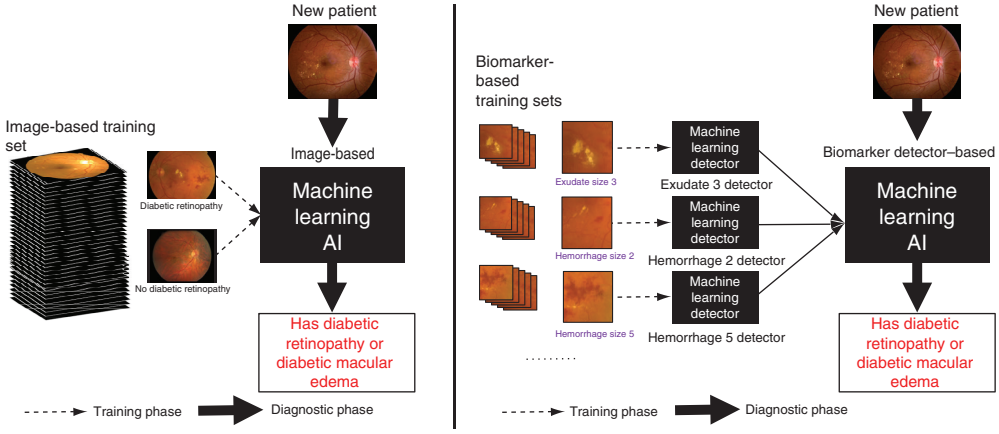


Figure 18-1 Image-based *(left)* and biomarker-based *(right)* deep learning artificial intelligence (AI) algorithms. The AI deep learning algorithm or model (represented by the black rectangles) for diagnosing diabetic retinopathy is built during the training phase and outputs the diagnosis in the clinical phase.

The AI algorithm is trained using a set of retinal images *(left)* or image regions containing biomarkers *(right)*. The training set also contains the "ground truth" or "reference standard" for each image, such as the diagnosis (eg, "diabetic retinopathy") or the biomarker type (eg, "hemorrhage"). Multiple biomarker detectors are typically trained for biomarker-based AI. During the training phase, the partially trained algorithm is offered an input image and creates an output. If the generated output is incorrect compared to the ground truth, some of the AI parameters are adjusted (not shown). Thus, the algorithm becomes increasingly accurate with each additional training image from the training set. During the clinical phase, a previously unseen image ("new patient") is input, and the fully trained AI, incorporating either the algorithm trained with complete images *(left)* or multiple detectors for the different pathology biomarkers *(right)*, provides the diagnosis. *(Courtesy of Michael D. Abràmoff, MD, PhD. New patient photo courtesy of Dominik Thomas and Damien Luviano, MD; diabetic retinopathy photo courtesy of Damien Luviano, MD, and Nishant Kumar, FRCOphth; no diabetic retinopathy photo courtesy of Vikram S. Brar, MD; biomarker-based training set photos courtesy of Michael D. Abràmoff, MD, PhD.)*

unknown associations, such as research into a potential new disease mechanism. However, if the goal is to accurately identify patients with a retinal disease on fundus photographs, which may appear different between various racial and ethnic groups, bias can be introduced.

For example, consider a training set that is inadvertently skewed toward images of patients with darkly pigmented retinas and a lower incidence of disease than patients with lightly pigmented retinas. After machine learning from this training set, a black box AI will associate a lightly pigmented retina more with a "disease" output than a darkly pigmented retina. After all, it has no other information to learn that this association is incorrect. This biased AI is more likely to diagnose a previously unseen patient with darkly pigmented retinas as not having the disease, resulting in a missed diagnosis.

Such bias can be mitigated by AI conceptualization, design, careful development, prior analysis of the training set, and validation with a test set. Prior knowledge can be introduced, such as the fact that diabetic retinopathy is characterized by hemorrhages, exudates, and new vessels, independent of race or ethnicity. Using machine learning to create lesion detectors can result in AI systems that are better understood, are more robust to noisy inputs, and may have reduced risk of bias based on fundus appearance, provided lesion identification is

not affected by fundus pigmentation. Regardless of the AI design, careful evaluation of the algorithm's performance in relevant subpopulations is essential.

Reference standards can be labels created by a single clinician, the consensus of several experts, an independent reading center, or a prognostic standard associated with clinical outcomes. Developing strict reference standards for the labels used in AI algorithm training sets is fundamental to the algorithm's accuracy, safety, and efficacy on new, previously unseen input data.

Conclusions

Digital ophthalmology can improve the quality of care, reduce disparity, and improve physician well-being while reducing the cost of care delivery. EHRs, telemedicine, big data, and AI may each play a crucial role in reaching these goals. Ophthalmology has been a leader in the adoption of AI and obtained the first US Food and Drug Administration De Novo authorization ("approval") for an autonomous AI system for clinical use. Now that such AI systems are commercially available, they can be scaled to hundreds of millions of patients, thereby increasing the potential for patient benefit as well as the risk of harm. Therefore, addressing safety, equity, and other ethical issues of AI is crucial—these issues are as important as, or more important than, an AI system's technical details. Our profession is tasked to ensure that ophthalmological AI systems are designed, developed, validated, and introduced in a safe and equitable manner. Engagement and the development of skills and understanding in these domains, as well as vigilance about equity and bias, are essential for ushering in the benefits of digital ophthalmology.

Additional Materials and Resources

Related Academy Materials

The American Academy of Ophthalmology is dedicated to providing a wealth of high-quality clinical education resources for ophthalmologists.

Print Publications and Electronic Products

For a complete listing of Academy products related to topics covered in this BCSC Section, including the BCSC Self-Assessment Program, visit our online store at https://store.aao.org/clinical-education/topic/comprehensive-ophthalmology.html.

Or call Customer Service at 866.561.8558 (toll free, US only) or +1 415.561.8540, Monday through Friday, between 8:00 AM and 5:00 PM (PST).

Online Resources

Visit the **Ophthalmic News and Education (ONE®) Network** at aao.org/comprehensive-ophthalmology to find relevant videos, podcasts, webinars, online courses, journal articles, practice guidelines, self-assessment quizzes, images, and more. The ONE Network is a free Academy-member benefit.

The **Residents page** on the ONE Network (aao.org/residents) offers resident-specific content, including courses, videos, flashcards, and OKAP and Board Exam study tools.

Find comprehensive **resources for diversity, equity, and inclusion** in ophthalmology on the ONE Network at aao.org/diversity-equity-and-inclusion.

Access free, trusted articles and content with the Academy's collaborative online encyclopedia, **EyeWiki,** at aao.org/eyewiki.

Get mobile access to the *Wills Eye Manual* and *EyeWiki,* watch the latest 1-minute videos, challenge yourself with weekly Diagnose This activities, and set up alerts for clinical updates relevant to you with the free **AAO Ophthalmic Education App.** Download today: search for "AAO Ophthalmic Education" in the Apple app store or in Google Play.

Basic Texts and Additional Resources

General Ophthalmology

Forrester JV, Dick AD, McMenamin PG, Roberts F, Pearlman E. *The Eye: Basic Sciences in Practice.* 5th ed. Elsevier; 2021.

Anatomy and Histology

Bron AJ, Tripathi RC, Tripathi BJ, eds. *Wolff's Anatomy of the Eye and Orbit.* 8th ed. Chapman & Hall; 1997.

Dutton JJ. *Atlas of Clinical and Surgical Orbital Anatomy.* 2nd ed. Saunders; 2011.*

Hogan MJ, Alvarado JA, Weddell JE. *Histology of the Human Eye: An Atlas and Textbook.* Saunders; 1971.

Miller NR, Newman NJ, eds. *Walsh & Hoyt's Clinical Neuro-Ophthalmology, Volume 1.* 6th ed. Lippincott Williams & Wilkins; 2005.*

Snell RS, Lemp MA. *Clinical Anatomy of the Eye.* 2nd ed. Wiley-Blackwell; 1998.*

Spalton DJ, Hitchings RA, Hunter PA, eds. *Atlas of Clinical Ophthalmology.* 3rd ed. Elsevier; 2005.

Tasman W, Jaeger EA, eds. *Duane's Ophthalmology on DVD-ROM, 2013 Edition.* Lippincott Williams & Wilkins; 2013.

Zide BM, ed. *Surgical Anatomy Around the Orbit: The System of Zones.* Lippincott Williams & Wilkins; 2006.

Embryology and Genetics

Couser NL. *Ophthalmic Genetic Diseases: A Quick Reference Guide to the Eye and External Ocular Adnexa Abnormalities.* Elsevier; 2019.

Jakobiec FA, ed. *Ocular Anatomy, Embryology, and Teratology.* Harper & Row; 1982.

Merin S. *Inherited Eye Diseases: Diagnosis and Management.* 2nd ed. Taylor & Francis; 2005.

Nussbaum RL, McInnes RR, Willard HF. *Thompson & Thompson Genetics in Medicine.* 8th ed. Elsevier/Saunders; 2016.

Schoenwolf GC, Bleyl SB, Brauer PR, Francis-West PH, eds. *Larsen's Human Embryology.* 6th ed. Elsevier/Churchill Livingstone; 2021.

Traboulsi EI, ed. *Genetic Diseases of the Eye.* 2nd ed. Oxford University Press; 2012.

Biochemistry and Metabolism

Levin LA, Nilsson SFE, Ver Hoeve J, Wu SM, eds. *Adler's Physiology of the Eye.* 11th ed. Elsevier/Saunders; 2011.

Whikehart DR. *Biochemistry of the Eye.* 2nd ed. Butterworth-Heinemann; 2003.

Ocular Pharmacology

Bartlett JD, Jaanus SD, eds. *Clinical Ocular Pharmacology.* 5th ed. Elsevier/Butterworth-Heinemann; 2008.

Brunton LL, Knollman BC, Goodman LS, eds. *Goodman & Gilman's The Pharmacological Basis of Therapeutics.* 14th ed. McGraw-Hill Education; 2022.

Fraunfelder FT, Fraunfelder FW. *Drug-Induced Ocular Side Effects: Clinical Ocular Toxicology.* 8th ed. Elsevier; 2020.

Zimmerman TJ, Karanjit K, Mordechaie S, Fechtner RD, eds. *Textbook of Ocular Pharmacology.* 3rd ed. Lippincott Williams & Wilkins; 1997.

Imaging

Bhatti MT, Schmalfuss I. *Handbook of Neuroimaging for the Ophthalmologist.* JP Medical; 2014.

Dutton JJ. *Radiology of the Orbit and Visual Pathways.* Elsevier/Saunders; 2010.

Müller-Forell WS. *Imaging of Orbital and Visual Pathway Pathology.* Springer; 2006.

Singh AD, Hayden BC. *Ophthalmic Ultrasonography.* Elsevier/Saunders; 2012.

*Also see the Embryology section in this book.

Requesting Continuing Medical Education Credit

The American Academy of Ophthalmology is accredited by the Accreditation Council for Continuing Medical Education (ACCME) to provide continuing medical education for physicians.

The American Academy of Ophthalmology designates this enduring material for a maximum of 15 *AMA PRA Category 1 Credits*™. Physicians should claim only the credit commensurate with the extent of their participation in the activity.

To claim *AMA PRA Category 1 Credits*™ upon completion of this activity, learners must demonstrate appropriate knowledge and participation in the activity by taking the posttest for Section 2 and achieving a score of 80% or higher.

There is no formal American Board of Ophthalmology (ABO) approval process for self-assessment activities. Any CME activity that qualifies for ABO Continuing Certification credit may also be counted as "self-assessment" as long as it provides a mechanism for individual learners to review their own performance, knowledge base, or skill set in a defined area of practice. For instance, grand rounds, medical conferences, or journal activities for CME credit that involve a form of individualized self-assessment may count as a self-assessment activity.

To take the posttest and request CME credit online:

1. Go to www.aao.org/cme-central and log in.
2. Click on "Claim CME Credit and View My CME Transcript" and then "Report AAO Credits."
3. Select the appropriate media type and then the Academy activity. You will be directed to the posttest.
4. Once you have passed the test with a score of 80% or higher, you will be directed to your transcript. *If you are not an Academy member, you will be able to print out a certificate of participation once you have passed the test.*

CME expiration date: June 1, 2026. *AMA PRA Category 1 Credits*™ may be claimed only once between June 1, 2023 (original release date), and the expiration date.

For assistance, contact the Academy's Customer Service department at 866.561.8558 (US only) or +1 415.561.8540 between 8:00 AM and 5:00 PM (PST), Monday through Friday, or send an e-mail to customer_service@aao.org.

Study Questions

Please note that these questions are not part of your CME reporting process. They are provided here for your own educational use and for identification of any professional practice gaps. The required CME posttest is available online (see "Requesting Continuing Medical Education Credit"). Following the questions are answers with discussions. Although a concerted effort has been made to avoid ambiguity and redundancy in these questions, the authors recognize that differences of opinion may occur regarding the "best" answer. The discussions are provided to demonstrate the rationale used to derive the answer. They may also be helpful in confirming that your approach to the problem was correct or, if necessary, in fixing the principle in your memory. The Section 2 faculty thanks the Resident Self-Assessment Committee for developing these self-assessment questions and the discussions that follow.

1. Loss of what structure due to increasing age can lead to conjunctivochalasis?
   a. levator aponeurosis
   b. Müller muscle
   c. tarsus
   d. Tenon capsule

2. What is the approximate volume of the orbit in an adult?
   a. 5 mL
   b. 15 mL
   c. 30 mL
   d. 50 mL

3. In what condition does a pathogenic variant in the fibrillin-1 gene cause lens subluxation due to zonular weakness?
   a. homocystinuria
   b. Marfan syndrome
   c. pseudoexfoliation syndrome
   d. recurrent uveitis

4. What vessels perfuse the choroid?
   a. central retinal artery
   b. choriocapillaris
   c. long and short posterior ciliary arteries
   d. major arterial circle

5. What is the normal density of corneal endothelial cells centrally in young adults?
   a. 8000 cells/mm^2
   b. 3000 cells/mm^2
   c. 1000 cells/mm^2
   d. 500 cells/mm^2

6. What ocular structure is susceptible to damage from a nasopharyngeal carcinoma that extends into the skull base?
   a. cranial nerve (CN) IV (the trochlear nerve)
   b. CN VI (the abducens nerve)
   c. CN VII (the facial nerve)
   d. sympathetic fibers traveling along the carotid artery

7. What is the sensory function of CN VII?
   a. sensation from the external auditory meatus
   b. sensation from the preauricular skin
   c. preganglionic sympathetic innervation of the ciliary ganglion
   d. taste from the posterior one-third of the tongue

8. What congenital cranial dysinnervation disorder is characterized by innervation of the levator muscle by CN V (the trigeminal nerve)?
   a. congenital fibrosis of the extraocular muscles
   b. Duane syndrome
   c. Marcus Gunn jaw-winking syndrome
   d. Möbius syndrome

9. A pathogenic variant of what gene leads to the development of Waardenburg syndrome?
   a. *BAX*
   b. *PAX2*
   c. *PAX3*
   d. *PAX6*

10. What is the cellular function of the gene product that is defective in cases of retinoblastoma?
    a. contribution to cellular structure
    b. production of energy
    c. regulation of the cell cycle
    d. transportation of cell wall proteins

11. Patients with xeroderma pigmentosum are at increased risk for which ocular cancers?
    a. choroidal melanoma and retinoblastoma
    b. squamous cell carcinoma and choroidal melanoma
    c. squamous cell carcinoma and ocular surface melanoma
    d. squamous cell carcinoma and retinoblastoma

12. An ophthalmologist is consulted to provide a complete eye evaluation for a patient. The patient, who has very light hair and skin color, has reported experiencing mild chronic photosensitivity and blurring in both eyes but no other symptoms. Recently, the patient had a dental procedure that resulted in excessive bleeding. His sister has a similar history and symptoms. What is the most likely diagnosis?
    a. achromatopsia with myopia
    b. Hermansky-Pudlak syndrome
    c. Niemann-Pick disease
    d. oculocutaneous albinism

13. What 2 medications have been approved by the US Food and Drug Administration (FDA) for treatment of the inflammatory component of dry eye syndrome?
    a. prednisolone acetate and doxycycline
    b. topical cyclosporine A emulsion and doxycycline
    c. topical cyclosporine A emulsion and lifitegrast
    d. topical cyclosporine A emulsion and prednisolone acetate

14. What is the maximum amount of fluid an eye can hold prior to tearing?
    a. 5–10 μL
    b. 15–20 μL
    c. 25–30 μL
    d. 35–40 μL

15. What type of collagen production is associated uniquely with corneal stromal wound healing?
    a. type I
    b. type III
    c. type V
    d. type VII

16. Soft contact lenses with low oxygen permeability can cause corneal edema via the accumulation of what substance?
    a. aldehyde dehydrogenase
    b. carbon dioxide
    c. lactic acid
    d. proteoglycans

17. The disruption of what corneal layer during laser subepithelial keratomileusis (LASEK) is thought to be the cause of increased risk for visual complications postoperatively due to central corneal haze?
    a. Bowman layer
    b. endothelium
    c. epithelium
    d. stroma

18. In the healthy human eye, which of the following components of the aqueous humor is always higher in concentration in the aqueous than it is in plasma?
    a. calcium
    b. glucose
    c. lactate
    d. urea

19. In the Goldmann equation, IOP = (F − U) / C + EVP, what variable represents the rate of aqueous humor drainage via the pressure-insensitive pathway?
    a. C
    b. EVP
    c. F
    d. U

20. Alterations in glucose metabolism can result in cataract formation. Under normal physiologic conditions, what is the primary pathway by which glucose is converted into adenosine triphosphate (ATP) in the human lens?
    a. aerobic metabolism
    b. glycolysis
    c. pentose phosphate pathway (also called hexose monophosphate shunt)
    d. polyol pathway (also called sorbitol pathway)

21. What is the thickness of the posterior lens capsule?
    a. 1–2 μm
    b. 2–4 μm
    c. 11–12 μm
    d. 13.5–14.5 μm

22. Proteins constitute what percentage of the weight of the lens?
    a. 11%
    b. 22%
    c. 33%
    d. 44%

23. What role does the vitreous exert on oxygen tension in the vitreous cavity?
    a. Oxygen tension is unrelated to the presence of vitreous.
    b. Oxygen tension is lower in the presence of vitreous.
    c. Oxygen tension is higher in the presence of vitreous.
    d. Eyes that have undergone vitrectomy contain decreased amounts of free radicals.

24. What condition is characterized by a pathogenic variant in a gene encoding type II collagen and leads to premature liquefaction of vitreous with peripheral condensation, which may induce retinal detachment?
    a. familial exudative vitreoretinopathy
    b. Marfan syndrome
    c. retinitis pigmentosa
    d. Stickler syndrome

25. What is the major soluble vitreous protein?
    a. albumin
    b. collagen fibers
    c. tissue plasminogen activator
    d. transferrin

26. What type of cells are retinal horizontal cells?
    a. antagonistic interneurons
    b. bipolar cells
    c. glial cells
    d. photoreceptors

27. What vitamin is most critical for a photoreceptor's response to light?
    a. A
    b. B
    c. C
    d. E

28. What class of retinal cells functions as the resident macrophage and is activated under stress?
    a. amacrine cells
    b. macroglia
    c. microglia
    d. pericytes

29. In what clinical presentation is genetic testing for a pathogenic variant in the gene *RPE65* indicated?
    a. bilateral central scotomas with optic disc pallor
    b. bilateral central scotomas with vitelliform macular lesions
    c. bilateral ring scotomas with bone spicule retinal lesions
    d. bilateral superior arcuate scotomas with optic disc cupping

30. The retinal pigment epithelium is the first developmental site of melanogenesis in the body. In which of the following ocular processes has ocular melanin been shown to participate?
    a. pathogenesis of retinitis pigmentosa
    b. retinal adhesion
    c. retinal development and neuronal migration
    d. vitamin A metabolism

31. The adverse effects of reactive oxygen species (ROS) have been proposed as causal factors in which ocular conditions?
    a. cataract
    b. conjunctivitis
    c. strabismus
    d. posterior capsule opacification

32. What characteristic of the retina makes it more vulnerable to damage from lipid peroxidation?
    a. high number of mitochondria in the rod inner segments
    b. high levels of saturated fatty acids in the rod outer segments
    c. low light exposure at night
    d. poor oxygen supply through the choroid

33. Assuming a ratio of 20 drops per milliliter (mL), how many milligrams (mg) of atropine are found in 1 drop of a 1% solution?
    a. 1 mg
    b. 0.5 mg
    c. 0.1 mg
    d. 0.05 mg

34. How much epinephrine is present in 1 mL of 1:10,000 epinephrine solution?
    a. 1 mg of epinephrine
    b. same amount of epinephrine as in 1 mL of 0.01% epinephrine
    c. same amount of epinephrine as in 1 mL of 1:1000 epinephrine
    d. same amount of epinephrine as in 1 mL of 0.1% epinephrine

35. What cycloplegic agent has the longest duration of action?
    a. atropine sulfate, 1%
    b. cyclopentolate HCl, 1%
    c. homatropine hydrobromide, 5%
    d. scopolamine hydrobromide, 0.25%

36. What US FDA–approved drug is a growth factor?
    a. aflibercept
    b. cenegermin
    c. ranibizumab
    d. teprotumumab

37. An orbital floor fracture is suspected in a 23-year-old patient examined in the emergency department following trauma. What imaging modality is best suited to evaluate the orbit in this case?
    a. computed tomography
    b. magnetic resonance imaging
    c. optical coherence tomography
    d. ultrasound biomicroscopy

38. What are the standard probe positions used in ocular B-scan ultrasonography?
    a. axial, sagittal, and radial
    b. axial, tangential, and radial
    c. axial, transverse, and longitudinal
    d. coronal, transverse, and sagittal

39. What term describes a deep learning training set labeled with disease state?
    a. algorithm
    b. ground truth
    c. spatial coherence
    d. temporal coherence

40. What represents the digital data standard for diagnostic images and measurements?
    a. Current Procedural Terminology
    b. Digital Imaging and Communications in Medicine
    c. Logical Observations, Identifiers, Names, and Codes
    d. Picture Archiving and Communications System

Answers

1. **d.** Conjunctivochalasis is characterized by redundant folds of conjunctiva between the globe and the eyelid margin. Because the bulbar conjunctiva fuses with the Tenon capsule as it inserts at the limbus, conjunctivochalasis results from loss of Tenon capsule caused by increasing age. Dehiscence of the levator aponeurosis with increasing age can lead to ptosis but is not the cause of conjunctivochalasis. Although the palpebral conjunctiva adheres firmly to the tarsus, and the forniceal conjunctiva of the upper eyelid is enmeshed in fibrous elements of Müller muscle, loss of these structures is not the cause of conjunctivochalasis.
2. **c.** Each eye lies within the bony orbit, the volume of which is slightly less than 30 mL. The orbital entrance averages approximately 35 mm in height and 45 mm in width at its widest point. The depth of the orbit varies from 40 mm to 45 mm. Race and sex affect each of these measurements.
3. **b.** Each zonular fiber suspending the lens is made up of multiple filaments of fibrillin. In patients with Marfan syndrome, a pathogenic variant in the fibrillin-1 gene leads to weakness of the zonular fibers and lens subluxation. Homocystinuria may cause lens subluxation, but the pathologic variant in this condition is in a gene that regulates cystathionine β-synthase production. Although pseudoexfoliation syndrome and uveitis also may cause lens subluxation, occurrence of these conditions has not been associated with the fibrillin-1 gene.
4. **c.** The long and short posterior ciliary arteries, in addition to the perforating anterior ciliary arteries, perfuse the choroid. The choroid is drained by the vortex veins. The choroid is approximately 0.25 mm thick and comprises 3 layers: the choriocapillaris, the middle layer of small vessels, and the outer layer of large vessels. The choriocapillaris perfuses the outer retinal layers. The central retinal artery perfuses the nerve fibers that form the optic nerve. The major arterial circle perfuses the iris and ciliary body.
5. **b.** The corneal endothelium is composed of a single layer of hexagonal cells derived from the neural crest. Therefore, the corneal endothelium is of neuroectodermal origin. In young adult eyes, approximately 500,000 cells are present, at a density of about 3000/mm^2 centrally and up to 8000/mm^2 peripherally. Mitosis of the endothelium is limited in humans, and the overall number of endothelial cells decreases with age. The principal function of the corneal endothelium is to regulate transmission of nutrients and solutes from the aqueous humor to the stroma. The active transport of ions by these cells leads to the transfer of water from the corneal stroma and the maintenance of stromal deturgescence and transparency. Endothelial cell dysfunction and loss—through surgical injury, inflammation, or disease (eg, Fuchs endothelial corneal dystrophy)—may cause endothelial decompensation, stromal edema, and vision loss. Because endothelial mitosis is limited in humans, destruction of cells causes cell density to decrease and residual cells to spread and enlarge.
6. **b.** Cranial nerve (CN) VI, the abducens nerve, leaves the brainstem at the pontomedullary junction, follows a vertical course along the ventral face of the pons, and continues in the subarachnoid space along the surface of the clivus. Nasopharyngeal carcinomas that extend through the skull base can impact CN VI along the surface of the clivus, prior to its entry into the cavernous sinus via the Dorello canal. Extension into the cavernous sinus can affect CN III, CN IV, CN V, and CN VI. Similarly, sympathetic fibers traveling along

the carotid artery would only be affected if there is extension into the cavernous sinus. Like CN VI, CN VII also exits the brainstem at the pontomedullary junction. However, CN VII enters the internal auditory meatus and is not present at the skull base.

7. **a.** CN VII (the facial nerve) is a complex, mixed sensory and motor nerve. Its motor root contains special visceral efferent fibers that innervate the muscles of facial expression. Its sensory root conveys the sense of taste from the anterior two-thirds of the tongue and sensation from the external auditory meatus and the retroauricular skin. It also supplies preganglionic parasympathetic innervation by way of the sphenopalatine and submandibular ganglia to the lacrimal, submaxillary, and sublingual glands. CN V_3 (the mandibular division of the trigeminal nerve) provides sensation for the preauricular skin. Preganglionic sympathetic fibers (second-order neurons) run in the sympathetic chain, where they eventually synapse at the superior cervical ganglion. Taste and sensation from the posterior one-third of the tongue are provided by CN IX (the glossopharyngeal nerve).
8. **c.** Congenital cranial dysinnervation disorders are thought to result from delayed muscle innervation during development, which can provide a window for inappropriate innervation (by a different nerve) to develop. In Marcus Gunn jaw-winking syndrome, the levator muscle is innervated by CN V (the trigeminal nerve), consistent with the eyelid elevation that occurs with engagement of the pterygoid muscle, thus giving the appearance of "winking" when chewing. Similarly, in Duane syndrome, CN III (the oculomotor nerve) inappropriately innervates the lateral rectus muscle. Alternatively, delayed muscle innervation may lead to premature differentiation of the mesenchyme into connective tissue (ie, fibrosis), as in congenital fibrosis of the extraocular muscles and in Möbius syndrome.
9. **c.** Transcription factors are proteins that bind to specific DNA sequences and control the flow of genetic information at the level of transcription of DNA to messenger RNA. Homeobox genes, like *PAX,* represent highly conserved transcription factors dedicated to embryologic development. Many ophthalmic diseases are caused by pathogenic variants of homeobox genes, including Waardenburg syndrome with dystopia canthorum, which is caused by a *PAX3* variant. *PAX2* variants may lead to optic nerve coloboma and renal hypoplasia. *PAX6* variants lead to aniridia. The *BAX* gene promotes apoptosis in the patients with DNA damage (thus preventing tumor development).
10. **c.** The retinoblastoma protein regulates the cell cycle at the G_1 checkpoint and functions as a tumor suppressor. Pathogenic variants in the retinoblastoma gene *(RB1)* are found not only in other related tumors, such as osteosarcoma, but also in unrelated tumors such as breast cancer and lung cancer. The hereditary pattern of familial retinoblastoma is autosomal dominant. However, at the cellular level, it is autosomal recessive; a pathogenic variant on both chromosomes in a given cell is required in order for tumorigenesis to occur.
11. **c.** Xeroderma pigmentosum is a severe condition caused by a pathogenic variation that affects DNA repair enzymes. Patients with this disorder have diffuse pigmented anomalies on their sun-exposed skin and are at high risk for squamous cell carcinoma and melanoma of the ocular surface. The risks for choroidal melanoma and retinoblastoma are not increased in these individuals.
12. **b.** All the listed diseases may be concentrated in various racial/ethnic groups. Hermansky-Pudlak syndrome is more common in certain Puerto Rican communities, but has also been found in India, Japan, the United Kingdom, and Western Europe. Hermansky-Pudlak syndrome is an autosomal recessively inherited disorder characterized by oculocutaneous albinism and platelet abnormalities that lead to increased bleeding time and

abnormal platelet aggregation (easy bruising and higher bleeding tendency, but normal platelet counts). Several types of achromatopsia (complete color blindness) with myopia are common on the South Pacific island of Pingelap. Niemann-Pick disease is a rare inherited metabolic disorder of fat metabolism with different subtypes (varying severity and presentations); type A is associated with increased incidence among the Ashkenazi Jewish population. Oculocutaneous albinism occurs at a higher rate in the Kuna Indian population in Panama.

13. **c.** Topical cyclosporine A emulsion and lifitegrast have both been approved by the US Food and Drug Administration (FDA) to treat the inflammatory component of dry eye syndrome. Prednisolone acetate may be used in the treatment of dry eye syndrome but is not US FDA approved for this use. Although doxycycline has ocular anti-inflammatory effects, it is not US FDA approved for the treatment of the inflammatory component of dry eye syndrome.

14. **c.** The maximum amount of fluid an eye can hold prior to tearing is 25–30 microliters (μL). The volume of the average eyedrop is 45 μL; therefore, it is not helpful to use more than 1 drop on an eye at a time.

15. **b.** Type III collagen production is associated uniquely with stromal wound healing. Type I is the major collagen component of the corneal stroma; it constitutes approximately 70% of the total stromal dry weight. Immunohistochemical and biochemical studies have shown that normal adult corneal stroma also contains collagen types V, VI, VII, XII, and XIV.

16. **c.** Under anaerobic (low-oxygen) conditions, glucose, the main metabolic substrate for the cornea, is converted to pyruvic acid and then to lactic acid. Lactic acid accumulation in the stroma increases the osmotic load, which draws water into the cornea and causes corneal edema. Aldehyde dehydrogenase, carbon dioxide, and proteoglycans do not accumulate in the cornea in hypoxic conditions. Aldehyde dehydrogenase is a soluble protein found in the cornea that absorbs ultraviolet-B (UVB) radiation. Carbon dioxide is a product of glucose metabolism via glycolysis under aerobic conditions. Proteoglycans confer hydrophilic properties to the corneal stroma and interact with collagen fibrils to provide corneal clarity.

17. **a.** It is thought that Bowman layer, by virtue of its acellularity and packing distribution, serves to prevent exposure of stromal corneal keratocytes to growth factors secreted by corneal epithelial cells. This effect is notable because, during photorefractive keratectomy (PRK) or laser subepithelial keratomileusis (LASEK), Bowman layer is removed, along with the anterior corneal stromal tissue. In these procedures, corneal haze is a potentially significant postoperative visual complication, presumably because the stromal keratocytes are exposed to regenerating epithelial growth factors and take on fibroblastic behaviors. In contrast, during laser in situ keratomileusis (LASIK), Bowman layer is transected but still retained, and thus central corneal haze is extremely rare.

18. **c.** The aqueous humor is the major nutrient source for the avascular lens and cornea and provides a route for the removal of waste products. Ocular fluids are separated from blood by barriers formed by tight junctions between epithelial and endothelial cells. These junctions make up the blood–aqueous barrier. Aqueous enters the posterior chamber from the ciliary processes by means of active and passive physiologic mechanisms, resulting in specific concentrations of various ions to maintain a specific composition of the fluid. In order of highest to lowest concentration, the components of aqueous humor are:

    - Na^+ (163 mmol/kg H_2O)
    - Cl^- (134 mmol/kg H_2O)

- HCO_3^- (20 mmol/kg H_2O)
- glucose (3 mmol/kg H_2O)
- ascorbate (1.06 mmol/kg H_2O)

Lactate is the most abundant organic anion in the aqueous humor, and its concentration there is always higher than that in plasma. The high lactate level in the aqueous is a result of glycolysis in the lens. Ascorbate is another anion that is more abundant in the aqueous than the plasma. It has antioxidant properties and blocks UV light. Calcium is generally 50% less concentrated in the aqueous versus plasma, and aqueous concentration of glucose is 50%–70% of the concentration found in plasma (glucose levels in the aqueous can be higher in individuals with diabetes, which can lead to problems with refraction due to lens retention of glucose short-term, and cataract formation long-term). Urea's concentration in the aqueous is about 80%–90% of that in plasma.

19. **d.** The Goldmann equation represents the factors that determine intraocular pressure (IOP). U represents the rate of aqueous drainage through the uveoscleral pathway, which is pressure-insensitive. C represents the outflow facility through the trabecular (pressure-sensitive) pathway. EVP signifies the episcleral venous pressure. F represents the rate of aqueous humor production.
20. **b.** Glucose typically enters the lens via diffusion from the aqueous humor and is phosphorylated to glucose-6-phosphate before passing through glycolysis to generate adenosine triphosphate (ATP). This provides the majority of the energy for the lens. Hexokinase is the rate-limiting enzyme of the glycolytic pathway. Due to the poor oxygen saturation in the lens, aerobic metabolism is not possible. A small amount of glucose-6-phosphate enters the pentose phosphate pathway (also called hexose monophosphate shunt). This pathway is responsible for replenishing nicotinamide adenine dinucleotide phosphate (NADPH) stores, which are depleted by redox reactions. The polyol pathway (also called sorbitol pathway) becomes important in cases of hyperglycemia, in which glucose is metabolized through the polyol pathway and sorbitol is generated. Sorbitol does not readily traverse cell membranes, and its accumulation is thought to play a role in the development of sugar cataracts.
21. **b.** The posterior lens capsule is 2–4 microns (μm) thick, whereas the anterior lens capsule is approximately 11–15 μm thick. The anterior portion of the capsule is thicker due to epithelial cells continuing to secrete capsular material throughout life, whereas no epithelium is present in the posterior capsule. Because of its relative thinness, the posterior capsule is at risk for inadvertent tear or rupture during cataract surgery, which can lead to vitreous loss and other surgical complications.
22. **c.** Proteins constitute 33% of the weight of the lens, an unusually high protein content for any tissue in the body. The lens has 2–3 times more protein by weight than any other body tissue.
23. **b.** Most of the changes in ocular physiology after vitrectomy result from altered viscosity in the vitreous cavity; when the vitreous is removed, the viscosity decreases. This results in the diffusion of oxygen more rapidly from the well-oxygenated anterior segment to the posterior segment and increased oxygen tension at the retina. The increased oxygen tension exceeds the capacity of clearance by ascorbate, increasing the potential for oxidative stress. Additionally, antibiotic transfer from anterior segment to posterior segment is increased and antibiotics are cleared more rapidly from the vitreous cavity after vitrectomy.
24. **d.** Stickler syndrome is caused by a pathogenic variant in the gene *COL2A1,* which codes for type II collagen (a major component of vitreous collagen fibers). Affected patients have an optically empty vitreous due to premature liquefaction centrally with peripheral condensation,

which may induce retinal detachment. Wagner syndrome is also characterized by an optically empty vitreous but is due to a pathogenic variant in the *VCAN* (versican) gene, which participates in formation of the vitreous gel. However, patients with Wagner syndrome do not have increased risk of retinal detachment as do those with Stickler syndrome. Familial exudative vitreoretinopathy is an inherited disease (resulting from defects in Wnt signaling) that leads to abnormal retinal angiogenesis and incomplete vascularization of the peripheral retina. Marfan syndrome is an inherited disease caused by a pathogenic variant in the gene that encodes fibrillin-1. Its ocular manifestations include ectopia lentis, high myopia, scleral thinning, and retinal detachment. Retinitis pigmentosa refers to a group of inherited diseases characterized by diffuse, progressive dysfunction of predominantly rod photoreceptors. In the United States, 10% of retinitis pigmentosa cases are due to a pathogenic variant in the rhodopsin *(RHO)* gene.

25. **a.** After the collagen fibers and other insoluble elements present in the vitreous gel are removed by filtration or centrifugation, many proteins remain in solution. Serum albumin is the major soluble vitreous protein, followed by transferrin. Other proteins include neutrophil elastase inhibitor and tissue plasminogen activator. The concentration of serum proteins in the vitreous gel depends on the integrity of the retinal vasculature and the degree of intraocular inflammation.

26. **a.** Horizontal cells are antagonistic (inhibitory) interneurons that provide negative feedback to photoreceptors. Their dendrites synapse with cones, receiving glutamate from the cones and releasing γ-aminobutyric acid (GABA) back onto them, thus providing negative feedback. When light causes cone hyperpolarization and cessation of glutamate release, then neighboring horizontal cells are also hyperpolarized and stop releasing GABA. When GABA release onto the cone ceases, the cone then depolarizes. This feedback inhibition allows for visualization of low-contrast details against background luminance.

    Bipolar cells are neurons that transmit neural signals from photoreceptors to the inner retina. Glial cells, which provide neuronal support, include Müller cells, macroglia (mainly astrocytes), and microglia. Photoreceptors are neurons and include rods and cones.

27. **a.** 11-*cis*-retinal is a vitamin A derivative. Light activation of rhodopsin starts a series of reactions that lead to hyperpolarization of the photoreceptor's membrane potential. Once rhodopsin absorbs a quantum of light, the 11-*cis* double bond of retinal (vitamin A) is reconfigured (creating all-*trans*-retinal, also called all-*trans*-retinaldehyde), and the opsin molecule undergoes a series of rapid configurational changes to an activated state known as metarhodopsin II, initiating a signal transduction cascade. Vitamin B does not participate in the phototransduction cascade. However, members of the vitamin B family do play supportive roles in biochemical processes in the eye. For example, vitamin B_{12} deficiency can lead to optic atrophy. Vitamins C and E play antioxidant roles in the retina, but do not participate in the light response of the retina.

28. **c.** Microglia are a class of retinal cells that are related to tissue macrophages and are activated when retinal homeostasis is disturbed. Amacrine cells are inhibitory interneurons that mediate interactions among bipolar and ganglion cells. Macroglia provide physical support to neuronal and vascular cells, regulate the ionic and chemical composition of the extracellular milieu, participate in the blood–retina barrier, form the myelin sheath of the optic nerve, guide neuronal migration during development, and exchange metabolites with neurons. Pericytes are modified smooth muscle cells that surround the endothelial cells and play a role in autoregulation of retinal blood vessels.

29. **c.** The *RPE65* gene encodes the enzyme RPE65 isomerohydrolase, which converts all-*trans*-retinyl ester to 11-*cis*-retinal. A pathogenic variant in this gene may result in Leber congenital amaurosis or retinitis pigmentosa, which present clinically as bilateral ring scotomas with bone spicule retinal lesions. The US FDA has approved gene therapy to treat diseases caused by pathogenic variants in *RPE65*; thus, genetic testing is indicated for patients with this clinical presentation. None of the other conditions have been attributed to a pathogenic variant in *RPE65*. Answer choice (a) describes a bilateral optic neuropathy, such as dominant optic atrophy. Answer choice (b) describes the clinical presentation of Best disease, which is caused by heterozygous variants of the bestrophin gene. Answer choice (d) is most suggestive of glaucoma.

30. **c.** Melanin absorbs all wavelengths of light. Patients with oculocutaneous albinism have foveal hypoplasia and more contralateral projections of the retinal ganglion cells, thought to be due to reduced melanin levels resulting from defects in the tyrosinase gene. Additional functions of melanin include stabilization of free radicals and detoxification. Melanin is not known to be involved in the pathogenesis of retinitis pigmentosa, retinal adhesion, or vitamin A metabolism.

31. **a.** The adverse effects of reactive oxygen species (ROS) are thought to be causal factors in many vision-threatening diseases, including cataract, age-related macular degeneration (AMD), diabetic retinopathy, and glaucoma. Lipid peroxides are formed when ROS react with unsaturated fatty acids. Lipid peroxidation causes not only direct damage to the cell membrane but also secondary damage to cells through its breakdown products. Lipid peroxides are unstable, and they break down to form many aldehydes, such as malondialdehyde and 4-hydroxyalkenals. These aldehydes can quickly react with proteins, inhibiting the proteins' normal functions. Both the lens and the retina are susceptible to such oxidative damage. Although repair and regeneration mechanisms are active in the lens epithelium and superficial cortex, no such mechanisms exist in the deep cortex and the nucleus, where any damage to lens proteins and membrane lipids is irreversible. One result of this damage can be crosslinking and insolubilization of proteins, leading to loss of transparency. Conjunctivitis, strabismus, and posterior capsule opacification are not associated with ROS damage.

32. **a.** Several distinctive characteristics make the retina vulnerable to damage from lipid peroxidation:
    - Rod inner segments are rich in mitochondria, which may leak activated oxygen species.
    - Rod outer segments possess high levels of polyunsaturated fatty acids (PUFAs), making them susceptible to damage by oxygen. PUFAs are sensitive to peroxidation in proportion to their number of double bonds.
    - The outer retina contains many chromophores. Light exposure may trigger photooxidative processes mediated by singlet oxygen.
    - The abundant oxygen supply through the choroid and retinal vessels elevates the risk of oxidative damage.

33. **b.** A 1% solution has 1 g/100 mL, or 1000 mg/100 mL, of active ingredient. Assuming there are 20 drops/mL, 1 drop contains 0.05 mL of drug. Multiplying 1000 mg/100 mL × 0.05 mL yields 0.5 mg per drop of atropine available for systemic absorption. Ophthalmologists need to be particularly aware of the risk of atropine-related systemic side effects; the relatively high drop concentration and long half-life of the drug might lead to cardiac or psychiatric complications depending on the frequency of use and the age/size of patient.

34. **b.** A 1:10,000 dilution has 1 g of drug in 10,000 mL (or 1000 mg/10,000 mL). This concentration is equivalent to a 0.01% solution (0.01 g/100 mL, or 10 mg/100 mL). One milliliter of the 1:10,000 dilution of epinephrine contains 0.1 mg of epinephrine. If the concentration of the solution increases to 1:1000, 0.1 mL of it contains the same amount of epinephrine as in 1 mL of the 1:10,000 solution.

35. **a.** In patients with uveitis, topical mydriatic and cycloplegic agents are used to prevent posterior synechiae and to relieve pain due to ciliary spasm. Atropine sulfate has the longest duration of action (7–14 days), followed by scopolamine (4–7 days), homatropine (3 days), and cyclopentolate (2 days).

36. **b.** Cenegermin, a recombinant human nerve growth factor (NGF), is the first drug approved by the US FDA for the management of neurotrophic keratopathy. Both aflibercept and ranibizumab are *inhibitors* of vascular endothelial growth factor (VEGF) and are used in ophthalmology to treat various retinal diseases, including diabetic retinopathy, retinal vein occlusion, and neovascular AMD. Teprotumumab is an *inhibitor* of the insulin-like growth factor-1 receptor (IGF-1R) and is used in the treatment of active thyroid eye disease (TED).

37. **a.** Computed tomography (CT) is the modality of choice for assessing bony abnormalities. Magnetic resonance imaging (MRI) is better suited for assessment of soft-tissue abnormalities than is CT. Optical coherence tomography and ultrasound biomicroscopy are useful for assessing ocular structures but not for assessing the orbit.

38. **c.** The standard B-scan probe positions are axial, transverse, and longitudinal. Coronal, sagittal, radial, and tangential are not standard B-scan probe positions.

39. **b.** Labeled data sets are considered the "ground truth" for machine learning algorithms to identify patterns that predict those labels on new data. Similarities in data points over time (eg, a single pixel in an image) are referred to as temporal coherence, whereas similarities among groups of data points (eg, a group of pixels having similar coloring in an image of a retinal hemorrhage) are referred to as spatial coherence. During machine learning, algorithms learn to differentiate between relevant and irrelevant spatial and temporal coherences in the training images and, ultimately, to predict disease state in new data sets.

40. **b.** Digital Imaging and Communications in Medicine (DICOM) is the digital data standard for diagnostic images and measurements (eg, visual fields, biometry). A Picture Archiving and Communications System (PACS) is required for the storage and display of patient images and can also help facilitate image analysis. Logical Observations, Identifiers, Names, and Codes (LOINC) represents the digital data standard for lab results and clinical observations/measurements, whereas Current Procedural Terminology (CPT) represents the digital data standard for procedures and services.

Index

(*f* = figure; *t* = table)

A-scan ultrasound/ultrasonography, 489*f*, 489–490, 490*t*
AAO. *See* American Academy of Ophthalmology
Abatacept, 427*t*
ABCA4, 321, 336, 338
Abducens nerve
  anatomy of, 109*f*, 137–138
  palsy of, 502*t*
Abetalipoproteinemia, 247
ACAID. *See* Anterior chamber–associated immune deviation
Acanthamoeba infections, 459
Accessory ophthalmic artery, 25*f*
Accommodation
  in children, 82
  direct-acting cholinergic agonists' effect on, 394
Accommodative esotropia, 398
Accommodative power, 82
Acetazolamide sodium, 381, 411*t*, 412
Acetylcholine
  degradation of, 396*f*
  intracameral use of, 379*t*, 394
  synthesis of, 396*f*
Acetylcholine receptors, 392, 393*f*, 394*t*
Acetylcholinesterase, 394, 396*f*
Acetylcysteine, 389*t*
Acetyltransferase, 244
Achromatopsia, 237
Actin, 297
Acular. *See* Ketorolac tromethamine
Acular LS. *See* Ketorolac tromethamine
Acular PF. *See* Ketorolac tromethamine
Acuvail. *See* Ketorolac tromethamine
Acyclovir sodium, 454–456, 455*t*
Adalimumab, 426*t*
Adenine, 185
Adeno-associated virus vectors, 206
Adenosine triphosphate (ATP), 240, 299, 301*f*, 321
Adenoviral conjunctivitis, 39
Adenylate cyclase, 405
Adherence, 391–392
Adie (tonic) pupil, 395
Adrenergic agonists
  α_1-, direct-acting, 402–404
  α_2-, 404–406
  β_2-, 404*t*, 408
  indirect-acting, 406–407
Adrenergic drugs
  β-, 408–410, 409*t*
  overview of, 402–404
Adrenergic receptors
  α_1, 402
  α_2, 402
  β_1, 402
  β_2, 402
  β_3, 402
  categories of, 402
  sites of, 402
Advanced glycation end products (AGEs), 358
Aflibercept, 474, 474*t*
Age-Related Eye Disease Study (AREDS), 351, 358–359
Age-related macular degeneration (AMD)
  indocyanine green applications in, 467
  Manhattan plot for, 204*f*
  neovascular, 473
  oxidative stress in, 358–359
  vascular endothelial growth factor inhibitors for, 473
  "wet," 473
AGEs. *See* Advanced glycation end products
Agonists
  definition of, 364
  direct-acting
    acetylcholine, 394
    actions of, 394
    adverse effects of, 397
    indications for, 396
    pilocarpine, 395–396
  indirect-acting, 398–399
  mechanism of action, 393
  muscarinic
    adverse effects of, 397
    direct-acting, 394–398, 395–396*f*
    indirect-acting, 398–399
  types of, 395*f*
AI. *See* Artificial intelligence
Aicardi syndrome, 223–225, 224*f*
Air–eye interface, 262
AK-Cide. *See* Prednisolone sodium phosphate/sulfacetamide sodium
AK-Con. *See* Naphazoline hydrochloride
AK-Dilate. *See* Phenylephrine hydrochloride
AK-Pentolate. *See* Cyclopentolate hydrochloride
AK-Poly-Bac. *See* Polymyxin B sulfate/bacitracin zinc
AK-Spore. *See* Hydrocortisone/neomycin sulfate/polymyxin B sulfate/bacitracin zinc
AK-Tob. *See* Tobramycin sulfate
AK-Tracin. *See* Bacitracin zinc
AK-Trol. *See* Dexamethasone/neomycin sulfate/polymyxin B sulfate
Akten. *See* Lidocaine
Alamast. *See* Pemirolast potassium
Alaway. *See* Ketotifen fumarate
Albalon. *See* Naphazoline hydrochloride
Albinism
  description of, 215
  enzymes that cause, 216*t*
  oculocutaneous, 101, 238, 249
Albumin, serum, 307
Alcaftadine, 434*t*, 436
Alcaine. *See* Proparacaine
Aldehyde dehydrogenase, 272
Alkaptonuria, 216*t*
Alkylating agents, 425*t*
All-*trans*-retinaldehyde, 318, 336
Alleles
  definition of, 183
  independent assortment of, 183

Allergic conjunctivitis, 434*t*, 435
Alocril. *See* Nedocromil sodium
Alomide. *See* Lodoxamide tromethamine
α-Adrenergic drugs
  α_2-adrenergic agonists, 404–406
  direct-acting α_1-adrenergic agonists, 402–404
  indirect-acting, 406–407
α_1-Adrenergic receptors, 402
α_2-Adrenergic receptors
  description of, 402
  ligand binding to, 405
α_1-Antitrypsin, 289
α_2-Macroglobulin, 289
Alphagan P. *See* Brimonidine tartrate
Alport syndrome, 197
Alrex. *See* Loteprednol etabonate
Altacaine. *See* Tetracaine
Altafrin. *See* Phenylephrine hydrochloride
Alternative splicing, 190
Alu sequence, 185
Alymsys. *See* Bevacizumab-maly
Amacrine cells, 327
Amaurosis fugax, 501*t*
AMD. *See* Age-related macular degeneration
American Academy of Ophthalmology (AAO)
  aspirin recommendations by, 433
  compounding recommendations by, 391
  Diabetic Retinopathy Preferred Practice Pattern, 509
  IRIS (Intelligent Research Into Sight) Registry, 388, 507
  maintenance of certification, 505
  Task Force on Genetic Testing, 212, 252
Amikacin, 425, 440*t*, 448
Aminoglycosides, 448
Amniocentesis, 250
Amoxicillin, 441
Amphipathic, 363
Amphotericin B, 451, 452*t*
Ampicillin sodium, 440*t*, 441
Anakinra, 427*t*
Anaphase, 180, 180*f*
Anaphylactoid reactions, 440
Ancobon. *See* Flucytosine
Anestacaine. *See* Lidocaine
Anesthesia
  peribulbar, 465
  retrobulbar, 465
  sub-Tenon, 465
Anesthetics, local
  composition of, 461
  intraocular surgery use of, 464–466
  mechanism of action, 462
  overview of, 460–462
  peribulbar anesthesia, 465
  regional, 461*t*
  retrobulbar anesthesia, 465
  topical, 462, 462*t*, 464
  toxic manifestations of, 462
  types of, 463–464
Aneuploidy, of autosomes, 228–229
Angelman syndrome, 190
Angiogenesis, vitreous effects on, 311
Angular artery, 25*f*, 39*f*
Angular vein, 28*f*
Anidulafungin, 453*t*
Aniridia, 172*f*, 219, 231–232
Annulus of Zinn, 12, 18–19, 18–19*f*, 21, 21*f*, 118, 129*f*, 131
Antagonists
  cholinergic, 399–400
  definition of, 365
  muscarinic, 399–400
  nicotinic, 401*t*, 401–402
Anterior cerebral artery, 145*f*
Anterior chamber
  anatomy of, 48*f*, 60–63*f*, 60–64
  aqueous humor of, 60
  depth of, 48, 60
  development of, 168, 168*f*
  dimensions of, 49*t*
  dysgenesis of, 168
  structures of, 60–63*f*, 60–64
  ultrasound biomicroscopy of, 62*f*, 498–499*f*
  volume of, 48
Anterior chamber angle
  anatomy of, 48*f*, 57*f*, 60–63*f*, 60–64
  development of, 168
  structures of, 60–63*f*, 60–64
Anterior chamber–associated immune deviation (ACAID), 308
Anterior ciliary arteries, 23, 26*f*, 44
Anterior clinoid, 108*f*
Anterior clinoid process, 11*f*
Anterior colobomas, 159
Anterior communicating artery, 108*f*
Anterior cranial fossa, 485*t*
Anterior ethmoidal artery, 25*f*, 27*f*
Anterior ethmoidal foramen, 7*f*, 11
Anterior facial vein, 28*f*
Anterior hyaloid face, 499*f*
Anterior lacrimal crest, 7*f*
Anterior lens capsule, 83
Anterior pigmented epithelium, 73*f*, 73–74
Anterior segment, 485*t*
Anterior uveitis, muscarinic antagonists for, 400
Anti-inflammatory drugs
  glucocorticoids. *See* Glucocorticoids
  nonsteroidal. *See* Nonsteroidal anti-inflammatory drugs
  types of, 420*t*
Anti-interleukins, 427*t*
Antiallergic drugs, 434–436
Antibiotic resistance, 193
Anticipation, 195
Antifibrinolytic agents, 470
Antifibrotic drugs, 436–437
Antifungal drugs, 451–454, 452–453*t*, 460
Antiglaucoma agents, 404*t*
Antihistamines
  description of, 435
  mast-cell stabilizers and, 436
Antimetabolites, 425*t*, 436–437
Antimicrobial drugs
  aminoglycosides, 448
  antifungal drugs, 451–454, 452–453*t*
  cephalosporins, 439–442, 440*t*

chloramphenicol, 447–448
fluoroquinolones, 443–445
macrolide antibiotics, 450
penicillins, 439–441, 440*t*
sulfonamides, 445–446
systemically administered, ocular penetration of, 459–460, 460*t*
tetracyclines, 446–447
types of, 440*t*
vancomycin, 449
Antioncogenes, 194
Antioxidants
age-related macular degeneration and, 359
ascorbate, 353–354
carotenoids, 354
catalase, 353
description of, 470
glutathione. *See* Glutathione
glutathione peroxidase, 352
macula localization of, 355*f*
pathways of, 347*f*
in retinal pigment epithelium, 352–354
selenium, 352
superoxide dismutase, 353
vitamin E, 342, 351, 355*f*
Antiporters, 283
Antiretroviral therapy (ART), 458
Antisense oligonucleotides, 207*f*
Anti–vascular endothelial growth factor, 379*t*
Antiviral drugs
description of, 454–457
systemic, 454, 456–458, 460
topical, 454
types of, 455–456*t*
Aplastic anemia, 412
Apolipoprotein D, 289
Apoptosis
atrophy caused by, 192
definition of, 177, 192
in embryogenesis, 192
Apraclonidine hydrochloride, 404*t*, 404–405
Aquaporin, 297
Aqueous humor
ascorbate levels in, 287
blood–aqueous barrier, 282
calcium in, 287
carbohydrates in, 288
carbon dioxide in, 290
composition of, 285*t*, 285–291
dynamics of, 282–284
enzymes in, 289
flow of, 61*f*, 101
formation of, 282–284, 286*f*
glucose concentration in, 288
glutathione in, 288
growth-modulatory factors in, 289–290
inorganic ions in, 287
inositol in, 288
insulin-like growth factor binding proteins in, 290
in iris stroma, 72
lactate in, 287
magnetic resonance imaging of, 485*t*
neuroendocrine proteins in, 289
neurotrophic proteins in, 289
nonpigmented epithelium secretion of, 283
organic anions in, 287
oxygen in, 291
phosphate in, 287
production of, 60, 281, 286*f*
proteinase inhibitors in, 289
proteinases in, 289
proteins in, 288–289
secretion of, 282–284, 286*f*
vascular endothelial growth factors in, 290
Aqueous misdirection, 396
Aqueous vein, 68*f*
Arachidonic acid
derivatives of, 430
description of, 419
prostaglandin synthesis from, 431*f*
Arachnoid sheath, 116, 117*f*
AREDS. *See* Age-Related Eye Disease Study
Arrestin, 323*t*
ART. *See* Antiretroviral therapy
Artificial insemination, 250
Artificial intelligence (AI)
bias in, 510–512
black box, 510–511
clinical example of, 509–510
definition of, 508–509
design standards, 510–512
digital retinal images, 509–510
machine learning, 510–511
reference standards, 510–512
Artificial tears, 437
Ascorbate
in aqueous humor, 287
description of, 351, 353–354
in vitreous cavity, 311, 312*f*
Aspirin, 431–433, 432*t*
Astrocytes, 113, 115
Ataxia-telangiectasia, 191, 236*t*
ATM gene, 191
ATP. *See* Adenosine triphosphate
ATPase-6 gene, 243
Atropine-Care. *See* Atropine sulfate
Atropine sulfate, 245, 372, 399*t*
Auto-oxidation, 347
Autophagy
description of, 295
in retinal pigment epithelium, 342
Autosomal dominant inheritance, 219–221, 220*t*
Autosomal dominant retinitis pigmentosa, 323
Autosomal recessive inheritance
carrier heterozygotes, 218
characteristics of, 219*t*
consanguinity, 219
description of, 215
enzyme defects as cause of, 215, 218
pseudodominance, 219
Autosomal recessive retinitis pigmentosa, 323
Autosomes
aneuploidy of, 228–229
definition of, 183
Axenfeld loops, 59, 60*f*
Axenfeld-Rieger syndrome, 247

Axial hyperopia, 497*f*
Axial proptosis, 110
Axial scans
  B-scan ultrasound, 490, 491–492*f*
  computed tomography, 480, 482*f*
  ultrasound biomicroscopy, 494, 498*f*
AzaSite. *See* Azithromycin
Azathioprine, 425*t*
Azelastine hydrochloride, 434*t*, 436
Azithromycin, 444*t*, 450
Azlocillin, 441
Azopt. *See* Brinzolamide

B-scan ultrasound/ultrasonography
  axial scans, 490, 491–492*f*
  dynamic, 492, 496*t*, 497–498*f*
  longitudinal scans, 490, 495–496*f*
  probe for, 489*f*
  tissue-specific gain setting for, 496*t*
  transverse scans, 490–491, 491*f*, 493*f*
  types of, 490, 492*f*
Bacampicillin hydrochloride, 441
Bacitracin zinc, 440*t*, 444*t*, 450
Bacteroides spp, 442
Balanced salt solution, 379*t*
Bardet-Biedl syndrome, 197
Baricitinib, 428*t*
Baroreceptors, 404
Basal cells, of corneal epithelium, 273
Basal lamina, of cornea, 52, 52*f*
Base pairs, 192
Basic fibroblast growth factor, 471–472
Basilar artery, 108*f*, 128, 143
BAX gene, 191
BBG. *See* Brilliant blue G
Benoxinate, 464
Benzalkonium chloride, 366–367
Bepotastine besilate, 434*t*
Bepreve. *See* Bepotastine besilate
Besifloxacin, 444*t*
Besivance. *See* Besifloxacin
Bestrophin, 343*t*
β-Adrenergic antagonists, 408–410, 409*t*
β_2-Adrenergic agonists, 404*t*, 408
β_1-Adrenergic receptors, 402, 403*f*
β_2-Adrenergic receptors, 402, 403*f*
β_3-Adrenergic receptors, 402
β-Blockers. *See* β-Adrenergic antagonists
β-Lactamases, 439
Betagan. *See* Levobunolol hydrochloride
Betaxolol hydrochloride, 409*t*, 410
Betimol. *See* Timolol hemihydrate
Betoptic S. *See* Betaxolol hydrochloride
Bevacizumab, 389*t*, 473, 474*t*
Bevacizumab-abcd, 475
Bevacizumab-maly, 475
Bias, 510–512
Bicarbonate, in tear film, 263
Big data, 507
Bimatoprost
  description of, 413*t*, 414
  implant, 414
Bimatoprost/timolol maleate, 413*t*, 417*t*
Bioavailability, 363
Biologic agent, 363
Biologic response modifiers, 426–428*t*
Biologics Price Competition and Innovation Act, 475
Biosimilar drugs, 475, 476*t*
Bipolar cells, 89, 326, 326*f*
Bipolar dendrites, 89
Bitemporal hemianopia, 501*t*
Black box algorithms, 510
Bleph-10. *See* Sulfacetamide sodium
Blephamide. *See* Prednisolone acetate/sulfacetamide sodium
Blepharoptosis, 36
Blepharospasm, 378
Blessig-Iwanoff cysts, 103
Blinking, 372
Bloch-Sulzberger syndrome, 223, 236*t*
Blood pressure, phenylephrine hydrochloride effects on, 403
Blood–aqueous barrier
  description of, 282
  functions of, 288
Blood–ocular barrier, 471
Blood–retina barrier, 92–93*f*, 101, 282, 331
Blue zone, 57
Bolus administration, 380
Bony orbit, 6, 7*f*
Botulinum toxin, 378
  type A, 466
Bourneville disease, 235*t*
Bowman layer
  anatomy of, 50*f*, 52–53, 275
  Descemet membrane versus, 53
Brainstem, 111*f*
Brilliant blue G (BBG), 468
Brimonidine tartrate
  characteristics of, 404*t*
  in infants, 406
  intraocular pressure reductions using, 406
  neuroprotective effects of, 406
Brimonidine tartrate/timolol maleate, 404*t*, 409*t*, 417*t*
Brinzolamide, 374, 411*t*, 413
Brinzolamide/brimonidine tartrate suspension, 417*t*
British anti-Lewisite, 247
Broad-spectrum penicillins, 441
Brodmann area 17, 119
Brolucizumab, 474, 474*t*
Bromday. *See* Bromfenac sodium
Bromfenac sodium, 420*t*
Bruch membrane, 100, 102, 332*f*
Bulbar conjunctiva, 30*f*, 44
Bupivacaine, 461*t*, 463
Butyrylcholinesterase, 398
Byooviz. *See* Ranibizumab-nuna

C4, 289
CAIs. *See* Carbonic anhydrase inhibitors
Calcarine fissure, 120
Calcarine sulcus, 120
Calcitonin gene–related peptide (CGRP), 64
Calcium, in aqueous humor, 287
CALT. *See* Conjunctiva-associated lymphoid tissue
cAMP. *See* Cyclic adenosine monophosphate

Canakinumab, 427*t*
Canaliculus, punctum of, 29
Cancer genes, 194
Candidate gene screening, 199
Capsulopalpebral fascia, 36
Capsulopalpebral head, 30*f*
Carbachol
  characteristics of, 397*t*
  intracameral use of, 379*t*, 394–395
  intraocular pressure affected by, 395
Carbenicillin sodium, 440*t*, 441
Carbocaine. *See* Mepivacaine
Carbohydrate cataracts, 302
Carbohydrates, in aqueous humor, 288
Carbon dioxide, in aqueous humor, 290
Carbonic anhydrase, 283, 365
Carbonic anhydrase inhibitors (CAIs), 410–413
Carotenoids, 354
Carotid canal, 108*f*
Carotid cavernous sinus, 503*t*
Carteolol hydrochloride, 409*t*, 410
Caruncle, 29*f*, 45
Caspofungin, 453, 453*t*
Catalase, 353
Cataracts
  carbohydrate, 302
  cortical, 247
  galactose metabolism defects as cause of, 302
  sugar, 302
  ultrasonographic findings in, 497*f*
Cavernous sinus, 137–138, 142
Cavernous sinus syndrome, 502*t*
CDKs. *See* Cyclin-dependent kinases
Cefadroxil, 442
Cefamandole, 442
Cefazolin sodium, 440*t*, 442
Cefepime hydrochloride, 442
Cefoperazone, 442
Cefotaxime, 442
Cefoxitin, 442
Cefpirome, 442
Ceftazidime, 440*t*, 442, 449
Ceftriaxone sodium, 440*t*
Cefuroxime, 379*t*, 442
Celecoxib, 432*t*
Cell cycle
  checkpoints in, 181
  cytokinesis, 180
  meiosis, 181–183
  mitosis, 179
  phases of, 179–180, 180*f*
  regulation of, 180–181
Cell-free fetal DNA, 251
Cellophane maculopathy, 308
Cellular retinol-binding protein 1 (CRBP1), 336
Cenegermin, 472
Central colobomas, 159
Central cornea, 51
Central retinal artery
  description of, 112
  lumen of, 123
Central retinal vein, 28*f*, 112, 123
Central supporting connective tissue strand, 114*f*
Cephalexin, 442
Cephalosporins, 439–442, 440*t*
Cephradine, 442
Ceramide trihexoside, 247
Cerebral aqueduct, 109*f*
Cerebral arterial circle, 143, 145*f*
Cerebral peduncle, 109*f*
Cerebral vascular system
  cavernous sinus, 142
  description of, 142
  venous sinuses, 142, 144*f*
Cerebral venous sinus thrombosis, 142
Cerebrospinal fluid, 485*t*
Cetirizine, 434*t*
CGRP. *See* Calcitonin gene–related peptide
Chaperone-mediated autophagy, 342
Checkpoint inhibitors, 181
Checkpoints, 180–181
Children
  accommodation in, 82
  aspirin in, 432–433
  tetracycline contraindications in, 447
Chlorambucil, 425*t*
Chloramphenicol, 444*t*, 447–448
Chlortetracycline, 446
Cholesterol, 295
Cholinergic agents
  agonists
    direct-acting
      acetylcholine, 394
      actions of, 394
      adverse effects of, 397
      indications for, 396
      pilocarpine, 395–396
    indirect-acting, 398–399
    mechanism of action, 393
    types of, 395*f*
  antagonists, 399–400
  nicotinic
    antagonists, 401–402
    indirect-acting agonists, 401
Cholinergic innervation, 41
Cholinergic receptors, 393, 393*f*, 394*t*
Cholinesterase inhibitors
  characteristics of, 397*t*
  irreversible, 398
  pralidoxime reversal of, 398
  reversible, 398
Chondroitin sulfate, 305–307
Choriocapillaris
  anatomy of, 80–82, 81*f*
  development of, 168
  fenestrations of, 82
  retinal pigment epithelium and, 332*f*
Choroid
  blood flow in, 80
  choriocapillaris, 80–82, 81*f*
  development of, 168
  gyrate atrophy of, 217*t*
  layers of, 79
  magnetic resonance imaging of, 485*t*
  melanoma of, 498*f*
  neovascularization of, 473

perfusion of, 79
stroma of, 82
ultrasound biomicroscopy of, 499*f*
venous circulation of, 80*f*
vessels of, 80–82
Chromosomal crossing over, 182
Chromosomal defects, 227
Chromosomal microarray, 200*t*
Chromosome(s)
abnormalities of, 231–232
description of, 183
gene assignments, 198–199
homologous, 184
nonhomologous, 184
numbering of, 185
sex
aneuploidy of, 228
mosaicism, 230
structure of, 186*f*
Chromosome analysis
aneuploidy of autosomes, 228–229
description of, 227–228
mosaicism, 229–231
Chronic progressive external ophthalmoplegia (CPEO)
description of, 41
features of, 242*t*
mitochondrial DNA mutations in, 41
Cidofovir, 455*t*, 458
Ciliary arteries
anatomy of, 23
anterior, 23, 26*f*
posterior, 25–26*f*
Ciliary body
anatomy of, 48*f*
apex of, 74
aqueous humor production by, 281
arterial supply to, 76
cytochrome P450, 282
definition of, 74
development of, 166–167, 167*f*
drug targeting of, for glaucoma, 281
epithelial cells of, 75, 76*f*
functions of, 74, 281
neuroendocrine peptides in, 289
oxidative stress and, 281
pars plana of, 75
pars plicata of, 75, 77*f*, 499*f*
physiology of, 281–282
pigmented epithelium of, 75
protein synthesis in, 288
reduction-oxidation enzymes in, 281
smooth muscle fibers in, 78*f*
stroma of, 75
supraciliary space, 79
ultrasound biomicroscopy of, 498–499*f*
Ciliary epithelium
description of, 282, 285
neuroendocrine properties of, 287, 289
secretory properties of, 285
Ciliary ganglion
anatomy of, 17*f*, 109*f*
branches of, 16–17
motor root of, 16, 17*f*
parasympathetic fibers in, 16–17
roots of, 16, 17*f*
sensory root of, 16, 17*f*
sympathetic fibers in, 16–17
sympathetic root of, 16, 17*f*
Ciliary muscles
contraction of, 82
development of, 167
direct-acting cholinergic agonists' effect on, 394
fibers of, 76, 78, 394
layers of, 76, 78
muscarinic antagonists' effect on, 400
stimulation of, for accommodative esotropia, 398
Ciliary nerves
branches of, 58
long, 266*f*
short, 17
Ciliary neurotrophic factor, 342
Ciliary process
description of, 75
development of, 167*f*
Ciliary sulcus, 62*f*
Ciloxan. *See* Ciprofloxacin hydrochloride
Cimerli. *See* Ranibizumab-eqrn
Ciprofloxacin hydrochloride, 443, 444*t*
Circle of Willis, 143, 145*f*
Circle of Zinn-Haller, 123, 126*f*
Circular ciliary muscle, 27*f*
11-*cis*-retinaldehyde, 318, 336, 343*t*
CLs. *See* Contact lenses
Clarithromycin, 450
Clindamycin, 440*t*
Clinical genetics
chromosome analysis. *See* Chromosome analysis
chromosomes, 183–185
expressivity, 196
genes, 183–185
inheritance patterns. *See* Inheritance
lyonization, 238–240, 239*f*
overview of, 211–212
pathogenic variants, 192–197
pedigree analysis in, 212–213, 213*f*
penetrance, 195–196
pleiotropism, 196–197
terminology associated with, 225–227
Clinical Laboratories Improvement Amendments, 252
Cloquet canal, 166
Clostridium botulinum, 466
CME. *See* Cystoid macular edema
Coats disease, 497*f*
Cocaine, 462*t*, 464
Codominant, 214
Coenzyme Q_{10}, 347
Cohesive ophthalmic viscosurgical devices, 468
COL2A1, 313
Colistimethate sodium, 440*t*
Collagen fibers
in Bowman layer, 275
in corneal stroma, 275, 276*f*
in Descemet membrane, 277

scleral, 59
in vitreous
age-related breakdown of, 309
description of, 103, 304*f*, 304–305, 306*f*
proteins associated with, 307
Collector channels, 67, 68*f*
Colobomas, 159
Color blindness, 225
Color vision defects, 323
Combigan. *See* Brimonidine tartrate/timolol maleate
Complementary DNA, 201
Compounded pharmaceuticals, 390–391
Compounding, 390–391
Computed tomography (CT)
axial scans, 480, 482*f*
contrast agents with, 483
coronal scans, 482*f*
description of, 479–480
diagnostic uses of, 234
disadvantages of, 482–483
indications for, 480, 501*t*, 503*t*
iodinated contrast agents with, 483
magnetic resonance imaging versus, 481*t*, 483
periorbital sinuses, 16*f*
posterior fossa on, 482
radiation exposure from, 482
Computed tomography (CT) angiography, 480, 481*t*, 484
Computed tomography (CT) venography, 480, 481*t*
Cones
anatomy of, 90*f*
bipolar cells, 326, 326*f*
cells of, 326, 326*f*
circuitry of, 326*f*
foveal, 99
gene defects associated with, 324*t*
L, 323, 326–327
light effects on, 329, 329*f*
M, 323, 326
neuronal elements of, 89
number of, 89
pedicle of, 89
phototransduction of, 321–322
rods versus, 315
S, 323
synaptic body of, 89
trivariant color vision, 323
Congenital, 231
Congenital hypertrophy of retinal pigment epithelium, 213, 214*f*
Conjunctiva
anatomy of, 38, 38*f*, 44–45
bulbar, 30*f*, 44
epithelium of, 44
fornices of, 30*f*, 38, 38*f*, 44
innervation of, 44
palpebral, 38, 38*f*, 44
topical agent absorption in, 372
Conjunctiva-associated lymphoid tissue (CALT), 44
Conjunctival artery, 26*f*
Conjunctivitis, allergic, 434*t*, 435
Consanguinity, 219, 249
Conserved base-pair variants, 192
Contact lenses (CLs), 384
Contiguous gene-deletion syndrome, 231
Contrast agents
adverse effects of, 484
gadolinium-based, 484
iodinated, 483
Copper, in aqueous humor, 287
Copper-zinc superoxide dismutase (CuZnSOD), 353
Cornea
air–tear film interface, 48
aldehyde dehydrogenase in, 272
anatomy of, 48, 48*f*
avascularity of, 271
basal lamina of, 52, 52*f*
biochemistry of, 271–273
Bowman layer of. *See* Bowman layer
central, 51
collagen fibrils of, 53
Descemet membrane of. *See* Descemet membrane
development of, 168, 169*f*
edema of, 263
epithelial cells of, 274, 274*f*
epithelium of, 52, 52*f*, 56, 273–275, 274*f*, 394
glucose metabolism by, 271
glycosaminoglycans in, 277
ground substance of, 53
hyperprolate, 51*f*
innervation of, 55
keratocytes of, 53
lactic acid accumulation in, 272
layers of, 50*f*, 50–55, 52*f*
matrix metalloproteinases in, 277
nerves of, 55–56
neural penetration of, 56*f*
oblate, 51*f*
peripheral, 51
physiology of, 271–273
posterior, 54*f*
prolate, 51*f*
proteinase inhibitors of, 277
proteoglycans in, 53
radius of curvature of, 51
refractive index of, 51
stroma of
anatomy of, 53
collagen fibers in, 275, 276*f*
composition of, 53, 59
keratocytes, 275
tear film of, 49–50, 271
tight junctions of, 52
transketolase in, 272
ultrasound biomicroscopy of, 498*f*
Corneal endothelium
anatomy of, 54–55, 54–55*f*
cells of, 54–55, 278*f*, 279, 279*t*
definition of, 277
Corneal haze, 275
Corneoscleral junction, 56
Corneoscleral trabecular meshwork, 65
Corrugator supercilii muscle, 33*f*
Cortical vision loss, 502*t*
Cortical vitreous, 305

Corticosteroids
intravitreal administration of, 379*t*, 421*t*
ocular allergies treated with, 435
types of, 420*t*
Cortisporin suspension. *See* Hydrocortisone/neomycin sulfate/polymyxin B sulfate
Cosopt Ocumeter Plus. *See* Dorzolamide hydrochloride/timolol maleate
Cotransport, 283
COVID-19, 508
COX. *See* Cyclooxygenase
CPEO. *See* Chronic progressive external ophthalmoplegia
CPEO-plus syndromes, 241
CPT. *See* Current Procedural Terminology
Cranial nerve(s)
anatomic relationships of, 108*f*
anatomy of, 16
cerebrovascular system effects on, 142
I. *See* Olfactory nerve
II. *See* Optic nerve
III. *See* Oculomotor nerve
intracavernous course of, 143*f*
IV. *See* Trochlear nerve
palsy of, 142, 502*t*
V. *See* Trigeminal nerve
VI. *See* Abducens nerve
VII. *See* Facial nerve
Craniofacial development, 151*f*
CRBP1. *See* Cellular retinol-binding protein 1
Crigler-Najjar syndrome, 217*t*
CRISPR–Cas9, 208
Crolom. *See* Cromolyn sodium
Cromolyn sodium, 434*t*
Crossing over, 182, 184–185
Crystallins
α-, 296
β,γ-, 296–297
description of, 293, 296–297
CT. *See* Computed tomography
CT angiography. *See* Computed tomography (CT) angiography
CT venography. *See* Computed tomography (CT) venography
Current Procedural Terminology (CPT), 506, 507*t*
CuZnSOD. *See* Copper-zinc superoxide dismutase
Cyclic adenosine monophosphate (cAMP), 408
Cyclic nucleotide–gated channels, 318, 319*f*
Cyclin-dependent kinases (CDKs), 181
Cyclins, 181
Cyclogyl. *See* Cyclopentolate hydrochloride
Cyclomydril. *See* Cyclopentolate hydrochloride/phenylephrine hydrochloride
Cyclooxygenase (COX), 432*t*
Cyclopentolate hydrochloride, 399*t*
Cyclopentolate hydrochloride/phenylephrine hydrochloride, 399*t*
Cyclophosphamide, 425*t*
Cycloplegia, 400
Cycloplegics, 399*t*
Cyclosporine, 425*t*, 438
Cyclosporine A, 269, 389*t*
Cylate. *See* Cyclopentolate hydrochloride
Cystine, 247
Cystinosis, 247
Cystoid macular edema (CME), 410, 414, 433
Cytochrome P450, 365
Cytogenetics, 227
Cytokines, in tear film, 264
Cytomegalovirus retinitis, 383, 457–458
Cytosine, 185
Cytoskeletal proteins, in lens, 297
Cytovene IV. *See* Ganciclovir sodium

Dapiprazole hydrochloride, 408
Data, 506–508
DCCT (Diabetes Control and Complications Trial), 358
Decamethonium, 401
Decongestants, ocular, 439
Deep learning algorithms, 510, 511*f*
Deep plexus, 58
Demyelination optic neuritis, 501*t*
Depolarizing agents, 402
Depressor supercili muscle, 33*f*
DES. *See* Dry eye syndrome
Descemet membrane
age-related thickening of, 278*f*
anatomy of, 53–54, 54*f*
Bowman layer versus, 53
definition of, 277
Hassall-Henle warts of, 54
thickness of, 53–54
Desmosomes, 52*f*, 76*f*
Dexacidin. *See* Dexamethasone/neomycin sulfate/polymyxin B sulfate
Dexamethasone implant, 383, 421*t*
Dexamethasone/neomycin sulfate/polymyxin B sulfate, 445*t*
Dexamethasone phosphate, 421*t*
Dexamethasone sodium phosphate, 420*t*, 423*t*
Dexamethasone/tobramycin, 445*t*
Dexasporin. *See* Dexamethasone/neomycin sulfate/polymyxin B sulfate
Diabetes Control and Complications Trial (DCCT), 358
Diabetes insipidus, diabetes mellitus, optic atrophy, and neural deafness (DIDMOAD) syndrome, 197
Diabetic retinopathy
AAO Preferred Practice Pattern, 509
proliferative, 311
reactive oxygen species in, 358
Diabetic teleretinal screening, 508
Diamox Sequels. *See* Acetazolamide
Diclofenac sodium, 420*t*, 432*t*
DICOM. *See* Digital Imaging and Communications in Medicine
DIDMOAD. *See* Diabetes insipidus, diabetes mellitus, optic atrophy, and neural deafness (DIDMOAD) syndrome
Diet, genetic diseases managed with, 247
Diffusible ligands, 172–173
Diffusion, 283
Diffusion-weighted imaging (DWI), 484
Diflucan. *See* Fluconazole
Diflunisal, 432*t*
Difluprednate, 420*t*, 424
Digital Imaging and Communications in Medicine (DICOM), 506–507, 507*t*

Digital ophthalmology
applications of, 505
artificial intelligence. *See* Artificial intelligence
big data, 507
data, 506–508, 507*t*
electronic health records, 506
summary of, 512
teleophthalmology, 508
Diisopropyl phosphofluoridate, 398
Dinitrophenol, 340
Dipivefrin hydrochloride, 404*t*
Diquafosol tetrasodium, 438
Direct-acting agonists
α_1-adrenergic agonists, 402–404
cholinergic
acetylcholine, 394
actions of, 394
adverse effects of, 397
indications for, 396
pilocarpine, 395–396
Direct sequencing, 201
Direct-to-consumer genetic testing, 252
Disciform macular degeneration, 498*f*
Dispersive ophthalmic viscosurgical devices, 468
DNA
coding region of, 187
complementary, 201
damage to, 191–192
direct sequencing of, 201
methylation of, 190
noncoding, 187
repair of, 191–192
sequencing of, 201
telomeric, 187
DNA gyrase, 443
Docosahexaenoic acid, 334, 348
Dominant diseases, gene therapy for, 207–208
Dominant inheritance
autosomal, 219–221, 220*t*
description of, 214–215
X-linked, 223, 223*t*
Dominant-negative effect, 207
Dorello canal, 137
Dorsal midbrain syndrome, 502*t*
Dorsal nasal artery, 25*f*, 39*f*
Dorzolamide hydrochloride, 411*t*, 413
Dorzolamide hydrochloride/timolol maleate, 409*t*, 411*t*, 417*t*
Down syndrome
clinical features of, 229, 230*t*
genetic errors in, 229
ocular features of, 230*t*
pharmacogenetics and, 244–245
Doxycycline
description of, 389*t*, 446
ocular rosacea treated with, 389
Drug(s). *See also specific drug*
compounding of, 390–391
as diagnostic agents, 467–468
dry eye treated with, 437–439
nonadherence to, 391–392, 392*t*
topical. *See* Topical drugs
Drug delivery
bolus administration, 380
contact lenses for, 384
gel-forming drops for, 385
implants for, 383
intracameral, 369*t*, 378, 379*t*
intraocular, 378–380
intraocular lenses for, 384
intravitreal, 369*t*, 379*t*, 379–380
liposomes for, 385
local administration, 377–380
nanotechnology for, 385–386
ocular inserts for, 382–383
periocular injections, 377–378
posterior juxtascleral, 369*t*
punctal plug–mediated, 384–385
retrobulbar, 369*t*
routes for, 369*t*, 370*f*
sub-Tenon, 369*t*
subconjunctival, 369*t*
sustained-release, 382–386
systemic administration, 380–381
topical. *See* Topical drugs
vehicles for, 374
Drug Quality and Security Act (2013), 390–391
Drusen, 102
Dry eye syndrome (DES)
cyclosporine A for, 269
description of, 265
lifitegrast for, 269
medications for, 437–439
ocular surface inflammation in, 268*f*, 269
tear substitutes for, 269
vicious circle theory of, 265, 267*f*
Duchenne muscular dystrophy, 223
DuoTrav. *See* Travoprost/timolol maleate
Dural fistula, 503*t*
Durezol. *See* Difluprednate
DWI. *See* Diffusion-weighted imaging
Dynamic B-scan ultrasonography, 492, 496*t*, 497–498*f*
Dystrophin, 190

Echinocandins, 453, 453*t*
Echo time (TE), 483
Echothiophate iodide, 397*t*
Econopred Plus. *See* Prednisolone acetate
Ectoderm
derivatives of, 155*t*
description of, 149–150, 151*f*
in embryologic development, 156*f*
Ectomesenchyme, 155
Ectropion, 74
Ectropion uveae, 75
Edetate disodium, 389*t*
Edinger-Westphal nucleus, 16, 74, 127, 130*f*, 130–131
Edrophonium, 401
EFEMP1, 343*t*
Ehlers-Danlos syndrome, 217*t*
EHRs. *See* Electronic health records
Elderly patients, 367–368
Electro-oculogram, 340
Electrolytes, in tear film, 263
Electron transport chain, 345

Electronic health records (EHRs), 506
Electroretinogram, 329, 329*f*
11-*cis*-retinaldehyde, 318, 336, 343*t*
ELM. *See* External limiting membrane
Emadine. *See* Epinastine hydrochloride
Embryogenesis
  early stages of, 149, 150*f*
  steps involved in, 149
Emedastine difumarate, 434*t*, 435
Emissaria, 59
Emotional lacrimation, 142
Emulsion, 363, 374
Encephalofacial angiomatosis, 236*t*, 237
Endoderm, 149, 151*f*
Endoperoxides, 430
Endophthalmitis, postoperative, 450
Endothelial cells, of cornea, 54–55, 278*f*, 279, 279*t*
Endothelial meshwork, 65, 66*f*
Endothelial nitric oxide synthase (eNOS), 414
Enterobacter aerogenes, 442
Enucleation, for retinoblastoma, 115
Enzyme(s)
  in aqueous humor, 289
  posterior vitreous detachment induced by, 313
  vitreolysis using, 313
Enzyme replacement therapy, 247
EOG. *See* Electro-oculogram
Epigenetics, 188
Epinastine hydrochloride, 434*t*, 436
Epinephrine hydrochloride
  description of, 404*t*
  intracameral administration of, 379*t*
  L-, 408
Epiretinal membranes, 308
Episclera, 58
Episcleral arterial circle, 26*f*
Episcleral vessels, 59, 59*f*
Episcleritis, 58
Epithelium, corneal, 52, 52*f*, 56, 273–275, 274*f*
ε-Aminocaproic acid, 470
Erythromycin, 440*t*, 444*t*, 449–450
Escherichia coli, 441
Esotropia, accommodative, 398
Ethmoid bone, 7*f*, 8
Ethmoid sinus, 13, 15–16*f*
Ethmoid sinusitis, 8
Etodolac, 432*t*
Excision repair, 191
Exons, 186
Exophthalmometry, 6*t*
Expiration dates on biologics, 391
Expressivity, 196
External limiting membrane (ELM)
  definition of, 96
  development of, 162
Extraocular muscles. *See also specific muscle*
  anatomy of, 17–18, 18–19*f*
  blood supply to, 23
  congenital cranial dysinnervation disorders involving, 170
  development of, 168–170
  fine structure of, 24
  formation of, 168–170
  innervation of, 24
  insertions of, 21–22, 22*f*
  magnetic resonance imaging of, 485*t*
  names of, 17–18
  orbital distribution of, 22–23
  origins of, 18, 21*f*
Eye. *See also specific ocular entries*
  compartments of, 47
  embryologic development of, 149–150, 150–154*f*, 158*t*. *See also* Ocular development
  glands of, 32*t*
Eyeball. *See* Globe
Eyelashes, 30
Eyelid(s)
  anatomy of, 28–38, 30*f*
  arterial supply to, 39*f*
  blood supply to, 38–39, 39*f*
  lower
    anatomy of, 29
    development of, 170–171, 171*f*
    muscles of, 36
    punctum of, 42
  lymphatics of, 39, 40*f*
  margin of, 29, 31*f*
  movement of, 266
  muscles of, 30, 33*f*, 33–36
  palpebral fissure of, 28, 29*f*, 37*f*
  racial variations in, 31*f*
  skin of, 29–30, 31*f*
  upper
    anatomy of, 29
    development of, 170–171, 171*f*
    muscles of, 33–36
  vascular supply of, 38–39, 39*f*
Eyelid–globe incongruity, 268

Fabry disease, 216*t*, 247
Facial artery, 25*f*, 39*f*
Facial colliculus, 140
Facial nerve
  anatomy of, 138–140
  branches of, 140
  infranuclear anatomy of, 139*f*
  motor nucleus of, 138
  nuclear anatomy of, 139*f*
  palsy of, 140
  supranuclear anatomy of, 139*f*
  temporal branch of, 140
Famciclovir, 455*t*, 457
Familial adenomatous polyposis, congenital hypertrophy of retinal pigment epithelium in, 213, 214*f*
Familial cerebello retinal angiomatosis. *See* von Hippel–Lindau syndrome
Familial disorder, 226
Familial dysautonomia, 217*t*
Familial exudative vitreoretinopathy, 173
Family history, in genetic counseling, 248–249
Famvir HZV. *See* Famciclovir
Fanconi syndrome, 447
Faricimab, 474*t*, 474–475
Fascia bulbi, 46
Fast Healthcare Interoperability Resources (FHIRs), 507*t*
FAZ. *See* Foveal avascular zone
FDA. *See* Food and Drug Administration
FDCA. *See* Food, Drug, and Cosmetic Act

Fenoprofen, 432*t*
FHIRs. *See* Fast Healthcare Interoperability Resources
Fibrillar opacities, 309
Fibrillin, 308
Fibrin sealant, 389*t*, 469
Fibrinolytic agents, 469
Fibroblast growth factors, 173
Fibronectin, 313
Filensin, 297
First-generation cephalosporins, 442
FISH. *See* Fluorescent in situ hybridization
5-Fluorocytosine, 453
5-FU. *See* Fluorouracil
Fixed-combination medications, 417, 417*t*
Flarex. *See* Fluorometholone acetate
Flicker fusion threshold, 327
Fluconazole, 452*t*, 453
Flucytosine, 453*t*, 453–454
Fluocinolone acetonide
  description of, 429
  implant, 383, 421*t*
Fluor-Op. *See* Fluorometholone acetate
Fluorescein sodium/benoxinate, 462*t*
Fluorescent in situ hybridization (FISH), 200*t*, 201
Fluorescent polymerase chain reaction, 251
Fluorinated pyrimidine, 453–454
Fluorometholone acetate, 420*t*, 423, 423*t*
Fluorometholone/sulfacetamide, 445*t*
Fluoroquinolones, 443–445
Fluorouracil (5-FU), 378, 389*t*, 436–437
Flurbiprofen sodium, 420*t*, 432*t*
Fluress. *See* Fluorescein sodium/benoxinate
Flurox. *See* Fluorescein sodium/benoxinate
FML Forte Liquifilm. *See* Fluorometholone acetate
FML Liquifilm. *See* Fluorometholone acetate
FML-S. *See* Fluorometholone/sulfacetamide
FML S.O.P. *See* Fluorometholone acetate
fMRI. *See* Functional magnetic resonance imaging
Food and Drug Administration (FDA)
  artificial intelligence approval by, 512
  biosimilars as defined by, 475
  description of, 388–389
  expiration dates on biologics, 391
Food, Drug, and Cosmetic Act (FDCA), 391
Foramen rotundum, 108*f*
Foramina, orbital, 11–12
Foscarnet sodium, 379*t*, 455*t*, 458
Foscavir. *See* Foscarnet sodium
Fourth-generation cephalosporins, 442
Fovea
  anatomy of, 87
  definition of, 97
  optical coherence tomography of, 99*f*
  perifovea, 100
  schematic section of, 96*f*
Fovea ethmoidalis, 15, 16*f*
Foveal avascular zone (FAZ), 99–100, 100*f*
Foveal cones, 89
Foveola
  borders of, 99
  definition of, 99
  photoreceptor layer of, 99
FOXC1 gene, 198
Frontal bone, 7*f*, 9*f*, 11*f*
Frontal nerve, 13*f*, 135
Frontalis muscle, 30*f*, 33*f*
Frontoethmoidal suture, 7*f*, 9*f*
Frontosphenoid suture, 11*f*
Frontozygomatic suture, 10, 11*f*
Fuchs endothelial corneal dystrophy, 54
Functional magnetic resonance imaging (fMRI), 484
Fundus autofluorescence, 340*f*
Fundus coloboma, 497*f*
Fundus oculi, 86, 87*f*
Fungizone. *See* Amphotericin B

G_2 phase, 180–181
Gadolinium-based contrast agents, 484
Gain of function, 193
Galactokinase, 302
Galactokinase deficiency, 216*t*
Galactosemia
  description of, 215, 217*t*, 302
  galactose-free diet for, 247
Gallamine, 401
Gametes, 182
Ganciclovir sodium, 379*t*, 455*t*, 457
Ganfort. *See* Bimatoprost/timolol maleate
Ganglion-blocking drugs, 401*t*
Ganglion cell layer (GCL), 97
Ganglion cells
  axons of, 92
  description of, 327
Gasserian ganglion, 134
Gastrulation, 149–150
Gatifloxacin, 444*t*
GCL. *See* Ganglion cell layer
Gel-forming drops, 385
Gelatinase, 304
Gene(s)
  definition of, 183, 185
  disease association for, 198–199
  independent assortment of, 184–185
  linkage studies of, 198
  recessive, 214
  segregation of, 184
  size variations among, 183
  structure of, 185–187
  word origin of, 183
Gene assignments, 198–199
Gene dosage, 198
Gene mapping, 198
Gene therapy
  adeno-associated virus vectors, 206
  dominant diseases treated with, 207–208
  genetic diseases treated with, 248
  replacement of absent gene product in X-linked and recessive diseases, 205–206
Gene transcription and translation
  definition of, 188
  overview of, 187–189
Genetic, 225–227
Genetic counseling
  description of, 205, 248–249
  family history in, 248–249
  issues in, 249–250
  preimplantation genetic diagnosis, 251
  prenatal diagnosis, 250–251

referrals for providers of support for persons with disabilities, 251
for reproductive issues, 250–251
requirements of, 248–249
Genetic diseases and disorders. *See also specific disease or disorder*
chelation of excessive metabolites, 247
clinical management of, 245–248
complications of, 248
dietary control of, 247
drug therapy for, 248
enzyme replacement therapy for, 247
ethnic concentration of, 237–238
explanation of, 245
gene therapy for, 248
genetic testing for, 249–250
multifactorial inheritance of, 243–244
polygenic inheritance of, 243–244
prevalence of, 177
racial concentration of, 237–238
sequelae of, 248
single-gene, 194
treatment of, 246–248
variability of, 195
vitamin therapy for, 247
vitreous affected by, 313
Genetic heterogeneity, 227
Genetic linkage, 183
Genetic map, 183
Genetic markers, 197–198
Genetic test(s), 200*t*
Genetic testing
AAO Task Force on Genetic Testing recommendations for, 212, 252
description of, 249–250
direct-to-consumer, 252
of minors, 252
Genetics
clinical
chromosome analysis. *See* Chromosome analysis
chromosomes, 183–185
expressivity, 196
genes, 183–185
inheritance patterns. *See* Inheritance
lyonization, 238–240, 239*f*
overview of, 211–212
pathogenic variants, 192–197
pedigree analysis in, 212–213, 213*f*
penetrance, 195–196
pleiotropism, 196–197
terminology associated with, 225–227
definition of, 177
molecular
cell cycle, 179–183, 180*f*
DNA damage and repair, 191–192
gene structure, 185–187
gene therapy. *See* Gene therapy
gene transcription and translation. *See* Gene transcription and translation
mitochondrial diseases. *See* Mitochondrial diseases
noncoding DNA, 187
pharmacogenetics, 244–245
Geniculocalcarine radiation, 119*f*
Genome, 193, 226
Genome editing, 208
Genome-wide association studies (GWAS), 193, 201–205
Genotype, 193
Gentamicin sulfate, 440*t*, 448
Gevokizumab, 427*t*
GFR. *See* Glomerular filtration rate
Gillespie syndrome, 231
Gland of Krause, 30*f*, 32*t*, 41–42, 263, 265
Gland of Moll, 30, 31*f*, 32*t*
Gland of Wolfring, 32*t*, 41–42, 263, 265
Gland of Zeis, 30, 31*f*, 32*t*, 262
Glaucoma
angle-closure, 407–408
oxidative stress in, 358–359
primary open-angle, 244, 356, 395, 400, 407–408
reactive oxygen species in, 355
Glial cells, 327
Globe
layers of, 48
posterior view of, 26*f*
topographic features of, 48–49
Glomerular filtration rate (GFR), 368
Glucocorticoids
administration of, 424, 429*t*
adverse effects of, 422–424
cell-specific effects of, 419
in elderly patients, 422
immune-mediated inflammation effects of, 419
indications for, 419
intraocular pressure elevation by, 422, 423*t*
regimens for, 424–430
types of, 424–430
Glucose
aqueous humor concentration of, 288
lens metabolism of, 301*f*
in retinal pigment epithelium, 333
Glutathione (GSH)
in aqueous humor, 288
description of, 352
reactive oxygen species and, 349
reduction-oxidation cycle, 351
Glutathione peroxidase, 352
Glycerin, 417–418, 418*t*
Glycocalyx, 273
Glycopyrronium bromide, 400
Glycosaminoglycans, 53, 160, 277, 305–307
GM_1 gangliosidosis, 216*t*
GM_2 gangliosidosis
type I, 216*t*
type II, 216*t*
Goblet cells
description of, 32*t*, 44
mucin production by, 264
Goldenhar syndrome, 152
Goldmann equation, 284
Graves orbitopathy, 497*f*
Gray line, 29
Gray matter, 484, 485*t*, 486*f*
Gray zone, 57
Greater superficial petrosal nerve, 141

Greater wing of sphenoid bone, 7–8*f*, 10–11*f*
Ground substance, of cornea, 53
Growth factors
  in aqueous humor, 289–290
  definition of, 471
  in ocular development, 172–173
  in tear film, 264
  types of, 471–473
GSH. *See* Glutathione
Guanine, 185
Guanine nucleotide-binding proteins, 415
Guanylate cyclase, 323*t*
Guanylyl cyclase, 318
GWAS. *See* Genome-wide association studies
Gyrus rectus, 110, 111*f*

Haemophilus influenzae, 441–442
Haller layer, 79
Haploid insufficiency, 207
Haploinsufficiency, 231
HapMap, 201–202, 202*f*
Hassall-Henle warts, 54
Healon, 468
Healon5, 468
Healon GV, 468
Health information technology, 505
Heavy eye syndrome, 46
Helicases, 191
Hemidesmosomes, 52, 52*f*
Hemifacial spasm, 378, 502*t*
Hemorrhage, 311
Henle fiber layer, 88, 96
Hereditary, 225–227
Hereditary retinoblastomas, 232
Hering's law of equal innervation, 127
Heritability, 226
Hermansky-Pudlak syndrome, 238
Herpes simplex keratitis, 471
Herpes simplex virus (HSV), 454, 456
Herpes zoster virus (HZV), 456
Herpetic keratitis, 414
hESCs. *See* Human embryonic stem cells
Heteroplasmy, 186
Heterozygous, 184
Hexose monophosphate pathway, 272
Hexose monophosphate shunt, 301
High-frequency ultrasound, 488
HL7 Fast Healthcare Interoperability Resources, 507*t*
Homatropaire. *See* Homatropine hydrobromide
Homatropine hydrobromide, 399*t*
Homeobox genes
  description of, 172
  functions of, 177
Homocystinuria, 217*t*
Homologous chromosomes, 182, 184
Homonymous hemianopia, 501*t*
Homozygous, 183
Horizontal cells, 325*f*, 326–327
Horner muscle, 32, 34*f*
Horner syndrome
  apraclonidine for diagnosis of, 405
  imaging studies for, 502*t*
HSV. *See* Herpes simplex virus
Human embryonic stem cells (hESCs), 173
Human Genome Project, 198
Hunter syndrome, 216*t*
Hurler syndrome, 184, 216*t*
Hutchinson sign, 136
Hyalocytes, 103, 304, 308, 309*f*
Hyaloid artery, 165*f*
Hyaloideocapsular ligament, 166
Hyaluronan
  description of, 303
  in vitreous, 305–306
Hyaluronic acid, 303, 389*t*
Hyaluronidase, 463
Hydrocortisone, 423*t*
Hydrocortisone/neomycin sulfate/polymyxin B sulfate, 445*t*
Hydrocortisone/neomycin sulfate/polymyxin B sulfate/bacitracin zinc, 445*t*
Hydrogen peroxide (H_2O_2), 345, 347*t*
Hydrophilic (lipophobic), 363
Hydroxyamphetamine hydrobromide, 399*t*
Hydroxyamphetamine hydrobromide/tropicamide, 399*t*
Hydroxyl radical, 347*t*
Hyperglycinemia, 217*t*
Hyperosmolar drugs, 466
Hyperprolate cornea, 51*f*
Hypotension, 404
Hypoxia-inducible factor, 234
HZV. *See* Herpes zoster virus

Ibuprofen, 432*t*
ICAM-1. *See* Intercellular adhesion molecule 1
ICD-10. *See International Classification of Diseases*, Tenth Revision
ICG. *See* Indocyanine green
ICSI. *See* Intracytoplasmic sperm injection
Idoxuridine, 454, 455*t*
IFIS. *See* Intraoperative floppy iris syndrome
IgA. *See* Immunoglobulin A
IgE. *See* Immunoglobulin E
IgE–mediated hypersensitivity reaction. *See* Immunoglobulin E (IgE)–mediated hypersensitivity reaction
IgG. *See* Immunoglobulin G
Ilevro. *See* Nepafenac
ILM. *See* Internal limiting membrane
Imaging studies
  computed tomography. *See* Computed tomography
  indications for, 480, 483, 501–503*t*
  magnetic resonance imaging. *See* Magnetic resonance imaging
  ordering of, 495, 499, 501–503*t*
  ultrasound/ultrasonography. *See* Ultrasound/ultrasonography
Imidazoles, 451–453, 452*t*
Imipenem/cilastatin sodium, 440*t*
Immunoglobulin A (IgA), 263
Immunoglobulin E (IgE), 420
Immunoglobulin E (IgE)–mediated hypersensitivity reaction, 366
Immunoglobulin G (IgG), 420
Immunomodulatory therapy (IMT), 424, 425–428*t*

Implants, for drug delivery, 383
Imprinting
  definition of, 190
  diseases caused by abnormalities in, 190
IMT. *See* Immunomodulatory therapy
In vitro fertilization, 250
Inborn errors of metabolism, 215
Incomplete penetrance, 220
Incontinentia pigmenti, 224*f*, 236*t*
Indels, 187
Independent assortment, 183–185
Indirect-acting adrenergic agonists, 406–407
Indirect-acting agonists
  cholinergic, 398–399
  nicotinic, 401
Indirect traumatic optic neuropathy, 118
Indocyanine green (ICG), 381, 467
Indomethacin, 432*t*, 433
INDs. *See* Investigational new drugs
Induced pluripotent stem cells
  CRISPR–Cas9 and, 208
  description of, 173
Inducible nitric oxide synthase (iNOS), 414–415
Infectious keratitis, 449
Inferior canaliculus, 34*f*
Inferior oblique muscle
  anatomy of, 18*f*, 30*f*, 109*f*
  characteristics of, 20*t*
  magnetic resonance imaging of, 486*f*
  origins of, 19
Inferior ophthalmic vein, 13, 13*f*, 28*f*
Inferior orbital fissure, 7*f*, 11*f*, 12–13
Inferior punctum, 29
Inferior rectus muscle
  anatomy of, 18*f*, 21*f*, 30*f*, 109*f*
  characteristics of, 20*t*
  computed tomography of, 482*f*
  magnetic resonance imaging of, 486*f*
Inferior tarsal muscle, 36
Inferior turbinate, 16*f*
Inferomedial orbital strut, 15
Inferotemporal fossa, 12
Inflamase Forte. *See* Prednisolone sodium phosphate
Inflammation, orbital
  imaging studies for, 503*t*
  nonsteroidal anti-inflammatory drugs for, 433
Infliximab, 426*t*
Information technology (IT), 508
Infraorbital artery, 25*f*
Infraorbital canal, 12
Infraorbital foramen, 10*f*
Infraorbital groove, 7*f*, 9, 10*f*
Infraorbital vein, 28*f*
Infundibulum, 111*f*
Inheritance
  codominant patterns of, 214
  dominant
    autosomal, 219–221, 220*t*
    description of, 214–215
    X-linked, 223, 223*t*
  maternal, 194, 225
  multifactorial, 243–244
  polygenic, 243–244
  recessive
    autosomal, 215–219
    description of, 214–215
    X-linked, 221–222, 222*t*
  X-linked
    description of, 221
    disorders associated with, 223–225
    dominant, 223, 223*t*
    recessive, 221–222, 222*t*
Inner neuroblastic layer, 163*f*
Inner nuclear layer, 97
Inner plexiform layer, 97
iNOS. *See* Inducible nitric oxide synthase
Inositol, 288
Institute of Medicine
  electronic health records and, 506
  quality and, 505
Insulin-like growth factor, 472
Insulin-like growth factor 1 receptor inhibitors, 475
Insulin-like growth factor binding proteins, 290
Intelligent Research Into Sight (IRIS) Registry, 388, 507
Intercellular adhesion molecule 1 (ICAM-1), 264, 438
Interdigitations, 298, 298*f*
Interferon, 428*t*, 470–471
Interferon alfa-2a, 428*t*
Interferon alfa-2b, 428*t*, 471
Intermarginal sulcus, 29
Intermittent ataxia, 217*t*
Intermuscular septum, 46
Internal carotid artery
  anatomy of, 108*f*
  description of, 143
  magnetic resonance imaging of, 486*f*
Internal limiting membrane (ILM)
  anatomy of, 76*f*
  development of, 162
  vitreoretinal interface, 305
Internal reflectivity, 489
International Classification of Diseases, Tenth Revision (ICD-10), 506, 507*t*
International HapMap Project, 201–202
Internuclear ophthalmoplegia, 502*t*
Interphotoreceptor retinoid-binding protein (IRBP), 336
Intersexes, 231
Intracameral drug delivery, 369*t*, 378, 379*t*
Intracytoplasmic sperm injection (ICSI), 251
Intramuscular injections, 381
Intraocular gases, 379*t*
Intraocular injections, 378–380
Intraocular lenses, for drug delivery, 384
Intraocular pressure
  apraclonidine hydrochloride effects on, 404
  β-agonist effects on, 408
  brimonidine effects on, 406
  carbachol effects on, 395
  carbonic anhydrase inhibitors' effect on, 412
  factors that affect, 283
  glucocorticoid-induced elevation of, 422, 423*t*
  Goldmann equation and, 284
  maintenance of, 284
  netarsudil effects on, 416
Intraoperative floppy iris syndrome (IFIS), 404
Intravenous injections, 381

Intravitreal drug delivery, 369*t*, 379*t*, 379–380, 421*t*
Introns
  description of, 186
  excision of, 189
Investigational new drugs (INDs), 390
Iodinated contrast agents, 483
Ionization constant, 275
Iontophoresis, 385
Iopidine. *See* Apraclonidine hydrochloride
IPE. *See* Iris pigment epithelium
IRBP. *See* Interphotoreceptor retinoid-binding protein
Iridocyclitis, 400, 456
Iris
  anatomy of, 48*f*, 70–71*f*
  anterior pigmented epithelium of, 73*f*, 73–74
  blood vessels of, 73
  collarette of, 73
  development of, 166–167, 166–167*f*
  dilator muscles of
    description of, 73–74, 169*f*
    phenylephrine hydrochloride effects on, 403
  functions of, 281
  intramuscular circle of, 27
  layers of, 73*f*
  nerves of, 73
  parasympathetic innervation of, 74
  physiology of, 281–282
  posterior pigmented epithelium of, 74
  prostaglandin analogues' effect on, 414
  sphincter muscles of
    anatomy of, 73*f*, 169*f*
    direct-acting cholinergic agonists' effect on, 394
  stroma of, 72
  structures of, 72
  surfaces of, 73*f*
  sympathetic innervation of, 74
  ultrasound biomicroscopy of, 498–499*f*
IRIS (Intelligent Research Into Sight) Registry, 388, 507
Iris pigment epithelium (IPE), 74
Iron, in aqueous humor, 287
Irreversible cholinesterase inhibitors, 398
Irrigating solutions, 466–467
Isoforms, 190
Isoniazid, 244
Isopto Atropine. *See* Atropine sulfate
Isopto Homatropine. *See* Homatropine hydrobromide
Isopto Hyoscine. *See* Scopolamine hydrobromide
Isosorbide, 419
Istalol. *See* Timolol maleate
IT. *See* Information technology
Itraconazole, 452*t*, 453

JAK inhibitors, 428*t*
Junctional scotoma, 501*t*
Juxtacanalicular trabecular meshwork
  definition of, 65
  Schlemm canal and, 66*f*

Kanamycin sulfate, 440*t*, 448
Karyotype, 200*t*, 201, 204*f*
Karyotyping, 228
K_{cat}, 410
Kearns-Sayre syndrome, 241, 242*t*
Kennedy disease, 195
Keratocytes, 53, 271, 275
Ketoconazole, 452*t*, 453
Ketoprofen, 432*t*
Ketorolac tromethamine, 420*t*, 432*t*, 433
Ketotifen fumarate, 434*t*, 436
Klebsiella spp, 441
Klippel-Trénaunay-Weber syndrome, 236*t*
K_m, 410
Knudson's hypothesis, 233–234
Krabbe disease, 216*t*

L cones, 323, 326
Lacrimal artery, 25*f*, 27*f*, 41
Lacrimal bone, 10*f*
Lacrimal canaliculi, 43
Lacrimal crest, 9*f*
Lacrimal drainage system, 34*f*, 40*f*, 42*f*, 42–44
Lacrimal glands
  accessory, 41–42, 265. *See also specific gland*
  anatomy of, 39–41
  cells of, 41
  characteristics of, 32*t*
  development of, 171
  fossa of, 7, 8*f*
  innervation of, 263
  lobule of, 42*f*
  magnetic resonance imaging of, 485*t*
  orbital lobe of, 263
  palpebral, 39
  palpebral lobe of, 263
  secretions produced by, 41
  tear production from, 171
Lacrimal nerve, 13*f*, 135
Lacrimal puncta, 42, 43
Lacrimal reflex arc, 141*f*
Lacrimal sac, 43
  anatomy of, 33*f*
  fossa of, 7*f*, 8
Lactate, in aqueous humor, 287
Lamina cribosa, 113, 115
Lamina fusca, 59
Lamina papyracea, 8
Laminin, 313
Lantoprostene bunod (LBN), 413*t*, 415
Laser subepithelial keratomileusis, 275
Lastacaft. *See* Alcaftadine
Latanoprost, 382, 386, 413, 413*t*
Latanoprost/timolol maleate, 413*t*, 417*t*
Lateral canthus, 29*f*
Lateral geniculate nucleus
  anatomic relationships with, 129*f*
  anatomy of, 119, 120, 121*f*
  blood supply of, 124*t*
Lateral orbital wall, 10–11, 11*f*
Lateral palpebral artery, 39*f*
Lateral rectus muscle
  anatomy of, 109*f*
  blood supply to, 23
  characteristics of, 20*t*
  computed tomography of, 482*f*
  innervation of, 24
  magnetic resonance imaging of, 486*f*

Lateral transverse B-scan, 491
LBN. *See* Lantoprostene bunod
Leber congenital amaurosis
  genetic heterogeneity of, 227
  RPE65 pathogenic variants as cause of, 206, 343*t*
Leber hereditary optic neuropathy (LHON)
  causes of, 347
  description of, 242–243
  family history of, 212
  features of, 242*t*
Lecithin retinol acyltransferase (LRAT), 336, 337*f*
Legionella pneumophila, 450
Legionnaires' disease, 450
Leigh necrotizing encephalopathy, 217*t*
Leigh syndrome, 242*t*
Lens
  anatomy of, 82
  bow zone/bow region of, 295
  capsule of, 83, 83*f*
  chemical composition of, 295–297
  cortex of, 295
  crystallins in, 293, 296–297
  cytoskeletal proteins in, 297
  definition of, 82, 293
  embryologic development of, 160–161, 161*f*
  epithelium of, 83, 85
    development of, 161*f*
    structure of, 294–295
  fibers of, 85, 295
  formation of, 160–161, 161*f*
  germinative zone of, 85
  glucose metabolism in, 301*f*
  interdigitations, 298, 298*f*
  magnetic resonance imaging of, 485*t*, 486*f*
  major intrinsic protein expression by, 295, 297
  metabolism in, 300–302
  microscopic appearance of, 83*f*
  nucleus of, 295
  organization of, 84*f*
  oxidative damage to, 350–351
  physiology of, 299–300
  plasma membranes of, 295–296
  potassium in, 299
  proteins of
    description of, 296–297
    posttranslational modifications to, 297
  pump–leak hypothesis of solute movement in, 300*f*
  refractive index of, 293
  sodium in, 299
  sorbitol accumulation in, 302
  structure of, 293–295, 294*f*
  sutures of, 85
  transparency of, 298–299
  zonular fibers of, 85–86, 86*f*, 294
Lens capsule
  anatomy of, 293–294, 294*f*
  formation of, 160, 161*f*
  structure of, 293–294, 294*f*
  ultrasound biomicroscopy of, 498*f*
Lens equator, 295
Lens pit, 160
Lens vesicle, 160, 161*f*
Lesser wing of sphenoid bone, 7–8*f*, 11
Leukotrienes, 431*f*
Levator aponeurosis, 30*f*, 33–35
Levator palpebrae superioris
  anatomy of, 18*f*, 21*f*, 30*f*, 33–35, 109*f*
  characteristics of, 20*t*
  computed tomography of, 482*f*
  innervation of, 24, 127
  magnetic resonance imaging of, 486*f*
  origins of, 19
Levobunolol hydrochloride, 409, 409*t*
Levocabastine hydrochloride, 434*t*
Levofloxacin, 444*t*
LFA-1. *See* Lymphocyte function–associated antigen-1
LHON. *See* Leber hereditary optic neuropathy
Lidocaine, 378, 379*t*, 461*t*, 463–465
Lifitegrast, 264, 269, 438
Ligament of Weiger, 166
Light reflex, 128
Likelihood ratio, 199
Limbal palisades of Vogt, 58*f*
Limbus
  anatomy of, 56–57, 58*f*
  definition of, 48
LINEs. *See* Long interspersed elements
Linkage disequilibrium, 185
Lipid layer of tear film, 262
Lipid peroxidation, 347–349
Lipid solubility, 375
Lipid strip, 262
Lipids, 334
Lipofuscin, 102, 338
Lipophilic (lipophobic), 363
Liposomes, for drug delivery, 385
Lisch nodules, 196
Local administration, of drugs, 377–380
Local anesthetics
  composition of, 461
  intraocular surgery use of, 464–466
  mechanism of action, 462*t*
  overview of, 460–462
  peribulbar anesthesia, 465
  regional, 461*t*
  retrobulbar anesthesia, 465
  topical, 462, 462*t*, 464
  toxic manifestations of, 462*t*
  types of, 463–464
Lockwood ligament, 36
Lodoxamide tromethamine, 434*t*, 435–436
Logarithm of odds score, 199
Logical Observations, Identifiers, Names, and Codes (LOINC), 507*t*
Long arm 13 deletion syndrome, 232
Long interspersed elements (LINEs), 187
Long posterior ciliary artery, 26*f*
Longitudinal ciliary muscle, 27*f*
Longitudinal scans, 490, 495–496*f*
Loss of heterozygosity, 194
Lotemax. *See* Loteprednol etabonate
Loteprednol etabonate, 420*t*, 424, 435
Loteprednol etabonate/tobramycin, 445*t*
Louis-Bar syndrome, 191, 236*t*
Low-frequency ultrasound, 488

Lower eyelids
anatomy of, 29
development of, 170–171, 171*f*
muscles of, 36
punctum of, 42
LOXL1 gene, 205
LRAT. *See* Lecithin retinol acyltransferase
Lumigan. *See* Bimatoprost
Lutein, 97
Lymphatics, of eyelids, 39, 40*f*
Lymphocyte function–associated antigen-1 (LFA-1), 269, 438
Lymphocyte inhibitors, 427*t*
Lyonization, 191, 238–240, 239*f*

M cones, 323, 327
Machine learning, 510–511
Macroautophagy, 342
Macroglia, 328
Macrolide antibiotics, 450
Macula
anatomy of, 87, 97
antioxidant localization in, 355*f*
B-scan ultrasonography of, 496*f*
fibers of, 113
fovea of. *See* Fovea
Macula lutea, 97
Macular degeneration
age-related
genome-wide association studies for, 202
indocyanine green applications in, 467
Manhattan plot for, 204*f*
neovascular, 473
oxidative stress in, 358–359
vascular endothelial growth factor inhibitors for, 473
disciform, 498*f*
ultrasonographic findings in, 497*f*
Macular pucker, 308
Magnetic resonance angiography (MRA), 481*t*, 484
Magnetic resonance imaging (MRI)
computed tomography versus, 481*t*, 483
concerns regarding, 484, 486
description of, 479
diffusion-weighted imaging, 484
disadvantages of, 484
echo time, 483
gray matter on, 484, 485*t*, 486*f*
indications for, 483, 501–503*t*
metallic foreign bodies and, 484
ocular anatomy on, 485*t*, 486*f*
principles of, 483
repetition time, 483
T1-weighted images, 483, 486*f*
T2-weighted images, 483–484, 486*f*
Magnetic resonance venography (MVA), 481*t*
Main sensory nucleus, 133
Maintenance of certification (MOC), 505
Major arterial circle, 26*f*, 75
Major intrinsic protein, 295, 297
MAK-associated retinitis pigmentosa, 237
MALT. *See* Mucosa-associated lymphoid tissue
Mammillary body, 111*f*
Manganese superoxide dismutase (MnSOD), 353
Manhattan plot, 202–203
Mannitol, 417–418, 418*t*
Mannosidosis, 216*t*
Maple syrup urine disease, 217*t*
Marcaine. *See* Bupivacaine
Marfan syndrome, 227
fibrillin defects in, 308
lens zonular fibers in, 86
pleiotropism in, 196
Marginal arterial cascade, 38
Massively parallel sequencing, 201
Mast cell(s), 434
Mast-cell stabilizers, 434–436
Maternal inheritance, 194, 225, 225*f*
Maternally inherited diabetes and deafness (MIDD), 241, 242*t*
Matrix metalloproteinase(s) (MMPs)
-9, 263–264
in cornea, 277
in tear film, 263–264
in vitreous from myopia patients, 310
Maxidex. *See* Dexamethasone sodium phosphate
Maxillary antrum, 9
Maxillary artery, 25*f*
Maxillary bone, 7*f*, 10–11*f*
Maxillary sinus, 11*f*, 12, 15–16*f*
Maxilloethmoidal suture, 9*f*
Maxitrol. *See* Dexamethasone/neomycin sulfate/polymyxin B sulfate
Mechanism of action, 364–365
Meckel cave, 135
Medial canthus, 29*f*
Medial lemniscus, 109*f*
Medial longitudinal fasciculus, 137
Medial margin, of orbit, 9
Medial orbital wall, 9, 9*f*
Medial palpebral artery, 25*f*
Medial rectus muscle
anatomy of, 18*f*, 109*f*
characteristics of, 20*t*
computed tomography of, 482*f*
magnetic resonance imaging of, 486*f*
Medical therapy, 388–390
Medrysone, 420*t*, 423*t*
Meibomian glands
anatomy of, 30*f*, 32*t*, 37*f*
dysfunction of, 262
innervation of, 265
phospholipid secretion by, 262
Meiosis, 181–183, 182*f*
Melanin
magnetic resonance imaging of, 483
in retinal pigment epithelium, 101, 341
Melanocytes, 168, 414
Melanogenesis, 341
Melanosomes, 101, 414
MELAS. *See* Mitochondrial encephalomyopathy, lactic acidosis, and stroke-like episodes
Meloxicam, 432*t*
Membrane proteins, in lens, 297
Membrane-spanning mucins, 264

Mendel, Gregor, 214
Mendelian diseases, 194
Meningeal sheaths, 117*f*
Meningiomas, 110
Mepivacaine, 461*t*, 463
Merlin, 234
MERRF. *See* Myoclonic epilepsy with ragged red fibers
Mesencephalic nucleus, 132
Mesencephalon, 126, 151*f*
Mesoderm
  derivatives of, 155*t*
  description of, 149, 151*f*
  in embryologic development, 156*f*
  hyaloid artery arising from, 165*f*
Messenger RNA (mRNA)
  description of, 186
  intron excision, 189
  proteins, 287
Metabolic acidosis, 412
Metachromatic leukodystrophy, 216*t*
Metaphase, 180, 180*f*
Metarhodopsin II, 318
Methazolamide, 411*t*, 412
Methicillin-resistant *Staphylococcus aureus* (MRSA), 378, 449
Methicillin sodium, 440*t*
Methotrexate, 425*t*
Methylation, 190
Methylprednisolone, 419
Metipranolol hydrochloride, 409*t*, 410
Meyer loop, 120, 122*f*
Mezlocillin sodium, 441
mGy. *See* Milligray
Micafungin, 453*t*
Miconazole nitrate, 452*t*, 453
Microautophagy, 342
Microglia, 327
Microinvasive glaucoma surgery (MIGS), 487
Microphthalmia-associated transcription factor (MITF), 173
Micropinocytotic vesicles, 65
Microsatellites, 187
Microsomal triglyceride transfer protein, 325*t*
MIDD. *See* Maternally inherited diabetes and deafness
Middle cerebral artery, 108*f*, 145*f*
Middle cranial fossa, 108*f*, 486*f*
Middle limiting membrane (MLM), 96
Middle turbinate, 16*f*
MIGS. *See* Microinvasive glaucoma surgery
Milligray (mGy), 482
Millisievert (mSv), 482
Minocycline, 446
Minors, genetic testing of, 252
Miotics, 396, 397*t*
Mismatch repair, 191
MITF. *See* Microphthalmia-associated transcription factor
Mitochondria, 185–186
Mitochondrial diseases
  causes of, 241
  chronic progressive external ophthalmoplegia, 241, 242*t*
  description of, 240–241
  features of, 242*t*
  Leber hereditary optic neuropathy. *See* Leber hereditary optic neuropathy
  maternally inherited diabetes and deafness, 241, 242*t*
  mitochondrial encephalomyopathy, lactic acidosis, and stroke-like episodes, 241, 242*t*
  myoclonic epilepsy with ragged red fibers, 242*t*, 243*f*
  neurogenic muscle weakness, ataxia, and retinitis pigmentosa, 242*t*
Mitochondrial DNA
  acquisition of, 186
  diseases associated with. *See* Mitochondrial diseases
  replicative segregation of, 241
  spontaneous deletions and mutations of, 240
Mitochondrial encephalomyopathy, lactic acidosis, and stroke-like episodes (MELAS), 241, 242*t*
Mitomycin C, 389*t*, 436–437
Mitophagy, 342
Mitosis, 179
Mitotic nondisjunction, 228, 230
MLM. *See* Middle limiting membrane
MMPs. *See* Matrix metalloproteinase(s)
MnSOD. *See* Manganese superoxide dismutase
MOC. *See* Maintenance of certification
Molecular genetics
  cell cycle, 179–183, 180*f*
  DNA damage and repair, 191–192
  gene structure, 185–187
  gene therapy. *See* Gene therapy
  gene transcription and translation. *See* Gene transcription and translation
  mitochondrial diseases. *See* Mitochondrial diseases
  noncoding DNA, 187
Monoamine oxidase inhibitors, α_2-adrenergic agonist interactions with, 406
Monogenic diseases, 194
Monosomy, 228
Morphogenic gradients, 171–173
Morphogens, 173
Mosaicism, 229–231
Mosaics, 229
Moxeza. *See* Moxifloxacin hydrochloride
Moxifloxacin hydrochloride, 379*t*, 444*t*
MPSs. *See* Mucopolysaccaridoses
MRA. *See* Magnetic resonance angiography
MRI. *See* Magnetic resonance imaging
mRNA. *See* Messenger RNA
MRSA. *See* Methicillin-resistant *Staphylococcus aureus*
mSv. *See* Millisievert
Mucin glycoproteins, 273
Mucins, 264–265
Mucopolysaccharidoses (MPSs), 184, 216*t*
Mucosa-associated lymphoid tissue (MALT), 44
Müller cells
  description of, 93, 97, 113, 114*f*
  development of, 163*f*
Müller muscle, 29, 33, 35
Multifactorial inheritance, 243–244
Muscarinic drugs
  adverse effects of, 397
  agonists
    adverse effects of, 397
    direct-acting, 394–398, 395–396*f*
    indirect-acting, 398–399
  antagonists, 399–400

Muscarinic receptors, 393, 393*f*, 394*t*
Muscle of Riolan, 31*f*, 32, 33*f*
Mutagens, 192
Mutations. *See* Pathogenic variants
MVA. *See* Magnetic resonance venography
Myasthenia gravis, neostigmine methylsulfate for, 401
Mycophenolate mofetil, 425*t*
Mycoplasma pneumoniae, 450
Mydfrin. *See* Phenylephrine hydrochloride
Mydral. *See* Tropicamide
Mydriacyl. *See* Tropicamide
Mydriasis, 399, 399*t*
Myoclonic epilepsy with ragged red fibers (MERRF), 242*t*, 243*f*
Myopia, 310
Myosin VIIA, 324*t*
Myositis, 497*f*
Myotonic dystrophy, 195

N-retinylidene-phosphatidylethanolamine, 338
Nabumetone, 432*t*
NADH reductase. *See* Nicotinamide adenine dinucleotide (NADH) reductase
NADPH. *See* Nicotinamide adenine dinucleotide phosphate
Nafcillin, 441
Na^+,K^+-ATPase
  description of, 278, 283, 299
  in retinal pigment epithelium, 334
Nanotechnology, for drug delivery, 385–386
Naphazoline hydrochloride, 434*t*
Naphazoline hydrochloride/antazoline phosphate, 434*t*
Naphazoline hydrochloride/pheniramine maleate, 434*t*
Naphcon-A. *See* Naphazoline hydrochloride/pheniramine maleate
Naproxen, 432*t*
NARP. *See* Neurogenic muscle weakness, ataxia, and retinitis pigmentosa
Nasal vein, 28*f*
Nasociliary nerve, 13*f*, 55, 135–136, 136*f*
Nasofrontal vein, 28*f*
Nasolacrimal duct
  anatomy of, 10*f*, 12, 43
  obstruction of, 43
Natacyn. *See* Natamycin
Natamycin, 451, 452*t*
NDP gene, 227
Near reflex, 130–131
Near synkinesis, 130
Near triad, 130
Nedocromil sodium, 434*t*
Neisseria spp, 441–442
Neo-Synephrine. *See* Phenylephrine hydrochloride
Neofrin. *See* Phenylephrine hydrochloride
Neomycin sulfate, 440*t*, 448
Neomycin sulfate/polymyxin B sulfate/prednisolone acetate, 445*t*
Neosporin. *See* Polymyxin B sulfate/neomycin sulfate/gramicidin
Neostigmine methylsulfate, 401
Nepafenac, 420*t*, 433
Nephrogenic systemic fibrosis, 484
Nervus intermedius, 141
Netarsudil, 416
Nettleship-Falls ocular albinism, 238
Neural crest cells
  definition of, 150
  ectomesenchymal cells derived from, 169*f*
  migration of, 152–153*f*
  types of, 150
Neural retina
  anatomy of, 48*f*
  development of, 162, 163*f*
  lamination of, 162
Neurocutaneous syndromes, 234–237
Neuroectoderm, 155*t*, 156*f*, 167
Neuroectodermal cells, 163
Neuroendocrine proteins, in aqueous humor, 289
Neurofibromatosis 1
  expressivity in, 196
  features of, 235*t*
  genetics of, 233–234
Neurofibromatosis 2, 235*t*
Neurogenic muscle weakness, ataxia, and retinitis pigmentosa (NARP), 242*t*
Neuromuscular blocking drugs, 401*t*
Neuronal nitric oxide synthase (nNOS), 414-415
Neurons, retinal, 326–328, 338
Neuropeptide Y (NPY), 262
Neurosensory retina
  cells of, 315
  definition of, 87
  description of, 87
  embryology of, 161
  external limiting membrane of, 96
  ganglion cell layer of, 97
  glial elements of, 92
  inner nuclear layer of, 97
  inner plexiform layer of, 97
  internal limiting membrane of, 97
  layers of, 88*f*, 88–89
  middle limiting membrane of, 96
  nerve fiber layer of, 97
  neuronal elements of, 89–92, 90*f*
  outer nuclear layer of, 96
  outer plexiform layer of, 96
  retinal pigment epithelium and, 96
  stratification of, 94–97, 96*f*
  vascular elements of, 92–94, 94–95*f*
Neurotransmitters, 374*f*
Neurotrophic proteins, 289
Nevanac. *See* Nepafenac
Nicotinamide adenine dinucleotide hydrogen dehydrogenase, 243
Nicotinamide adenine dinucleotide (NADH) reductase, 353
Nicotinamide adenine dinucleotide phosphate (NADPH), 321, 345
Nicotinic drugs
  antagonists, 401*t*, 401–402
  indirect-acting agonists, 401
Nicotinic receptors, 393, 393*f*, 394*t*
Niemann-Pick disease, 217*t*
Nitric oxide (NO), 414–415
Nitric oxide donors, 414–415
Nizoral. *See* Ketoconazole
nNOS. *See* Neuronal nitric oxide synthase

NO. *See* Nitric oxide
Nonadherence, 391–392, 392*t*
Noncoding DNA, 187
Nondepolarizing agents, 401
Nondisjunction
  meiotic, 228
  mitotic, 228, 230
Nonhomologous chromosomes, 184
Noninvasive prenatal screening, 251
Nonpenetrance, 195
Nonpigmented epithelium (NPE)
  definition of, 282
  tight junctions of, 282, 288
Nonsteroidal anti-inflammatory drugs (NSAIDs). *See also specific drugs*
  corneal complications of, 433
  cyclooxygenase inhibition by, 430
  cystoid macular edema treated with, 433
  derivatives of, 430
  types of, 420*t*, 431–433, 432*t*
Norflox. *See* Norfloxacin
Norfloxacin, 444*t*
Norrie disease, 227
Note bloat, 506
Novocain. *See* Procaine
NPE. *See* Nonpigmented epithelium
NPY. *See* Neuropeptide Y
Nrf2. *See* Nuclear factor erythroid 2–related factor
Nrl, 162
NSAIDs. *See* Nonsteroidal anti-inflammatory drugs
Nuclear factor erythroid 2–related factor (Nrf2), 349
Nucleic acids, in retinal pigment epithelium, 334
Nucleotides, 185
Null allele, 205
Null variants, 193
Nystagmus, 502*t*

Oblate cornea, 51*f*
Ocriplasmin, 313
Ocu-Dex. *See* Dexamethasone sodium phosphate
Ocufen. *See* Flurbiprofen sodium
Ocuflox. *See* Ofloxacin
Ocular adnexa
  anatomy of, 5–15, 7–16*f*
  development of, 170–171, 171*f*
  extraocular muscles. *See* Extraocular muscles
  glands of, 32*t*
  orbit. *See* Orbit
Ocular albinism
  definition of, 249
  description of, 101
  X-linked, 238–239
Ocular decongestants, 439
Ocular development
  adnexa, 170–171, 171*f*
  anterior chamber, 168
  choroid, 168
  ciliary body, 166–167, 167*f*
  cornea, 168, 169*f*
  diffusible ligands in, 172–173
  embryogenesis in, 149–150, 150–154*f*
  extraocular muscles, 168–170
  genetic cascades, 171–173
  growth factors in, 172–173
  homeobox genes, 172
  iris, 166–167, 166–167*f*
  lacrimal gland, 171
  lens, 160–161, 161*f*
  morphogenic gradients, 171–173
  morphogens in, 173
  neural crest cell migration in, 152–153*f*
  optic nerve, 163, 164*f*
  orbit, 171
  retina, 162, 163*f*
  retinal pigment epithelium, 163
  sclera, 168
  timeline of, 154, 156–157*f*, 158*t*
  uvea, 166
  vitreous, 163, 165*f*, 166
Ocular drug design, 382–386
Ocular emollients, 437
Ocular foreign bodies, 484
Ocular hypotony, 497*f*
Ocular inserts, 382–383
Ocular pharmacotherapeutics. *See* Pharmacotherapeutics
Ocular surgery, anesthetics in, 464–466
Oculoauriculovertebral dysplasia, 152
Oculocardiac reflex, 133, 400
Oculocutaneous albinism, 101, 238
Oculomotor foramen, 21*f*
Oculomotor nerve
  anatomy of, 111*f*, 126–128
  extraocular muscles innervated by, 24
  fascicular portion of, 127
  inferior division of, 128
  muscles innervated by, 126
  nucleus complex of, 126, 127*f*
  palsy of, 502*t*
  subnuclei of, 126
  superior division of, 128
Oculomotor nerve palsy, 128
Ocumeter, 409*t*
Ocupress. *See* Carteolol hydrochloride
Off-bipolar cells, 326
Off-label drug use, 389*t*, 389–390
Ofloxacin, 443, 444*t*
Oguchi disease, 237, 323*t*
Ointments, 377
Olfactory bulb, 111*f*
Olfactory fossa, 486*f*
Olfactory nerve, 110, 111*f*
Olfactory tract, 110
Oligodendrocytes, 163
Olopatadine hydrochloride, 436
Omidria, 404
OMIM. *See* Online Mendelian Inheritance in Man
Omnipred. *See* Prednisolone acetate
On-bipolar cells, 326–327
"On-label" prescribing, 389
Oncogenes, 194
ONH. *See* Optic nerve head
ONL. *See* Outer nuclear layer
Online Mendelian Inheritance in Man (OMIM), 198
Opcon-A. *See* Naphazoline hydrochloride/pheniramine maleate

Open reading frame (ORF), 186
Ophthalmic artery
  anatomy of, 23, 25*f*, 27*f*, 108*f*, 123
  branches of, 23
Ophthalmic viscosurgical devices (OVDs), 379*t*, 468
Ophthetic. *See* Proparacaine
OPL. *See* Outer plexiform layer
Optic atrophy, in DIDMOAD syndrome, 197
Optic canal
  anatomy of, 7*f*, 11
  computed tomography of, 12*f*, 482*f*
Optic chiasm
  anatomy of, 111*f*, 119–120
  blood supply of, 124*t*
Optic cup, 112
  anatomy of, 166*f*
  formation of, 315
  invagination of, 159
Optic cup margin, 166*f*
Optic disc, 87
  anatomy of, 48*f*
  definition of, 111
  edema of, 497*f*
Optic foramen, 11
Optic nerve
  anatomy of, 9, 21*f*, 48*f*, 110, 112*f*
  blood supply of, 123–125, 124–126*f*
  computed tomography of, 482*f*
  development of, 163, 164*f*
  embryologic development of, 163, 164*f*
  intracanalicular region of, 118
  intracranial region of, 118
  intraocular region of, 111–116, 114–115*f*
  intraorbital region of, 116–118, 125
  lateral geniculate nucleus of, 119, 120, 121*f*
  magnetic resonance imaging of, 485*t*
  meningeal sheaths of, 116–118, 117*f*
  regional differences in, 113*t*
  topographic areas of, 110
  vascular supply of, 125*f*
Optic nerve drusen, 501*t*
Optic nerve head (ONH), 99
  description of, 110
  laminar area of, 115
  prelaminar area of, 115
  retrolaminar area of, 116
  schematic representation of, 114*f*
  size of, 110
  spontaneous venous pulsation of, 117
  superficial nerve fiber layer of, 113, 115*f*
Optic nerve sheath, 117*f*
  description of, 485*t*
  dural, 116
  fenestration of, 116
Optic neuritis, 501*t*
Optic neuropathy, 501*t*
Optic radiations, 120, 122*f*, 124*t*
Optic stalk, 156*f*, 163
Optic sulci, 154
Optic tract
  anatomy of, 120
  blood supply of, 124*t*
  visual pathways in, 119
Optic vesicles, 154
Opticin, 307
OptiPranolol. *See* Metipranolol hydrochloride
Optivar. *See* Azelastine hydrochloride
Ora serrata
  anatomy of, 48*f*, 102, 103*f*
  description of, 87
Orbicularis oculi muscle
  anatomy of, 30*f*, 31–32, 33*f*
  innervation of, 31
  palpebral, 31
  tarsal, 43
Orbit
  anatomy of, 5–15, 7–16*f*
  arteries of, 25*f*, 27*f*
  bony, 6, 7*f*
  canals of, 7*f*, 12
  computed tomography of, 12*f*
  connective tissues of, 46*f*
  depth of, 6
  development of, 171
  dimensions of, 6
  entrance to, 6
  extraocular muscle distribution in, 22–23
  fissures of, 12–13, 12–13*f*
  foramina of, 11–12
  inflammation of
    imaging studies for, 503*t*
    nonsteroidal anti-inflammatory drugs for, 433
  margin of, 6, 8*f*
  neoplasms of, 497*f*
  periorbital sinuses and, 13–15
  rim of, 6
  roof of, 7–8, 8*f*
  trauma to, 503*t*
  tumors of, 503*t*
  vascular supply and drainage of, 24–28, 25–28*f*
  veins of, 28*f*
  vortex veins of, 26*f*, 27–28, 28*f*
Orbital apex, 6, 13*f*
Orbital cellulitis, 503*t*
Orbital diseases, 503*t*
Orbital fat, 30*f*, 32, 35*f*, 485*t*
Orbital floor
  anatomy of, 9*f*, 9–10
  fractures of, 10
  right, 9–10*f*
Orbital pseudotumor, 497*f*
Orbital septum, 30*f*, 32
Orbital wall
  lateral, 10–11, 11*f*
  medial, 8, 9*f*
ORF. *See* Open reading frame
Organic anions, in aqueous humor, 287
Ornithine aminotransferase, 325*t*
Osmitrol. *See* Mannitol
Osmotic drugs, 417–419, 418*t*
Osmotic hypothesis, 302
Ouabain, 300, 340
Outer neuroblastic layer, 163*f*
Outer nuclear layer (ONL), 96
Outer plexiform layer (OPL), 96
OVDs. *See* Ophthalmic viscosurgical devices

Oxaprozin, 432*t*
Oxidative stress
  in age-related macular degeneration, 358–359
  causes of, 345
  ciliary body and, 281
  in diabetic retinopathy, 357–358
  in glaucoma, 358–359
  in vision-threatening ophthalmic diseases, 354–359
  after vitrectomy, 311
Oxybuprocaine. *See* Benoxinate
Oxygen
  in aqueous humor, 291
  retinal consumption of, 316
  in vitreous, 311, 312*f*

p53, 191
PACS. *See* Picture archiving and communications systems
Palatine bone, 7*f*
Palisades of Vogt, 271, 274
Palmitic acid, 334
Palpebral conjunctiva, 30*f*, 38, 38*f*, 44
Palpebral fissure, 28, 37*f*
Palpebral lacrimal gland, 39
Pancuronium, 401
Papilledema, 501*t*
Papillomacular fibers, 92
para-Aminobenzenesulfonamide, 445
Parafovea, 100
Parcaine. *See* Proparacaine
Paremyd. *See* Hydroxyamphetamine hydrobromide/tropicamide
Parinaud oculoglandular syndrome, 39
Pars plana of ciliary body, 75
Pars plicata of ciliary body, 75, 77*f*, 499*f*
Pathogenic variants
  description of, 192–193
  identification of, 199–205
  polymorphisms versus, 193
  screening for, 199–205
PAX2 pathologic variants, 189
PAX6, 172
  in aniridia, 231–232
  description of, 189
  pathogenic variants of, 231
PCAB. *See* Pharmacy Compounding Accreditation Board
PCR. *See* Polymerase chain reaction
PE. *See* Pigmented epithelium
Pearson syndrome, 241, 242*t*
Pedigree analysis, 212–213, 213*f*
Pegaptanib, 473, 474*t*
Pemirolast potassium, 434*t*
Penetrance, 195–196
Penicillin(s), 439–441, 440*t*
Penicillinase-resistant penicillins, 441
Pentose phosphate pathway, 301
Perfluorocarbon, 379*t*
Peribulbar anesthesia, 465
Pericytes, 83, 328
Perifovea, 100
Periocular injections, 377–378
Periorbital lacerations, 32
Periorbital sinuses
  anatomy of, 13–15
  computed tomography of, 16*f*
  orbit and, 13–15
Periorbital space–occupying lesions, 497*f*
Peripheral arterial cascade, 30*f*, 38
Peripheral cornea, 51
Peripheral vitreous, 305
Peripherin, 321, 324*t*
Peroxin, 325*t*
Persistent fetal vasculature, 160, 166, 497*f*
Persistent hyperplastic primary vitreous, 303
Persons with disabilities, referrals for providers of support for, 251
PET-CT. *See* Positron emission tomography (PET)–computed tomography
Peters anomaly, 231
Petroclinoid ligament, 137
PGD. *See* Preimplantation genetic diagnosis
$PGF_{2\alpha}$. *See* Prostaglandin $F_{2\alpha}$
Phagosomes, 102, 333
Phakinin, 297
Phakomatoses, 211
Pharmacodynamics, 363–365, 364
Pharmacogenetics, 244–245, 386
Pharmacogenomics, 386
Pharmacokinetics
  definition of, 363–364
  topical eyedrops, 373*f*
Pharmacologic principles
  in elderly patients, 367–368
  mechanism of action, 364–365
  pharmacodynamics, 363–365, 364
  pharmacokinetics. *See* Pharmacokinetics
  pharmacotherapeutics, 364–365
  terminology associated with, 363
  toxicity, 365–366
Pharmacology, 363
Pharmacotherapeutics. *See also specific drug*
  biosimilar drugs, 475, 476*t*
  compounded pharmaceuticals, 390–391
  definition of, 364–365
  legal aspects of, 388–390
  nonadherence, 391–392
Pharmacy Compounding Accreditation Board (PCAB), 390
Phenethicillin, 439–441
Phenocopy, 194
Phenotype, 193–194
Phenylephrine hydrochloride
  blepharoptosis contraindications for, 36
  blood pressure affected by, 403
  description of, 398, 399*t*
  intracameral use of, 379*t*, 403
Phosphate, in aqueous humor, 287
Phosphatidylcholine, 334
Phosphatidylethanolamine, 334
Phosphodiesterase, 318, 320*f*
Phospholine iodide, 398
Phospholipase A_2, 430, 447
Photo-oxidation, 347–348

Photoreceptor(s)
cones. *See* Cones
depolarized state of, 318, 319*f*
inner segments of, 328, 331
outer segments of, 315, 317*f*, 320*f*, 331
retinal degeneration caused by gene alterations in, 323
rods. *See* Rod(s)
Photoreceptor cells
anatomy of, 90*f*
description of, 89
synaptic bodies of, 91*f*
Phototransduction
cone, 321–322
definition of, 315
rod, 316–321
Physostigmine, 397*t*
Phytanoyl-CoA hydroxylase, 325*t*
Pial sheath, 118
Picture archiving and communications systems (PACS), 506
PIGF. *See* Placental growth factor
Pigment epithelium–derived factor, 342
Pigmented epithelium (PE), 282
PIK3CA-related overgrowth spectrum (PROS), 236*t*
Pilocarpine hydrochloride
Adie (tonic) pupil diagnosed using, 395
characteristics of, 397*t*
ocular inserts for delivery of, 383
ointment, 397*t*
primary open-angle glaucoma treated with, 395
Pineal gland, 119*f*
Piperacillin sodium, 441
Piroxicam, 432*t*
Placental growth factor (PIGF), 472
Plasma, 285*t*
Plasma proteins, in aqueous humor, 288–289
Pleiotropism, 196–197
PLGA. *See* Poly(lactic-*co*-glycolic acid)
Plica semilunaris, 29*f*, 46
POAG. *See* Primary open-angle glaucoma
Polar amphiphilic phospholipids, 262
Poly-Dex. *See* Dexamethasone/neomycin sulfate/polymyxin B sulfate
Poly-Pred. *See* Neomycin sulfate/polymyxin B sulfate/prednisolone acetate
Polyallelism, 184
Polyenes, 451, 452*t*
Polyhexamethylene biguanide, 459
Polyinosinic acid–polycytidylic acid, 470
Poly(lactic-*co*-glycolic acid) (PLGA), 379*t*
Polymerase chain reaction (PCR)
advantages of, 200*t*
disadvantages of, 200*t*
fluorescent, 251
principles of, 197
thermal cycling in, 197
Polymorphisms
definition of, 193
pathogenic variants versus, 193
single-nucleotide, 193, 205, 386
Polymyxin B sulfate, 440*t*, 450
Polymyxin B sulfate/bacitracin zinc, 444*t*
Polymyxin B sulfate/neomycin sulfate/bacitracin zinc, 444*t*
Polymyxin B sulfate/neomycin sulfate/gramicidin, 444*t*
Polymyxin B sulfate/trimethoprim sulfate, 444*t*, 450
Polyquaternium-1, 366
Polytrim. *See* Polymyxin B sulfate/trimethoprim sulfate
Polyunsaturated fatty acids (PUFAs), 348, 351
Polyvinyl alcohol (PVA), 375
Positional candidate gene screening, 199
Positron emission tomography (PET)–computed tomography, 480
Posterior cerebral artery, 108*f*, 111*f*, 145*f*
Posterior chamber
anatomy of, 48
dimensions of, 49*t*
ultrasound biomicroscopy of, 498*f*
Posterior ciliary arteries, 25–26*f*, 125
Posterior clinoid, 108*f*
Posterior colobomas, 159
Posterior communicating artery
anatomy of, 108–109*f*, 127, 145*f*
aneurysms of, 145
Posterior cornea, 54*f*
Posterior ethmoidal artery, 25*f*
Posterior ethmoidal foramen, 7*f*, 11
Posterior hyaloid, 305, 306*f*
Posterior juxtascleral drug delivery, 369*t*
Posterior lacrimal crest, 7*f*
Posterior nonpigmented epithelium of the iris, 167*f*
Posterior pigmented epithelium, 74
Posterior pole, 305
Posterior scleritis, 490
Posterior synechiae, 399
Posterior vitreous detachment (PVD)
description of, 310, 310*f*
enzymes that induce, 313
ultrasonographic findings in, 498*f*
Postganglionic fibers, 16
Potassium, in lens, 299
Povidone-iodine solution, 450
Prader-Willi syndrome, 190
Pralidoxime, 398
Precorneal tear film. *See* Tear film
Precursor RNA, 187
Pred-G. *See* Prednisolone acetate/gentamicin sulfate
Pred Mild. *See* Prednisolone acetate
Prednisol. *See* Prednisolone sodium phosphate
Prednisolone acetate, 374, 420*t*, 423*t*
Prednisolone acetate/gentamicin sulfate, 445*t*
Prednisolone acetate/sulfacetamide sodium, 445*t*
Prednisolone sodium phosphate, 420*t*
Prednisolone sodium phosphate/sulfacetamide sodium, 445*t*
Preimplantation genetic diagnosis (PGD), 251
Prenatal diagnosis, 250–251
Presbyopia, 78
Preservatives, 366, 367*t*
Primary open-angle glaucoma (POAG), 244, 356, 395, 400, 407–408
Primary visual cortex, 120, 123*f*, 124*t*
Primary vitreous, 163, 166*f*
Primers, 197
Probabilistic training, 510

Procaine, 461*t*
Procerus muscle, 33*f*
Prodrugs, 382
Prolate cornea, 51*f*
Prolensa. *See* Bromfenac sodium
Proliferative diabetic retinopathy, 311
Proliferative retinopathy, 498*f*
Proliferative vitreoretinopathy (PVR), 343
Proparacaine, 462*t*, 463
Prophase, 180, 180*f*
Propine. *See* Dipivefrin hydrochloride
PROS. *See PIK3CA*-related overgrowth spectrum
Prostaglandin analogues, 413*t*, 413–414
Prostaglandin-endoperoxide synthase, 430
Prostaglandin $F_{2\alpha}$ ($PGF_{2\alpha}$), 431*f*
Prostaglandin $F_{2\alpha}$ receptor gene *(PTGFR),* 386
Protein(s)
  in aqueous humor, 288–289
  cytoskeletal, 297
  in lens, 296–297
  membrane, 297
  in retinal pigment epithelium, 333–334
  in tear film, 263
  in vitreous, 307
Proteinase inhibitors, 289
Proteinases, 289
Proteoglycans, 53
Proteus spp, 441–442
Pseudocholinesterase, 245, 398
Pseudodominance, 219
Pseudohermaphrodites, 231
Pseudomonas aeruginosa, 443
Pseudotumor cerebri, 410
Pseudoxanthoma elasticum, 249
Pterygoid venous plexus, 28*f*
Pterygopalatine fossa, 13, 136
Pterygopalatine ganglion, 13
PTGFR. See Prostaglandin $F_{2\alpha}$ receptor gene
Ptosis, 192
PUFAs. *See* Polyunsaturated fatty acids
Punctal plug–mediated drug delivery, 384–385
Punctum of canaliculus, 29
Pupil reflexes
  light reflex, 128, 130*f*
  near reflex, 130–131
  pathways for, 128–131, 130*f*
Pupillary light reflex, 128, 130*f*
Purified neurotoxin complex, 466
PVA. *See* Polyvinyl alcohol (PVA)
PVD. *See* Posterior vitreous detachment
PVR. *See* Proliferative vitreoretinopathy

Quixin. *See* Levofloxacin

Rab escort protein 1, 325*t*
Racemose angioma, 236*t*
Radial ciliary muscle, 27*f*
Radial ultrasound biomicroscopy scans, 495, 499*f*
Radiation retinopathy, 358
Ranibizumab, 473, 474*t*
Ranibizumab-eqrn, 475
Ranibizumab-nuna, 475
RB1 gene pathogenic variants, 233
RBP. *See* Retinol-binding protein
RCFM. *See* Retrocorneal fibrous membrane
RDH. *See* Retinol dehydrogenase
Reactive oxygen species (ROS)
  cell protection from, 350
  defense mechanisms and, 349–350
  description of, 345
  detoxification of, 346*f*
  generation of, 346*f*
  in glaucoma, 355
  oxidative stress caused by, 345
  pathways of, 347*t*
  radiation retinopathy caused by, 358
  retinal vulnerability to, 351–352
  sources of, 346
  UV light as source of, 350
Rebamipide, 439
Recessive diseases, 205–206
Recessive inheritance
  autosomal, 215–219
  description of, 214–215
  X-linked, 221–222, 222*f*, 222*t*
Recessive tumor suppressor genes, 232
Recombination frequency, 199
Red nucleus, 109*f*
Reference standards, 510–512
Reflectance, 509
Reflex tearing, 376
Refsum disease, 217*t*, 325*t*
Regional anesthetics, 461*t*
Remote patient monitoring, 508
Repetition time (TR), 483
Replicative segregation, 241
Residence time, 372, 384
Respiratory burst, 346
Retina
  adhesion of, 341
  anatomy of, 48, 86–87
  anomalies of, ultrasonographic findings in, 497*f*
  antioxidant localization in, 355*f*
  arterioles of, 94
  blood vessels of, 94
  blood–retina barrier, 92, 94*f*
  cells of, 315
    amacrine cells, 327
    bipolar cells, 326, 326*f*
    classes of, 326*f*, 326–328
    ganglion cells, 327–328
    glial cells, 328
    horizontal cells, 325*f*, 326–327
    neurons, 326–328, 338
    vascular cells, 328
  circulation of, 94
  development of, 162, 162*f*
  electrophysiology of, 329, 330*f*
  embryologic development of, 87, 162, 162*f*
  gyrate atrophy of, 217*t*
  layers of, 92–93*f*, 98*f*
  magnetic resonance imaging of, 485*t*
  neural
    anatomy of, 48*f*
    development of, 162, 162*f*
    lamination of, 162

neurosensory
cells of, 315
definition of, 87
description of, 87
external limiting membrane of, 96
ganglion cell layer of, 97
glial elements of, 92
inner nuclear layer of, 97
inner plexiform layer of, 97
internal limiting membrane of, 97
layers of, 88*f*, 88–89
middle limiting membrane of, 96
nerve fiber layer of, 97
neuronal elements of, 89–92, 90*f*
outer nuclear layer of, 96
outer plexiform layer of, 96
retinal pigment epithelium and, 96
stratification of, 94–97, 96*f*
vascular elements of, 92–94, 94–95*f*
oxygen consumption by, 316
reactive oxygen species vulnerability of, 351–352
"Rim" proteins, 321
thickness of, 97
topography of, 97–100, 98*f*
vascular supply of, 162
veins of, 94
visual pathways of, 118–119
Retinal break, 498*f*
Retinal degeneration
gene alterations that cause, 323
gene defects that cause, 325*t*
Retinal detachment
definition of, 101
description of, 341
rhegmatogenous, 342
Retinal ganglion cells (RGCs), 345
Retinal organoids, 174
Retinal pigment epithelium (RPE)
antioxidants in, 352–354
apical membrane of, 340
autophagy in, 342
basal surface of, 331
biochemical composition of, 333–334
cells of
11-*cis*-retinaldehyde generation by, 336
cytoplasm of, 102
description of, 100
functions of, 101–102
illustration of, 332*f*
melanin granules in, 331, 333
Na^+,K^+-ATPase in, 334
number of, 331
choriocapillaris and, 332*f*
congenital hypertrophy of, in familial adenomatous polyposis, 213, 214*f*
development of, 163, 331
in disease, 343, 343*t*
embryology of, 100, 161
functions of, 100
genetic defects in, 343
glucose in, 333
histology of, 339*f*
lipids in, 334
melanin pigment in, 101, 341
net ionic fluxes in, 340
neurosensory retina and, 96
nucleic acids in, 334
phagocytosis of shed photoreceptor outer-segment discs by, 338
phosphatidylcholine in, 334
phosphatidylethanolamine in, 334
physiologic roles of, 334–342, 335*f*
pigmentation in, 341
proteins in, 333–334
in retinal adhesion, 341
RPE65 protein expression in, 334
secretions by, 342
structure of, 331–333
tight junctions in, 89
transport proteins in, 340
vitamin A regeneration in, 336–338, 337*f*
Retinitis pigmentosa
autosomal dominant, 220, 323
autosomal recessive, 323
description of, 191
inheritance patterns for, 220, 226
MAK-associated, 237
X-linked, 239*f*
Retinoblastoma
aniridia versus, 231
enucleation for, 115
genetics of, 232
hereditary, 232
Knudson's hypothesis and, 233–234
sporadic, 233*f*
tumorigenesis in, 232
ultrasonographic findings in, 497*f*
Retinocerebral angiomatosis, 236*t*
Retinoid cycle, 336, 337*f*
Retinol-binding protein (RBP), 336
Retinol dehydrogenase (RDH), 337*f*
Retinopathy of prematurity, 497*f*
Retrobulbar anesthesia, 465
Retrobulbar drug delivery, 369*t*
Retrocorneal fibrous membrane (RCFM), 279
Retrolaminar area, 116
Retrovir. *See* Zidovudine
Reversible cholinesterase inhibitors, 398
Reye syndrome, 432–433
RGCs. *See* Retinal ganglion cells
Rhegmatogenous retinal detachment, 342
Rho guanosine triphosphate hydrolase (Rho GTPase), 415
Rho kinase (ROCK), 415–416
Rho kinase inhibitors, 415–416
Rhodopsin, 317*f*, 317–318, 336
Rhodopsin kinase, 323*t*
Rhodopsin *(RHO)* gene pathogenic variant, 323
Ribozymes, 207–208
Riley-Day syndrome, 217*t*, 237
"Rim" proteins, 321
Rimexolone, 429
Ripasudil, 416
Rituximab, 427*t*

RNA
  messenger
    description of, 186
    intron excision, 189
    proteins, 287
  precursor, 187
  retinal pigment epithelium synthesis of, 334
  short interfering, 208
ROCK. *See* Rho kinase
Rocuronium, 401
Rod(s)
  anatomy of, 89, 90*f*
  cones versus, 316–317
  inner segment of, 89
  light effects on, 329, 329*f*
  neuronal elements of, 89
  number of, 89
  phototransduction of, 316–321
Rod ABC transporter, 323*t*
Rod cGMP-gated channel, 323*t*
Rod cGMP phosphodiesterase, 323*t*
Rod monochromatism, 324*t*
Rod outer segment protein 1, 308, 324*t*
Rod transducin, 323*t*
Romycin. *See* Erythromycin
ROS. *See* Reactive oxygen species
Rose bengal, 467
RPE. *See* Retinal pigment epithelium
RPE65 gene
  description of, 334, 343*t*
  gene therapy trials with, 206
  Leber congenital amaurosis caused by, 206, 343*t*
Rubeosis iridis, 27, 74
"Rule of twelves," 9
RxNorm, 507*t*

S cones, 322
Sandhoff disease, 216*t*
Sanfilippo syndrome, 216*t*
Sanger sequencing, 199, 201
Satellites, 187
Sattler layer, 79
Scheie syndrome, 184, 216*t*
Schlemm canal, 168
  anatomy of, 64, 65
  collector channels from, 67, 68*f*
  endothelial lining of, 67*f*
  juxtacanalicular trabecular meshwork and, 66*f*
  schematic representation of, 68*f*
Schwalbe line, 57, 61*f*, 64, 103
Schwann cells, 163
Schwannomin, 234
Sclera
  anatomy of, 48, 48*f*, 57–59, 276*f*
  avascular nature of, 58, 59*f*
  collagen fibers of, 59
  composition of, 276*f*
  development of, 168
  emissaria of, 58
  episcleral vessels of, 59, 59*f*
  magnetic resonance imaging of, 485*t*
  rupture of, 58
  stroma of, 59
  uveal attachment to, 69
Scleral spur, 167*f*
  anatomy of, 61*f*
  cells of, 64
  formation of, 168
Scleral sulcus, internal, 64
Scopolamine hydrobromide, 399*t*
Seafood allergy, 450
Second-generation cephalosporins, 442
Secondary vitreous, 163, 165*f*, 166, 303
Secretory IgA (sIgA), 263
Secukinumab, 427*t*
Segregation, genetic, 184
Selenium, 352
Selenoprotein P, 289
Sella turcica, 108*f*
Semilunar ganglion, 134
Sensorcaine. *See* Bupivacaine
Sequencing, 200*t*
Sex chromosomes
  aneuploidy of, 228
  mosaicism, 230
Sex-determining region Y (SRY), 221
sFlt-1, 271
SFT. *See* "Store-and-forward" telemedicine
Short arm 11 deletion syndrome, 231–232
Short ciliary arteries, 25*f*, 124*f*
Short ciliary nerves, 17, 78
Short interfering RNA. *See* siRNA
Short interspersed elements (SINEs), 187
Short posterior ciliary artery, 26*f*
Sickle cell disease, 184
sIgA. *See* Secretory IgA
Silicone oil, 379*t*
Simbrinza. *See* Brinzolamide/brimonidine tartrate suspension
SINEs. *See* Short interspersed elements
Single-gene disorders, 193
Single-nucleotide polymorphisms, 193, 205, 386
Single-photon emission computed tomography (SPECT), 480
Singlet oxygen, 347*t*
Sinusitis, 8
siRNA (short interfering RNA), 189, 208
Sirolimus, 426*t*
Skipped generation, 196, 220
Skull, 108*f*
Slow inactivators, 244
SMAS. *See* Superficial musculoaponeurotic system
SNOMED CT. *See* Standard Nomenclature of Medicine Clinical Terms
SNRPN gene, 190
Sodium, in lens, 299
Sodium fluorescein, 381, 467
Sodium-potassium pump, 299, 318, 334
Soluble proteins, in vitreous, 307
Soluble vascular endothelial growth factor receptor 1 (SVEGFR-1), 190
Solutes
  low-molecular-weight, 308
  pump–leak hypothesis of, 300*f*
Somatic development, 159*f*
Somatic variants, 192
Sondermann channels, 68*f*
Sorbitol, 302

Southern blotting, 200*t*
Spatial coherence, 509
SPECT. *See* Single-photon emission computed tomography
Sphenoid bone
  greater wing of, 7–8*f*, 10–11*f*
  lesser wing of, 7–8*f*, 11
Sphenoid sinus, 486*f*
Spherule, 89
Sphingomyelin, 295
Spiral of Tillaux, 21, 22*f*, 103
Spliceosomes, 189
Splicing
  alternative, 190
  definition of, 189
Sporadic retinoblastoma, 233*f*
Sporanox. *See* Itraconazole
SRY. *See* Sex-determining region Y
Standard Nomenclature of Medicine Clinical Terms (SNOMED CT), 507*t*
Standardization of Uveitis Nomenclature, 70
Staphylococcus aureus, 443
Staphylococcus epidermidis, 443
Stargardt disease, 321
Stearic acid, 334
Steinert disease, 195
Stem cells
  definition of, 173
  human embryonic, 173
  induced pluripotent, 173
Stickler syndrome, 313
"Store-and-forward" telemedicine (SFT), 508
Strabismus, 46
Streptococcus bovis, 449
Streptococcus mitis, 450
Streptococcus orientalis, 449
Streptococcus pneumoniae, 443
Streptococcus pyogenes, 449
Streptococcus viridans, 448
Streptokinase, 469
Streptomyces caespitosus, 436
Streptomycin, 448
Striate cortex, 119, 119*f*
Stroma
  choroidal, 82
  ciliary body, 75
  corneal
    anatomy of, 53
    composition of, 53, 59
  glucose delivery to, 271
  iris, 72
  keratocytes of, 271
Sturge-Weber syndrome. *See* Encephalofacial angiomatosis
Sub-Tenon
  anesthesia, 465
  drug delivery, 369*t*
Subconjunctival drug delivery, 369*t*
Subepithelial plexus, 55
Suborbicularis oculi fat, 30*f*
Subretinal space, 340
Substantia nigra, 109*f*
Succinylcholine, 245, 398, 401
Sugar cataracts, 302
Sulfacetamide ophthalmic solutions, 446
Sulfacetamide sodium, 444*t*
Sulfite oxidase deficiency, 217*t*
Sulfonamides, 380, 445–446
Sulindac, 432*t*
Superficial musculoaponeurotic system (SMAS), 140
Superficial nerve fiber layer, 113, 115*f*
Superficial plexus, 58
Superficial temporal artery, 38
Superior cerebellar artery, 109*f*
Superior eyelid crease, 29
Superior oblique muscle
  anatomy of, 8, 18*f*, 21*f*, 30*f*, 109*f*
  characteristics of, 20*t*
  innervation of, 24
  magnetic resonance imaging of, 486*f*
  origins of, 19
Superior oblique tendon, 18*f*
Superior ophthalmic vein, 28*f*
Superior orbital fissure
  anatomy of, 7*f*, 12, 108*f*, 136
  computed tomography of, 12*f*
Superior punctum, 29
Superior rectus muscle
  anatomy of, 18*f*, 21*f*, 30*f*, 109*f*
  characteristics of, 20*t*
  computed tomography of, 482*f*
  magnetic resonance imaging of, 486*f*
Superior rectus tendon, 18*f*
Superior turbinate, 16*f*
Superoxide anion, 347*t*
Superoxide dismutase, 353
Supraciliary space, 79
Supraorbital artery, 25*f*, 39*f*
Supraorbital foramen, 8*f*, 11
Supraorbital notch, 6, 8*f*
Supraorbital vein, 28*f*
Supratrochlear artery, 25*f*, 39*f*
Supratrochlear nerve, 135
Surface-active agents, 376
Surfactants, 376
Surgery, anesthetics in, 464–466
Suspension, 364, 374
Sustained-release drug delivery, 382–386
Sustained-release oral preparations, 381
sVEGFR-1. *See* Soluble VEGF receptor 1
Symporters, 283
Synaptic body, 89
Syntenic traits, 185
Systemically administered antimicrobial drugs, ocular penetration of, 459–460, 460*t*

T-cell inhibitors, 425*t*
T1-weighted images, 483, 486*f*
T2-weighted images, 483–484, 486*f*
Tachyphylaxis, 409
Tacrolimus, 426*t*
Tafluprost, 382, 413, 413*t*
Taq polymerase, 197
Tarsal glands, 249
Tarsal plates, 37
Tarsus, 30*f*, 37
TASS. *See* Toxic anterior segment syndrome

Tay-Sachs disease
description of, 216*t*
ethnic characteristics of, 237
TDF. *See* Testis-determining factor
TE. *See* Echo time
Tear(s), artificial, 437
Tear film
antimicrobial components of, 263
aqueous component of, 263–264
components of, 259
description of, 49–50, 259, 271
dysfunction of, 264, 267–269. *See also* Dry eye syndrome
electrolytes in, 263
functions of, 259
glucose levels in, 263
growth factors in, 264
layers of, 260, 261*f*
lipid layer of, 262
matrix metalloproteinase 9 levels in, 263–264
mucoaqueous layer of, 262–265
osmolarity of, 268
peptide hormones in, 265
properties of, 261*t*
proteins in, 263
secretion of, 265–266
solutes of, 263
steroid hormones in, 265
thickness of, 260, 261*t*
Tear lake, 371
Tear meniscus, 259, 260*f*
Tear reflex pathway, 141
Tear substitutes, 269
Teleconsultations, 508
Telemedicine, 508
Teleophthalmology, 508
Telepresenter, 508
Telomeric DNA, 187
Telophase, 180, 180*f*
Temporal coherence, 510
Temporal lobe, 486*f*
Tenon capsule
anatomy of, 45, 45*f*
functions of, 57
Teprotumumab, 475
Terson syndrome, 498*f*
Tertiary vitreous, 165*f*, 166, 303
Testis-determining factor (TDF), 221
Tetracaine, 462*t*, 464
Tetrahydrotriamcinolone, 423*t*
TetraVisc. *See* Tetracaine
Thalamus, 119*f*
Thermal cycling, 197
Third-generation cephalosporins, 442
3' untranslated region, 186
Thrombin, 469
Thrombospondin 1, 311
Thymidine kinase, 454
Thymine, 185
Thymoxamine hydrochloride, 407–408
Thyroid eye disease, 475, 503*t*
Ticarcillin sodium, 440*t*, 441
Tight junctions, 52, 52*f*, 282
Timolol hemihydrate, 409*t*
Timolol maleate, 409, 409*t*
Timoptic, 409*t*
Timoptic-XE, 409*t*
TIMP3, 343*t*
Tissue inhibitor of metalloproteinase, 342
Tissue plasminogen activator (tPA), 379*t*, 389*t*, 469
Tobradex. *See* Dexamethasone/tobramycin
Tobramycin sulfate, 440*t*, 444*t*, 448
Tobrasol. *See* Tobramycin sulfate
Tobrex. *See* Tobramycin sulfate
Tocilizumab, 427*t*
Tofacitinib, 428*t*
Tolmetin, 432*t*
Tonic cells, 328
Topical anesthetics, 464
Topical drugs
absorption of, 373
binding of, 377
concentration of, 374
delivery of, 369*t*
eyedrops, 368–377
ionic charge of, 375–376
lipid solubility of, 375
ointments, 377
pH, 375
pharmacokinetics of, 373*f*
reflex tearing, 376
retention of, 371–373
solubility of, 374
surfactants, 376
viscosity of, 375
Toxic anterior segment syndrome (TASS), 378, 379*t*
Toxicity, 365–366
tPA. *See* Tissue plasminogen activator
TR. *See* Repetition time
Trabecular meshwork
aging changes to, 64–65
anatomy of, 63*f*
composition of, 64
corneoscleral, 65
juxtacanalicular, 65
layers of, 64
nitric oxide production in, 415
uveal, 65
Trabeculectomy, limbus-based, 58*f*
Trabeculocytes, 65
Training set, 510, 511*f*
Trait
definition of, 214
dominant, 214–215
recessive, 214
syntenic, 185
Tranexamic acid, 470
Transcription factors, 188
Transducin, 318
Transfer RNA, mitochondrial DNA–encoded, 241
Transferrin, in vitreous, 307
Transforming growth factor β, 471
Transketolase, 272
Translation, 188
Transthyretin, 336
Transverse facial artery, 39*f*
Transverse scans, 490–491, 491*f*, 493*f*

"Trapdoor"-type fractures, 10
Travatan. *See* Travoprost
Travatan Z. *See* Travoprost
Travoprost, 382, 413*t*
Travoprost/timolol maleate, 413*t*, 417*t*
Triamcinolone acetonide, 379*t*, 389*t*, 421*t*, 429, 467
Triazoles, 451–453, 452*t*
Trifluridine, 454, 455*t*
Trigeminal ganglion, 134
Trigeminal nerve
  anatomy of, 109*f*, 111*f*, 132
  branches of, 109*f*
  divisions of, 135–137
  innervations by, 132, 132*f*
  intracranial pathway of, 134–135
  main sensory nucleus of, 133
  mandibular division of, 137
  maxillary division of, 136–137
  mesencephalic nucleus of, 133
  motor nucleus of, 134
  nuclear complex of, 133
  ophthalmic division of, 133, 135–136, 136*f*
  pathways of, 132*f*
  sensory nucleus of, 133
  spinal nucleus and tract of, 133–134
Trinucleotides, 185, 187
Trisomy, 228
Trisomy 21
  genetic errors in, 229
  mosaicism, 225
  pharmacogenetics and, 245
Trivariant color vision, 322
Trochlea, 18*f*
Trochlear fossa, 8, 8*f*
Trochlear nerve
  anatomy of, 13*f*, 131
  extraocular muscles innervated by, 24
  fascicles of, 131
  palsy of, 502*t*
Tropicacyl. *See* Tropicamide
Tropicamide, 399*t*
Tropocollagen, 304
Trusopt Ocumeter Plus. *See* Dorzolamide hydrochloride
Trypan blue, 379*t*, 467
TSC1, 237
TSC2, 237
Tuberous sclerosis, 235*t*, 237
Tubulin, 297
Tumor necrosis factor inhibitors, 426*t*
Tumor suppressor genes, 194
Tunica vasculosa lentis, 160, 165*f*
Turner syndrome, 231
2-hit hypothesis, 194
Tyrosinemia, 217*t*

Ubiquinone, 347
UBM. *See* Ultrasound biomicroscopy
Ultrafiltration, 283
Ultrasound biomicroscopy (UBM)
  of anterior chamber, 62*f*
  axial scans, 494, 498*f*
  characteristics of, 494
  ocular anatomy on, 498–499*f*
  radial scans, 495, 499*f*
Ultrasound/ultrasonography
  A-scan probe, 489*f*, 489–490, 490*t*
  B-scan
    axial scans, 490, 491–492*f*
    dynamic, 492, 496*t*, 497–498*f*
    longitudinal scans, 490, 495–496*f*
    probe for, 489*f*
    tissue-specific gain setting for, 496*t*
    transverse scans, 490–491, 491*f*, 493*f*
    types of, 490, 492*f*
  definition of, 488
  devices for, 488, 489*f*
  disease-/disorder-specific findings, 497–498*f*
  high-frequency, 488
  indications for, 488
  low-frequency, 488
  macula imaging on, 496*f*
Ultraviolet light. *See* UV (ultraviolet) light
Upper eyelids
  anatomy of, 29
  development of, 170–171, 171*f*
  muscles of, 33–36
Urea, 417, 418*t*
Uric acid, 248
Urinary stones, 412
Urine alkalinization, 412
Urokinase, 469
US Pharmacopeia (USP), 390
Usher syndrome, 246, 249
USP. *See* US Pharmacopeia
Ustekinumab, 427*t*
UV (ultraviolet) light
  blockage of, 299*f*, 349
  definition of, 299
  reactive oxygen species from, 350
Uvea
  anatomy of, 48, 69*f*
  choroid. *See* Choroid
  ciliary body. *See* Ciliary body
  development of, 166
  iris. *See* Iris
  parts of, 69, 69*f*
  scleral attachment of, 69
Uveal trabecular meshwork, 65
Uveal tract
  anatomy of, 166, 281
  venous circulation of, 80*f*
Uveitis
  anterior, 400
  classification of, 70
  immunomodulatory medications for, 425–428*t*
Uveoscleral pathway, 62

Valacyclovir hydrochloride, 455*t*, 457
Valcyte. *See* Valganciclovir
Valganciclovir, 455*t*, 457
Valtrex HZV. *See* Valacyclovir hydrochloride
Valve of Hasner, 43
van der Waals forces, 341, 364
Vancomycin, 378, 379*t*, 440*t*, 449
Vancomycin flushing syndrome, 449

Varenicline, 438
Vascular cells, 328
Vascular endothelial growth factor (VEGF)
  in aqueous humor, 290
  description of, 471–473
  VEGF-A, 271, 290
  in vitreous, 311
Vascular endothelial growth factor (VEGF) inhibitors, 473–476
Vascular endothelial growth factor (VEGF) receptors
  description of, 290
  sVEGFR-1, 190
Vasoactive intestinal polypeptide (VIP), 262
Vasocidin. *See* Prednisolone sodium phosphate/sulfacetamide sodium
Vasocon-A. *See* Naphazoline hydrochloride/antazoline phosphate
VCAID. *See* Vitreous cavity–associated immune deviation
VCAN gene, 307
Vecuronium, 401
VEGF. *See* Vascular endothelial growth factor
VEGF inhibitors. *See* Vascular endothelial growth factor (VEGF) inhibitors
VEGF receptors. *See* Vascular endothelial growth factor (VEGF) receptors
Vegzelma. *See* Bevacizumab-abcd
Vehicles, 374
Venous sinuses, 142, 144*f*
Vernal conjunctivitis, 263
Versican, 307
Vertebral artery, 111*f*
Vexol. *See* Rimexolone
Vfend. *See* Voriconazole
Vicious circle theory of dry eye syndrome, 265, 267*f*
Vidarabine monohydrate, 455*t*
Vigamox. *See* Moxifloxacin hydrochloride
Vimentin, 297
VIP. *See* Vasoactive intestinal polypeptide
Vira-A. *See* Vidarabine monohydrate
Viroptic. *See* Trifluridine
Viscosity, 375
Visine-A. *See* Naphazoline hydrochloride/pheniramine maleate
Vision loss, transient, 501*t*
Vistide. *See* Cidofovir
Visual cycle, 336, 337*f*
Visual pathways
  anatomy of, 118–119, 119*f*
  blood supply of, 123–125, 124*t*, 124–126*f*, 125*f*
  vascular supply of, 124*t*, 125*f*
VIT1, 307
Vitamin A, 336–338, 337*f*
Vitamin C. *See* Ascorbate
Vitamin E, 351–353, 355*f*
Vitamin supplements, 470
Vitamin therapy, 247
Vitrasert. *See* Ganciclovir sodium
Vitrectomy, 311
Vitreolysis, enzymatic, 313
Vitreoretinal interface, 305, 309
Vitreous
  age-related changes in, 309–313
  anatomy of, 104*f*
  as angiogenesis inhibitor, 311
  chondroitin sulfate in, 305–307
  collagen fibers in
    age-related breakdown of, 309
    description of, 103, 304*f*, 304–305, 306*f*
    proteins associated with, 307
  composition of, 285*t*, 304–308
  cortical, 305
  development of, 163, 165*f*, 166, 303
  functions of, 103
  genetic diseases involving, 313
  hemorrhage-related injury of, 311
  hyalocytes in, 308, 309*f*
  hyaluronan in, 305–306
  illustration of, 104*f*
  inflammation of, 311
  liquefaction of, 309–310
  low-molecular-weight solutes in, 308
  magnetic resonance imaging of, 485*t*, 486*f*
  myopia effects on, 310
  oxygen movement in, 311, 312*f*
  peripheral, 305
  posterior attachments of, 105*f*
  posterior vitreous detachment, 310, 310*f*
  primary, 163, 166, 166*f*, 303
  proteins in, 307
  secondary, 163, 165*f*, 166, 303
  soluble proteins in, 307
  tertiary, 165*f*, 166, 303
  vitrectomy effects on, 311
  zonular fibers of, 307
Vitreous base, 104, 104*f*
Vitreous body, 48
Vitreous cavity, 49*t*
  anatomy of, 48
  ascorbate in, 311, 312*f*
  description of, 103
Vitreous cavity–associated immune deviation (VCAID), 308
Vitreous humor, 48, 103
Voltaren. *See* Diclofenac sodium
von Hippel–Lindau syndrome, 234, 236*t*
von Recklinghausen disease. *See* Neurofibromatosis 1
Voretigene neparvovec, 206
Voriconazole, 452*t*, 453
Vortex veins, 26*f*, 27–28, 28*f*
Vyzulta. *See* Lantoprostene bunod

Waardenburg syndrome, 206
Wagner syndrome, 313
WAGR syndrome, 231
Watershed zone, 125
Wear-and-tear pigment, 102
Whitnall ligament, 30*f*, 33, 36*f*
Whitnall tubercle, 10
Whole-exome sequencing, 199, 200*t*
Whole-genome shotgun sequencing, 203*f*
Wilms tumor, aniridia versus, 231
Wilson disease, 247
Wnt signaling defects, 173
Wyburn-Mason syndrome, 236*t*

X-inactivation, 191
X-linked diseases, 205–206

X-linked inheritance
description of, 221
disorders associated with, 223–225
dominant, 223, 223*t*
recessive, 221–222, 222*f*, 222*t*
X-linked ocular albinism, 238–239
Xalacom. *See* Latanoprost/timolol maleate
Xalatan. *See* Latanoprost
Xeroderma pigmentosum, 191–192
Xibrom. *See* Bromfenac sodium
Xylocaine. *See* Lidocaine

Y-shaped suture, 85

Zaditor. *See* Ketotifen fumarate
Zeaxanthin, 97
Zidovudine, 455*t*, 458
Zinc, in aqueous humor, 287
Zioptan. *See* Tafluprost
Zirgan. *See* Ganciclovir sodium
Zonulae adherentes, 101
Zonulae occludentes, 101
Zonular fibers
of lens, 85–86, 86*f*
ultrasound biomicroscopy of, 499*f*
of vitreous, 307
Zovirax. *See* Acyclovir sodium
Zygomatic bone, 7*f*
Zygomaticofacial artery, 27*f*
Zygomaticofacial foramen, 11
Zygomaticotemporal artery, 27*f*
Zygomaticotemporal foramen, 11
Zylet. *See* Loteprednol etabonate/tobramycin
Zymar. *See* Gatifloxacin
Zymaxid. *See* Gatifloxacin